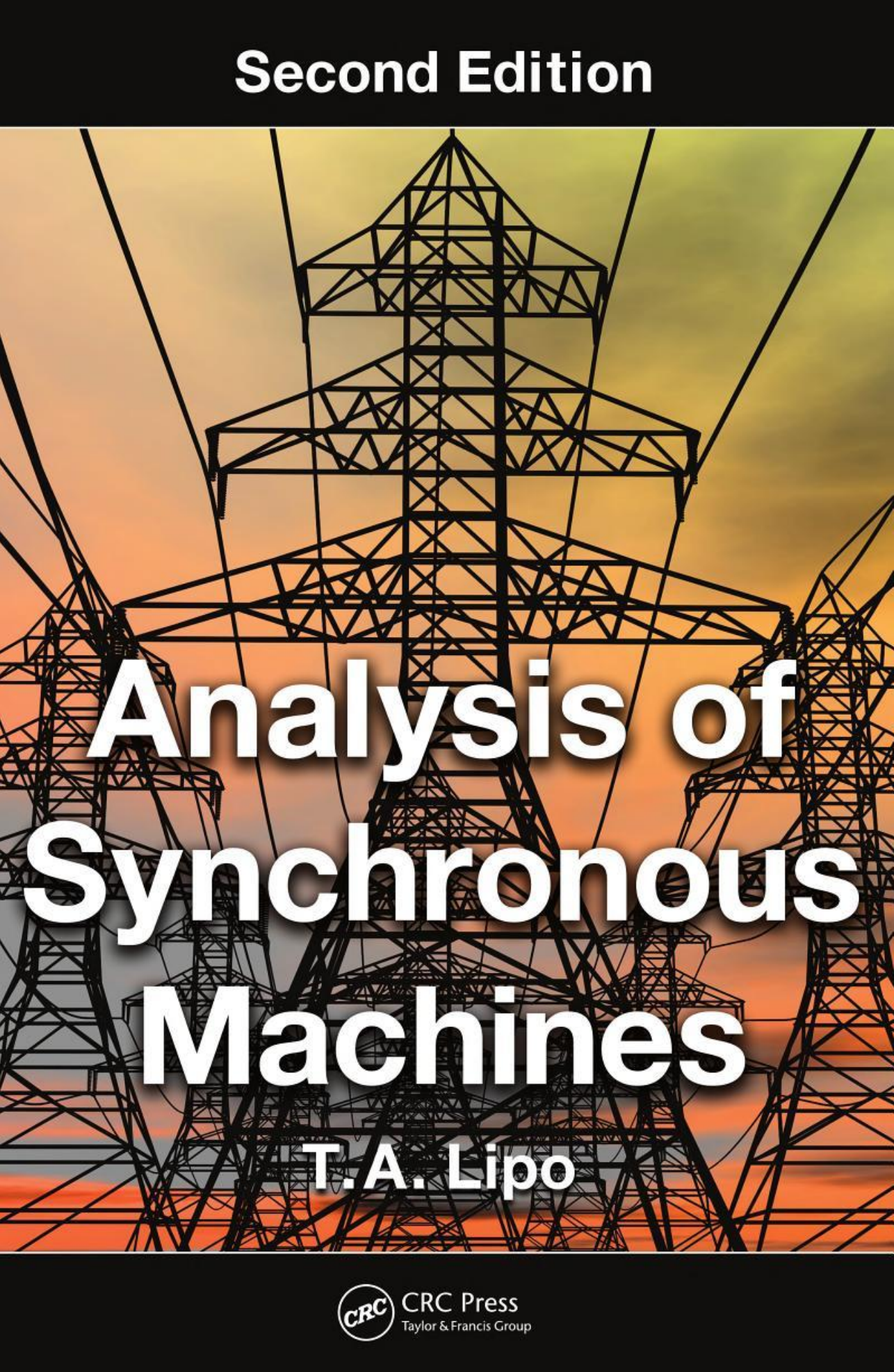


Second Edition



Analysis of Synchronous Machines

T. A. Lipo



CRC Press
Taylor & Francis Group

Second Edition

Analysis of Synchronous Machines

Second Edition

Analysis of Synchronous Machines

T.A. Lipo



CRC Press

Taylor & Francis Group

Boca Raton London New York

CRC Press is an imprint of the
Taylor & Francis Group, an **informa** business

MATLAB® and Simulink® are trademarks of The MathWorks, Inc. and are used with permission. The MathWorks does not warrant the accuracy of the text or exercises in this book. This book's use or discussion of MATLAB® and Simulink® software or related products does not constitute endorsement or sponsorship by The MathWorks of a particular pedagogical approach or particular use of the MATLAB® and Simulink® software.

CRC Press
Taylor & Francis Group
6000 Broken Sound Parkway NW, Suite 300
Boca Raton, FL 33487-2742

© 2012 by Taylor & Francis Group, LLC
CRC Press is an imprint of Taylor & Francis Group, an Informa business

No claim to original U.S. Government works
Version Date: 20120515

International Standard Book Number-13: 978-1-4398-8068-5 (eBook - PDF)

This book contains information obtained from authentic and highly regarded sources. Reasonable efforts have been made to publish reliable data and information, but the author and publisher cannot assume responsibility for the validity of all materials or the consequences of their use. The authors and publishers have attempted to trace the copyright holders of all material reproduced in this publication and apologize to copyright holders if permission to publish in this form has not been obtained. If any copyright material has not been acknowledged please write and let us know so we may rectify in any future reprint.

Except as permitted under U.S. Copyright Law, no part of this book may be reprinted, reproduced, transmitted, or utilized in any form by any electronic, mechanical, or other means, now known or hereafter invented, including photocopying, microfilming, and recording, or in any information storage or retrieval system, without written permission from the publishers.

For permission to photocopy or use material electronically from this work, please access www.copyright.com (<http://www.copyright.com/>) or contact the Copyright Clearance Center, Inc. (CCC), 222 Rosewood Drive, Danvers, MA 01923, 978-750-8400. CCC is a not-for-profit organization that provides licenses and registration for a variety of users. For organizations that have been granted a photocopy license by the CCC, a separate system of payment has been arranged.

Trademark Notice: Product or corporate names may be trademarks or registered trademarks, and are used only for identification and explanation without intent to infringe.

Visit the Taylor & Francis Web site at
<http://www.taylorandfrancis.com>

and the CRC Press Web site at
<http://www.crcpress.com>

CONTENTS

<i>Preface</i>	xiii
<i>Acknowledgments</i>	xv
<i>Chapter 1 Winding Distribution in an Ideal Machine</i>	1
1.1 Introduction	1
1.2 Winding Function.....	2
1.3 Calculation of the Winding Function	8
1.4 Multipole Winding Configurations	22
1.5 Inductances of an Ideal Doubly Cylindrical Machine.....	25
1.6 Calculation of Winding Inductances	29
1.7 Mutual Inductance Calculation—An Example	32
1.8 Winding Functions for Multiple Circuits	39
1.9 Analysis of a Shorted Coil—An Example	46
1.10 General Case for C Circuits	49
1.11 Winding Function Modifications for Salient-Pole Machines	53
1.12 Leakage Inductances of Synchronous Machines	64
1.12.1 Synchronous Machine Stator	64
1.12.2 Synchronous Machine Rotor.....	69
1.13 Practical Winding Design.....	70
1.14 Conclusion.....	75
1.15 References	75
<i>Chapter 2 Reference Frame Theory</i>	77
2.1 Introduction	77
2.2 Rotating Reference Frames	78
2.3 Transformation of Three-Phase Circuit Variables to a Rotating Reference Frame	81
2.3.1 Vector Approach Applied to $r-L$ Circuits.....	81
2.3.2 Transformation Equations	84
2.3.3 System Equations in the $d-q-n$ Coordinate System	92
2.3.4 Power Flow in the $d-q-n$ Equivalent Circuits	95

CONTENTS

2.4	Stationary Three-Phase $r-L$ Circuits Observed in a $d-q-n$ Reference Frame	96
2.4.1	Example	104
2.5	Matrix Approach to the $d-q-n$ Transformation	112
2.5.1	Example	117
2.6	The $d-q-n$ Transformation Applied to a Simple Three-Phase Cylindrical Inductor	121
2.7	Winding Functions in a $d-q-n$ Reference Frame	125
2.8	Direct Computation of $d-q-n$ Inductances of a Cylindrical Three-Phase Inductor.....	131
2.9	Conclusion	134
2.10	References.....	134
 <i>Chapter 3 The $d-q$ Equations of a Synchronous Machine</i>		137
3.1	Introduction.....	137
3.2	Physical Description	137
3.3	Synchronous Machine Equations in the Phase Variable or as -, bs -, cs - Reference Frame.....	138
3.3.1	Voltage Equations.....	140
3.3.2	Flux Linkage Equations	142
3.4	Transformation of the Stator Voltage Equations to a Rotating Reference Frame	143
3.5	Transformation of Stator Flux Linkages to a Rotating Reference Frame	144
3.6	Winding Functions of the Three-Phase Stator Windings in a $d-q-n$ Reference Frame	146
3.7	Winding Functions of the Rotor Windings.....	148
3.7.1	d -Axis Amortisseur Winding Function.....	148
3.7.2	q -Axis Amortisseur Circuit Winding Function.....	155
3.7.3	Field Circuit Winding Function	159
3.8	Calculation of Stator Magnetizing Inductances	160
3.9	Mutual Inductances between Stator and Rotor Circuits	164
3.10	$d-q$ Transformation of the Rotor Flux Linkage Equation	167

CONTENTS

3.11	Power Input.....	168
3.12	Torque Equation.....	169
3.13	Summary of Synchronous Machine Equations Expressed in Physical Units	171
3.14	Turns Ratio Transformation of the Flux Linkage Equations	172
3.15	System Equations in Physical Units Using Hybrid Flux Linkages .	180
3.16	Synchronous Machine Equations in Per Unit Form	181
3.16.1	Base Quantities	181
3.16.2	Voltage Equations	184
3.16.3	Flux Linkage Equations	184
3.16.4	Electromagnetic Torque Equation	185
3.16.5	Motional Equation	186
3.16.6	Power Equation.....	187
3.16.7	Summary	188
3.17	Conclusion	190
3.18	References.....	190

<i>Chapter 4 Steady-State Behavior of Synchronous Machines</i>	193	
4.1	Introduction.....	193
4.2	<i>d–q</i> Axes Orientation	193
4.3	Steady-State Form of Park's Equations	196
4.4	Steady-State Torque Equation	200
4.5	Steady-State Power Equation.....	202
4.6	Steady-State Reactive Power	204
4.7	Graphical Interpretation of the Steady-State Equations.....	204
4.8	Steady-State Vector Diagram	207
4.9	Vector Interpretation of Power and Torque	210
4.10	Phasor Form of the Steady-State Equations.....	216
4.11	Equivalent Circuits of a Synchronous Machine.....	217
4.12	Solutions of the Phasor Equations	221

CONTENTS

4.13	Solution of the Steady-State Synchronous Machine Equations Using MathCAD	223
4.14	Open-Circuit and Short-Circuit Characteristics.....	226
4.15	Saturation Modeling of Synchronous Machines under Load	233
4.16	Construction of the Phasor Diagram for a Saturated Round-Rotor Machine.....	237
4.17	Calculation of the Phasor Diagram for a Saturated Salient-Pole Synchronous Machine.....	240
4.18	Zero Power Factor Characteristic and the Potier Triangle.....	241
4.19	Other Reactance Measurements.....	247
4.20	Steady-State Operating Characteristics.....	250
4.21	Calculation of Pulsating and Average Torque during Starting of Synchronous Motors	253
4.22	Conclusion	262
4.23	References.....	263
<i>Chapter 5 Transient Analysis of Synchronous Machines</i>		265
5.1	Introduction.....	265
5.2	Theorem of Constant Flux Linkages.....	265
5.3	Behavior of Stator Flux Linkages on Short-Circuit.....	266
5.4	Three-Phase Short-Circuit, No Damper Circuits, Resistances Neglected	267
5.5	Three-Phase Short-Circuit from Open Circuit, Resistances and Damper Windings Neglected.....	270
5.6	Short-Circuit from Loaded Condition, Stator Resistance and Damper Winding Neglected	272
5.7	Three-Phase Short-Circuit from Open Circuit, Effect of Resistances Included, No Dampers.....	275
5.8	Extension of the Theory to Machines with Damper Windings.....	282
5.9	Short-Circuit of a Loaded Generator, Dampers Included.....	290
5.10	Vector Diagrams for Sudden Voltage Changes	291

CONTENTS

5.11	Effect of Exciter Response.....	295
5.12	Transient Solutions Utilizing Modal Analysis.....	297
5.13	Comparison of Modal Analysis Solution with Conventional Methods.....	306
5.14	Unsymmetrical Short-Circuits	310
5.15	Conclusion	312
5.16	References.....	312
 <i>Chapter 6 Power System Transient Stability</i>		315
6.1	Introduction.....	315
6.2	Assumptions.....	315
6.3	Torque Angle Curves	318
6.4	Mechanical Acceleration Equation in Per Unit Form.....	320
6.5	Equal Area Criterion for Transient Stability.....	322
6.6	Transient Stability Analysis.....	323
6.7	Transient Stability of a Two Machine System.....	331
6.8	Multi-Machine Transient Stability Analysis.....	333
6.9	Types of Faults and Effect on Stability.....	338
6.10	Step-by-Step Solution Methods Including Saturation	340
6.11	Machine Model Including Saturation	342
6.12	Summary Step-by-Step Method for Calculating Synchronous Machine Transients	347
6.13	Conclusion	348
6.14	References.....	348
 <i>Chapter 7 Excitation Systems and Dynamic Stability</i>		349
7.1	Introduction.....	349
7.2	Generator Response to System Disturbances	350
7.3	Sources of System Damping.....	352
7.4	Excitation System Hardware Implementations.....	353

CONTENTS

7.4.1	Basic Excitation System	353
7.4.2	Basic DC Exciter.....	353
7.4.3	Modeling of Saturation	357
7.4.4	AC Excitation Systems	362
7.4.5	Static Excitation Systems.....	363
7.5	IEEE Type 1 Excitation System	364
7.6	Excitation Design Principles.....	369
7.7	Effect of the Excitation System on Dynamic Stability	374
7.7.1	Generator Operating with Constant Field Flux Linkages.....	374
7.7.2	Generator with Variable Field Flux Linkages	380
7.7.3	Closed-Loop Representation.....	386
7.7.4	Excitation Control of Other Terminal Quantities	390
7.8	Conclusion	392
7.9	References.....	394
<i>Chapter 8 Naturally Commutated Synchronous Motor Drives</i>		395
8.1	Introduction.....	395
8.2	Load Commutated Inverter (LCI) Synchronous Motor Drives	395
8.3	Principle of Inverter Operation	397
8.4	Fundamental Component Representation	399
8.4.1	Phasor Diagram.....	399
8.4.2	Inverter Operation	401
8.4.3	Expression for Power and Torque.....	405
8.5	Control Considerations	406
8.5.1	Firing Angle Controller.....	406
8.6	Starting Considerations	408
8.7	Detailed Steady-State Analysis.....	408
8.7.1	Modes of Converter Operation	411
8.7.2	State Equations.....	413
8.7.3	Conduction Mode 1 State Equations.....	414
8.7.4	Commutation Mode 2 State Equations	417
8.7.5	Calculation of Initial Conditions.....	421

CONTENTS

8.8	Time Step Solution	424
8.9	Sample Calculations.....	425
8.10	Torque Capability Curves	427
8.11	Constant Speed Performance	432
8.12	Comparison of State Space and Phasor Diagram Solutions	434
8.13	Conclusion	436
8.14	References.....	437
 <i>Chapter 9 Extension of $d-q$ Theory to Unbalanced Operation</i>		439
9.1	Introduction.....	439
9.2	Source Voltage Formulation	439
9.3	System Equations to Be Solved	443
9.4	System Formulation with Non-Sinusoidal Stator Voltages	446
9.5	Solution for Currents.....	451
9.6	Solution for Electromagnetic Torque.....	453
9.7	Example Solutions	462
9.8	Conclusion	464
 <i>Chapter 10 Linearization of the Synchronous Machine Equations</i>		467
10.1	Introduction.....	467
10.2	Park's Equations in Physical Units	467
10.3	Linearization Process	469
10.4	Transfer Functions of a Synchronous Machine	474
10.4.1	Transfer Function Inputs.....	474
10.4.2	Transfer Function Outputs	475
10.5	Solution of the State Space and Measurement Equations.....	479
10.6	Design of a Terminal Voltage Controller	485
10.7	Design of a Classical Regulator.....	492
10.8	Conclusion	496
10.9	References.....	496

CONTENTS

<i>Chapter 11 Computer Simulation of Synchronous Machines</i>	497
11.1 Introduction.....	497
11.2 Simulation Equations	497
11.3 MATLAB® Simulation of Park's Equations	500
11.4 Steady-State Check of Simulation	503
11.5 Simulation of the Equations of Transformation.....	507
11.6 Simulation Study.....	519
11.7 Consideration of Saturation Effects.....	520
11.8 Air Gap Saturation	525
11.9 Field Saturation.....	529
11.10 Approximate Models of Synchronous Machines.....	531
11.11 Conclusion	543
 <i>Appendix 1 Identities Useful in AC Machine Analysis</i>	547
 <i>Appendix 2 Time Domain Solution of the State Equation</i>	549
A2.1 Reduction to Explicit Form.....	549
A2.2 Complex Eigenvalues	552
A.2.3 References.....	553
 <i>Appendix 3 Three-Phase Fault</i>	555
 <i>Appendix 4 TrafunSM</i>	563
 <i>Appendix 5 SMHB—Synchronous Machine Harmonic Balance</i>	571
 <i>Index.....</i>	583

PREFACE

The material in this book has evolved from a course taught yearly to senior/graduate students entitled “Theory and Control of Synchronous Machines” at the University of Wisconsin. Begun in 1980, the essence of the course material has not changed substantially. However, the means by which the course is taught has changed dramatically with the evolution of computing tools. The ready availability of MATLAB® and MATHCAD® has rendered many of the traditional methods of problem solving, such as analog simulation, FORTRAN programming, constructional phasor diagrams and so forth, to be mere anecdotes. As a result of these powerful tools, over the years material has been increasingly added to challenge the student and provide a deeper appreciation of the underlying theory of the subject. In particular, the material contained in Chapters 8–11 is rarely included in an introductory course and, if desired, could easily be omitted from a 3-credit course on this subject. These chapters are typically presented by the author as the background material for a lengthy “class problem” near the end of the semester which serves to cap the student’s learning experience. I might add, with some delight, that these computational tools have even added to the “fun” of learning a challenging new subject.

Thomas A. Lipo

Madison, WI

MATLAB ® is a registered trademark of The MathWorks, Inc. For product information, please contact:

The MathWorks, Inc.
3 Apple Hill Drive
Natick, MA 01760-2098 USA
Tel: 508 647 7000
Fax: 508-647-7001
E-mail: info@mathworks.com
Web: www.mathworks.com

ACKNOWLEDGMENTS

The author is indebted to his many graduate students, some of whom have contributed to the production of this book via their MSc. and Ph.D. theses. In addition, numerous other graduate students have also assisted both through their technical contributions as well as thorough proofreading of this text. The author also wishes to thank the David Grainger Foundation for funding and facilities provided at the University of Wisconsin. He is also indebted for facilities provided by the Center for Applied Power Systems, Florida State University during final rewrite of the text. Finally, this book is dedicated to Christine Lipo, wonderful and loving wife, who passed away August 18, 2004.

Chapter 1

Winding Distribution in an Ideal Machine

1.1 Introduction

All conventional machines rely upon magnetic fields for the purpose of energy conversion. Windings are arranged on the periphery of a stationary member (stator) and a rotating member (rotor) so as to set up a field distribution of magnetic flux density in the space which separates them (air gap). By appropriate excitation of the windings, this field can be made to rotate relative to the stationary member (synchronous machine), relative to the rotating member (DC machine) or relative to both members (induction machine). The interaction of the flux components produced by the stator and rotor members result in the production of torque. Subsequent rotation of the rotor results in electromechanical energy conversion.

A valid approach to the study of electric machines is to deal directly with the electromagnetic fields. Knowledge of the field distribution leads to a deeper understanding of where flux is concentrated, where currents flow, where forces appear, and where heat is generated within the machine. Such detailed information is very important, since relatively small alterations in the design can often lead to substantial improvements in efficiency, cost, or reliability of the machine. The serious student of machine design must eventually be required to delve into the electromagnetic fields associated with rotating machines. Unfortunately, the analysis of machines as a fields problem involves the solution of Laplace's or Poisson's equation. The geometry of machines leads to complicated boundary conditions even for simplified cases. A digital computer must generally be used to find complete field distributions.

The approach of this book is to characterize the machine in terms of coupled magnetic circuits rather than magnetic fields. Our interest is then restricted primarily to the terminal rather than internal characteristics of machines. Although one loses sight of the exact spatial distribution of currents

and fluxes, the problem becomes immensely simplified. However, to ensure an understanding of the simplifying assumptions, one must initially deal directly with the fields. The significant effects of the rotating fields must be expressed properly in terms of flux linkages in rotating coupled circuits. Since flux linkage is proportional to inductance, the ability to characterize winding distributions and utilize this characterization in the calculation of winding inductances is of central importance.

1.2 Winding Function

It is useful to begin a study of winding distribution by considering what is generally termed a doubly cylindrical machine. In such a machine a cylindrical rotor is assumed which is axially aligned within a cylindrical stator shell. Such a device is shown in Figure 1.1. In this device the air gap separating the stator and rotor members is assumed to be uniform and is also considered to be small relative to the rotor radius. The inner stator radius is R_s and the rotor radius is R_r .

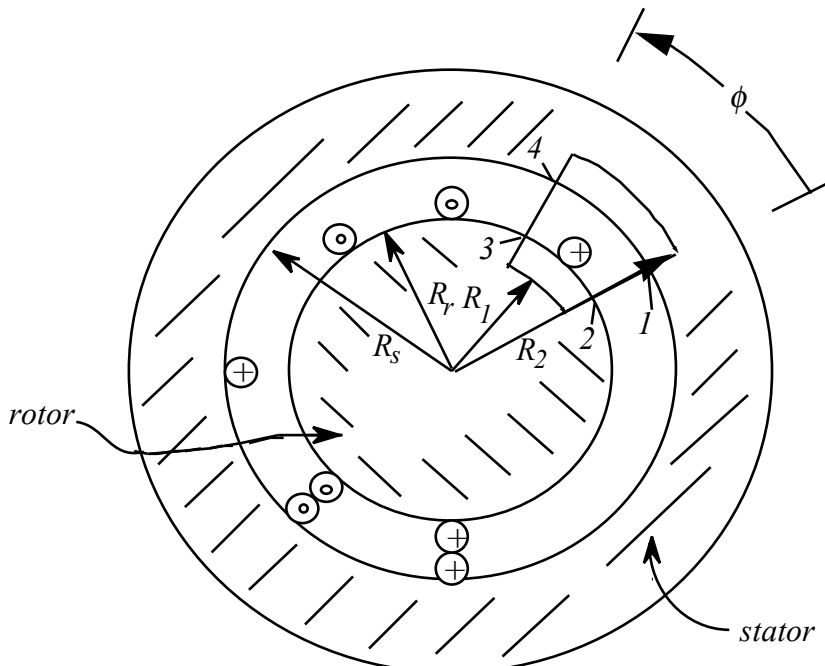


Figure 1.1 Elementary doubly cylindrical device with arbitrary placement of windings in the gap.

Consider initially a single wire carrying current i which is looped continuously back and forth through the gap of the machine an arbitrary number of times N_t . It is assumed that the conductor is located around the gap in a completely general manner. Each winding section is, however, considered to be aligned axially within the gap. That is, the wire is neither slanted in the circumferential direction (“skewed”) nor “tilted” in the radial direction as it passes through the gap. [Figure 1.1](#) shows a typical case where $N_t = 4$.

Since the motor is assumed at this point to be non-rotating, it will not be necessary to immediately associate this winding with either the stator or rotor. In [Figure 1.1](#) the winding has been idealized by locating it within the air gap of the machine. For small motors, such as servomotors, this may actually be the case since the winding can be rigidly attached to the rotor or stator surface by means of an epoxy binding. In most cases, however, the actual winding is embedded in slots in order to reduce the size of the forces impressed on the winding arising from current flow and also to reduce the size of the air gap as much as possible.

Although not strictly necessary, each turn is also assumed to have a negligible cross-sectional area. A reference point along the gap periphery is arbitrarily chosen to denote the reference point for the angular (circumferential) measure ϕ along the air gap. The angle ϕ is assumed to increase in the counter-clockwise direction. Consider the path 12341 shown in [Figure 1.1](#), where the path 12 is taken across the gap from stator to rotor at the reference ($\phi = 0$) point and the portion 34 returns across the gap at an arbitrary value, $0 < \phi < 2\pi$. By Ampere’s Law

$$\oint_{12341} H \cdot dl = \int_S J \cdot dS \quad (1.1)$$

where S is that surface enclosed by the path 12341. Since all windings carry the same current i , this equation can be expressed as

$$\oint_{12341} H \cdot dl = n(\phi)i \quad (1.2)$$

The function $n(\phi)$ is called the *turns function* and expresses the number of turns enclosed by the path 12341. Since the line integral is taken in the clockwise direction, by the right-hand rule convention $n(\phi)$ specifically corresponds to the net number of conductors enclosed by the path 12341 carrying currents into the page. Turns carrying current out of the page are considered as nega-

tive. The turns function for the elementary device of [Figure 1.1](#), for the path shown is +1. The turns function for any value of ϕ , $0 < \phi < 2\pi$, as shown in [Figure 1.2](#). In order not to confuse $n(\phi)$ with the total number of turns N_t , in future work the functional dependence of the turns function on the angle ϕ will always be shown explicitly.

When Eq. (1.2) is broken into its four components, each of the four integrals can be interpreted as magnetomotive force (*MMF*) drops in a magnetic circuit. In terms of *MMFs*, Eq. (1.2) can be written

$$\mathcal{F}_{12} + \mathcal{F}_{23} + \mathcal{F}_{34} + \mathcal{F}_{41} = n(\phi)i \quad (1.3)$$

If ϕ is considered as a particular (but arbitrary) point around the gap then it is clear that upon taking the proper vector dot products

$$\mathcal{F}_{12} = \int_{R_s}^{R_r} H_r(r, 0) dr \quad (1.4)$$

$$\mathcal{F}_{23} = - \int_{R_1}^{R_r} H_r(r, 0) dr + \int_{R_1}^{\phi} R_1 H_\phi(R_1, u) du + \int_{\phi}^{R_r} H_r(r, \phi) dr \quad (1.5)$$

$$\mathcal{F}_{34} = \int_{R_r}^{R_s} H_r(r, \phi) dr \quad (1.6)$$

$$\mathcal{F}_{41} = \int_{R_s}^{R_2} H_r(r, \phi) dr - \int_{R_s}^{\phi} R_2 H_\phi(r_2, u) du - \int_{\phi}^{R_2} H_r(r, 0) dr \quad (1.7)$$

where u is simply a dummy variable of integration. If effects at each end of the machine (axial direction) are neglected, both the r and ϕ components of H can be assumed independent of z . However, in general, both components are a function of both r and ϕ so that the integrals implied by Eq. (1.3) can not be carried out without additional assumptions.

Since the relative permeability of iron is several thousand times greater than that of air, one might be tempted to assume the reluctance of the iron portion of the flux path negligible compared to the air portion. However, since the gap length is very small compared to the length of path that flux must traverse in the iron, the reluctance of the iron flux path is not necessarily small com-

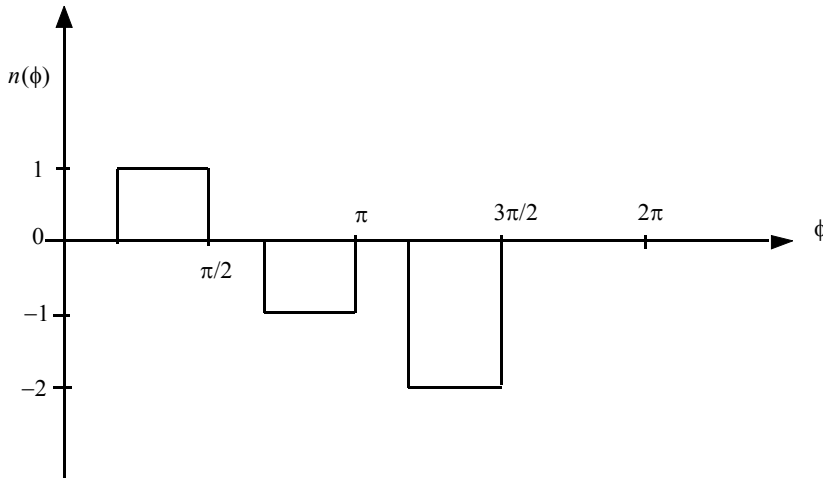


Figure 1.2 Turns function for the elementary device of Fig. 1.1.

pared to the air path. In fact, for a well designed machine the *MMF* drop in the iron can not be calculated without resorting to semi-empirical equations, field plotting, or numerical methods. In general, the approach is to include correction factors for the *MMF* consumed in the teeth and yoke portions of the iron by replacing the physical air gap g by an effective g_e which incorporates the effect of *MMF* drop in the teeth and yoke. The interested reader is referred to advanced books on the subject [1]. It will be assumed that gap length corresponds to the effective gap. With this simplification the *MMF* drops \mathcal{F}_{23} and \mathcal{F}_{41} are incorporated into the air gap *MMFs* \mathcal{F}_{12} and \mathcal{F}_{34} and the actual iron is replaced with a fictitious iron of infinite permeability. In this case, Eq. (1.3) reduces to

$$\mathcal{F}_{12}(0) + \mathcal{F}_{34}(\phi) = n(\phi)i \quad (1.8)$$

If the effective gap g_e remains small compared to R_s , then H_r can be considered constant across the gap and in particular

$$\mathcal{F}_{12}(0) + \mathcal{F}_{34}(\phi) = n(\phi)i \quad (1.9)$$

Equations (1.4) and (1.6) become

$$\mathcal{F}_{12}(0) = -H_r(R_s, 0)g_e \quad (1.10)$$

$$\mathcal{F}_{34}(\phi) = H_r(R_s, \phi)g_e \quad (1.11)$$

Unfortunately, the fields $H_r(R_s, 0)$ and $H_r(R_s, \phi)$ are still not known. It is not possible to solve uniquely for either $\mathcal{F}_{12}(0)$ or $\mathcal{F}_{34}(\phi)$ without an additional

equation. The additional equation that is needed is available from Gauss' Theorem applied to magnetic fields, which states that the net flux leaving any closed surface is zero, or

$$\oint_S \mathbf{B} \cdot d\mathbf{S} = 0 \quad (1.12)$$

In particular, one can choose the surface S to be a closed cylindrical surface enclosing the rotor but not the stator of the elementary device of [Figure 1.1](#). The “top” and “bottom” of the cylinder correspond to the circular ends of the rotor. The cylinder “wall” is positioned within the air gap of the machine. Since all flux is assumed to link the rotor via the air gap, the flux flowing through the two ends of the cylinder (i.e., the two ends of the rotor) is zero. Since the permeability of the iron is now assumed to be infinite, all flux is directed normal to the cylindrical surface, and Eq. (1.12) reduces to

$$\mu_0 \int_0^{l/2\pi} \int r H_r(r, \phi) d\phi dz = 0 \quad R_r \leq r \leq R_s \quad (1.13)$$

where l is the effective length of the rotor. The effective gap accounts for the bowing of the flux lines on each end of the machine and is again examined in more detail in [1]. Since H_r is independent of the axial direction, and r is constant, Eq.(1.13) becomes

$$\int_0^{2\pi} H_r(r, \phi) d\phi = 0 \quad (1.14)$$

From Eqs. (1.9) and (1.11), this result can be written equivalently as

$$\int_0^{2\pi} \mathcal{F}_{34}(\phi) d\phi = 0 \quad (1.15)$$

Equation (1.15) states that in order for the net flux linking the rotor to be zero, the function $\mathcal{F}_{34}(\phi)$ must have no average component. Equation (1.15) can be utilized to solve uniquely for $\mathcal{F}_{34}(\phi)$ and $\mathcal{F}_{12}(0)$. Integrating Eq. (1.8) from 0 to 2π ,

$$\int_0^{2\pi} \mathcal{F}_{12}(0) d\phi + \int_0^{2\pi} \mathcal{F}_{34}(\phi) d\phi = \int_0^{2\pi} n(\phi) i d\phi \quad (1.16)$$

From Eq. (1.15) the second term is identically zero. Also, since \mathcal{F}_{12} and i are independent of ϕ

$$\mathcal{F}_{12} = i \left[\frac{1}{2\pi} \int_0^{2\pi} n(\phi) d\phi \right] \quad (1.17)$$

The quantity in the brackets is clearly the average value of the turns function $n(\phi)$. Defining

$$\langle n(\phi) \rangle = \frac{1}{2\pi} \int_0^{2\pi} n(\phi) d\phi \quad (1.18)$$

then,

$$\mathcal{F}_{12} = \langle n(\phi) \rangle i \quad (1.19)$$

From Eq. (1.8), the *MMF* at any point along the air gap is

$$\mathcal{F}_{34}(\phi) = (n(\phi) - \langle n(\phi) \rangle) i \quad (1.20)$$

The function inside the brackets is simply the turns function $n(\phi)$ without its average value. This quantity is used so frequently in machine analysis that it is also given a name, the *winding function*,¹ and is formally defined as

$$N(\phi) = n(\phi) - \langle n(\phi) \rangle \quad (1.21)$$

Dropping the numerical subscript, the *MMF* at any point in the gap is then given simply by

$$\mathcal{F}(\phi) = N(\phi) i \quad (1.22)$$

Hence, the *MMF* is related directly to the winding function. In fact, it is apparent that the winding function can be considered as the *MMF* distribution for unity winding current. Derivation of the winding function is an important aspect of machine analysis since knowledge of the winding functions for all windings, together with the winding current, essentially describe the spatial field distribution in the gap of the machine. Moreover, it will be shown that the winding function forms the basis by which most machine inductances can be calculated.

1. First defined by A. W. Rankin. The Fourier series corresponding to this function was originally termed the “turns series” by Rankin. For an alternative development, see [2].

In this book the total number of winding turns is designated with the symbol N_t . In order not to confuse the winding function with the total number of turns, the winding function will also be designated with its functional dependence on the independent variable explicitly shown as for the turns function.

Because the turns function $n(\phi)$ depends on the reference position selected for the angle ϕ , the amplitude and phase of this function vary with the choice of $\phi = 0$ and clearly are not unique. It is apparent that the reference location for ϕ also affects the winding function $N(\phi)$ in that it introduces an arbitrary “phase shift” in the function. In general, this phase shift is of little consequence. However, for the purpose of comparing one winding configuration to another, it is useful to define ϕ such that $N(\phi)$ will be unique for a given winding distribution. For most winding distributions the coil sides are located such that a positive turn is situated diametrically opposite the corresponding negative turn. In such cases the requirement of Eq. (1.24) is satisfied if the reference position ϕ^* is chosen such that

$$N(\phi^*) = N(-\phi^*) \quad (1.23)$$

that is, such that $N(\phi^*)$ has even (cosine) symmetry.

In any case,

$$\int_0^{2\pi} N(\phi^*) d\phi^* = 0 \quad (1.24)$$

and $\phi^* = 0$ can always be chosen so that $N(0)$ is a positive maximum. An asterisk is used to denote the variable for this unique reference location. The radial direction corresponding to $\phi^* = 0$ is termed the *winding magnetic axis*.

1.3 Calculation of the Winding Function

It is now useful to illustrate the above procedure by means of several practical examples. Consider initially the cylindrical structure of Figure 1.3. Here, one continuous winding with N_t turns is assumed to be concentrated at two points within the machine, as shown. It can be noted that the positive coil side is diametrically opposite to the negative coil side. Such a winding, said to span π radians, is called a *full pitch winding*.

The reference position for the angle ϕ is arbitrarily chosen in the horizontal direction. One can mentally visualize a line integral 12341 crossing the air gap

from stator to rotor at the reference point, then crossing back over from rotor to stator at an arbitrary angle measured counter-clockwise from the reference position. A typical line integral is shown in Figure 1.3 wherein $\phi = 40^\circ$. It should be noted that the line integral 12341 is always taken in the clockwise direction. The number of turns enclosed by the line integral for the case illustrated is clearly zero. When $\phi = 60^\circ$ the line integral suddenly encloses N_t turns. Since the line integral is taken in the clockwise direction by the right-hand rule, positive current enclosed by the path is directed into the page. However, since the winding current has been defined as out of the page, the number of turns enclosed is negative and the turns function $n(\phi)$ abruptly jumps from zero to $-N_t$ at $\phi = 60^\circ$. The function remains at N_t until ϕ reaches 240° , at which point N_t positive turns are enclosed so that the function jumps back to zero. The resulting function is plotted in Figure 1.4.

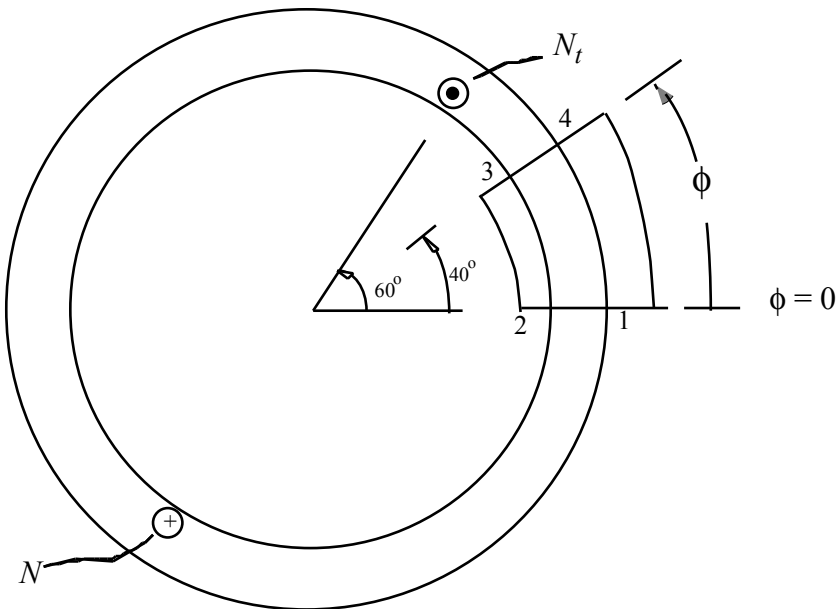


Figure 1.3 Arbitrary closed path crossing the airgap at $\phi=0$ and $\phi=40^\circ$.

Since $n(\phi)$ is non-zero only over the range $\pi / 3 < \phi < 4\pi / 3$, the average value of $n(\phi)$ is

$$\langle n \rangle = \frac{1}{2\pi} \int_{-\frac{\pi}{3}}^{\frac{4\pi}{3}} (-N_t) d\phi = -\frac{N_t}{2} \quad (1.25)$$

From Eq. (1.21) the winding function is simply the turns function $n(\phi)$ translated upwards by $N_t/2$. The function will have even symmetry if ϕ^* is chosen such that $\phi^* = \phi + \pi/6$. The unshifted and shifted winding functions are plotted in Figure 1.4(b) and (c). In the case of the shifted winding function, the subscript “*c*” has been appended since this function for the case of N_t turns concentrated in a single slot (*concentrated winding*) has a special significance.

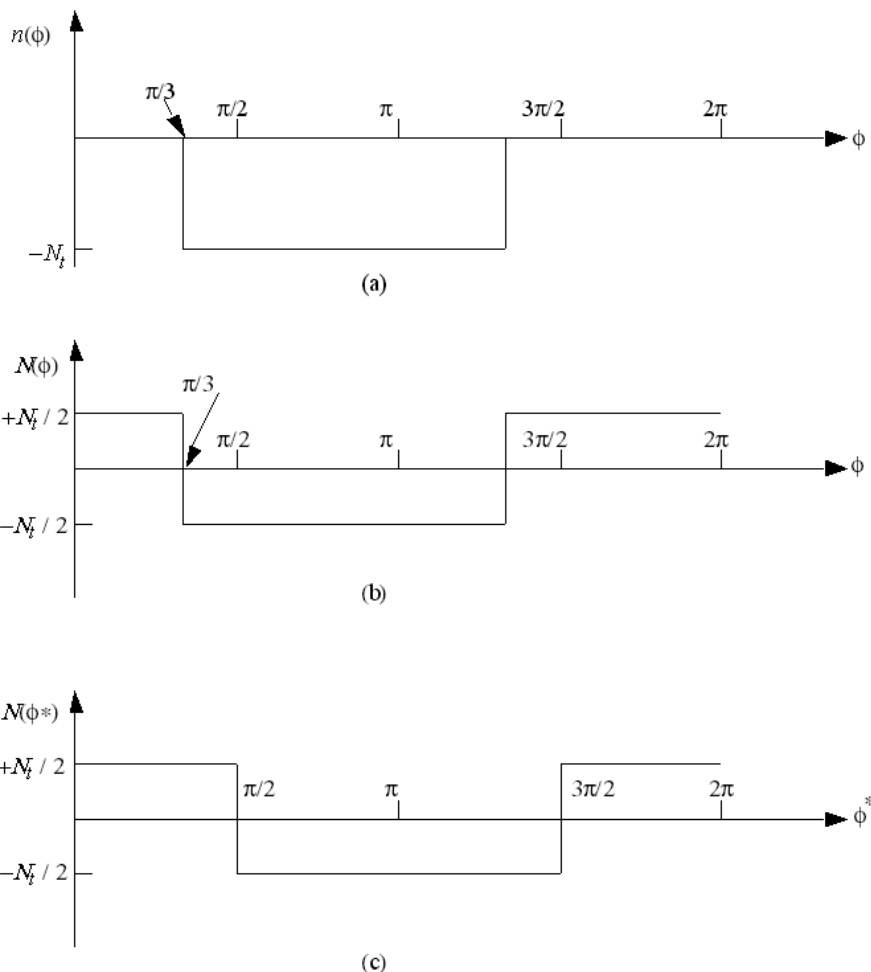


Figure 1.4 Turn and winding functions for an N_t turn, full pitch coil.

In order to help facilitate analysis it is useful to express $N_c(\phi^*)$ in terms of its Fourier components. It is clear that the winding function is completely defined over the entire stator periphery when ranges are from 0 to 2π . However, it is possible to consider the function to be repeated when ϕ^* ranges over the value 2π to 4π , 4π to 6π , etc. Specifically, it is useful to assume $N_c(\phi^*)$ as the periodic function shown in Figure 1.5. This function can then be described by a Fourier series and the resulting series is commonly termed the *winding series*. It can be noted that since the function of Figure 1.5 has the desired even symmetry about $\phi^* = 0$, that is, $N_c(\phi^*) = N_c(-\phi^*)$, the winding series for this function will contain only cosine terms. The Fourier series for this function is

$$N_c(\phi^*) = N_{c1} \cos \phi^* + N_{c2} \cos 2\phi^* + N_{c3} \cos 3\phi^* + \dots \quad (1.26)$$

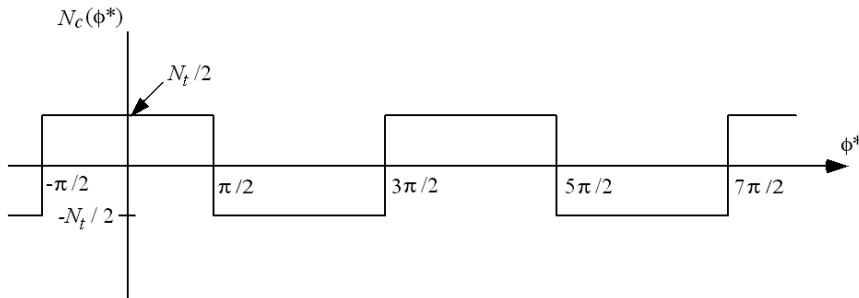


Figure 1.5 Cosine symmetric winding function $N_c(\phi^*)$.

where

$$N_{ch} = \frac{1}{\pi} \int_0^{2\pi} N_c(\phi^*) \cos(h\phi^*) d\phi^* \quad h = 1, 2, 3, \dots \quad (1.27)$$

Upon integrating,

$$N_{ch} = (-1)^{\frac{h-1}{2}} \left(\frac{2N_t}{h\pi} \right) \quad \text{for } h = 1, 3, 5, 7, \dots \quad (1.28)$$

$$N_{ch} = 0 \quad \text{for } h = 2, 4, 6, \dots \quad (1.29)$$

The fact that all even harmonics are zero is also evident by noting that $N_c(\phi^*) = -N_c(\phi^* + \pi)$. The winding series for an N_t turn, concentrated coil is

$$N_c(\phi^*) = \frac{2N_t}{\pi} \left[\cos \phi^* - \frac{1}{3} \cos 3\phi^* + \frac{1}{5} \cos 5\phi^* - \dots \right] \quad (1.30)$$

Because the factor $N_t/2$ appears continuously as the amplitude for the winding function of a two-pole winding, the coefficient of Eq. (1.30) is sometimes written

$$\frac{2N_t}{\pi} = \frac{4N_p}{\pi} \quad (1.31)$$

where $N_p = N_t/2$ is the number of series connected turns per pole. (For this example the winding only possesses two poles).

As a second example, suppose now that the concentrated winding is split up into two equal portions, as shown in [Figure 1.6](#). The two winding sections are separated by an angle ε . Such a winding is termed a *short pitch* or *fractional pitch* winding. If the reference position is located midway between windings, the resulting function $n(\phi)$ is as shown in [Figure 1.7\(a\)](#). It is readily established that in this case the average value $\langle n \rangle$ of $n(\phi)$ is $N_t/2$. The function $N(\phi^*)$ is obtained by shifting $N(\phi)$ by $\pi+\varepsilon/2$ radians, that is $\phi^* = \phi - \pi - \varepsilon/2$. [Figure 1.7\(b\)](#) and [\(c\)](#) show winding functions for $N(\phi)$ and $N(\phi^*)$ for this case.

The Fourier components for this winding distribution are of considerable interest. Again

$$N(\phi^*) = -N(\phi^* + \pi) \quad (1.32)$$

and since

$$N(\phi^*) = N(-\phi^*) \quad (1.33)$$

the Fourier expansion again contains only odd cosine terms. The h harmonic component can be expressed as the integral

$$N_h = \frac{2N_t}{\pi} \int_{-\frac{\pi}{2} + \frac{\varepsilon}{2}}^{\frac{\pi}{2} - \frac{\varepsilon}{2}} \cos(h\phi) d\phi \quad (1.34)$$

so that

$$N(\phi^*) = \frac{2N_t}{\pi} \left[\cos \frac{\varepsilon}{2} \cos \phi^* - \frac{1}{3} \cos \frac{3\varepsilon}{2} \cos 3\phi^* + \frac{1}{5} \cos \frac{5\varepsilon}{2} \cos 5\phi^* - \dots \right] \quad (1.35)$$

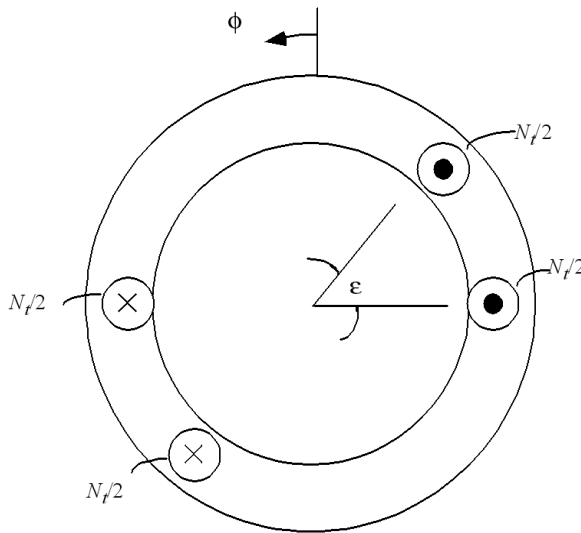


Figure 1.6 Winding placement for a fractional pitch concentrated winding.

It is useful to express N_h in terms of the corresponding harmonic coefficients for a concentrated winding. That is,

$$N_h = k_h N_{ch} \quad (1.36)$$

The factors k_h are termed the harmonic winding factors and are a means of relating the harmonic components of a winding of arbitrary distribution to a common reference. For the winding under consideration

$$k_h = \frac{(-1)^{\frac{(h-1)}{2}} \frac{2N_t}{\pi h} \cos \frac{h\varepsilon}{2}}{(-1)^{\frac{h-1}{2}} \frac{2N_t}{\pi h}} \quad (1.37)$$

or simply

$$k_h = \cos\left(\frac{h\varepsilon}{2}\right) \quad (1.38)$$

It will be learned shortly that it is of interest to eliminate harmonics in the winding function. It is evident that by the symmetry of the winding placement, all even harmonics have been eliminated. Moreover, if ε is properly selected, then one additional odd harmonic can be eliminated. For example, if $\varepsilon = \pi/3$, then

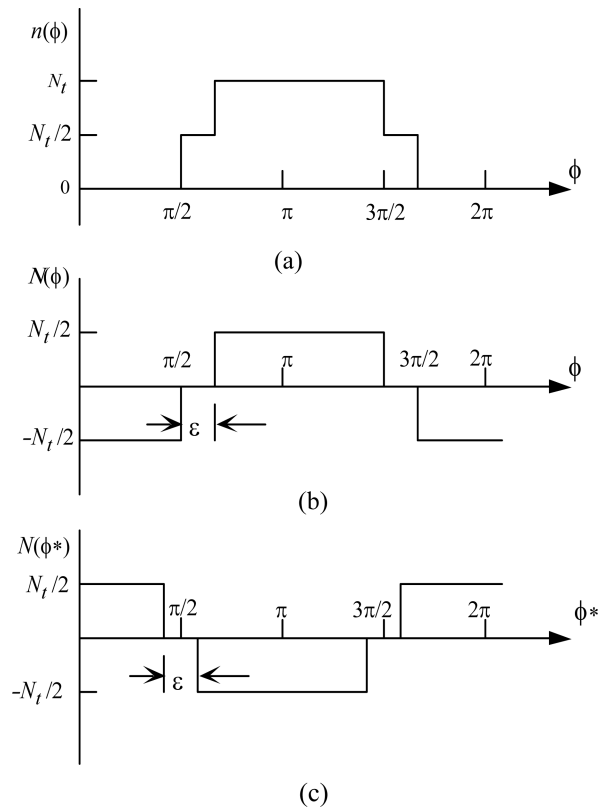


Figure 1.7 Turns and winding functions for a N_t turn, fractional pitch winding.

$$k_3 = \cos\left(\frac{3\pi}{3 \cdot 2}\right) = 0 \quad (1.39)$$

Similarly, if $\epsilon = \pi/5$, then $k_5 = 0$, etc.

It can be shown that two odd harmonics can be eliminated with three $N_t/3$ turn coils displaced by unequal values of ϵ_1 and ϵ_2 . However, since the spacing between windings is uniform, such an arrangement is generally impractical. Another possibility is to utilize equispaced slots but vary the number of turns per coil. However, since the number of turns per coil is discrete and space in the slot is limited, specific harmonics can generally only be minimized and not eliminated. In the case just considered, the concentrated winding has been divided into two equal sections. In general, when the winding is separated into k sections (or coils), then $k-1$ odd harmonics can be limited.

It is important to note that harmonic elimination is not without its penalties. When $\epsilon = \pi / 3$, the winding factor for the first harmonic corresponding to a two-coil, fractional pitch winding is

$$k_1 = \cos \frac{\pi}{6} = 0.866$$

That is, the fundamental component of *MMF* in the gap of the machine is reduced by 13%. This is equivalent to stating that the current must be increased by 15% (and hence copper losses by roughly 32%) in order to obtain the same fundamental component of *MMF* as for a full pitch concentrated winding.

As additional coils are added, the concentrated nature of the windings becomes less and less significant so that in the limit one can assume a continuous rather than discrete distribution of windings. In this case, it is logical to define a winding density η . A most important example of continuous winding distribution is when η is constant over some portion of the air gap. Such a winding is said to be *uniformly distributed*. [Figure 1.8](#) illustrates this case. Here, the N_t turns are assumed to be uniformly distributed over β radians, and the winding density is therefore a constant equal to

$$\eta = \frac{N_t}{\beta} \quad (1.40)$$

Assume the reference axis to be the horizontal axis. The number of turns enclosed by the hypothetical line integral crossing the air gap from stator to rotor at $\phi = 0$ and returning across the air gap at ϕ is

$$n(\phi) = \frac{N_t}{\beta} \phi \quad (1.41)$$

when $0 \leq \phi \leq \beta$. Hence, $n(\phi)$ changes linearly over this region. When ϕ reaches β , all of the N_t turns are enclosed. The turns function $n(\phi)$ remains fixed at N_t until it reaches π at which point negative turns start being enclosed. The function $n(\phi)$ is plotted in [Figure 1.9\(a\)](#).

It is readily established that $\langle n \rangle$ is $N_t/2$ so that $N(\phi)$ is the same as $n(\phi)$ shifted downward by $N_t/2$. In order to obtain $N(\phi)$, $N(\phi^*)$ is shifted to the left by $\pi/2 + \beta/2$ radians, or

$$\phi^* = \phi - \frac{\pi}{2} - \frac{\beta}{2}$$

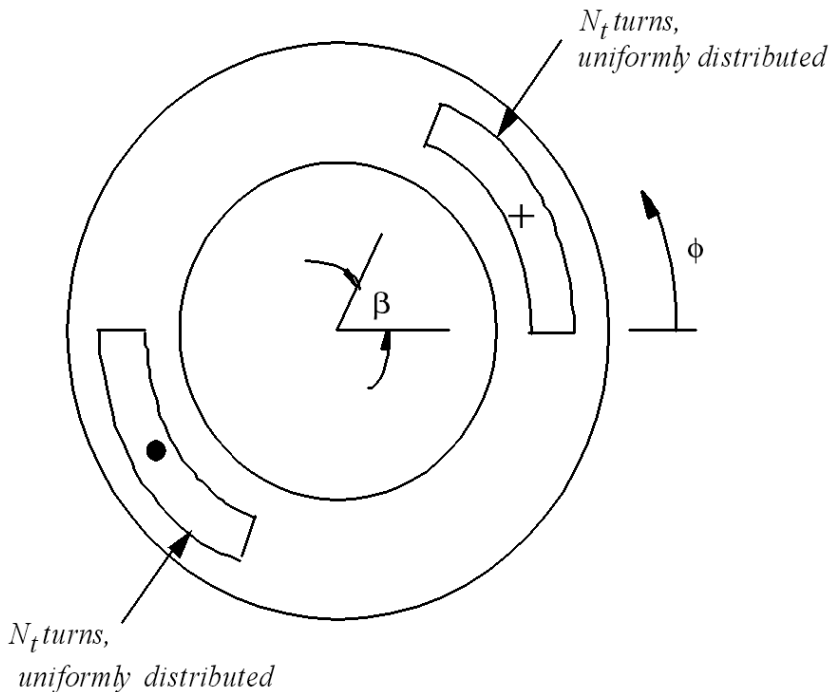


Figure 1.8 A uniformly distributed winding.

Due to the symmetry of the function, the coefficients of the winding series N_h are given by

$$N_h = \frac{4N_t}{\pi} \int_0^{\frac{\pi-\beta}{2}} \cos(h\phi^*) d\phi^* + \frac{4}{\pi} \int_{\frac{(\pi-\beta)}{2}}^{\frac{\pi}{2}} \frac{N_t/2}{(\beta/2)} \left(\frac{\pi}{2} - \phi^* \right) \cos(h\phi^*) d\phi^* \quad (1.42)$$

The first term is the same as for the fractional pitch winding example, Eq. (1.34). Thus, the first right-hand term of Eq. (1.42) is

$$\text{(first term)} = \frac{2N_t}{\pi h} (-1)^{\frac{h-1}{2}} \cos\left(\frac{h\beta}{2}\right) \quad (1.43)$$

The complexity of the second term can be reduced if a change of variable is used. In this second integral let $\rho = \pi/2 - \phi^*$. The second term of Eq. (1.42) becomes

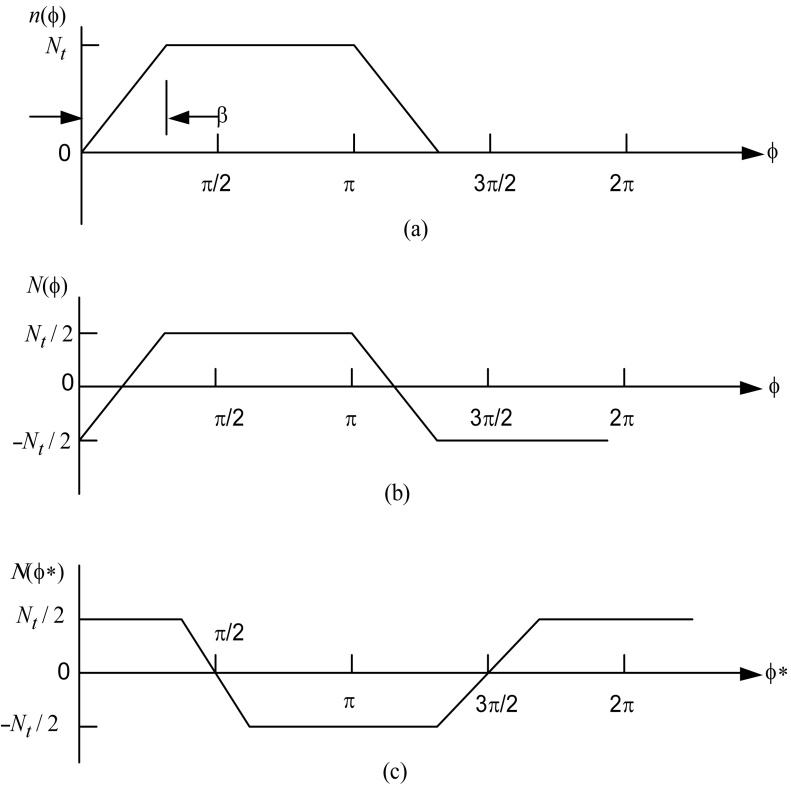


Figure 1.9 Turns and winding functions for the uniformly distributed winding of Fig. 1.7, (a) turns function, (b) winding function, (c) cosine symmetric winding function.

$$\text{(second term)} = \frac{4N_t}{\pi\beta} \int_0^{\beta/2} \rho \cos\left[h\left(\rho - \frac{\pi}{2}\right)\right] d\rho \quad (1.44)$$

Since Eq. (1.44) only applies for odd h , this term reduces to

$$\text{(second term)} = (-1)^{\frac{h-1}{2}} \frac{4N_t}{\pi\beta} \int_0^{\beta/2} \rho \sin(h\rho) d\rho \quad (1.45)$$

Upon integrating and evaluating the limits

$$\text{(second term)} = (-1)^{\frac{h-1}{2}} \frac{4N_t}{\pi\beta} \left[\frac{\sin\left(\frac{h\beta}{2}\right)}{h^2} - \frac{\beta}{2h} \cos\frac{h\beta}{2} \right] \quad (1.46)$$

Upon adding the two terms, Eqs. (1.43) and (1.46), the coefficient for the h harmonic is

$$N_h = (-1)^{\frac{h-1}{2}} \frac{2N_t}{\pi h} \frac{\sin\left(\frac{h\beta}{2}\right)}{\left(\frac{h\beta}{2}\right)} \quad (h \text{ odd}) \quad (1.47)$$

Comparing Eq. (1.47) to Eq. (1.31), it is readily seen that the harmonic winding k_h for a uniformly distributed winding spread over β/π pole pitch is

$$k_h = \frac{\sin\left(\frac{h\beta}{2}\right)}{\left(\frac{h\beta}{2}\right)} \quad (1.48)$$

For a practical application of this equation, it can be recalled that the distribution of current over a slot pitch has been neglected in the computation of the winding function for a concentrated winding. As the width of the slot increases, the winding function changes linearly across the slot. In this case β corresponds to a slot width and Eq.(1.48) describes the effect of a finite slot width on the winding series.

As a final example, assume now that the winding turns are continuously distributed around the gap such that the winding density can be considered as sinusoidal, as shown in [Figure 1.10](#). That is,

$$\eta = \eta_m |\sin\phi| \quad (1.49)$$

where, in this case, $\phi = 0$ has been located where $\eta = 0$. Again it is assumed that the total number of turns is N_t . Since the turns are distributed over a pole pitch, the total number of turns is related to the maximum value of the winding density by

$$N_t = - \int_0^{\pi} \eta_m \sin\phi d\phi \quad (1.50)$$

Hence, $\eta_m = N_t/2$ and the turns function is found as

$$n(\phi) = \int_0^{\phi} \eta(\phi) d\phi \quad (1.51)$$

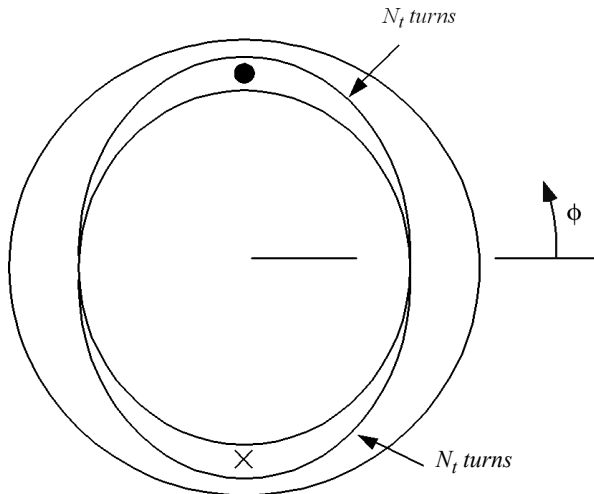


Figure 1.10 Sinusoidally distributed winding.

or

$$n(\phi) = \frac{N_t}{2}(\cos\phi - 1) \quad (1.52)$$

The average value of $n(\phi)$ is clearly $N_t/2$, and hence

$$N(\phi) = \frac{N_t}{2}(\cos\phi - 1) - \left(-\frac{N_t}{2}\right) = \frac{N_t}{2}\cos\phi \quad (1.53)$$

The turn and winding functions for a sinusoidally distributed winding are shown in [Figure 1.11](#). Since all harmonic terms other than the fundamental are zero, the winding series for $N(\phi^*)$ is clearly the winding function itself. Since the polarity of the result varies with choice of $\phi = 0$, the harmonic winding factors depend only on the amplitude of the harmonic coefficients and for this case are

$$k_1 = \frac{\pi}{4}$$

$$k_h = 0 \quad k \neq 1 \quad (1.54)$$

Therefore a sinusoidal distribution of N_t total turns produces an *MMF* with approximately 3/4 the fundamental component of a concentrated winding with the same number of turns.

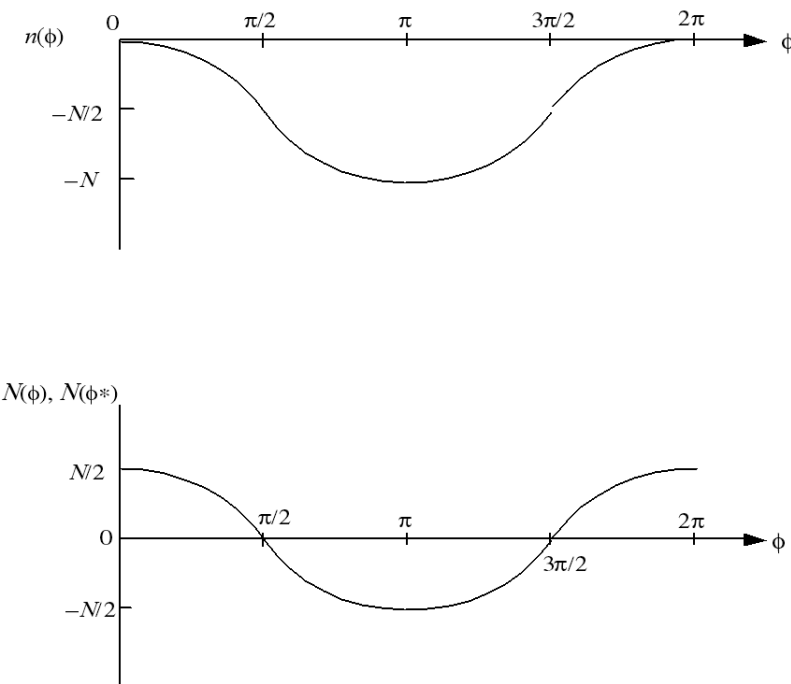


Figure 1.11 Turns and winding functions for a sinusoidally distributed winding.

The procedure that has been outlined can clearly be extended to windings of increasing complexity. The results for a large number of winding configurations are given in [Table 1.1](#). In all cases it can be noted that $N(\phi) = N(\phi^*)$. Therefore, all the functions shown contain only odd harmonics. It is clear that the approach could be extended to configurations wherein this symmetry does not exist. However, since the reference winding (concentrated winding) has only odd cosine components, the harmonic winding factors k_h are not readily defined in such cases.

In many texts the harmonic winding factor k_h is split into two terms, the distribution factor k_{dh} and the pitch factor k_{ph} to account for fractional pitch (if any). Hence, for any symmetric winding distribution

$$k_h = k_{dh} k_{ph} \quad (1.55)$$

For example, k_h for Table 1.1(b) can be considered a pitch factor k_{ph} . The corresponding distribution factor is unity since the winding is concentrated. On the other hand, k_h for Table 1.1(e) can be interpreted as a distribution factor k_{dh} . The pitch factor for this winding is unity. Also, the first term of k_h for the

stepped distribution, Table 1.1(d), has a winding factor and the second term of the product a pitch factor. A similar interpretation applies for the other windings. The interested reader is referred to Langsdorf [3].

Table 1.1 Winding function and harmonic winding factors of various types of two-pole windings

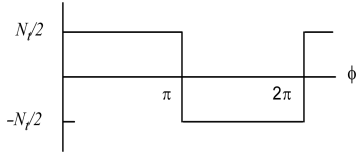
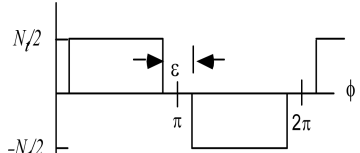
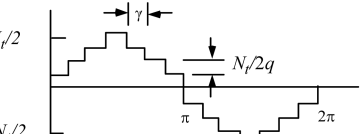
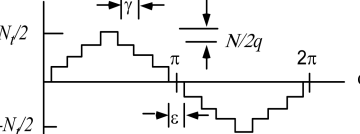
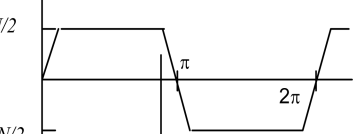
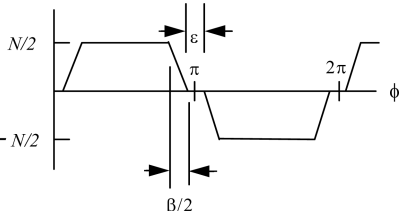
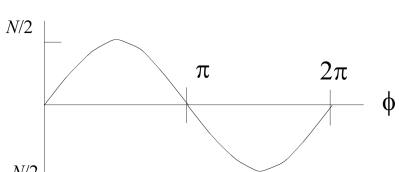
Winding Type	Winding Function	Harmonic Winding Factor k_h (h odd)
a) Full Pitch Concentrated		1
b) Fractional Pitch, Concentrated		$\cos\left(\frac{h\varepsilon}{2}\right)$
c) Full Pitch Stepped Distribution ($2q$ Coils)		$\frac{\sin\left(\frac{hq\gamma}{2}\right)}{q \sin\left(\frac{h\gamma}{2}\right)} \cos\left[h(q-1)\frac{\gamma}{2}\right]$
d) Fractional Pitch, Stepped Distribution ($2q$ Coils)		$\frac{\sin\left(\frac{hq\gamma}{2}\right)}{q \sin\left(\frac{h\gamma}{2}\right)} \cos\left(\frac{h\varepsilon}{2} + h(q-1)\frac{\gamma}{2}\right)$
e) Full Pitch Uniformly Distributed		$\frac{\sin\left(\frac{h\beta}{2}\right)}{\frac{h\beta}{2}}$

Table 1.1 Winding function and harmonic winding factors of various types of two-pole windings (continued)

Winding Type	Winding Function	Harmonic Winding Factor k_h (h odd)
g) Fractional Pitch, Uniformly Distributed		$\frac{\sin\left(\frac{h\beta}{4}\right)}{\frac{h\beta}{4}} \cos\left[h\left(\frac{\beta}{4} + \frac{\varepsilon}{2}\right)\right]$
h) Full Pitch, Sinusoidally Distributed		$\begin{cases} \frac{\pi}{4}, & h = 1 \\ 0, & h \neq 1 \end{cases}$

1.4 Multipole Winding Configurations

In previous sections, winding arrangements for a two-pole machine were considered. That is, the winding function (or equivalently the *MMF*) has a first harmonic winding factor which is non-zero. For full pitch windings each coil spans π radians and the complete winding arrangement forms a two-pole system. In a multipole machine, the windings are arranged to span sub-multiples of π radians. Since each span of the winding creates a complete magnetic system, the additional poles must occur in pairs. The number of poles is generally determined by application considerations. Large, low-speed hydroelectric generators may have as many as 60 or more poles while high-speed steam turbine generators are wound with only two or at most four poles.

The modifications necessary to extend these results for two-pole machines to multipole machines may be established by considering the four-pole concentrated winding shown in Figure 1.12 Again the winding has N_t total turns. Half the coil sides are assumed to lie in each of the four slots. The turns function and winding function for an angle referenced from the horizontal axis are shown in Figure 1.12(b, c). The winding function referred to a point of even symmetry

$N(\phi^*)$ is plotted in [Figure 1.12\(d\)](#). Since two locations of even symmetry exist, it is apparent that ϕ^* is not uniquely defined. That is, $\phi^* = \phi - 3\pi/4$ or $\phi^* = \phi + \pi/4$. However, $N(\phi^*)$ is identical for either reference location. The winding series is readily established as

$$N(\phi^*) = \frac{N_t}{\pi} \left[\cos 2\phi^* - \frac{1}{3} \cos 6\phi^* + \frac{1}{5} \cos 10\phi^* - \dots \right] \quad (1.56)$$

From Eq. (1.56) it is apparent that the winding function is a periodic function having period π radians. It is possible to define a new variable ϕ_e such that the winding function is a periodic function over 2π radians of the new variable. That is,

$$\phi_e^* = 2\phi^* \quad (1.57)$$

Equation (1.56) can now be written as

$$N(\phi^*) = \frac{4N_t}{\pi P} \left[\cos \phi_e^* - \frac{1}{3} \cos 3\phi_e^* + \frac{1}{5} \cos 5\phi_e^* - \dots \right] \quad (1.58)$$

where P is the number of poles (four in this case).

Comparing Eq. (1.58) to Eq. (1.30), it can be observed that the form of the equation is identical except that angle ϕ^* has been replaced by ϕ_e^* and $N_t/2$ by $N_t/4$. The factor 2 in the definition of ϕ_e^* is the number of winding pole pairs. What has been derived is actually a general result. For a concentrated winding with P poles or $P/2$ pole pairs, the electrical angle ϕ_e^* is defined by

$$\phi_e^* = \frac{P}{2}\phi^* \quad (1.59)$$

The angle ϕ_e^* uses the subscript “e” to designate the electrical angle so as to be distinguished from the mechanical angle ϕ^* . In order to emphasize the fact that when the angle ϕ refers to a physical mechanical angular measurement, the symbol ϕ_m^* will sometimes be used as well. The angle ϕ or ϕ_m always varies from zero to 2π for one traversal around the air gap. The angle ϕ_e^* completes a 2π change when $2/P$ of the air gap has been traversed. It is now easy to see how it is possible extend [Table 1.1](#) to include multipole machines. In each case all one need do is replace the variable ϕ by ϕ_e^* and modify the amplitude of the function from $N_t/2$ to N_t/P . In all cases the angles which appear in the definition of the various functions are now simply

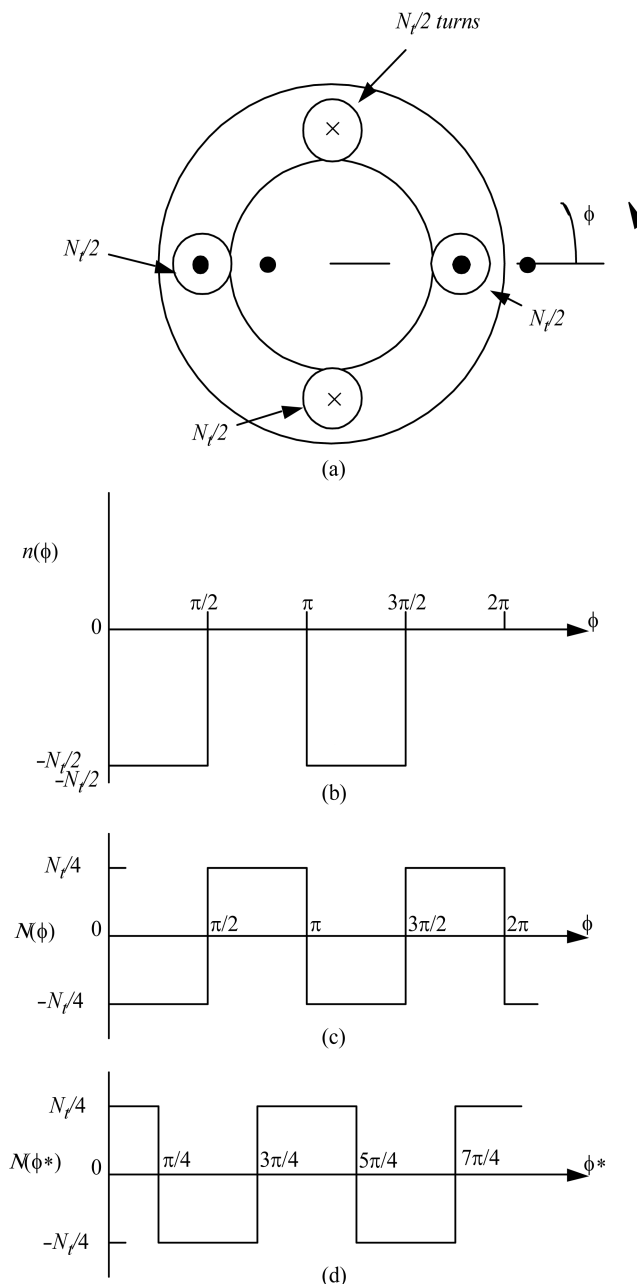


Figure 1.12 Four pole concentrated winding. (a) winding placement, (b) turns function, (c) winding function, (d) cosine symmetric winding function.

expressed in terms of the electrical angle ϕ_e^* rather than the mechanical angle ϕ .

1.5 Inductances of an Ideal Doubly Cylindrical Machine

Up to this point, it has been shown that if the *MMF* in the iron is neglected, the *MMF* between any two points along the air gap of a doubly cylindrical machine can be expressed simply as the product of the winding function times the current flowing through the winding. It will now be assumed that such an *MMF* distribution exists in the air gap resulting from current i_A flowing in a winding A having N_A turns and winding function $N_A(\phi)$. That is,

$$\mathcal{F}_A(\phi) = N_A(\phi)i_A \quad (1.60)$$

This winding is idealized as the dashed concentrated winding in [Figure 1.13](#), but can be any arbitrary distribution.

Consider now a second winding B having N_B turns arranged along the gap in an arbitrary fashion, as shown in [Figure 1.13](#). Again, the rotor is assumed to be stationary so that it is not necessary at this point to associate winding B with either the stator or rotor. It should be noted that since the reference position for the angle ϕ has been previously selected to define $N_A(\phi)$, one is not free to choose this reference point relative to winding B .

It is useful to calculate the flux linking this second winding due to current flowing in the A winding. From elementary magnetic circuits, the flux in the gap is related to the *MMF* by

$$\Phi = \mathcal{F}\mathcal{P} \quad (1.61)$$

where \mathcal{P} is the permeance of the flux of cross-section A and length l and \mathcal{F} is the *MMF* drop across the length l . Referring to [Figure 1.1](#), the differential flux across the gap from rotor to stator through a differential volume of length g and cross section $(rd\phi)l$ is

$$d\Phi = \mathcal{F}_A(\phi)\mu_0 r l \frac{d\phi}{g} \quad (1.62)$$

where \mathcal{F}_A is the *MMF* due to winding A . It is recalled from [Section 1.2](#) that the *MMF* drop (and hence flux) is considered positive from rotor to stator. What is desired is the total flux linkage of winding B from current in winding A . Thus

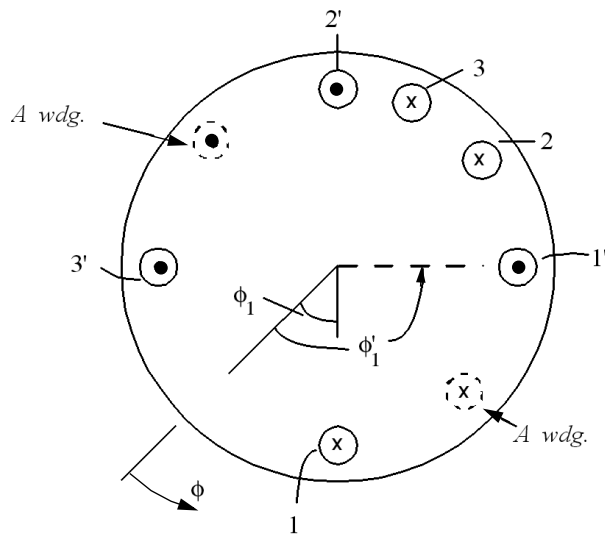


Figure 1.13 Winding placement for mutual inductance calculation.

far the placement of winding B has been assumed arbitrary so that an expression for the total flux linkage appears rather hopeless. Note, however, that regardless of the distribution one must have an equal number of conductors directed into the page (x) as out of the page as (\bullet). One can assign the number “1” to the first conductor carrying current into the page and “1’” to the first conductor encountered defined as carrying current out of the page. Similarly, the second conductor encountered with current into the page is labeled 2 and the second with current in the opposite direction as 2’. One can continue with the procedure until all N_B conductors have been accounted for. Clearly, this process is unambiguous and one will wind up labeling the last two conductors N_B and N_B' . In Figure 1.13 the labeling procedure has been carried out for a simple three-turn winding, $N_B = 3$.

Consider now the flux linking coil $1 - 1'$. If coil side 1 is encountered first around the gap before 1’, then the positive flux linking the one-turn coil $1 - 1'$ is

$$\Phi_{1-1'} = \frac{\mu_0 r l}{g} \int_{\phi_1}^{\phi_1'} \mathcal{F}_A(\phi) d\phi \quad (1.63)$$

Alternatively, if coil side 1' is situated before 1, then the flux linking the coil is in the negative sense so that

$$\Phi_{1-1'} = -\frac{\mu_0 r l}{g} \int_{\phi_1}^{\phi'_1} \mathcal{F}_A(\phi) d\phi \quad (1.64)$$

Either situation can be accounted for if a turns function $n_{B1}(\phi)$ is defined which is zero from $\phi = 0$ until ϕ_1 or ϕ'_1 whichever comes first. When $\phi = \phi_1$ (or ϕ'_1) the turns function then jumps from 0 to 1 (or -1) and remains at 1 (or -1) until ϕ reaches ϕ'_1 (ϕ_1), at which point $n_{B1}(\phi)$ abruptly returns to zero. With this definition of the turns function $n_{B1}(\phi)$, the flux linking turn #1 for either case is

$$\Phi_{1-1'} = \frac{\mu_0 r l}{g} \int_{\phi_1}^{\phi'_1} n_{B1}(\phi) \mathcal{F}_A(\phi) d\phi \quad (1.65)$$

Since $n_{B1}(\phi)$ is zero when ϕ takes on value outside the span of the integral, Eq. (1.63) can also be written

$$\Phi_{1-1'} = \frac{\mu_0 r l}{g} \int_0^{2\pi} n_{B1}(\phi) \mathcal{F}_A(\phi) d\phi \quad (1.66)$$

This process can be continued for all turns. The flux linking the N_B^{th} turn is

$$\Phi_{N_b-N'_b} = \frac{\mu_0 r l}{g} \int_0^{2\pi} n_{N_b}(\phi) \mathcal{F}_A(\phi) d\phi \quad (1.67)$$

The total flux linking the winding is found by summing all N_A fluxes defined as above, or

$$\lambda_{BA} = \sum_{j=1}^{N_B} \Phi_{j-j'} = \frac{\mu_0 r l}{g} \left[\sum_{j=1}^{N_B} \int_0^{2\pi} n_{Bj}(\phi) \mathcal{F}_A(\phi) d\phi \right] \quad (1.68)$$

$$= \frac{\mu_0 r l}{g} \int_0^{2\pi} \left[\sum_{j=1}^{N_B} n_{Bj}(\phi) \right] \mathcal{F}_A(\phi) d\phi \quad (1.69)$$

The term in the brackets, however, is simply the turns function for the B winding. Defining,

$$N_B = \sum_{j=1}^J n_{Bj}(\phi) \quad (1.70)$$

the flux linkage of winding B due to a current winding A becomes

$$\lambda_{BA} = \frac{\mu_0 r l}{g} \int_0^{2\pi} n_B(\phi) \mathcal{F}_A(\phi) d\phi \quad (1.71)$$

The mutual inductance L_{BA} is defined as the flux linkage of winding B divided by the current flowing in winding A . Substituting Eq. (1.60) into Eq. (1.71)

$$L_{BA} = \frac{\lambda_{BA}}{i_A} = \frac{\mu_0 r l}{g} \int_0^{2\pi} n_B(\phi) N_A(\phi) d\phi \quad (1.72)$$

However, from [Section 1.2](#) the turns function can be represented as

$$n_B(\phi) = N_B(\phi) + \langle n_B \rangle \quad (1.73)$$

where $N_B(\phi)$ is the winding function for the B winding and $\langle n_B \rangle$ is the average value of the turns function. Substituting this relationship into Eq. (1.72)

$$L_{BA} = \frac{\mu_0 r l}{g} \int_0^{2\pi} N_B(\phi) N_A(\phi) d\phi + \frac{\mu_0 r l}{g} \int_0^{2\pi} \langle n_B \rangle N_A(\phi) d\phi \quad (1.74)$$

Since $\langle n_B \rangle$ is simply a constant, it can be removed from inside the second integral. Moreover, the winding function $N_A(\phi)$ is periodic with zero average value, so that the second term of Eq. (1.74) is zero. Hence, finally,

$$L_{BA} = \frac{\mu_0 r l}{g} \int_0^{2\pi} N_B(\phi) N_A(\phi) d\phi \quad (1.75)$$

From Eq. (1.75) it is clear that reciprocity holds, since the order of the two winding functions may be interchanged. Therefore, $L_{AB} = L_{BA}$. Alternatively, if one had started the problem assuming instead an *MMF* distribution for winding B and calculated the flux linking winding A , the result would have been the same. Equations (1.72) and (1.75) are equivalent expressions for mutual inductance. Although use of Eq. (1.75) is generally preferred, Eq.(1.72) will be of use when considering the mutual inductance of concentrated windings.

It should be noted that through this analysis, no restrictions were made on winding placement. That is, either winding (or both) can be located on the rotor as well as the stator. Moreover, the results that have been derived are clearly valid for cases where windings A and B are one and the same. Hence, the self inductance of winding A associated with flux crossing the air gap (magnetizing inductance) is given by the integral

$$L_{AA} = \frac{\mu_0 r l}{g} \int_0^{2\pi} N_A^2(\phi) d\phi \quad (1.76)$$

1.6 Calculation of Winding Inductances

As a simple introduction to the calculation of winding inductances, reconsider the case of the N_t turn concentrated, full pitched winding shown in [Figure 1.3](#). The winding function which has been derived has been plotted in [Figure 1.4](#) for a two-pole winding. Note that Eq. (1.76) is valid whether or not the winding is attached to the stator or rotor. Since $N_A^2(\phi)$ is simply a constant equal to $N_t^2/4$, integration of Eq. (1.76) yields

$$L_{AA} = \frac{\mu_0 r l}{g} N_t^2 \frac{\pi}{2} \quad (1.77)$$

As a second example, consider the case of the distributed winding in [Figure 1.8](#). The corresponding function $N_A(\phi)$ is plotted in [Figure 1.9](#). Because of the symmetry of the function $N_A^2(\phi)$, it is sufficient to integrate Eq.(1.76) from zero to $\pi/2$ and multiply by 4, or

$$L_{AA} = \frac{\mu_0 r l}{g} (4) \int_0^{\pi/2} N_A^2(\phi) d\phi \quad (1.78)$$

Equation (1.78) is given explicitly by

$$L_{AA} = 4 \frac{\mu_0 r l}{g} \left[\int_0^{\left(\frac{\pi}{2} - \frac{\beta}{2}\right)} \left(\frac{N_t}{2} \right)^2 d\phi + \int_{\left(\frac{\pi}{2} - \frac{\beta}{2}\right)}^{\frac{\pi}{2}} \left[\frac{N_t}{2} \frac{\left(\frac{\pi}{2} - \phi\right)}{\frac{\beta}{2}} \right]^2 d\phi \right] \quad (1.79)$$

Proceeding with the integration, Eq. (1.79) breaks up into the two integrals

$$L_{AA} = \frac{\mu_0 r l}{g} N_t^2 \left[\int_0^{\beta/2} \left(\frac{p}{\beta/2} \right)^2 dp + \int_0^{\left(\frac{\pi}{2} - \frac{\beta}{2}\right)} d\phi \right], \quad p = \frac{\pi}{2} - \phi \quad (1.80)$$

Thus, the inductance of a winding, uniformly distributed over pole pitch $\beta\pi/2$, is

$$L_{AA} = \frac{\mu_0 r l N_t^2}{g} \left[\frac{\pi}{2} - \frac{\beta}{3} \right] \quad (1.81)$$

As a final example of self inductance, consider the case where the winding turns have been distributed sinusoidally (Figure 1.11). The self inductance is found in a straightforward manner as

$$\begin{aligned} L_{AA} &= \frac{\mu_0 r l}{g} \left(\frac{N_t}{2} \right)^2 \int_0^{2\pi} \cos^2 \phi d\phi \\ L_{AA} &= \frac{\mu_0 r l}{g} N_t^2 \left(\frac{\pi}{4} \right) \end{aligned} \quad (1.82)$$

It should be noted that the self inductance for this case is exactly one-half that of a concentrated winding having the same number of turns. Since the winding functions for the two configurations have the same amplitude, each winding distribution produces the same maximum *MMF* and consequently the same peak flux density along the air gap of the machine. However, it is clear that since the inductance for a sinusoidally distributed winding is half the value for a concentrated winding, the flux linkage of the winding is halved and hence the amplitude of the sinusoidal voltage that can be safely applied across this winding without saturation is halved. This is equivalent to stating that the sinusoidally distributed winding utilizes effectively only a portion of the available iron in the machine. In a similar manner the resulting inductance of all wind-

ings shown in Table 1.1 can be computed. The values are shown in Table 1.2.

Table 1.2 Magnetizing inductances for various series connected P pole distributions

Winding Type	Winding Function	Magnetizing Inductance
a) Full pitch concentrated		$\mu_o \frac{rl}{g} (2\pi) \left(\frac{N_t}{P} \right)^2$
b) Fractional pitch concentrated		$\mu_o \frac{rl}{g} (2\pi) \left(\frac{N_t}{P} \right)^2 \left(1 - \frac{\epsilon}{\pi} \right)$
c) Full pitch uniformly distributed		$\mu_o \frac{rl}{g} (2\pi) \left(\frac{N_t}{P} \right)^2 \left(1 - \frac{2\beta}{3\pi} \right)$
d) Fractional pitch uniformly distributed		$\mu_o \frac{rl}{g} (2\pi) \left(\frac{N_t}{P} \right)^2 \left(1 - \frac{2\beta}{3\pi} - \frac{\epsilon}{\pi} \right)$
e) Full pitch sinusoidally distributed		$\mu_o \frac{rl}{g} \pi \left(\frac{N_t}{P} \right)^2$

If the number of poles is greater than two, Eqs. (1.75) and (1.82) can be readily modified. If all of the poles remain connected such that the same current flows through all of the coils, then the winding is said to be *series connected* (the issue of parallel connection of windings will be taken up shortly). In this case, if N_t continues to signify the total number of turns (series connected turns) then it is not difficult to show that the number of series connected

turns for one pole of a P pole machine is simply N_t/P . From Eq. (1.59), the electrical angle ϕ_e is defined to vary from zero to π when ϕ varies from 0 to $2\pi/P$. That is,

$$\phi_e = \frac{P}{2}\phi \quad (1.83)$$

In terms of the electrical angle, Eq. (1.75) becomes

$$L_{AB} = \frac{\mu_0 r l \pi^P}{g} \int_0^{2\pi} N_A(\phi_e) N_B(\phi_e) d\phi_e \quad (1.84)$$

If the winding is regular, that is, if the winding is constructed so that the distribution of turns over each pole is identical, then it is necessary to only compute Eq. (1.84) over 2π electrical radians and the result multiplied by $P/2$ or

$$L_{AB} = \frac{\mu_0 r l}{g} \left(\frac{P}{2}\right)^2 \int_0^{\pi} N_A(\phi_e) N_B(\phi_e) d\phi_e \quad (1.85)$$

Similarly, for a regular P pole machine

$$L_{AA} = \frac{\mu_0 r l}{g} \left(\frac{P}{2}\right)^2 \int_0^{\pi} N_A^2(\phi_e) d\phi_e \quad (1.86)$$

Recall that the gap g and length l can be modified to account for an *MMF* drop in the stator (or rotor) iron. When desired, g and l can be replaced by g_e and l_e , respectively.

1.7 Mutual Inductance Calculation—An Example

As an example of a mutual inductance calculation, suppose now that two concentrated full pitch windings A and B having N_A and N_B turns, respectively, are arranged along the gap. The B winding is pitched counter-clockwise to the A winding by an angle γ , as shown in [Figure 1.14](#). In [Figure 1.15](#) winding functions $N_A(\phi)$ and $N_B(\phi)$ are given for a reference position along the horizontal axis where it is assumed that $0 < \gamma < \pi$. Since the product function $N_A(\phi)N_B(\phi)$ clearly repeats at $\phi = \pi$, the mutual inductance is defined by the integral

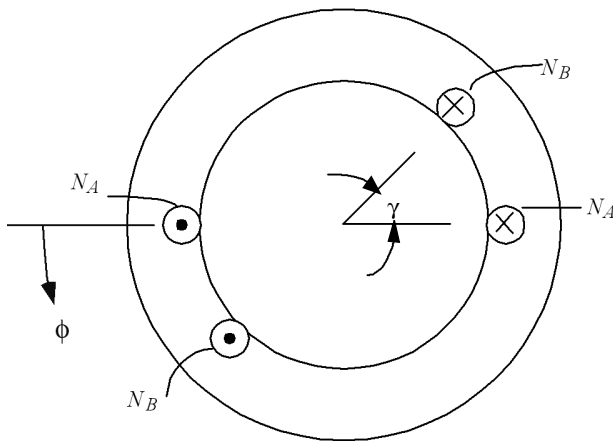


Figure 1.14 Two concentrated full pitch windings.

$$L_{AB} = \frac{\mu_0 r l}{g} \int_0^\pi N_A(\phi) N_B(\phi) d\phi \quad (1.87)$$

$$= \frac{\mu_0 r l}{g} \left[-\frac{N_A N_B \gamma}{4} + \frac{N_A N_B (\pi - \gamma)}{4} \right] \quad (1.88)$$

Thus,

$$L_{AB} = \frac{\mu_0 r l}{g} N_A N_B \left(\frac{\pi}{2} \right) \left[1 - \frac{2\gamma}{\pi} \right] \quad (1.89)$$

However, when the negative and positive parts of the product function are interchanged, the mutual inductance becomes

$$L_{AB} = -\frac{\mu_0 r l}{g} N_A N_B \frac{\pi}{2} \left(3 - \frac{2\gamma}{\pi} \right) \quad (1.90)$$

which corresponds to reversing one of the two currents in Figure 1.14.

Thus far, no distinction has been made between windings associated with the stator and windings associated with the rotor. It is useful to now reconsider the previous case where the concentrated *A* winding is rigidly attached to the stator (or lies in a stator slot). Winding *B* is fixed to the rotor. Since the rotor is free to rotate, the mutual inductance L_{AB} changes with rotor position. In practice, the rotor winding is generally located relative to the stator winding by specifying a mechanical angle θ_{rm} between the winding axes, as shown in Figure 1.16(a). Since both winding axes are in this case located 90° counter-clock-

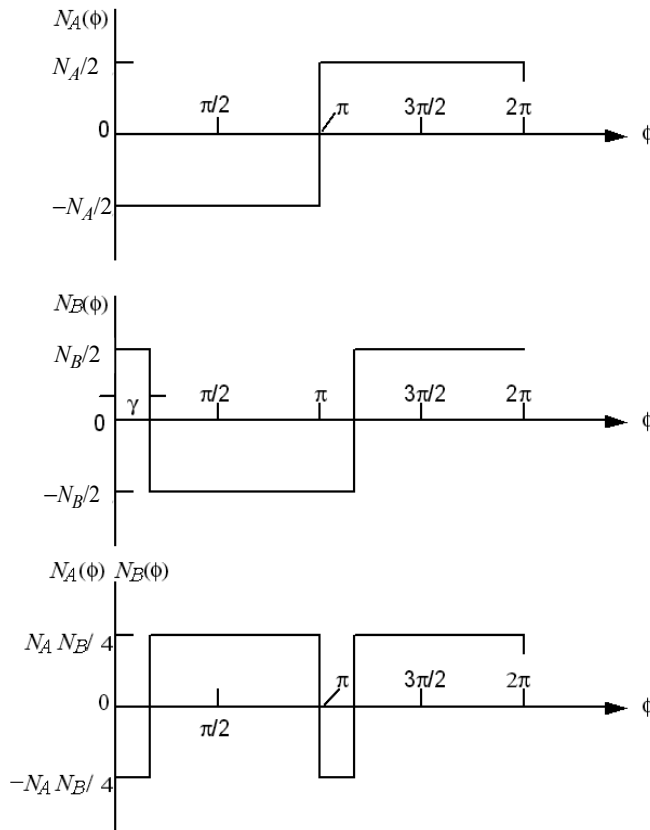


Figure 1.15 Mutual inductance example with concentrated coils.

wise to the coil side directed into the page, it is evident that $\gamma = \theta_{rm}$ so that Eqs. (1.88) and (1.90) can also be used to describe this condition. The inductance $L_{AB}(\theta_r)$ is plotted as a function of rotor position in [Figure 1.16\(b\)](#).

The triangular nature of L_{AB} can be more easily visualized if the expression for mutual inductance in the form of Eq. (1.91) is chosen. That is,

$$L_{AB} = \frac{\mu_0 r l^2 \pi}{g} \int_0^{2\pi} N_A(\phi) n_B(\phi) d\phi \quad (1.91)$$

Since the turns function $n_B(\phi)$ is a non-zero constant over the range θ_{rm} to $\theta_{rm} + \pi$, and zero elsewhere, it can be interpreted as a function which specifies which portions of the function N_A are to be evaluated in the integral. [Figure](#)

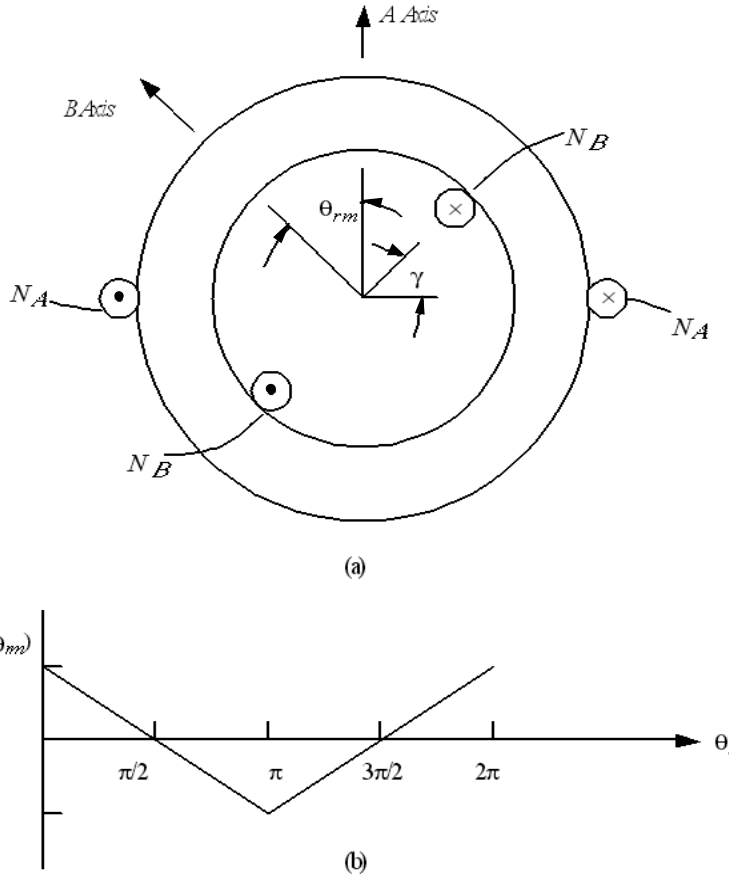


Figure 1.16 Mutual inductance example with rotating coil. (a) showing coil placement and (b) resulting mutual inductance.

1.17 shows $N_A(\phi)$ and $n_B(\phi)$ for three positions of θ_{rm} . The inductance L_{AB} at each position is proportional to the cross-hatched area.

One can proceed with the process of calculating mutual inductances for many combinations of windings shown in Table 1.2. However, it is apparent that the process rapidly becomes very difficult for complicated winding distributions. One can, of course, always resort to numerical integration and the definitions of self and mutual inductance, Eqs. (1.72) and (1.76) are ideally suited for this purpose. Mutual inductance relations can, however, always be obtained when the winding is expressed in terms of its winding series.

Assume that it is desired to calculate the mutual inductance between winding A located on the stator and winding B fixed to the rotor. If it is assumed that

the axis of winding B is positioned θ_{rm} radians counter-clockwise from winding A , then the winding series for the A and B windings are

$$N_A(\phi^*) = \frac{2N_A}{\pi} \left[k_{1A} \cos \phi^* + \frac{1}{3} k_{3A} \cos 3\phi^* + \dots \right] \quad (1.92)$$

$$N_B(\phi^*) = \frac{2N_B}{\pi} \left[k_{1B} \cos(\phi^* - \theta_{rm}) + \frac{1}{3} k_{3B} \cos 3(\phi^* - \theta_{rm}) + \dots \right] \quad (1.93)$$

Equations (1.92) and (1.93) can now be substituted into Eq. (1.72). It should be

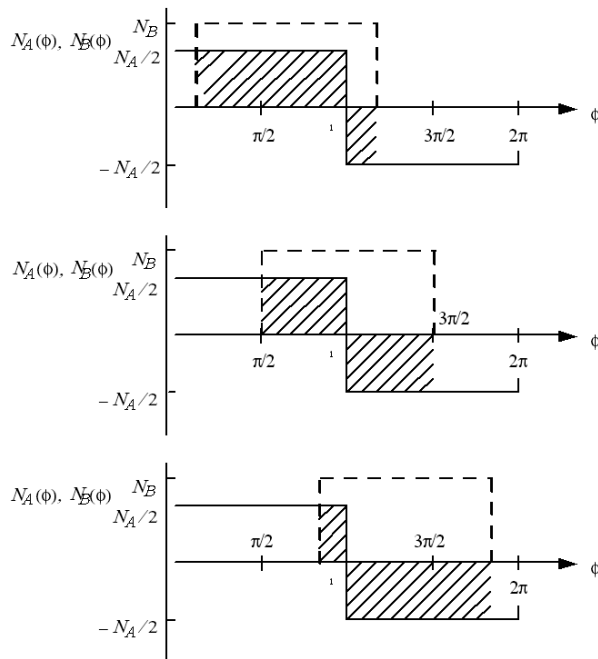


Figure 1.17 Graphical interpretation of Eq. (1.87). $N_A(\phi)$ – solid line, $n_B(\phi)$ – dashed line. (a) $\theta_{rm} = 30^\circ$, L_{AB} positive, (b) $\theta_{rm} = 90^\circ$, $L_{AB} = 0$, (c) $\theta_{rm} = 150^\circ$.

noted immediately that since L_{AB} is defined as an integral whose range is from zero to 2π , all product terms containing non-similar frequencies will be zero. That is,

$$\int_0^{2\pi} \cos n\phi^* \cos m(\phi^* - \theta_{rm}) d\phi = 0, \quad m \neq n \quad (1.94)$$

Excluding these terms, the mutual inductance may be expressed as

$$L_{AB} = \frac{\mu_0 r l}{g} N_A N_B \frac{4}{\pi^2} \int_0^{2\pi} \left[\sum_{h=1, h \text{ odd}}^{\infty} \left(\frac{k_{hA} k_{hB}}{h^2} \right) \cosh h\phi^* \cosh(h\phi^* - \theta_{rm}) \right] d\phi^* \quad (1.95)$$

Upon integrating

$$L_{AB} = \frac{\mu_0 r l}{g} N_A N_B \left(\frac{4}{\pi} \right) \left[\sum_{h=1, h \text{ odd}}^{\infty} \left(\frac{k_{hA} k_{hB}}{h^2} \right) \cosh \theta_{rm} \right] \quad (1.96)$$

For a P pole machine the result is

$$L_{AB} = \frac{\mu_0 r l N_A N_B}{g P^2} \left(\frac{16}{\pi} \right) \left[\sum_{h=1, h \text{ odd}}^{\infty} \left(\frac{k_{hA} k_{hB}}{h^2} \right) \cosh \theta_r \right] \quad (1.97)$$

where $\theta_r = (P/2)\theta_{rm}$ is the displacement of the rotor in electrical degrees.

In a similar manner it can be shown that the magnetizing inductance is

$$L_{AA} = \frac{\mu_0 r l}{g} \left(\frac{N_A}{P} \right)^2 \left(\frac{16}{\pi} \right) \left[\sum_{h=1, h \text{ odd}}^{\infty} \left(\frac{k_{hA}}{h} \right)^2 \right] \quad (1.98)$$

The summation on the right hand side of Eq. (1.98) is sometimes called the *winding series*. Note that the harmonics drop off rapidly since the higher harmonics vary not only as $(1/h)^2$ but also decrease by the square of the harmonic winding factor.

If desired, Eq. (1.96) can be used to derive the mutual inductance between any two windings of interest. For example, from [Table 1.1\(e\)](#), the mutual inductance between two full pitched, uniformly distributed windings displaced by an electrical angle θ_r is

$$L_{AB} = \frac{\mu_0 r l}{g} N_A N_B \left(\frac{4}{\pi} \right) \left[\frac{\sin^2 \left(\frac{\beta}{3} \right)}{\left(\frac{\beta}{2} \right)^2} \cos \theta_r + \frac{\sin^2 \left(\frac{3\beta}{2} \right)}{9 \left(\frac{3\beta}{2} \right)^2} \cos 3\theta_r + \dots \right] \quad (1.99)$$

In many simpler cases the Fourier series approach is not needed and mutual inductance can be calculated directly by application of Eq. (1.72). A number of mutual inductance functions for various winding configurations have been tabulated in Table 1.3.

Table 1.3 Mutual inductances for various series connected P pole winding configurations $\phi_e = (P/2)^*\phi$

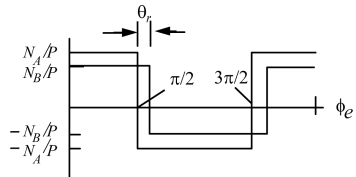
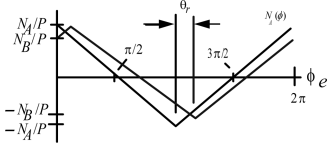
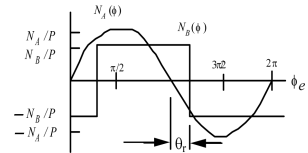
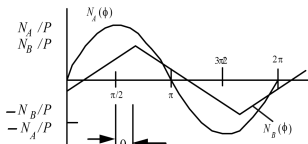
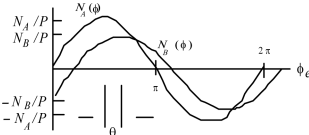
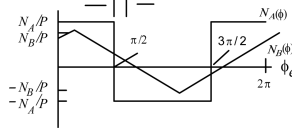
Winding Types	Winding Functions	Mutual Inductance
a) Two full pitch concentrated windings		$L_{AB} = \frac{\mu_0 r l}{g} \left(\frac{N_A N_B}{P^2} \right) (2\pi) \left(1 - \frac{2\theta_r}{\pi} \right)$ for $0 \leq \theta_r \leq \pi$
b) Two uniformly distributed windings		$L_{AB} = \frac{\mu_0 r l}{g} \left(\frac{N_A N_B}{P^2} \right) (2\pi) \left(\frac{4\theta_r^3}{3\pi^2} - \frac{2\theta_r^2}{\pi^2} + \frac{1}{3} \right)$ for $0 \leq \theta_r \leq \pi$
c) Full pitch concentrated and sinusoidally distributed windings		$L_{AB} = \frac{\mu_0 r l}{g} \left(\frac{N_A N_B}{P^2} \right) 4 \cos \theta_r$
d) Uniformly distributed and sinusoidally distributed windings		$L_{AB} = \frac{\mu_0 r l}{g} \left(\frac{N_A N_B}{P^2} \right) \left(\frac{8}{\pi} \right) \cos \theta_r$

Table 1.3 Mutual inductances for various series connected P pole winding configurations $\phi_e = (P/2)^*\phi$

Winding Types	Winding Functions	Mutual Inductance
e) Two sinusoidally distributed windings		$L_{AB} = \frac{\mu_0 r l N_A N_B}{g} \frac{(4\pi)}{P^2} \cos \theta_r$
f) One concentrated and one uniformly distributed winding		$L_{AB} = \frac{\mu_0 r l}{g} N_A N_B \left(\frac{\pi}{P} \right) \left(1 - \frac{4\theta_r^2}{\pi^2} \right)$ for $-\pi/2 \leq \theta_r \leq \pi/2$

1.8 Winding Functions for Multiple Circuits

Thus far it has been assumed that the windings of all of the “poles” of the machine are connected in series. However, the practical need to produce a wide range of machines with different voltage and power ratings with only a few sizes of conductors often leads to the need for parallel circuits in most machines. In the manufacture of coils it is desirable to keep the cross section of each individual turn around a nominal value so that each turn can be readily worked into the desired shape. As the number of poles of the machine increases, this requirement implies a corresponding increase in the voltage which must be applied to the machine unless steps are taken to reduce the number of series connected turns by connecting groups of windings in parallel.

To illustrate the procedure, consider the general case of a P pole structure with P independent circuits, as shown in Figure 1.18. For simplicity only the fundamental component of the turns function is considered. The current is assumed directed into the terminal of each coil which produces the same polarity of air gap flux. The dotted line represents the density of turns along the air gap η , while the solid line indicates the turns function $n(\phi)$ resulting from counting (integrating) the turns density as one progresses along the air gap in a manner similar to Figure 1.8. The winding functions are found by taking the average value of the turns function and subtracting it from the turns function. For this case, using winding A1, for example,

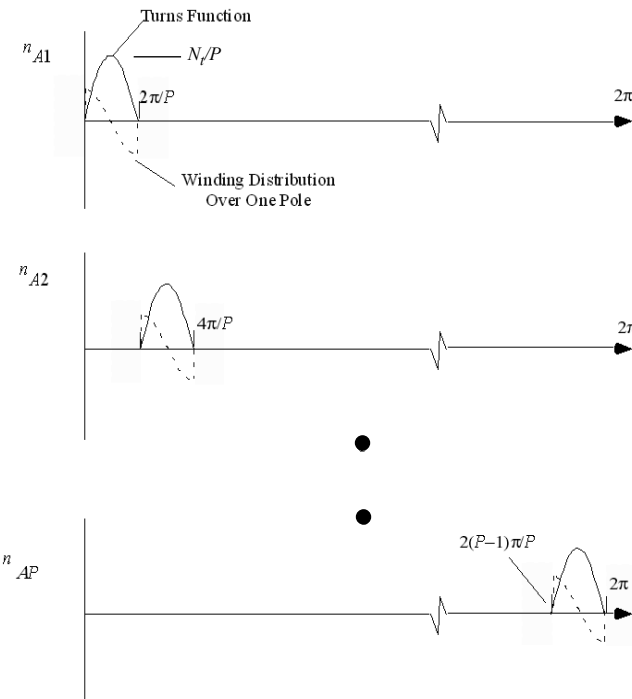


Figure 1.18 Sinusoidal winding distribution and resulting turns functions with equispaced P independent circuits.

$$\langle n_{A1} \rangle = \frac{\int_0^{\frac{2\pi}{P}} \frac{N_t}{P} \sin\left(P \frac{\phi}{2}\right) d\phi}{2\pi} = \frac{2N_t}{\pi P^2} \quad (1.100)$$

The corresponding winding function is

$$N_{A1}(\phi) = \frac{N_t}{P} \sin\left(P \frac{\phi}{2}\right) - \frac{2N_t}{\pi P^2} \quad \text{for } 0 \leq \phi \leq \frac{2\pi}{P} \quad (1.101)$$

and

$$N_{A1}(\phi) = -\frac{2N_t}{\pi P^2} \quad \text{for } \frac{2\pi}{P} \leq \phi \leq 2\pi \quad (1.102)$$

A plot of the winding functions corresponding to Figure 1.18 is shown in [Figure 1.19](#).

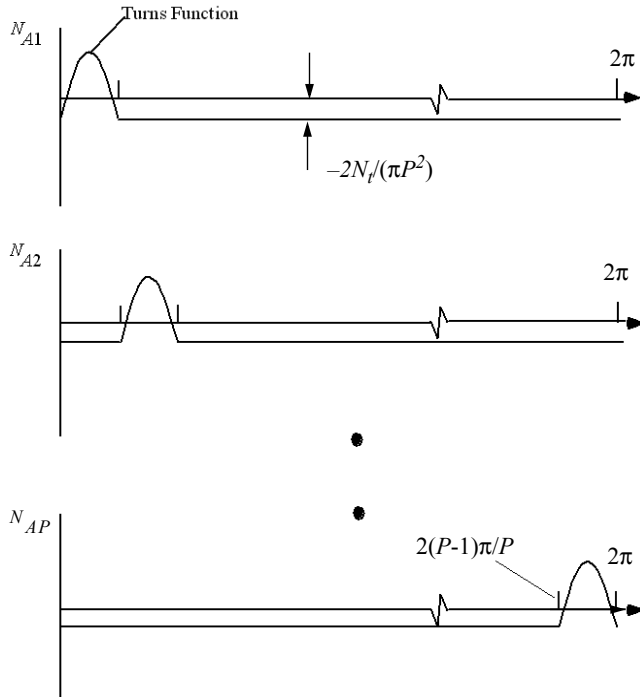


Figure 1.19 Winding functions corresponding to [Figure 1.18](#).

The self inductance of any of the P windings can be most easily computed by the form for inductance expressed as the product of the turns and the winding function, or, for winding A1,

$$L_{A1} = \mu_o \frac{rl}{g} \int_0^{2\pi} N_{A1}(\phi) n_{A1}(\phi) d\phi \quad (1.103)$$

Since the turns function is non-zero only over the span of the winding,

$$L_{A1} = \mu_o \frac{rl}{g} \int_0^{\frac{2\pi}{P}} \left[\frac{N_t}{P} \sin\left(P\frac{\phi}{2}\right) - \frac{2N_t}{\pi P^2} \right] \frac{N_t}{P} \sin\left(P\frac{\phi}{2}\right) d\phi \quad (1.104)$$

which results in

$$L_{A1} = \mu_o \frac{rl}{g} N_t^2 \left[\frac{\pi}{P^3} - \frac{8}{\pi P^4} \right] \quad (1.105)$$

The result is, of course, the same for all of the other $P-1$ windings.

The mutual inductance between any two circuits, say i and j , is

$$L_{Aij} = \mu_o \frac{rl}{g} \int_0^{2\pi} N_{Ai}(\phi) n_{Aj}(\phi) d\phi \quad (1.106)$$

which reduces to

$$L_{Aij} = \mu_o \frac{rl}{g} \int_{2\pi\left(\frac{j-1}{P}\right)}^{2\pi\left(\frac{j}{P}\right)} N_{Ai}(\phi) n_{Aj}(\phi) d\phi \quad (1.107)$$

and then finally to

$$L_{Aij} = -\mu_o \frac{rl}{g} N_t^2 \left(\frac{8}{\pi P^4} \right) \quad (1.108)$$

where it is assumed that the fluxes produced by the two circuits have the same polarity. If the fluxes produced by the two circuits have opposite polarity, then

$$L_{Aij} = \mu_o \frac{rl}{g} N_t^2 \left(\frac{8}{\pi P^4} \right) \quad (1.109)$$

Equations (1.105) and (1.108) can now be used to calculate the net inductance for any combination of coils spaced by one pole pitch.

Consider, for example, the case of a four-pole machine. In general, four connections of the four windings are possible, as illustrated in [Figure 1.20](#). In the first case the windings are simply connected in series. Attention must be paid to the “dots”, which indicate the resulting polarity of the magnetic flux in the gap. For example, currents into the dots produce, for example, north poles (i.e. A1 and A3) while currents out of the dots produce south poles (A2 and A4). Hence the mutual inductance between coils A1 and A2 is positive while the mutual inductance between coils A1 and A3 is negative.

In general, the total flux linking winding A for a P pole series connection is

$$\psi_A = \sum_{i=1}^P L_{Ai} i_A + \sum_{i=1}^P \sum_{\substack{j=1 \\ (i \neq j)}}^P (-1)^{i+j+1} L_{Aij} i_A \quad (1.110)$$

whereupon, for the four-pole example of [Figure 1.20\(a\)](#),

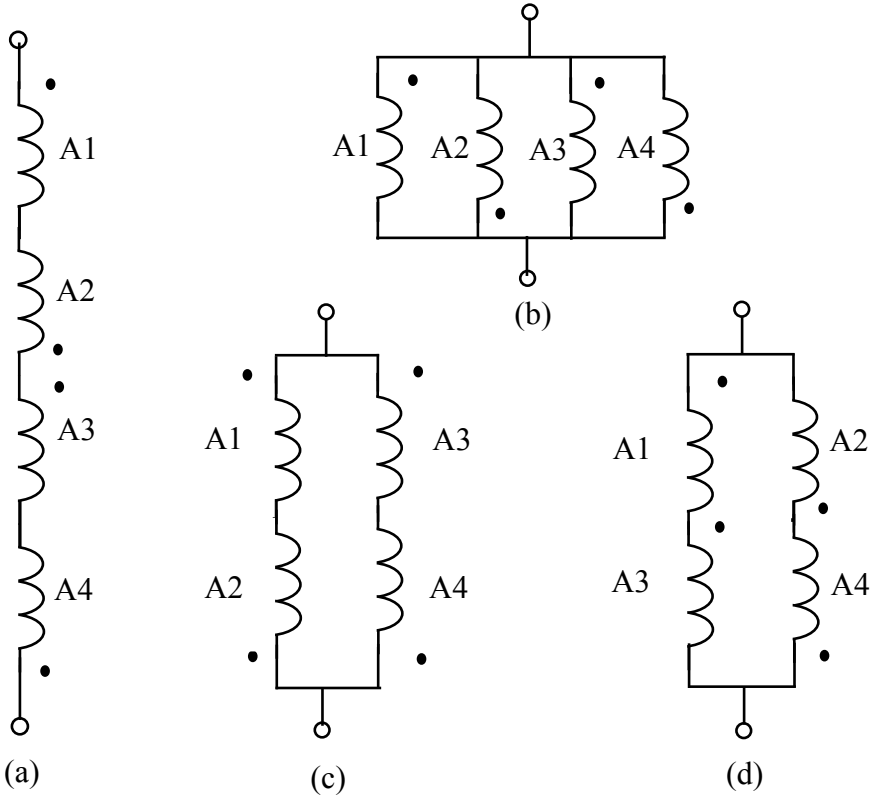


Figure 1.20 Four possible methods of connecting a four pole machine which retains balanced four-pole fields, (a) series connection, (b) parallel connection, (c) series/parallel connection #1, (d) series/parallel connection #2.

$$\lambda_A = \mu_o \frac{rl i_A}{g} (4) N_t^2 \left[\frac{\pi}{P^3} - \frac{8}{\pi P^4} \right] + \mu_o \frac{rl i_A}{g} (4) N_t^2 \left(\frac{8}{\pi P^4} \right) \quad (1.111)$$

where $P = 4$, which leads to

$$L_A = \mu_o \frac{rl}{g} \left[N_t^2 \frac{\pi}{16} \right] \quad (1.112)$$

It is interesting that the contribution of the average value of the turns function, i.e., $2N_t/(\pi P^2)$, does not enter into the final expression for self inductance. The same result can be obtained in a more straightforward manner if the net inductance of only one north and one south pole is computed, say A1 and A2 in Figure 1.20. In this simpler case, the total flux linkages are, observing proper polarities for the mutual flux components,

$$\lambda_{A1, A2} = L_{A1, A2} I_{A1} = (L_{A1} + L_{A2} + 2L_{A12}) I_{A1} \quad (1.113)$$

Substituting Eqs. (1.105) and (1.108), and assuming that the number of turns per pole is $N_t/4$, finally,

$$L_{A1, A2} = \mu_o \frac{rl}{g} \left[N_t^2 \frac{\pi}{32} \right] \quad (1.114)$$

In a similar manner

$$L_{A3, A4} = L_{A1, A2} = \mu_o \frac{rl}{g} \left[N_t^2 \frac{\pi}{32} \right] \quad (1.115)$$

Equation (1.115) can now be used to find the total inductance of the four-coil series string. In this case

$$L_{A1, A2, A3, A4} = L_{A1, A2} + L_{A3, A4} + L_{(A1, A2), (A3, A4)} + L_{(A3, A4), (A1, A2)} \quad (1.116)$$

The two mutual inductances can be easily resolved by taking the integral of the two winding functions,

$$L_{(A1, A2), (A3, A4)} = \mu_o \frac{rl}{g} \int_0^{2\pi} N_{A1, A2}(\phi) N_{A3, A4}(\phi) d\phi \quad (1.117)$$

However, the winding function $N_{A1, A2}$ is zero over pole pitches corresponding to the position of windings A3 and A4 (and vice versa). As a result, the mutual inductance between any two pairs of windings having both a north and south pole is zero. The total inductance for the four-pole series string (Figure 1.20(a)) is therefore

$$L_{A1, A2, A3, A4} = L_{A1, A2} + L_{A3, A4} = \mu_o \frac{rl}{g} \frac{N_t^2}{16} (\pi) \quad (1.118)$$

which is the same as Eq. (1.112).

In the analysis above strict attention has been paid to the correct definition of the mutual and self inductances when the four poles of the circuit are considered individually (each having both a positive and negative portion in their winding functions). However, it should now be clear from the above that when windings of the circuit are taken in pairs (i.e., one north and one south pole), the total inductance of each pair is much more easily computed since the net winding function has a simple sinusoidal distribution in the gap associated with the two poles under consideration and is zero elsewhere. In most cases the

detail outlined above is not necessary when the machine is wound in a conventional manner. However, the approach shown is general and is applicable to an arbitrary winding distribution with an unequal number of north and south producing poles or with an unequal number of turns per pole. This situation occurs most frequently when, for example, a machine coil develops an open- or short-circuit while the remaining poles remain excited normally.

Since the mutual inductance between any two windings having both a north and south pole is always zero, the inductances for the remaining winding configurations can be rapidly determined. For the parallel string, [Figure 1.20\(b\)](#),

$$L_{A1, A2, A3, A4} = \mu_o \frac{rl}{g} \left[\left(\frac{N_t^2}{16} \right) \frac{\pi}{16} \right] \quad (1.119)$$

For the series/parallel strings, [Figure 1.20\(c\)](#) or [\(d\)](#),

$$L_{A1, A2, A3, A4} = \mu_o \frac{rl}{g} \left[\left(\frac{N_t^2}{16} \right) \frac{\pi}{4} \right] \quad (1.120)$$

It is important to recall that N_t represents the total number of turns used to wind the entire configuration. It is more conventional to express these results in terms of the total number of series connected turns N_s . This corresponds to N_t turns for [Figure 1.20\(a\)](#), $N_t/4$ for [Figure 1.20\(b\)](#), and $N_t/2$ for [Figure 1.20\(c\)](#) and [\(d\)](#). In terms of the number of series connected turns, for the series, parallel or series parallel strings

$$L_{A1, A2, A3, A4} = \mu_o \frac{rl}{g} N_s^2 \left(\frac{\pi}{16} \right) \quad (1.121)$$

The general case with an arbitrary number of parallel circuits can now be considered. The practical need to produce a wide range of machines with different voltage and power ratings with only a few sizes of conductors often leads to the need for parallel circuits in most machines. In the manufacture of coils it is desirable to keep the cross section of each individual turn around a nominal value so that each turn can be readily worked into the desired shape. As the number of poles of the machine increases this requirement implies a corresponding increase in the voltage which must be applied to the machine unless steps are taken to reduce the number of series connected turns by connecting groups of windings in parallel.

1.9 Analysis of a Shorted Coil—An Example

Since electrical machines inevitably are equipped with windings which have an equal number of coils intended for north and south poles, it might be questioned what purpose is served by allowing for a more general situation. Such situations occur most frequently during abnormal operation of an electrical machine in which portions of the machine are either short-circuited or open circuited. A typical example is shown in Figure 1.21, in which one of the four poles of the series connected winding of Figure 1.20(a) has been shorted. In this case the situation now changes to a network having two independent currents one flowing in the three healthy series connected poles and one flowing in the shorted winding. The condition can be modeled using the circuit of Figure 1.21(b).

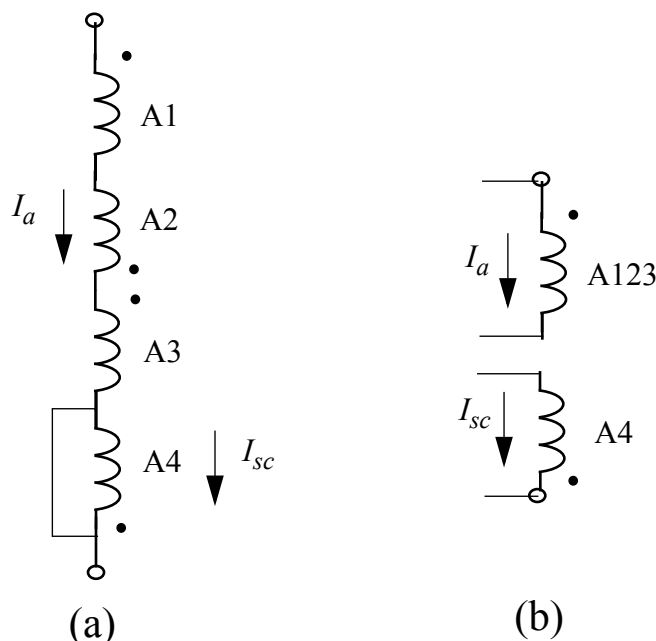


Figure 1.21 Series connected four-pole winding with one shorted pole.

The turns and winding functions for the 123 circuit can be expressed by

$$n_{123}(\phi) = \frac{N_t}{4} \sin 2\phi \quad 0 \leq \phi \leq \frac{3\pi}{2}$$

$$= 0 \quad \frac{3\pi}{2} < \phi \leq 2\pi \quad (1.122)$$

$$\begin{aligned} N_{123}(\phi) &= \frac{N_t}{4} \sin 2\phi - \frac{N_t}{8\pi} \quad 0 \leq \phi \leq \frac{3\pi}{2} \\ &= -\frac{N_t}{8\pi} \quad \frac{3\pi}{2} < \phi \leq 2\pi \end{aligned} \quad (1.123)$$

The self inductance of the 123 winding is then

$$\begin{aligned} L_{123} &= \frac{\mu_0 r l}{g} \int_0^{2\pi} N_{123}(\phi) n_{123}(\phi) d\phi \\ &= \frac{\mu_0 r l}{g} \int_0^{\frac{3\pi}{2}} \left(\frac{N_t}{4} \right)^2 \sin^2 2\phi d\phi - \frac{\mu_0 r l}{g} \int_0^{\frac{3\pi}{2}} \left(\frac{N_t}{4} \right) \sin 2\phi d\phi \end{aligned} \quad (1.124)$$

which ultimately results in

$$L_{123} = \frac{\mu_0 r l}{g} \left(\frac{N_t^2}{32} \right) \left(\frac{3\pi}{2} - \frac{1}{\pi} \right) \quad (1.125)$$

The turns and winding functions for circuit 4 are

$$\begin{aligned} n_4(\phi) &= 0 \quad 0 < \phi \leq \frac{3\pi}{2} \\ n_4(\phi) &= \frac{N_t}{4} \sin 2\phi \quad \frac{3\pi}{2} \leq \phi \leq 2\pi \end{aligned} \quad (1.126)$$

$$\begin{aligned} N_4(\phi) &= \frac{N_t}{8\pi} \\ N_4(\phi) &= \frac{N_t}{4} \sin 2\phi + \frac{N_t}{8\pi} \end{aligned} \quad (1.127)$$

The self inductance of the winding 4 is then

$$L_4 = \frac{\mu_0 r l}{g} \int_0^{2\pi} N_4(\phi) n_4(\phi) d\phi \quad (1.128)$$

$$= \frac{\mu_0 r l}{g} \int_{\frac{3\pi}{2}}^{2\pi} \left(\frac{N_t}{4} \right)^2 \sin^2 2\phi d\phi - \frac{\mu_0 r l}{g} \left(\frac{N_t}{8\pi} \right) \int_{\frac{3\pi}{2}}^{2\pi} \left(\frac{N_t}{4} \right) \sin 2\phi d\phi \quad (1.129)$$

which becomes, ultimately,

$$L_4 = \frac{\mu_0 r l}{g} \left(\frac{N_t^2}{32} \right) \left(\frac{\pi}{2} - \frac{1}{\pi} \right) \quad (1.130)$$

Finally, the mutual inductance between the 123 and 4 circuits is

$$L_{123,4} = \frac{\mu_0 r l}{g} \int_0^{2\pi} N_{123}(\phi) n_4(\phi) d\phi \quad (1.131)$$

or

$$L_{123,4} = \frac{\mu_0 r l}{g} \left(\frac{N_t}{8\pi} \right) \int_{\frac{3\pi}{2}}^{2\pi} \sin 2\phi d\phi \quad (1.132)$$

which becomes, finally,

$$L_{123,4} = \frac{\mu_0 r l}{g} \left(\frac{N_t^2}{32} \right) \left(\frac{1}{\pi} \right) \quad (1.133)$$

The overall behavior of the circuit can be obtained from the equivalent circuit of [Figure 1.22](#), which follows the normal procedure for circuit modeling of a two-winding transformer.

The inductances of the equivalent circuit are

$$L_{123} - L_{123,4} = \frac{\mu_0 r l}{g} \left(\frac{N_t^2}{32} \right) \left(\frac{3\pi}{2} - \frac{2}{\pi} \right) \quad (1.134)$$

$$L_4 - L_{123,4} = \frac{\mu_0 r l}{g} \left(\frac{N_t^2}{32} \right) \left(\frac{\pi}{2} - \frac{2}{\pi} \right) \quad (1.135)$$

It is useful to compare these inductances with the inductance viewed from the terminals of the phase when the phase is healthy (no short-circuit). In this case, from Eq. (1.112),

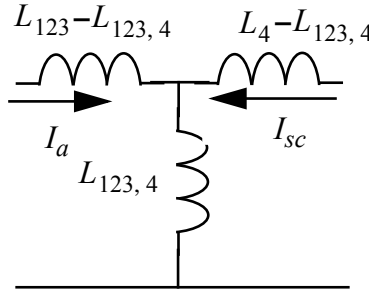


Figure 1.22 Equivalent circuit of four-pole winding with one short-circuited pole.

$$L_{1234} = \frac{\mu_0 r l}{g} \left(\frac{N_t^2}{32} \right) (2\pi) \quad (1.136)$$

In per unit of the inductance L_{1234} , the circuit impedances are

$$(L_{123} - L_{123,4})_{pu} = \frac{3}{4} - \frac{1}{\pi^2} = 0.6487 \quad (1.137)$$

$$(L_{123,4})_{pu} = \frac{1}{2\pi^2} = 0.0507 \quad (1.138)$$

$$(L_4 - L_{123,4})_{pu} = \frac{1}{4} - \frac{1}{\pi^2} = 0.1487 \quad (1.139)$$

The inductance for a short-circuit as seen from the terminals as a per unit of the healthy case is

$$L_{sc} = 0.6487 + \frac{0.0507 \times 0.1487}{0.0507 + 0.1487} = 0.6865 \quad (1.140)$$

Hence, if the AC current flow through the healthy case is one per unit and if the resistance of the coils is neglected, then when the short occurs the current can be expected to rise to $1/0.6865$ or 1.4567 per unit.

1.10 General Case for C Circuits

The general case of a winding with C parallel circuits with an even number of poles is shown in [Figure 1.23](#) for the case of two poles per circuit. For simplicity only the fundamental components are again shown. Since the mutual induc-

tance is calculated by obtaining the product of the winding functions and then integrating the result from zero to 2π , it is now evident that the mutual inductance between any two parallel circuits having an even number of poles is zero. If $L_{A,1}$ is the inductance of the parallel circuit located between $0 \leq \phi \leq 2\pi/C$, then the self inductance of one of the circuits can be expressed as

$$L_{A,1} = \frac{\mu_0 r l}{g} \int_0^{\frac{2\pi}{C}} N_{A1}^2(\phi) d\phi \quad (1.141)$$

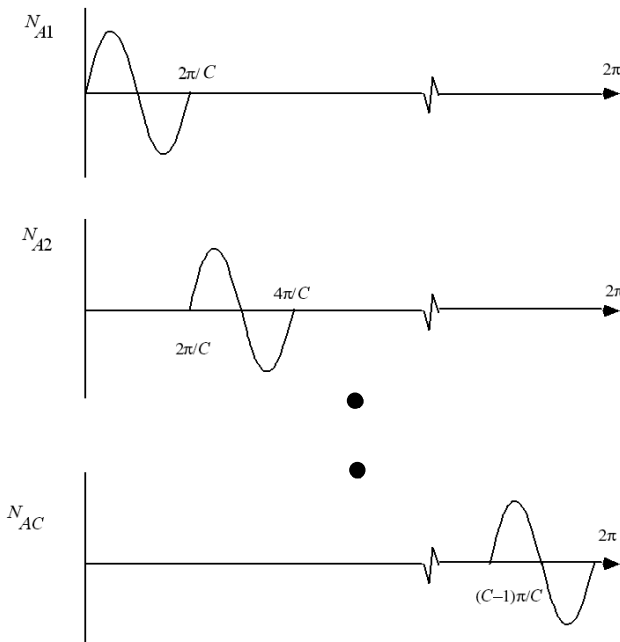


Figure 1.23 Sinusoidal winding distribution with C parallel circuits.

where

$$N_{A,1} = \frac{N_t}{P} \sin\left(\frac{P\phi}{2}\right) \quad (1.142)$$

Upon integrating,

$$L_{A,1} = \frac{\mu_0 r l}{g} \left(\frac{N_t}{P}\right)^2 \left[-\frac{1}{4P} \sin\left(\frac{4\pi P}{C}\right) + \frac{\pi}{C} \right] \quad (1.143)$$

It is easily shown that the first term in the square bracket is zero for both even and odd values of P/C , so that

$$L_{A,1} = \frac{\mu_0 r l}{g} \left(\frac{N_t}{P} \right)^2 \left(\frac{\pi}{C} \right) \quad (1.144)$$

The self inductance of all of the other circuits is the same so that the fundamental component of inductance as seen from the terminals is

$$\frac{\lambda_a}{I_A} = \frac{L_{A,1}}{C} \quad (1.145)$$

where the total input current I_A is related to the current in an individual circuit by $I_A = CI_{A,1}$. Hence, for a winding with C circuits, each having P/C poles, the self inductance is

$$L_A = \frac{L_{A,1}}{C} = \frac{\mu_0 r l}{g} \left(\frac{N_t}{CP} \right)^2 \pi \quad (1.146)$$

In general, when each individual winding has additional, equal harmonics, see Eq. (1.98), the solution is

$$L_A = \frac{L_{A,1}}{C} = \frac{\mu_0 r l}{g} \left(\frac{N_t}{CP} \right)^2 \left(\frac{16}{\pi} \right) \left[\sum_{h=1,3,5,\dots}^{\infty} \left(\frac{k_{hA}}{h} \right)^2 \right] \quad (1.147)$$

It is interesting to examine more carefully the case where the number of poles connected in series within each circuit is odd. The additional poles, over and above the nearest even number, can be visualized as shown in Figure 1.24 for the case of four parallel circuits. Since the number of poles in each circuit is odd, the number of circuits must be even since $(P/C)*C = P$ and P is necessarily even. If the number of circuits is even, the number of “additional” poles is also even (four in the case of this example). Two of these poles are obviously north poles and two are south poles. However, it has already been shown previously (Figure 1.20), that an even number of single poles connected in parallel result in an inductance

$$L_{A1-4} = \mu_0 \frac{rl}{g} \left[\left(\frac{N_t}{P} \right)^2 \frac{\pi}{16^2} \right] \quad (1.148)$$

which is the same as if mutual coupling were ignored. That is, the inductance resulting from these coils again does not contain an additional term due to coupling between coils. Hence, Eq. (1.146) expresses the correct inductance for

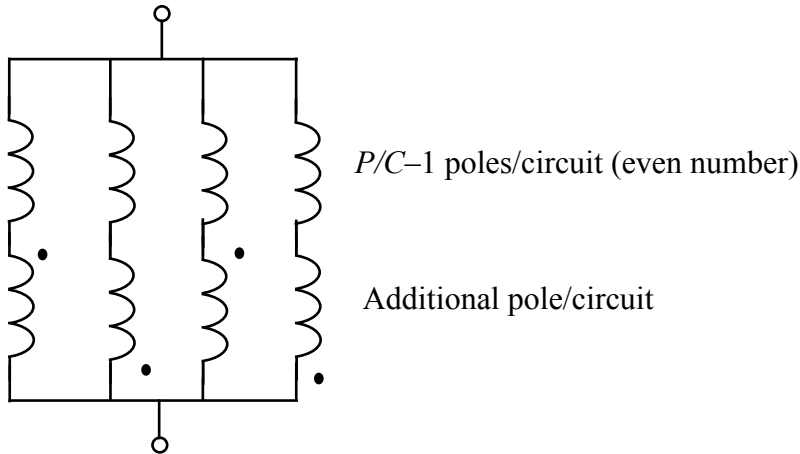


Figure 1.24 Four circuits with an odd number of series connected poles.

the case of a P pole, C circuit system for both even and odd numbers of magnetic poles per circuit.

In practical design situations it is again useful to define the total number of series connected turns which, in this case, is $N_s = N_t/C$. In terms of series connected turns, the general expression for a P pole C circuit winding is

$$L_A = \frac{\mu_0 r l}{g} \left(\frac{N_s}{P} \right)^2 \pi \quad (1.149)$$

The result can be compared with [Table 1.2\(e\)](#).

When the same analysis is applied to a non-sinusoidally distributed winding, then from Eq. (1.98)

$$L_A = \frac{\mu_0 r l}{g} \left(\frac{N_s}{P} \right)^2 \left(\frac{16}{\pi} \right) \left[\sum_{h=1,3,5...}^{\infty} \left(\frac{k_{hA}}{h} \right)^2 \right] \quad (1.150)$$

Comparing the fundamental component of Eq. (1.150) to the ideal case of Eq. (1.149) becomes, after some simplification,

$$N_{s,ideal} = \frac{4}{\pi} k_{1A} N_s = \frac{4}{\pi} k_{1A} \left(\frac{N_t}{C} \right) \quad (1.151)$$

where $N_{s,ideal}$ corresponds to the number of series connected turns on the ideal sinusoidally distributed winding. Generally, this quantity is denoted as N_e , which now denotes the “equivalent” or “effective” number of turns of a

practical winding which produces the fundamental component of *MMF* produced by the winding.

In terms of N_e , the corresponding expression for the fundamental component of L_A corresponding to a non-ideal winding is

$$L_A = \mu_o \frac{rl}{g} \left(\frac{N_e}{P} \right)^2 \pi$$

as in [Table 1.2\(e\)](#).

1.11 Winding Function Modifications for Salient-Pole Machines

Up to now only machines having the so-called doubly cylindrical configuration have been considered. That is, it is assumed the radial air gap between the rotor and the stator is independent of the angle ϕ measured along the stator-rotor periphery. This type of gap configuration finds its application primarily in induction motors and round-rotor synchronous motors. Other machines, notably *dc* machines and salient-pole synchronous machines, utilize configurations in which either the stator inner radius or rotor outer radius is a function of position. In this case the gap length must now be expressed as a function of the angle ϕ .

Consider now the two-pole stator-rotor configuration of [Figure 1.25](#). Here, the stator is again cylindrically shaped. However, the air gap is now assumed to have a non-uniform cross section. A single conductor is again threaded back and forth through the gap and since the winding need not be associated with either the stator or rotor, it is again assumed to be located, for simplicity, in the gap. In order to simplify the analysis it is assumed that each pole has an identical shape. Although this tends to limit somewhat the generality of the result, such symmetry is typical of nearly all types of salient-pole synchronous machines. Also, each winding turn is assumed to be full pitch so that, in the case of a two-pole machine, every conductor in the gap with current in a specified direction is diametrically opposite a conductor carrying current in the opposite direction. This also is true for all practical winding distributions including all of those listed in [Table 1.1](#).

As for the case of the uniform air gap, the gap dimensions have been adjusted so as to account for *MMF* drop in the iron. Hence, the effective per-

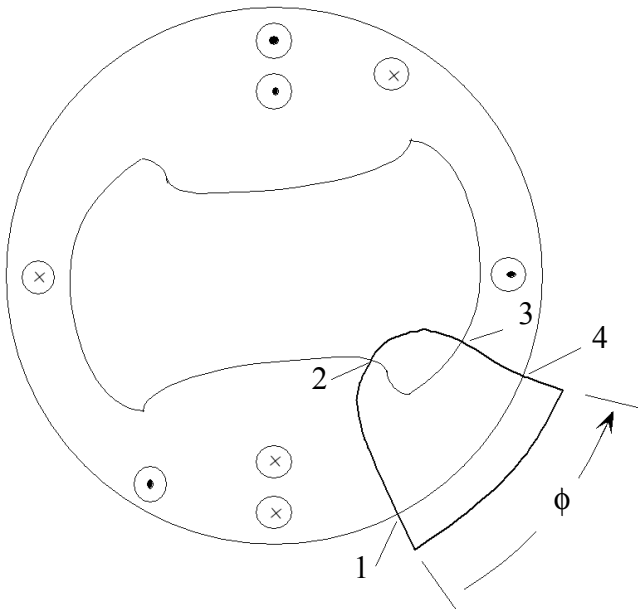


Figure 1.25 Elementary salient-pole device with symmetric placement of windings in the gap.

meability of the iron can now be considered as infinite. Although saliency on the rotor has been assumed, the analysis will hold equally for saliency on the stator (dc machines). The results can be easily extended to (even positive integer) multiple machines by the techniques of [Section 1.8](#).

The reference position for the angle ϕ is located at an arbitrary point along the gap and again a point 1 is defined on the stator corresponding to $\phi = 0$. Point 4 is located on the stator at an arbitrary angle ϕ . In the case of the uniform air gap, points 2 and 3 were located on the rotor radially from the stator points 1 and 4, respectively. Although not explicitly stated, it was implicit in the analysis that all flux lines cross the gap in the radial direction. In the case of the salient-pole machine, this is clearly not the case, since flux lines will assume an irregular shape in the air gap so as to continue to intersect both the stator and rotor iron at right angles. Paths 12 and 34 are in this case defined to lie along lines of flux. Although these flux lines can not be uniquely determined without a flux plot, it is clear that when points 1 and 4 on the stator are fixed, then by Gauss' Law for magnetic fields points 2 and 3 are uniquely defined since two flux lines can never emanate from the same point.

Since the gap has been adjusted for *MMF* drops in the iron, the iron is considered infinitely permeable. Hence, by Ampere's Law

$$\int_{12341} \mathbf{H} \cdot d\mathbf{l} = \int_{12} \mathbf{H} \cdot d\mathbf{l} + \int_{34} \mathbf{H} \cdot d\mathbf{l} = n(\phi)i \quad (1.152)$$

where $d\mathbf{l}$ is defined to be along flux lines originating (or terminating) at points 1 and 4. Again, $n(\phi)$ is the turns function corresponding to the number of turns enclosed by path 12341. Since the line integral of \mathbf{H} is by definition the *MMF*

$$\mathcal{F}_{12}(0) + \mathcal{F}_{34}(\phi) = n(\phi)i \quad (1.153)$$

Gauss' Law for magnetic fields, which can again be invoked, states that

$$\oint_S \mathbf{B} \cdot d\mathbf{S} = 0$$

Taking the surface S to be the side of a cylindrical "can" located just at the inside of the stator inner surface together with its top and bottom, the flux passing through the top and bottom of the can is again negligible. Since B does not vary with respect to the axial length,

$$\int_0^{2\pi} \int_0^l (\mu_o H) R_s(d\mathbf{l})(d\phi) = 0 \quad (1.154)$$

where R_s is the stator inner radius. Eliminating constants results in the fact that

$$\int_0^{2\pi} H(\phi) d\phi = 0 \quad (1.155)$$

However, one can assign $\mathcal{F}(\phi)$ to be the *MMF* at the inner surface of the stator with respect to the rotor pole the entire surface of which can be taken to be at the same magnetic potential. The stator surface is where the field intensity $H(\phi)$ is evaluated in Eq. (1.155). This equation can then also be written as

$$\int_0^{2\pi} \frac{\mathcal{F}(\phi)}{g(\phi)} d\phi = 0 \quad (1.156)$$

where $g(\phi)$ describes the flux line emanating from the stator at the angle ϕ . Hence, in the case of a salient-pole machine, the ratio of the two functions $\mathcal{F}(\phi)/g(\phi)$ must have no average value.

Dividing Eq. (1.153) by $g(\phi)$ and integrating from zero to 2π produces

$$\int_0^{2\pi} \frac{\mathcal{F}_{12}(0) + \mathcal{F}_{34}(\phi)}{g(\phi)} d\phi = \int_0^{2\pi} \frac{n(\phi)I}{g(\phi)} d\phi \quad (1.157)$$

Since the second term on the left hand side is zero from Eq. (1.156) the equation reduces to

$$2\pi\mathcal{F}_{12}(0) \langle g^{-1} \rangle = \int_0^{2\pi} \frac{n(\phi)I}{g(\phi)} d\phi \quad (1.158)$$

where $\langle g^{-1} \rangle$ denotes the average value of the function $1/g(\phi)$.

It has already been noted that practical *MMF* distributions have only odd harmonics. If one assumes that the north and south poles of the salient-pole machine are identical and furthermore are symmetric about the center line of the poles, then it follows that the inverse gap function will have only *even* harmonics (including “dc”). If the turns function and the inverse of the gap function are expanded into their Fourier components, it can now be argued that the only term remaining on the right hand side of Eq. (1.158) is the product of the dc components of the two terms. Thus Eq. (1.158) becomes

$$2\pi\mathcal{F}_{12}(0) \langle g^{-1} \rangle = 2\pi \langle n \rangle \langle g^{-1} \rangle I \quad (1.159)$$

or simply

$$\mathcal{F}_{12}(0) = \langle n \rangle I \quad (1.160)$$

One can now establish the definition of the winding function as

$$N(\phi) = n(\phi) - \langle n \rangle \quad (1.161)$$

Comparing these results with [Section 1.5](#), it is apparent that saliency has no influence on the form of the winding function.

In order to calculate the winding inductance, the flux linkages arising either from the winding itself or another winding must be computed. Again the first conductor encountered with current into the page will be labeled with the numeric 1 and the first conductor with current out of the page with 1'. The process is continued for the second, third, etc., conductors until all turns have been accounted for. A flux distribution in the gap arising from current in a winding not explicitly shown in [Figure 1.25](#) is assumed. In general the flux

passing through a differential cross-sectional area $(rd\phi)l$ and length g is

$$d\Phi = (d\mathcal{P})\mathcal{F} = \mu_0 \frac{rl d\phi}{g} \mathcal{F} \quad (1.162)$$

In this instance the cross-sectional area $rl d\phi$ of interest must be defined at the stator surface so that r corresponds to the inner radius of the stator shell R_s . In the remainder of this book the symbol r will be used for this quantity rather than R_s to avoid confusion with the stator resistance, which will soon be denoted by the same symbol.

A typical “flux tube” defined by Eq. (1.162) is shown in Figure 1.26. It

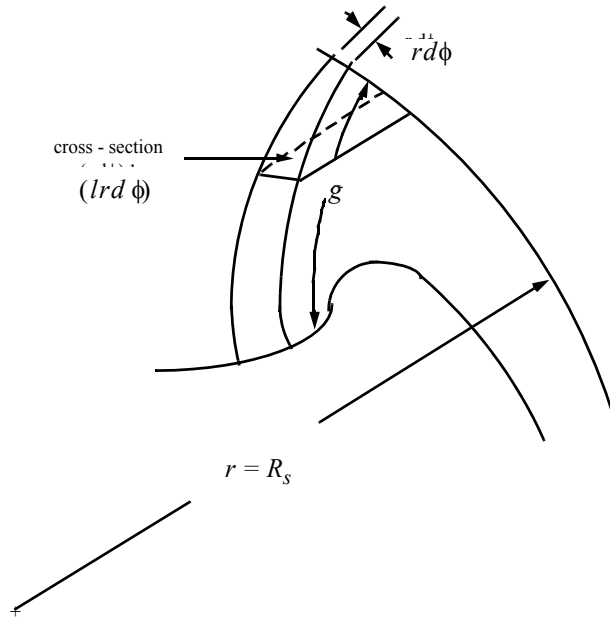


Figure 1.26 Typical flux tube.

should be noted that the gap length g is now a function of ϕ . With the aid of flux plots, the gap length g can be measured as a function of ϕ . A typical flux plot is shown in Figure 1.27(a). Because the gap g appears in the denominator of Eq. (1.162), it is more direct to plot the inverse of g vs. ϕ . Such a plot for the flux map shown for one half a pole pitch is given in Figure 1.27(b).

The total flux passing through the one-turn coil $1 - 1'$ having a span $\phi_1 - \phi'_1$ is given by

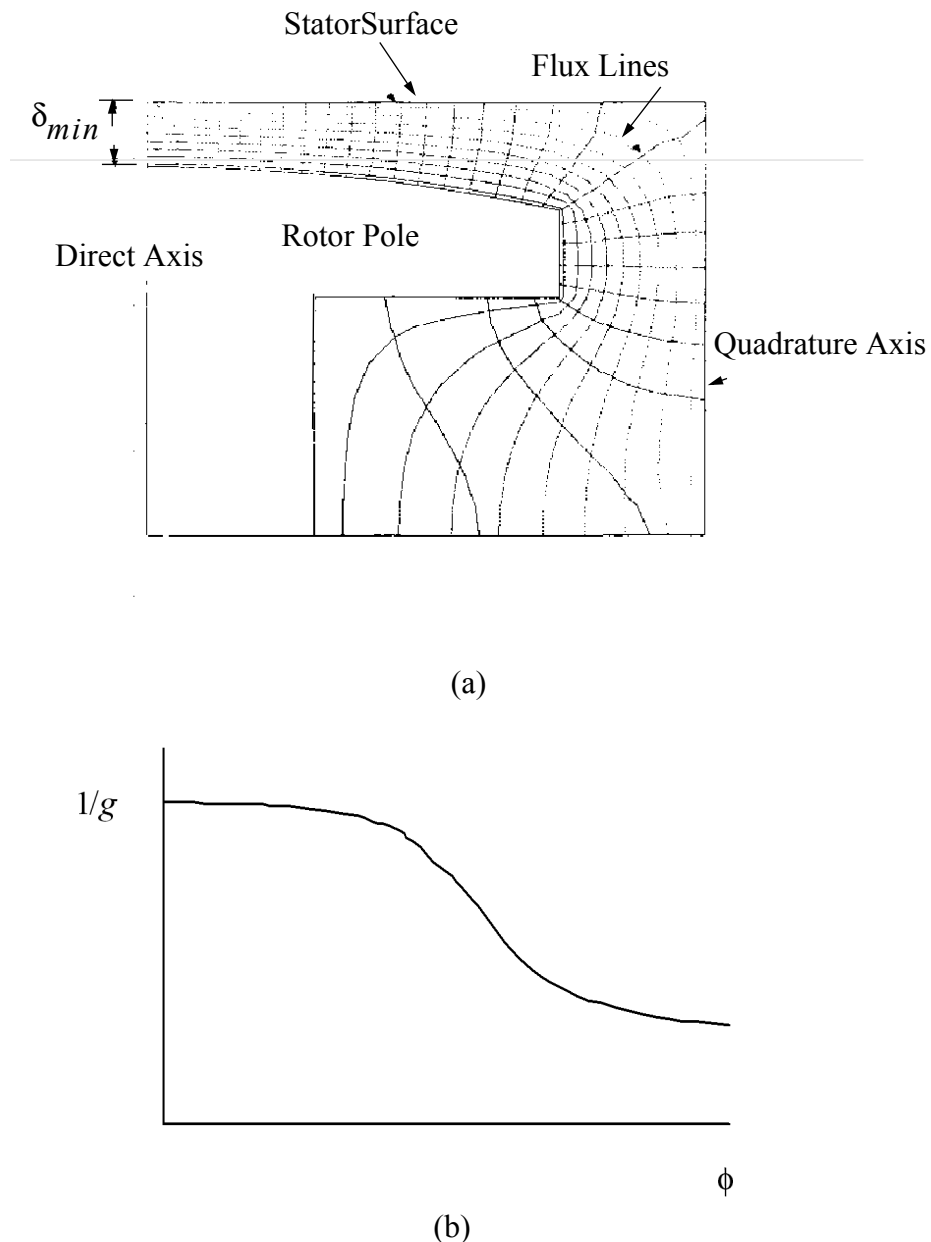


Figure 1.27 (a) Air gap flux plot for a salient-pole machine and (b) corresponding inverse gap function.

$$\Phi_{1-1'} = \mu_0 r l \int_{\phi_1}^{\phi'_1} \frac{\mathcal{F}(\phi)}{g(\phi)} d\phi \quad (1.163)$$

where the gap g must now be retained under the integral sign. This result should be compared to Eq. (1.63). Repeating the procedure and computing the flux linking coils $2 - 2'$, $3 - 3'$ to $N - N'$, the total flux linking the winding can be computed. It is evident from the work in [Section 1.4](#) that the total flux linkages for a N_A turn winding due to current in a N_B turn winding can be expressed as

$$\lambda_{AB} = \mu_0 r l I \int_0^{2\pi} \frac{n_A(\phi)N_B(\phi)}{g(\phi)} d\phi \quad (1.164)$$

where $n_A(\phi)$ is the turns function for winding A .

The mutual inductance is therefore

$$L_{AB} = \mu_0 r l \int_0^{2\pi} n_A(\phi)N_B(\phi)g^{-1}(\phi)d\phi \quad (1.165)$$

When the problem is reversed and the flux linking the B winding due to current in the A winding is considered, then

$$L_{BA} = \mu_0 r l \int_0^{2\pi} N_A(\phi)n_B(\phi)g^{-1}(\phi)d\phi \quad (1.166)$$

Similarly, the magnetizing inductance is given by

$$L_{AA} = \mu_0 r l \int_0^{2\pi} n_A(\phi)N_A(\phi)g^{-1}(\phi)d\phi \quad (1.167)$$

Note that these equations employ a product of the turns and winding functions. In general, it is more convenient to visualize multiplication of functions rather than division of functions. Hence, in these equations the term $1/g(\phi)$ has been written $g^{-1}(\phi)$ since it is easier to find the product of three functions than the product of two functions divided by a third.

From Eq. (1.163) the mutual inductance can also be expressed as

$$L_{AB} = \mu_0 r l \int_0^{2\pi} N_A(\phi)N_B(\phi)g^{-1}(\phi)d\phi + \mu_0 r l \langle n_a \rangle \int_0^{2\pi} N_B(\phi)g^{-1}(\phi)d\phi \quad (1.168)$$

In the practical cases considered here, the rotor is designed to have an even number of symmetrically shaped poles and an equal number of north and south poles. Here, the inverse gap function $g^{-1}(\phi)$ consists of a constant term plus even harmonics of the form

$$g^{-1}(\phi) = \frac{1}{g_0} + \left(\frac{1}{g_2}\right)\cos 2(\phi - \phi_0) + \left(\frac{1}{g_4}\right)\cos 4(\phi - \phi_0) + \dots \quad (1.169)$$

where ϕ_0 is the point at which the gap is a minimum ($g^{-1}(\phi)$ a maximum). It is recalled that the winding function was assumed to contain only odd harmonics. Hence, when $g(\phi)$ (and thus $g^{-1}(\phi)$) contains only even harmonics and when the winding functions are expressed only in terms of odd harmonics, the second term of Eq. (1.168) is identically zero. An equivalent expression for mutual inductance is

$$L_{AB} = \mu_0 r l \int_0^{2\pi} N_A(\phi) N_B(\phi) g^{-1}(\phi) d\phi \quad (1.170)$$

Similarly, for magnetizing inductance

$$L_{AA} = \mu_0 r l \int_0^{2\pi} N_A^2(\phi) g^{-1}(\phi) d\phi \quad (1.171)$$

In order to illustrate the use of these results, consider calculation of the self and mutual inductance of a simple type of salient-pole machine. [Figure 1.28](#) shows a cross-section of an elementary synchronous-reluctance machine, that is, a synchronous machine without rotor excitation. Two identical N turn, concentrated windings are located orthogonal to each other on the stator. Although the gap is generally tapered at the pole tips so as to approximate a sinusoidal inverse gap function, it will be assumed here for simplicity that the inverse gap function $g^{-1}(\phi)$ is piece-wise constant with sudden changes in the function only at the pole tips. The area covered by each pole (pole span) is taken as 120° . So as not to become initially involved with flux maps, the effect of fringing will be neglected. Hence, all flux lines are assumed to be radially directed.

The winding functions and assumed inverse gap function are plotted in [Figure 1.29](#). The reference position for the angle ϕ has been selected as the axis of phase A . The location of a point of symmetry on one of the two-pole faces relative to the axis of phase A is defined as θ_r .

The magnetizing inductance of phase A is defined by

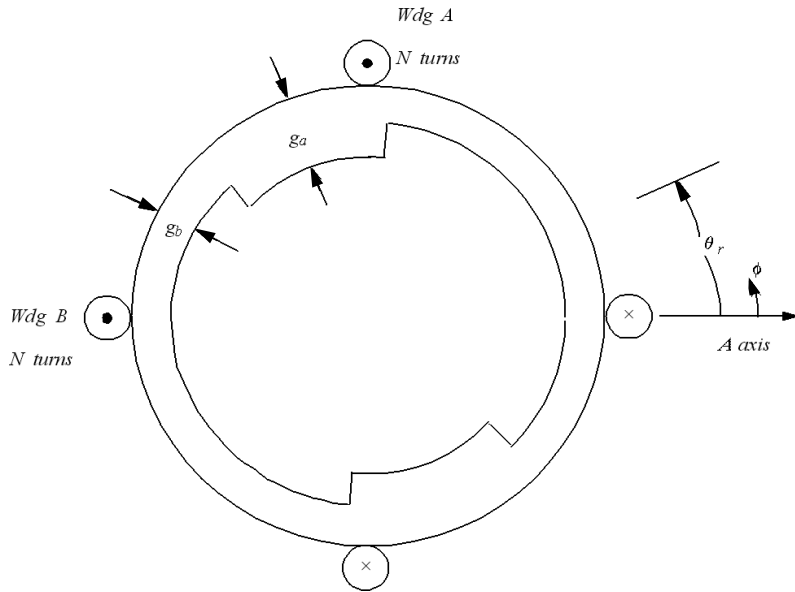


Figure 1.28 Elementary synchronous-reluctance machine.

$$L_{AA} = \mu_0 r l \int_0^{2\pi} N_A^2(\phi) g^{-1}(\phi, \theta_r) d\phi \quad (1.172)$$

where the dependence of the inverse gap function on the rotor position is explicitly shown. Since $N_A^2(\phi)$ is a constant equal to $N_t^2/4$, Eq. (1.172) reduces to

$$L_{AA} = \mu_0 r l \left(\frac{N_t^2}{4} \right) \int_0^{2\pi} g^{-1}(\phi, \theta_r) d\phi \quad (1.173)$$

Upon integrating, since $g^{-1}(\phi, \theta_r)$ is piece-wise constant,

$$L_{AA} = \mu_0 r l N_t^2 \frac{\pi}{2} \left(\frac{2}{3g_a} + \frac{1}{3g_b} \right) \quad (1.174)$$

In a similar manner it is evident that the magnetizing inductance of phase *B* is identical. That is,

$$L_{BB} = L_{AA} \quad (1.175)$$

The computation of mutual inductance is clearly more involved than self inductance. Regardless of the complexity, these inductances can, of course, always be computed by numerical integration using the definition, Eq. (1.170).

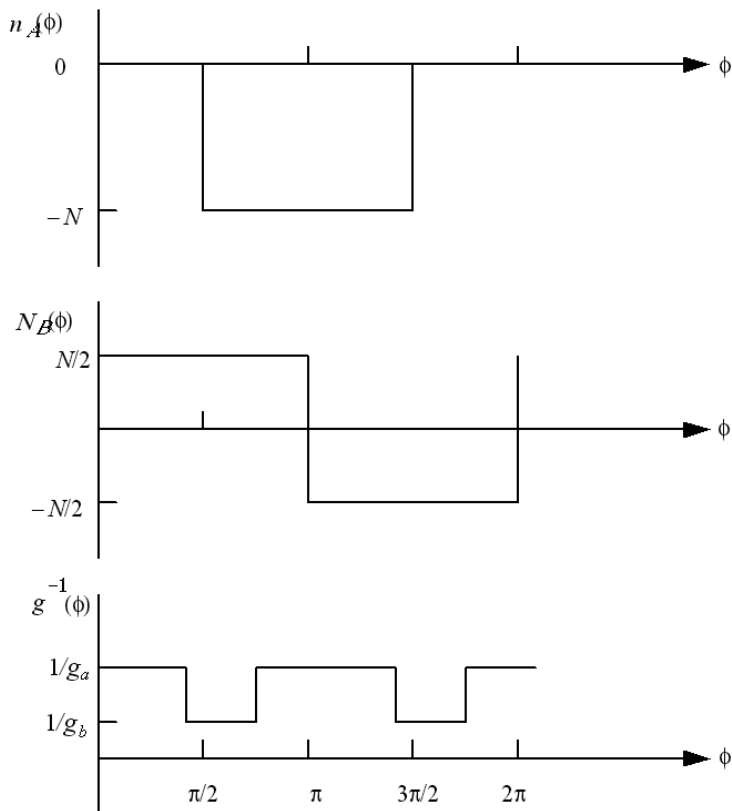


Figure 1.29 Winding and gap functions for the elementary synchronous-reluctance machine of Fig. 1.22.

In simplified examples such as this, mutual inductance can be readily sketched if a few key points are evaluated. In such cases it is useful if Eq. (1.165) rather than Eq. (1.170) is used. That is,

$$L_{AB} = \mu_0 r l \int_0^{2\pi} n_A(\phi) N_B(\phi) g^{-1}(\phi, \theta_r) d\phi \quad (1.176)$$

The turns function for winding A and winding function for winding B are shown in Figure 1.29 together with their product. The inverse gap function is plotted for an arbitrary value of $0 < \theta_r < \pi/2$. As the rotor moves (increases), the function $g^{-1}(\phi, \theta_r)$ moves to the right in the figure. For any θ_r , the mutual inductance is the area resulting from the multiplication of the function $n_A(\phi)N_B(\phi)$. Typical areas for several values of inductance are shown in Figure 1.30.

From the form of the inverse gap function, it is easy to see that as θ_r increases, the product function $n_A(\phi)N_B(\phi)g^{-1}(\phi, \theta_r)$ will begin to repeat at $\theta_r =$

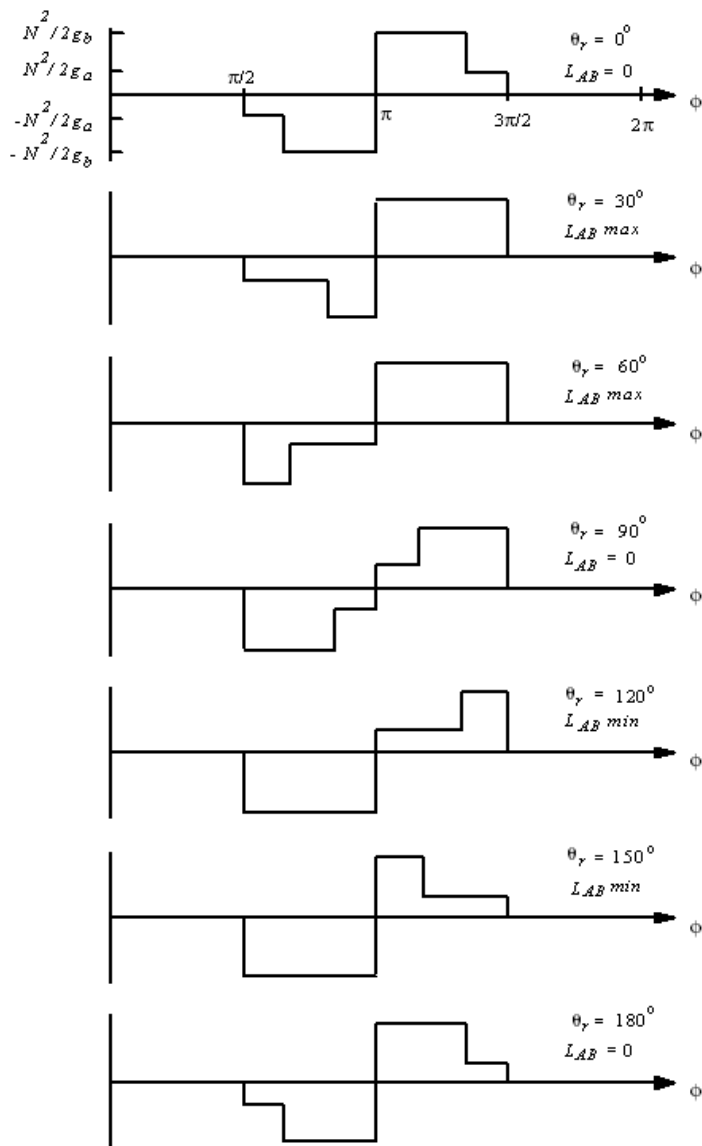


Figure 1.30 Product of function $n_A(\phi)$, $N_B(\phi)$, and $g^{-1}(\phi)$ for various values of θ_r .

π . Also, from the plots in Figure 1.30, the function θ_r is piece-wise linear. The maximum inductance position occurs between $30^\circ < \theta_r < 60^\circ$. At the position $\theta_r = 30^\circ$

$$L_{AB}\left(\frac{\pi}{3}\right) = \mu_0 r l \int_{\frac{\pi}{2}}^{\frac{5\pi}{6}} \left(-\frac{N_t^2}{2}\right) \frac{1}{g_b} d\phi + \mu_0 r l \int_{\frac{5\pi}{6}}^{\pi} \left(-\frac{N_t^2}{2}\right) \frac{1}{g_a} d\phi \quad (1.177)$$

The minimum inductance clearly occurs between $120^\circ < \theta_r < 150^\circ$ and is the negative of the maximum inductance value. The mutual inductance is plotted as a function of θ_r in [Figure 1.31](#).

1.12 Leakage Inductances of Synchronous Machines

As was pointed out previously, use of iron as a magnetic conductor is nowhere near as efficient as the use of copper for an electric conductor. Attempts to direct flux in desirable paths are always accompanied by stray or unwanted flux which flows in undesirable directions. In general, if one ignores certain types of reluctance-synchronous machines, flux which links both a stator and a rotor winding, that is, mutual flux, can be considered as the useful component of flux. Flux which links only a single stator or rotor winding does not enter into energy conversion and can be called stray or leakage flux. The inductance associated with this component of flux is termed *leakage inductance*. Because the air gap is a necessary part of the flux path in an electric machine, leakage flux forms a much greater portion of the total flux produced by a winding than for a static transformer.

1.12.1 Synchronous Machine Stator

The various sources of leakage inductance can best be described by considering first the stator or armature of the machine. The two main subdivisions of leakage are: 1) the *end-winding leakage* and 2) the *gap leakage*.

End-winding leakage L_{ew} , shown in [Figure 1.32](#), occurs because each coil side which forms the useful working portion of the coil must exit from the core body and be bent in a circumferential path in order to be directed back into a different slot for the return path. Its value depends upon a number of complex factors including arrangement of the windings and proximity of either magnetic or conductive components such as core stiffeners, vent covers, housings, and end shields. In general, closed form expressions for end-winding leakage are nearly impossible to obtain and empirical formulas are widely used. More recently, field plotting using either finite difference or finite element tech-

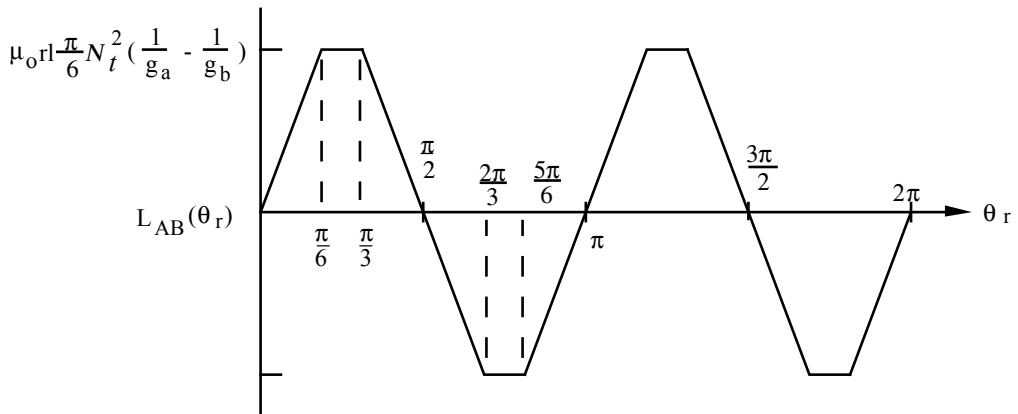


Figure 1.31 Mutual inductance L_{AB} of the elementary synchronous-reluctance machine as a function of rotor position θ_r .

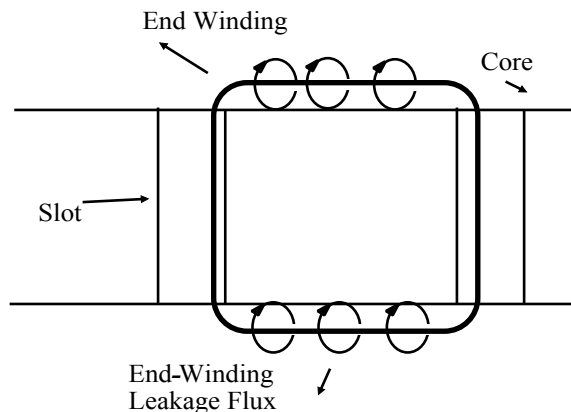


Figure 1.32 End-winding leakage flux.

niques has been used successfully to produce more accurate values. A very comprehensive treatment of end-winding leakage is given by Alger [4].

Gap leakage can be further subdivided into a number of components, namely slot leakage, tooth-top (or zig-zag) leakage, and differential leakage. Slot leakage corresponds to that flux which crosses a conductor circumferentially from tooth to tooth, closing its path around the iron beneath the slot and never crossing the air gap. When the tooth tips are not saturated, reasonably accurate closed form expressions for slot leakage can be obtained. Consider the simple case of a single coil of N turns occupying a slot as in Figure 1.33.

From Ampere's Law the ampere turns enclosed by the path 12341 are

$$\int_{12341} \mathbf{H} \cdot d\mathbf{l} = Ni \frac{x}{h_c} \quad (1.178)$$

where h_c is the height of the conductor and x is measured from the bottom of

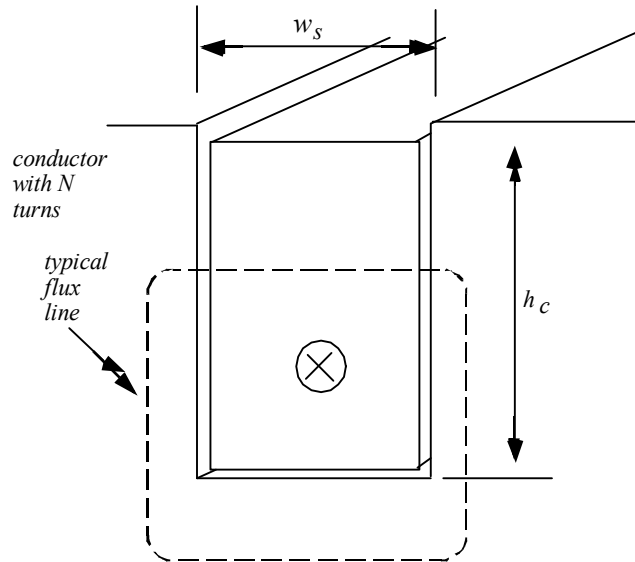


Figure 1.33 Example for slot leakage inductance calculation.

the conductor. If the permeability of the iron path is much larger than the air portion of the closed path, then

$$\int_{2341} \mathbf{H} \cdot d\mathbf{l} = 0 \quad (1.179)$$

so that

$$\int_{12} \mathbf{H} \cdot d\mathbf{l} = N_{slot} I \frac{x}{h_c} = \mathcal{F}_{12} \quad (1.180)$$

If it is assumed that the effective length of the core is l and w_s is the width of the slot, then the flux passing through an elemental area is

$$d\Phi = \mathcal{F}_{12} dP = \mu_0 \mathcal{F}_{12} l \frac{dx}{w_s} \quad (1.181)$$

Substituting Eq. (1.180),

$$d\Phi = \mu_0 N_{slot} I \frac{l}{w_s} x \frac{dx}{h_c} \quad (1.182)$$

However, this differential flux element links only (x/h_c) of the total turns in the slot so that the differential flux linkage corresponding to $d\Phi$ is

$$d\lambda = \frac{Nx}{h_c} d\Phi = \mu_0 N_{slot}^2 \frac{Il}{w_s} \left(\frac{x}{h_c}\right)^2 dx \quad (1.183)$$

The total flux linkage is found by integrating λ from zero to h_c .

$$\lambda = \int_0^{h_c} d\lambda = \int_0^{h_c} \mu_0 N_{slot}^2 I \frac{l}{w_s} \left(\frac{x}{h_c}\right)^2 dx \quad (1.184)$$

The slot leakage inductance for one slot is therefore

$$\frac{\lambda}{I} = L_{sl1} = \mu_0 N_{slot}^2 \frac{lh_c}{3w_s} \quad (1.185)$$

Since an entire winding occupies many slots, the total slot leakage is found by combining terms like L_{sl1} in series and parallel as the case may be. Using the above approach, a slot leakage for numerous different slot configurations can be readily found. A number of practical examples are given in the exercises. When coil sides from two or more different windings occupy a single slot, the leakage inductances must be modified somewhat since some of the slot leakage flux is common to other stator or rotor circuits. The reader is referred to Lipo [1] or Brosan and Hayden [5] for a more detailed presentation.

The second component of gap leakage is termed *zig-zag leakage* L_{zz} since it tends to cross back and forth across the gap utilizing the high permeance paths of the rotor and stator teeth. This component is addressed in books such as [1]. The term is much smaller for a synchronous machine than an induction machine in which the air gap is usually much smaller.

The third type of gap leakage flux, *differential leakage*, also termed *harmonic* or *belt leakage*, arises from quite a different cause. The cause of differential leakage reactance can best be described by means of a simple example. Consider two idealized windings N_A and N_B located on the stator and rotor, respectively which have the following winding functions

$$N_A(\phi) = \frac{N_A}{2} \cos \phi \quad (1.186)$$

$$N_B(\phi) = \frac{N_B}{2} \cos 3(\phi - \theta_r) \quad (1.187)$$

From [Table 1.2](#) the magnetizing inductances of the two windings are both constants.

$$L_{AA} = \frac{\mu_0 r l}{g} N_A^2 \frac{\pi}{4} \quad (1.188)$$

$$L_{BB} = \frac{\mu_0 r l}{g} N_B^2 \frac{\pi}{4} \quad (1.189)$$

From either of the two definitions of mutual inductance, Eq. (1.72) or Eq. (1.97), it is a simple matter to show that

$$L_{AB}(\theta_r) = 0 \quad (1.190)$$

From these equations it can clearly be seen that although the flux produced by winding *A* clearly crosses the air gap it does not link *B* and vice versa. Since the flux produced by the two windings does not link any other windings the corresponding inductances are by definition leakage inductance, namely, differential leakage inductances.

In most cases, only the inductance corresponding to the first harmonic of the winding function is considered as a “useful” torque producing component. In fact, the higher order terms are formally defined as the so-called “belt leakage flux or “differential” flux. That is, the belt leakage inductance is all of the terms in Eq. (1.150) except the first so that

$$L_{belt} = \frac{\mu_0 r l}{g} \left(\frac{N_s}{P} \right)^2 \frac{16}{\pi} \left[\sum_{h=3,5,7\dots}^{\infty} \left(\frac{k_{hA}}{h} \right)^2 \right] \quad (1.191)$$

The total stator leakage inductance of the machine is simply the net sum of the individual leakage components. That is,

$$L_l = L_{ew} + L_{zz} + L_{sl} + L_{belt}$$

Other components of leakage flux that are generally of minor importance can be identified. For the interested reader, Alger has an entire chapter on the calculation of induction motor leakage inductances [4].

1.12.2 Synchronous Machine Rotor

The two categories of synchronous machines which exist, namely, round-rotor and salient-pole machines, have different leakage components and must be discussed separately. The leakage inductances of a round-rotor synchronous machine are handled in nearly the same manner as the stator of the machine although the rotor is excited with direct current, the conductors again lie in slots around a uniform air gap.

In the salient-pole synchronous machine, the stator MMF can be split into two components acting along the poles (direct or d -axis) and at right angles to this axis (quadrature or q -axis). Both components again produce slot leakage and end-winding leakage exactly as inductance machines. There is no zig-zag leakage, however, since the rotor pole surface is generally smooth and without slots. Instead, a type of leakage shown in Figure 1.34, called *tooth-top leakage*,

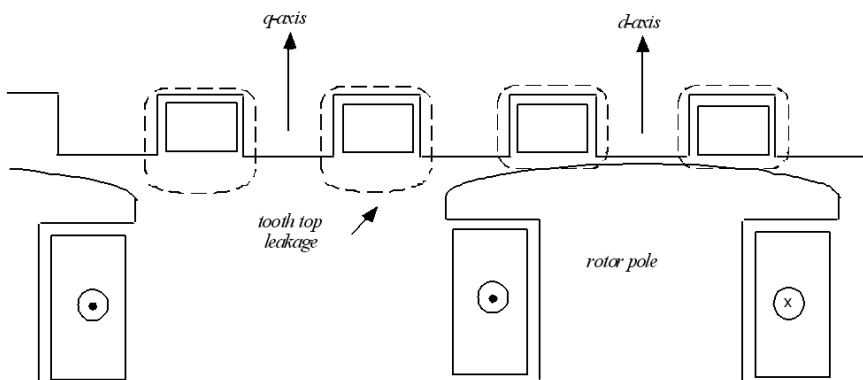


Figure 1.34 Tooth-top leakage flux.

occurs which takes on slightly different values in the two axes due to the presence of the salient poles.

Because the rotor winding is wound around the poles rather than through slots, neither rotor slot leakage nor tooth-top leakage adequately describe the phenomenon. The main component of rotor leakage is interpole leakage, as shown in Figure 1.35. The problem is treated analytically in much the same manner as slot leakage except that the problem is three, rather than two dimensional. Calculation of interpole leakage is also dealt with directly in terms of the field distribution because of the availability of high speed digital computa-

tion. The interested reader is referred to [1], [5] or [6].

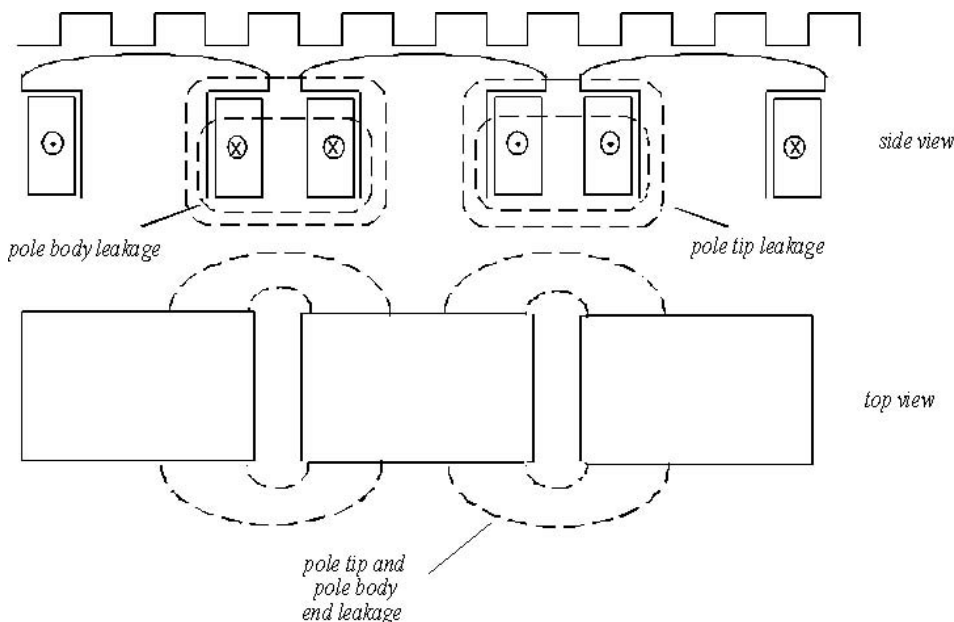


Figure 1.35 Interpole leakage flux.

1.13 Practical Winding Design

The theory that has been developed thus far has enabled the determination of the winding function and *MMF* at any point in the air gap for an arbitrary (but specified) winding distribution. It was shown that these functions enable one to calculate all the associated magnetizing and mutual inductances of the machine. It has been determined that a sinusoidal winding function is most desirable, but no attention has been paid as to why winding functions assume various non-sinusoidal forms. Because of the numerous ramifications of this subject, it is best left to the advanced student. However, a brief discussion of winding design will give an indication of the difficulties involved.

In practice, a phase winding is generally broken down into C individual loops of wire (groups or coils) having N_t/C turns. These coils are then linked up by means of end connections. That portion of the coil which extends beyond the slots forms the end-winding. Each half of the coil which lies in a slot is termed a coil side. When coil sides are spaced by a pole pitch (180 electrical

degrees), they are said to be of full pitch. When the pitch of a coil is less than a full pitch, it is said to be short-pitched and when greater, over-pitched. The pitch of an individual coil should be distinguished from the winding pitch, which is the composite effect after all coils have been connected. In most cases, coils are usually short-pitched in order to reduce the amount of copper used to form the coil.

In nearly all machines slots are punched uniformly around the gap periphery. Also, slots are generally occupied by one coil side (*single layer winding*) or two coil sides (*double layer winding*). It has been explained that proper winding design of an AC machine requires approximately the sinusoidal *MMF* in the air gap. The problem of winding design is to produce a sinusoidal *MMF* in the air gap and to arrange and connect the coils in order to obtain symmetric phase groupings. This must be done while also maximizing the fundamental component of *MMF* in the air gap per ampere relative to its harmonic components for each phase. That is to say, it is desirable to maximize the fundamental component of the winding function relative to its harmonics.

As a typical example of winding design, suppose that a stator winding for a three-phase, four-pole machine is to be designed and the plan is to use a punching having 24 slots. Perhaps the simplest arrangement is to reserve eight slots for each phase or two slots/pole/phase. To produce one phase, four single layer groups of coils can be inserted in the slots and connected, as shown in [Figure 1.36\(a\)](#). Because the coils, in this case, enclose only north and not both north and south poles, the production of the south poles is a “consequence” of the coils producing north poles. The winding is normally termed a *consequent pole* winding arrangement. It can be noted that there are four reversals in flux, resulting in four poles. Since the total number of turns per phase is always assumed as N_t , each coil (indicated by the heavy line) has $N_t/4$ turns. The end connections between coils have “one turn” and are shown as a light line. Since there are 12 slots for each pole pair, there are 30 electrical degrees per slot pitch. The coil sides which lie in adjacent slots are said to span (in this case) two slot pitches or 60° and are called a 60° group. It can also be noted that the inner coil is short-pitched by 15° and the outer coil over-pitched by 15° . This type of coil arrangement, which can be extended to any number of coils, is termed a single layer concentric winding.

Another possibility is shown in [Figure 1.36\(b\)](#). Here, the two coils overlap each other and are full-pitched. Again the winding forms consequent poles.

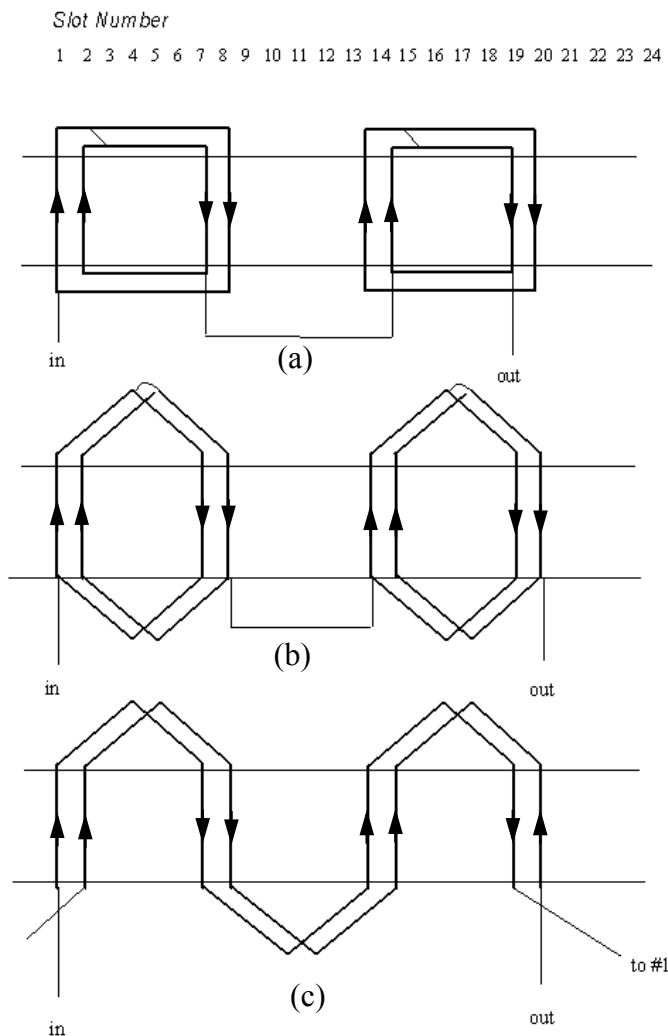


Figure 1.36 Possible single layer winding configurations for a four pole, three-phase machine with 24 slots (a) concentric consequent, (b) lapped consequent and (c) wave windings.

Because of its overlapping nature, such a coil configuration is called a single layer lap winding. A third possibility is shown in Figure 1.36(c). In this case the winding continues around the stator periphery without ever circling back to form a coil. Such a layout is called a single layer wave winding.

Since the currents in the slots are the same in all three cases, the winding functions are clearly identical. However, the three types are quite different in their manufacture. In most cases coils are preformed to the desired shape prior to the assembly process. It is apparent that the concentric winding is composed

of two shapes, namely, the under-pitched and over-pitched coil. Six coils of each shape are used to wind the entire stator winding set. The lap winding requires only one shape of coil, a full-pitched diamond-shaped coil, 12 of which are used to mechanize a three-phase winding configuration. Clearly, costs associated with coil manufacture are reduced if only one type of coil rather than two has to be produced. Also, inspection of [Figure 1.36\(a\)](#) will show that when all three-phases of the concentric windings are inserted, the end windings will form two “tiers” when the machine is viewed from the side (axially). Proper positioning of the windings in the slots requires that the coils in one of the tiers be bent so that both tiers can be accommodated.

Because of its nature, the wave winding presents special problems. The wave winding can not be constructed in coils but in coil sides which must generally be butted together during assembly. Hence, this type of construction is limited to windings having a small number of turns per coil side (preferably one). It is used primarily in cases where the number of pole pairs is large, for example, large low speed hydroelectric generators.

Another possible winding strategy for this 24 slot machine is to use a double layer winding in which each coil making up the phase will share the slot with a coil comprising a portion of some other phase. Such double layer windings are generally preferred in larger horsepower ratings, since the smaller number of turns per coil results in less difficulty in fitting the coil into the required slot. Moreover, this type of winding arrangement can be easily extended to more advanced configurations, where the number of slots per pole per phase is not an integer, as is the case here, resulting in *fractional slotting*.

A double layer lap configuration comprised of four coils per pole pair (120° span) with $N_t/8$ turns per coil is shown in [Figure 1.37\(a\)](#). In order to produce complete symmetry between phases (and hence balanced voltages) each individual coil is always placed with one side on the top of the slot and one side on the bottom. The coil sides on the bottom of the slot correspond, for example, to the downward pointing arrows of [Figure 1.37\(a\)](#). Although this four coil double layer winding would seem a logical choice, examination of the winding function would indicate that the winding factor for the fundamental component is reduced. Also, since the magnetizing inductance is reduced, the voltage required to produce normal “rated” current is less so that the voltage rating for this winding configuration is less than for the single layer windings.

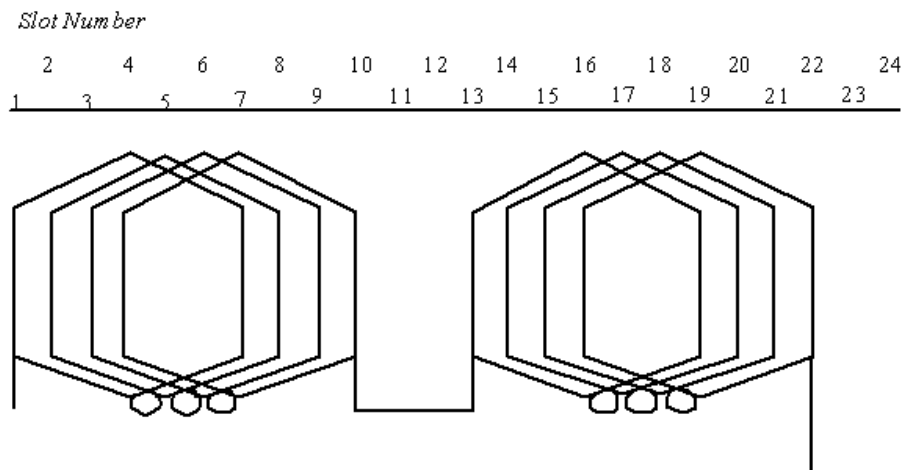
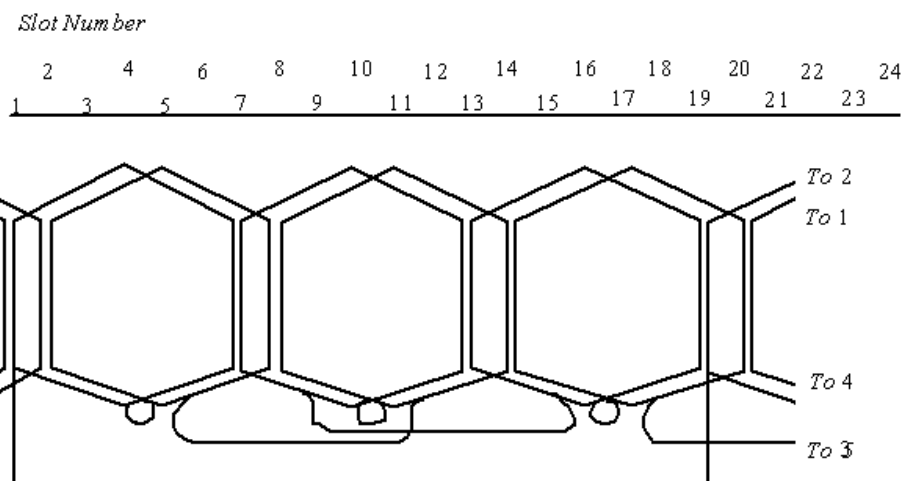
(a) Double Layer Lap Winding 120° Coil Group(b) Double Layer Lap Winding 60° Coil Group

Figure 1.37 Double layer winding configurations for a four-pole, three-phase machine with 24 slots.

The advantages of the single layer winding can be discerned if the eight coils are rearranged in 60° groups, as shown in Figure 1.37(b). Here, coil sides from two different coils making up the same phase share the same slot. Since the voltage induced in each successive coil is 180° out of phase, successive windings are connected in the opposite sense so as to obtain voltage addition. The winding function for this case is again the same as the single layer wind-

ings, [Figure 1.36\(a–c\)](#). In this case little is to be gained by the double layer lap connection of [Figure 1.37\(b\)](#) over the single layer connection, [Figure 1.36\(b\)](#), except, perhaps, ease of manufacture. Note that the number of connections to be made between coils has been doubled which offsets somewhat the advantage in handling the smaller two-layer coils. The real benefit of two layer windings is in cases where there is a fractional number of slots per pole per phase. Such machines enjoy wide use particularly in synchronous machines, since they tend to run at reduced noise levels and alleviate telephone interference problems.

This section has served merely as an introduction to winding design. Certainly the winding function is not the starting point but the end result of a considerable amount of engineering judgment. The interested reader is referred to excellent books which treat the subject by Alger [4], Say [6] and Hindmarsh [7].

1.14 Conclusion

This chapter has served to introduce the necessary mathematical tools to enable the calculation of the inductances of a salient-pole or round-rotor synchronous machine. The use of these tools will be deferred until the third chapter in order to introduce another important concept in the analysis of synchronous machines, that of reference frame theory. These two fundamental concepts will then be employed in Chapter 3 to find the proper winding inductances of the salient-pole synchronous machine.

1.15 References

- [1] T.A. Lipo, “Introduction to AC Machine Design,” Wisconsin Power Electronics Research Center, University of Wisconsin, Madison WI, 3rd Edition, 2012.
 - [2] N.L. Schmitz and D.W. Novotny, “Introductory Electromechanics,” Ronald Press, New York, 1965.
 - [3] A. Langsdorf, “Theory of Alternating-Current Machinery,” McGraw-Hill, New York 1955.
-

- [4] P.L. Alger, "Induction Machines—Their Behavior and Uses," Gordon and Breach Science Publishers, New York, 2nd Edition, 1970, (First Edition Entitled "The Nature of Induction Machines").
- [5] G.S. Brosan and J.T. Hayden, "Advanced Electrical Power and Machines," Pitman, London, 1966.
- [6] M.G. Say, "The Performance and Design of Alternating Current Machines," Pitman, London, 1958.
- [7] J. Hindmarsh, "Electrical Machines and Their Applications," Pergamon Press, Oxford, Second Edition, 1970.

Chapter 2

Reference Frame Theory

2.1 Introduction

The subject of electric machinery involves essentially the study of circuits in relative motion. Unfortunately, the analysis of AC machines becomes involved at an early stage due to the nature of the numerous coupled magnetic circuits. Historically, this difficulty was overcome only in 1929 by R. H. Park, who formulated equations of transformation (Park's transformation) from actual stator currents and voltages to different, equivalent currents and voltages. Prior to this time only steady-state phasor diagrams or very simplified models involving second or third order differential equations had been used to describe synchronous machine behavior. The differential equations describing behavior of the synchronous machine, resulting from this transformation, are called Park's equations. Subsequent work by Stanley, Kron, Krause, and Thomas extended Park's approach to induction machines. The innovation by Park has had a profound effect on our understanding of AC machines.

The topic of transformations or reference frame theory constitutes an essential aspect of machine analysis. In many texts, each type of electric machine is presented separately and a specific change of variables appropriate for each machine is introduced. In other treatments, the so-called primitive (generalized) machine is analyzed and the equations for each type of machine derived by constraining the primitive machine equations. The approach used in this text is somewhat the reverse of this latter method in that the reference frames are introduced initially and the theory underlying a generalized reference frame rather than a generalized machine is developed. This transformation, referred to as the arbitrary reference frame, constitutes a change in variables to a reference frame rotating at an arbitrary velocity. The conventional transformations may be derived from this general transformation by simply specifying the speed of rotation of the arbitrary reference frame. Although this transformation might be applied to a generalized type of machine, the two classes of practical AC machines can be considered directly: namely, synchronous and induction machines.

Since the transformation to the arbitrary reference frame is simply a change of variables, the essential idea can be established without the complexities of machine equations. In this chapter the theory of the arbitrary rotating reference frame will be introduced using the voltage equations of simple $r-L$ circuits. In this manner, one has the opportunity to relate the physical variables associated with the $r-L$ circuits, which can be readily visualized, to the substitute variables in the arbitrary reference frame. The complexities of machine theory and AC machine equations will be deferred to a later stage.

2.2 Rotating Reference Frames

It might be stated that one lives in a world of reference frames. The world as one perceives it, is observed in a reference frame fixed by our senses. As we seat ourselves in the family car, one can say that we change reference frames and attach ourselves to a reference frame fixed in the automobile. Changes of reference frames are clearly an everyday experience. In most cases the reference frame to which we attach ourselves is associated with linear rather than rotational motion (notable exceptions include a number of rides at the amusement park!). It should come as no surprise that rotational reference frames are a part of life since the earth itself is a rotating reference frame.

Rotating reference frames are of central importance in the analysis of electric machines. But first, before one delves into this subject, it is useful to consider a few more general aspects. For simplicity, first consider two Cartesian reference frames whose z -axis and origins coincide. Let the (x_0, y_0, z_0) axes be fixed in space. Let an (x, y, z) system, on the other hand, rotate with angular velocity ω about the $z_0(z)$ axis. This situation is shown in Figure 2.1 where $\hat{u}_x, \hat{u}_y, \hat{u}_z$ are vectors along x, y , and z , respectively, in the rotating system. The location of a point P in the rotating system is then

$$\hat{r} = x\hat{u}_x + y\hat{u}_y + z\hat{u}_z \quad (2.1)$$

where, in general, as P moves so also does $x, y, z, \hat{u}_x, \hat{u}_y$, and \hat{u}_z . The lengths of x, y, z are called the *coordinates* of the point P .

Suppose that P moves in the (x, y, z) system with a velocity

$$\hat{v} = \frac{dx}{dt}\hat{u}_x + \frac{dy}{dt}\hat{u}_y + \frac{dz}{dt}\hat{u}_z \quad (2.2)$$

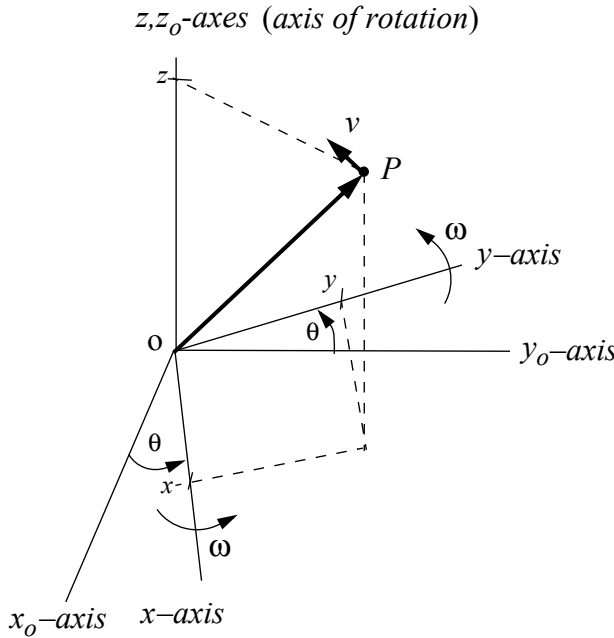


Figure 2.1 Rotating (x, y, z) and fixed (x_o, y_o, z_o) Cartesian coordinate systems.

This would be the velocity measured by an observer rotating with this system. To an outsider, that is, one in the (x_o, y_o, z_o) reference frame, the point P would appear to have a motion

$$\hat{v}_o = \frac{d\hat{r}}{dt} = \frac{dx}{dt}\hat{u}_x + \frac{dy}{dt}\hat{u}_y + \frac{dz}{dt}\hat{u}_z + x\frac{d\hat{u}_x}{dt} + y\frac{d\hat{u}_y}{dt} + z\frac{d\hat{u}_z}{dt} \quad (2.3)$$

From geometric considerations, the two coordinate systems are related by the equations

$$\hat{u}_x = \cos\theta\hat{u}_{xo} + \sin\theta\hat{u}_{yo} \quad (2.4)$$

$$\hat{u}_y = -\sin\theta\hat{u}_{xo} + \cos\theta\hat{u}_{yo} \quad (2.5)$$

$$\hat{u}_z = \hat{u}_{zo} \quad (2.6)$$

Since \hat{u}_{xo} , \hat{u}_{yo} and \hat{u}_{zo} are stationary,

$$\frac{d\hat{u}_x}{dt} = (-\sin\theta\hat{u}_{xo} + \cos\theta\hat{u}_{yo})\frac{d\theta}{dt} = \hat{u}_y\frac{d\theta}{dt} \quad (2.7)$$

$$\frac{d\hat{u}_y}{dt} = (-\cos\theta\hat{u}_{xo} - \sin\theta\hat{u}_{yo})\frac{d\theta}{dt} = -\hat{u}_x\frac{d\theta}{dt} \quad (2.8)$$

$$\frac{d\hat{u}_z}{dt} = 0 \quad (2.9)$$

Note that the derivative of the unit vectors is expressed in terms of $\sin\theta$ and $\cos\theta$ as well as the unit vectors themselves. Recalling the definition of cross product, the derivatives can be expressed directly in terms of the unit vectors themselves if written in the form

$$\frac{d\hat{u}_x}{dt} = \frac{d\theta}{dt}\hat{u}_{zo} \times (\cos\theta\hat{u}_{xo} + \sin\theta\hat{u}_{yo}) = \frac{d\theta}{dt}\hat{u}_z \times \hat{u}_x \quad (2.10)$$

$$\frac{d\hat{u}_y}{dt} = \frac{d\theta}{dt}\hat{u}_{zo} \times (-\sin\theta\hat{u}_{xo} + \cos\theta\hat{u}_{yo}) = \frac{d\theta}{dt}\hat{u}_z \times \hat{u}_y \quad (2.11)$$

$$\frac{d\hat{u}_z}{dt} = \frac{d\theta}{dt}\hat{u}_{zo} \times \hat{u}_{zo} = \frac{d\theta}{dt}\hat{u}_z \times \hat{u}_z = 0 \quad (2.12)$$

Since the term appears in all three equations, it is useful to define the vector

$$\hat{\omega} = \frac{d\theta}{dt}\hat{u}_z \quad (2.13)$$

Equation (2.3) can then be written

$$\hat{v}_o = \hat{v} + \hat{\omega} \times (x\hat{u}_x + y\hat{u}_y + z\hat{u}_z) \quad (2.14)$$

Hence, from Eq. (2.1), the velocity of the point P as viewed in the stationary system is

$$\hat{v}_o = \hat{v} + \hat{\omega} \times \hat{r} \quad (2.15)$$

It is now apparent that in the stationary reference frame, the point P appears to have two types of motions, one described by \hat{v} , the velocity in the rotation reference frame, and the other an angular velocity defined by $\hat{\omega} \times \hat{r}$ due to the rotating axes. Although it has, for simplicity, been assumed that the z and z_o axes are aligned, it can be shown that Eq. (2.15) is equally valid for the general case where the origins of the two coordinate systems coincide but are otherwise independent [1].

An important special case occurs when the point P is stationary in the rotating reference frame. In this case, $\hat{v} = 0$ and the apparent velocity as seen by the stationary observer (in the stationary reference frame) is

$$\hat{v}_o = \hat{\omega} \times \hat{r} \quad (2.16)$$

where $|\hat{r}|$ is a constant. By definition of the cross product it is clear from Eq. (2.16) that $\hat{\omega}$ and \hat{r} are always perpendicular to \hat{v}_o . By inverse reasoning it is apparent that if the velocity in the stationary reference frame can be expressed in the form of Eq. (2.16) then there must exist at least one rotating reference frame for which the P defined by the vector \hat{r} is stationary. More will be stated concerning this point in later sections.

2.3 Transformation of Three-Phase Circuit Variables to a Rotating Reference Frame

2.3.1 Vector Approach Applied to $r-L$ Circuits

Because of economies gained in the cost of transmission and distribution, three-phase networks are used almost exclusively in the generation and utilization of electrical power. Because of this widespread use, it is useful to investigate how the rotating reference frame theory of [Section 2.2](#) can be applied to three-phase networks.

One can begin the study of coordinate transformations by considering three identical $r-L$ networks, as shown in [Figure 2.2](#). The mutual coupling between circuits is assumed to be zero. The three circuit equations are clearly

$$v_{as} = i_{as}r_s + L_s \frac{di_{as}}{dt} \quad (2.17)$$

$$v_{bs} = i_{bs}r_s + L_s \frac{di_{bs}}{dt} \quad (2.18)$$

$$v_{cs} = i_{cs}r_s + L_s \frac{di_{cs}}{dt} \quad (2.19)$$

where the subscript s denotes, here, that the circuits are stationary.

In general, the voltages v_{as} , v_{bs} and v_{cs} can be arbitrary time functions. However, in order to suggest a change of reference frame, it will be assumed (initially) that the voltages form a balanced three-phase set. That is,

$$v_{as} = V_s \cos \omega_e t \quad (2.20)$$

$$v_{bs} = V_s \cos \left(\omega_e t - \frac{2\pi}{3} \right) \quad (2.21)$$

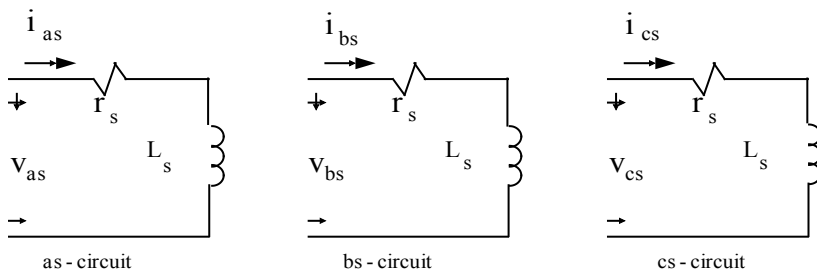


Figure 2.2 Identical r - L networks: $as-$, $bs-$, $cs-$ variables.

$$v_{cs} = V_s \cos\left(\omega_e t + \frac{2\pi}{3}\right) \quad (2.22)$$

If these voltages are applied to the three networks, then after the three networks have settled into the steady-state,

$$i_{as} = I_s \cos(\omega_e t - \xi_s) \quad (2.23)$$

$$i_{bs} = I_s \cos\left(\omega_e t - \frac{2\pi}{3} - \xi_s\right) \quad (2.24)$$

$$i_{cs} = I_s \cos\left(\omega_e t + \frac{2\pi}{3} - \xi_s\right) \quad (2.25)$$

where

$$I_s = \frac{V_s}{Z_s} \quad (2.26)$$

$$Z_s = \sqrt{r_s^2 + (\omega_e L_s)^2} \quad (2.27)$$

$$\xi_s = \tan^{-1}\left(\frac{\omega_e L_s}{r_s}\right) \quad (2.28)$$

In a manner similar to [Section 2.2](#), one may view the three voltages as representing a point in a three dimensional space. It is then convenient to define a voltage vector having components, v_{as} , v_{bs} , and v_{cs} locating this point in a Cartesian coordinate system having units (length) of volts. That is,

$$\hat{v}_{abcs} = v_{as} \hat{u}_{as} + v_{bs} \hat{u}_{bs} + v_{cs} \hat{u}_{cs} \quad (2.29)$$

It is important to keep in mind that the vector \hat{v}_{abcs} locates a point in an orthogonal three dimensional coordinate system and should not be confused with vectors oriented relatively by 120° on a plane as in a phasor plot. Similarly, the current response vector can be defined as,

$$\hat{i}_{abcs} = i_{as}\hat{u}_{as} + i_{bs}\hat{u}_{bs} + i_{cs}\hat{u}_{cs} \quad (2.30)$$

Because the problem is now three, rather than two dimensional, the motion of the vectors \hat{v}_{abcs} and \hat{i}_{abcs} becomes more difficult to visualize. It is possible, however, to derive a considerable amount of information regarding their motion by application of vector algebra. Concentrate, initially, on the voltage vector \hat{v}_{abcs} . The magnitude (or length) of the vector is

$$|\hat{v}_{abcs}| = \sqrt{v_{as}^2 + v_{bs}^2 + v_{cs}^2} \quad (2.31)$$

$$|\hat{v}_{abcs}| = V_s \sqrt{\cos^2 \omega_e t + \cos^2\left(\omega_e t - \frac{2\pi}{3}\right) + \cos^2\left(\omega_e t + \frac{2\pi}{3}\right)} \quad (2.32)$$

Since three-phase trigonometric quantities such as the one above will appear so often in this book, a table of identities is given for convenience in Appendix 1. From trigonometric identity #9 in Appendix 1, it is evident that Eq. (2.32) reduces simply to

$$|\hat{v}_{abcs}| = \sqrt{\frac{3}{2}} V_s \quad (2.33)$$

Hence, the length of vector \hat{v}_{abcs} is constant when the voltages form a balanced fixed amplitude three-phase set.

In the case where the applied voltages are balanced, it is also apparent that

$$v_{as} + v_{bs} + v_{cs} = 0 \quad (2.34)$$

It should now be recalled from analytic geometry that the general equation of a plane in three dimensional space is

$$ax + by + cz = d \quad (2.35)$$

Upon comparing Eqs. (2.34) and (2.35), it is apparent that the particular plane of interest is where $a = b = c = 1$ and $d = 0$. That is, Eq. (2.34) is the equation of a plane in the as -, bs -, cs - coordinate system which has equal directional cosines with respect to the as -, bs -, cs - axes and which passes through the origin. As a result, the excitation vector moves on a plane, and, since the ampli-

tude of \hat{v}_{abcs} is fixed, the vector clearly traces out a circle (or segment of a circle) in this plane. In order to aid in visualization of the plane of rotation, a number of points of the locus described by \hat{v}_{abcs} have been calculated and summarized in Table 2.1. The $d-q$ plane of rotation is sketched in Figure 2.3.

Table 2.1 Voltage components of the vector \hat{v}_{abcs} at various time instants

$\omega_e t$	v_{as}	v_{bs}	v_{cs}
$\pi/6$	$\sqrt{3/2} V_s$	0	$-\sqrt{3/2} V_s$
$\pi/2$	0	$\sqrt{3/2} V_s$	$-\sqrt{3/2} V_s$
$5\pi/6$	$-\sqrt{3/2} V_s$	$\sqrt{3/2} V_s$	0
$7\pi/6$	$-\sqrt{3/2} V_s$	0	$\sqrt{3/2} V_s$
$3\pi/2$	0	$-\sqrt{3/2} V_s$	$\sqrt{3/2} V_s$
$11\pi/6$	$\sqrt{3/2} V_s$	$-\sqrt{3/2} V_s$	0

Again it is useful to make a change in coordinate systems. It should be recalled from Section 2.2 that since the amplitude of the vector \hat{v}_{abcs} is constant, the velocity of the position vector, in this case \hat{v}_{abcs} , as viewed in the non-rotating (physical) system, can be expressed in the form

$$\frac{d\hat{v}_{abcs}}{dt} = \hat{\omega}_e \times \hat{v}_{abcs} \quad (2.36)$$

where $\hat{\omega}_e$ is the angular velocity of the rotating vector relative to the frame of reference.

2.3.2 Transformation Equations

From Section 2.2 it was also demonstrated that since the plane of motion passes through the origin, the three vectors \hat{v}_{abcs} , $d\hat{v}_{abcs}/dt$ and $\hat{\omega}$ are mutually perpendicular. Hence, they can be used as the basis vectors to define a rotating coordinate system in which the vector \hat{v}_{abcs} is stationary. Recall from vector algebra that the plane of rotation defined by Eq. (2.34) can be expressed

in the equivalent form

$$\hat{n} \cdot \hat{v}_{abcs} = 0 \quad (2.37)$$

where

$$\hat{n} = \hat{u}_{as} + \hat{u}_{bs} + \hat{u}_{cs} \quad (2.38)$$

From Eq. (2.37), the vector \hat{n} is normal to the plane of rotation so that it is clearly parallel to $\hat{\omega}$. The unit vector in the \hat{n} (or $\hat{\omega}$) direction is defined by

$$\hat{u}_n = \frac{\hat{n}}{|\hat{n}|} = \frac{1}{\sqrt{3}}(\hat{u}_{as} + \hat{u}_{bs} + \hat{u}_{cs}) \quad (2.39)$$

The use of the subscript “ n ” is intended to signify that the n -axis is “normal” to the $d-q$ plane and that it is associated with current flowing in the “neutral” of the load back to the source. Except for a difference in magnitude, the quantity, in effect, defines the “zero sequence” component of Fortescue [3].

One unit vector which is in the plane defined by Eq. (2.39) is readily located by recalling from Eqs. (2.20), (2.21), and (2.22), that the vector \hat{v}_{abcs} is defined by

$$\hat{v}_{abcs} = V_s \left[\cos(\omega_e t) \hat{u}_{as} + \cos\left(\omega_e t - \frac{2\pi}{3}\right) \hat{u}_{bs} + \cos\left(\omega_e t + \frac{2\pi}{3}\right) \hat{u}_{cs} \right] \quad (2.40)$$

Consequently, by utilizing Eq. (2.33), the unit vector in the direction defined by \hat{v}_{abcs} is clearly

$$\frac{\hat{v}_{abcs}}{|\hat{v}_{abcs}|} = \frac{\hat{v}_{abcs}}{\sqrt{\frac{3}{2}}V_s} \quad (2.41)$$

If this unit vector is defined as \hat{u}_q then

$$\hat{u}_q = \sqrt{\frac{2}{3}} \left[\cos\theta \hat{u}_{as} + \cos\left(\theta - \frac{2\pi}{3}\right) \hat{u}_{bs} + \cos\left(\theta + \frac{2\pi}{3}\right) \hat{u}_{cs} \right] \quad (2.42)$$

where $\theta = \omega_e t$.

In a similar manner it is readily shown that the other vector in the plane of rotation which, by virtue of Eq. (2.36), is clearly perpendicular to \hat{v}_{abcs} is

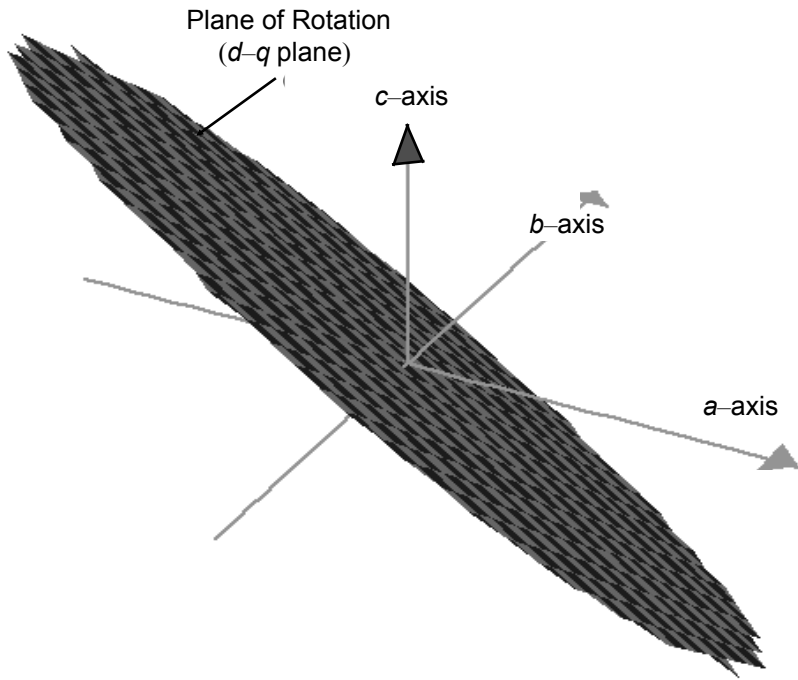


Figure 2.3 Plane of rotation of the vector \hat{v}_{abcs} in the as -, bs -, cs -coordinate system.

$$-\frac{\frac{d\hat{v}_{abcs}}{dt}}{\left| \frac{d\hat{v}_{abcs}}{dt} \right|} = \frac{\omega_e V_s}{\sqrt{\frac{3}{2}} \omega_e V_s} \left[\sin \theta \hat{u}_{as} + \sin \left(\theta - \frac{2\pi}{3} \right) \hat{u}_{bs} + \sin \left(\theta + \frac{2\pi}{3} \right) \hat{u}_{cs} \right] \quad (2.43)$$

or

$$\hat{u}_d = \sqrt{\frac{2}{3}} \left[\sin \theta \hat{u}_{as} + \sin \left(\theta - \frac{2\pi}{3} \right) \hat{u}_{bs} + \sin \left(\theta + \frac{2\pi}{3} \right) \hat{u}_{cs} \right] \quad (2.44)$$

The negative sign in Eq. (2.43) has been chosen such that $\hat{u}_d \times \hat{u}_q = \hat{u}_n$. That is, the vector \hat{u}_d has been located 90° clockwise from the \hat{u}_q vector in the plane of rotation.

It should be pointed out that the particular alignment chosen for the voltage vector at $t = 0$ has permitted one to employ a conventional definition for the \hat{u}_q and \hat{u}_d vectors. However, once having defined these three unit vectors it is important to realize that this particular orientation of the new axes with respect to the voltage vector is not necessary. In fact, the initial orientation of \hat{v}_{abcs} in a particular application is arbitrary. However, for consistency the unit vectors will now remain defined by Eqs. (2.39), (2.43), and (2.44) regardless of their orientation relative to the actual voltage vector. It is an interesting exercise to verify that the three unit vectors are truly orthogonal. That is,

$$\hat{u}_n \cdot \hat{u}_q = \hat{u}_n \cdot \hat{u}_d = \hat{u}_q \cdot \hat{u}_d = 0 \quad (2.45)$$

It is instructive to visualize the location of the unit vector $\hat{u}_{as}, \hat{u}_{bs}, \hat{u}_{cs}$ with respect to the axes $\hat{u}_d, \hat{u}_q, \hat{u}_n$ at the time instant $t = 0$. When the $d-q-n$ vectors do not move from this position (setting $\omega = 0$), these vectors form what is termed the *stationary reference frame*. In this case the projections of unit vectors $\hat{u}_{as}, \hat{u}_{bs}, \hat{u}_{cs}$ onto the $d-q-n$ frame of reference are

$$\hat{u}_{as} = \sqrt{\frac{2}{3}}\hat{u}_q + \sqrt{\frac{1}{3}}\hat{u}_n \quad (2.46)$$

$$\hat{u}_{bs} = -\sqrt{\frac{1}{2}}\hat{u}_d - \sqrt{\frac{1}{6}}\hat{u}_q + \sqrt{\frac{1}{3}}\hat{u}_n \quad (2.47)$$

$$\hat{u}_{cs} = \sqrt{\frac{1}{2}}\hat{u}_d - \sqrt{\frac{1}{6}}\hat{u}_q + \sqrt{\frac{1}{3}}\hat{u}_n \quad (2.48)$$

When the $d-q$ plane as sketched in Figure 2.3 is rotated so as to be in the plane of the paper, the n -axis is then normal to the plane of the paper. The sketch of Figure 2.4 is obtained. Note that in this case the unit vectors $\hat{u}_{as}, \hat{u}_{bs}, \hat{u}_{cs}$ project upwards out of the paper. The angles between these three vectors as viewed from the n -axis are 120° . The projection of these unit vector on the n -axis is clearly the coefficient of the \hat{u}_n term of Eqs. (2.46)–(2.48) namely, $\sqrt{1/3}$. The angle between the unit vector \hat{u}_n and any one of the three unit vectors $\hat{u}_{as}, \hat{u}_{bs}, \hat{u}_{cs}$ is $\cos^{-1}(\sqrt{1/3}) = 54.7^\circ$. In analytic geometry the coefficient $\sqrt{1/3}$ is termed a *direction cosine* of vector $\hat{u}_{as}, \hat{u}_{bs}$, or \hat{u}_{cs} . It is important to observe the fact that the projections of these vectors on the n -axis are a natural consequence of identifying the $d-q$ plane and need not be defined separately from the $d-q$ components in a more or less arbitrary fashion as was done originally by Fortesque. It can be further shown that the projections of the

unit vectors \hat{u}_{as} , \hat{u}_{bs} , \hat{u}_{cs} on the $d-q$ plane are all the same, with a direction cosine of $\sqrt{2}/3$ corresponding to an angle of 35.3° .

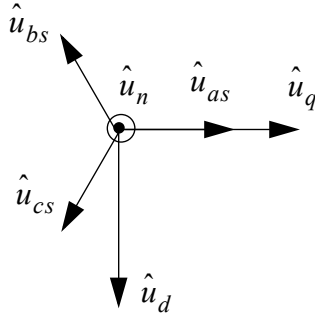


Figure 2.4 Orientation of the $as-bs-cs$ axes with respect to the $d-q-n$ axes at time $t = 0$ and when the $d-q$ axis is located in the plane of the paper. Vectors \hat{u}_{as} , \hat{u}_{bs} and \hat{u}_{cs} have components normal to the plane.

In the analysis thus far it has been assumed that the new reference frame located on the plane of rotation rotates at an angular velocity ω_e such that the vector \hat{v}_{abcs} appears to be stationary. From previous work, however, one should realize that it is not necessary to let the reference frame rotate synchronously but that the speed of rotation can be arbitrary. That is, one can permit Eqs. (2.39), (2.42), and (2.44) to describe the unit vectors of a reference frame rotating at any arbitrary velocity wherein $\omega = \omega(t)$. This reference has been termed in the literature the *arbitrary* or *freely rotating reference frame* [2]. When the reference frame is synchronously rotating with the “electrical” angular velocity of the source, that is, when $\theta = \theta_e = \omega_e t$, the letter “*e*” will be appended as a superscript to the unit vectors as a reminder. The relationships between the unit vectors are summarized in Eqs. (2.49) to (2.54).

$$\hat{u}_d = \sqrt{\frac{2}{3}} \left[\sin \theta \hat{u}_{as} + \sin \left(\theta - \frac{2\pi}{3} \right) \hat{u}_{bs} + \sin \left(\theta + \frac{2\pi}{3} \right) \hat{u}_{cs} \right] \quad (2.49)$$

$$\hat{u}_q = \sqrt{\frac{2}{3}} \left[\cos \theta \hat{u}_{as} + \cos \left(\theta - \frac{2\pi}{3} \right) \hat{u}_{bs} + \cos \left(\theta + \frac{2\pi}{3} \right) \hat{u}_{cs} \right] \quad (2.50)$$

$$\hat{u}_n = \sqrt{\frac{1}{3}} [\hat{u}_{as} + \hat{u}_{bs} + \hat{u}_{cs}] \quad (2.51)$$

where

$$\theta = \int_0^t \omega(t) dt$$

and, in general, $\theta(0) \neq 0$. The inverse relations to these equations are readily found to be

$$\hat{u}_{as} = \sqrt{\frac{2}{3}} \left[\sin \theta \hat{u}_d + \cos \theta \hat{u}_q + \frac{1}{\sqrt{2}} \hat{u}_n \right] \quad (2.52)$$

$$\hat{u}_{bs} = \sqrt{\frac{2}{3}} \left[\sin \left(\theta - \frac{2\pi}{3} \right) \hat{u}_d + \cos \left(\theta - \frac{2\pi}{3} \right) \hat{u}_q + \frac{1}{\sqrt{2}} \hat{u}_n \right] \quad (2.53)$$

$$\hat{u}_{cs} = \sqrt{\frac{2}{3}} \left[\sin \left(\theta + \frac{2\pi}{3} \right) \hat{u}_d + \cos \left(\theta + \frac{2\pi}{3} \right) \hat{u}_q + \frac{1}{\sqrt{2}} \hat{u}_n \right] \quad (2.54)$$

Although only the excitation vector \hat{v}_{abcs} has been considered thus far, comparison with the response vector \hat{i}_{abcs} indicates that the entire derivation is equally valid for \hat{i}_{abcs} since, in the steady-state, it also describes a circle on a $d-q$ plane which passes through the origin. Although the unit vectors \hat{u}_q and \hat{u}_d are defined by Eqs. (2.49) and (2.50), they also describe orthogonal vectors in the same plane defined by the equation

$$i_{as} + i_{bs} + i_{cs} = 0 \quad (2.55)$$

The unit vector \hat{u}_n is normal to this plane as well. It is evident that although the voltage and current vectors are properly viewed in coordinate systems having different units these two quantities can be considered as rotating on the same $d-q$ plane.

In this analysis it has been assumed, initially, that the source voltages are balanced. This assumption has led to a coordinate system located on the plane of rotation of the voltage and current vectors. It should be emphasized, however, that this change of coordinate system remains valid regardless of the form of the source voltages. One would not, of course, expect the same amount of simplification as has been achieved in the case of balanced voltages.

When Eqs. (2.52) to (2.54) are substituted into Eq. (2.29), the excitation vector expressed in the $d-, q-, n-$ rotating reference frame is

$$\begin{aligned}
\hat{v}_{abcs} = & \sqrt{\frac{2}{3}} \left[v_{as} \sin \theta + v_{bs} \sin \left(\theta - \frac{2\pi}{3} \right) + v_{cs} \sin \left(\theta + \frac{2\pi}{3} \right) \right] \hat{u}_d \\
& + \sqrt{\frac{2}{3}} \left[v_{as} \cos \theta + v_{bs} \cos \left(\theta - \frac{2\pi}{3} \right) + v_{cs} \cos \left(\theta + \frac{2\pi}{3} \right) \right] \hat{u}_q \\
& + \frac{1}{\sqrt{3}} [v_{as} + v_{bs} + v_{cs}] \hat{u}_n
\end{aligned} \tag{2.56}$$

It has already been shown, in effect, that when the $r-L$ circuits are supplied with balanced sinusoidal three-phase voltages, the vector representing these voltages has a constant amplitude and rotates with a constant angular velocity. Hence, the vector traces out a circle in the $d-q$ plane. The corresponding vector amplitude is, from Eq. (2.33),

$$|\hat{v}_{abcs}| = \sqrt{\frac{3}{2}} V_s = 1.225 V_s$$

In the case where the voltages are balanced, the \hat{u}_n component of voltage is zero and it would be desirable for purposes of visualization if the amplitude of the vector corresponded to the amplitude of the sine wave V_s . Such a needless complication can be eliminated if one simply introduces a scale factor $\sqrt{2/3}$ between the as, bs, cs system and the d, q, n system. This factor is simply the value of the direction cosine of the $\hat{u}_{as}, \hat{u}_{bs}, \hat{u}_{cs}$ unit vectors with respect to the $d-q$ plane. Now, by definition,

$$\hat{v}_{dqns} \equiv \left(\sqrt{\frac{2}{3}} \right) \hat{v}_{abcs} \tag{2.57}$$

Because of the scale change, a vector on the $d-q$ plane can be measured by either its projection on the $d-q$ axes or on the $as-bs/cs$ axes which now can also be considered as located on the $d-q$ plane, as shown in [Figure 2.5](#) when the neutral component of the three-phase variable is zero. The position of the axes in Figure 2.5 are fixed when $\theta = 0$, that is, when the reference frame is stationary. Because of the change in scale of the $d-q$ components, the projection of the vector on the $q-$ and $as-$ axes are now identical.

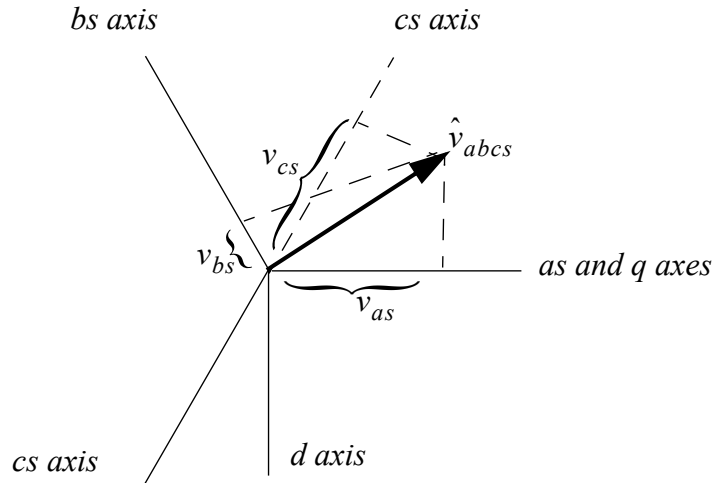


Figure 2.5 Superimposed $a-b-c$ and $d-q$ axes located on the $d-q$ plane when $\theta = 0$.

When balanced voltages are now applied to the three-phase network, the magnitude of \hat{v}_{dqns} is equal to V_s , the amplitude of the phase voltage. The components of the vector \hat{v}_{dqns} are now clearly

$$v_{ds} = \frac{2}{3} \left[v_{as} \sin \theta + v_{bs} \sin \left(\theta - \frac{2\pi}{3} \right) + v_{cs} \sin \left(\theta + \frac{2\pi}{3} \right) \right] \quad (2.58)$$

$$v_{qs} = \frac{2}{3} \left[v_{as} \cos \theta + v_{bs} \cos \left(\theta - \frac{2\pi}{3} \right) + v_{cs} \cos \left(\theta + \frac{2\pi}{3} \right) \right] \quad (2.59)$$

$$v_{ns} = \frac{\sqrt{2}}{3} [v_{as} + v_{bs} + v_{cs}] \quad (2.60)$$

Analogous expressions apply for the components of the current vector \hat{i}_{abcs} and any other three dimensional vector transformed to the $d-q-n$ coordinate system.

The difference between the $n-$ component and Fortescue's zero sequence component now becomes clear, since the "1/3" factor in Fortescue's zero component has been replaced by $\sqrt{2}/3$ in the case of the $n-$ component. Since the use of the zero sequence component would imply a different scale factor associated with one of the three new axes it has not been adopted here. If v_n is replaced by v_0 , no simple relationship such as Eq. (2.57) exists between the as , bs , cs and the qs , ds , ns variables. It could be mentioned that the choice of the "1/3" factor was essentially arbitrary since it was proposed as the third component of the symmetrical component approach as applied to analysis of the sinu-

soidal steady-state and predated Park's landmark paper, which defined the *d*- and *q*-axis quantities by 20 years [4].

The quantities v_{ds} , v_{qs} , and v_{ns} are termed the “direct axis,” “quadrature axis,” and “neutral axis” components of voltage, respectively. The terms *direct* and *quadrature* result from considerations in machine analysis which have yet to be addressed. The significance of these terms will become clear in subsequent chapters. The term *neutral* arises due to the fact that this component results in current flow in the neutral or return path of a three-phase network. For those readers referring to other books on the subject, it should be remembered that the neutral component differs by $\sqrt{2}$ from the zero sequence component of Fortesque. That is,

$$v_{ns} = \sqrt{2}v_{0s} \quad (2.61)$$

The inverse relations to Eqs. (2.58) to (2.60) are

$$v_{as} = v_{ds}\sin\theta + v_{qs}\cos\theta + \frac{v_{ns}}{\sqrt{2}} \quad (2.62)$$

$$v_{bs} = v_{ds}\sin\left(\theta - \frac{2\pi}{3}\right) + v_{qs}\cos\left(\theta - \frac{2\pi}{3}\right) + \frac{v_{ns}}{\sqrt{2}} \quad (2.63)$$

$$v_{cs} = v_{ds}\sin\left(\theta + \frac{2\pi}{3}\right) + v_{qs}\cos\left(\theta + \frac{2\pi}{3}\right) + \frac{v_{ns}}{\sqrt{2}} \quad (2.64)$$

2.3.3 System Equations in the *d*-*q*-*n* Coordinate System

The system differential equations described by Eqs. (2.5) to (2.7) can be written in the vector form

$$\hat{v}_{abcs} = r_s \hat{i}_{abcs} + L_s \frac{d\hat{i}_{abcs}}{dt} \quad (2.65)$$

Because of the change in scale factor between the *as*, *bs*, *cs* and *ds*, *qs*, *ns* variables,

$$\hat{v}_{dqns} = \sqrt{\frac{2}{3}} \hat{v}_{abcs} \quad (2.66)$$

Similarly,

$$\hat{i}_{dqns} = \sqrt{\frac{2}{3}} \hat{i}_{abcs} \quad (2.67)$$

in the d - q - n system. Substituting these variables into the system differential equation, Eq. (2.65) is written

$$\hat{v}_{dqns} = r_s \hat{i}_{dqns} + L_s \frac{d\hat{i}_{dqns}}{dt} \quad (2.68)$$

Note that the $\sqrt{2/3}$ term can be cancelled out since it is common to all factors.

The derivative term can be expanded to the form

$$\frac{d\hat{i}_{dqns}}{dt} = \frac{di_{ds}}{dt}\hat{u}_d + \frac{di_{qs}}{dt}\hat{u}_q + \frac{di_{ns}}{dt}\hat{u}_n + i_{ds}\frac{d\hat{u}_d}{dt} + i_{qs}\frac{d\hat{u}_q}{dt} + i_{ns}\frac{d\hat{u}_n}{dt} \quad (2.69)$$

From Eqs. (2.49) to (2.51)

$$\frac{d\hat{u}_d}{dt} = \sqrt{\frac{2}{3}} \left[\cos\theta \hat{u}_{as} + \cos\left(\theta - \frac{2\pi}{3}\right) \hat{u}_{bs} + \cos\left(\theta + \frac{2\pi}{3}\right) \hat{u}_{cs} \right] \frac{d\theta}{dt} \quad (2.70)$$

$$\frac{d\hat{u}_q}{dt} = -\sqrt{\frac{2}{3}} \left[\sin\theta \hat{u}_{as} + \sin\left(\theta - \frac{2\pi}{3}\right) \hat{u}_{bs} + \sin\left(\theta + \frac{2\pi}{3}\right) \hat{u}_{cs} \right] \frac{d\theta}{dt} \quad (2.71)$$

$$\frac{d\hat{u}_n}{dt} = 0 \quad (2.72)$$

Comparing the bracketed quantities in Eqs. (2.67) and (2.68) to \hat{u}_d and \hat{u}_q , it is apparent that

$$\frac{d\hat{u}_d}{dt} = \hat{u}_q \frac{d\theta}{dt} \quad (2.73)$$

$$\frac{d\hat{u}_q}{dt} = -\hat{u}_d \frac{d\theta}{dt} \quad (2.74)$$

However, since

$$\hat{\omega} = \frac{d\theta}{dt} \hat{u}_n \quad (2.75)$$

the time derivative of the unit vectors can be written in the equivalent form

$$\frac{d\hat{u}_d}{dt} = \hat{\omega} \times \hat{u}_d \quad (2.76)$$

$$\frac{d\hat{u}_q}{dt} = -\hat{\omega} \times \hat{u}_q \quad (2.77)$$

$$\frac{d\hat{u}_n}{dt} = \hat{\omega} \times \hat{u}_n \quad (2.78)$$

Substituting these three relations into Eq. (2.69), the time derivative of the current vector in a rotating *d-q-n* reference frame is

$$\frac{d\hat{i}_{dqns}}{dt} = \left(\frac{d\hat{i}}{dt} \right)_{dqns} + \hat{\omega} \times \hat{i}_{dqns} \quad (2.79)$$

This result might have now been expected since the form of Eq. (2.79) arises basically due to viewing the problem in a rotating reference frame. The first term again denotes the relative velocity of the current vector as viewed in the *d-q-n* arbitrary reference frame. The second term accounts for the velocity of the new reference frame relative to the stationary *as, bs, cs* frame of reference. Substituting Eq. (2.79) into Eq. (2.68) results in the following vector differential equation for the behavior of the “stationary” circuits expressed in a reference frame rotating at an arbitrary velocity ω .

$$\hat{v}_{dqns} = r_s \hat{i}_{dqns} + L_s \left(\frac{d\hat{i}}{dt} \right)_{dqns} + L_s \hat{\omega} \times \hat{i}_{dqns} \quad (2.80)$$

If one defines a flux linkage vector

$$\hat{\lambda}_{dqns} = L_s \hat{i}_{dqns} \quad (2.81)$$

then Eq. (2.80) can be written in the equivalent form

$$\hat{v}_{dqns} = r_s \hat{i}_{dqns} + L_s \frac{d\hat{i}_{dqns}}{dt} + \hat{\omega} \times \hat{\lambda}_{dqns} \quad (2.82)$$

Expanding Eq. (2.82) into its components, this vector equation is equivalent to the three scalar equations

$$v_{ds} = r_s i_{ds} + L_s \frac{di_{ds}}{dt} - \omega L_s i_{qs} \quad (2.83)$$

$$v_{qs} = r_s i_{qs} + L_s \frac{di_{qs}}{dt} + \omega L_s i_{ds} \quad (2.84)$$

$$v_{ns} = r_s i_{ns} + L_s \frac{di_{ns}}{dt} \quad (2.85)$$

When expressed in terms of flux linkages, the voltage equations take the form

$$v_{ds} = r_s i_{ds} + \frac{d\lambda_{ds}}{dt} - \omega \lambda_{qs} \quad (2.86)$$

$$v_{qs} = r_s i_{qs} + \frac{d\lambda_{qs}}{dt} + \omega \lambda_{ds} \quad (2.87)$$

$$v_{ns} = r_s i_{ns} + \frac{d\lambda_{ns}}{dt} \quad (2.88)$$

The equivalent circuits suggested by these equations are shown in Figure 2.6. Note the presence of two so-called “speed voltages” in the d - and q -axis

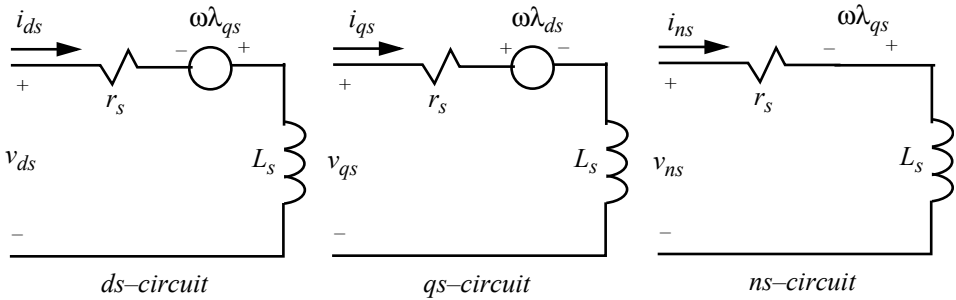


Figure 2.6 Equivalent circuit in d - q - n freely rotating reference frame, ds - $,$ qs - $,$ ns - variables.

circuits which arise because the physical as , bs , cs circuits are being represented in the rotating frame. Since rotation is restricted to the d - q plane, however, the extra voltage generator is not present in the ns circuit. Since the neutral axes equation is not coupled to the d - or q -axis equations nor does it affect their solution, the neutral circuit equation can be solved independently in a straightforward manner.

2.3.4 Power Flow in the d - q - n Equivalent Circuits

The instantaneous power into the as , bs , cs circuits is by definition

$$P_{abcs} = v_{as} i_{as} + v_{bs} i_{bs} + v_{cs} i_{cs} \quad (2.89)$$

In equivalent vector form the power is

$$P_{abcs} = \hat{v}_{abcs} \cdot \hat{i}_{abcs} \quad (2.90)$$

Expressing the voltage and current vectors in terms of the ds –, qs –, ns – variables from Eqs. (2.66), (2.67), the power expression becomes

$$P_{abcs} = \sqrt{\frac{3}{2}} \hat{v}_{dqns} \cdot \sqrt{\frac{3}{2}} \hat{i}_{dqns} \quad (2.91)$$

$$= \frac{3}{2} (v_{ds} i_{ds} + v_{qs} i_{qs} + v_{ns} i_{ns}) \quad (2.92)$$

$$= \frac{3}{2} P_{dqns} \quad (2.93)$$

Hence, the power into the ds , qs , ns equivalent circuits must be multiplied by $3/2$ in order to obtain the power flow into the actual as , bs , cs circuits. The $3/2$ factor is clearly a result of the scale factor used in the transformation to the rotating axes.

It should be mentioned that the $3/2$ term is often a confusing point since some authors preserve the magnitude of the voltage and current vectors in the rotating reference frame, thereby eliminating the need for the $3/2$ term in the power expression. Although such a choice seems ideal, confusion is merely transferred to interpretation of the amplitude of the ds – qs voltage and current components for balanced operation, which now differ by 1.225 from the amplitude of components in the real system. Elimination of the $3/2$ factor is said to result in conservation of power which is probably a moot question since the ds , qs , ns circuits do not physically exist anyway. In any case, the choice results only in conservation of the form of the power equation. Power is clearly “conserved” if defined by Eq. (2.93). In general, the notation for electrical power typically does not use the convention of Eq. (2.93), but instead, by definition

$$P_{es} \equiv P_{abcs} = \frac{3}{2} P_{dqns} \quad (2.94)$$

2.4 Stationary Three-Phase r – L Circuits Observed in a d – q – n Reference Frame

It is interesting to now solve a simple static network problem involving an electrical transient. In particular, consider the solution for the transient response of the three uncoupled networks of Figure 2.2 when the sources are applied suddenly to the load, assuming zero initial conditions. It will again be assumed that balanced voltages are applied to the circuit wherein

$$v_{as} = V_s \cos \omega_e t \quad (2.95)$$

$$v_{bs} = V_s \cos \left(\omega_e t - \frac{2\pi}{3} \right) \quad (2.96)$$

$$v_{cs} = V_s \cos \left(\omega_e t + \frac{2\pi}{3} \right) \quad (2.97)$$

and where V_s and ω_e are constants.

If Eqs. (2.95), (2.96), and (2.97) are substituted into Eqs. (2.58) to (2.60) and if $\theta = \omega t$ where ω is constant, then the applied voltages can be written

$$\begin{aligned} v_{ds} &= \frac{2}{3} V_s \left[\cos \omega_e t \sin \omega t + \cos \left(\omega_e t - \frac{2\pi}{3} \right) \sin \left(\omega t - \frac{2\pi}{3} \right) \right. \\ &\quad \left. + \cos \left(\omega_e t + \frac{2\pi}{3} \right) \sin \left(\omega t + \frac{2\pi}{3} \right) \right] \end{aligned} \quad (2.98)$$

$$\begin{aligned} v_{qs} &= \frac{2}{3} V_s \left[\cos \omega_e t \cos \omega t + \cos \left(\omega_e t - \frac{2\pi}{3} \right) \cos \left(\omega t - \frac{2\pi}{3} \right) \right. \\ &\quad \left. + \cos \left(\omega_e t + \frac{2\pi}{3} \right) \cos \left(\omega t + \frac{2\pi}{3} \right) \right] \end{aligned} \quad (2.99)$$

$$v_{ns} = \frac{2}{3} V_s \left[\cos \omega_e t + \cos \left(\omega_e t - \frac{2\pi}{3} \right) + \cos \left(\omega_e t + \frac{2\pi}{3} \right) \right] \quad (2.100)$$

Again, the “three-phase” identities in Appendix 1 are most useful in reducing these equations. Utilizing identities #18, #16, and #7 in reducing Eqs. (2.98), (2.99), and (2.100), respectively, the voltage quantities in the arbitrary or freely rotating reference frame become

$$v_{ds} = -V_s \sin(\omega_e - \omega)t \quad (2.101)$$

$$v_{qs} = V_s \cos(\omega_e - \omega)t \quad (2.102)$$

$$v_{ns} = 0 \quad (2.103)$$

Note that the ds and qs voltages are equivalent to a voltage applied to a balanced two-phase circuit when modeled in the new frame of reference. Although strictly not necessary, an explicit solution for the currents is most readily obtained if ω is assumed as constant. In this case any of the usual

approaches to solving linear, constant coefficient, differential equations can be used (i.e., undetermined coefficients, Laplace transforms, etc.). Using any of these techniques, if the voltages are applied to the circuits at $t = 0$, the ds , qs currents flowing in the equivalent circuit, [Figure 2.6](#) are

$$i_{ds} = \frac{V_s}{Z_s} \left\{ e^{-\frac{r_s t}{L_s}} \sin(\omega t + \xi_s) - \sin[(\omega_e - \omega)t - \xi_s] \right\} \quad (2.104)$$

$$i_{qs} = -\frac{V_s}{Z_s} \left\{ e^{-\frac{r_s t}{L_s}} \cos(\omega t + \xi_s) - \cos[(\omega_e - \omega)t - \xi_s] \right\} \quad (2.105)$$

where

$$Z_s = \sqrt{r_s^2 + \omega_e^2 L_s^2} \quad (2.106)$$

$$\xi_s = \tan^{-1} \left(\frac{\omega_e L_s}{r_s} \right) \quad (2.107)$$

Substituting these expressions for currents into the inverse transformation and again reducing the resulting expressions by the identities of Appendix 1, it can be shown that the actual three-phase currents are simply

$$i_{as} = \frac{V_s}{Z_s} \left[e^{-\frac{r_s t}{L_s}} \cos \xi_s + \cos(\omega_e t - \xi_s) \right] \quad (2.108)$$

$$i_{bs} = \frac{V_s}{Z_s} \left[e^{-\frac{r_s t}{L_s}} \cos \left(\xi_s - \frac{2\pi}{3} \right) + \cos \left(\omega_e t - \xi_s - \frac{2\pi}{3} \right) \right] \quad (2.109)$$

$$i_{cs} = \frac{V_s}{Z_s} \left[e^{-\frac{r_s t}{L_s}} \cos \left(\xi_s + \frac{2\pi}{3} \right) + \cos \left(\omega_e t - \xi_s + \frac{2\pi}{3} \right) \right] \quad (2.110)$$

The constants Z_s and ξ_s are the magnitude and phase of the load impedance normally defined with phasor analysis.

It is apparent that this simple static network can be solved directly in terms of its natural (or “phase”) variables and no real benefit has been gained over solving the static network equations directly. However, it is interesting to con-

sider how the solution behaves in various reference frames. For example, consider the case where the angular velocity of the $d-q-n$ reference frame is fixed, that is, $\omega = 0$. In this case

$$i_{ds}^s = \frac{V_s}{Z_s} \left\{ e^{-\frac{r_s}{L_s} t} \sin(\xi_s) - \sin[\omega_e t - \xi_s] \right\} \quad (2.111)$$

$$i_{qs}^s = -\frac{V_s}{Z_s} \left\{ e^{-\frac{r_s}{L_s} t} \cos(\xi_s) - \cos[\omega_e t - \xi_s] \right\} \quad (2.112)$$

where the superscript “ s ” has been attached to the $d-q$ currents as a reminder that one is employing the “stationary” reference frame. The electrical response is shown in [Figure 2.7](#) using the parameters $r_s = 0.216 \Omega$, $L_s = 2.88 \text{ mh}$, $V_s = 10 \text{ V}_s$, $\omega_e = 377 \text{ rad/s}$. It is important to observe that the q -axis current and voltage are, in this case, identical to the phase *as* current and voltage. This is a natural consequence of the initial alignment of the $d-q$ axes used and the choice of the $\sqrt{2/3}$ scale factor taken in the definition of the $d-q-n$ variables (Eqs (2.66) and (2.67)). In many cases, when stator currents are to be examined, it is sufficient to view only one of the three variables. In this case, the solution of the q -axis current in the stationary reference frame can be calculated since it is the same as the phase *as* current.

The applied voltage and solution for current is represented as the locus of a vector as shown in [Figure 2.8](#). The d -axis is located in the negative vertical direction as is commonly used in the analysis of synchronous machines. Observe that the voltage traces out a circle in the $d-q$ plane (the ns component is zero) while the current spirals outward until it too traces out a circle in the steady-state. The instantaneous angular position of the current vector with respect to the current vector is clearly the phase angle in the steady-state and with this representation of the circuit, variables can even be defined for transient conditions. At the time instant $t = 0.015$, the instantaneous phase angle between the voltage and current vectors is actually slightly greater than 90 degrees, indicating that energy is being returned to the supply at this instant. The period of time during which energy is returned to the supply is also evident in [Figure 2.7](#) where the power briefly goes negative. This result is somewhat surprising since a balanced set of inductors as a load is (incorrectly) assumed

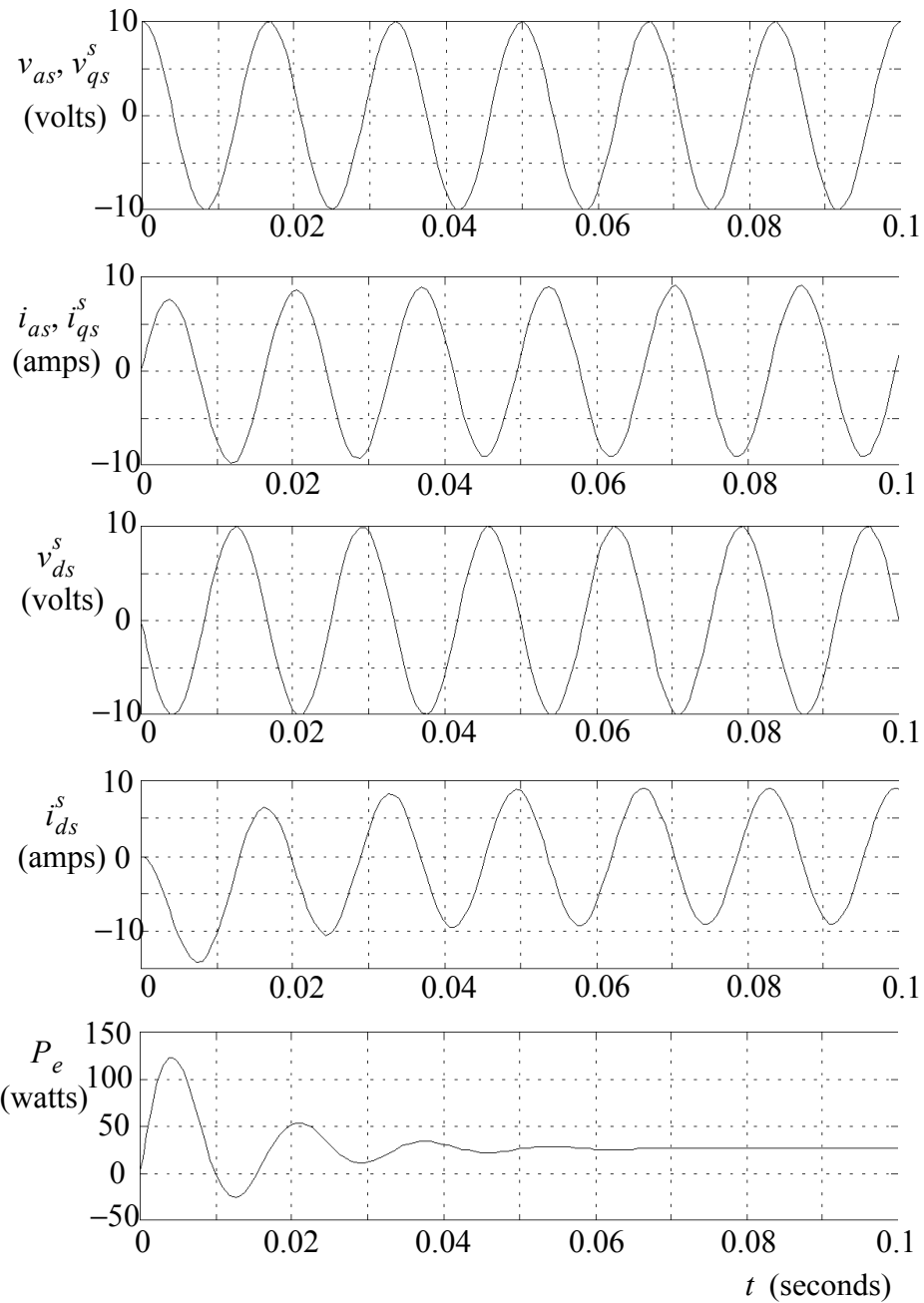


Figure 2.7 Response of electric system for $t > 0$ with $v_{as} = 10 \cos(377t)$ viewed in the stationary reference frame.

to only accept energy from the supply and never return the energy when being energized.

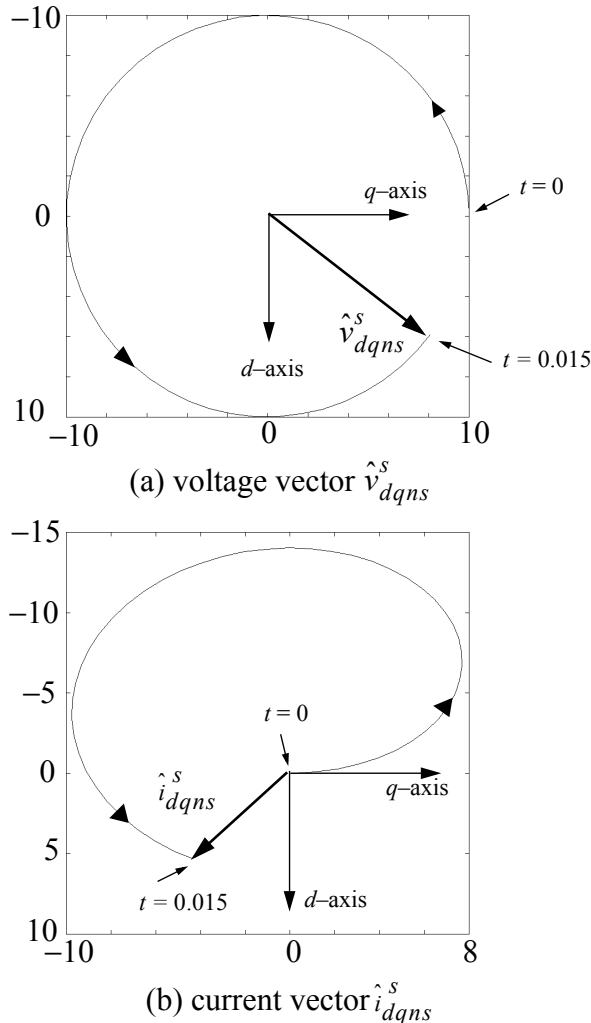


Figure 2.8 Evolution of the locus of the voltage vector \hat{v}_{dqns}^s and current vector \hat{i}_{dqns}^s in the stationary reference frame, $\omega = 0$, during the interval $0 \leq t \leq 0.015$ seconds.

In Figure 2.9 the solution is obtained in the so-called “synchronous” reference frame in which the angular velocity of the reference frame is set equal to the angular frequency of the supply, i.e., $\omega = \omega_e$. In addition, since the voltage vector location at $t = 0$ has been arranged so that it is the same as the position of the q -axis, the projection of the voltage vector on the q -axis is always the length of the vector itself while the d -axis component is necessarily zero.

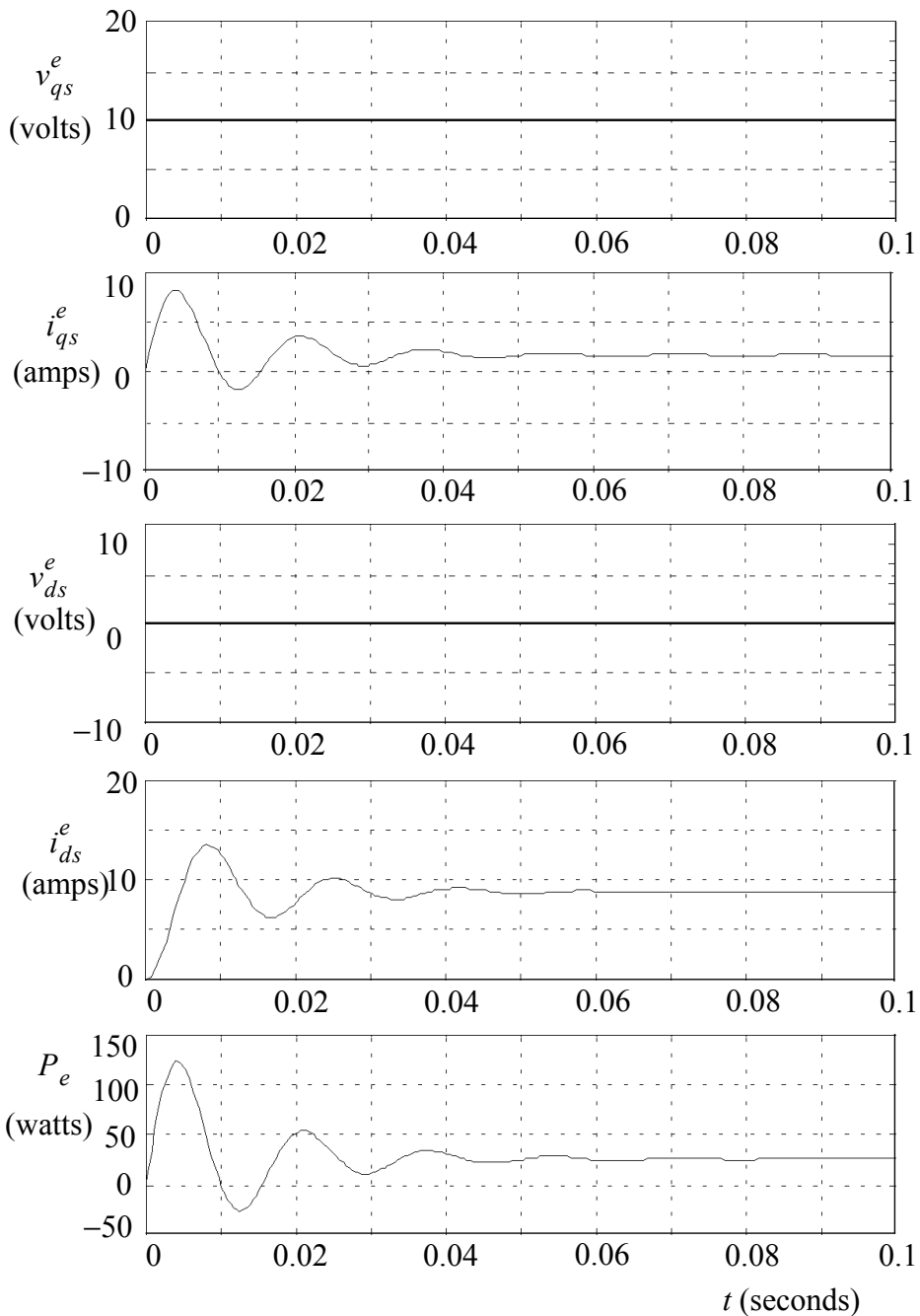


Figure 2.9 Response of electric system for $t > 0$ with $v_{as} = 10 \cos(377t)$ in the synchronously rotating reference frame, $\omega = \omega_e$.

Whereas the current variables in the stationary frame undergo a DC transient on their way to a sinusoidal steady-state, the current vector in the synchronous

reference behaves in just the opposite manner. That is, the currents undergo a sinusoidal transient while the steady-state components become constant. This type of behavior is further illustrated by Figure 2.10. In this case the voltage

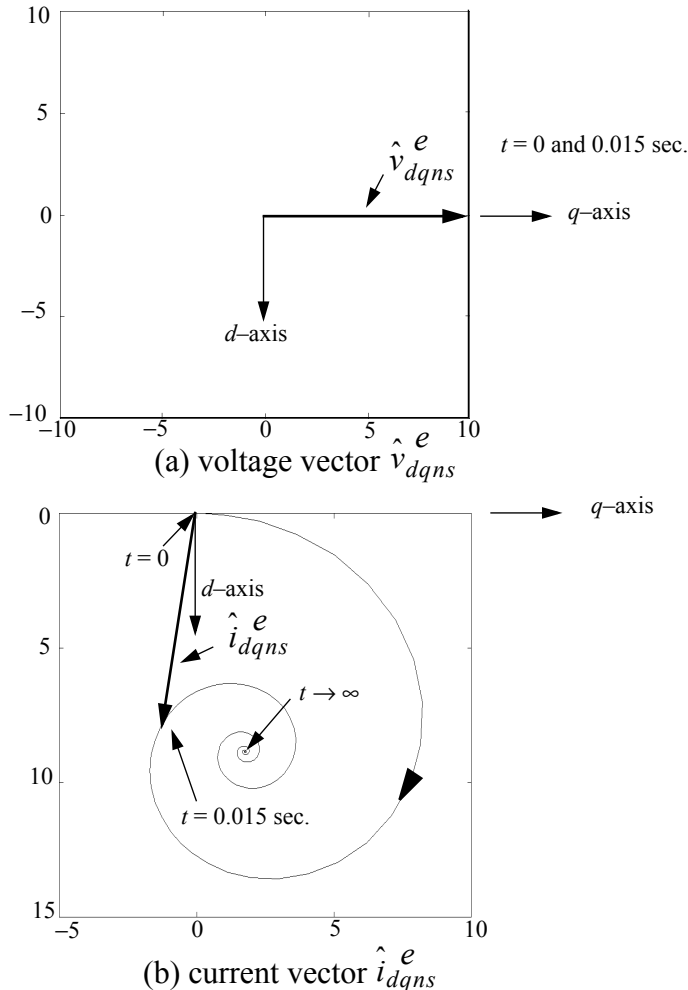


Figure 2.10 Evolution of the locus of the voltage vector \hat{v}_{dqns}^e and current vector \hat{i}_{dqns}^e in the synchronously rotating reference frame, $\omega = \omega_e$, during the interval $0 \leq t \leq 0.15$ seconds.

vector remains “frozen” on the q -axis while the current vector spirals inward until it reaches a constant value. It is interesting to note that the phase angle between the voltage and current is clearly visible during the entire transient interval. Initially the current is in phase with the voltage and then becomes progressively more lagging as the inductors receive reactive energy. Ultimately,

during the first cycle, the current again lags the voltage instantaneously by more than 90 degrees, clearly indicating that energy is temporarily being returned to the supply. The “overshoot” in power is also apparent from the plot of input power in [Figure 2.9](#) as well, which is identical to the input power in [Figure 2.7](#).

In [Figure 2.11](#) the speed of the reference frame is first rotated in the negative (clockwise) direction relative to the positive (counter-clockwise) rotation of the voltage vector. Midway through the transient, the reference frame is commanded to jump to zero and, after a short period, the reference frame is commanded to increase linearly to synchronous speed. Note that the frequency of the voltage takes on the “difference frequency” between that of the reference frame and that of the voltage vector. That is, when the reference frame rotates backwards, the frequency of the $d-q$ voltages is 120 Hz, jumping to 60 Hz when the reference speed jumps to zero. The frequency linearly decreases from 60 to zero as the reference frame speed increases to synchronous speed. The currents basically follow the frequency variation of the voltage but, because of the dc transient in the solution, the waveform is complicated. Nonetheless, the power, as computed from the general expression Eq. (2.92), remains invariant.

2.4.1 Example

As a slightly more complex example of reference frame theory it will be assumed now that the voltages are unbalanced. In particular consider the three-wire circuit shown in [Figure 2.12](#). The three source voltages are expressed by

$$e_{ag} = \epsilon E_s \cos \theta_e \quad (2.113)$$

$$e_{bg} = E_s \cos\left(\theta_e - \frac{2\pi}{3}\right) \quad (2.114)$$

$$e_{cg} = E_s \cos\left(\theta_e + \frac{2\pi}{3}\right) \quad (2.115)$$

where $\theta_e = \omega_e t$ and ϵ is an arbitrary constant. Note that when ϵ is equal to unity the applied voltages are balanced.

Since the neutral return path in this case is absent, the load voltages are now not readily unknown but must be solved from the network equations. If v_{sg} is defined as the voltage between neutral points, then clearly

$$e_{ag} = v_{as} + v_{sg} \quad (2.116)$$

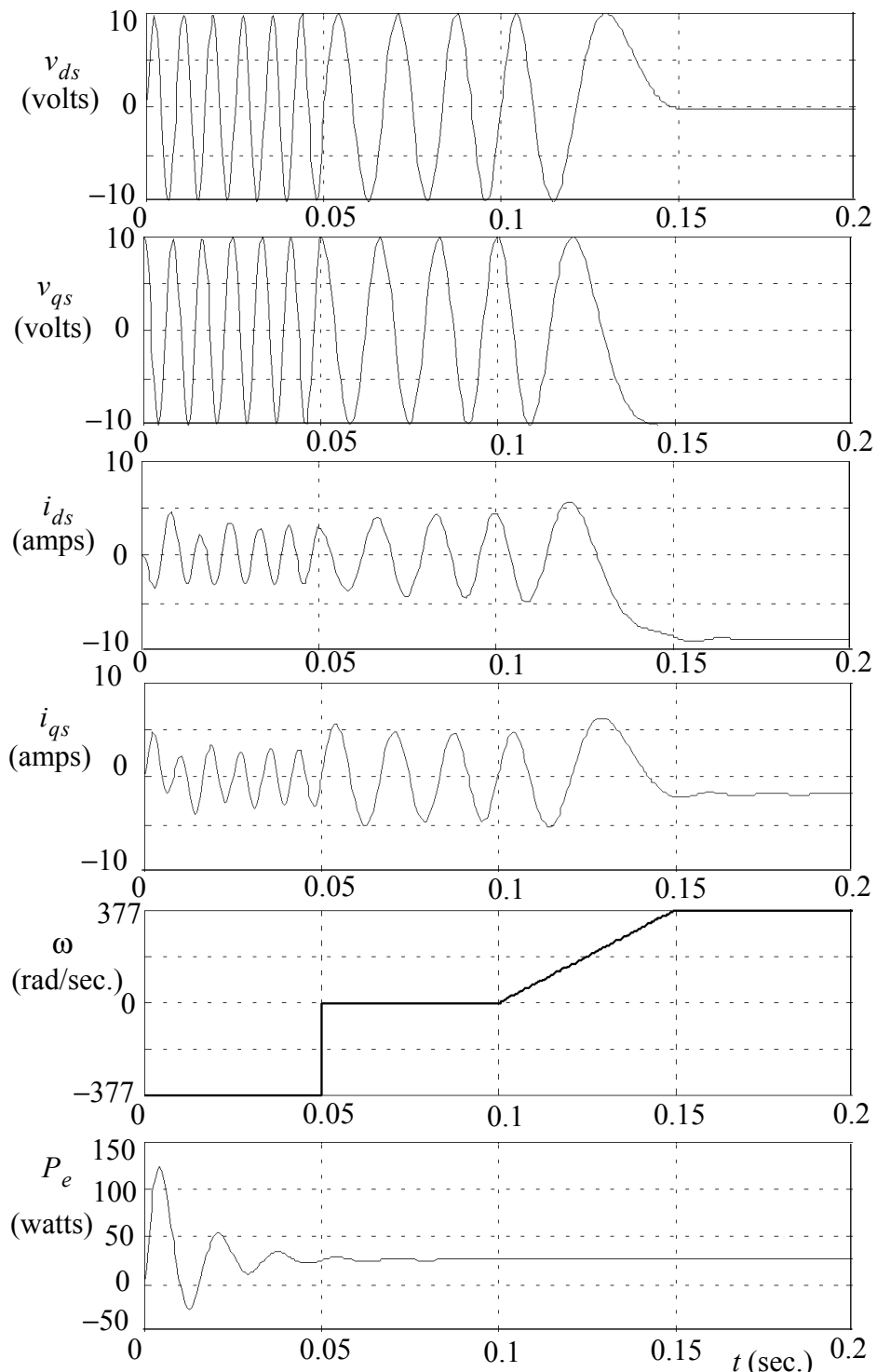


Figure 2.11 Response of electric system for $t > 0$ with phase a s voltage $v_{as} = 10\cos(377t)$; step change in reference frame speed followed by a ramp increase.

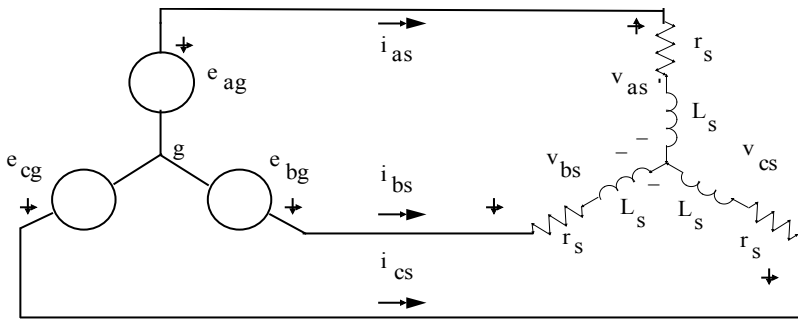


Figure 2.12 Three-wire system with identical r - L networks.

$$e_{bg} = v_{bs} + v_{sg} \quad (2.117)$$

$$e_{cg} = v_{cs} + v_{sg} \quad (2.118)$$

If these three voltage equations are summed, then

$$e_{ag} + e_{bg} + e_{cg} = v_{as} + v_{bs} + v_{cs} + 3v_{sg} \quad (2.119)$$

Since the load is again assumed to be balanced, then Eq. (2.119) can be written

$$e_{ag} + e_{bg} + e_{cg} = r_s(i_{as} + i_{bs} + i_{cs}) + L_s \frac{d}{dt}(i_{as} + i_{bs} + i_{cs}) + 3v_{sg}$$

$$(2.120)$$

However, the load has no neutral return, so that

$$i_{as} + i_{bs} + i_{cs} = 0 \quad (2.121)$$

Equation (2.120) reduces to simply

$$v_{sg} = \frac{1}{3}(e_{ag} + e_{bg} + e_{cg}) \quad (2.122)$$

Substituting Eq. (2.122) into Eqs. (2.116) to (2.118), the load voltages expressed in terms of the source voltages are

$$v_{as} = \frac{2}{3}e_{ag} - \frac{1}{3}e_{bg} - \frac{1}{3}e_{cg} \quad (2.123)$$

$$v_{bs} = -\frac{1}{3}e_{ag} + \frac{2}{3}e_{bg} - \frac{1}{3}e_{cg} \quad (2.124)$$

$$v_{cs} = -\frac{1}{3}e_{ag} - \frac{1}{3}e_{bg} + \frac{2}{3}e_{cg} \quad (2.125)$$

It can be noted that this result is general and is valid regardless of the form of the source voltages.

Substituting the assumed expressions for the source voltages into Eqs. (2.123) to (2.125) yields the following expressions for the load voltages:

$$v_{as} = \frac{2\epsilon + 1}{3} E_s \cos \theta_e \quad (2.126)$$

$$v_{bs} = \frac{1 - \epsilon}{3} E_s \cos \theta_e + E_s \cos \left(\theta_e - \frac{2\pi}{3} \right) \quad (2.127)$$

$$v_{cs} = \frac{1 - \epsilon}{3} E_s \cos \theta_e + E_s \cos \left(\theta_e + \frac{2\pi}{3} \right) \quad (2.128)$$

Referring to Eq. (2.87), the q -axis voltage component in the arbitrary reference frame is

$$v_{qs} = \frac{2}{3} \left[v_{as} \cos \theta + v_{bs} \cos \left(\theta - \frac{2\pi}{3} \right) + v_{cs} \cos \left(\theta + \frac{2\pi}{3} \right) \right] \quad (2.129)$$

Substituting the above expressions for the phase voltages, this expression can be arranged in the form

$$\begin{aligned} v_{qs} = & \frac{2E_s}{3} \left(\frac{1 - \epsilon}{3} \right) \cos \theta_e \left[\cos \theta + \cos \left(\theta - \frac{2\pi}{3} \right) + \cos \left(\theta + \frac{2\pi}{3} \right) \right] \\ & + \left(\frac{2E_s}{3} \right) \left[\epsilon \cos \theta_e \cos \theta \cos \left(\theta_e - \frac{2\pi}{3} \right) \cos \left(\theta - \frac{2\pi}{3} \right) \right. \\ & \left. + \cos \left(\theta_e + \frac{2\pi}{3} \right) \cos \left(\theta + \frac{2\pi}{3} \right) \right] \end{aligned} \quad (2.130)$$

From identity #7 in Appendix 1, the term in the first square bracket is identically zero. The remaining portion of the expression can be reduced to the form

$$\begin{aligned} v_{qs} = & \frac{2E_s}{3} \left[(\epsilon - 1) \cos \theta_e \cos \theta + \cos \theta_e \cos \theta + \cos \left(\theta_e - \frac{2\pi}{3} \right) \cos \left(\theta - \frac{2\pi}{3} \right) \right. \\ & \left. + \cos \left(\theta_e + \frac{2\pi}{3} \right) \cos \left(\theta + \frac{2\pi}{3} \right) \right] \end{aligned} \quad (2.131)$$

Using identity #16 in Appendix 1, the last three terms inside the brackets of Eq. (2.131) reduce to $(3/2) \cos(\theta_e - \theta)$ so that

$$v_{qs} = E_s \left[\frac{2(\epsilon - 1)}{3} \cos \theta_e \cos \theta + \cos(\theta_e - \theta) \right] \quad (2.132)$$

Expanding the first term using identity #5 yields the final result

$$\begin{aligned} v_{qs} &= \frac{\epsilon + 2}{3} E_s \cos(\theta_e - \theta) + \frac{\epsilon - 1}{3} E_s \cos(\theta_e + \theta) \\ &= \frac{\epsilon + 2}{3} E_s \cos(\theta - \theta_e) + \frac{\epsilon - 1}{3} E_s \cos(\theta + \theta_e) \end{aligned} \quad (2.133)$$

In a similar manner it can be shown that

$$\begin{aligned} v_{ds} &= -\frac{\epsilon + 2}{3} E_s \sin(\theta_e - \theta) + \frac{\epsilon - 1}{3} E_s \sin(\theta_e + \theta) \\ &= \frac{\epsilon + 2}{3} E_s \sin(\theta - \theta_e) + \frac{\epsilon - 1}{3} E_s \sin(\theta + \theta_e) \end{aligned} \quad (2.134)$$

Also, it is a relatively straightforward matter to show that

$$v_{ns} = 0 \quad (2.135)$$

so that the voltage vector \hat{v}_{abcs} again rotates on a plane defined by the constraint $v_{as} + v_{bs} + v_{cs} = 0$. A similar interpretation is valid for the current vector \hat{i}_{abcs} .

It is interesting to note the fact that the $d-q$ voltages form two balanced sets. When $\epsilon = 1$ the expressions reduce to the previous result for balanced voltages. When $\epsilon = -2$ only the second of the two terms remain for v_{qs} and v_{ds} . In general, the amplitude of the voltage vector is no longer constant. However, the vector v_{abcs} can be considered as being made up of two vectors of constant amplitude corresponding to the first terms of Eqs. (2.133) and (2.134) and the second terms, respectively. A simple sketch will quickly demonstrate that whereas the first term of the ds, qs voltages represent components of a vector rotating in the counterclockwise direction, the second terms correspond to a vector rotating in the clockwise direction on the $d-q$ plane. Since counterclockwise rotation is generally assumed as the reference or positive direction, these voltage components are sometimes called positively rotating or *positive sequence* components.

In order to better visualize system response, the equations describing the behavior of the system in the $d-q-n$ reference frame were simulated with

SIMULINK®. The parameters used were $r_s = 0.216\Omega$ and $L_s = 2.88\text{ mh}$. Also, it was assumed that

$$e_{ag} = \varepsilon 10 \cos(377t) \quad (2.136)$$

$$e_{bg} = 10 \cos\left(377t - \frac{2\pi}{3}\right) \quad (2.137)$$

$$e_{cg} = 10 \cos\left(377t + \frac{2\pi}{3}\right) \quad (2.138)$$

Consider now first the case, where the $d-q$ axes do not rotate, that is, the circuits are viewed from a stationary reference frame wherein $\omega = 0$, $\theta = 0$. When $\omega = 0$, the ds , qs , ns variables are again simply algebraically related to the as , bs , cs variables. In particular, from Eqs. (2.133) to (2.135),

$$v_{ds}^s = -E_s \sin \omega_e t \quad (2.139)$$

$$v_{qs}^s = \frac{(2\varepsilon + 1)}{3} E_s \cos \omega_e t \quad (2.140)$$

$$v_{ns}^s = 0 \quad (2.141)$$

Here, the superscript “ s ” is used as a reminder that the reference frame is stationary. Comparing Eq. (2.139) to (2.126), it can be noted that $v_{qs}^s = v_{as}$. Similarly, $i_{qs}^s = i_{as}$. This is a very useful feature of the stationary reference frame as formulated, since one of the three physical variables has been arranged to be identical to the q -axis component when the $d-q$ frame is fixed at its reference position ($\theta = 0$). The d -axis voltage is lagging in phase from the q -axis voltage by 90° . However, in this case the amplitudes of the two voltages are not equal unless $\varepsilon = 1.0$ or -2 . Figure 2.13 shows the response of the system in the stationary reference frame. In particular, ε has been set to zero so that $e_{ag} = 0$. In the steady-state, the d -axis current again lags the q -axis current by 90° . The neutral n -axis variables have not been plotted since the excitation vector \hat{v}_{dqns} and response vector \hat{i}_{dqns} again rotate on the $d-q$ plane.

It has already been observed that the $d-q-n$ voltages can be separated into components, one rotating in the positive (counterclockwise) direction and one rotating negatively (clockwise) in the $d-q$ plane. In Figure 2.14, the computer run has been repeated with v_{qs} plotted versus v_{ds} and i_{qs} versus i_{ds} . Figure 2.14(a) shows the response of the equivalent circuit when only the positive rotating voltage component is applied, that is, when the first terms in Eqs. (2.133) and (2.134) are used wherein $\theta = \omega = \varepsilon = 0$, $E_s = 10\text{ V}$. and $\theta_e = 377t$.

Figure 2.14(b) gives the transient response when only the negatively rotating component (second term) is applied to the equivalent circuit. In Figure 2.14(c) both components have been applied simultaneously to the circuits, Eqs. (2.133)

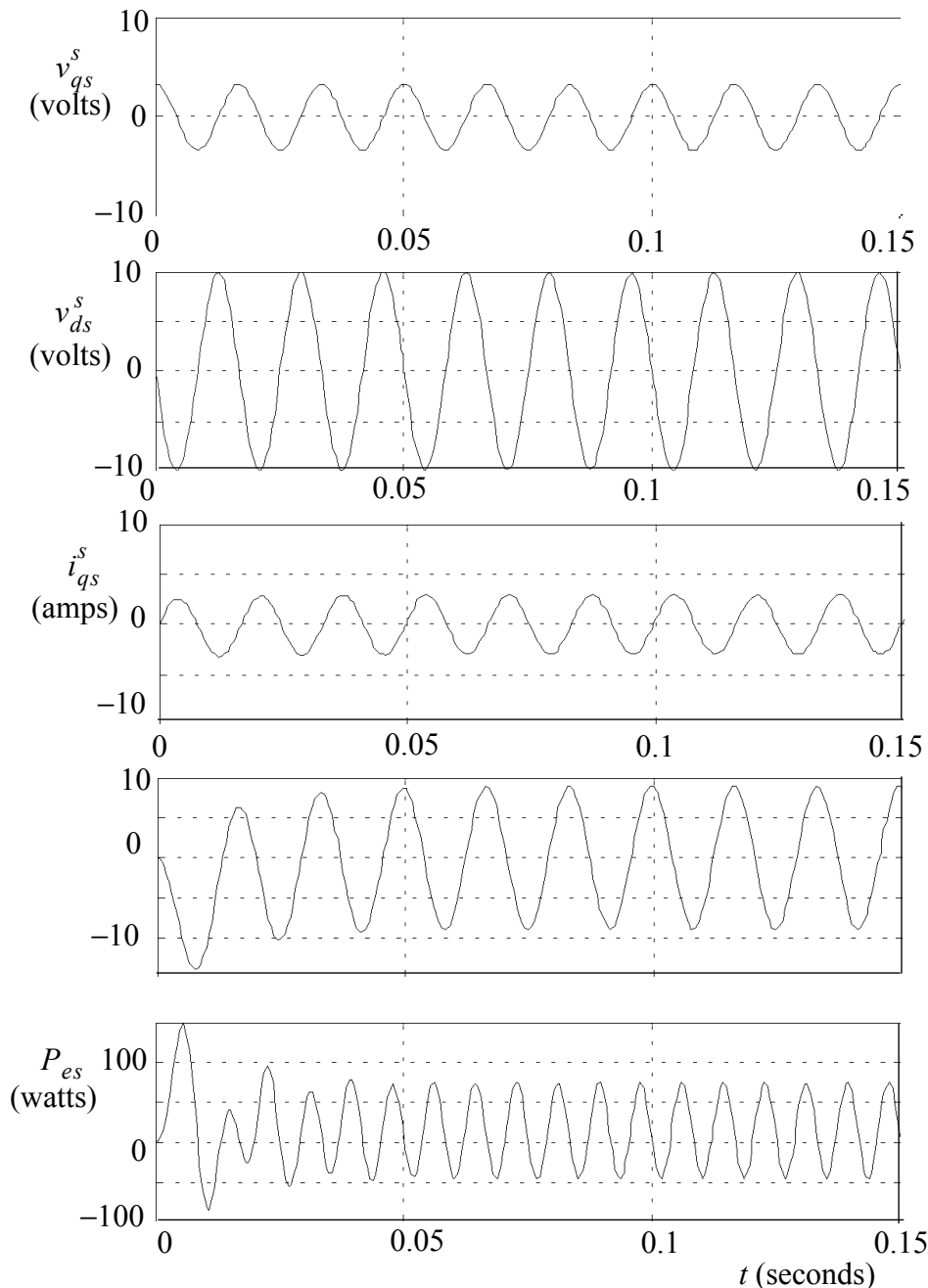


Figure 2.13 Components voltage vector \hat{v}_{qdns} and current vector \hat{i}_{qdns} in the stationary reference frame, $\omega = 0$.

and (2.134). The two constant amplitude voltage vectors rotating in opposite directions clearly add to produce an ellipse when both components are applied simultaneously. The positively and negatively rotating portions of the voltage vector rotate in the $d-q$ plane with constant magnitude at a uniform angular velocity ω_e . The corresponding current vectors also rotate in the $d-q$ plane with a constantly changing amplitude and angular velocity. Since the angular velocity of the negatively and positively rotating current vectors are not fixed, the speed of rotation has not been explicitly noted in [Figure 2.14](#). However, in the steady-state the two current vector components approach vectors of constant amplitude rotating at a constant angular velocity ω_e which also trace out circles in the $d-q$ plane.

In [Figure 2.17](#) the computer run has been repeated with the $d-q$ axes rotating about the n -axis at synchronous speed or $\omega = \omega_e$ (synchronously rotating reference frame). In this case the positive rotating components of the voltage and current vectors become stationary so that the ds , qs variables are constant. However, the negatively rotating vectors now appear to rotate relative to this reference frame at $2\omega_e$, since the vector and the reference frame are rotating relative to each other in opposite directions. [Figure 2.11](#) further illustrates this behavior. It can be observed that the positive rotating voltage vector is stationary and the positive rotating current vector becomes stationary in the steady-state. The negatively rotating vectors, however, in the steady-state rotate clockwise with constant amplitudes at twice synchronous speed. The net result is that the voltage vector containing both components traces out a circle offset from the origin. As a matter of interest, [Figure 2.17](#) shows how the voltage and current vectors appear at the intermediate speed of $\omega = \omega_e/2$. It is suggested that the reader attempt to sketch the path of the voltage vector for another reference frame speed, say $\omega = -\omega_e$ or $\omega = \omega_e/3$.

Although the emphasis in this chapter has centered primarily on the solution of sinusoidal sources, it is important to realize that the transformation to the arbitrary reference frame is valid regardless of the form of the source voltages. That is, the voltage for phase *as* could just as well have been a sine wave, phase *bs* a square wave, and phase *cs* a triangle wave all of different frequencies! If the currents in the $d-q-n$ coordinate system are obtained, then the result referred to the stationary frame, one would arrive at the same answer as if one solved the three networks directly.

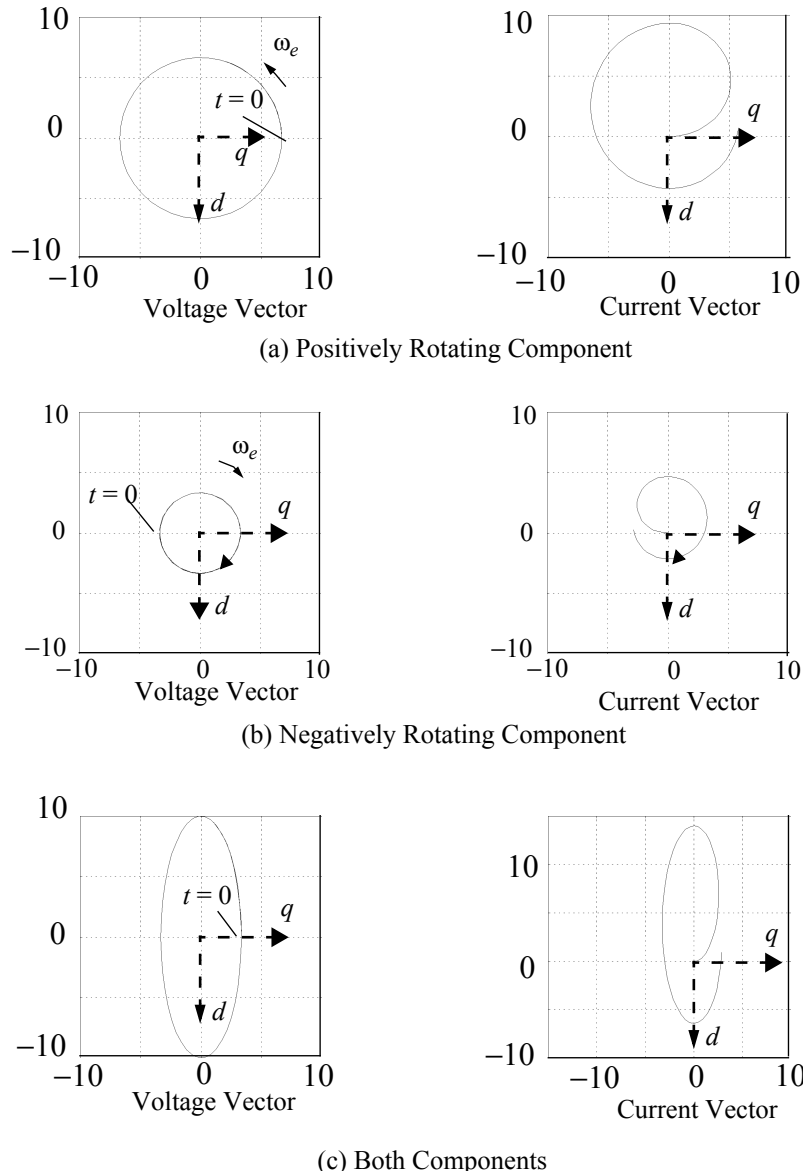


Figure 2.14 Voltage vector \hat{v}_{qdns} and current vector \hat{i}_{qdns} in the stationary reference frame, $\omega = 0$ for $0 < t < 0.02$ sec.

2.5 Matrix Approach to the $d-q-n$ Transformation

Although the derivation of the $d-q-n$ equivalent circuit using vector algebra went quite smoothly, when one encounters electric machinery, inductive coupling will occur between circuits. A considerable amount of algebraic manipu-

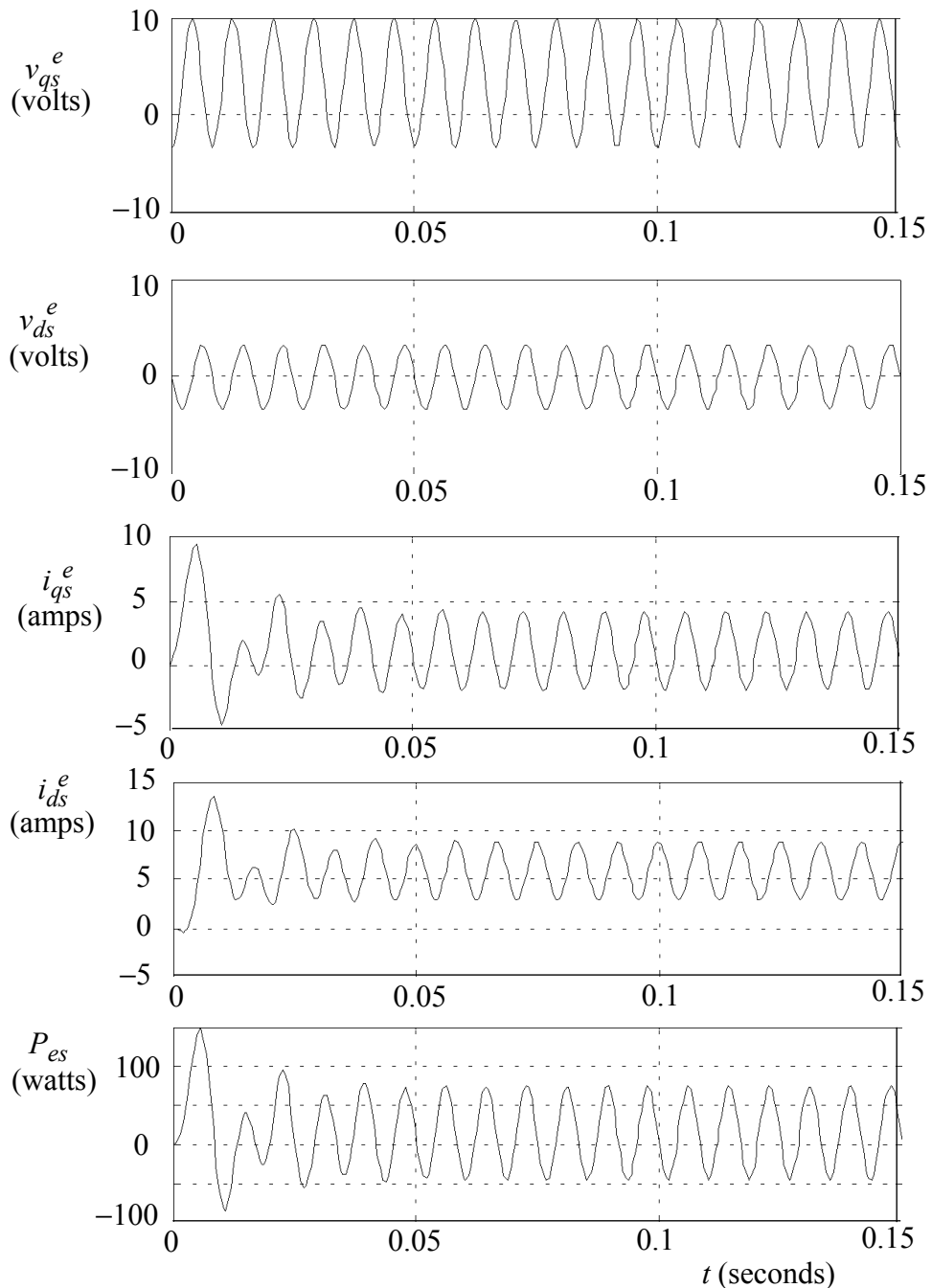


Figure 2.15 Response of three-phase electric system with unbalanced voltages viewed in the synchronously rotating reference frame, $\omega = \omega_e$

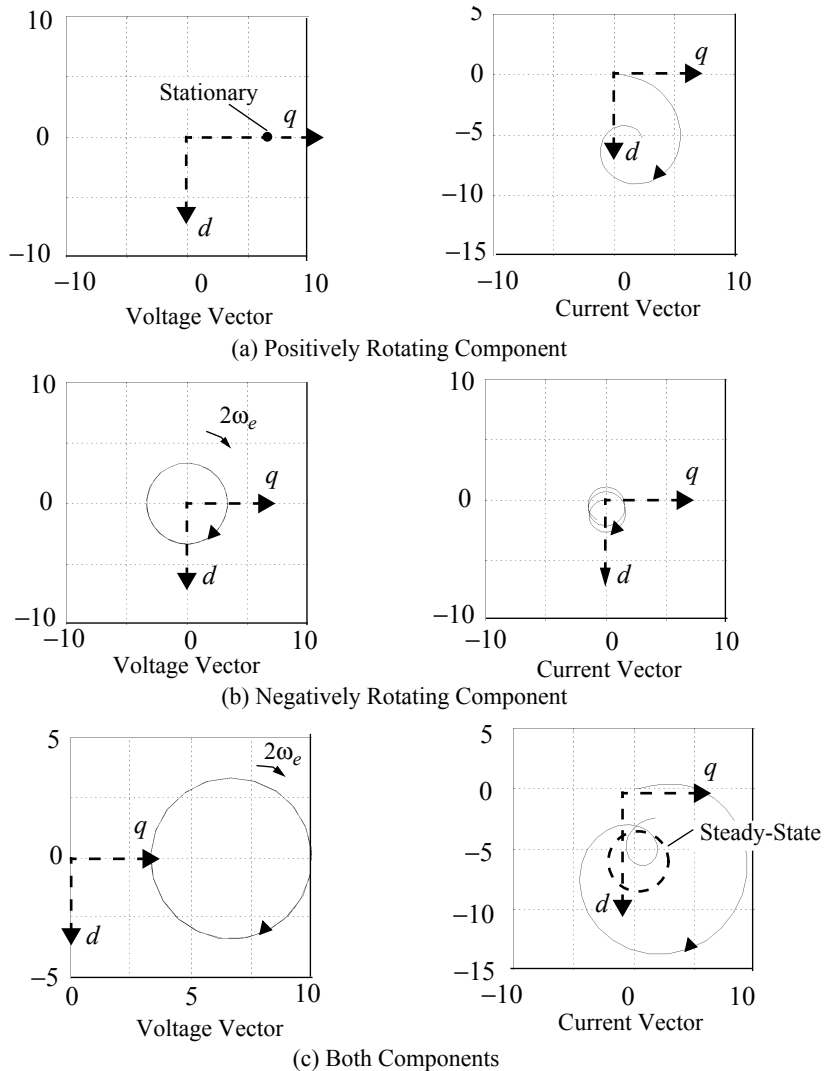


Figure 2.16 Voltage vector \hat{v}_{dqns} and current vector \hat{i}_{dqns} in a reference frame rotating at synchronous speed, $\omega = \omega_e$ for $0 < t < 0.02$ seconds.

lation will be necessary to convert the machine equations to a similar $d-q-n$ format. In order to pave the way for this task it is useful to adopt an equivalent matrix formulation. Define now the following three-element matrix vectors

$$\mathbf{f}_{abcs} = \begin{bmatrix} f_{as} \\ f_{bs} \\ f_{cs} \end{bmatrix} \quad (2.142)$$

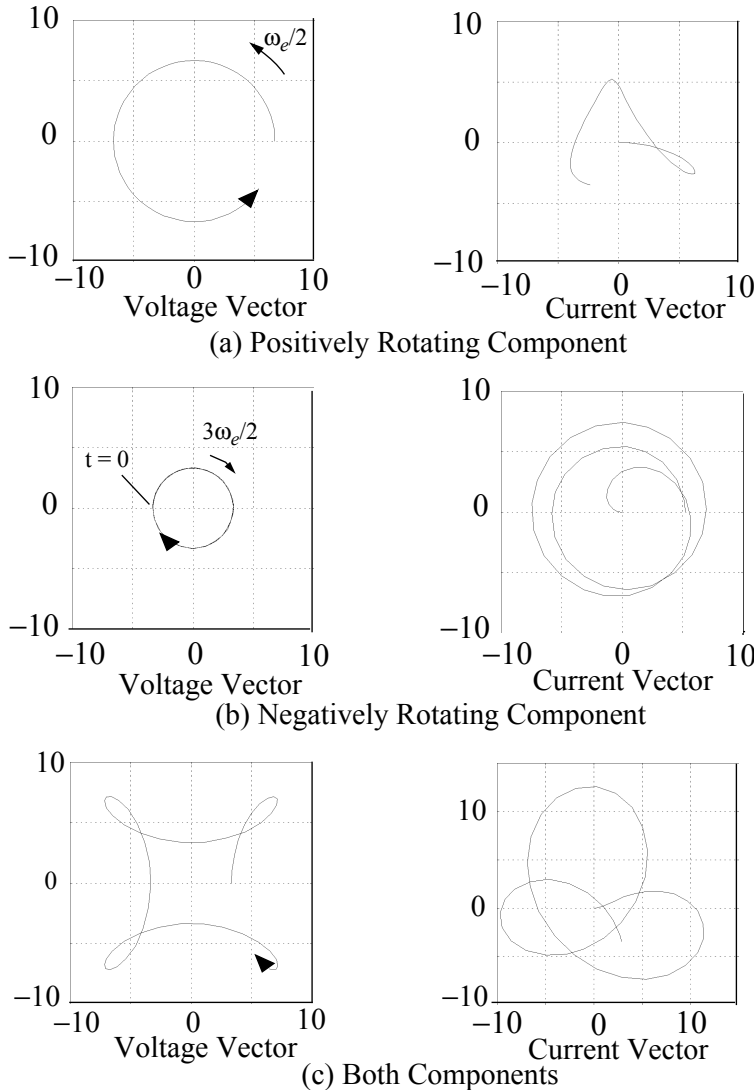


Figure 2.17 Voltage vector \hat{v}_{qdns} and current vector \hat{i}_{qdns} in a reference frame rotating at one-half synchronous speed, $\omega = \omega_e/2$ for $0 < t < 0.03$ seconds.

$$f_{dqns} = \begin{bmatrix} f_{ds} \\ f_{qs} \\ f_{ns} \end{bmatrix} \quad (2.143)$$

where “ f ” denotes either “ v ”, “ i ”, or “ λ ”. In matrix format, the voltage equations defining the balanced $r-L$ circuits of Figure 2.6 are

$$v_{abcs} = r_s i_{abcs} + L_s \frac{di_{abcs}}{dt} \quad (2.144)$$

Again r_s and L_s are simple scalar constants. In order to transform to the $d-q-n$ axes, the transformation equations expressed by Eqs. (2.58), (2.59), and (2.51)(2.60) must be expressed in matrix form. Let

$$f_{dqns} = T(\theta) f_{abcs} \quad (2.145)$$

where

$$T(\theta) = \frac{2}{3} \begin{bmatrix} \sin\theta & \sin\left(\theta - \frac{2\pi}{3}\right) & \sin\left(\theta + \frac{2\pi}{3}\right) \\ \cos\theta & \cos\left(\theta - \frac{2\pi}{3}\right) & \cos\left(\theta + \frac{2\pi}{3}\right) \\ \frac{1}{\sqrt{2}} & \frac{1}{\sqrt{2}} & \frac{1}{\sqrt{2}} \end{bmatrix} \quad (2.146)$$

and f denotes any three-phase quantity such as v , i , or λ (flux linkage).

Again the argument of the transformation matrix $T(\theta)$ will always again be denoted explicitly. As for the two-phase case, it can be shown that $T(\theta)$ has the following important properties.

$$1) T(\theta)^{-1} = \frac{3}{2} T(\theta)^t \quad (2.147)$$

$$2) T(\theta) \frac{dT(\theta)^{-1}}{dt} = \begin{bmatrix} 0 & -\omega & 0 \\ \omega & 0 & 0 \\ 0 & 0 & 0 \end{bmatrix} \equiv \omega \times \quad (2.148)$$

$$3) \frac{dT(\theta)}{dt} T(\theta)^{-1} \equiv -\omega \times \quad (2.149)$$

Note the appearance of the $3/2$ term in matrix identity #1 which results from the choice of the $\sqrt{3/2}$ scale factor between the as , bs , cs and ds , qs , ns variables. Because of this fact the transformation matrix T is not orthogonal.

Multiplying Eq. (2.144) by $T(\theta)$ and observing the definition of the voltage and current components in the $d-q-n$ reference frame from Eq. (2.145) yields

$$v_{dqns} = r_s i_{dqns} + L_s T(\theta) \frac{d}{dt} [T(\theta)^{-1} i_{dqns}] \quad (2.150)$$

Carrying out the differentiation of the last term results in

$$v_{dqns} = r_s i_{dqns} + L_s T(\theta) \frac{dT(\theta)^{-1}}{dt} i_{dqns} + L_s T(\theta) T(\theta)^{-1} \frac{di_{dqns}}{dt} \quad (2.151)$$

From the matrix property #2 above, Eq. (2.151) reduces to

$$v_{dqns} = r_s i_{dqns} + L_s \omega \times i_{dqns} + L_s \frac{di_{dqns}}{dt} \quad (2.152)$$

where $\omega = d\theta/dt$ and the matrix $\omega \times$ is defined by the matrix operation of Eq. (2.148).

It is apparent that although the three-phase case is potentially a considerably more complex problem, matrix analysis reduces the work to the same degree of difficulty as for a two-phase case. In fact, when the neutral component of voltage and current is zero, these equations reduce identically to their two-phase counterpart. In such cases the three-phase problem can be solved by finding the solution to a two-phase problem of reduced complexity.

Although only three-phase circuits have been investigated in this chapter, one could now extend this approach to any number of circuits. However, it would then be necessary to adopt the matrix approach entirely, since vector algebra is normally limited to three dimensions.

2.5.1 Example

As an example of how the matrix approach becomes extremely useful, consider the coupled magnetic circuit shown in Figure 2.18. These three windings

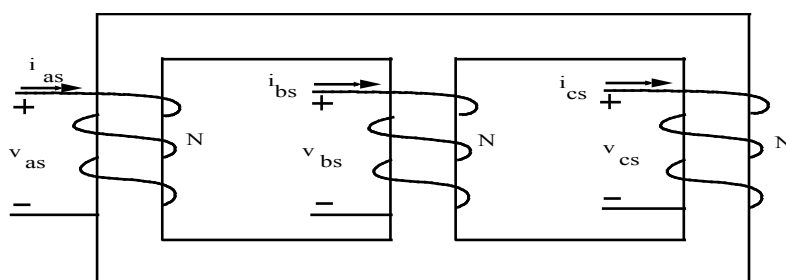


Figure 2.18 Three winding coupled magnetic circuit.

can be considered as the primary portion of a three-phase transformer. The three circuit equations are

$$v_{as} = i_{as}r_s + \frac{d\lambda_{as}}{dt} \quad (2.153)$$

$$v_{bs} = i_{bs}r_s + \frac{d\lambda_{bs}}{dt} \quad (2.154)$$

$$v_{cs} = i_{cs}r_s + \frac{d\lambda_{cs}}{dt} \quad (2.155)$$

Although the permeance of the magnetic path of the center leg is different from the outer two legs, it can be assumed to a first approximation that

$$\lambda_{as} = L_s i_{as} - L_m i_{bs} - L_m i_{cs} \quad (2.156)$$

$$\lambda_{bs} = -L_m i_{as} + L_s i_{bs} - L_m i_{cs} \quad (2.157)$$

$$\lambda_{cs} = -L_m i_{as} - L_m i_{bs} + L_s i_{cs} \quad (2.158)$$

Since all inductances are again constants, Eqs. (2.153) to (2.155) can be written in matrix form as

$$v_{abcs} = r_s i_{abcs} + L_s \frac{di_{abcs}}{dt} \quad (2.159)$$

where it is now necessary to define an inductance matrix L_s as

$$L_s = \begin{bmatrix} L_s & -L_m & -L_m \\ -L_m & L_s & -L_m \\ -L_m & -L_m & L_s \end{bmatrix} \quad (2.160)$$

Consider now a transformation of Eq. (2.159) to a stationary $d-q-n$ set of axes. Setting $\theta = 0$ in Eq. (2.146), the required transformation is

$$T(0) = \frac{2}{3} \begin{bmatrix} 0 & -\frac{\sqrt{3}}{2} & \frac{\sqrt{3}}{2} \\ 1 & -\frac{1}{2} & -\frac{1}{2} \\ \frac{1}{\sqrt{2}} & \frac{1}{\sqrt{2}} & \frac{1}{\sqrt{2}} \end{bmatrix} \quad (2.161)$$

whereby

$$T(0)^{-1} = \begin{bmatrix} 0 & 1 & \frac{1}{\sqrt{2}} \\ -\frac{\sqrt{3}}{2} & \frac{1}{2} & \frac{1}{\sqrt{2}} \\ \frac{\sqrt{3}}{2} & -\frac{1}{2} & \frac{1}{\sqrt{2}} \end{bmatrix} \quad (2.162)$$

The process of changing variables can be simplified if Eq. (2.159) is written in the form

$$v_{abcs} = r_s i_{abcs} + (L_s + L_m) I \frac{di_{abcs}}{dt} - L_m U \frac{di_{abcs}}{dt} \quad (2.163)$$

where U is a matrix filled with ones and is called the *unit matrix*. That is,

$$U = \begin{bmatrix} 1 & 1 & 1 \\ 1 & 1 & 1 \\ 1 & 1 & 1 \end{bmatrix} \quad (2.164)$$

Multiplying Eq. (2.163) by $T(0)$ and observing that it is not time dependent,

$$T(0)v_{abcs} = r_s T(0)i_{abcs} + (L_s + L_m) \frac{d}{dt}[T(0)i_{abcs}] - L_m T(0)U \frac{di_{abcs}}{dt} \quad (2.165)$$

Noting $T(0)v_{abcs} = v_{dqns}^s$ etc. one obtains

$$v_{dqns}^s = r_s i_{dqns}^s + (L_s + L_m) \frac{di_{dqns}^s}{dt} - L_m T(0)U T(0)^{-1} \frac{di_{dqns}^s}{dt} \quad (2.166)$$

where the superscript s has been added to the voltage and current variables to signify that the $d-q-n$ axes are *stationary*.

In order to reduce the last term of this equation, it can be shown without much difficulty that

$$T(0)U = \begin{bmatrix} 0 & 0 & 0 \\ 0 & 0 & 0 \\ \sqrt{2} & \sqrt{2} & \sqrt{2} \end{bmatrix} \quad (2.167)$$

and

$$[T(0)U]T(0)^{-1} = \begin{bmatrix} 0 & 0 & 0 \\ 0 & 0 & 0 \\ 0 & 0 & 3 \end{bmatrix} \quad (2.168)$$

Hence Eq. (2.166) reduces to

$$v_{dqns}^s = r_s i_{dqns}^s + L_{dqns} \frac{di_{dqns}^s}{dt} \quad (2.169)$$

wherein

$$L_{dqns} = \begin{bmatrix} L_s + L_m & 0 & 0 \\ 0 & L_s + L_m & 0 \\ 0 & 0 & L_s - 2L_m \end{bmatrix} \quad (2.170)$$

In scalar form, Eq. (2.169) is equivalent to the three equations

$$v_{ds}^s = r_s i_{qs}^s + (L_s + L_m) \frac{di_{ds}^s}{dt} \quad (2.171)$$

$$v_{qs}^s = r_s i_{qs}^s + (L_s + L_m) \frac{di_{qs}^s}{dt} \quad (2.172)$$

$$v_{ns}^s = r_s i_{ns}^s + (L_s - 2L_m) \frac{di_{ns}^s}{dt} \quad (2.173)$$

Clearly, by expressing the three-phase circuit of [Figure 2.18](#) in the *d-q-n* reference frame, it has been possible to simplify remarkably the complexity of the equations to be solved. Since the three circuits defined by Eqs. (2.171) to (2.173) are uncoupled, the *ds*, *qs*, *ns* currents can be solved without difficulty. The actual *as*, *bs*, *cs* currents are then readily reconstructed by inverting the transformation procedure.

Although it should again be mentioned that the use of rotating reference frames to formulate the solution of static networks is only rarely of practical interest, one case has been shown where a stationary *d-q-n* axes orientation has proven useful. This chapter has primarily served as a familiarization with the concept of rotating frames. This knowledge will prove indispensable in the future analysis of electric machinery. Before it is possible to commence with this analysis, one must be able to properly set down the differential equations which describe their behavior. In order to gain a deeper appreciation for these

equations which will serve as a springboard for an analysis of electrical machines, it is necessary to first turn attention to some of the details that go into the design of a rotating machine.

2.6 The d - q - n Transformation Applied to a Simple Three-Phase Cylindrical Inductor

It has already been demonstrated that the d - q - n transformation has utility beyond that of AC machine analysis. As a further example of the use of the d - q - n transformation, consider the inductances of the double cylindrical structure shown in [Figure 2.19](#). This device is assumed to have a three-phase set of concentrated windings placed symmetrically around the gap, each having N_t total turns. The device can be considered as a type of coupled three-phase inductor. When excitation windings (or magnets) are placed on the rotor, the device becomes a primitive type of AC machine.

The magnetizing inductances of the three windings have already been determined previously. They are

$$L_{am} = L_{bm} = L_{cm} = \frac{\mu_0 r l}{g} \int_0^{2\pi} \left(\frac{N_t}{2}\right)^2 d\phi \quad (2.174)$$

$$= \frac{\mu_0 r l}{g} N_s^2 \left(\frac{\pi}{2}\right) \quad (2.175)$$

It is useful to define this term as simply the magnetizing inductance L_m .

The mutual inductance between windings A and B is readily found by sketching the winding functions of the two windings and calculating their product. The mutual inductance is

$$L_{ab} = \mu_0 \frac{r l}{g} \int_0^{2\pi} N_a(\phi) N_b(\phi) d\phi \quad (2.176)$$

which can be readily evaluated by integrating over the portions of the winding function products that are piecewise constant:

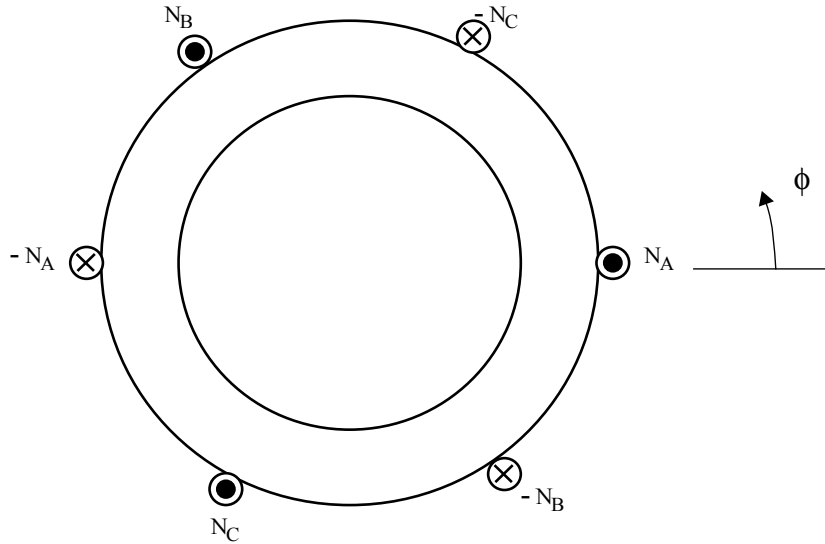


Figure 2.19 Three-phase cylindrical inductor with concentrated coils.

$$L_{ab} = \mu_0 \frac{rl}{g} \left[\int_0^{\frac{2\pi}{3}} \left(-\frac{N^2}{4} \right) d\phi + \int_{\frac{2\pi}{3}}^{\pi} \frac{N^2}{4} d\phi + \int_{\pi}^{\frac{5\pi}{3}} \left(-\frac{N^2}{4} \right) d\phi + \int_{\frac{5\pi}{3}}^{2\pi} \frac{N^2}{4} d\phi \right] \quad (2.177)$$

$$= \mu_0 \frac{rlN^2}{g} \left(-\frac{2\pi}{3} + \frac{\pi}{3} - \frac{2\pi}{3} + \frac{\pi}{3} \right) \quad (2.178)$$

$$= \mu_0 \frac{rl}{g} N^2 \left(-\frac{\pi}{6} \right) \quad (2.179)$$

$$= -\frac{1}{3} L_m \quad (2.180)$$

By symmetry it is evident that also

$$L_{bc} = L_{ca} = -\frac{1}{3} L_m \quad (2.181)$$

Because the mutual inductances between windings are not zero, solution for the currents which flow in this cylindrical inductor is again involved. Again it is interesting to consider what happens to this problem when a transformation is made to d - q - n components. In the physical set of axes, one has

$$v_{abc} = r_s i_{abcs} + \frac{d\lambda_{abcs}}{dt} \quad (2.182)$$

where

$$\lambda_{abcs} = L_s i_{abcs} \quad (2.183)$$

and where

$$L_s = \begin{bmatrix} L_{ls} + L_m & -\frac{1}{3}L_m & -\frac{1}{3}L_m \\ -\frac{1}{3}L_m & L_{ls} + L_m & -\frac{1}{3}L_m \\ -\frac{1}{3}L_m & -\frac{1}{3}L_m & L_{ls} + L_m \end{bmatrix} \quad (2.184)$$

When the voltage vector differential equation is transformed to a stationary reference frame (stationary d - q axes) exactly the same result will be obtained as developed previously. That is

$$v_{dqns}^s = r_s i_{dqns}^s + \frac{d\lambda_{dqns}^s}{dt} \quad (\omega = 0) \quad (2.185)$$

When the flux linkage equation is transformed the result is

$$\lambda_{dqns}^s = [T(0)L_s T(0)^{-1}] i_{dqns}^s \quad (2.186)$$

where

$$\lambda_{qns}^s = T(0)\lambda_{abcs} \quad (2.187)$$

$$i_{dqns}^s = T(0)i_{abcs} \quad (2.188)$$

and

$$T(0) = \begin{bmatrix} 0 & -\frac{1}{\sqrt{3}} & \frac{1}{\sqrt{3}} \\ \frac{2}{3} & -\frac{1}{3} & -\frac{1}{3} \\ \frac{\sqrt{2}}{3} & \frac{\sqrt{2}}{3} & \frac{\sqrt{2}}{3} \end{bmatrix} \quad (2.189)$$

It is necessary to now reduce the curly bracketed expression of the transformed flux linkage equation. Upon expanding the coefficient of i_{dqns}^s in Eq. (2.186), one obtains, in progressive steps

$$\begin{aligned} & T(0)L_s T(0)^{-1} \\ &= \begin{bmatrix} 0 & -\frac{1}{\sqrt{3}} & \frac{1}{\sqrt{3}} \\ \frac{2}{3} & -\frac{1}{3} & -\frac{1}{3} \\ \frac{\sqrt{2}}{3} & \frac{\sqrt{2}}{3} & \frac{\sqrt{2}}{3} \end{bmatrix} \begin{bmatrix} L_{ls} + L_m & -\frac{L_m}{3} & -\frac{L_m}{3} \\ -\frac{L_m}{3} & L_{ls} + L_m & -\frac{L_m}{3} \\ -\frac{L_m}{3} & -\frac{L_m}{3} & L_{ls} + L_m \end{bmatrix} \times \begin{bmatrix} 0 & 1 & \frac{1}{\sqrt{2}} \\ -\frac{\sqrt{3}}{2} & -\frac{1}{2} & \frac{1}{\sqrt{2}} \\ \frac{\sqrt{3}}{2} & -\frac{1}{2} & \frac{1}{\sqrt{2}} \end{bmatrix} \end{aligned} \quad (2.190)$$

$$= \begin{bmatrix} 0 & -\frac{1}{\sqrt{3}}L_{ls} - \frac{4}{3\sqrt{3}}L_m & \frac{1}{\sqrt{3}}L_{ls} + \frac{4}{3\sqrt{3}}L_m \\ \frac{2}{3}L_{ls} + \frac{8}{9}L_m & -\frac{1}{3}L_{ls} - \frac{4}{9}L_m & -\frac{1}{3}L_{ls} - \frac{4}{9}L_m \\ \frac{\sqrt{2}}{3}L_{ls} + \frac{1}{3}L_m & \frac{\sqrt{2}}{3}L_{ls} + \frac{1}{3}L_m & \frac{\sqrt{2}}{3}L_{ls} + \frac{1}{3}L_m \end{bmatrix} \times \begin{bmatrix} 0 & 1 & \frac{1}{\sqrt{2}} \\ -\frac{\sqrt{3}}{2} & -\frac{1}{2} & \frac{1}{\sqrt{2}} \\ \frac{\sqrt{3}}{2} & -\frac{1}{2} & \frac{1}{\sqrt{2}} \end{bmatrix} \quad (2.191)$$

$$= \begin{bmatrix} L_{ls} + \frac{4}{3}L_m & 0 & 0 \\ 0 & L_{ls} + \frac{4}{3}L_m & 0 \\ 0 & 0 & L_{ls} + \frac{1}{3}L_m \end{bmatrix} \quad (2.192)$$

Again one has arrived at a decoupled network so that the equations to be solved for this network become simply

$$v_{ds}^s = r_s i_{ds}^s + \left(L_{ls} + \frac{4}{3} L_m \right) \frac{di_{ds}^s}{dt} \quad (2.193)$$

$$v_{qs}^s = r_s i_{qs}^s + \left(L_{ls} + \frac{4}{3} L_m \right) \frac{di_{qs}^s}{dt} \quad (2.194)$$

$$v_{ns}^s = r_s i_{ns}^s + \left(L_{ls} + \frac{1}{3} L_m \right) \frac{di_{ns}^s}{dt} \quad (2.195)$$

where

$$L_m = \mu_0 \frac{rl}{g} N_t^2 \left(\frac{\pi}{2} \right) \quad (2.196)$$

The physical circuit in which physical voltages are impressed on physical circuits having resistances and inductances has again been transformed to an equivalent network in which equivalent voltages are impressed on equivalent circuits having equivalent resistances and inductances. In doing so it has been possible to achieve a decoupling between the three circuits in the equivalent network. Unfortunately, the process of reducing the transformed inductance matrix $T(\theta)L_sT(\theta)^{-1}$ has been rather tedious.

It has already been shown in Chapter 1 that the physical inductances can be calculated from winding functions which describe the physical placement of the windings through which flow the physical phase currents. The winding functions are used to calculate the physical winding inductances. It is useful to question whether there perhaps exist equivalent windings through which flow the equivalent *d-q-n* currents. The inductances corresponding to the *d-q-n* currents could then be computed directly. The next section will show that such equivalent winding functions do indeed exist.

2.7 Winding Functions in a *d-q-n* Reference Frame

Consider again the simple three-phase cylindrical inductor. In the physical coordinate system the flux linkages are related to the currents in the windings by

$$\lambda_{abcs} = (L_{ls}I + L_{ms})i_{abcs} \quad (2.197)$$

where L_{ls} represents the leakage component of inductance, which is assumed the same for all three windings, and I is the identity matrix. The matrix L_{ms} which describes the air gap components of flux linkage has the form

$$L_{ms} = \begin{bmatrix} L_{aa} & L_{ab} & L_{ac} \\ L_{ab} & L_{bb} & L_{bc} \\ L_{ac} & L_{bc} & L_{cc} \end{bmatrix} \quad (2.198)$$

Upon transforming this equation to general rotating d - q - n axes, one has

$$T(\theta)\lambda_{abcs} = [L_{ls}T(\theta)IT(\theta)^{-1} + T(\theta)L_{ms}T(\theta)^{-1}]T(\theta)i_{abcs} \quad (2.199)$$

or

$$\lambda_{dqns} = \{L_{ls}I + [T(\theta)L_{ms}T(\theta)^{-1}]\}i_{dqns} \quad (2.200)$$

It is instructive to consider the second term of this expression in more detail. Recall that in terms of winding functions the inductances L_{aa} , L_{ab} , ..., L_{cc} are defined by

$$L_{aa} = \mu_0 \frac{rl}{g} \int_0^{2\pi} N_a^2(\phi) d\phi \quad (2.201)$$

$$L_{ab} = \mu_0 \frac{rl}{g} \int_0^{2\pi} N_a(\phi)N_b(\phi) d\phi \quad (2.202)$$

•

•

$$L_{cc} = \mu_0 \frac{rl}{g} \int_0^{2\pi} N_c^2(\phi) d\phi \quad (2.203)$$

Hence, the second term in the flux linkage expression, Eq. (2.200), may be written as

$$T(\theta)L_{ms}T(\theta)^{-1} =$$

$$T(\theta) \begin{bmatrix} \mu_0 \frac{rl}{g} \int\limits_0^{2\pi} N_a^2(\phi) d\phi & \mu_0 \frac{rl}{g} \int\limits_0^{2\pi} N_a(\phi) N_b(\phi) d\phi & \mu_0 \frac{rl}{g} \int\limits_0^{2\pi} N_a(\phi) N_c(\phi) d\phi \\ \mu_0 \frac{rl}{g} \int\limits_0^{2\pi} N_a(\phi) N_b(\phi) d\phi & \mu_0 \frac{rl}{g} \int\limits_0^{2\pi} N_b^2(\phi) d\phi & \mu_0 \frac{rl}{g} \int\limits_0^{2\pi} N_b(\phi) N_c(\phi) d\phi \\ \mu_0 \frac{rl}{g} \int\limits_0^{2\pi} N_a(\phi) N_c(\phi) d\phi & \mu_0 \frac{rl}{g} \int\limits_0^{2\pi} N_b(\phi) N_c(\phi) d\phi & \mu_0 \frac{rl}{g} \int\limits_0^{2\pi} N_c^2(\phi) d\phi \end{bmatrix} T(\theta)^{-1}$$
(2.204)

Since the operations on the angles θ and ϕ are independent they can be interchanged in which case it is possible to first integrate and then operate with the transformation matrix $T(\theta)$. This expression can also be written as

$$T(\theta)L_{ms}T(\theta)^{-1} = \mu_0 \frac{rl}{g} \int\limits_0^{2\pi} T(\theta) \begin{bmatrix} N_a^2(\phi) & N_a(\phi)N_b(\phi) & N_a(\phi)N_c(\phi) \\ N_a(\phi)N_b(\phi) & N_b^2(\phi) & N_b(\phi)N_c(\phi) \\ N_a(\phi)N_c(\phi) & N_b(\phi)N_c(\phi) & N_c^2(\phi) \end{bmatrix} T(\theta)^{-1} d\phi$$
(2.205)

This expression can be arranged in the form

$$T(\theta)L_{ms}T(\theta)^{-1} =$$

$$\mu_0 \frac{rl}{g} \int\limits_0^{2\pi} \left\{ T(\theta) \begin{bmatrix} N_a(\phi) & N_a(\phi) & N_a(\phi) \\ N_b(\phi) & N_b(\phi) & N_b(\phi) \\ N_c(\phi) & N_c(\phi) & N_c(\phi) \end{bmatrix} \times \begin{bmatrix} N_a(\phi) & 0 & 0 \\ 0 & N_b(\phi) & 0 \\ 0 & 0 & N_c(\phi) \end{bmatrix} T(\theta)^{-1} \right\} d\phi$$
(2.206)

However,

$$\begin{aligned}
T(\theta) \begin{bmatrix} N_a(\phi) & N_a(\phi) & N_a(\phi) \\ N_b(\phi) & N_b(\phi) & N_b(\phi) \\ N_c(\phi) & N_c(\phi) & N_c(\phi) \end{bmatrix} = \\
\frac{2}{3} \begin{bmatrix} \sin\theta & \sin\left(\theta - \frac{2\pi}{3}\right) & \sin\left(\theta + \frac{2\pi}{3}\right) \\ \cos\theta & \cos\left(\theta - \frac{2\pi}{3}\right) & \cos\left(\theta + \frac{2\pi}{3}\right) \\ \frac{1}{(\sqrt{2})} & \frac{1}{\sqrt{2}} & \frac{1}{\sqrt{2}} \end{bmatrix} \times \begin{bmatrix} N_a(\phi) & N_a(\phi) & N_a(\phi) \\ N_b(\phi) & N_b(\phi) & N_b(\phi) \\ N_c(\phi) & N_c(\phi) & N_c(\phi) \end{bmatrix}
\end{aligned} \tag{2.207}$$

Multiplication of these two matrices results in an equation of the form

$$\begin{bmatrix} a & a & a \\ b & b & b \\ c & c & c \end{bmatrix} \tag{2.208}$$

where

$$\begin{aligned}
a &= \frac{2}{3} \left[N_a(\phi) \sin(\theta) + N_b(\phi) \sin\left(\theta - \frac{2\pi}{3}\right) + N_c(\phi) \sin\left(\theta + \frac{2\pi}{3}\right) \right] \\
b &= \frac{2}{3} \left[N_a(\phi) \cos(\theta) + N_b(\phi) \cos\left(\theta - \frac{2\pi}{3}\right) + N_c(\phi) \cos\left(\theta + \frac{2\pi}{3}\right) \right] \\
c &= \frac{\sqrt{2}}{3} [N_a(\phi) + N_b(\phi) + N_c(\phi)]
\end{aligned}$$

Note the strong resemblance of the elements a , b , c , in this matrix expression to the definition of the $d-q-n$ variables, Eqs. (2.58) to (2.60). Indeed, it is logical to define

$$N_d(\phi) = a = \frac{2}{3} \left[N_a(\phi) \sin(\theta) + N_b(\phi) \sin\left(\theta - \frac{2\pi}{3}\right) + N_c(\phi) \sin\left(\theta + \frac{2\pi}{3}\right) \right] \tag{2.209}$$

$$N_q(\phi) = b = \frac{2}{3} \left[N_a(\phi) \cos(\theta) + N_b(\phi) \cos\left(\theta - \frac{2\pi}{3}\right) + N_c(\phi) \cos\left(\theta + \frac{2\pi}{3}\right) \right] \quad (2.210)$$

$$N_n(\phi) = c = \frac{\sqrt{2}}{3} [N_a(\phi) + N_b(\phi) + N_c(\phi)] \quad (2.211)$$

The expression for the entire inductance matrix then becomes

$$T(\theta) L_{ms} T(\theta)^{-1} =$$

$$\mu_0 \frac{rl}{g} \int_0^{2\pi} \begin{bmatrix} N_d(\phi) & N_d(\phi) & N_d(\phi) \\ N_q(\phi) & N_q(\phi) & N_q(\phi) \\ N_n(\phi) & N_n(\phi) & N_n(\phi) \end{bmatrix} \times \begin{bmatrix} N_a(\phi) & 0 & 0 \\ 0 & N_b(\phi) & 0 \\ 0 & 0 & N_c(\phi) \end{bmatrix} \times \begin{bmatrix} \sin\theta & \cos\theta & \frac{1}{\sqrt{2}} \\ \sin\left(\theta - \frac{2\pi}{3}\right) & \cos\left(\theta - \frac{2\pi}{3}\right) & \frac{1}{\sqrt{2}} \\ \sin\left(\theta + \frac{2\pi}{3}\right) & \cos\left(\theta + \frac{2\pi}{3}\right) & \frac{1}{\sqrt{2}} \end{bmatrix} \quad (2.212)$$

$$= \mu_0 \frac{rl}{g} \int_0^{2\pi} \begin{bmatrix} N_d(\phi) N_a(\phi) & N_d(\phi) N_b(\phi) & N_d(\phi) N_c(\phi) \\ N_q(\phi) N_a(\phi) & N_q(\phi) N_b(\phi) & N_q(\phi) N_c(\phi) \\ N_n(\phi) N_a(\phi) & N_n(\phi) N_b(\phi) & N_n(\phi) N_c(\phi) \end{bmatrix} \times \begin{bmatrix} \sin\theta & \cos\theta & \frac{1}{\sqrt{2}} \\ \sin\left(\theta - \frac{2\pi}{3}\right) & \cos\left(\theta - \frac{2\pi}{3}\right) & \frac{1}{\sqrt{2}} \\ \sin\left(\theta + \frac{2\pi}{3}\right) & \cos\left(\theta + \frac{2\pi}{3}\right) & \frac{1}{\sqrt{2}} \end{bmatrix} d\phi \quad (2.213)$$

$$= \mu_0 \frac{rl}{g} \int_0^{2\pi} \begin{bmatrix} N_d(\phi) \left[N_a(\phi) \sin\theta + N_b(\phi) \sin\left(\theta - \frac{2\pi}{3}\right) + N_c(\phi) \sin\left(\theta + \frac{2\pi}{3}\right) \right] \\ N_q(\phi) \left[N_a(\phi) \sin\theta + N_b(\phi) \sin\left(\theta - \frac{2\pi}{3}\right) + N_c(\phi) \sin\left(\theta + \frac{2\pi}{3}\right) \right] \\ N_n(\phi) \left[N_a(\phi) \sin\theta + N_b(\phi) \sin\left(\theta - \frac{2\pi}{3}\right) + N_c(\phi) \sin\left(\theta + \frac{2\pi}{3}\right) \right] \end{bmatrix}$$

(1st column)

$$\begin{aligned}
& N_d(\phi) \left[N_a(\phi) \cos \theta + N_b(\phi) \cos \left(\theta - \frac{2\pi}{3} \right) + N_c(\phi) \cos \left(\theta + \frac{2\pi}{3} \right) \right] \\
& N_q(\phi) \left[N_a(\phi) \cos \theta + N_b(\phi) \cos \left(\theta - \frac{2\pi}{3} \right) + N_c(\phi) \cos \left(\theta + \frac{2\pi}{3} \right) \right] \\
& N_n(\phi) \left[N_a(\phi) \cos \theta + N_b(\phi) \cos \left(\theta - \frac{2\pi}{3} \right) + N_c(\phi) \cos \left(\theta + \frac{2\pi}{3} \right) \right] \\
& \quad (2\text{nd column}) \\
& \left. \begin{aligned}
& N_d(\phi) \frac{[N_a(\phi) + N_b(\phi) + N_c(\phi)]}{\sqrt{2}} \\
& N_q(\phi) \frac{[N_a(\phi) + N_b(\phi) + N_c(\phi)]}{\sqrt{2}} \\
& N_n(\phi) \frac{[N_a(\phi) + N_b(\phi) + N_c(\phi)]}{\sqrt{2}}
\end{aligned} \right] d\phi \\
& \quad (3\text{rd column}) \tag{2.214}
\end{aligned}$$

The inductance matrix becomes, finally, using the already defined expressions for $N_d(\phi)$, $N_q(\phi)$, and $N_n(\phi)$

$$T(\theta) L_{ms} T(\theta)^{-1} = \mu_0 \frac{rl}{g} \int_0^{2\pi} \left(\frac{3}{2} \right) \begin{bmatrix} N_d(\phi)^2 & N_d(\phi)N_q(\phi) & N_d(\phi)N_n(\phi) \\ N_d(\phi)N_q(\phi) & N_q(\phi)^2 & N_q(\phi)N_n(\phi) \\ N_d(\phi)N_n(\phi) & N_q(\phi)N_n(\phi) & N_n(\phi)^2 \end{bmatrix} d\phi \tag{2.215}$$

It now becomes apparent that one is now in a position to calculate the $d-q-n$ inductances directly. That is, it is possible to now let

$$T(\theta) L_{ms} T(\theta)^{-1} = \begin{bmatrix} L_{dd} & L_{dq} & L_{dn} \\ L_{dq} & L_{qq} & L_{qn} \\ L_{dn} & L_{qn} & L_{nn} \end{bmatrix} \tag{2.216}$$

where the self and mutual inductances in the $d-q-n$ plane are defined by

$$L_{dd} = \left(\frac{3}{2} \right) \mu_0 \frac{rl}{g} \int_0^{2\pi} N_d^2(\phi) d\phi \tag{2.217}$$

$$\begin{aligned}
 L_{dq} &= \left(\frac{3}{2}\right)\mu_0 \frac{rl}{g} \int_0^{2\pi} N_d(\phi)N_q(\phi)d\phi \\
 &\bullet \\
 &\bullet \\
 L_{nn} &= \left(\frac{3}{2}\right)\mu_0 \frac{rl}{g} \int_0^{2\pi} N_n^2(\phi)d\phi
 \end{aligned} \tag{2.218}$$

Note that while the inductances remain defined in rotating orthogonal axes, no simplification can be guaranteed unless certain symmetry exists between the physical windings. It is left to the student to verify that this concept remains valid for salient-pole geometries in which the gap is also a function of the angle ϕ . The use of the above equations to calculate the motor inductances in the d - q - n axes directly is an important concept which will enable the avoidance of considerable labor when the time comes to analyze AC machines.

2.8 Direct Computation of d - q - n Inductances of a Cylindrical Three-Phase Inductor

In order to illustrate the method by which inductances in a d - q - n frame of reference can be computed directly, it is useful to return to the simple three-phase reactor problem. In a stationary d - q - n reference frame, the d - q - n winding functions are related to the physical a - b - c winding functions by

$$N_q^s(\phi) = \frac{2}{3}N_a(\phi) - \frac{1}{3}N_b(\phi) - \frac{1}{3}N_c(\phi) \tag{2.219}$$

$$N_d^s(\phi) = \frac{1}{\sqrt{3}}[N_c(\phi) - N_b(\phi)] \tag{2.220}$$

$$N_n^s(\phi) = \frac{\sqrt{2}}{3}[N_a(\phi) + N_b(\phi) + N_c(\phi)] \tag{2.221}$$

where θ has been set equal to zero in the general expressions derived previously. The non-transformed and corresponding transformed winding functions are sketched in [Figure 2.20](#).

Utilizing this figure as an aid, the d -axis magnetizing inductance is readily computed to be

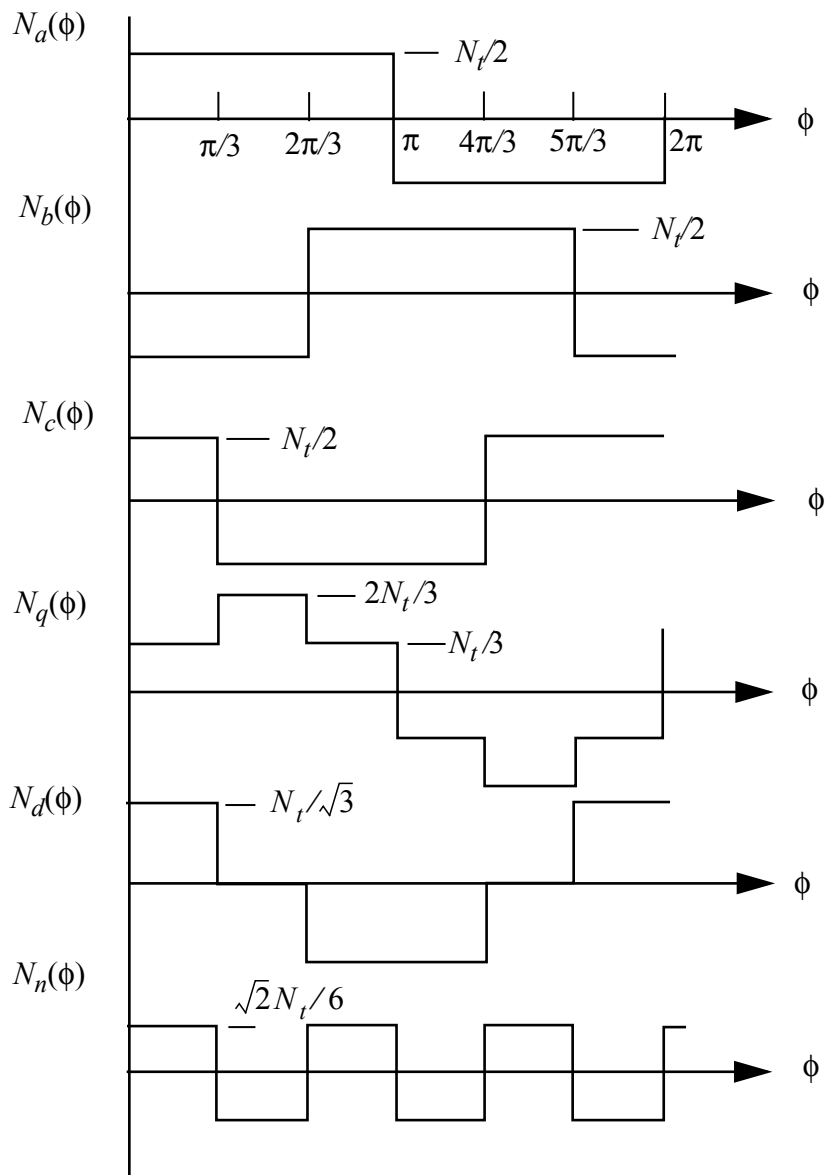


Figure 2.20 Actual and equivalent winding functions for cylindrical inductors.

$$L_{dd} = \mu_0 \left(\frac{rl}{g} \right) \left(\frac{3}{2} \right) (2) \int_{-\pi/3}^{\pi/3} \left(\frac{N_t}{\sqrt{3}} \right)^2 d\phi \quad (2.222)$$

$$= \mu_0 \left(\frac{rl}{g}\right) \left(\frac{3}{2}\right) (2)(N_t)^2 \left(\frac{2\pi}{9}\right) \quad (2.223)$$

$$= \mu_0 \frac{rl}{g} N_t^2 \left(\frac{2\pi}{3}\right) = L_{qq} = \left(\frac{4}{3}\right) L_m \quad (2.224)$$

Similarly,

$$L_{qq} = \mu_0 \frac{rl}{g} \left(\frac{3}{2}\right) (2) \left[\int_0^{\frac{\pi}{3}} \left(\frac{N_t}{3}\right)^2 d\phi + \int_{\frac{\pi}{3}}^{\frac{2\pi}{3}} \left(\frac{2N_t}{3}\right)^2 d\phi + \int_{\frac{2\pi}{3}}^{\pi} \left(\frac{N_t}{3}\right)^2 d\phi \right] \quad (2.225)$$

$$= \mu_0 \frac{rl}{g} (3) \left[\left(\frac{\pi}{27}\right) + \left(\frac{4\pi}{27}\right) + \left(\frac{\pi}{27}\right) \right] N_t^2 \quad (2.226)$$

$$= \mu_0 \frac{rl}{g} N_t^2 \left(\frac{2\pi}{3}\right) = \frac{4}{3} L_m \quad (2.227)$$

Finally,

$$L_{nn} = \mu_0 \frac{rl}{g} \left(\frac{3}{2}\right) (6) \int_0^{\frac{\pi}{3}} \left(\frac{\sqrt{2}N_t}{6}\right)^2 d\phi \quad (2.228)$$

$$= \mu_0 \frac{rl}{g} \left(\frac{3}{2}\right) (6) \left(\frac{\pi}{54}\right) N_t^2 \quad (2.229)$$

$$= \mu_0 \frac{rl}{g} N_t^2 \left(\frac{\pi}{6}\right) = \frac{L_m}{3} \quad (2.230)$$

By reference to the figure illustrating the winding functions, it is easy to see that

$$L_{dq} = \mu_0 \frac{rl}{g} \int_0^{\frac{2\pi}{3}} \frac{3}{2} N_d(\phi) N_q(\phi) d\phi = 0 \quad (2.231)$$

$$L_{dn} = \mu_0 \frac{rl}{g} \int_0^{\frac{2\pi}{3}} \frac{3}{2} N_d(\phi) N_n(\phi) d\phi = 0 \quad (2.232)$$

$$L_{qn} = \mu_0 \frac{rl}{g} \int_0^{2\pi} \frac{3}{2} N_q(\phi) N_n(\phi) d\phi = 0 \quad (2.233)$$

The approach of calculating the $d-q-n$ inductances is clearly much more straightforward than first calculating the $a-b-c$ inductances (which takes the same amount of effort) and then referring the inductances to the $d-q$ plane. This technique will be put to good use in the next chapter when it is finally time to tackle the analysis of synchronous machines.

2.9 Conclusion

This chapter has developed a systematic means for calculating the inductances of synchronous machines based on the concept of winding functions. In more traditional treatments of this subject, only the inductances associated with the physical $a-b-c$ (phase variable) circuits are computed. The inductances associated with a representation in a $d-q$ plane are then obtained by a series of complicated trigonometric manipulations. In this presentation, the concept of winding functions has been extended to include their representation in the $d-q$ plane. Hence, the needed inductances for proper representation of the machine in the $d-q$ plane can be directly calculated and these trigonometric complications avoided. The stage has now been set for the derivation of the defining differential equations of the synchronous machine, Park's equations, which will be the subject of the next chapter.

2.10 References

- [1] H. Goldstein, "Classical Mechanics," Addison-Wesley Publ. Co, Boston MA, 1959.
- [2] P.C. Krause and C.H. Thomas, "Simulation of Symmetrical Induction Machinery," *IEEE Trans. on Power Apparatus and Systems*, vol. PAS-84, November 1965, pp. 1025-1037.
- [3] C.L. Fortescue, "Method of Symmetrical Co-ordinates Applied to the Solution of Polyphase Networks," *Proc. 34th Ann. Conv. of AIEE*, 1918, pp. 1027.

- [4] R.H. Park, “Two-Reaction Theory of Synchronous Machines, Generalized Method of Analysis - Part I,” *Trans. of the AIEE*, 1929, pp. 716–730.

Chapter 3

The $d-q$ Equations of a Synchronous Machine

3.1 Introduction

The winding function approach to inductance computation of Chapter 1 combined with the concept of a three dimensional Cartesian space of Chapter 2 forms the essential building blocks for the analysis of any AC electrical machine. It is now time to put these concepts to work by developing the model of a synchronous machine, the so-called Park's model.

3.2 Physical Description

A synchronous machine consists essentially of two elements, first an element to produce a rotating magnetic field and a second element to couple with the field and rotate relative to the first and thereby produce electromechanical energy conversion. For constructional reasons the first element, which produces the magnetic field, is usually wound on the rotor and is called the *field winding*. The second element which couples with the field winding is wound in slots on the stator and is called the *armature winding*. The armature winding is typically but not always wound as a three-phase “wye” winding. When used as a generator the neutral of the wye is usually grounded, frequently through a reactor, which is used to limit certain types of fault currents and over voltages. Hence, a zero sequence or “neutral axis” current can flow. The armature coils are inserted in slots and the distribution of the coils arranged to approximate a sinusoidal distribution of conductors for each phase (sinusoidal winding function).

The rotor can be configured in two distinct styles called “round-rotor” construction and “salient-pole” construction. The round rotor shape, shown in [Figure 3.1](#), is used primarily for high speed turbo generators and is usually either a two-pole or four-pole construction. The field winding of the round-rotor machine is imbedded in slots similar to the armature winding. However, in this

case the winding is not sinusoidally distributed but arranged to produce a trapezoidal *MMF* distribution (trapezoidal winding function).

Nearly all synchronous motors and slower speed generators utilize the salient-pole construction illustrated in [Figure 3.2](#). Salient-pole machines also have the symmetric polyphase set of stator windings as for the round-rotor machine. The field winding, however, is formed by winding concentrated coils around projecting or salient rotor poles. The air gap between the stator and rotor is non-uniform. In effect, the *MMF* distribution (or winding function) set up by the field winding is quasi-rectangular (as in Table 1.1(b)). Additional rotor windings (amortisseur windings) are often used with salient-pole machines and less frequently with round-rotor machines. These windings take the form of bars which are inserted along the periphery of the rotor poles. The bars are shorted by means of end rings in much the same manner as for squirrel cage induction machines. The short-circuiting end ring can be continuous or interrupted, as shown in [Figure 3.3](#).

3.3 Synchronous Machine Equations in the Phase Variable or *as*-, *bs*-, *cs*- Reference Frame

After the introductory Chapters 1 and 2, one is now in a position to calculate the inductances of a synchronous machine in some detail. It is convenient for this purpose to consider the idealized salient two-pole synchronous machine shown in [Figure 3.4](#). In this figure only an equivalent full pitch turn is shown in order to locate the magnetic axes of each winding. Note that the stator is assumed to be wound in symmetric three-phase fashion such that the magnetic axes of the three stator windings are mutually displaced by 120° . The rotor is arranged effectively in a “two-phase” configuration whereas the stator is a three-phase connection. The magnetic axes for each winding are chosen such that the *MMF* is assumed to be positive when directed across the gap from rotor to stator. The equivalent rotor phase winding, qr is assumed to be displaced, in general, with respect to the reference *as*-axis by the electrical angle θ_r . Note that the reference axis for the spatial angle ϕ is also taken with respect to the *as*-axis.

In this analysis the following assumptions will be made:

1. The stator inner periphery has a uniform radius (i.e., the radius is not a function of position around the air gap).

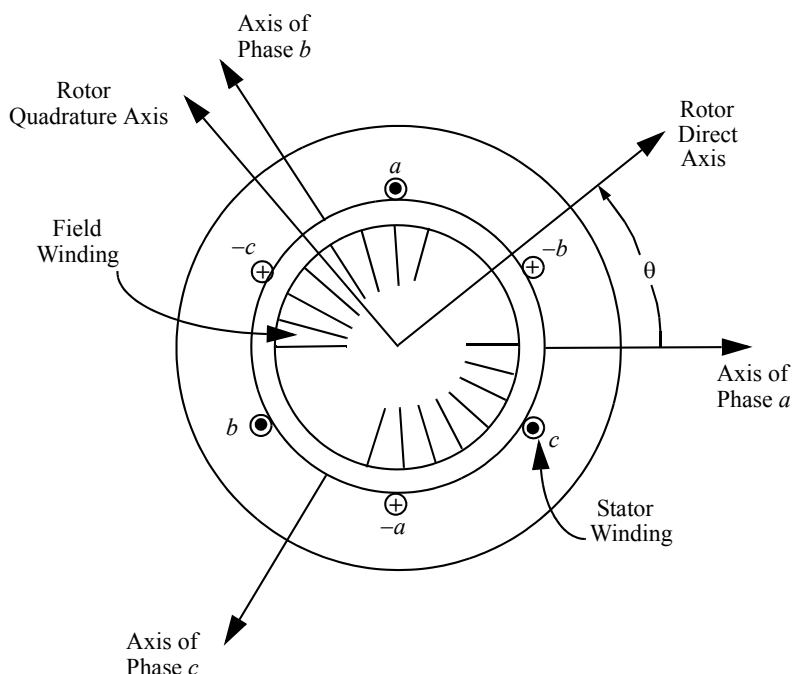


Figure 3.1 Round-rotor synchronous machine construction.

2. The rotor outer periphery has a non-uniform radius shaped such that when the stator axis excited by a single, full pitched, concentrated winding the flux which exits from the stator into the air gap is a even, symmetric function of gap position.
3. The rotor is equipped with shorted rotor coils or bars called damper or amortisseur (“killer”) windings which, although not sinusoidally distributed, can ultimately be replaced by two sinusoidally distributed windings.
4. A third (field) winding is located on one axis of rotor symmetry (the *d*-axis). Although this winding is generally concentrated, its effect can also be represented by an equivalent sinusoidally distributed winding which produces the same fundamental component of MMF in the air gap. This is permissible since the stator windings are generally nearly an ideal sinusoidal distribution. Harmonic components of MMF then give rise merely to a *differential* leakage flux component.
5. The magnetic circuit is assumed to be linear (no saturation).

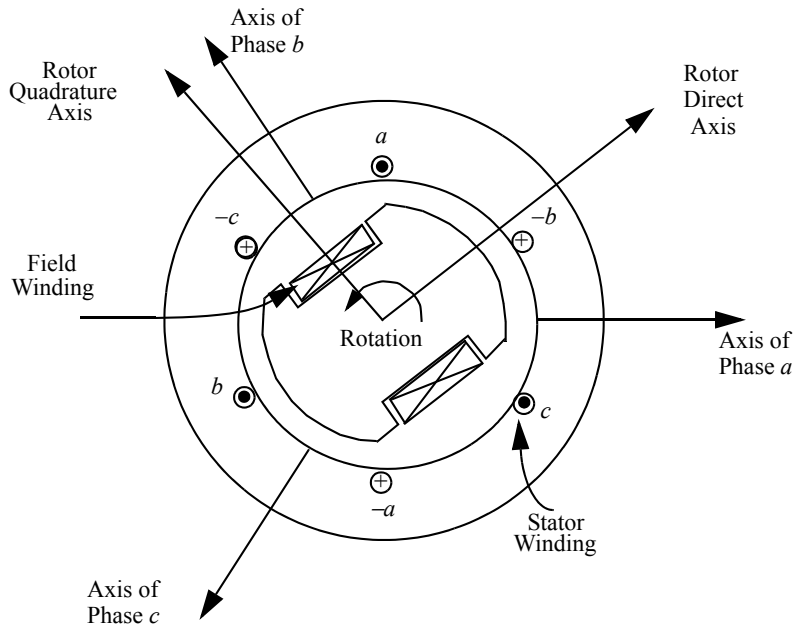


Figure 3.2 Salient-pole synchronous machine construction.

6. All electrical parameters are assumed constant, independent of temperature and frequency.

3.3.1 Voltage Equations

An equivalent schematic representation of the machine is shown on [Figure 3.5](#). In general, the stator and rotor voltages can be expressed in vector-matrix form as

$$\mathbf{v}_{abcs} = r_s \mathbf{i}_{abcs} + p_{abcs} \quad (\text{In the stator frame}) \quad (3.1)$$

$$\mathbf{v}_{dqfr} = r_r \mathbf{i}_{dqfr} + p_{dqfr} \quad (\text{In the rotor frame}) \quad (3.2)$$

In these equations the operator $p = d/dt$ and

$$\mathbf{v}_{abcs} = \begin{bmatrix} v_{as} \\ v_{bs} \\ v_{cs} \end{bmatrix}$$

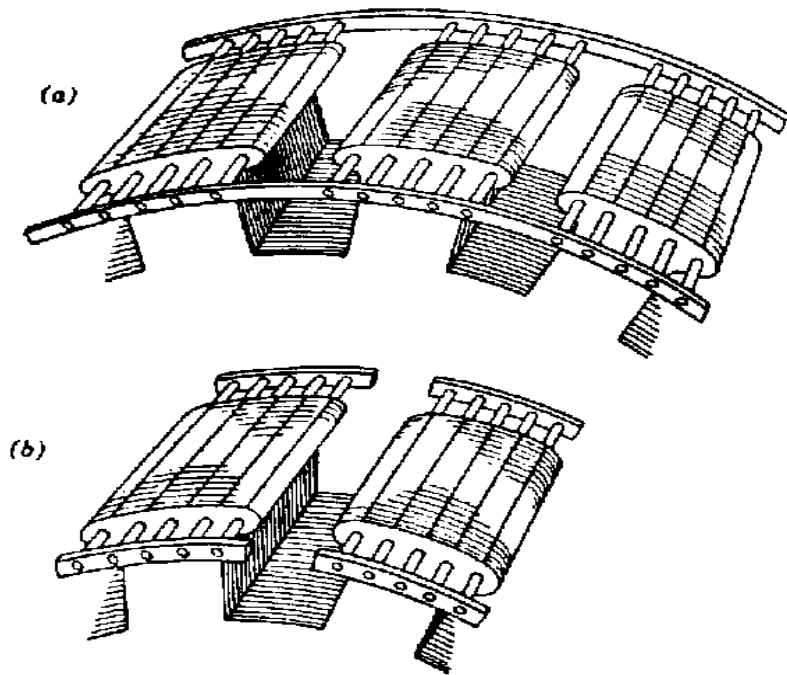


Figure 3.3 Continuous and interrupted end ring construction.
 (a) continuous, (b) interrupted end ring [1].

$$\boldsymbol{v}_{dqfr} = \begin{bmatrix} v_{dr} \\ v_{qr} \\ v_{fr} \end{bmatrix}$$

Similar definitions apply for current vectors \boldsymbol{i}_{abcs} , \boldsymbol{i}_{dqfr} and the flux linkages $\boldsymbol{\psi}_{abcs}$ and $\boldsymbol{\psi}_{dqfr}$. In general, the rotor is unsymmetrical so that the rotor resistances must now be defined by a matrix \boldsymbol{r}_r , where

$$\boldsymbol{r}_r = \begin{bmatrix} r_{dr} & 0 & 0 \\ 0 & r_{qr} & 0 \\ 0 & 0 & r_{fr} \end{bmatrix} \quad (3.3)$$

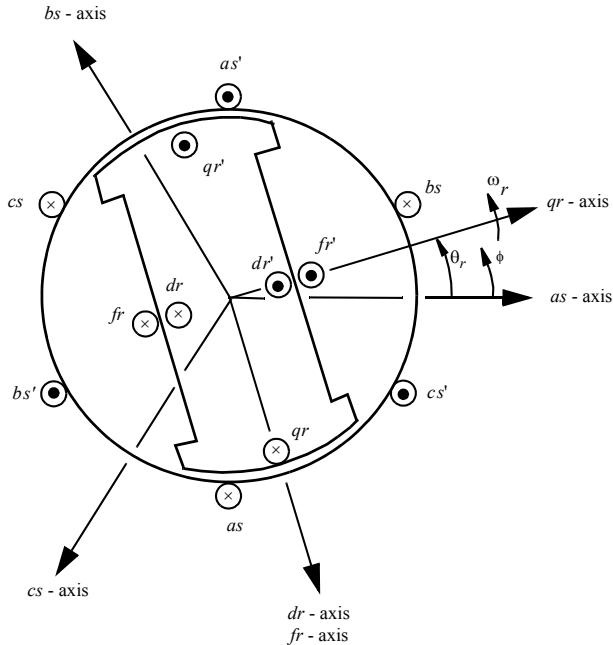


Figure 3.4 Idealized two-pole synchronous machine.

3.3.2 Flux Linkage Equations

Since three stator and three rotor windings exist with mutual coupling between each possible pair of windings, the problem to be solved is formidable. In general, the flux linkages for any orientation of the rotor θ_r can be written in matrix form as

$$abcs = \mathbf{L}_{abcs} i_{abcs} + \mathbf{L}_{abcsr} i_{dqfr} \quad (3.4)$$

$$dqfr = \mathbf{L}_{abcsr}^t i_{abcs} + \mathbf{L}_{dqfr} i_{dqfr} \quad (3.5)$$

where

$$\mathbf{L}_{abcs} = \begin{bmatrix} L_{asas} & L_{asbs} & L_{ascas} \\ L_{asbs} & L_{bsbs} & L_{bscas} \\ L_{ascas} & L_{bscas} & L_{ccas} \end{bmatrix} \quad (3.6)$$

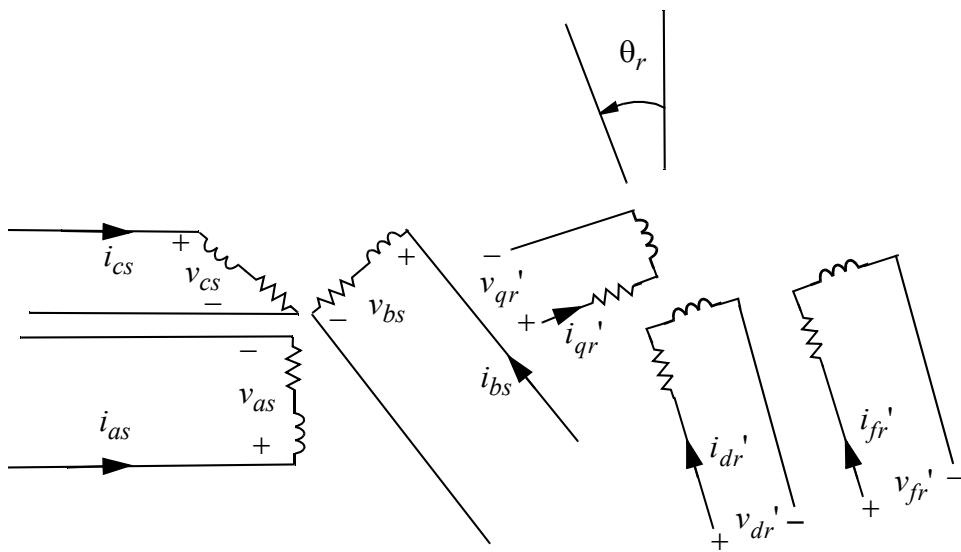


Figure 3.5 Schematic representation of synchronous machine windings.

$$\mathbf{L}_{abcsr} = \begin{bmatrix} L_{asdr} & L_{asqr} & L_{asfr} \\ L_{bsdr} & L_{bsqr} & L_{bsfr} \\ L_{csdr} & L_{csqr} & L_{csfr} \end{bmatrix} \quad (3.7)$$

3.4 Transformation of the Stator Voltage Equations to a Rotating Reference Frame

Recall from previous work that the necessary algebra has already been carried out to transform the vector form of the stator voltage equations to a rotating reference frame. Although the flux linkages are now a much more complicated function of the currents, this complexity does not prevent the transformation of the equations to a rotating frame. The result remains simple as long as the windings contain equal resistances. As done previously, if one multiplies the stator voltage equation by the transformation matrix $\mathbf{T}(\theta)$,

$$\mathbf{T}(\theta)\mathbf{v}_{abcs} = r_s \mathbf{T}(\theta)\mathbf{i}_{abcs} + \mathbf{T}(\theta)\mathbf{p}_{abcs} \quad (3.8)$$

However, it can be recalled that, if \mathbf{M} is an $n \times n$ matrix and \mathbf{v} is an $n \times 1$ vector,

$$\mathbf{M} \frac{d\mathbf{v}}{dt} = \frac{d}{dt}(\mathbf{M}\mathbf{v}) - \frac{d\mathbf{M}}{dt}\mathbf{v} \quad (3.9)$$

Hence Eq. (3.8) can be expanded to the form

$$\mathbf{T}(\theta)\mathbf{v}_{abcs} = r_s \mathbf{T}(\theta)\mathbf{i}_{abcs} + p[\mathbf{T}(\theta)_{abcs} - [p\mathbf{T}(\theta)\mathbf{T}(\theta)^{-1}\mathbf{T}(\theta)_{abcs}]] \quad (3.10)$$

where $p = d/dt$. However, from identity 3 of the previous chapter,

$$[p\mathbf{T}(\theta)]\mathbf{T}(\theta)^{-1} = - \quad (3.11)$$

Therefore, if one formally defines

$$\mathbf{T}(\theta)\mathbf{v}_{abcs} = \mathbf{v}_{dqns} \quad (3.12)$$

$$\mathbf{T}(\theta)\mathbf{i}_{abcs} = \mathbf{i}_{dqns} \quad (3.13)$$

$$\mathbf{T}(\theta)_{abcs} = \mathbf{v}_{dqns} \quad (3.14)$$

the stator voltage vector equation in the *d-q-n* rotating reference frame again reduces to

$$\mathbf{v}_{dqns} = r_s \mathbf{i}_{dqns} + p \mathbf{v}_{dqns} + \mathbf{v}_{dqns} \quad (3.15)$$

3.5 Transformation of Stator Flux Linkages to a Rotating Reference Frame

Because the stator flux linkage variation is complicated by the saliency of the rotor, the manipulation of the stator flux linkage equation is much more difficult than for the stator voltage equation. Much of the work can be avoided, however, if one proceeds to calculate the necessary machine inductances directly in a rotating reference frame. A preliminary investigation of this procedure has already been carried out in the previous chapter for a simple cylindrical inductor. The process this time is very much the same except that now one has a “secondary,” i.e., the rotor windings of the synchronous machine.

Multiplying the stator flux linkage vector, Eq. (3.4), by $\mathbf{T}(\theta)$ and manipulating the result,

$$\mathbf{T}(\theta)_{abcs} = \mathbf{T}(\theta)\mathbf{L}_{abcs}\mathbf{T}(\theta)^{-1}[\mathbf{T}(\theta)\mathbf{i}_{abcs}] + \mathbf{T}(\theta)\mathbf{L}_{abcsr}\mathbf{i}_{dqfr} \quad (3.16)$$

or

$$d_{qns} = \mathbf{T}(\theta) \mathbf{L}_{abcs} \mathbf{T}(\theta)^{-1} \mathbf{i}_{dqns} + \mathbf{T}(\theta) \mathbf{L}_{abcsr} \mathbf{i}_{dqfr} \quad (3.17)$$

It has already been shown that the coefficient of \mathbf{i}_{dqns} can be written as

$$\mathbf{T}(\theta) \mathbf{L}_{abcs} \mathbf{T}(\theta)^{-1} = \begin{bmatrix} L_{ls} + L_{dsds} & L_{dsqs} & L_{dns} \\ L_{qsqs} & L_{ls} + L_{qsqs} & L_{qsns} \\ L_{dns} & L_{qsns} & L_{ls} + L_{nsns} \end{bmatrix} \quad (3.18)$$

where L_{ls} represents that portion of the leakage inductance which is not associated with flux in the air gap (slot and end winding leakage). Since this component of leakage inductance is identical for all three-phases it passes unchanged under the $d-q-n$ transformation in much the same manner as the stator resistance (compare the ir terms in Eqs. (3.1) and (3.15)). In practice, an additional leakage term occurs due to the higher winding function harmonics, i.e., *spatial harmonics* or *belt harmonics*. Calculation of these inductances is considered beyond the scope of this course. A more detailed presentation of leakage inductances and their calculation is given in a machine design text such as [2] and the interested reader is encouraged to refer to such information there.

Also in Eq. (3.13), from winding function theory

$$L_{dsds} = \left(\frac{3}{2}\right) \mu_0 r l \int_0^{2\pi} N_{ds}^2(\phi, \theta) g^{-1}(\phi, \theta_r) d\phi \quad (3.19)$$

$$L_{dsqs} = \left(\frac{3}{2}\right) \mu_0 r l \int_0^{2\pi} N_{ds}(\phi, \theta) N_{qs}(\phi, \theta) g^{-1}(\phi, \theta_r) d\phi \quad (3.20)$$

•

•

•

$$L_{nsns} = \left(\frac{3}{2}\right) \mu_0 r l \int_0^{2\pi} N_{ns}^2(\phi, \theta) g^{-1}(\phi, \theta_r) d\phi \quad (3.21)$$

The second term in Eq. (3.12) is similarly represented by inductances in a $d-q-n$ reference frame. In Chapter 2 the transformation of such a term was not specifically examined. However, it is not difficult to show that the coefficient

of the rotor current vector \mathbf{i}_{dqfr} of the transformed flux linkage equation is represented in the *d-q-n* reference frame by

$$\mathbf{T}(\theta) \mathbf{L}_{abcsr} = \begin{bmatrix} L_{dsqr} & L_{dsdr} & L_{dsfr} \\ L_{qsqr} & L_{qsdr} & L_{qsfr} \\ L_{nsdr} & L_{nsfr} & L_{nsfr} \end{bmatrix} \quad (3.22)$$

$$= \mathbf{L}_{dqnsr} \quad (3.23)$$

where

$$L_{dsqr} = \mu_0 r l \int_0^{2\pi} N_{ds}(\phi, \theta) N_{qr}(\phi, \theta_r) g^{-1}(\phi, \theta_r) d\phi \quad (3.24)$$

$$L_{dsdr} = \mu_0 r l \int_0^{2\pi} N_{ds}(\phi, \theta) N_{dr}(\phi, \theta_r) g^{-1}(\phi, \theta_r) d\phi \quad (3.25)$$

•

•

•

$$L_{nsfr} = \mu_0 r l \int_0^{2\pi} N_{ns}(\phi, \theta) N_{fr}(\phi, \theta_r) g^{-1}(\phi, \theta_r) d\phi \quad (3.26)$$

It is important to note the absence of the “3/2” term in these expressions. This results from the fact that Eq. (3.21) is the coefficient of non-transformed currents (\mathbf{i}_{dqfr}) rather than currents which have been transformed by the *d-q-n* transformation (\mathbf{i}_{dqns}).

3.6 Winding Functions of the Three-Phase Stator Windings in a *d-q-n* Reference Frame

In order to evaluate the inductance expressions of Section 3.5, it is first necessary to find the winding functions of both the stator and rotor circuits in the *d-q-n* rotating reference frame. Recall that the winding functions $N_{ds}(\phi, \theta)$, $N_{qs}(\phi, \theta)$, and $N_{ns}(\phi, \theta)$ describe the placement of equivalent windings in rotating *d-q-n* axes. By definition they are related to the winding functions $N_{as}(\phi)$,

$N_{bs}(\phi)$, $N_{cs}(\phi)$ which describe the distribution of the actual stator windings by the following equations of transformation.

$$N_{ds}(\phi, \theta) = \frac{2}{3} \left[N_{as}(\phi) \sin \theta + N_{bs}(\phi) \sin \left(\theta - \frac{2\pi}{3} \right) + N_{cs}(\phi) \sin \left(\theta + \frac{2\pi}{3} \right) \right] \quad (3.27)$$

$$N_{qs}(\phi, \theta) = \frac{2}{3} \left[N_{as}(\phi) \cos \theta + N_{bs}(\phi) \cos \left(\theta - \frac{2\pi}{3} \right) + N_{cs}(\phi) \cos \left(\theta + \frac{2\pi}{3} \right) \right] \quad (3.28)$$

$$N_{ns}(\phi, \theta) = \frac{\sqrt{2}}{3} [N_{as}(\phi) + N_{bs}(\phi) + N_{cs}(\phi)] \quad (3.29)$$

It is assumed in this analysis that only the fundamental components of the winding functions are of interest. Hence, for this specific case,

$$N_{as}(\phi) = \frac{N_{s1}}{2} \cos(\phi) \quad (3.30)$$

$$N_{bs}(\phi) = \frac{N_{s1}}{2} \cos \left(\phi - \frac{2\pi}{3} \right) \quad (3.31)$$

$$N_{cs}(\phi) = \frac{N_{s1}}{2} \cos \left(\phi + \frac{2\pi}{3} \right) \quad (3.32)$$

where N_{s1} denotes the number of stator turns of the fundamental component of the three winding functions. From previous work in Chapter 1 it is clear that the fundamental number of turns N_{s1} is related to the total number of series connected turns per phase N_t by

$$N_{s1} = \frac{4}{\pi} k_{p1} k_{d1} \left(\frac{2N_t}{PC_s} \right) \quad (3.33)$$

where P is the number of poles, C_s is the number of parallel stator circuits, and k_{p1} and k_{d1} are the fundamental component pitch and distribution factors respectively. The winding functions $N_{ds}(\phi, \theta)$, $N_{qs}(\phi, \theta)$, $N_{ns}(\phi, \theta)$ corresponding to the special case of sinusoidally distributed stator windings are therefore, for $N_{ds}(\phi, \theta)$,

$$\begin{aligned}
 N_{ds}(\phi, \theta) = & \left(\frac{2}{3}\right)\left(\frac{N_{s1}}{2}\right) \left[\cos\phi\sin\theta + \cos\left(\phi - \frac{2\pi}{3}\right) \right. \\
 & \left. + \cos\left(\phi + \frac{2\pi}{3}\right)\sin\left(\theta + \frac{2\pi}{3}\right) \right]
 \end{aligned} \tag{3.34}$$

From Identity # 18 of Appendix 1, this reduces to the simple expression

$$N_{ds}(\phi, \theta) = \frac{N_{s1}}{2} \sin(\theta - \phi) \tag{3.35}$$

The q -axis winding function is, similarly,

$$\begin{aligned}
 N_{qs}(\phi, \theta) = & \left(\frac{2}{3}\right)\left(\frac{N_{s1}}{2}\right) \left[\cos\phi\cos\theta + \cos\left(\phi - \frac{2\pi}{3}\right)\cos\left(\theta - \frac{2\pi}{3}\right) \right. \\
 & \left. + \cos\left(\phi + \frac{2\pi}{3}\right)\cos\left(\theta + \frac{2\pi}{3}\right) \right]
 \end{aligned} \tag{3.36}$$

and, from Identity #16, Appendix 1,

$$N_{qs}(\phi, \theta) = \left(\frac{N_{s1}}{2}\right) \cos(\theta - \phi) \tag{3.37}$$

Finally, for the n -axis stator winding function,

$$\begin{aligned}
 N_{ns}(\phi, \theta) = & \left(\frac{\sqrt{2}}{3}\right)\left(\frac{N_{s1}}{2}\right) \left[\cos\phi + \cos\left(\phi - \frac{2\pi}{3}\right) + \cos\left(\phi + \frac{2\pi}{3}\right) \right] \\
 = & 0
 \end{aligned} \tag{3.38}$$

3.7 Winding Functions of the Rotor Windings

3.7.1 d -Axis Amortisseur Winding Function

Because the bars of the amortisseur winding are simply shorted together, the amortisseur winding does not follow the pattern of previous cases. In previous work, each winding was made from discrete, insulated conductors so that the exact current in each slot could be uniquely determined. In this case, different currents can clearly flow in each of the shorted bars and the problem to be solved seems to defy analysis by use of the winding function technique. However, with certain assumptions it can be shown that an “effective” winding function can still be identified.

First, consider calculation of the effective number of turns in an equivalent dr amortisseur winding. For this purpose Figure 3.6 shows a conceptual layout of the amortisseur winding having six bars per pole. For simplicity, a uniform air gap over the rotor pole surfaces will be assumed. It is useful to let $\alpha\pi$ denote the pole arc in electrical radians. In this case α is generally referred to as the *per unit pole arc*.

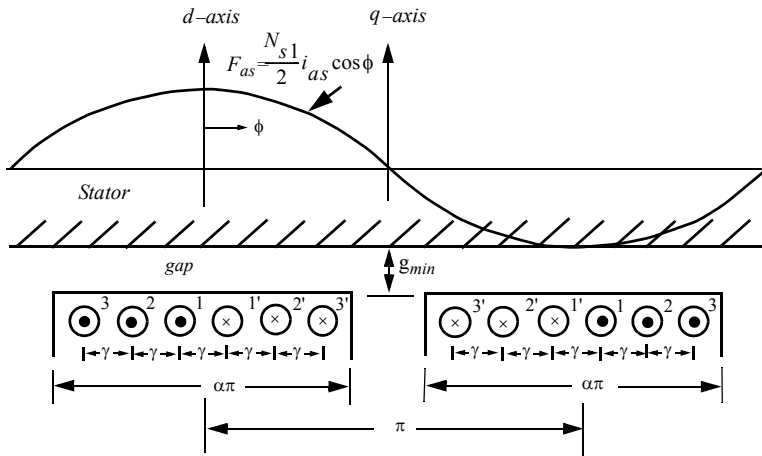


Figure 3.6 Amortisseur bar arrangement with six bars per pole illustrating direct axis stator winding coupling.

Since the bars are shorted, it is clear that current can flow in the bars only by virtue of a time rate of change of flux linkage set up by current in another winding. For simplicity, it will be assumed that the direct axis of the rotor (dr -axis in Figure 3.6) is aligned with the axis of phase as , i.e., $\theta_r = \pi/2$. Also, it is assumed that stator phase as is excited with a sinusoidal voltage and therefore the resulting flux pulsates sinusoidally in the gap. It has already been assumed that the actual winding functions for any of the three stator phase windings can be replaced by equivalent sinusoidal winding functions, Eqs. (3.35), (3.37), and (3.38). Hence, because of the uniform air gap over the pole surface, the flux in the gap will be sinusoidal over the pole face and zero between the poles. The entire flux wave will alternate sinusoidally in time since the excitation current varies sinusoidally.

Note that since the excitation is centered about the d -axis, the currents that flow in the 1 and $1'$ bars are equal and opposite. It is useful, for purposes of analysis, to assume that the six bars form three independent circuits, as shown

in [Figure 3.6](#). If N_{s1} is the effective number of turns of stator phase a_s and I_s is the maximum amplitude of the sinusoidal current in the phase, the flux linking the 1-1' circuit is

$$\Phi_{1,1'} = \frac{\mu_0 r l}{g_{min}} \int_{-\gamma/2}^{\gamma/2} \frac{N_{s1}}{2} I_s \sin \omega_e t \cos \phi d\phi \quad (3.39)$$

$$= \frac{\mu_0 r l}{g_{min}} N_{s1} I_s \sin \omega_e t \left(\sin \frac{\gamma}{2} \right) \quad (3.40)$$

Similarly, the flux linkages of the 2-2' and 3-3' circuits are

$$\Phi_{2,2'} = \frac{\mu_0 r l}{g_{min}} N_{s1} I_s \sin \omega_e t \left(\sin \frac{3\gamma}{2} \right) \quad (3.41)$$

$$\Phi_{3,3'} = \frac{\mu_0 r l}{g_{min}} N_{s1} I_s \sin \omega_e t \left(\sin \frac{5\gamma}{2} \right) \quad (3.42)$$

In general, for a machine with n pairs of bars per pole

$$\Phi_{n,n'} = \frac{\mu_0 r l}{g_{min}} N_{s1} I_s \sin \omega_e t \sin \left[\frac{(2n-1)\gamma}{2} \right] \quad (3.43)$$

It is important to observe that the fluxes in the three circuits of [Figure 3.6](#) differ only by the factor, $\sin(\gamma/2)$, $\sin(3\gamma/2)$, and $\sin(5\gamma/2)$ respectively. Since all of the bars are identical, the resistance and leakage inductance associated with the slot portion of the bar are identical in each case. However, because the “sides” of the three circuits do not have identical lengths, the resistance and leakage inductance, over this portion of the path of the circuit are different. Fortunately, since this portion of the circuit is in air, the leakage inductance is relatively small. Hence, the impedance of each bar can be approximated by its slot impedance. In this case the current induced in the three circuits, being proportional to the induced voltage, also varies in the proportion $\sin(\gamma/2)$, $\sin(3\gamma/2)$, and $\sin(5\gamma/2)$ and are in time phase.

Unless the bar impedances are known, it is not possible, of course, to solve uniquely for the current in the bars. However, the current in circuit 1-1' can be denoted as simply $I_{dr} \sin(\omega_e t + \alpha) \sin(\gamma/2)$ where α represents the phase of the current in each circuit relative to the excitation voltage. The *MMF* distribution produced by the three circuits can be sketched as shown in [Figure 3.7](#) for the case where $\omega_e t + \alpha = \pi/2$. Observe that the *MMFs* are also related by the same factors as the flux linkages.

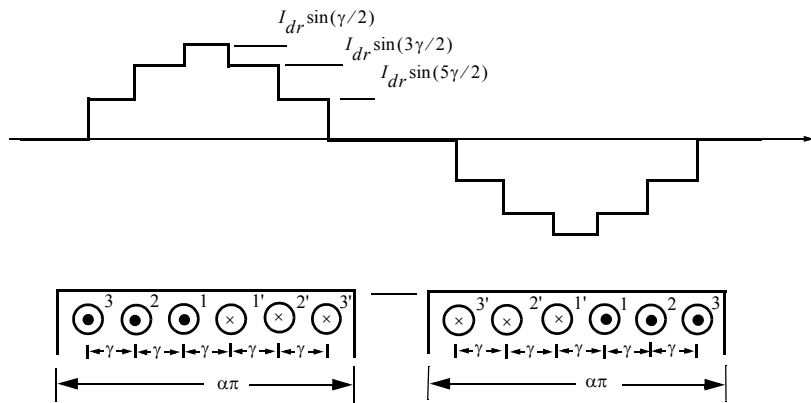


Figure 3.7 Direct axis rotor *MMF* distribution due to stator coupling for an amortisseur cage having six bars per pole.

In order to use the concept of winding functions, it is necessary that the same current flow in each individual conductor. This requirement can fortunately be arranged. In particular, Figure 3.8 shows an equivalent set of windings functions which will result in exactly the same *MMF* as the actual case. Note that in this case each winding carries the same current $I_{dr}\sin(\omega_e t + \alpha)$ and the number of turns is assumed to vary as $\sin(\gamma/2)$, $\sin(3\gamma/2)$, and $\sin(5\gamma/2)$ respectively. Also, note that rectangular distributions are set up by each of the three circuits since they are, in effect, concentrated coils.

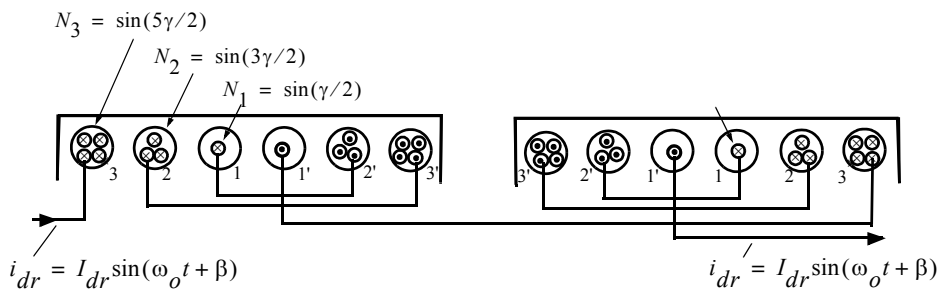
Although the three winding functions of Figure 3.8 are rectangular, only the fundamental component actually couples the sinusoidal winding function representing stator phase *as*. The fundamental component of the winding function of circuit 1-1' is clearly

$$N_{1(1, 1')} = \frac{2}{\pi} \sin\left(\frac{\gamma}{2}\right) \int_{-\gamma/2}^{\gamma/2} \cos \phi d\phi \quad (3.44)$$

$$= \frac{4}{\pi} \sin^2\left(\frac{\gamma}{2}\right) \quad (3.45)$$

Similarly

$$N_{1(2, 2')} = \frac{4}{\pi} \sin^2\left(\frac{3\gamma}{2}\right) \quad (3.46)$$



Equivalent Winding Distribution to Describe Coupling of the Amortisseur Winding in the Direct Axis

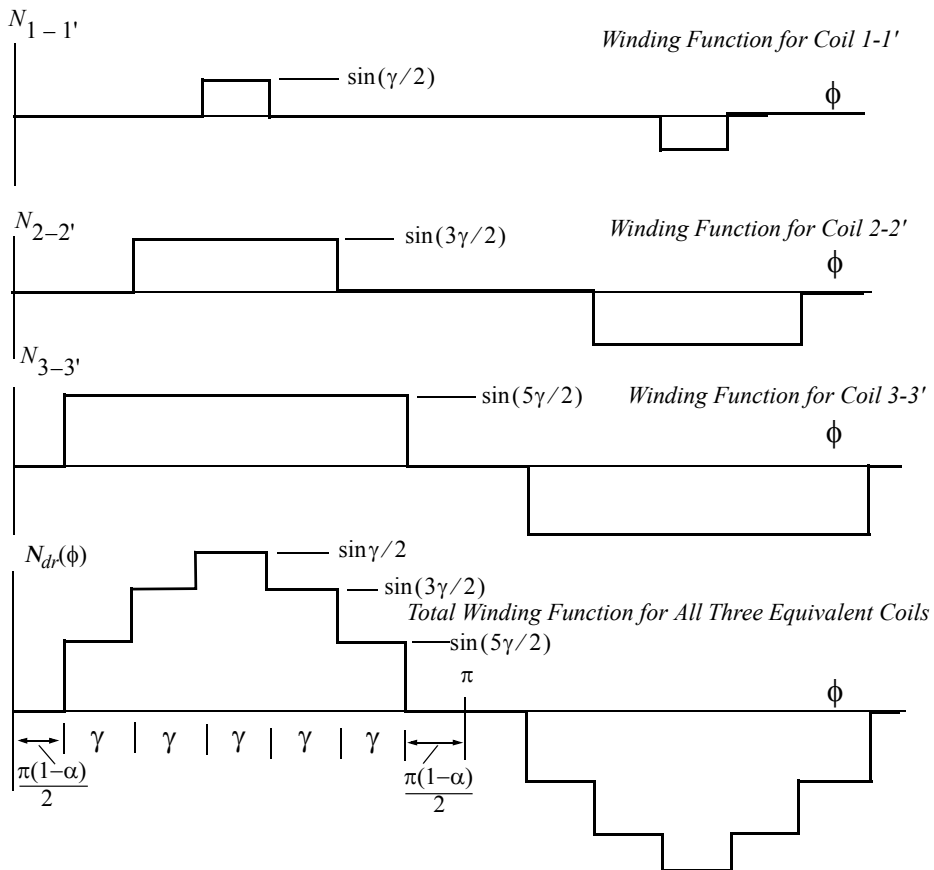


Figure 3.8 Equivalent direct axis winding and winding functions for an amortisseur cage having six bars per pole.

$$N_{1(3, 3')} = \frac{4}{\pi} \sin^2 \left(\frac{5\gamma}{2} \right) \quad (3.47)$$

In general, for an amortisseur with n bars per pole the fundamental component of the $n-n'$ circuit is

$$N_{1(n, n')} = \frac{4}{\pi} \sin^2 \left[\frac{(2n-1)\gamma}{2} \right] \quad (3.48)$$

Since all of the first harmonic components are in phase, the total first harmonic component of the overall d -axis amortisseur winding having n pairs of bars per pole is

$$N_{dr1} = \frac{4}{\pi} \left[\sin^2 \left(\frac{\gamma}{2} \right) + \sin^2 \left(\frac{3\gamma}{2} \right) + \sin^2 \left(\frac{5\gamma}{2} \right) + \dots + \sin^2 \left[(2n-1)\gamma/2 \right] \right] \quad (3.49)$$

Equation (3.49) can be written in the form

$$\begin{aligned} N_{dr1} = & \frac{4}{\pi} [\sin^2 \gamma/2 + \sin^2(\gamma/2 + \gamma) + \sin^2(\gamma/2 + 2\gamma) + \dots \\ & + \sin^2[\gamma/2 + (n-1)\gamma]] \end{aligned} \quad (3.50)$$

which can be expanded to the form (Dwight 401.01)[3]

$$\begin{aligned} N_{dr1} = & \frac{4}{\pi} \sin^2 \left(\frac{\gamma}{2} \right) [1 + \cos^2 \gamma + \cos^2 2\gamma + \dots + \cos^2(n-1)\gamma] \\ & + \frac{4}{\pi} \cos^2 \left(\frac{\gamma}{2} \right) [\sin^2 \gamma + \sin^2 2\gamma + \dots + \sin^2(n-1)\gamma] \\ & + \frac{8}{\pi} \sin \left(\frac{\gamma}{2} \right) \cos \left(\frac{\gamma}{2} \right) [\sin \gamma \cos \gamma + \sin 2\gamma \cos 2\gamma + \dots \\ & + \sin(n-1)\gamma \cos(n-1)\gamma] \end{aligned} \quad (3.51)$$

Again, by trigonometric identities (Dwight 404.22, 404.12, and 401.05)

$$\begin{aligned}
N_{dr1} = & \frac{4}{\pi} \sin^2\left(\frac{\gamma}{2}\right) \left\{ 1 + \frac{n-1}{2} + \frac{1}{2} [\cos 2\gamma + \cos 4\gamma + \dots + \cos 2(n-1)\gamma] \right\} \\
& + \frac{4}{\pi} \cos^2\left(\frac{\gamma}{2}\right) \left\{ \frac{n-1}{2} - \frac{1}{2} [\cos 2\gamma + \cos 4\gamma + \dots + \cos 2(n-1)\gamma] \right\} \\
& + \frac{4}{\pi} \sin\frac{\gamma}{2} \cos\frac{\gamma}{2} [\sin 2\gamma + \sin 4\gamma + \dots + \sin 2(n-1)\gamma]
\end{aligned} \tag{3.52}$$

which becomes (Dwight 420.1 and 420.2)

$$\begin{aligned}
N_{dr1} = & \frac{4}{\pi} \sin^2\left(\frac{\gamma}{2}\right) \left\{ 1 + \frac{n-1}{2} + \frac{1}{2} \frac{\cos[n\gamma] \sin[(n-1)\gamma]}{\sin\gamma} \right\} \\
& + \frac{4}{\pi} \cos^2\left(\frac{\gamma}{2}\right) \left\{ \frac{n-1}{2} - \frac{1}{2} \frac{\cos[n\gamma] \sin[(n-1)\gamma]}{\sin\gamma} \right\} \\
& + \frac{4}{\pi} \sin\left(\frac{\gamma}{2}\right) \cos\left(\frac{\gamma}{2}\right) \left\{ \frac{\sin[n\gamma] \sin[(n-1)\gamma]}{\sin\gamma} \right\}
\end{aligned} \tag{3.53}$$

This expression reduces finally to

$$\begin{aligned}
V_{dr1} = & \frac{2}{\pi} \left[2N_b - \cos\gamma \left(1 + \frac{\cos[2N_b\gamma] \sin[(2N_b-1)\gamma]}{\sin\gamma} \right) \right. \\
& \left. + \sin[2N_b\gamma] \sin[(2N_b-1)\gamma] \right]
\end{aligned} \tag{3.54}$$

where, for convenience, the number of pairs of bars per pole n has been replaced by N_b , the number of bars per pole. It should be noted that this result is identical for both the continuous end ring and the interrupted end ring construction of [Figure 3.3](#). Since the d -axis amortisseur is fixed on the rotor, its winding function is given by, finally

$$N_{dr}(\phi, \theta_r) = N_{dr1} \sin(\theta_r - \phi) \tag{3.55}$$

where N_{dr1} is given by Eq. (3.54).

3.7.2 q -Axis Amortisseur Circuit Winding Function

The equivalent turns for the q -axis amortisseur is found in much the same manner as for the d -axis. In this case, the interpolar axis is aligned with phase as by setting $\theta_r = 0$, i.e., the qr -axis of Figure 3.4. Phase as is again impressed with a sinusoidal current and can be used to deduce the current distribution in the rotor bars. However, it can be noted from Figure 3.9 that the solution will now differ depending upon whether or not the end ring is closed. The particular case where the end ring is interrupted will be studied here. The case of the non-interrupted circuit will be left for homework. Six bars per pole will again be used as an illustrative example. Notice from Figure 3.9 that for convenience the reference point for the measurement of ϕ has now been moved to coincide with the q -axis. In order to determine the stator coupling, the stator phase as is again excited with a sinusoidal voltage so that a sinusoidal current of amplitude I_s flows in the winding.

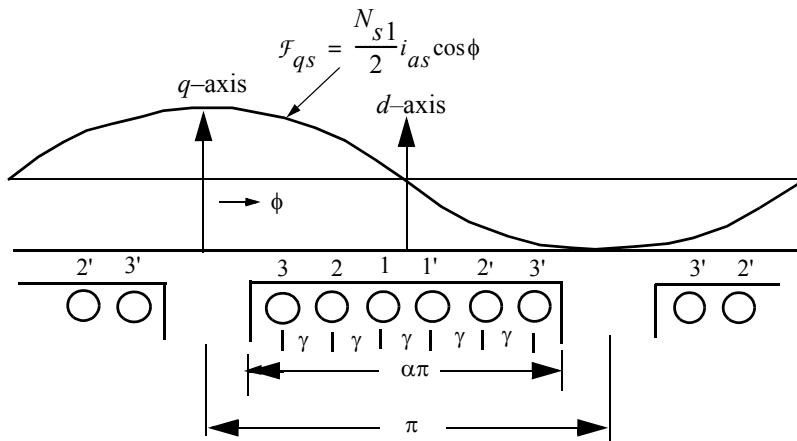


Figure 3.9 Amortisseur bar configuration with six bars per pole illustrating quadrature axis stator winding coupling.

Proceeding as before, the flux linking the quadrature axis between bars 3 and 3' is

$$\Phi_{3,3'} = \frac{\mu_0 r l}{g_{min}} (2) \int_{\pi(\frac{1-\alpha}{2})}^{\left(\frac{\pi}{2} - \frac{5\gamma}{2}\right)} \frac{N_{s1}}{2} I_s \sin \omega_e t \cos \phi d\phi \quad (3.56)$$

Equation (3.56) reduces to

$$\Phi_{3,3'} = \frac{\mu_0 r l}{g_{min}} N_{s1} I_s \sin \omega_e t \left[\cos \frac{5\gamma}{2} - \cos \frac{\alpha\pi}{2} \right] \quad (3.57)$$

Note that in this case a current does not flow around the circuit defined by bars 3-3' since the end ring is interrupted. In a similar manner, the fluxes linking the 2-2' and 1-1' pairs of bars are

$$\Phi_{2,2'} = \frac{\mu_0 r l}{g_{min}} N_{s1} I_s \sin \omega_e t \left[\cos \frac{3\gamma}{2} - \cos \frac{\alpha\pi}{2} \right] \quad (3.58)$$

$$\Phi_{1,1'} = \frac{\mu_0 r l}{g_{min}} N_{s1} I_s \cos \omega_e t \left[\cos \left(\frac{\gamma}{2} \right) - \cos \left(\frac{\alpha\pi}{2} \right) \right] \quad (3.59)$$

In the general case for the $n-n'$ bar circuit

$$\Phi_{n,n'} = \frac{\mu_0 r l}{g_{min}} N_{s1} I_s \sin \omega_e t \left[\cos \left(\frac{(2n-1)\gamma}{2} \right) - \cos \left(\frac{\alpha\pi}{2} \right) \right] \quad (3.60)$$

Although current can not flow from pole to pole due to the interrupted end ring, current flow can occur, for example, between circuits defined by bars 1 and 2 and also 2 and 3. Symmetric currents will simultaneously flow between bars 1' and 2' and also 2' and 3' on the adjacent pole. The flux linking the circuit formed by shorted bars 3 and 2 (and also 3' and 2') is

$$\Phi_{2,3} = \frac{1}{2} (\Phi_{2,2'} - \Phi_{3,3'}) \quad (3.61)$$

$$= \frac{\mu_0 r l}{2g_{min}} N_{s1} I_s \sin \omega_e t \left[\cos \frac{3\gamma}{2} - \cos \frac{5\gamma}{2} \right] \quad (3.62)$$

Similarly for bars 1 and 2 (and also 1' and 2')

$$\Phi_{1,2} = \frac{\mu_0 r l}{2g_{min}} N_{s1} I_s \sin \omega_e t \left[\cos \frac{\gamma}{2} - \cos \frac{3\gamma}{2} \right] \quad (3.63)$$

In the general case for n bars per pole,

$$\Phi_{n-1,n} = \frac{\mu_0 r l}{2g_{min}} N_{s1} I_s \sin \omega_e t \left[\cos \frac{(2n-3)\gamma}{2} - \cos \frac{(2n-1)\gamma}{2} \right] \quad (3.64)$$

Again the impedances presented by each shorted bar are assumed to be equal. Therefore, current flows in time phase in all of the rotor bars. If $I_{qr}[\cos(3\gamma/2) - \cos(5\gamma/2)]$ denotes the current amplitude in the circuit formed

by bars 2 and 3, then examination of Eq. (3.58) indicates that the current in the circuit defined by bars 1 and 2 is simply proportional to the current in the circuit formed by bars 2 and 3 multiplied by the bracketed factors of Eqs. (3.62) and (3.63). [Figure 3.10](#) shows a plot of the *MMF* formed by this current distribution at the instant when the current in the amortisseur bars is a maximum. It is apparent that it is again possible to identify an equivalent winding function having unequal numbers of turns per slot but carrying the same current. The two component parts of the winding function for the six bar case together with the composite winding function is shown in [Figure 3.11](#).

Again only the fundamental component of the winding distributions of Figure 3.11 are of interest, since only this component links the stator in any significant way. The fundamental components of the two partial winding functions of Figure 3.11 are

$$N_{2,3} = \frac{4}{\pi} \left[\cos \frac{3\gamma}{2} - \cos \frac{5\gamma}{2} \right] \int_{\left(\frac{\pi}{2} - \frac{3\gamma}{2}\right)}^{\left(\frac{\pi}{2} - \frac{5\gamma}{2}\right)} \cos \phi d\phi \quad (3.65)$$

$$= \frac{4}{\pi} \left[\cos \frac{3\gamma}{2} - \cos \frac{5\gamma}{2} \right]^2 \quad (3.66)$$

Similarly

$$N_{1,2} = \frac{4}{\pi} \left[\cos \frac{\gamma}{2} - \cos \frac{3\gamma}{2} \right]^2 \quad (3.67)$$

For the general case with n pairs of bars per pole

$$N_{n-1,n} = \frac{4}{\pi} \left[\cos \left(\frac{2n-3}{2} \right) \gamma - \cos \left(\frac{2n-1}{2} \right) \gamma \right]^2 \quad (3.68)$$

The total fundamental component of the winding function is therefore

$$N_{qr1} = \frac{4}{\pi} \left\{ \left(\cos \frac{\gamma}{2} - \cos \frac{3\gamma}{2} \right)^2 + \left(\cos \frac{3\gamma}{2} - \cos \frac{5\gamma}{2} \right)^2 + \dots \right. \\ \left. + \left[\cos \left(\frac{2n-3}{2} \right) \gamma - \cos \left(\frac{2n-1}{2} \right) \gamma \right]^2 \right\} \quad (3.69)$$

By means of identities (Dwight 401.11), Eq. (3.69) can be manipulated to form

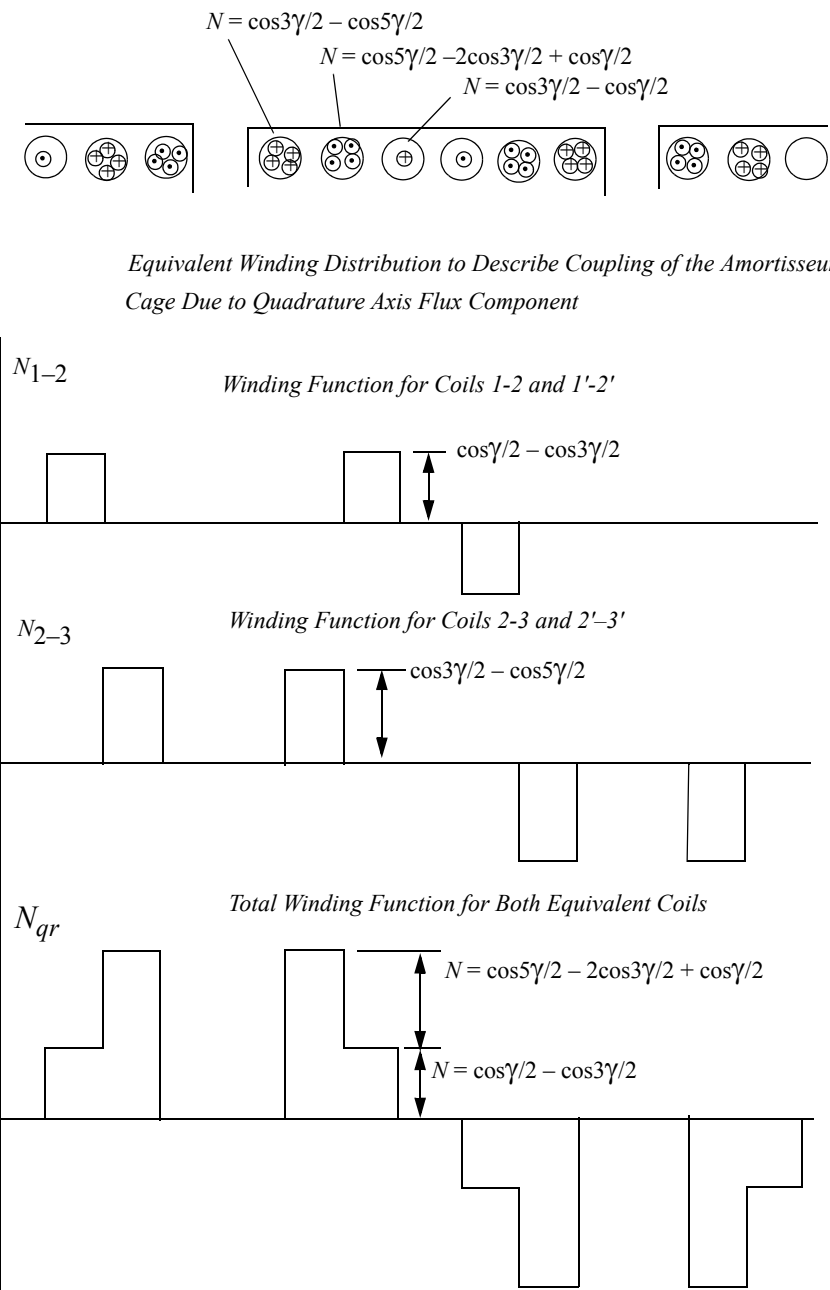


Figure 3.10 Equivalent quadrature axis winding and winding functions for an amortisseur having six bars per pole.

$$N_{qr1} = \frac{4}{\pi} \left\{ \left(2 \sin \gamma \sin \frac{\gamma}{2} \right)^2 + \left(2 \sin 2\gamma \sin \frac{\gamma}{2} \right)^2 + \dots + \left[2 \sin(n-1)\gamma \sin \frac{\gamma}{2} \right]^2 \right\} \quad (3.70)$$

which can be written as

$$N_{qr1} = \frac{16}{\pi} \sin^2 \frac{\gamma}{2} [\sin^2 \gamma + \sin^2 2\gamma + \dots + \sin^2(n-1)\gamma] \quad (3.71)$$

From Dwight 404.12, Eq. (3.71) can also be written as

$$N_{qr1} = \frac{8}{\pi} \sin^2 \frac{\gamma}{2} [(n-1) - \cos 2\gamma - \cos 4\gamma - \dots - \cos 2(n-1)\gamma] \quad (3.72)$$

Finally, using Dwight 420.2,

$$N_{qr1} = \frac{8}{\pi} \sin^2 \frac{\gamma}{2} \left[\frac{N_b}{2} - 1 - \frac{\cos \left[N_b \frac{\gamma}{2} \right] \sin \left[(N_b/2 - 1)\gamma \right]}{\sin \gamma} \right] \quad (3.73)$$

Again the number of pairs of bars n has been replaced by the number of bars per pole N_b . It is important to take note that although the end ring is interrupted in the quadrature axis and the current does not flow from pole to pole, a quadrature axis current is still induced in the amortisseur cage. The reader may wish to calculate the functions defined by Eqs. (3.54) and (3.73) for various numbers of bars per pole. The case of the continuous end ring is only slightly more complicated than for the interrupted ring. In this case the additional flux linking the circuits due to the flux entering the pole tips must be included. The solution is left to the reader.

With the axis alignment implied by Figure 3.2, the overall winding function for the q -axis amortisseur winding is given by

$$N_{qr}(\phi, \theta_r) = N_{qr1} \cos(\theta_r - \phi) \quad (3.74)$$

3.7.3 Field Circuit Winding Function

Since the current flow in the field winding is through discrete conductors, the calculation of the field circuit winding function is blessedly simple. It can be

recalled that the field is wound in concentrated fashion around the rotor saliences. In effect, the interpolar space between poles can be considered as simply an enormous slot. The concentrated winding located in the slots has the winding function as shown in Figure 3.11. The effective number of turns for the field winding corresponding to the fundamental component is simply

$$N_{fr1} = \frac{2}{\pi} \frac{N_{fr}}{PC_f} \int_{-\pi/2}^{\pi/2} \cos \phi d\phi \quad (3.75)$$

$$= \frac{4}{\pi} \frac{N_{fr}}{PC_f} \quad (3.76)$$

where C_f denotes the number of parallel circuits used to wind the field. The winding function for the field circuit is simply

$$N_{fr}(\phi, \theta_r) = N_{fr1} \sin(\theta_r - \phi) \quad (3.77)$$

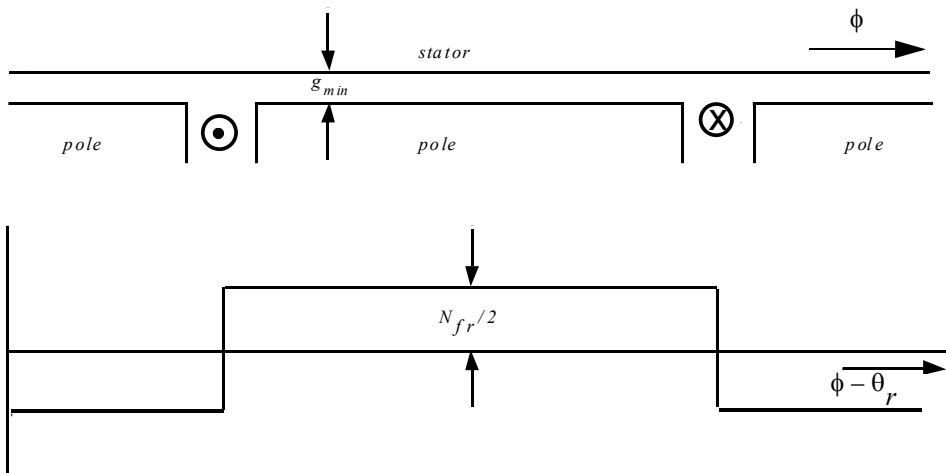


Figure 3.11 Equivalent winding and resulting winding function for the field winding.

3.8 Calculation of Stator Magnetizing Inductances

It is now possible to proceed to directly calculate the stator magnetizing inductances in a $d-q-n$ rotating reference frame. From previous work in [Section 3.5](#), the quadrature axis magnetizing inductance is expressed by

$$L_{qsqs} = \mu_0 r l \left(\frac{3}{2} \right) \int_0^{2\pi} N_{qs}^2(\phi, \theta) g^{-1}(\phi, \theta_r) d\phi \quad (3.78)$$

As yet, the inverse gap function has not been defined. In practice, the exact shape of the inverse gap function is a design variable. The taper of the poles is selected so as to maximize the fundamental component of air gap flux produced by the field winding. Contrary to what might be expected, the pole is not necessarily shaped so as to produce a sinusoidal distribution of flux in the air gap. As a result, the inverse gap function is not sinusoidal. In this study a uniform gap has been assumed uniform under the entire pole surface. This pole shape is characteristic of many smaller synchronous motors. Larger machines, however, are designed with tapered poles. In this case the functional variation of the inverse gap function must be computed from flux plots.

The inverse gap function for a salient-pole machine with a uniform air gap beneath the poles is described by [Figure 3.12](#). Note that since the effective gap over the interpolar space is assumed to be infinite, the inverse gap function is zero over this same interval. Because the poles are identical, the g^{-1} function is also periodic over π radians.

As yet, no restriction has been made on the speed or position of the rotating $d-q-n$ reference frame. It is probably apparent to the reader by now that the rotor asymmetry severely restricts the flexibility of the $d-q-n$ representation. While the $d-q-n$ representation continues to be a useful concept, the orientation of the $d-q$ axis must now accommodate the rotor saliency. For the present, however, assume that the rotating $d-q$ axis is not related in any way to the angular position of the rotor θ_r . Incorporating the assumptions implicit in [Figure 3.12](#), Eq. (3.78) becomes

$$L_{qsqs} = \mu_0 r l \left(\frac{3}{2} \right) \int_{-\frac{\alpha\pi}{2} + \theta_r}^{\frac{\alpha\pi}{2} + \theta_r} \left(\frac{N_{s1}}{2} \right)^2 \cos^2(\theta - \phi) \left(\frac{1}{g_{min}} \right) d\phi \quad (3.79)$$

$$= 3 \frac{\mu_0 r l}{g_{min}} \left(\frac{N_{s1}}{2} \right)^2 \left[\frac{\alpha\pi}{2} - \frac{1}{2} \sin[\alpha\pi] \cos[2(\theta - \theta_r)] \right] \quad (3.80)$$

which can be written as

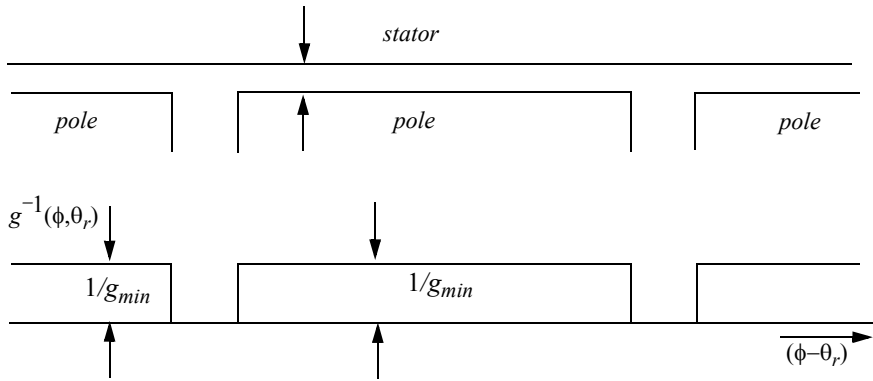


Figure 3.12 Inverse gap function for the idealized machine.

$$= \frac{\mu_0 r l}{g_{min}} \left(\frac{3}{2}\right) N_{s1}^2 \frac{\pi}{4} \left[\alpha - \frac{\sin[\alpha\pi]}{\pi} \cos[2(\theta - \theta_r)] \right] \quad (3.81)$$

In a similar manner the direct axis magnetizing inductance is

$$L_{dsds} = \mu_0 r l \left(3\right) \int_{\left(-\frac{\alpha\pi}{2} + \theta\right)}^{\left(\frac{\alpha\pi}{2} + \theta\right)} \left(\frac{N_{s1}}{2}\right)^2 \cos^2(\theta - \phi) \left(\frac{1}{g_{min}}\right) d\phi \quad (3.82)$$

$$= 3 \frac{\mu_0 r l}{g_{min}} \left(\frac{N_{s1}}{2}\right)^2 \left[\frac{\alpha\pi}{2} + \frac{1}{2} \sin[\alpha\pi] \cos[2(\theta - \theta_r)] \right] \quad (3.83)$$

which can be written as

$$\begin{aligned} L_{dsds} &= \frac{\mu_0 r l}{g_{min}} \left(\frac{3}{2}\right) N_{s1}^2 \left(\frac{\pi}{4}\right) \left[\alpha + \frac{\sin[\alpha\pi]}{\pi} \cos[2(\theta - \theta_r)] \right] \\ &= \frac{\mu_0 r l}{g_{min}} \left(\frac{3}{2}\right) N_{s1}^2 \left(\frac{\pi}{4}\right) k_d \end{aligned} \quad (3.84)$$

Finally, it is obvious that

$$L_{nsns} = 0 \quad (3.85)$$

since the winding function associated with the ns -axis is identically zero, Eq. (3.38).

Using the same approach, it is not difficult to show that the mutual inductance between the direct and quadrature axis stator circuits is

$$L_{qsds} = \left(\frac{3}{2}\right) \frac{\mu_0 r l}{g_{min}} N_{s1}^2 \left(\frac{\pi}{4}\right) \left[\frac{\sin \alpha \pi}{\pi} \sin 2(\theta - \theta_r) \right] \quad (3.86)$$

The completed magnetizing inductance matrix represented in a $d-q$ plane rotating at an arbitrary speed θ is summarized below

$$\mathbf{L}_{dqns} = \left(\frac{3}{2}\right) \frac{\mu_0 r l}{g_{min}} N_{s1}^2 \left(\frac{\pi}{4}\right) \begin{bmatrix} \alpha + \frac{1}{\pi} \sin \alpha \pi \cos 2(\theta - \theta_r) & \frac{1}{\pi} \sin \alpha \pi \sin 2(\theta - \theta_r) & 0 \\ \frac{1}{\pi} \sin \alpha \pi \sin 2(\theta - \theta_r) & \alpha - \frac{1}{\pi} \sin \alpha \pi \cos 2(\theta - \theta_r) & 0 \\ 0 & 0 & 0 \end{bmatrix} \quad (3.87)$$

Clearly, there is considerable benefit in transforming to the $d-q-n$ coordinate system even though coupling still exists between the d - and q -axis components. It is apparent from this result, however, that the simplest inductance relationships are obtained if one simply sets $\theta = \theta_r$. In this case one can say that the $d-q$ axes have been *attached to the rotor*. Alternatively, it is often stated that in order to obtain non-time-varying inductance coefficients, it is necessary to choose a *rotor reference frame*. Upon incorporating this constraint, the inductance matrix \mathbf{L}_{qdns} reduces to:

$$\mathbf{L}_{dqns} = \begin{bmatrix} L_{ls} & 0 & 0 \\ 0 & L_{ls} & 0 \\ 0 & 0 & L_{ls} \end{bmatrix} + \left(\frac{3}{2}\right) \frac{\mu_0 r l}{g_{min}} N_{s1}^2 \left(\frac{\pi}{4}\right) \begin{bmatrix} k_d & 0 & 0 \\ 0 & k_d & 0 \\ 0 & 0 & 0 \end{bmatrix} \quad (3.88)$$

where

$$k_d = \alpha + \frac{1}{\pi} \sin \alpha \pi \quad (3.89)$$

and

$$k_q = \alpha - \frac{1}{\pi} \sin \alpha \pi \quad (3.90)$$

The quantities k_d and k_q are frequently called the *direct axis* and *quadrature axis armature form factors*. Note that when $\alpha = 1$, both k_d and k_q are equal to unity. The magnetizing inductances become equal to that of a symmetrical induction machine.

It is apparent that for the general case of a tapered gap

$$k_d = \frac{2g_{min}}{\pi} \int_0^{\pi} \cos^2 \phi g^{-1}(\phi, 0) d\phi \quad (3.91)$$

and

$$k_q = \frac{2g_{min}}{\pi} \int_0^{\pi} \sin^2 \phi g^{-1}(\phi, 0) d\phi \quad (3.92)$$

where it is assumed that the inverse gap function is periodic over π electrical radians and that the rotor polar axis (d -axis) is aligned with the magnetic axis of phase *as*, i.e., $\theta_r = 0$. Note that multiplying the inverse gap function by g_{min} effectively normalizes the maximum value of $g^{-1}(\phi, \theta_r)$ to unity.

For most practical machine geometries, the functions k_d and k_q can only be calculated by an exhaustive number of field plots. [Figure 3.13](#) shows curves for determination of k_d and k_q measured by Kostenko and Konit and taken from the book by Kostenko and Piotrovsky [4]. The curves are plotted as a function of the per unit pole arc α , the ratio of maximum gap to minimum gap g_{max}/g_{min} and the ratio of minimum gap to pole pitch g_{min}/τ_p . The minimum air gap is the gap at the center line of the pole while, in this case, the maximum gap is measured at the edge of the pole. The pole pitch is related to the machine stator inner radius r and the number of poles by

$$\tau_p = \frac{2\pi r}{P} \quad (3.93)$$

3.9 Mutual Inductances between Stator and Rotor Circuits

It has already been shown that the stator self and mutual inductances simplify to a constant only if the d - q axes rotate synchronously with the rotor. If one now specifies that $\theta = \theta_r$, the mutual inductances which exist between the

equivalent rotating d - q - n stator windings and the rotating windings on the rotor can be solved as

$$\mathbf{L}_{dqnsr} = \begin{bmatrix} L_{dsdr} & L_{dsqr} & L_{dsfr} \\ L_{qsdr} & L_{qsqr} & L_{qsfr} \\ L_{nsdr} & L_{nsqr} & L_{nsfr} \end{bmatrix} \quad (3.94)$$

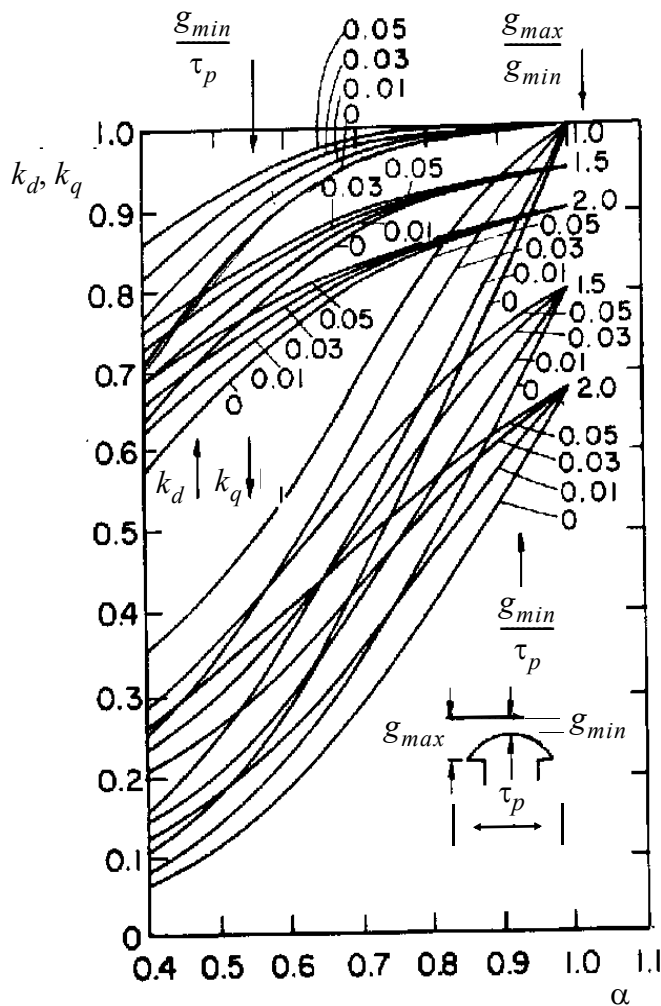


Figure 3.13 Curves for determination of k_q and k_d form factors [4].

It has also been demonstrated in the previous section that the maximum simplification of the inductance coefficients occurs if the rotor reference is employed, that is, if one sets $\theta = \theta_r$ in the transformation matrix $\mathbf{T}(\theta)$. In this case the inductance representing coupling between the q -axis stator winding and the q -axis amortisseur winding is, for example,

$$\begin{aligned} L_{qsqr} &= \mu_0 r l \int_{-\frac{\alpha\pi}{2} + \theta_r}^{\frac{\alpha\pi}{2} + \theta_r} N_{qs}(\phi, \theta_r) N_{qr}(\phi, \theta_r) g^{-1}(\phi, \theta_r) d\phi \\ &= \frac{\mu_0 r l}{g_{min}} (2) \int_{-\frac{\alpha\pi}{2} + \theta_r}^{\frac{\alpha\pi}{2} + \theta_r} \left(\frac{N_{s1}}{2} \right) \left(\frac{N_{qr1}}{2} \right) \cos^2(\phi - \theta_r) d\phi \\ &= \frac{\mu_0 r l}{g_{min}} N_{s1} N_{qr1} \left(\frac{\pi}{4} \right) \left[\alpha - \frac{\sin \alpha \pi}{\pi} \right] \end{aligned} \quad (3.95)$$

$$= \frac{\mu_0 r l}{g_{min}} N_{s1} N_{qr1} \left(\frac{\pi}{4} \right) k_q \quad (3.96)$$

In general, k_q is defined by Eq. (3.92).

In a similar manner,

$$\begin{aligned} L_{dsdr} &= \mu_0 r l \int_{-\frac{\alpha\pi}{2} + \theta_r}^{\frac{\alpha\pi}{2} + \theta_r} N_{ds}(\phi, \theta_r) N_{dr}(\phi, \theta_r) g^{-1}(\phi, \theta_r) d\phi \\ L_{dsdr} &= \frac{\mu_0 r l}{g_{min}} (2) \int_{-\frac{\alpha\pi}{2} + \theta_r}^{\frac{\alpha\pi}{2} + \theta_r} \frac{N_{s1}}{2} \frac{N_{dr1}}{2} \sin^2(\theta_r - \phi) d\phi \end{aligned} \quad (3.97)$$

$$= \frac{\mu_0 r l}{g_{min}} N_{s1} N_{dr1} \left(\frac{\pi}{4} \right) k_d \quad (3.98)$$

where k_d is, in general, given by Eq. (3.91). Finally,

$$L_{dsfr} = \frac{\mu_0 r l}{g_{min}} N_{s1} N_{fr1} \left(\frac{\pi}{4} \right) k_d \quad (3.99)$$

It is not difficult to show that all of the remaining coupling terms between the stator and rotor circuits are identically zero. Hence, the stator flux linkage referred to a $d-q-n$ coordinate system “attached to the rotor” reduces finally to:

$$\lambda_{dqns} = \mathbf{L}_{dqns} \mathbf{i}_{dqns} + \mathbf{L}_{dqnsr} \mathbf{i}_{dqfr} \quad (3.100)$$

or, explicitly,

$$\begin{bmatrix} \lambda_{ds} \\ \lambda_{qs} \\ \lambda_{ns} \end{bmatrix} = \begin{bmatrix} L_{ls} + L_{dsds} & 0 & 0 \\ 0 & L_{ls} + L_{qsqs} & 0 \\ 0 & 0 & L_{ls} \end{bmatrix} \begin{bmatrix} i_{ds} \\ i_{qs} \\ i_{ns} \end{bmatrix} + \begin{bmatrix} L_{dsdr} & 0 & L_{dsfr} \\ 0 & L_{qsqr} & 0 \\ 0 & 0 & 0 \end{bmatrix} \begin{bmatrix} i_{dr} \\ i_{qr} \\ i_{fr} \end{bmatrix} \quad (3.101)$$

3.10 $d-q$ Transformation of the Rotor Flux Linkage Equation

Because the $a-b-c$ stator currents have been transformed to the $d-q-n$ axes, the rotor flux linkage equation must also be changed to account for this change of variable. With the new variables, the rotor flux linkage equation can be written

$$dqfr = \mathbf{L}_{abcsr}^t \mathbf{T}(\theta_r)^{-1} [\mathbf{T}(\theta_r) \mathbf{i}_{abcs}] + \mathbf{L}_{dqfr} \mathbf{i}_{dqfr} \quad (3.102)$$

or, in terms of previously defined variables,

$$dqfr = \mathbf{L}_{abcsr}^t \mathbf{T}(\theta_r)^{-1} \mathbf{i}_{dqns} + \mathbf{L}_{dqfr} \mathbf{i}_{dqfr} \quad (3.103)$$

It can be recalled from Chapter 2 that

$$\mathbf{T}(\theta)^{-1} = \frac{3}{2} \mathbf{T}(\theta)^t$$

Equation (3.98) can therefore be written as

$$dqfr = \frac{3}{2} \mathbf{L}_{abcsr}^t \mathbf{T}(\theta_r)^t \mathbf{i}_{dqns} + \mathbf{L}_{dqfr} \mathbf{i}_{dqfr} \quad (3.104)$$

and, since $\mathbf{A}^t \mathbf{B}^t = (\mathbf{B}\mathbf{A})^t$,

$$dqfr = \frac{3}{2} [\mathbf{T}(\theta_r) \mathbf{L}_{abcsr}]^t + \mathbf{L}_{dqfr} \mathbf{i}_{dqfr}$$

The coefficient of \mathbf{i}_{dqns} is nothing more than the transpose of $\mathbf{T}(\theta) \mathbf{L}_{abcsr}$, which was evaluated previously, Eq. (3.22). Hence, Eq. (3.102) becomes, finally,

$$dqfr = \frac{3}{2} \mathbf{L}_{dqnsr}^t \mathbf{i}_{dqns} + \mathbf{L}_{dqfr} \mathbf{i}_{dqfr} \quad (3.105)$$

Note the presence of the “3/2” term in Eq. (3.104), which can be compared with Eq. (3.100).

The final inductance matrix to be determined is \mathbf{L}_{dqfr} . In this case the procedure is straightforward. It is readily determined that

$$\mathbf{L}_{dqfr} = \begin{bmatrix} L_{ldr} + L_{drdr} & 0 & L_{drfr} \\ 0 & L_{lqr} + L_{qrqr} & 0 \\ L_{drfr} & 0 & L_{lfr} + L_{frfr} \end{bmatrix} \quad (3.106)$$

where

$$L_{drdr} = \frac{\mu_0 r l}{g_{min}} N_{dr1}^2 \left(\frac{\pi}{4}\right) k_d \quad (3.107)$$

$$L_{qrqr} = \frac{\mu_0 r l}{g_{min}} N_{qr1}^2 \left(\frac{\pi}{4}\right) k_q \quad (3.108)$$

$$L_{frfr} = \frac{\mu_0 r l}{g_{min}} N_{fr1}^2 \left(\frac{\pi}{4}\right) k_d \quad (3.109)$$

$$L_{drfr} = \frac{\mu_0 r l}{g_{min}} N_{dr1} N_{fr1} \left(\frac{\pi}{4}\right) k_d \quad (3.110)$$

The above flux linkage vector equation is equivalent to the three scalar equations

$$\lambda_{dr} = \frac{3}{2} L_{dsdr} i_{ds} + (L_{ldr} + L_{drdr}) i_{dr} + L_{drfr} i_{fr} \quad (3.111)$$

$$\lambda_{qr} = \frac{3}{2} L_{qsqr} i_{qs} + (L_{lqr} + L_{qrqr}) i_{qr} \quad (3.112)$$

$$\lambda_{fr} = \frac{3}{2} L_{dsfr} i_{ds} + (L_{lfr} + L_{frfr}) i_{fr} + L_{drfr} i_{dr} \quad (3.113)$$

3.11 Power Input

In general, the power input to the machine is expressed in matrix form by the vector “dot product” equation

$$P_e = \mathbf{v}_{abcs}^t \cdot \mathbf{i}_{abcs} + \mathbf{v}_{dqfr}^t \cdot \mathbf{i}_{dqfr} \quad (3.114)$$

Upon referring the *a-b-c* stator variables the *q-d-n* variables

$$P_e = \frac{3}{2} \mathbf{v}_{dqns}^t \cdot \mathbf{i}_{dqns} + \mathbf{v}_{dqfr}^t \cdot \mathbf{i}_{dqfr} \quad (3.115)$$

Writing this equation in scalar form, one obtains

$$P_e = \frac{3}{2} (v_{ds} i_{ds} + v_{qs} i_{qs} + v_{ns} i_{ns}) + v_{dr} i_{dr} + v_{qr} i_{qr} + v_{fr} i_{fr} \quad (3.116)$$

Notice that since the rotor circuits are already expressed in “*d-q*” form, the input power supplied from the rotor side does not contain a “3/2” term, as needed for the stator.

3.12 Torque Equation

Because the stator self inductances and mutual inductances are functions of θ_r , as well as the stator-rotor mutual inductances, computation of the electromagnetic torque in terms of phase variables becomes quite involved. However, the solution is much more palatable in *d-q* form. It has already been demonstrated that in matrix form in the rotor reference frame, the stator voltage equation can be expressed by

$$\mathbf{v}_{dqns} = r_s \mathbf{i}_{dqns} + \frac{d}{dt} \mathbf{dqns} + \mathbf{r}_r \times \mathbf{dqns} \quad (3.117)$$

and the rotor equations by

$$\mathbf{v}_{dqfr} = \mathbf{r}_r \mathbf{i}_{dqfr} + \frac{d}{dt} \mathbf{dqfr} \quad (3.118)$$

Substituting these equations into the *d-q* power equation

$$\begin{aligned} P_e = & \frac{3}{2} \left[r_s \mathbf{i}_{dqns}^t \cdot \mathbf{i}_{dqns} + \frac{d}{dt} \left(\frac{t}{dqns} \right) \cdot \mathbf{i}_{dqns} + \left(\mathbf{r}_r \times \mathbf{dqns} \right) \cdot \mathbf{i}_{dqns} \right] \\ & + \mathbf{r}_r \mathbf{i}_{dqfr}^t \cdot \mathbf{i}_{dqfr} + \frac{d}{dt} \left(\frac{t}{dqfr} \right) \cdot \mathbf{i}_{dqfr} \end{aligned} \quad (3.119)$$

It is clear that the first and fourth terms account for the copper losses in the stator and rotor, respectively. The second and fifth terms represent the time rate of change of stored magnetic energy. By a process of elimination, the third term therefore has to correspond to the energy conversion term. It is useful to

view this third term as a space vector. Since the power output is equal to the torque times mechanical speed, one can write in space vector form

$$T_e \omega_{rm} = \left(\frac{3}{2}\right) (\hat{\omega}_r \times \hat{\lambda}_{dqns})^t \cdot \hat{i}_{dqns} \quad (3.120)$$

where ω_{rm} represents the actual mechanical speed of the rotor. The actual speed is related to the speed of an equivalent two-pole machine by

$$\omega_{rm} \hat{u}_{ns} = \frac{2\omega_r}{P} \hat{u}_{ns} \quad (3.121)$$

Hence, this equation becomes

$$T_e = \left(\frac{3}{2}\right) \left(\frac{P}{2}\right) (\hat{u}_{ns} \times \hat{\lambda}_{dqns})^t \cdot \hat{i}_{dqns} \quad (3.122)$$

However, if \hat{a} , \hat{b} and \hat{c} are vectors, then

$$(\hat{a} \times \hat{b})^t \cdot \hat{c} = \hat{a}^t \cdot \hat{b} \times \hat{c}$$

this equation can be written as

$$T_e = \left(\frac{3}{2}\right) \left(\frac{P}{2}\right) \hat{u}_{ns}^t \cdot \hat{\lambda}_{dqns} \times \hat{i}_{dqns} \quad (3.123)$$

Equation (3.123) states that the electromagnetic torque can be viewed as the instantaneous cross product of the stator flux linkage vector and the stator current vector. Because of the dot product taken with respect to the \hat{u}_{ns} direction, only the cross product of the flux linkage and current components in the *a d-q* plane contributes to torque production since it is only the cross product of these components which results in a vector in the *n*-axis direction and therefore is non-zero when dotted with the unit vector in the direction of the *n*-axis.

If this equation is reduced to vector form, it can be readily shown that the scalar version for electromagnetic torque is

$$T_e = \frac{3P}{22} (\lambda_{ds} i_{qs} - \lambda_{qs} i_{ds}) \quad (3.124)$$

This expression for torque is, in fact, valid in any reference frame and not restricted to the case where the rotating reference frame is tied to the rotor (rotor reference frame). It is important to mention, however, that

$$T_e \neq \frac{3P}{22} (\lambda_{qr} i_{dr} - \lambda_{dr} i_{qr}) \quad (3.125)$$

Although Eq. (3.125) is valid for induction machines, it is incorrect for synchronous machines.

3.13 Summary of Synchronous Machine Equations Expressed in Physical Units

A summary of the system equations for a synchronous machine in a rotor reference frame, typically called Park's equations after their originator R. H. Park [5]¹, are as follows:

Voltage Equations:

$$v_{ds} = r_s i_{ds} - \omega_r \lambda_{qs} + p \lambda_{ds} \quad (3.126)$$

$$v_{qs} = r_s i_{qs} + \omega_r \lambda_{ds} + p \lambda_{qs} \quad (3.127)$$

$$v_{ns} = r_s i_{ns} + p \lambda_{ns} \quad (3.128)$$

$$v_{dr} = r_{dr} i_{dr} + p \lambda_{dr} \quad (3.129)$$

$$v_{qr} = r_{qr} i_{qr} + p \lambda_{qr} \quad (3.130)$$

$$v_{fr} = r_{fr} i_{fr} + p \lambda_{fr} \quad (3.131)$$

Flux Linkage Equations:

$$\lambda_{ds} = [L_{ls} + L_{dsds}]i_{ds} + L_{dsdr}i_{dr} + L_{dsfr}i_{fr} \quad (3.132)$$

$$\lambda_{qs} = [L_{ls} + L_{qsqs}]i_{qs} + L_{qsqr}i_{qr} \quad (3.133)$$

$$\lambda_{ns} = L_{ls}i_{ns} \quad (3.134)$$

$$\lambda_{dr} = (L_{ldr} + L_{drdr})i_{dr} + \frac{3}{2}L_{dsdr}i_{ds} + L_{drfr}i_{fr} \quad (3.135)$$

$$\lambda_{qr} = (L_{lqr} + L_{qrqr})i_{qr} + \frac{3}{2}L_{dsdr}i_{ds} + L_{drfr}i_{fr} \quad (3.136)$$

$$\lambda_{fr} = (L_{lfr} + L_{frfr})i_{fr} + \frac{3}{2}L_{dsfr}i_{ds} + L_{drfr}i_{dr} \quad (3.137)$$

Torque and Power Equations:

$$T_e = \frac{3P}{2}(\lambda_{ds}i_{qs} - \lambda_{qs}i_{ds}) \quad (3.138)$$

1. Robert H. Park—b. 1902, d. 1994.

$$P_e = \frac{3}{2}(v_{ds}i_{ds} + v_{qs}i_{qs} + v_{ns}i_{ns}) + v_{dr}i_{dr} + v_{qr}i_{qr} + v_{fr}i_{fr} \quad (3.139)$$

It should be noted that in the attempt to be general, the possibility of the two damper windings being excited from external supplies (v_{qr} and v_{dr} non-zero) has been included. However, for all practical machines these two voltages are identically zero.

Note that the flux linking the “ qr ” circuit due to a unit current in the “ qs ” circuit is not the same as the flux linking the “ qs ” circuit due to a unit current in the “ qr ” circuit. This non-reciprocal mutual inductance results from starting with a “three-phase” stator and a “two-phase” rotor and then choosing a transformation T which does not preserve the length of the stator current and voltage vectors in the $d-q-n$ axes. An equivalent circuit which follows from the above equations is shown in [Figure 3.14](#).

3.14 Turns Ratio Transformation of the Flux Linkage Equations

The equivalent circuit that has been obtained is still rather complex, since a non-symmetrical mutual inductance now exists. In order to establish a simpler equivalent circuit, consider another change of variables such that the magnetizing inductance corresponding to each mesh current in a given axis is identical. Consider first the d -axis flux linkages. They are

$$\lambda_{ds} = (L_{ls} + L_{dsds})i_{ds} + L_{dsdr}i_{dr} + L_{dsfr}i_{fr} \quad (3.140)$$

$$\lambda_{dr} = \frac{3}{2}L_{dsdr}i_{ds} + (L_{ldr} + L_{drdr})i_{dr} + L_{drfr}i_{fr} \quad (3.141)$$

$$\lambda_{fr} = \frac{3}{2}L_{dsdr}i_{ds} + L_{drfr}i_{dr} + (L_{lfr} + L_{frfr})i_{fr} \quad (3.142)$$

In terms of physical dimensions, the d -axis mutual magnetizing inductances are defined as

$$L_{dsds} = \frac{3\mu_0 r l}{2g_{min}} N_{s1}^2 \frac{\pi}{4} k_d \quad (3.143)$$

$$L_{dsfr} = \frac{\mu_0 r l}{g_{min}} N_{s1} N_{fr1} \frac{\pi}{4} k_d \quad (3.144)$$

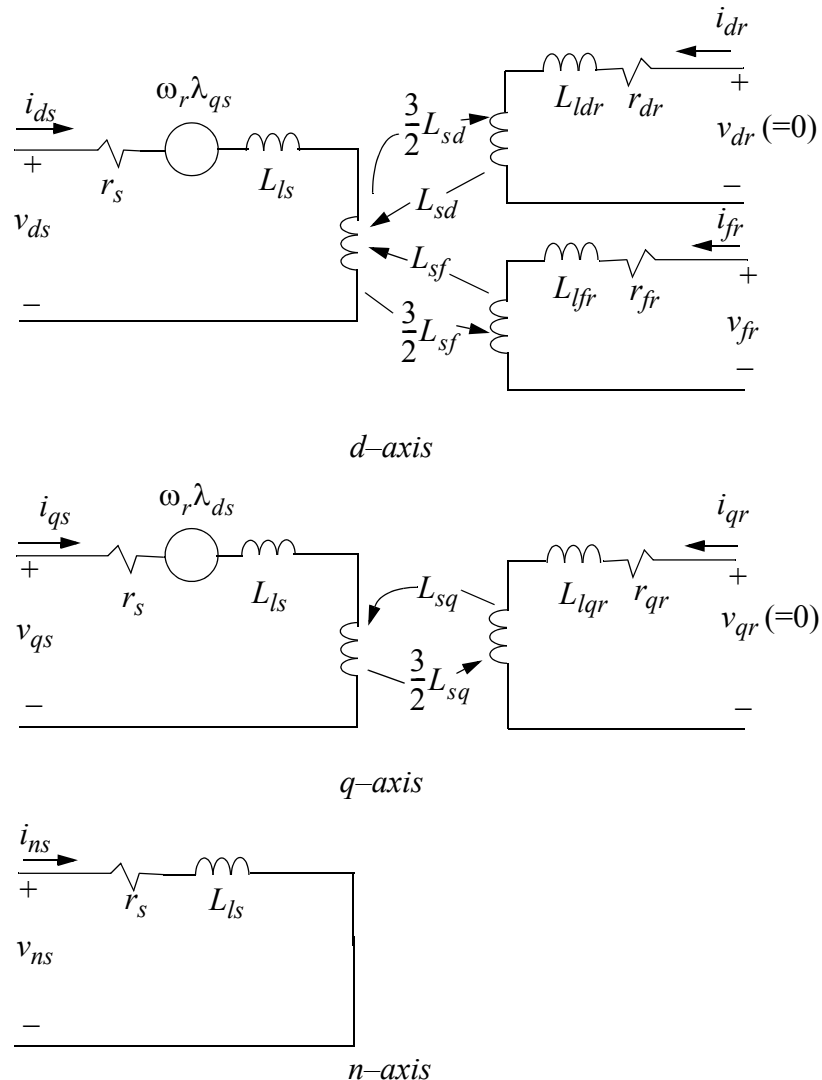


Figure 3.14 Equivalent circuit of synchronous machine represented in a rotor reference frame.

$$L_{dsdr} = \frac{\mu_0 r l}{g_{min}} N_{s1} N_{dr1} \frac{\pi}{4} k_d \quad (3.145)$$

$$L_{drdr} = \frac{\mu_0 r l}{g_{min}} N_{dr1}^2 \frac{\pi}{4} k_d \quad (3.146)$$

$$L_{frfr} = \frac{\mu_0 r l}{g_{min}} N_{fr1}^2 \frac{\pi}{4} k_d \quad (3.147)$$

$$L_{drfr} = \frac{\mu_0 r l}{g_{min}} N_{dr1} N_{fr1} \frac{\pi}{4} k_d \quad (3.148)$$

The quantity L_{dsds} will now be formally denoted as the direct axis magnetizing inductance L_{md} .

$$L_{md} \equiv L_{dsds} = \frac{3 \mu_0 r l}{2 g_{min}} N_{s1}^2 \frac{\pi}{4} k_d \quad (3.149)$$

It is apparent that all of the remaining *d*-axis mutual and magnetizing reactances are related to L_{md} . In fact, it can be verified that

$$L_{md} = \frac{3}{2} \frac{N_{s1}}{N_{dr1}} L_{dsdr} \quad (3.150)$$

$$= \frac{3}{2} \frac{N_{s1}}{N_{fr1}} L_{dsfr} \quad (3.151)$$

$$= \frac{3}{2} \frac{N_{s1}^2}{N_{dr1}} L_{drdr} \quad (3.152)$$

$$= \frac{3}{2} \frac{N_{s1}^2}{N_{dr1}^2} L_{frfr} \quad (3.153)$$

$$= \frac{3}{2} \frac{N_{s1}^2}{N_{dr1} N_{fr1}} L_{drfr} \quad (3.154)$$

Taking a hint from this, the *d*-axis flux linkage equations can be manipulated to the form

$$\begin{aligned} \lambda_{ds} &= [L_{ls} + L_{md}] i_{ds} + \left[\frac{3}{2} \frac{N_{s1}}{N_{dr1}} L_{dsdr} \right] \left[\frac{2}{3} \frac{N_{dr1}}{N_{s1}} i_{dr} \right] \\ &\quad + \left[\frac{3}{2} \frac{N_{s1}}{N_{fr1}} L_{dsfr} \right] \left[\frac{2}{3} \frac{N_{fr1}}{N_{s1}} i_{fr} \right] \end{aligned} \quad (3.155)$$

$$\begin{aligned} \frac{N_{s1}}{N_{dr1}} \lambda_{dr} = & \left[\frac{3}{2} \frac{N_{s1}^2}{N_{dr1}^2} (L_{ldr} + L_{drdr}) \right] \left[\frac{2}{3} \frac{N_{dr1}}{N_{s1}} i_{dr} \right] + \left[\frac{3}{2} \frac{N_{s1}}{N_{dr1}} L_{dsdr} \right] i_{ds} \\ & + \left[\frac{3}{2} \frac{N_{s1}}{N_{dr1} N_{fr1}} L_{drfr} \right] \left[\frac{2}{3} \frac{N_{fr1}}{N_{s1}} i_{fr} \right] \end{aligned} \quad (3.156)$$

$$\begin{aligned} \frac{N_{s1}}{N_{fr1}} \lambda_{fr} = & \left[\frac{3}{2} \frac{N_{s1}^2}{N_{fr1}^2} (L_{lfr} + L_{frfr}) \right] \left[\frac{2}{3} \frac{N_{fr1}}{N_{s1}} i_{fr} \right] + \left[\frac{3}{2} \frac{N_{s1}}{N_{fr1}} L_{dsfr} \right] i_{ds} \\ & + \left[\frac{3}{2} \frac{N_{s1}^2}{N_{fr1} N_{dr1}} L_{drfr} \right] \left[\frac{2}{3} \frac{N_{dr1}}{N_{s1}} i_{dr} \right] \end{aligned} \quad (3.157)$$

If one defines

$$\lambda_{dr}' = \frac{N_{s1}}{N_{dr1}} \lambda_{dr} \quad (3.158)$$

$$i_{dr}' = \frac{2}{3} \frac{N_{dr1}}{N_{s1}} i_{dr} \quad (3.159)$$

$$\lambda_{fr}' = \frac{N_{s1}}{N_{fr1}} \lambda_{fr} \quad (3.160)$$

$$i_{fr}' = \frac{2}{3} \frac{N_{fr1}}{N_{s1}} i_{fr} \quad (3.161)$$

$$L_{lfr}' = \frac{3}{2} \frac{N_{s1}^2}{N_{fr1}^2} L_{lfr} \quad (3.162)$$

$$L_{ldr}' = \frac{3}{2} \frac{N_{s1}^2}{N_{dr1}^2} L_{ldr} \quad (3.163)$$

the three direct axis flux linkage equations can now be written in the simplified form

$$\lambda_{ds} = L_{ls} i_{ds} + L_{md} (i_{ds} + i_{dr}' + i_{fr}') \quad (3.164)$$

$$\lambda_{dr}' = L_{ldr}' i_{dr}' + L_{md} (i_{ds} + i_{dr}' + i_{fr}') \quad (3.165)$$

$$\lambda_{fr}' = L_{lfr}' i_{fr}' + L_{md} (i_{ds} + i_{dr}' + i_{fr}') \quad (3.166)$$

In a similar fashion the q -axis flux linkage equations can be derived. They are

$$\lambda_{qs} = L_{ls} i_{qs} + L_{mq} (i_{qs} + i_{qr}')$$
 (3.167)

$$\lambda_{qr}' = L_{lqr}' i_{qr}' + L_{mq} (i_{qs} + i_{qr}')$$
 (3.168)

where

$$\lambda_{qr}' = \frac{N_{s1}}{N_{qr1}} \lambda_{qr}$$
 (3.169)

$$i_{qr}' = \frac{2N_{qr1}}{3N_{s1}} i_{qr}$$
 (3.170)

$$L_{lqr}' = \frac{3}{2} \frac{N_{s1}^2}{N_{qr1}^2} L_{lqr}$$
 (3.171)

and

$$L_{mq} = \frac{3\mu_0 r l}{2g_{min}} N_{s1}^2 \frac{\pi}{4} k_q$$
 (3.172)

The quantity L_{mq} is termed the *quadrature axis magnetizing inductance*. Note that the non-reciprocal mutual inductances have been eliminated from the five flux linkage equations.

Voltage Equations

The three d -axis voltage equations can be manipulated to form

$$v_{ds} = r_s i_{ds} - \omega_r \lambda_{qs} + \frac{d}{dt} \lambda_{ds} \quad (\text{no change})$$
 (3.173)

$$\frac{N_{s1}}{N_{dr1}} v_{dr} = \left[\frac{3}{2} \frac{N_{s1}^2}{N_{dr1}^2} r_{dr} \right] \left[\frac{2N_{dr1}}{3N_{s1}} i_{dr} \right] + \frac{d}{dt} \left(\frac{N_{s1}}{N_{dr1}} \lambda_{dr} \right)$$
 (3.174)

$$\frac{N_{s1}}{N_{fr1}} v_{fr} = \left[\frac{3}{2} \frac{N_{s1}^2}{N_{fr1}^2} r_{fr} \right] \left[\frac{2N_{fr1}}{3N_{s1}} i_{fr} \right] + \frac{d}{dt} \left(\frac{N_{s1}}{N_{fr1}} \lambda_{fr} \right)$$
 (3.175)

Defining

$$v_{dr}' = \frac{N_{s1}}{N_{dr1}} v_{dr}$$
 (3.177)

$$v_{fr}' = \frac{N_{s1}}{N_{fr1}} v_{fr} \quad (3.178)$$

$$r_{dr}' = \frac{3}{2} \frac{N_{s1}^2}{N_{dr1}^2} r_{dr} \quad (3.179)$$

$$r_{fr}' = \frac{3}{2} \frac{N_{s1}^2}{N_{fr1}^2} r_{fr} \quad (3.180)$$

and utilizing the already defined quantities, i'_{dr} , i'_{fr} , λ'_{dr} , λ'_{fr} , the voltage equations referred to the stator become

$$v_{ds} = r_s i_{ds} - \omega_r \lambda_{qs} + p \lambda_{ds} \quad (\text{no change}) \quad (3.181)$$

$$v_{dr}' = r_{dr}' i_{dr}' + \frac{d}{dt} \lambda_{dr}' \quad (3.182)$$

$$v_{fr}' = r_{fr}' i_{fr}' + \frac{d}{dt} \lambda_{fr}' \quad (3.183)$$

Similarly, the q -axis voltage equations referred to the stator are

$$v_{qs} = r_s i_{qs} + \omega_r \lambda_{ds} + \frac{d}{dt} \lambda_{qs} \quad (\text{no change}) \quad (3.184)$$

$$v_{qr}' = r_{qr}' i_{qr}' + \frac{d}{dt} \lambda_{qr}' \quad (3.185)$$

wherein

$$v_{qr}' = \frac{N_{s1}}{N_{qr1}} v_{qr} \quad (3.186)$$

$$r_{qr}' = \frac{3}{2} \frac{N_{s1}^2}{N_{qr1}^2} r_{qr} \quad (3.187)$$

Finally, note that the n -axis voltage and flux linkage equations are not altered by the turns ratio transformation, so that

$$v_{ns} = r_s i_{ns} + \frac{d}{dt} \lambda_{ns} \quad (\text{no change}) \quad (3.188)$$

Torque Equation

Since the stator variables are not altered by the turns ratio transformation, the torque equation is unaltered. That is, the torque equation remains as

$$T_e = \frac{3P}{22}(\lambda_{ds}i_{qs} - \lambda_{qs}i_{ds}) \quad (3.189)$$

Power Equation

The power equation is

$$P_e = \frac{3}{2}(v_{qs}i_{qs} + v_{ds}i_{ds} + v_{ns}i_{ns}) + v_{qr}i_{qr} + v_{dr}i_{dr} + v_{fr}i_{fr} \quad (3.190)$$

This expression can be manipulated to the form

$$\begin{aligned} P_e = & \frac{3}{2}(v_{ds}i_{ds} + v_{qs}i_{qs} + v_{ns}i_{ns}) + \frac{3}{2} \frac{N_{s1}}{N_{dr1}} v_{dr} \left(\frac{2}{3} \frac{N_{dr1}}{N_{s1}} i_{dr} \right) \\ & + \frac{3}{2} \left(\frac{N_{s1}}{N_{qr1}} v_{qr} \right) \frac{2}{3} \left(\frac{N_{qr1}}{N_{s1}} i_{qr} \right) + \frac{3}{2} \left(\frac{N_{s1}}{N_{fr1}} v_{fr} \right) \frac{2}{3} \left(\frac{N_{fr1}}{N_{s1}} i_{fr} \right) \end{aligned} \quad (3.191)$$

Upon incorporating the already defined variables, the power equation after the turns ratio transformation becomes

$$P_e = \frac{3}{2}(v_{ds}i_{ds} + v_{qs}i_{qs} + v_{ns}i_{ns} + v_{dr}'i_{dr}' + v_{qr}'i_{qr}' + v_{fr}'i_{fr}') \quad (3.192)$$

Note that the “3/2” term now operates on the entire power expression. It can be recalled that the rotor source voltages v_{dr} and v_{qr} are identically zero. Hence, the 3/2 issue is not particularly important here, since the power input to the machine from the rotor side is very small, often being only a small percentage, mainly from the field circuit. However, in computing losses the 3/2 must not be forgotten. The power lost in the stator and rotor copper is

$$P_{s(cu)} = \frac{3}{2}(r_s i_{ds}^2 + r_s i_{qs}^2) \quad (3.193)$$

$$P_{r(cu)} = \frac{3}{2}(r_{dr}' i_{dr}'^2 + r_{qr}' i_{qr}'^2 + r_{fr}' i_{fr}'^2) \quad (3.194)$$

[Figure 3.15](#) shows the synchronous machine equivalent circuit which results when the rotor circuits are referred to the stator by a turns ratio transformation. Note that reciprocity has now been reestablished. Also, the turns ratio

transformation permits the use of a transformer-like equivalent circuit in which the magnetizing inductance is common to all branches.

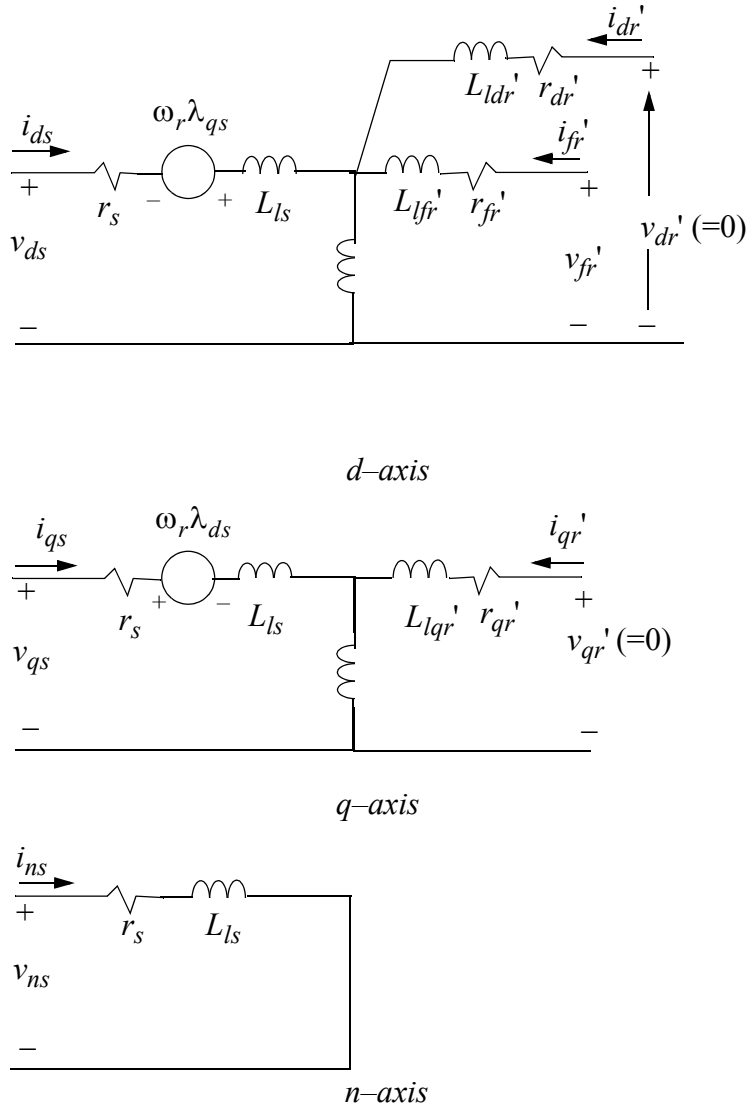


Figure 3.15 Equivalent circuit of a synchronous machine after turns ratio transformation.

3.15 System Equations in Physical Units Using Hybrid Flux Linkages

It is frequently useful for the purpose of analysis to define hybrid flux linkage variables by multiplying all flux linkages by a base angular frequency (generally $2\pi \cdot 60$ or $2\pi \cdot 50$). That is, let

$$\psi_{ds} = \omega_b \lambda_{ds} \quad (3.195)$$

$$\psi_{dr}' = \omega_b \lambda_{dr}' \quad (3.196)$$

and so forth for λ_{qs} , λ_{ns} , λ_{qr}' , and λ_{fr}' . The final resulting equations needed to define transient behavior of a synchronous machine expressed in a reference frame fixed in the rotor are:

$$v_{ds} = r_s i_{ds} + \frac{p}{\omega_b} \psi_{ds} - \frac{\omega_r}{\omega_b} \psi_{qs} \quad (3.197)$$

$$v_{qs} = r_s i_{qs} + \frac{p}{\omega_b} \psi_{qs} + \frac{\omega_r}{\omega_b} \psi_{ds} \quad (3.198)$$

$$v_{ns} = r_s i_{ns} + \frac{p}{\omega_b} \psi_{ns} \quad (3.199)$$

$$v_{dr}' = 0 = r_{dr}' i_{dr}' + \frac{P}{\omega_b} \psi_{dr}' \quad (3.200)$$

$$v_{qr}' = 0 = r_{qr}' i_{qr}' + \frac{p}{\omega_b} \psi_{qr}' \quad (3.201)$$

$$v_{fr}' = r_{fr}' i_{fr}' + \frac{p}{\omega_b} \psi_{fr}' \quad (3.202)$$

where

$$\psi_{ds} = x_{ls} i_{ds} + \psi_{md} \quad (3.203)$$

$$\psi_{qs} = x_{ls} i_{qs} + \psi_{mq} \quad (3.204)$$

$$\psi_{ns} = x_{ls} i_{ns} \quad (3.205)$$

$$\psi_{dr}' = x_{ldr}' i_{dr}' + \psi_{md} \quad (3.206)$$

$$\psi_{qr}' = x_{lqr}' i_{qr}' + \psi_{mq} \quad (3.207)$$

$$\psi_{fr}' = x_{lfr}' i_{fr}' + \psi_{md} \quad (3.208)$$

and wherein, for convenience, the air gap portions of the d - and q -axes flux linkages have been defined as

$$\Psi_{md} = x_{md}(i_{ds} + i_{dr}' + i_{fr}') \quad (3.209)$$

$$\Psi_{mq} = x_{mq}(i_{qs} + i_{qr}') \quad (3.210)$$

Note that the speed in Eqs. (3.197) to (3.202) has, in effect, been per unitized. Also it is important to observe that the hybrid flux linkages ψ ("pitchfork" flux linkages) have the units of volts and are related to the currents by reactances in ohms rather than by inductances. It should be emphasized that the normalization factor ω_b is a constant in this system of equations even if the applied frequency itself is a variable and remains constant even if the line frequency itself is a variable.

In Eqs. (3.203) to (3.210),

$$x_{ls} = \omega_b L_{ls} \quad (3.211)$$

$$x_{lqr}' = \omega_b L_{lqr}' \quad (3.212)$$

$$x_{ldr}' = \omega_b L_{ldr}' \quad (3.213)$$

$$x_{lfr}' = \omega_b L_{lfr}' \quad (3.214)$$

$$x_{md} = \omega_b L_{md} \quad (3.215)$$

$$x_{mq} = \omega_b L_{mq} \quad (3.216)$$

Finally in terms of the new hybrid flux linkage variable, the power and torque equations are

$$P_e = \frac{3}{2}(\nu_{ds}i_{ds} + \nu_{qs}i_{qs} + \nu_{ns}i_{ns} + \nu_{dr}'i_{dr}' + \nu_{qr}'i_{qr}' + \nu_{fr}'i_{fr}') \quad (3.217)$$

$$T_e = \frac{3P}{22}\frac{1}{\omega_b}(\Psi_{ds}i_{qs} - \Psi_{qs}i_{ds}) \quad (3.218)$$

3.16 Synchronous Machine Equations in Per Unit Form

3.16.1 Base Quantities

Thus far all of the machine equations have been written in terms of actual units. For purposes of analysis, it is convenient to convert these equations to a normalized or *per unit* form. The choice of reference or *base* quantities is arbitrary but is usually related to the nameplate rating of the machine. Assume that the nameplate (NP) specifies the following:

Stator Line Frequency:	f_{NP} (Hz)
Line-to-Line Voltage:	V_{NP} (Volts RMS)
Pole Number:	P_{NP}
Efficiency at Rated Output:	η_{NP}
Power Factor at Rated Output:	PF_{NP}

and either

$$\text{Horsepower: } HP_{NP} \text{ (Motor)}$$

or

$$\text{Volt Ampere Capacity: } VA_{NP} \text{ (Generator)}$$

or

$$\text{Electrical Power Capacity: } WATTS_{NP} \text{ (Generator)}$$

The base voltage and angular frequency are generally selected as

$$\text{Voltage Base} = V_b = \frac{\sqrt{2} V_{NP}}{\sqrt{3}} \quad (\text{Volts Peak})$$

$$\text{Base Electrical Angular Velocity} = \omega_b = 2\pi f_{NP} \quad (\text{rad/sec})$$

The choice for power base is the third variable needed to completely specify the per unit system. Unfortunately, there are many possibilities for base power. Consider first the machine operating as a motor. In this case many options for base power are possible. For example, if efficiency and power factor are included in the definition of the base power, then

$$\text{Volt Ampere Base} = S_b = \frac{746 HP_{NP}}{\eta_{NP} \cdot PF_{NP}} \quad (3.219)$$

In this case the per unit current will equal unity when rated input KVA is reached at rated frequency. Another definition is

$$S_b = 746 HP_{NP} \quad (3.220)$$

in which case base power is defined in terms of mechanical input (or output) power.

In applications where the machine operates as a generator, the choice is a little more straightforward. In such cases it is fairly standard to define the power base as

$$S_b = VA_{NP} \quad (3.221)$$

or

$$S_b = \frac{WATTS_{NP}}{PF_{NP}} \quad (3.222)$$

However, other definitions for base power or volt-amperes are again clearly possible.

The following additional base quantities can now be defined,

$$\text{Current Base} = I_b = \frac{2S_b}{3V_b} \quad (\text{amps peak}) \quad (3.223)$$

$$\text{Impedance Base} = Z_b = \frac{V_b}{I_b} = \frac{3V_b^2}{2S_b} \quad (\text{ohms}) \quad (3.224)$$

Base Mechanical Angular

$$\text{Velocity} = \omega_{mb} = 2\pi \frac{f_{NP}}{(P_{NP})/2} \quad (\text{rad/sec}) \quad (3.225)$$

$$\text{Torque Base} = T_b = \frac{S_b}{\omega_{mb}} = \left(\frac{P_{NP}}{2}\right) \frac{S_b}{\omega_b} (nt \cdot m) \quad (3.226)$$

It is important to realize that the definitions of S_b , V_b , and I_b are consistent. That is,

$$S_b = \frac{3}{2} V_b I_b \quad (3.227)$$

$$= \frac{3}{2} (\sqrt{2} V_{b(rms)}) (\sqrt{2} I_{b(rms)}) \quad (3.228)$$

$$= 3 V_{b(rms)} I_{b(rms)} \quad (3.229)$$

3.16.2 Voltage Equations

First consider the voltage equations expressed in per unit form. This can be done by dividing all of the voltage differential equations by V_b or $Z_b I_b$ as appropriate. For example, the qs -axis voltage equation can be written

$$\frac{v_{ds}}{V_b} = \frac{p}{\omega_b} \frac{\Psi_{ds}}{V_b} - \frac{\Psi_{qs}}{V_b} \frac{\omega_r}{\omega_b} + \frac{r_s}{Z_b} \frac{i_{ds}}{I_b} \quad (3.230)$$

Now define

$$v_{DS} = \frac{v_{ds}}{V_b} \quad (3.231)$$

$$\Psi_{DS} = \frac{\Psi_{ds}}{V_b} \quad (3.232)$$

$$\Psi_{QS} = \frac{\Psi_{qs}}{V_b} \quad (3.233)$$

$$i_{DS} = \frac{i_{ds}}{I_b} \quad (3.234)$$

$$r_S = \frac{r_s}{Z_b} \quad (3.235)$$

$$\omega_R = \frac{\omega_r}{\omega_b} \quad (3.236)$$

The d -axis stator voltage equation can now be written in per unit form as

$$v_{DS} = \frac{p}{\omega_b} \Psi_{DS} - \Psi_{QS} \omega_R + r_S i_{DS} \quad (3.237)$$

Note that this equation has exactly the same form as the original equation. The remaining four voltage equations can be handled in the same manner. Upon defining $v_{QS} = v_{qs}/V_b$, etc., three additional per unit voltage equations can be derived having the same form as their unnormalized counterparts.

3.16.3 Flux Linkage Equations

In the preferred “pitchfork” form, the flux linkages are given by Eqs. (3.203) to (3.210). Again dividing by $V_b = Z_b I_b$ one has, for example, for the q -axis stator flux linkage

$$\frac{\Psi_{ds}}{V_b} = \frac{x_{ls}}{Z_b} \frac{i_{ds}}{I_b} + \frac{x_m}{Z_b} \left(\frac{i_{ds}}{I_b} + \frac{i_{dr}'}{I_b} + \frac{i_{fr}'}{I_b} \right) \quad (3.238)$$

But $\psi_{ds}/V_b = \psi_{DS}$ and $i_{ds}/I_b = i_{DS}$. Upon defining the additional quantities

$$\frac{x_{ls}}{Z_b} = x_{LS} \quad (3.239)$$

$$\frac{x_m}{Z_b} = x_{MD} \quad (3.240)$$

the d -axis stator flux linkage can be written in per unit form as

$$\psi_{DS} = x_{LS} i_{DS} + x_{MD} (i_{DS} + i_{DR}' + i_{FR}') \quad (3.241)$$

Note that this equation again has the same form as the original flux linkage equation. One can continue in this fashion, defining five additional per unit flux expressions.

3.16.4 Electromagnetic Torque Equation

Consider now the torque equation. In this case it is clear that one must divide by base torque in order to per unitize the expression. From the definition of base power,

$$T_b = \left(\frac{P_{NP}}{2} \frac{S_b}{\omega_b} \right) = \frac{3}{2} \left(\frac{P_{NP}}{2} \right) \frac{V_b I_b}{\omega_b} \quad (3.242)$$

Dividing Eq. (3.228) by T_b results in

$$\frac{T_e}{T_b} = \frac{\frac{3}{2} \left(\frac{P_{NP}}{2} \right) \frac{1}{\omega_b} (\psi_{ds} i_{qs} - \psi_{qs} i_{ds})}{\frac{3}{2} \frac{P_{NP}}{2} \frac{1}{\omega_b} V_b I_b} \quad (3.243)$$

$$= \frac{\psi_{ds} i_{qs}}{V_b I_b} - \frac{\psi_{qs} i_{ds}}{V_b I_b} \quad (3.244)$$

or

$$T_E = \psi_{DS} i_{QS} - \psi_{QS} i_{DS} \quad (3.245)$$

where

$$T_E = \frac{T_e}{T_b} \quad (3.246)$$

Note that the form of the torque expression is different from the equivalent expression in physical units.

3.16.5 Motional Equation

The motional equation is also normalized by dividing by base torque, i.e.,

$$\frac{T_e}{T_b} - \frac{T_l}{T_b} = \frac{\frac{\omega_b}{(P_{NP}/2)}}{\frac{((P_{NP}/(2\omega_b))P_b)}{(P_{NP}/2)^2 P_b}} J \frac{d(\omega_r/\omega_b)}{dt} \quad (3.247)$$

or

$$\frac{T_e}{T_b} - \frac{T_l}{T_b} = \frac{\omega_b^2 J}{(P_{NP}/2)^2 P_b} \frac{d}{dt} \left(\frac{\omega_r}{\omega_b} \right) \quad (3.248)$$

The coefficient of the right hand side is generally termed the per unit inertia constant M

$$M = \frac{\omega_b^2 J}{(P_{NP}/2)^2 P_b} \quad (3.249)$$

Rather than utilize M in a per unit equation, it is conventional to define a related quantity H called the *inertia constant*.

$$H = \frac{\text{(Stored Kinetic Energy at Base Speed)}}{\text{Base Power}} \quad (3.250)$$

Comparing the definitions of M and H , it is apparent that

$$M = 2H \quad (3.251)$$

In per unit form, the motional equation is

$$T_E - T_L = 2H \frac{d}{dt} \omega_R \quad (3.252)$$

where $T_E = T_e / T_b$, $T_L = T_l / T_b$, and H is defined above.

Note that the motional equation has a different form in per unit form. Also, it is important to observe that H is *not* a unitless quantity but has units of seconds. Aside from scaling purposes, M (or H) plays an important role in studies

of dynamic performance. Significantly, it can be shown that when $T_L = 0$ and rated torque, $T_E = 1$, is exerted by the machine, then the time required to accelerate the rotor shaft to zero the rated speed is identically equal to M . The inertia constant can be expressed in numerous ways. Probably the most useful is

$$H = \frac{1}{1492} \left(\frac{2}{P}\right)_2^2 \frac{\omega_b^2}{HP_b} J \quad (3.253)$$

where P represents the number of poles, HP_b is base horsepower, and J is the moment of inertia in $nt \cdot m^2$. Alternatively,

$$H = \frac{5.48 \cdot 10^{-6} n^2 J}{KW_b} \quad (3.254)$$

where KW_b is the base power in *kilowatts*, n is rated mechanical speed in *RPM*, and J is again expressed in $nt \cdot m^2$, or

$$H = \frac{0.231 \cdot 10^{-6} n^2 (WK^2)}{KW_b} \quad (3.255)$$

where n and KW_b are as noted above and WK^2 is the moment of inertia in *lbf ft.²*.

3.16.6 Power Equation

As a final step, consider a change in the power equation to a per unit expression. Dividing Eq. (3.227) by $P_b = (3/2)V_b I_b$ results in

$$\frac{P_e}{P_b} = \frac{3/2}{3/2} \left(\frac{v_{ds} i_{ds}}{V_b I_b} + \frac{v_{qs} i_{qs}}{V_b I_b} + \frac{v_{ns} i_{ns}}{V_b I_b} + \frac{v_{dr'} i_{dr'}}{V_b I_b} + \frac{v_{qr'} i_{qr'}}{V_b I_b} + \frac{v_{fr'} i_{fr'}}{V_b I_b} \right) \quad (3.256)$$

or, simply,

$$P_E = v_{DS} i_{DS} + v_{QS} i_{QS} + v_{NS} i_{NS} + v_{DR'} i_{DR'} + v_{QR'} i_{QR'} + v_{FR'} i_{FR'} \quad (3.257)$$

where

$$P_E = \frac{P_e}{P_b} \quad (3.258)$$

It is important to recognize that the “3/2” coefficient disappears from the per unit power equation.

3.16.7 Summary

The per unit form of the synchronous machine equations (Park's equations) is summarized below.

$$v_{DS} = r_S i_{DS} + \frac{p}{\omega_b} \psi_{DS} - \omega_R \psi_{QS} \quad (3.259)$$

$$v_{QS} = r_S i_{QS} + \frac{p}{\omega_b} \psi_{QS} + \omega_R \psi_{DS} \quad (3.260)$$

$$v_{NS} = r_S i_{NS} + \frac{p}{\omega_b} \psi_{NS} \quad (3.261)$$

$$v_{DR}' = 0 = r_{DR}' i_{DR}' + \frac{p}{\omega_b} \psi_{DR}' \quad (3.262)$$

$$v_{QR}' = 0 = r_{QR}' i_{QR}' + \frac{p}{\omega_b} \psi_{QR}' \quad (3.263)$$

$$v_{FR}' = r_{FR}' i_{FR}' + \frac{p}{\omega_b} \psi_{FR}' \quad (3.264)$$

where

$$\psi_{DS} = x_{LS} i_{DS} + \psi_{MD} \quad (3.265)$$

$$\psi_{QS} = x_{LS} i_{QS} + \psi_{MQ} \quad (3.266)$$

$$\psi_{NS} = x_{LS} i_{NS} \quad (3.267)$$

$$\psi_{DR}' = x_{LDR}' i_{DR}' + \psi_{MD} \quad (3.268)$$

$$\psi_{QR}' = x_{LQR}' i_{QR}' + \psi_{MQ} \quad (3.269)$$

$$\psi_{FR}' = x_{LFR}' i_{FR}' + \psi_{MD} \quad (3.270)$$

$$\psi_{MD} = x_{MD} (i_{DS} + i_{FR}' + i_{FR}) \quad (3.271)$$

$$\psi_{MQ} = x_{MQ} (i_{QS} + i_{QR}') \quad (3.272)$$

$$T_E = \psi_{DS} i_{QS} + \psi_{QS} i_{DS} \quad (3.273)$$

$$P_E = v_{DS} i_{DS} + v_{QS} i_{QS} + v_{NS} i_{NS} \\ + v_{DR}' i_{DR}' + v_{QR}' i_{QR}' + v_{FR}' i_{FR}' \quad (3.274)$$

$$T_E - T_L = 2H_p \omega_R \quad (3.275)$$

The complete electrical equivalent circuit for the synchronous machine is shown in Figure 3.16.

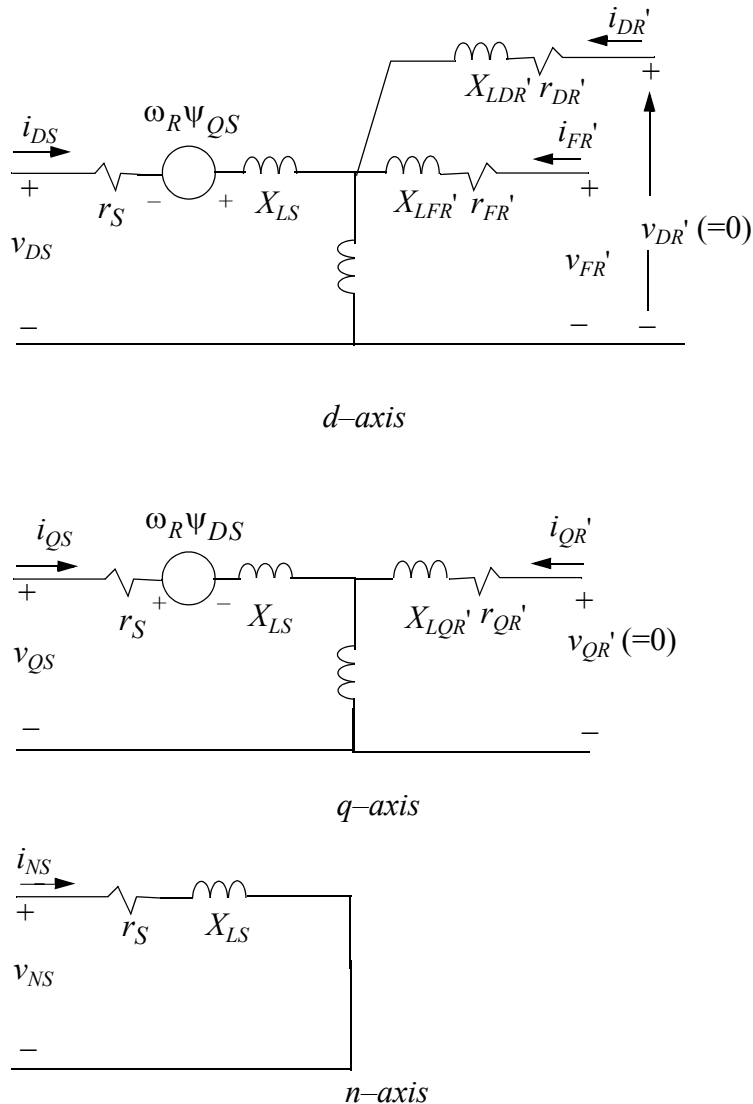


Figure 3.16 Equivalent circuit of synchronous machine with parameters in per unit. The time derivative operator is assumed to be $(1/\omega_b) \frac{d}{dt}$.

It should be mentioned before concluding that the urge to per unitize sometimes extends to normalizing time as well. In this case one could set

$$\begin{aligned} \frac{1}{\omega_b} \frac{d}{dt} &= \frac{d}{d(\omega_b t)} \\ &= \frac{d}{dT} \end{aligned} \tag{3.276}$$

In this case, for a 60 Hz base system, one per unit time corresponds to 1/377 sec. Alternatively, one could define t' such that

$$\begin{aligned} \frac{1}{\omega_b} \frac{d}{dt} &= \frac{d}{2\pi d(f_b t)} \\ &= \frac{d}{2\pi dT} \end{aligned} \tag{3.277}$$

One per unit time now would correspond to one cycle of base frequency (1/60 sec.) for a 60 Hz base. Such normalization typically leads to confusion in interpreting results, particularly when the frequency is a variable. The temptation to normalize time in this book will be resisted.

3.17 Conclusion

This chapter has served to combine the winding function theory and reference frame transformation principles learned in Chapters 1 and 2 in order to calculate the inductances of a synchronous machine directly in a freely rotating reference frame. It was then shown clearly the simplifications that can result from fixing the freely rotating $d-q$ reference frame of Chapter 1 with the rotor of the machine. In this manner, the use of *a priori* assumptions regarding selecting the appropriate reference frame was avoided until the benefits from doing so were made clear. The resulting equations, Park's equations, were formulated in both standard form and per unit form. These equations will now form the basis for the analysis of both round rotor and salient-pole machines for the remainder of the text.

3.18 References

- [1] E.W. Kimbark, "Power System Stability Vol. 3, Synchronous Machines," John Wiley, New York, 1956.

- [2] T.A. Lipo, "Introduction to AC Machine Design," University of Wisconsin, Madison, WI, 3rd Ed. 2011.
- [3] H.B. Dwight, Tables of Integrals and Other Mathematical Data," The MacMillan Co., New York, 1961.
- [4] M. Kostenko and I. Piotrovsky, "Electrical Machines Part II," Foreign Languages Publishing House, Moscow, 1968.
- [5] R.H. Park, "Two-Reaction Theory of Synchronous Machines, Generalized Method of Analysis—Part I," *Trans. of the AIEE*, 1929, pp. 716–730.

Chapter 4

Steady-State Behavior of Synchronous Machines

4.1 Introduction

Park's equations, derived in Chapter 3, form the basis for the analysis of any operating mode of a synchronous machine and can be employed for any situation that might be encountered, including starting transients, pole slipping, fault behavior, operation with a bridge inverter or rectifier, etc. However, since most synchronous machines operate nearly exclusively under balanced sinusoidal conditions, it is important that this important operating mode now be examined in some detail.

4.2 $d-q$ Axes Orientation

Recall that it has already been established that the voltages of any three-phase system can be viewed as a single vector in a three dimensional space. When the sum of the three voltages add to zero, the voltage vector then rotates on a plane (i.e., the $d-q$ plane). When the three-phase voltages form a balanced sinusoidal three-phase set then the voltage vector has a constant amplitude and therefore traces out a circle in the $d-q$ plane. Finally, when the d - and q -axes of the $d-q$ plane are made to rotate with the voltage vector itself, the projections of the voltage vector on the $d-q$ plane have been shown to become constants. When these balanced sinusoidal voltages are applied to the machine, a uniformly rotating armature flux in the gap is produced which rotates at the mechanical equivalent of synchronous speed. Normal steady-state operation is defined to be that condition in which the rotor of the machine rotates at the same mechanical angular velocity as the rotating stator flux (i.e., *synchronous speed*) and in which the currents in the machine have reached their steady-state condition.

For the purpose of analysis, it is convenient here to select the d -axis of such a synchronously rotating reference frame to locate the instantaneous position of the field pole which produces positively increasing field flux in the

armature phase as at time $t = 0$. Such an alignment of the d - q axes, in fact, also defines the rotor reference frame which, in this case, rotates at synchronous speed. Note that by convention, the positive q -axis is located horizontally to the right, while the positive d -axis is located vertically downward. The angle between the q -axis and the voltage vector \hat{V}_s at this instant of time is defined to be the angle δ . The alignment of the d - q axes and also the vector \hat{V}_s with respect to the magnetic axes of the stator phases as , bs , and cs at the instant $t = 0$ is shown in Figure 4.1. With these assumptions the three stator phase voltages

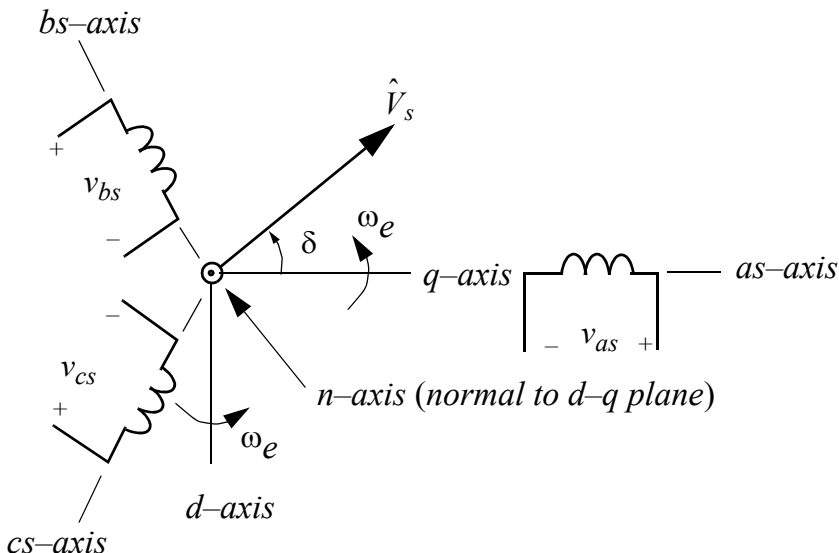


Figure 4.1 Alignment of rotating d - q axes and stationary as - $,$ bs - $,$ cs -axes on the d - q plane and the voltage vector \hat{V}_s at the instant $t = 0$.

can be expressed as functions of time as

$$v_{as} = V_s \cos(\omega_e t + \delta) \quad (4.1)$$

$$v_{bs} = V_s \cos\left(\omega_e t + \delta - \frac{2\pi}{3}\right) \quad (4.2)$$

$$v_{cs} = V_s \cos\left(\omega_e t + \delta + \frac{2\pi}{3}\right) \quad (4.3)$$

This set of voltages has been shown in Chapter 2 to trace out a circle on the d - q plane in the counter-clockwise direction, which will also be assumed to be the direction of rotating of the rotor of the machine itself.

The equations relating the as , bs , cs voltages to the ds , qs , ns voltages in the rotor reference frame rotating at synchronous speed are, in matrix form,

$$\mathbf{v}_{dqns} = \mathbf{T}(\omega_e t) \mathbf{v}_{abcs} \quad (4.4)$$

or, in expanded form,

$$\begin{bmatrix} v_{ds} \\ v_{qs} \\ v_{ns} \end{bmatrix} = \frac{2}{3} \begin{bmatrix} \sin \omega_e t & \sin \left(\omega_e t - \frac{2\pi}{3} \right) & \sin \left(\omega_e t + \frac{2\pi}{3} \right) \\ \cos \left(\omega_e t \right) & \cos \left(\omega_e t - \frac{2\pi}{3} \right) & \cos \left(\omega_e t + \frac{2\pi}{3} \right) \\ \frac{1}{\sqrt{2}} & \frac{1}{\sqrt{2}} & \frac{1}{\sqrt{2}} \end{bmatrix} \begin{bmatrix} V_s \cos(\omega_e t + \delta) \\ V_s \cos \left(\omega_e t + \delta - \frac{2\pi}{3} \right) \\ V_s \cos \left(\omega_e t + \delta + \frac{2\pi}{3} \right) \end{bmatrix} \quad (4.5)$$

When this matrix equation is multiplied out, one obtains, for the first row,

$$v_{ds} = \frac{2V_s}{3} \left[\cos(\omega_e t + \delta) \sin \omega_e t + \cos \left(\omega_e t + \delta - \frac{2\pi}{3} \right) \sin \left(\omega_e t - \frac{2\pi}{3} \right) + \cos \left(\omega_e t + \delta + \frac{2\pi}{3} \right) \sin \left(\omega_e t + \frac{2\pi}{3} \right) \right] \quad (4.6)$$

which, from Identity #18 of Appendix 1, becomes

$$v_{ds} = V_s \sin(-\delta) = (-V_s) \sin \delta \quad (4.7)$$

Similarly, evaluating the second row of this matrix equation yields

$$v_{qs} = \frac{2V_s}{3} \left[\cos \omega_e t \cos(\omega_e t + \delta) + \cos \left(\omega_e t - \frac{2\pi}{3} \right) \cos \left(\omega_e t + \delta + \frac{2\pi}{3} \right) + \cos \left(\omega_e t + \frac{2\pi}{3} \right) \cos \left(\omega_e t + \delta + \frac{2\pi}{3} \right) \right] \quad (4.8)$$

which, from Identity #16 in Appendix 1, reduces to

$$v_{qs} = V_s \cos(-\delta) = V_s \cos \delta \quad (4.9)$$

Finally, for the third row,

$$v_{ns} = \frac{\sqrt{2}V_s}{3} \left[\cos(\omega_e t + \delta) + \cos \left(\omega_e t + \delta - \frac{2\pi}{3} \right) + \cos \left(\omega_e t + \delta + \frac{2\pi}{3} \right) \right] \quad (4.10)$$

and from Identity #7,

$$v_{ns} = 0 \quad (4.11)$$

Since it has been assumed that the angle δ is positive, then the d -axis voltage v_{ds} is a negative quantity. This result is entirely consistent with our physical interpretation of the vector \hat{V}_s and its projections on the d - and q -axes.

In Figure 4.1, the angle δ is measured as the position of the vector \hat{V}_s with respect to the q -axis. As such, the angle δ is positive. In some texts, this particular orientation is taken to be a negative angle. It is apparent that the angle δ can readily be either positive or negative (meaning that δ is either oriented clockwise or counter-clockwise with respect to the q -axis). In order to avoid confusion it will be necessary to be very careful about the definition of the angle δ . In particular, counterclockwise rotation has already been defined to correspond to positive rotation in Chapter 1. In order to maintain the proper sign all angles are considered as “relative” angles. That is, the angle δ is assumed to be the angle that the vector \hat{V}_s makes with respect to the q -axis. In order to strictly define the polarity of δ , its polarity will be denoted by an arrow which has both a beginning and end as shown in , which shows a positive value in this case.

4.3 Steady-State Form of Park's Equations

In the sinusoidal steady-state at synchronous speed it has now been established that

$$v_{ds} = V_{ds} = -V_s \sin \delta \quad (4.12)$$

$$v_{qs} = V_{qs} = V_s \cos \delta \quad (4.13)$$

It addition, it will be assumed that the field excitation is constant, therefore, $v_{fr}' = V_{fr}'$ (a constant). Park's equations become

$$-V_s \sin \delta = V_{ds} = r_s i_{ds} + \frac{p}{\omega_b} \psi_{ds} - \frac{\omega_r}{\omega_b} \psi_{qs} \quad (4.14)$$

$$V_s \cos \delta = V_{qs} = r_s i_{qs} + \frac{p}{\omega_b} \psi_{qs} + \frac{\omega_r}{\omega_b} \psi_{ds} \quad (4.15)$$

$$0 = r_s i_{ns} + \frac{p}{\omega_b} \psi_{ns} \quad (4.16)$$

$$0 = r'_{dr} i'_{dr} + \frac{p}{\omega_b} \psi'_{dr} \quad (4.17)$$

$$0 = r'_{qr} i'_{qr} + \frac{p}{\omega_b} \psi'_{qr} \quad (4.18)$$

$$V'_{fr} = r'_{fr} i'_{fr} + \frac{p}{\omega_b} \psi'_{fr} \quad (4.19)$$

The solution of these differential equations clearly has both a transient (homogeneous) and steady-state (complementary) components. If one is concerned only with the steady-state portion of the solution (after all “initial conditions” have died away), then, since the left hand side of the equations contain only constants, the right-hand side must also be simple constants. Therefore, the derivative terms $p\psi_{ds}$, $p\psi_{qs}$, etc. become zero. Park’s equations reduce to

$$-V_s \sin \delta = r_s I_{ds} - \frac{\omega_r}{\omega_b} \psi_{qs} \quad (4.20)$$

$$V_s \cos \delta = r_s I_{qs} + \frac{\omega_r}{\omega_b} \psi_{ds} \quad (4.21)$$

$$0 = r_s I_{ns} \quad (4.22)$$

$$0 = r'_{dr} I'_{dr} \quad (4.23)$$

$$0 = r'_{qr} I'_{qr} \quad (4.24)$$

$$V'_{fr} = r'_{fr} I'_{fr} \quad (4.25)$$

where upper case letters have been used for all variables to denote the fact that they are simple constants.

From Eqs. (4.20) to (4.25) it is immediately evident that $I_{ns} = I'_{dr} = I'_{qr} = 0$ in the sinusoidal steady-state. Since ω_b has been chosen such that $\omega_b = \omega_e$ (synchronous frequency) and since $\omega_r = \omega_e$ at synchronous speed, Park’s equations reduce further to

$$-V_s \sin \delta = V_{ds} = r_s I_{ds} - \psi_{qs} \quad (4.26)$$

$$V_s \cos \delta = V_{qs} = r_s I_{qs} + \psi_{ds} \quad (4.27)$$

$$V'_{fr} = r'_{fr} I'_{fr} \quad (4.28)$$

where, during sinusoidal steady-state,

$$\psi_{ds} = x_{ds} I_{ds} + x_{md} I'_{fr} \quad (4.29)$$

$$\Psi_{qs} = x_{qs} I_{qs} \quad (4.30)$$

Hence, equivalently,

$$-V_s \sin \delta = r_s I_{ds} - x_{qs} I_{qs} \quad (4.31)$$

$$V_s \cos \delta = r_s I_{qs} + x_{ds} I_{ds} + x_{md} I'_{fr} \quad (4.32)$$

$$V'_{fr} = r'_{fr} I'_{fr} \quad (4.33)$$

Note that Eq. (4.33) simply describes Ohm's law and it is rather pointless to keep I'_{fr} as a variable. Therefore, it is traditional to define a new quantity,

$$E_i = x_{md} I'_{fr} \quad (4.34)$$

The subscript "i" is employed in Eq. (4.34) since the "internal" emf voltage E_i is proportional to field "current." In the *steady-state* it is evident that

$$I'_{fr} = \frac{V'_{fr}}{r'_{fr}} \quad (4.35)$$

so that *during steady-state*

$$E_i = \frac{x_{md} V'_{fr}}{r'_{fr}} \quad (4.36)$$

Utilizing Eq. (4.34), if Eqs. (4.31) and (4.32) are solved for I_{ds} and I_{qs} the following is obtained,

$$I_{ds} = \frac{V_s(x_{qs} \cos \delta - r_s \sin \delta) - E_i x_{qs}}{r_s^2 + x_{ds} x_{qs}} \quad (4.37)$$

$$I_{qs} = \frac{V_s(r_s \cos \delta + x_{ds} \sin \delta) - E_i r_s}{r_s^2 + x_{ds} x_{qs}} \quad (4.38)$$

When the synchronous machine is excited by sinusoidal voltages, the currents which flow in the steady-state form a vector of constant amplitude which also rotate on the $d-q$ plane at synchronous speed. In terms of $d-q$ currents, the phase currents can be readily found from the inverse $d-q-n$ transformation, that is,

$$\mathbf{i}_{abcs} = T(\omega_e t)^{-1} \mathbf{i}_{dqns} \quad (4.39)$$

which, upon evaluating, becomes

$$i_{as} = I_{ds} \sin(\omega_e t) + I_{qs} \cos(\omega_e t) \quad (4.40)$$

$$i_{bs} = I_{ds} \cos\left(\omega_e t - \frac{2\pi}{3}\right) + I_{qs} \sin\left(\omega_e t - \frac{2\pi}{3}\right) \quad (4.41)$$

$$i_{cs} = I_{ds} \cos\left(\omega_e t + \frac{2\pi}{3}\right) + I_{qs} \sin\left(\omega_e t + \frac{2\pi}{3}\right) \quad (4.42)$$

The current in phase as can be written equivalently as

$$i_{as} = I_s \sin(\omega_e t + \varepsilon) \quad (4.43)$$

where

$$I_s = \sqrt{I_{ds}^2 + I_{qs}^2}$$

and

$$\varepsilon = \tan^{-1} \left(\frac{I_{qs}}{I_{ds}} \right)$$

The quantity ε is called the *MMF angle* since it locates not only the position of the current vector on the d - q plane but also the position of the stator *MMF* with respect to the d -axis within the machine.

When written in terms of the position of the voltage vector, the three-phase currents are, alternatively,

$$i_{as} = I_s \cos(\omega_e t + \delta + \phi) \quad (4.44)$$

$$i_{bs} = I_s \cos\left(\omega_e t + \delta + \phi - \frac{2\pi}{3}\right) \quad (4.45)$$

$$i_{cs} = I_s \cos\left(\omega_e t + \delta + \phi + \frac{2\pi}{3}\right) \quad (4.46)$$

A diagram which illustrates a typical orientation of both the voltage vector \hat{V}_s and \hat{I}_s in the synchronously rotating d - q plane is shown in [Figure 4.2](#). Note that the current appears to *lag* the voltage vector by the angle ϕ . (The angle ϕ used here is clearly not the same entity as the ϕ used for spatial position of the winding function in Chapter 1). The head and tail of the arrow signifies that the angle ϕ measures the orientation of the current vector *with respect to* the voltage vector. Since the angle ϕ is measured clockwise in Figure 4.2, it has a negative value for this case. In addition, the vectors are drawn such that $\phi < -\delta$. Note that this interpretation is consistent with our concept of “phase lag.” That is, the vector \hat{I}_s is assumed to lag the vector \hat{V}_s when ϕ is negative. Comparing

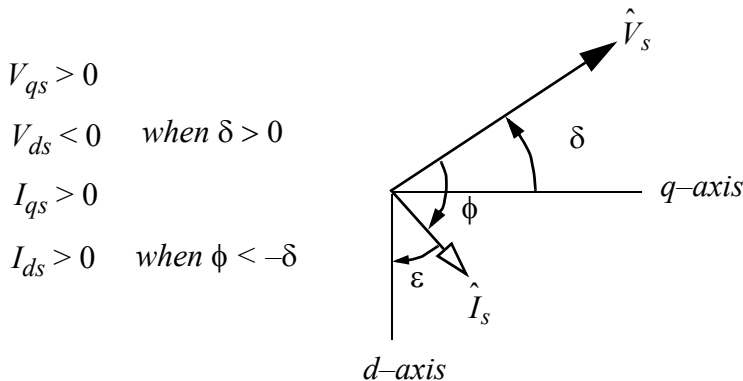


Figure 4.2 Alignment of the voltage vector \hat{V}_s and current vector \hat{I}_s on synchronously rotating d - q axes; the d -axis is assumed to be aligned with the field pole.

Eqs. (4.1) to (4.3) and (4.44) to (4.46), it is clear that under the same conditions the phase currents lag the voltages in time as well.

Since the d - q components of voltage and current become simple constants in the steady-state it is useful to distinguish between the cases where transient or steady-state conditions are implied. Henceforth, capital letters will be used to denote those conditions in which a given component is constant.

4.4 Steady-State Torque Equation

It can be recalled from Chapter 3 that the torque equation in SI units is

$$T_e = \frac{3P}{22} \frac{1}{\omega_b} (\psi_{ds} i_{qs} - \psi_{qs} i_{ds}) \quad (4.47)$$

In the steady-state $i_{qs} = I_{qs}$, $i_{ds} = I_{ds}$ and

$$\Psi_{ds} = x_{ds} I_{ds} + x_{md} I_{fr}'$$

$$= x_{ds} I_{ds} + E_i$$

Hence, in terms of steady-state stator currents, the torque equation becomes

$$T_e = \frac{3P}{22} \frac{1}{\omega_b} [E_i I_{qs} + (x_{ds} - x_{qs}) I_{qs} I_{ds}] \quad (4.48)$$

Note that Eq. (4.48) indicates that steady-state torque production in a synchronous machine can be viewed as comprised of two components. The first component can be considered as the interaction of the field flux ($x_{md}I_{fr}'$) with the component of stator current at a *right angle* to the field flux I_{qs} . The second component can be viewed as the interaction of the “salient” component of d -axis stator flux (i.e., the “excess” component of d -axis stator flux over and above the q -axis component, namely, $(x_{ds}-x_{qs})I_{ds}$) with the component of stator current at a *right angle* to this flux I_{qs} .

In terms of the *MMF* angle ε , the torque equation can be expressed as

$$T_e = \frac{3P}{22\omega_b} \left[E_i I_s \sin \varepsilon + \left(\frac{x_{ds} - x_{qs}}{2} \right) I_s^2 \sin(2\varepsilon) \right] \quad (4.49)$$

While not popular for the purpose of analyzing steady-state terminal characteristics, the *MMF* angle ε is a key parameter in the design of synchronous machines.

The torque equation can also be expressed in terms of stator voltages rather than stator currents. If Eqs. (4.37) and (4.38) are substituted into Eq. (4.48),

$$\begin{aligned} T_e = & \frac{3}{2} \left(\frac{P}{2\omega_b} \right) \left\{ E_i \frac{V_{qs}r_s - V_{ds}x_{ds} - E_i r_s}{r_s^2 + x_{ds}x_{qs}} + \frac{x_{ds} - x_{qs}}{(r_s^2 + x_{ds}x_{qs})^2} [r_s x_{qs} (V_{qs}^2 + E_i^2) \right. \\ & \left. + (r_s^2 - x_{ds}x_{qs}) V_{qs} V_{ds} - r_s x_{ds} V_{ds}^2 - 2r_s x_{qs} V_{qs} E_i - r_s^2 V_{ds} E_i + x_{qs} x_{ds} V_{ds} E_i] \right\} \end{aligned} \quad (4.50)$$

where

$$V_{ds} = -V_s \sin \delta$$

$$V_{qs} = V_s \cos \delta$$

If r_s is small compared to x_{ds} or x_{qs} , then Eq. (4.50) can be reduced to

$$T_e = \frac{3}{2} \left(\frac{P}{2\omega_b} \right) \left(\frac{E_i V_s}{x_{ds}} \sin \delta + \frac{x_{ds} - x_{qs}}{2x_{ds}x_{qs}} V_s^2 \sin 2\delta \right) \quad (4.51)$$

Again the torque is composed of two parts. The first term is often called the *synchronous torque* or *reaction torque* and clearly arises from the excitation of the machine. The second term is called the *reluctance torque* or *saliency torque*. The saliency torque again comes about due to the fact that $x_{ds} \neq x_{qs}$ in

a salient-pole machine. The term is zero in a round-rotor machine in which $x_{ds} = x_{qs}$. When $\delta > 0$, the torque is positive, meaning that the torque produced by the machine acts to rotate the machine in the positive direction of rotation (counter-clockwise), while when $\delta < 0$, the torque is negative, meaning that the torque acts to oppose operation in the preferred direction of rotation.

It is important to call attention to the fact that while the first and second terms in Eqs. (4.49) and (4.51) arise from the same phenomena, corresponding terms in the two equations are not equal to each other. In typical cases the excitation E_i and voltage amplitude V_s are constants. Hence, a change in load must be viewed as compensated within the machine by a change in the angle δ or the angle ε .

4.5 Steady-State Power Equation

It can be recalled that when expressed in $d-q-n$ components, the instantaneous power into the stator terminals is

$$P_{es} = \frac{3}{2}(v_{ds}i_{ds} + v_{qs}i_{qs} + v_{ns}i_{ns}) \quad (4.52)$$

When a three-wire system is assumed and specialized to the balanced sinusoidal steady-state, Eq. 4.52 becomes

$$P_{es} = \frac{3}{2}(V_{ds}I_{ds} + V_{qs}I_{qs}) \quad (4.53)$$

In the sinusoidal steady-state and in the synchronously rotating rotor reference frame,

$$V_{ds} = -V_s \sin \delta \quad (4.54)$$

$$V_{qs} = V_s \cos \delta \quad (4.55)$$

In addition, the currents are known in terms of the terminal voltages by Eqs. (4.37) and (4.38).

When these relationships are substituted into Eq. (4.53), the stator input power can be written in terms of the stator voltage amplitude, torque angle, and excitation voltage by

$$\begin{aligned}
 P_s = & \frac{3}{2} \left\{ \frac{V_s^2 (-x_{qs} \sin \delta \cos \delta + r_s \sin^2 \delta) + E_i V_s x_{qs} \sin \delta}{(r_s^2 + x_{ds} x_{qs})} \right. \\
 & \left. + \frac{V_s^2 (r_s \cos^2 \delta + x_{ds} \sin \delta \cos \delta) - E_i V_s r_s \cos \delta}{(r_s^2 + x_{ds} x_{qs})} \right\}
 \end{aligned} \tag{4.56}$$

Upon simplifying, this equation becomes

$$P_s = \frac{3}{2} \frac{V_s^2 \left[r_s + (x_{ds} - x_{qs}) \frac{\sin 2\delta}{2} \right] - E_i V_s (r_s \cos \delta - x_{qs} \sin \delta)}{r_s^2 + x_{ds} x_{qs}} \tag{4.57}$$

If r_s is again considered as small relative to x_{ds} and x_{qs} , then

$$P_s \approx \frac{3}{2} \frac{V_s E_i}{x_{ds}} \sin \delta + \frac{3}{2} V_s^2 \frac{(x_{ds} - x_{qs})}{2 x_{ds} x_{qs}} \sin 2\delta \tag{4.58}$$

Note that when $r_s = 0$, then the electrical power into the machine equals the mechanical power out of the machine. That is,

$$P_s \approx \left(\frac{2}{P} \right) \omega_r T_e \tag{4.59}$$

The validity of this result can be observed by comparing Eqs. (4.51) and Eq. (4.58).

Finally, if the currents are explicitly known, then

$$I_{ds} = -I_s \sin(\phi + \delta) \tag{4.60}$$

$$I_{qs} = I_s \cos(\phi + \delta) \tag{4.61}$$

Using Eqs. (4.60) and (4.61) together with (4.54) and (4.55) and substituting into Eq. (4.53), it is not difficult to show that

$$P_s = \frac{3}{2} V_s I_s \cos \phi \tag{4.62}$$

which is, of course, the expected result.

4.6 Steady-State Reactive Power

The reactive power corresponding to any operating point can be determined as the out-of-phase component of current multiplied by the terminal voltage. Assuming that the d - q voltage components are defined by Eqs. (4.7) and (4.9), the corresponding out-of-phase current components are i_{qs} and $-i_{ds}$, respectively, that is, in the steady-state

$$Q_s = \frac{3}{2}(V_{qs}I_{ds} - V_{ds}I_{qs}) \quad (4.63)$$

Substituting Eqs. (4.7), (4.9), (4.37) and (4.38) into this expression, results in

$$Q_s = \left(\frac{3}{2}\right) \frac{V_s^2(x_{qs}\cos^2\delta + x_{ds}\sin^2\delta) - E_i V_s(x_{qs}\cos\delta + r_s\sin\delta)}{r_s^2 + x_{ds}x_{qs}} \quad (4.64)$$

If the stator resistance is neglected, Eq. (4.64) reduces to the simpler expression

$$Q_s \approx \left(\frac{3}{2}\right) \left\{ \left(\frac{V_s^2}{2} \right) \left[\left(\frac{1}{x_{qs}} + \frac{1}{x_{ds}} \right) - \left(\frac{1}{x_{qs}} - \frac{1}{x_{ds}} \right) \sin 2\delta \right] - \frac{E_i V_s}{x_{ds}} \cos \delta \right\} \quad (4.65)$$

In this derivation it has been assumed that the reactive power is positive when the machine is absorbing reactive energy. When the machine is overexcited, reactive energy is “produced” by the machine and the reactive energy as computed by Eq. (4.65) becomes negative.

When the voltage and current are known in terms of magnitude and phase [Eqs. (4.54), (4.55), (4.60), and (4.61)], Eq. (4.63) can be written as

$$Q_s = \frac{3}{2}V_s I_s \sin\phi \quad (4.66)$$

which, again, is the expected result.

4.7 Graphical Interpretation of the Steady-State Equations

The concept of rotating vectors on a d - q plane has already been shown to be a powerful tool for analysis of three-phase networks. It was demonstrated that

the phase voltages form a balanced sinusoidal three-phase set and when the rotor of the machine rotates synchronously with this voltage vector, then both the stator voltage and the stator current vector become fixed amplitude, non-rotating vectors in the synchronously rotating reference frame. In effect, Park's equations describe how the inductive, resistive and *emf* voltage drops add up to produce the terminal voltage vector. In the steady-state Park's equations are, from [Section 4.3](#)

$$-V_s \sin \delta = V_{ds} = r_s I_{ds} - x_{qs} I_{qs} \quad (4.67)$$

$$V_s \cos \delta = V_{qs} = r_s I_{qs} + x_{ds} I_{ds} + E_i \quad (4.68)$$

where

$$E_i = x_{md} I'_{fr} \quad (4.69)$$

It is convenient, for the purpose used here, to neglect the stator resistance r_s . Setting $r_s = 0$ in the above two equations and solving for I_{ds} and I_{qs} ,

$$I_{ds} \approx \frac{V_s \cos \delta - E_i}{x_{ds}} \quad (4.70)$$

$$I_{qs} \approx \frac{V_s \sin \delta}{x_{qs}} \quad (4.71)$$

Recall now that when $\delta < 0$, the torque is negative (generator operation) and when $\delta > 0$, the torque is positive (motor action). Consider first the case where $\delta > 0$. This assumption places the voltage vector \hat{V}_s in the first quadrant of [Fig. 4.2](#), since

$$V_{ds} = -V_s \sin \delta < 0$$

$$V_{qs} = V_s \cos \delta > 0$$

From the above equations describing I_{ds} and I_{qs} it is apparent that when $\delta > 0$, the q -axis current $I_{qs} > 0$. The current vector \hat{I}_s must therefore be located either in the first or the fourth quadrant. In order to completely identify the quadrant containing \hat{I}_s , the sign of I_{ds} must be established. Clearly, when $E_i < V_s \cos \delta$, then I_{ds} is positive and the current vector \hat{I}_s is in the fourth quadrant. Since the d - q axes rotate synchronously in the counter-clockwise direction, the vector \hat{I}_s "lags" the vector \hat{V}_s in space as well as in time. In this case the motor is said to be *underexcited*.

For the case where $E_i > V_s \cos\delta$, then $I_{ds} < 0$, which implies that the current vector \hat{I}_s swings into the first quadrant. When $\phi > 0$, the current vector leads the voltage vector. The machine is said to be *overexcited*. Note that when the current vector enters the first quadrant, the current vector may still lag the terminal voltage vector. However, since \hat{I}_s leads the internal voltage E_i , this condition is sometimes called *leading internal power factor* operation. Construction of the voltage vector for these two cases follows from Eqs. (4.67) and (4.68) and is shown in Figure 4.3 and [Figure 4.4](#).

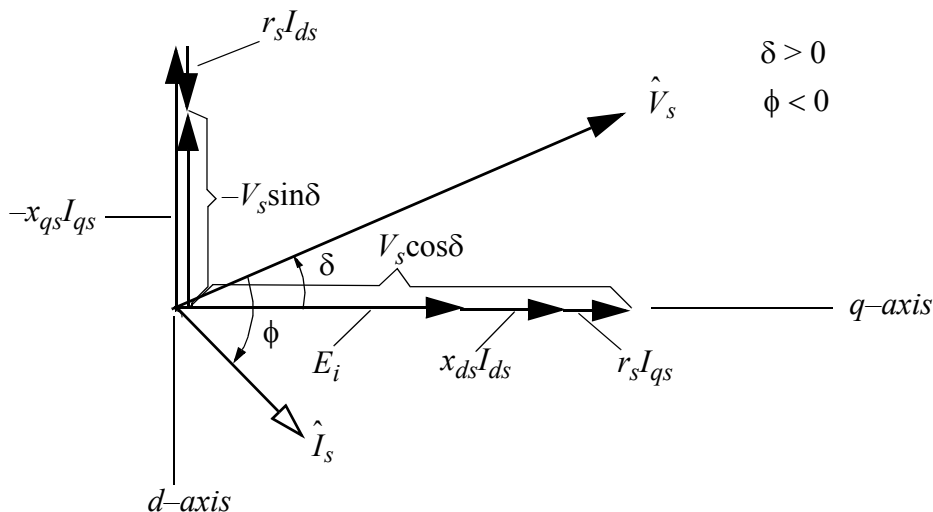


Figure 4.3 Voltage and current vector diagram for the case where $\delta > 0$ and $E_t < V_s \cos\delta$ (underexcited motor).

It is interesting to now investigate the case where $\delta < 0$, that is when the machine operates as a generator. In this case the vector \hat{V}_s is located in the fourth quadrant, since

$$V_{ds} = -V_s \sin\delta > 0$$

$$V_{qs} = V_s \cos\delta > 0$$

From the expression for I_{qs} , it is evident that this component of the current vector \hat{I}_s is negative placing the vector \hat{I}_s in either the second or third quadrant. Clearly, if $E_i < V_s \cos\delta$, then $I_{ds} > 0$ and \hat{I}_s is in the third quadrant. If $E_i > V_s \cos\delta$ then $I_{ds} < 0$ and the current vector \hat{I}_s is then in the second quadrant. Vector diagrams for these two cases are shown. Since the phase angle of the current with respect to the voltage is greater than 180° , determination of the

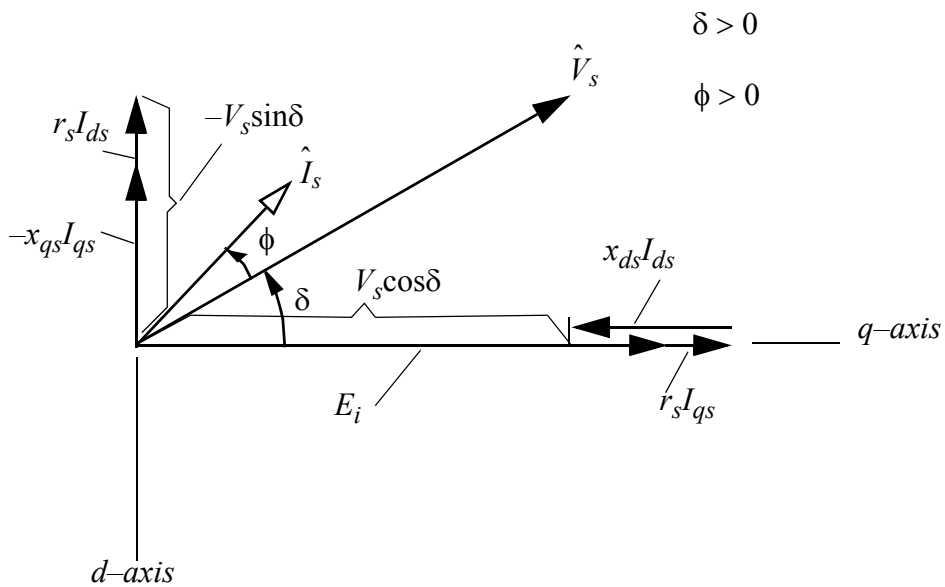


Figure 4.4 Voltage and current vector diagrams for the case where $\delta > 0$ and $E_i > V_s \cos \delta$ (overexcited motor).

sense of the power factor is somewhat difficult, (i.e., is it leading or lagging). However, if one defines, for generator action, current positive *out* of the machine rather than *into* the machine, the current vector becomes the dashed line in these two diagrams. The current is clearly then seen to be leading in the case of underexcitation ($E_i < V_s \cos \delta$) and is lagging in the case of overexcitation ($E_i > V_s \cos \delta$).

Vector diagrams for generator operation are shown in [Figure 4.5](#) and [Figure 4.6](#). [Figure 4.7](#) summarizes the operation in the four quadrants. Note that the sign of the *q*-axis current I_{qs} determines whether the machine is operating as a motor or generator, while the polarity of I_{ds} fixes whether the machine is over or underexcited. The four quadrants of operation and their corresponding modes are shown in Figure 4.7.

4.8 Steady-State Vector Diagram

It was demonstrated in Chapter 3 that Park's equations for the *d-q-n* stator circuits can be viewed as a single vector equation. That is,

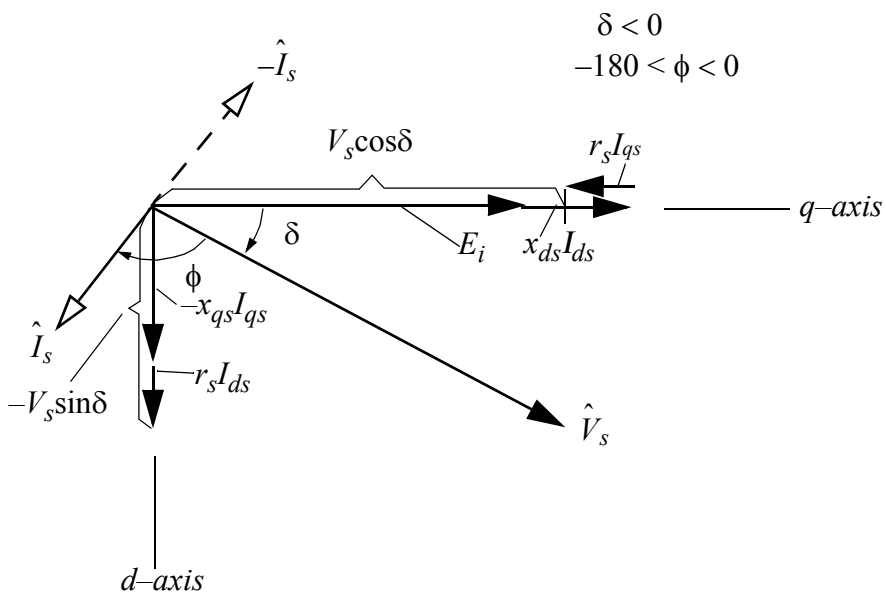


Figure 4.5 Voltage and current vector diagram for the case where $\delta < 0$ and $E_i < V_s$ (underexcited generator).

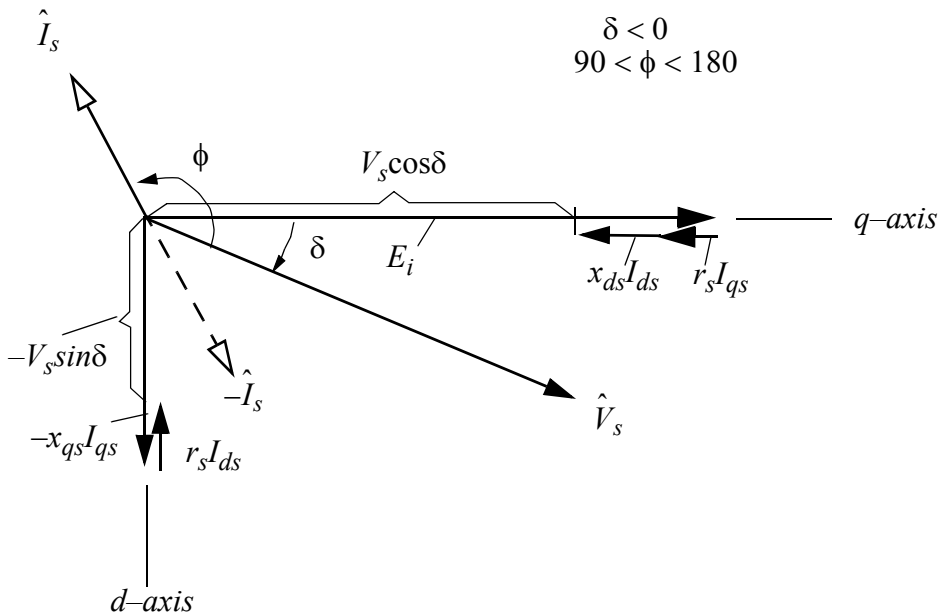


Figure 4.6 Voltage and current vector diagram for the case where $\delta < 0$ and $E_i > V_s$ (overexcited generator).

$$\hat{v}_{dqns} = r_s \hat{i}_{dqns} + p \hat{\lambda}_{dqns} + \hat{\omega}_r \times \hat{\lambda}_{dqns} \quad (4.72)$$

or, in terms of the hybrid flux linkages “ ψ ,”

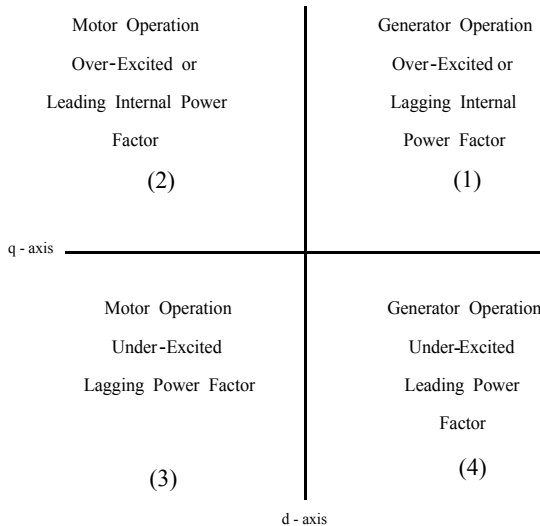


Figure 4.7 Directional sense of I_{ds} and I_{qs} for different operating conditions.

$$\hat{v}_{dqns} = r_s \hat{i}_{dqns} + \left(\frac{p}{\omega_b} \right) \hat{\psi}_{dqns} + \left(\frac{\hat{\omega}_r}{\omega_b} \right) \times \hat{\psi}_{dqns} \quad (4.73)$$

In the steady-state, $p\hat{\lambda}_{dqns} = 0$ and this equation reduces to

$$\hat{V}_s = r_s \hat{I}_s + \hat{u}_n \times \Psi_s \quad (4.74)$$

where

$$\hat{u}_n = \frac{\hat{\omega}_r}{\omega_b}$$

and

$$\Psi_s = (x_{ds} I_{ds} + E_i) \hat{u}_d + x_{qs} I_{qs} \hat{u}_q$$

Note that here it has also been assumed that the base frequency has been chosen such that synchronous rotation of the rotor corresponds to base frequency.

It is useful to separate the stator flux linkage into two components, one arising from the field current excitation $E_i \hat{u}_d$ and the other arising from armature reaction $x_{ds} I_{ds} \hat{u}_d + x_{qs} I_{qs} \hat{u}_q$. The steady-state vector equation for the stator voltage can then be written in the form

$$\hat{V}_s = r_s \hat{I}_s + \hat{u}_n \times \Psi_{s(ar)} + \hat{u}_n \times \Psi_{s(x)} \quad (4.75)$$

where

$$\Psi_{s(x)} = E_i \hat{u}_d$$

$$\Psi_{s(ar)} = x_{ds} I_{ds} \hat{u}_d + x_{qs} I_{qs} \hat{u}_q$$

A vector diagram illustrating these equations for the case of an overexcited motor is given in [Figure 4.8](#). Note that for an *overexcited* motor, the armature reaction flux tends to decrease the air gap flux. Such a flux is said to be *demagnetizing armature reaction*. Conversely, if the motor is underexcited, the armature reaction flux would tend to aid the air gap flux. The armature flux is then said to be *magnetizing armature reaction*. Note in the vector diagram that, neglecting the armature resistance, the angle between the total stator flux and the excitation component of flux is equal to the torque angle δ . This quantity is called the *internal torque angle* and is symbolized by δ' .

4.9 Vector Interpretation of Power and Torque

It has previously been shown that the power and torque can be computed by the following vector operations:

$$P_{es} = \frac{3}{2} \hat{v}_{dqns} \cdot \hat{i}_{dqns} \quad (4.76)$$

$$\hat{T}_e = \frac{3}{2} \left(\frac{P}{2\omega_b} \right) \hat{\psi}_{dqns} \times \hat{i}_{dqns} \quad (4.77)$$

In the steady-state these equations reduce to

$$P_{es} = \frac{3}{2} \hat{V}_s \cdot \hat{I}_s \quad (4.78)$$

$$\hat{T}_e = \frac{3}{2} \left(\frac{P}{2\omega_b} \right) \hat{\Psi}_s \times \hat{I}_s \quad (4.79)$$

The two vector operations can be readily visualized from the vector diagram of [Figure 4.8](#). The vector diagrams of [Figure 4.9](#) and [Figure 4.10](#) summarize torque and power production for the four possible modes of synchronous machine operation. In particular, note that the production of torque can be readily visualized, since the result of the cross product produces an axially directed (n -axis) torque which is the conventional definition of torque production. Careful interpretation of the direction of the cross product correctly yields the proper sense for motoring and generating conditions, i.e., counter-clock-

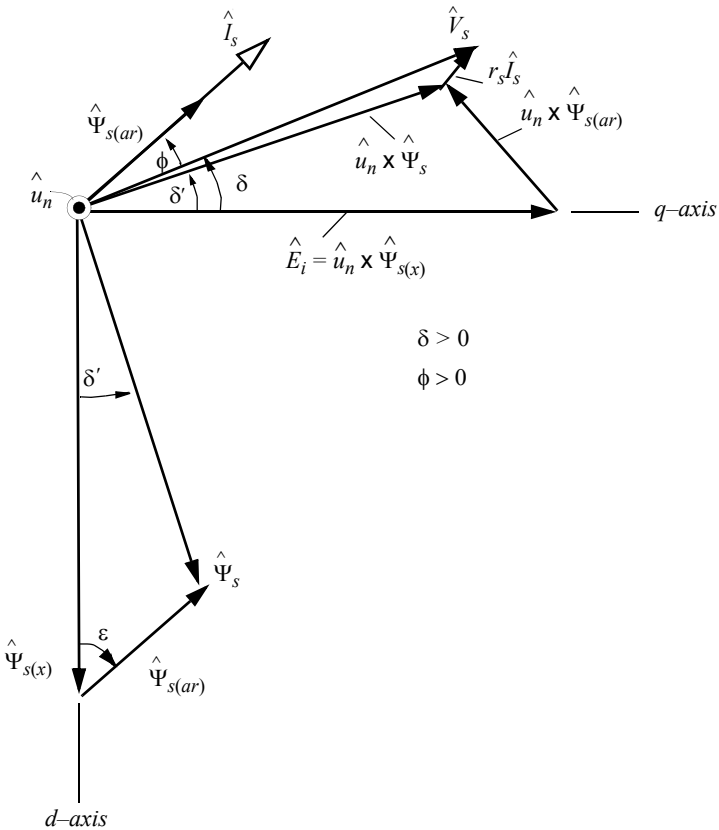


Figure 4.8 Vector diagram of a synchronous machine operating as an overexcited motor expressed in terms of the flux linkage vectors. Round-rotor machine assumed ($x_{ds} = x_{qs}$).

wise torque implying motoring and clockwise torque production implying generation.

It is useful to further consider separately the torque which arises from each component from the point of view of the vector description of Park's equations. Again, in general,

$$\hat{T}_e = \frac{3}{2} \left(\frac{P}{2} \right) \frac{1}{\omega_b} \hat{\Psi}_s \times \hat{I}_s \quad (4.80)$$

$$= \frac{3}{2} \left(\frac{P}{2} \right) \frac{1}{\omega_b} (\hat{\Psi}_{s(x)} \times \hat{I}_s + \hat{\Psi}_{s(ar)} \times \hat{I}_s) \quad (4.81)$$

$$\hat{T}_e = \hat{T}_{e1} + \hat{T}_{e2} \quad (4.82)$$

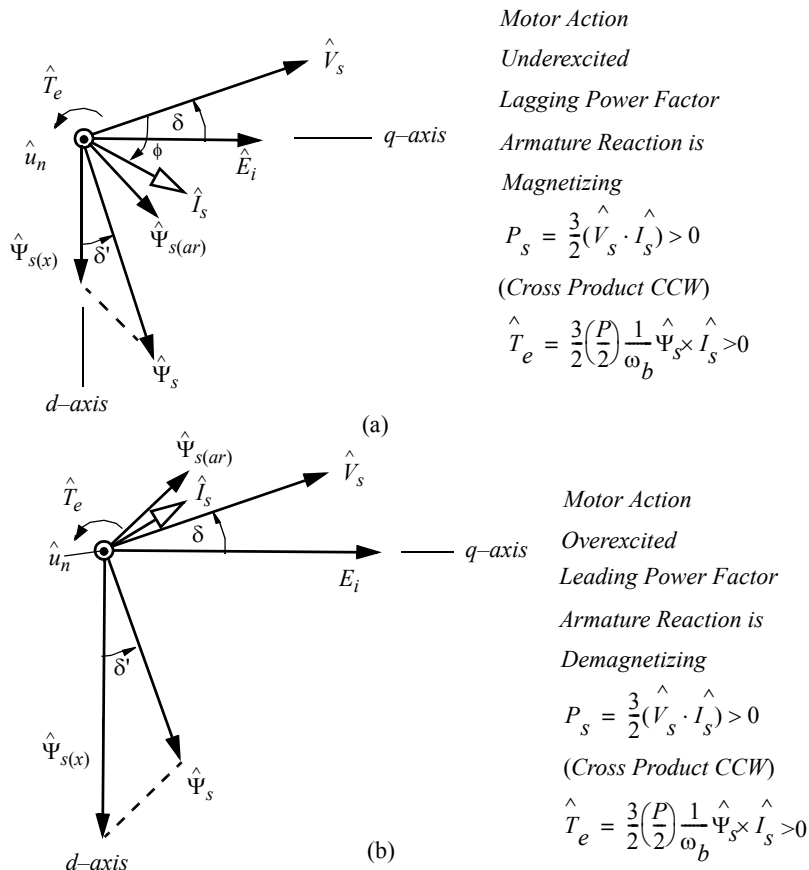


Figure 4.9 Vector diagram for motoring operation with (a) underexcitation and (b) overexcitation.

The first term corresponds to the torque produced by the field excitation, while the second results from the effect of armature current flow (armature reaction). Consider first the term involving the excitation flux. The excitation flux is related to the excitation voltage E_i by

$$\Psi_{s(x)} = E_i \hat{u}_d \quad (4.83)$$

whereupon,

$$\hat{T}_{e1} = \frac{3}{2}\left(\frac{P}{2}\right)\frac{1}{\omega_b}E_i(\hat{u}_d \times \hat{I}_s) \quad (4.84)$$

$$= \frac{3}{2}\left(\frac{P}{2}\right)\frac{1}{\omega_b}E_i \hat{u}_d \times (I_{qs} \hat{u}_q + I_{ds} \hat{u}_d) \quad (4.85)$$

After taking the indicated cross products, the result is the same as the first term of Eq. (4.48) except that the torque component is (properly) represented

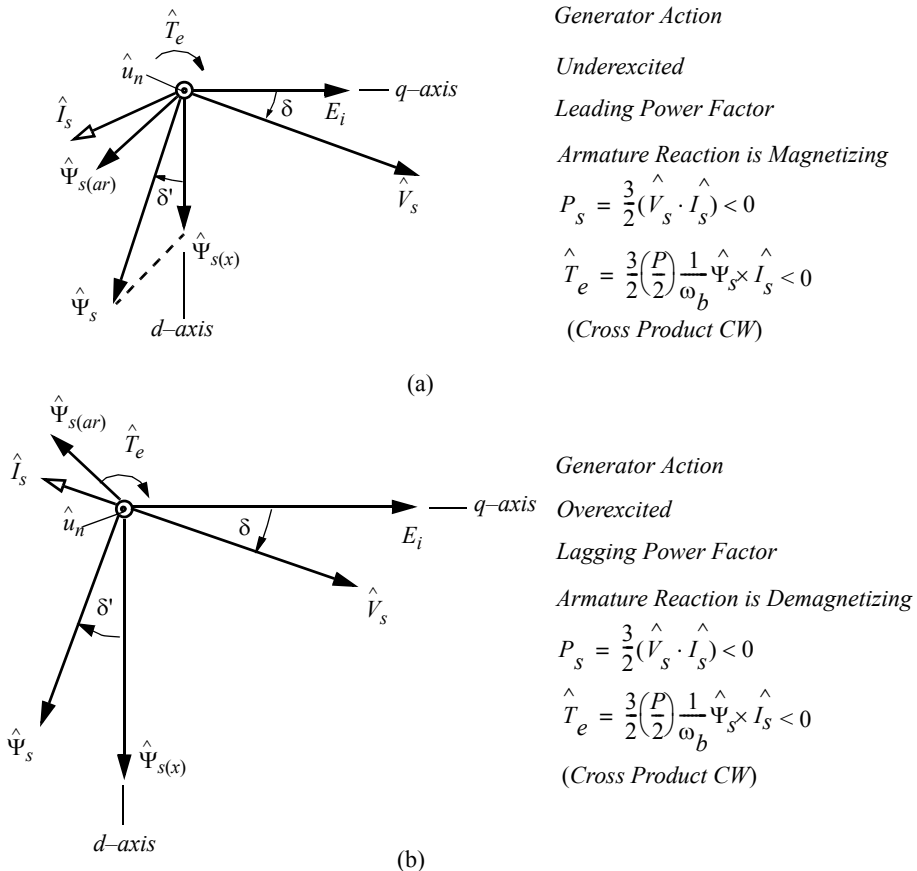


Figure 4.10 Vector diagrams for generator operating with
(a) underexcitation and (b) overexcitation.

in vector form. Also, note that this torque component arises from the interaction of the field flux $\hat{\Psi}_{s(x)}$, with the component of armature current *at a right angle* to the field flux. The component which is co-linear with the field flux, i.e., I_{ds} , does not contribute to torque production. Hence, this portion of torque production is identical to that of a DC machine. The directional sense of the torque is easily determined by crossing the field flux vector into the stator current vector. In the case of a motor this directional sense is counter-clockwise. Since the counter-clockwise direction has been selected as the positive direction of rotation, torques acting in this direction tend to accelerate the machine. This type of action is clearly motoring action.

The second component of torque can be expanded as

$$\hat{T}_{e2} = \frac{3}{2} \left(\frac{P}{2} \right) \frac{1}{\omega_b} (x_{ds} I_{ds} \hat{u}_d + x_{qs} I_{qs} \hat{u}_q) \times (I_{ds} \hat{u}_d + I_{qs} \hat{u}_q) \quad (4.86)$$

$$= \frac{3}{2} \left(\frac{P}{2} \right) \frac{1}{\omega_b} [(x_{ds} I_{ds} \hat{u}_d) \times (I_{qs} \hat{u}_q) + (x_{qs} I_{qs} \hat{u}_q) \times (I_{ds} \hat{u}_d)] \\ \quad (4.87)$$

$$= \frac{3}{2} \left(\frac{P}{2} \right) \frac{1}{\omega_b} (x_{ds} - x_{qs}) I_{ds} I_{qs} \hat{u}_n \quad (4.88)$$

This equation is the vector form of the second term of Eq. (4.48). Note from Eq. (4.87) that this component of torque can also be interpreted as the interaction of flux and current components again acting at right angles. In particular, the first term of Eq. (4.87) corresponds to the interaction of the d -axis armature reaction flux with the quadrature axis component of armature current, while the second term represents the interaction of the q -axis armature reaction flux with the direct axis component of armature current. The torques produced by the two terms clearly pull in opposite directions resulting in the minus sign in Eq. (4.88).

A complete example solution for the torque production by a salient-pole machine is shown in [Figure 4.11](#) for the case where the machine is overexcited. Stability conditions require that the torque angle remain within the range $-\pi/2 < \delta < \pi/2$ or else the machine will “pull out of step,” meaning that the rotor speed will decrease below synchronous speed if operating as a motor (stopping) or increase above synchronous speed if operating as a generator (increasing perhaps to dangerously high values). Clearly, this condition must be avoided in either case. The maximum value of torque that can be reached either in motor or generator operation is termed the *pull out torque*. The analysis of this condition, transient stability, will be covered in a later chapter. The solution shows that the d -axis current remains negative for any angle of δ (neglecting the effect of resistance), indicating that the machine remains overexcited (neglecting transient effects) even when operating beyond pull out. In an analogous manner the d -axis current remains positive when the machine operates underexcited.

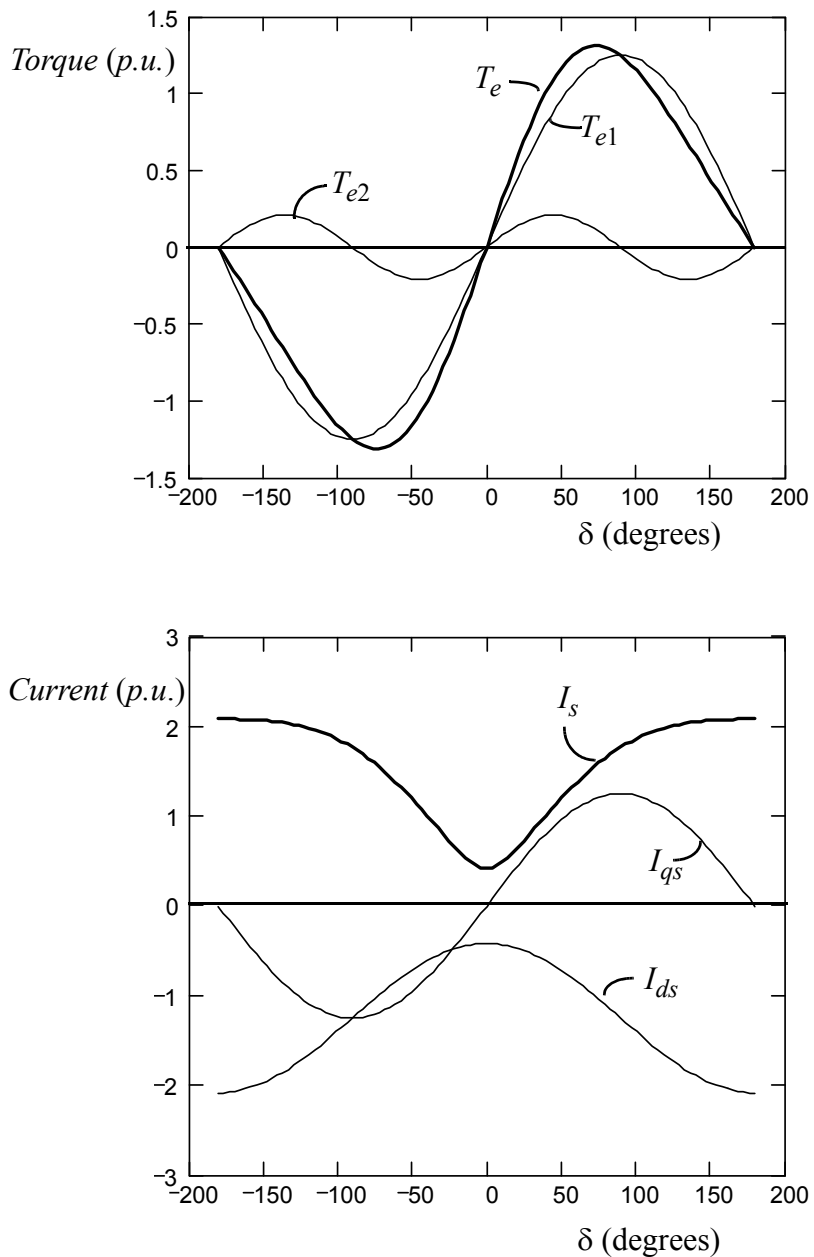


Figure 4.11 Per unit torque and current vs. torque angle δ for the case $x_{DS} = 1.2$, $x_{QS} = 0.8$, $r_S = 0$, $V_s = 1.0$, $E_i = 1.5$ (overexcited condition).

4.10 Phasor Form of the Steady-State Equations

It is now time to consider how to represent the steady-state machine equations by means of a phasor diagram. Recall that the phase voltages are assumed to be a sinusoidal set. That is, the phase *as* voltage is

$$v_{as} = V_s \cos(\omega_e t + \delta) \quad (4.89)$$

It is clear that in complex form this voltage is equivalently represented by the expression

$$v_{as} = \operatorname{Re}[V_s e^{j(\omega_e t + \delta)}] \quad (4.90)$$

In usual fashion, the term inside the bracket represents a complex quantity that rotates on the complex plane with an angular velocity ω_e . The phasor \tilde{V}_{as} is defined as the value of the complex vector when $t = 0$, or

$$\tilde{V}_{as} = V_s e^{j\delta} = V_s \angle \delta \quad (4.91)$$

Another form for the phase voltage v_{as} can be obtained from the equations of transformation, i.e.,

$$\mathbf{v}_{abcs} = \mathbf{T}(\omega_e t)^{-1} \mathbf{v}_{dqns} \quad (4.92)$$

where $\theta = \omega_e t$, in which case the *q*-axis is aligned with the phase *as*-axis at $t = 0$, as illustrated in [Figure 4.1](#). Recall that in the synchronous frame with balanced sinusoidal excitation that the *d*- and *q*-axes components are constants, denoted as V_{ds} and V_{qs} . Upon solving the above matrix equation for the first row, the phase *as* voltage is clearly

$$v_{as} = V_{ds} \sin(\omega_e t) + V_{qs} \cos(\omega_e t) \quad (4.93)$$

In complex form this equation corresponds to

$$\operatorname{Re}[\tilde{V}_{as} e^{j\omega_e t}] = \operatorname{Re}[V_{qs} e^{j\omega_e t}] + \operatorname{Re}[-jV_{ds} e^{j\omega_e t}] \quad (4.94)$$

If the operator Re is assumed and the $e^{j\omega_e t}$ is cancelled on both sides of the resulting equation, this expression reduces to

$$\tilde{V}_{as} = V_{qs} - jV_{ds} \quad (4.95)$$

Similarly, it can be established that for the phase *as* current, the corresponding phasor quantity is

$$\tilde{I}_{as} = I_{qs} - jI_{ds} \quad (4.96)$$

Having defined the phasor equivalent to the d - and q -components it is now possible to arrange the steady-state form of Park's equations such that the phasors \tilde{V}_{as} and \tilde{I}_{as} appear explicitly. Park's equations for steady-state are, from Eqs. (4.31) and (4.32),

$$V_{qs} = r_s I_{qs} + x_{ds} I_{ds} + E_i \quad (4.97)$$

$$V_{ds} = r_s I_{ds} - x_{qs} I_{qs} \quad (4.98)$$

Multiplying the second equation by $-j$ and adding the result to the first row, one has

$$V_{qs} - jV_{ds} = r_s(I_{qs} - jI_{ds}) + x_{ds}I_{ds} + jx_{qs}I_{qs} + E_i \quad (4.99)$$

where

$$\begin{aligned} V_{qs} - jV_{ds} &= V_s \cos \delta + jV_s \sin \delta \\ &= V_s e^{j\delta} \\ &= \tilde{V}_{as} \end{aligned} \quad (4.100)$$

Equation (4.99) is often written as

$$\tilde{V}_{as} = r_s \tilde{I}_{as} + jx_{ds}(-jI_{ds}) + jx_{qs}I_{qs} + \tilde{E}_i \quad (4.101)$$

or

$$\tilde{V}_{as} = r_s \tilde{I}_{as} + jx_{ds}\tilde{I}_{ds} + jx_{qs}\tilde{I}_{qs} + \tilde{E}_i \quad (4.102)$$

where

$$\tilde{I}_{qs} = I_{qs} \quad (\text{i.e., } \tilde{I}_{qs} \text{ is a real quantity}) \quad (4.103)$$

$$\tilde{I}_{ds} = -jI_{ds} \quad (\text{i.e., } \tilde{I}_{ds} \text{ is an imaginary quantity}) \quad (4.104)$$

$$\tilde{I}_{as} = \tilde{I}_{qs} + \tilde{I}_{ds} = I_{qs} - jI_{ds} \quad (4.105)$$

4.11 Equivalent Circuits of a Synchronous Machine

When $x_{ds} = x_{qs}$ Eq. (4.102) can be written as

$$\tilde{V}_{as} = r_s \tilde{I}_{as} + jx_{ds}(\tilde{I}_{ds} + \tilde{I}_{qs}) + \tilde{E}_i \quad (4.106)$$

or, simply

$$\tilde{V}_{as} = r_s \tilde{I}_{as} + jx_s \tilde{I}_{as} + \tilde{E}_i \quad (4.107)$$

resulting in the simple equivalent circuit of Figure 4.12. In this case the reactance of the machine is simply relabeled as x_s and termed the *synchronous reactance*, since it does not have $d-q$ component dependence. The voltage E_i in this case is frequently termed the *voltage behind synchronous reactance*.

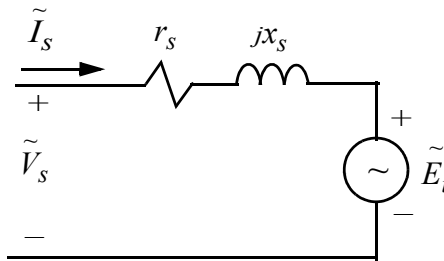


Figure 4.12 Per phase equivalent circuit of a round-rotor synchronous machine.

Because of the effect of saliency, the corresponding equivalent circuit for a salient-pole machine is somewhat more difficult but can still be created [1]. The development of the circuit is accomplished by expressing the power component (in phase with V_s) and reactive component (90° lagging V_s) of the stator current in terms of V_s , δ , x_{qs} , and x_{ds} . Referring to Figure 4.3, neglecting resistance and recalling that δ is positive for motor action, the components of the current in-phase and out-of-phase with the terminal voltage are

$$I_s \cos \phi = I_{qs} \cos \delta - I_{ds} \sin \delta \quad (4.108)$$

$$I_s \sin \phi = I_{qs} \sin \delta + I_{ds} \cos \delta \quad (4.109)$$

The d and q components of voltage are related to the currents by

$$V_s \cos \delta = x_{ds} I_{ds} + E_i \quad (4.110)$$

$$V_s \sin \delta = I_{qs} x_{qs} \quad (4.111)$$

Solving Eqs. (4.110) and (4.111) for currents and substituting into Eqs. (4.108) and (4.109) yields

$$I_s \cos \phi = \frac{V_s \sin \delta \cos \delta}{x_{qs}} - \frac{V_s \sin \delta \cos \delta}{x_{ds}} + \frac{E_i \sin \delta}{x_{ds}} \quad (4.112)$$

$$I_s \sin \phi = \frac{V_s \sin^2 \delta}{x_{qs}} + \frac{V_s \cos^2 \delta}{x_{ds}} - \frac{E_i \cos \delta}{x_{ds}} \quad (4.113)$$

$$= \frac{V_s}{x_{ds}} + V_s \sin^2 \delta \left(\frac{1}{x_{qs}} - \frac{1}{x_{ds}} \right) - \frac{E_i \cos \delta}{x_{ds}} \quad (4.114)$$

Combining the two current components to obtain the phasor stator current yields

$$\tilde{I}_s = I_s \cos \phi - j I_s \sin \phi \quad (4.115)$$

whereupon

$$\tilde{I}_s = V_s \sin \delta \cos \delta \left(\frac{1}{x_{qs}} - \frac{1}{x_{ds}} \right) + \frac{E_i \sin \delta}{x_{ds}} - j \frac{V_s}{x_{ds}} - j V_s \sin^2 \delta \left(\frac{1}{x_{qs}} - \frac{1}{x_{ds}} \right) + j \frac{E_i \cos \delta}{x_{ds}} \quad (4.116)$$

This equation can be rearranged to form

$$\tilde{I}_s = V_s \sin \delta (\cos \delta - j \sin \delta) \left(\frac{1}{x_{qs}} - \frac{1}{x_{ds}} \right) + \frac{V_s}{j x_{ds}} - \frac{E_i}{j x_{ds}} (\cos \delta - j \sin \delta) \quad (4.117)$$

However,

$$\sin \delta (\cos \delta - j \sin \delta) = \sin \delta (e^{-j\delta}) = \frac{\sin \delta}{e^{j\delta}} \quad (4.118)$$

$$= \frac{\sin \delta}{\cos \delta + j \sin \delta} = \frac{1}{\frac{1}{\tan \delta} + j 1} \quad (4.119)$$

The phasor equation for \tilde{I}_s can now be written as

$$\tilde{I}_s = \frac{V_s - \tilde{E}_i}{j x_{ds}} + \frac{V_s}{\frac{x_{ds} x_{qs}}{x_{ds} - x_{qs}} \frac{1}{\tan \delta} + j \frac{x_{ds} x_{qs}}{x_{ds} - x_{qs}}} \quad (4.120)$$

where $\tilde{E}_i = E_i e^{-j\delta}$.

The circuit described by this equation is shown in [Figure 4.13](#), where the stator resistance has now again been introduced to complete the result. The similarity of the equivalent circuit to that of the induction motor is interesting. The direct axis reactance x_{ds} is the equivalent magnetizing reactance of the induction motor, while the reactance $(x_{ds} x_{qs}) / (x_{ds} - x_{qs})$ is equivalent to both the leakage reactance and the rotor resistance of the equivalent induction

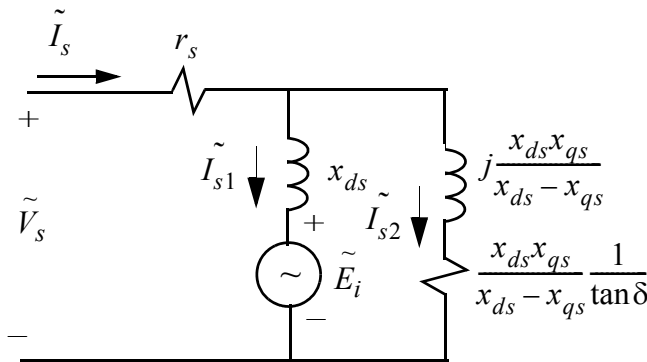


Figure 4.13 Per phase equivalent circuit of a salient-pole synchronous machine.

machine. The $\tan\delta$ is equivalent to the slip frequency of the induction machine. The obvious parallels between the induction machine equivalent circuit and the synchronous reluctance motor equivalent circuit provide a useful background when comparing issues between various other types of motors. For example, the peak reluctance torque will occur when the apparent rotor resistance is equal to the Thevenin impedance seen looking back toward the source. For ideal voltage source excitation, this impedance is equal to $j(x_{ds}x_{qs})/(x_{ds}-x_{qs})$ and the peak reluctance torque occurs when

$$\frac{x_{ds}x_{qs}}{x_{ds}-x_{qs}} \frac{1}{\tan\delta} = \frac{x_{ds}x_{qs}}{x_{ds}-x_{qs}} \quad (4.121)$$

or

$$\tan\delta = 1 \quad (4.122)$$

indicating $\delta = 45^\circ$, which is in agreement with earlier results. The reluctance torque can be computed by first solving for the current into the resistor. Again neglecting stator resistance,

$$\tilde{I}_{s2} = \frac{V_s}{\frac{x_{ds}x_{qs}}{x_{ds}-x_{qs}} \left(\frac{1}{\tan\delta} + j1 \right)} \quad (4.123)$$

In general, the power dissipated in the resistor is

$$P_{e2} = |\tilde{I}_{s2}|^2 \left(\frac{x_{ds}x_{qs}}{x_{ds}-x_{qs}} \frac{1}{\tan\delta} \right) \quad (4.124)$$

$$= \left| \frac{V_s \sin \delta}{\frac{x_{ds}x_{qs}}{x_{ds} - x_{qs}} (\cos \delta + j \sin \delta)} \right|^2 \left(\frac{x_{ds}x_{qs}}{x_{ds} - x_{qs}} \right) \frac{\cos \delta}{\sin \delta} \quad (4.125)$$

$$= \frac{V_s^2}{\frac{x_{ds}x_{qs}}{x_{ds} - x_{qs}}} \sin \delta \cos \delta \quad (4.126)$$

$$= V_s^2 \left(\frac{x_{ds} - x_{qs}}{2x_{ds}x_{qs}} \right) \sin 2\delta \quad (4.127)$$

which is the same as the second term of Eq. (4.58). In a similar manner it can be shown that the power corresponding to the reaction torque corresponds to the power flow into the voltage source E_i .

4.12 Solutions of the Phasor Equations

When δ is known, construction of the phasor diagram is straightforward. More often, however, only the stator voltage and current are known and it is desired to find the proper value of δ and excitation \tilde{E}_i needed to obtain these terminal conditions. In this case the d - q axis orientation must be developed around this information. Assuming that \tilde{V}_s and \tilde{I}_s are known, the necessary value of E_i can be found by simply solving Eq. (4.107) for \tilde{E}_i and performing the necessary computations in the complex plane. In the case of a salient-pole machine, however, the problem is not so easy, since the location of the d - q axes must be known to solve Eq. (4.102). The location of the q -axis relative to the voltage vector \tilde{V}_s can be accomplished by means of an artifice. If $x_{qs}I_{ds}$ is added and subtracted from the right hand side of the phasor voltage equation (4.99), then it may be written as

$$\begin{aligned} V_{qs} - jV_{ds} &= r_s(I_{qs} - jI_{ds}) + x_{ds}I_{ds} + jx_{qs}I_{qs} + E_i \\ \tilde{V}_{as} &= r_s \tilde{I}_{as} + x_{qs}(I_{ds} + jI_{qs}) + (x_{ds} - x_{qs})I_{ds} + E_i \end{aligned} \quad (4.128)$$

However, since

$$\tilde{I}_{as} = I_{qs} - jI_{ds} \quad (4.129)$$

then

$$\tilde{I}_{as} = I_{ds} + jI_{qs} \quad (4.130)$$

The phasor voltage equation therefore can be written as

$$\tilde{V}_{as} = (r_s + jx_{qs})\tilde{I}_{as} + [(x_{ds} - x_{qs})I_{ds} + E_i] \quad (4.131)$$

The quantity $(x_{ds} - x_{qs})I_{ds} + E_i$ is sometimes called *the voltage behind quadrature axis reactance* E_q . Note that E_q would be the internal emf of an equivalent round-rotor synchronous machine having a synchronous reactance of x_{qs} . A phasor diagram illustrating this construction technique is shown in Figure 4.14. The key idea of this manipulation is to establish the location of the q -axis or “Re” axis in complex notation. Thereafter, the proper lengths for the required I_x drops can be readily established. By use of the voltage E_q the electromag-

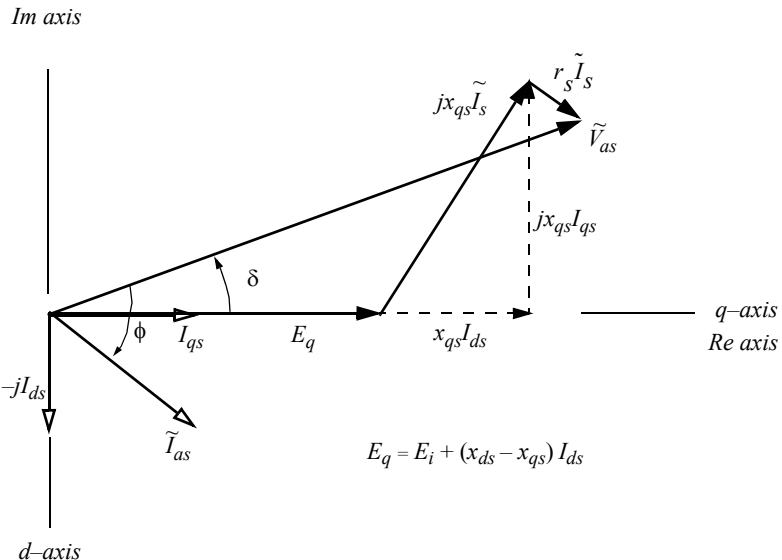


Figure 4.14 Phasor diagram of modified voltage equation for motor operation and lagging power factor.

netic torque can be computed directly. From Eq. (4.48) and the definition of E_q , it is apparent that an alternative expression for torque is

$$T_e = \frac{3P}{2} \frac{1}{2\omega_b} E_q I_{qs} \quad (4.132)$$

It is important to mention that, thus far, no mention has been made of any RMS quantities. That is, the length of the phasor \tilde{V}_{as} is assumed to be the peak

of the line to neutral phase voltage. Clearly, the lengths of the phase quantities in [Figure 4.14](#) can be scaled to represent voltage and current amplitudes or *RMS* voltage and current, since all of the lengths differ in the two cases by $\sqrt{2}$. However, to avoid confusion, vectors (and phasors) will always denote the amplitude of quantities in this book.

4.13 Solution of the Steady-State Synchronous Machine Equations Using MathCAD

The long history of the analysis of synchronous machines has led to lengthy discussions in most texts concerning the phasor solutions of steady-state for a wide variety of scenarios. Most often the stator resistance must be neglected to render the computational effort even tractable. However, with the emergence of powerful algorithms for solutions of non-linear algebraic equations in software such as MATLAB and MathCAD, almost any reasonably posed problem is now easily solved numerically.

Recall again that the two key equations to be solved for sinusoidal steady-state are Eqs. (4.14) and (4.15), i.e.,

$$V_{ds} = r_s I_{ds} - x_{qs} I_{qs} \quad (4.133)$$

$$V_{qs} = r_s I_{qs} + x_{ds} I_{ds} + E_i \quad (4.134)$$

where

$$E_i = x_{md} I_{fr}' = \frac{x_{md} V_{fr}'}{r_{fr}'} \quad (4.135)$$

When expressed in terms of amplitude and phase, the *d*-*q* voltages and currents are

$$V_{qs} = V_s \cos \delta \quad (4.136)$$

$$V_{ds} = -V_s \sin \delta \quad (4.137)$$

$$I_{qs} = I_s \cos(\delta + \phi) \quad (4.138)$$

$$I_{ds} = -I_s \sin(\delta + \phi) \quad (4.139)$$

Equations (4.133) and (4.134) can then be written as

$$V \sin \delta = r_s I_s \sin(\phi + \delta) + x_{qs} I_s \cos(\phi + \delta) \quad (4.140)$$

$$V \cos \delta = r_s I_s \cos(\phi + \delta) - x_{ds} \sin(\phi + \delta) + E_i \quad (4.141)$$

These two equations are, in general, clearly non-linear, since the torque angle δ and phase angle ϕ are a function of the sine and cosine. However, the equations become linear in some cases for example, if δ and ϕ are known or specified. In nearly all typical problems, the machine parameters, r_s , x_{qs} , and x_{ds} are assumed as given. The two equations contain five quantities that could be considered as variables, namely, V_s , δ , I_s , ϕ , and E_i . In general, any three of these variables must be defined, in which case Eqs. (4.140) and (4.141) can be used to find the remaining two.

In addition, having solved for the two desired variables, it is frequently desired to calculate the torque, electrical power, or reactive power, in which case, from Eqs. (4.53) and (4.63), incorporating Eqs. (4.136) to (4.139)

$$T_e = \frac{3P}{2} \frac{1}{2\omega_b} \left[E_i I_s \cos(\delta + \phi) - \frac{(x_{ds} - x_{qs})}{2} I_s^2 \sin 2(\phi + \delta) \right] \quad (4.142)$$

Also, if required

$$P_s = \frac{3}{2} V_s I_s \cos \phi \quad (4.143)$$

$$Q_s = \frac{3}{2} V_s I_s \sin \phi \quad (4.144)$$

As an example of such a solution consider the following problem. A salient-pole synchronous motor has the following per unit parameters $r_s = 0.02$, $x_{DS} = 1.2$, $x_{QS} = 0.8$. If it is desired that the stator current be at rated value and in phase with the stator voltage when the machine is supplied by rated voltage, what is the per unit excitation voltage E_i required? Note that this problem is essentially the one discussed using phasor notation in [Section 4.12](#). Three of the five variables are defined, namely, V_s , I_s , ϕ , and the solution of Eqs. (4.18) and (4.141) will provide a solution for the remaining two, E_i and δ . A brief conversation with the MathCAD program yields the following

Assumed Parameters

$rs := 0.02$

$Xqs := 0.8$

$Xds := 1.2$

Unity Power Factor Problem

$$Vs := 1.0$$

$$Is := 1.0$$

$$\phi := 0$$

Initial Guess

$$Ei := 1.3$$

$$\delta := 30. \pi/180$$

Given

$$-Vs \cdot \sin(\delta) = -rs \cdot Is \cdot \sin(\phi + \delta) - Xqs \cdot Is \cdot \cos(\phi + \delta)$$

$$Vs \cdot \cos(\delta) = rs \cdot Is \cdot \cos(\phi + \delta) - Xds \cdot Is \cdot \sin(\phi + \delta) + Ei$$

$$\text{Find}(Ei, \delta) = \begin{pmatrix} 1.518 \\ 0.6846 \end{pmatrix}$$

$$Te := Ei \cdot Is \cdot \cos(\delta + \phi) - (Xds - Xqs) \cdot Is^2 \cdot \frac{\sin[2.(\delta + \phi)]}{2}$$

$$Te = 0.98$$

The actual solution of the problem involves only the three lines of code following the statement “Given.” Although the answer is easily obtained, the reader is encouraged to construct the vector diagram, which yields additional insight not easily obtained from simple numerical answers.

More difficult problems can also be solved by this technique. For example, the torque equation above can be moved above the Find command to become a third equation to be solved. In this case one has six unknowns (including T_e) and three equations to be solved. In this case, however, care must be taken so as not to propose an impossible solution. For example, in the above case the input power has been effectively completely defined. It is not possible to search for a solution where T_e is also specified as a value other than 0.98. Many useful solutions can however, be obtained. As an example, assume the same machine as above, that the terminal voltage is again 1.0 per unit, and that the power factor is unity. What is the current required to obtain 1.1 per unit torque? In this case three quantities are specified (V_s , ϕ , and T_e) and three quantities are unknown (I_s , δ , and E_i). The proper answer is $I_s = 1.125$, $\delta = 42.645^\circ$, and $E_i = 1.634$. Solutions to problems of this type can not be readily obtained with a phasor approach unless one resorts to iterating the phasor solutions to converge on the desired torque.

4.14 Open-Circuit and Short-Circuit Characteristics

Whereas saturation effects are only of secondary importance in the analysis of induction machines, the iron in synchronous machines is nearly always saturated, particularly near the base of the field poles. Three basic sets of characteristic curves are involved in the evaluation of saturation effects, the *open-circuit characteristic*, the *short-circuit characteristic* and the *zero power factor characteristic*. The first two will be examined in this section and the third in the following section.

Figure 4.15 shows a typical open-circuit characteristic of a synchronous machine in which the open-circuit stator voltage is plotted against the field current when the machine is driven at synchronous speed. Essentially, the open-circuit curve represents the non-linear relationship between the fundamental component of field air gap flux and MMF impressed on the direct axis magnetic circuit which, in this case, comes completely from the field circuit. Note that the characteristic is linear when the field current is relatively small. The

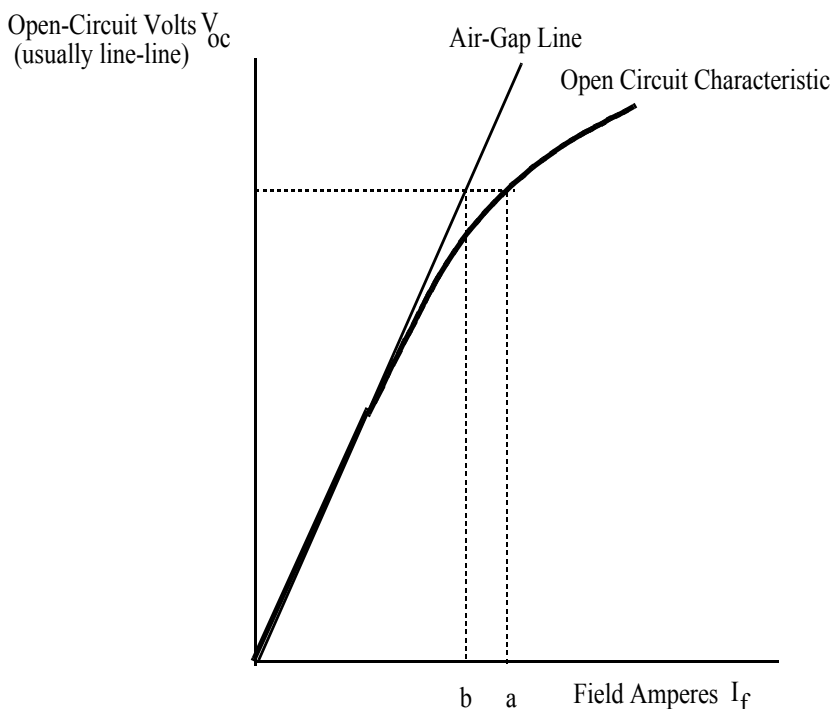


Figure 4.15 Open-circuit characteristic of a synchronous machine.

tangent to this linear portion of the curve is called the *air gap line*, since the MMF drop essentially appears across the air gap when the flux in the iron is small. The open-circuit characteristic is determined experimentally by driving the machine mechanically at synchronous speed with its armature terminals opened and reading the terminal voltage corresponding to a series of values of field current.

If the mechanical power required to drive the machine is measured, the no load rotational losses can be determined. These losses include not only friction and windage losses, but also the core loss corresponding to flux in the machine at various levels of field current. The distribution of losses between friction and windage losses and core loss can be determined by also measuring the mechanical power needed to drive the machine at synchronous speed with both the field and armature unexcited. The difference between the two loss measurements is the no load core loss. A typical plot of the open-circuit core loss as a function of the open-circuit voltage is shown in Figure 4.16. Note that this loss

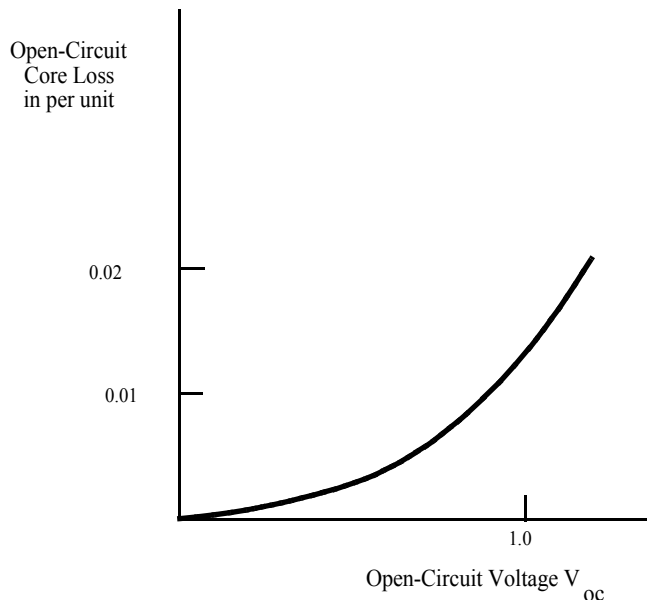


Figure 4.16 Open-circuit loss curve.

is typically only 1 or 2 percent of rated power for a large turbogenerator.

When the armature terminals of the synchronous machine are shorted with the machine driven at synchronous speed, and the field current is gradually increased from zero, data can be obtained from which the short-circuit armature current can be plotted against the field current. This relationship is known as the short-circuit characteristic. Although this measurement may seem to be rather drastic, the current that flows under such conditions is relatively small and data can safely be obtained up to about twice the rated armature current. A plot of the short-circuit characteristic together with an open-circuit characteristic is shown in Figure 4.17. Figure 4.18 shows a phasor diagram for such a short-circuit condition. Note that since the armature current very nearly lags the armature voltage by 90° , the armature flux is very nearly in direct opposition to the field flux. The current is related to the excitation voltage very nearly by

$$\tilde{E}_i = (r_s + jx_{ds})\tilde{I}_s \quad (4.145)$$

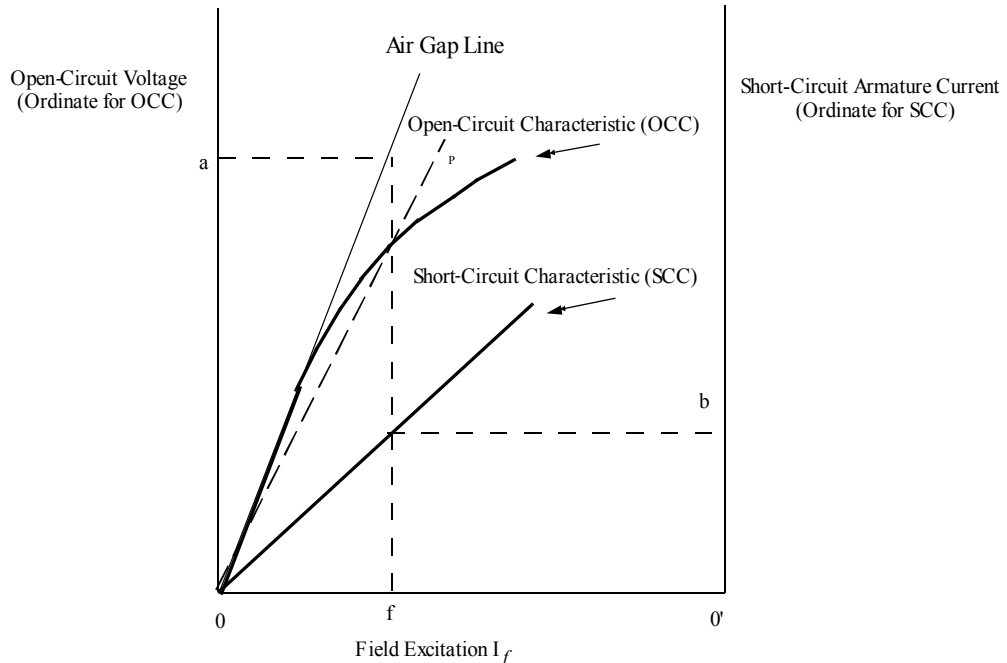


Figure 4.17 Open-circuit and short-circuit characteristics as a function of field current.

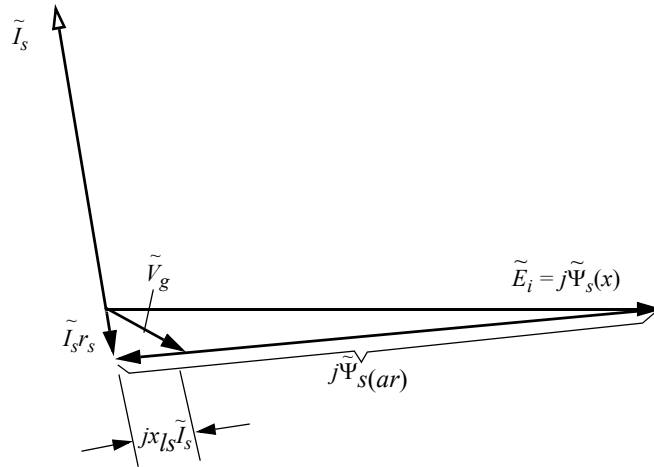


Figure 4.18 Phasor diagram for short-circuit condition.

It is apparent from Figure 4.18 that the resultant flux Ψ_s is very small and is only equal to that value necessary to support the stator *ir* drop. In actual fact the flux in the gap Ψ_g is slightly larger than Ψ_s as indicated on Figure 4.19. Since current is flowing out of the machine the time rate of change of air gap flux must be balanced essentially by the stator *ir* drop plus the stator leakage reactance drop. The air gap flux linkage at rated armature current on short-circuit is typically about 0.15 per unit so that the machine operates in an unsaturated condition. The short-circuit armature current is therefore directly proportional to the field current over the range from zero to well above the rated armature current.

The open- and short-circuit data can be used to measure the direct axis stator inductance. At any desired field excitation, such as O_f in Figure 4.17, the armature current on short-circuit $O'b$ and the excitation voltage for the same field current corresponds to Oa as read from the air gap line. The voltage on the air gap line is used, since the machine is assumed to be unsaturated. If the voltage per phase corresponding to Oa is $E_{i(oc)}$ and the armature current corresponding to $O'b$ is $I_{s(sc)}$, then, if armature resistance is neglected, the unsaturated value of *d*-axis synchronous reactance is

$$x_{ds(\text{unsat})} = \frac{E_{i(\text{ag-line})}}{I_{s(\text{sc})}} \quad (4.146)$$

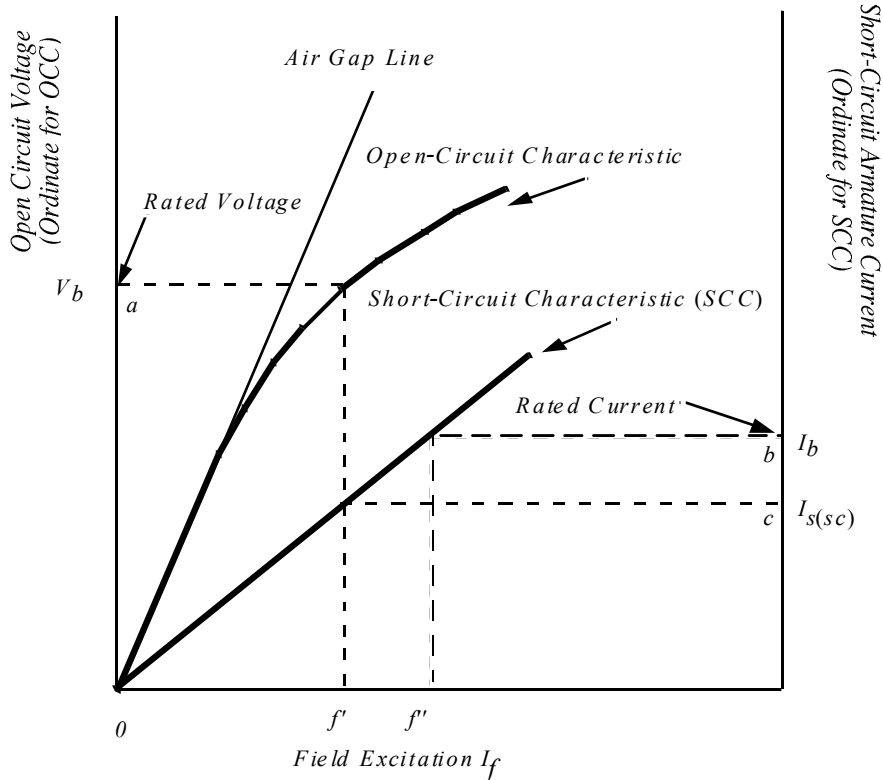


Figure 4.19 Open and short-circuit characteristics showing measurement of saturated direct axis reactance.

For operation near or at rated terminal voltage, it is sometimes assumed that the machine is equivalent to an unsaturated machine whose magnetization curve is a straight line through the origin and the rated voltage point on the open-circuit characteristic can be taken as a line such as the dashed line *Op* of Figure 4.17. The saturated value of direct axis synchronous reactance at rated voltage is taken as

$$x_{ds(sat)} = \frac{V_{s(oc)}}{I_{s(sc)}} \quad (4.147)$$

This method of handling saturation generally provides satisfactory results provided that the saturation is not too great.

Another useful quantity that can be derived from the short- and open-circuit characteristics is the *short-circuit ratio*. The short-circuit ratio is defined as the ratio of the field current required for rated voltage on open-circuit to the

field current required for rated armature current on short-circuit. That is, in Figure 4.19, the short-circuit ratio is

$$SCR = \frac{I_{sc}}{I_b} = \frac{Of}{Of'} \quad (4.148)$$

It can be shown that the short-circuit ratio is the reciprocal of the per unit value of saturated synchronous reactance. Specifically, recall that

$$x_{ds(sat)} = \frac{V_{s(oc)}}{I_{s(sc)}} \quad (4.149)$$

If $V_{s(oc)}$ corresponds to the base voltage V_b , then

$$x_{ds(sat)} = \frac{V_b}{I_{s(sc)}} \quad (4.150)$$

Equation 4.103 can be manipulated to

$$x_{ds(sat)} = \begin{pmatrix} \frac{V_b}{I_b} \\ \frac{I_b}{I_{s(sc)}} \\ \frac{I_{s(sc)}}{I_b} \end{pmatrix} \quad (4.151)$$

Hence, in per unit,

$$x_{DS(sat)} = \frac{1}{\frac{I_{s(sc)}}{I_b}} \quad (4.152)$$

$$= \frac{I_b}{I_{s(sc)}} \quad (4.153)$$

However, since the short-circuit ratio is simply a straight line, Eq. (4.152) is equivalently

$$x_{DS(sat)} = \frac{I_{fr}(\text{for base } I_{fr})}{I_{fr}(\text{for short circuit } I_{fr})} \quad (4.154)$$

$$= \frac{Of}{Of'} = \frac{1}{SCR} \quad (4.155)$$

If the mechanical power required to drive the machine is also measured while the short-circuit test is being made, information can also be obtained

concerning the losses arising from armature current flow. The mechanical power required to drive the machine during the short-circuit test is equal to the sum of the friction and windage loss plus the losses caused by the armature current. The armature current losses can be found by subtracting the friction and windage losses (determined previously by running the machine at synchronous speed with both the field and the armature open circuited) from the total losses measured. These losses are usually termed the *short-circuit load loss*. The short-circuit load loss comprises copper loss in the armature winding, the local core losses caused by the armature leakage flux, and also a very small core loss caused by the resultant flux. The loss due to armature copper loss can be computed if the dc resistance is quickly measured after the test and then corrected, when necessary, for the temperature which actually occurred in the copper conductors during a given short-circuit test.

This measurement is frequently done by performing a short-circuit test, then reading the temperature as a function of time beginning as soon after the test as possible. The temperature during the test can then be determined by extrapolating the curve back to “ $t = 0$.” The difference between the short-circuit load loss and the armature i^2r loss is called the *stray load loss* and corresponds to the loss due to skin effect and eddy currents in the stator conductors and to iron loss in the stator teeth due to armature current flow.

A curve of short-circuit load loss plotted against armature current is shown in [Figure 4.20](#). Note that it is approximately parabolic, i.e., it varies essentially as the square of the armature current. The stray load loss is commonly assumed to have the same value under normal load conditions as on short-circuit at the same load current. The effects of stray load loss are usually accounted for in an equivalent circuit by modifying the stator resistance appropriately. On the assumption that the stray load loss is a function of the square of the armature current, the effective stator resistance $r_{s(eff)}$ can be determined from the short-circuit load loss by the equation

$$r_{s(eff)} = \frac{\text{Short-Circuit Load Loss}}{(\text{Short-Circuit Armature Current})^2} \quad (4.156)$$

Usually it is sufficient to find the value of $r_{s(eff)}$ at rated current and then to assume this value to be constant as the load varies.

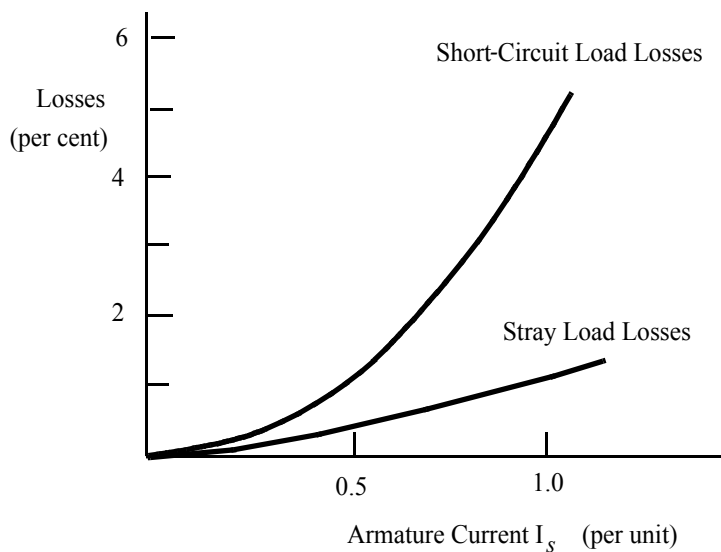


Figure 4.20 Short-circuit load loss and stray load loss plotted as a function of armature current.

4.15 Saturation Modeling of Synchronous Machines under Load

Thus far, the case where saturation occurs under load has yet to be handled. Since saturation is more readily managed with round-rotor synchronous machines this case will be considered first. [Figure 4.21](#) shows a phasor diagram for this case when the machine acts as an overexcited generator. Recall that with the scaling that has been chosen, a flux triangle involving the excitation flux $\Psi_{s(x)}$, the armature reaction flux $\Psi_{s(ar)}$, and the resultant flux Ψ_s can be located with the excitation flux $\Psi_{s(x)}$ lying along the direct axis. The time rate of change of these three fluxes produces corresponding voltage drops which are located as phasors (or vectors) oriented counter-clockwise by 90° . These voltage drops are termed the excitation voltage, the armature reaction voltage drop, and the voltage behind stator resistance. The stator iR drop is added onto the voltage behind stator resistance to form the terminal voltage and thereby completes the diagram.

When the iron becomes saturated, it is convenient to separate the stator flux vector into two components, one component corresponding to a leakage flux which does not enter into the saturation computation and a second component corresponding to flux in the air gap upon which the saturation depends. The air gap component of stator flux and corresponding air gap voltage are labeled Ψ_g and V_g respectively. In many cases the terminal voltage and current are known and hence, by subtracting the stator *ir* and leakage *ix* drop, the gap voltage V_g can be determined.

When the magnetic circuit remains linear, it is apparent that each flux component is exactly proportional to the *MMF*, which establishes this component of flux. Hence, paying proper attention to units, the flux linkage triangle of [Figure 4.8](#) can be used to represent *MMFs* as well as flux linkages. If \mathcal{F}_x is used to denote the field *MMF* (proportional to $\Psi_{s(x)}$), \mathcal{F}_{ad} the *d*-axis armature reaction *MMF* (proportional to the air gap portion of the *d*-axis armature reaction flux linkage $\Psi_{md(ar)}$), \mathcal{F}_{aq} the *q*-axis armature reaction *MMF* (proportional to the *q*-axis component of armature reaction flux linkage $\Psi_{mq(ar)}$), and \mathcal{F}_g the resultant air gap *MMF* (proportional to Ψ_g), the phasor diagram of [Figure 4.21\(a\)](#) can be constructed.

The proportionality constant between the hybrid flux linkage variable Ψ and the *MMF* \mathcal{F} is readily determined. For example, it can be recalled that the excitation flux is

$$\Psi_{s(x)} = x_{md} I_{fr}' \quad (4.157)$$

which, from Chapter 3, can be written as

$$\Psi_{s(x)} = x_{md} \left(\frac{2}{3} \frac{1}{N_s} \right) N_{fr} I_{fr} \quad (4.158)$$

$$= \omega_b \mathcal{P}_{md} N_s (N_{fr} I_{fr}) \quad (4.159)$$

where \mathcal{P}_{md} is the permeance of the direct axis magnetic circuit or, from Chapter 3,

$$\mathcal{P}_{md} = \frac{\mu_0 r l}{g_{min}} \left(\frac{\pi}{4} \right) k_d$$

In a similar manner it can be shown that the air gap portion of the stator flux resulting from armature reaction (i.e., stator current) is

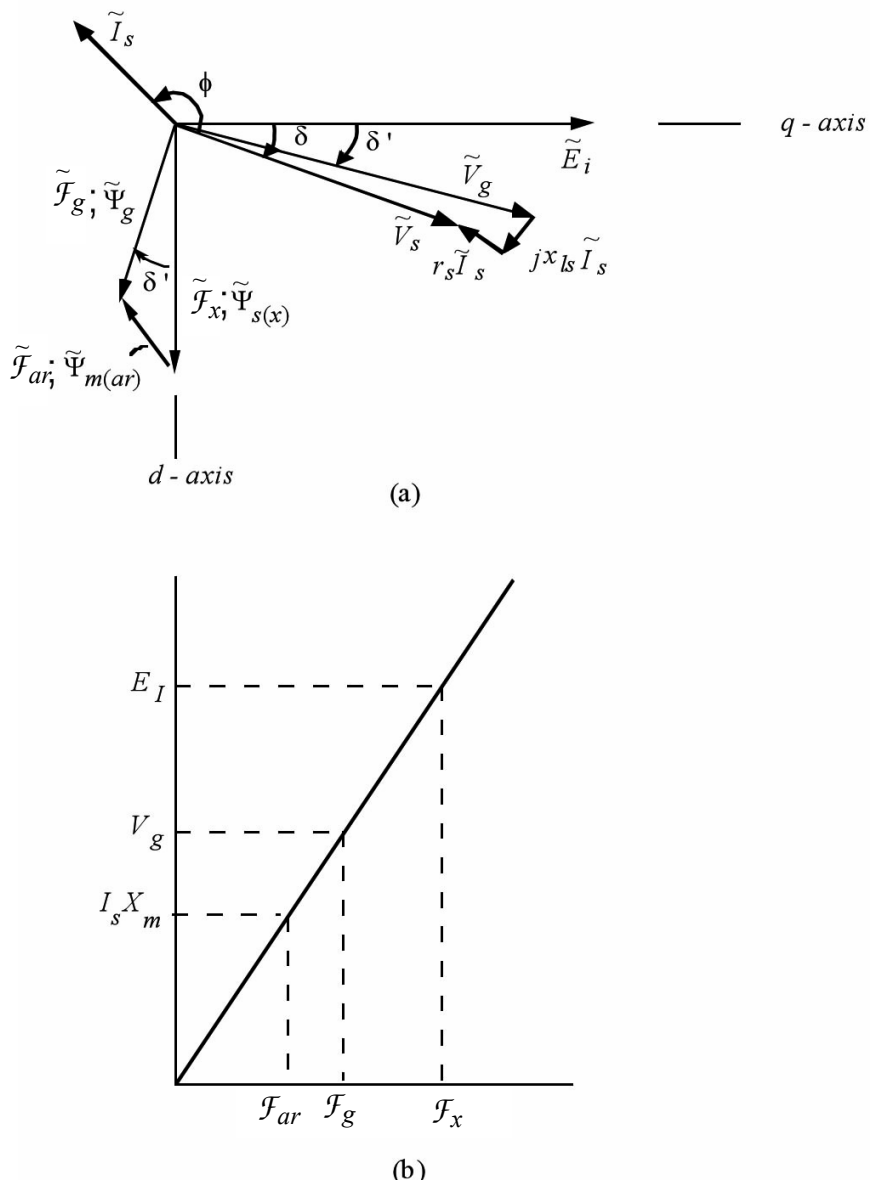


Figure 4.21 (a) Phasor diagram of a synchronous machine as an overexcited generator explicitly showing the *MMF* phasor diagram for the case of no saturation, (b) open-circuit characteristic used to identify *MMF* components and their respective voltage drops.

$$\Psi_{md(ar)} = \omega_b \mathcal{P}_{md}(N_s^2 I_{ds}) \quad (4.160)$$

The proportionality between the *MMFs* and the various induced voltage components can best be determined by providing an auxiliary *MMF* vs. voltage characteristic. Since the constants in Eqs. (4.159) and (4.160) are the same, this characteristic can clearly be used to determine the voltage drops resulting from either stator or rotor ampere turns.

The characteristic for the direct axis is conveniently obtained by measuring the open-circuit voltage as a function of field current, i.e., the *open-circuit characteristic*. Since the stator is open circuited, the measured voltage is, in reality, also the voltage drop across the air gap, i.e., across the magnetizing inductance of the direct axis. The abscissa of the open-circuit plot can be converted to *MMF* by multiplying the resulting field amps by the number of field turns. It is important to realize that while the abscissa represents *MMF* produced by the field circuit, when stator current flows, the *same axis* represents the net *MMF* produced by both the field current and *d*-axis stator current acting simultaneously.

The *d*-axis component of voltage, presumably the same if induced by a stator or rotor based *d*-axis *MMF*, can be used to find the effective turns ratio between the stator and the field winding from short-circuit data. Referring to [Figure 4.18](#), if the stator resistance and stator leakage inductance are neglected, then the voltage drop due to armature reaction exactly opposes the voltage induced due to the excitation, or

$$\Psi_{md(ar)} = \Psi_{s(x)}$$

If the stator *Ir* and leakage reactance drop are accounted for, then the armature reaction voltage drop is slightly less than the excitation voltage, or

$$\Psi_{md(ar)} = k_s \Psi_{s(x)} \quad (4.161)$$

where k_s is roughly 0.85 to 0.9. From Eqs. (4.159) and (4.160), it can be determined that

$$\frac{N_s}{N_f} = \frac{k_s I_f}{I_s} \quad (4.162)$$

Thus, if the stator and rotor currents are measured upon short-circuit and if the stator resistance and leakage inductance are known, the turns ratio can be determined. Means for measuring the stator leakage inductance will be discussed later in this chapter.

In cases where the number of field turns is not known, the abscissa of the d -axis characteristic can be simply scaled in terms of field amps, although the abscissa variable is now interpreted as *MMF*. The d -axis *MMFs* can then be said to be *referred to one field turn*. In a similar manner the q -axis excitation curve can be plotted against stator amps, i.e., volts vs. amps, referred to one *stator turn*.

Figure 4.21(b) shows the three *MMF* components, \mathcal{F}_x , \mathcal{F}_{ar} , and \mathcal{F}_g for the linear case and their resulting induced voltages. Since the *MMF* is simply proportional to the corresponding flux linkage in the unsaturated case, the *MMF* “ \mathcal{F} ” vectors and flux linkage “ Ψ ” vectors form similar triangles which, with due respect to scaling, can be represented by the same triangle in Figure 4.21(b).

Establishing a similar quadrature axis magnetizing characteristic in the case of a salient-pole machine is more difficult. It must be obtained by instrumenting the machine with a torque angle sensor (or position sensor). After the resistive and leakage inductance drops are subtracted from the terminal voltage, the resulting air gap voltage must then be resolved into its d - and q -axis components. The q -axis voltage component is then plotted against the q -axis component of current.

In cases where the motor becomes saturated, the principle remains the same except that the *MMFs* are no longer linearly related to the corresponding induced voltages. Figure 4.22 shows such a situation. Care must now be taken in the addition of *MMFs* to accurately reflect what is taking place inside the machine. Unfortunately, in the general case of saturation in both the d - and q -axes, the non-linearities of the saturation curves necessitate an iterative solution to obtain a phasor diagram solution for a given terminal voltage and current.

4.16 Construction of the Phasor Diagram for a Saturated Round-Rotor Machine

In many cases one is confronted with the following problem. Given that a certain machine is operating at specified voltage, current, and power factor, what is the excitation needed to realize this terminal condition? Consider answering this question first for a saturated round-rotor machine operating as a generator. It is assumed that the terminal voltage and current of Figure 4.22 are specified with generator operation assumed.

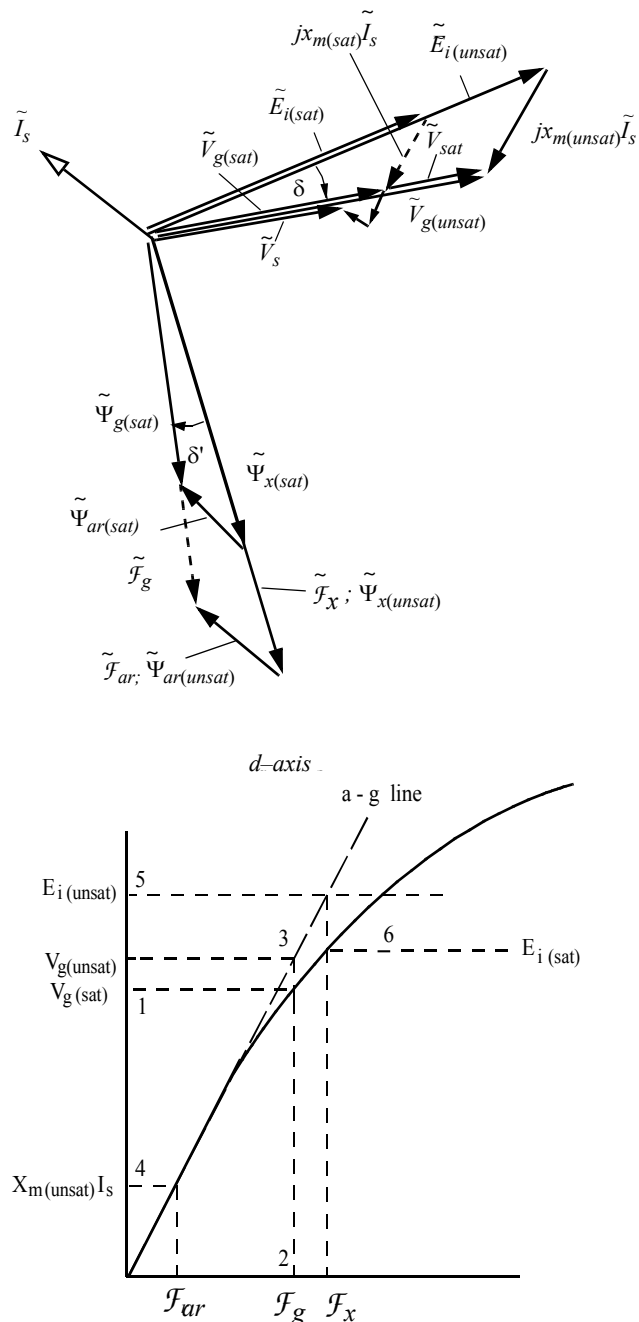


Figure 4.22 Construction diagram of saturated round-rotor synchronous generator.

A step by step procedure to obtain the phasor solution is as follows. First subtract the stator resistive $r_s I_s$ and leakage reactance $jx_{ls} I_s$ drop from the terminal voltage V_s to obtain the air gap voltage $V_{g(sat)}$ (see point #1 on the saturation curve, Figure 4.22). Locate the corresponding saturated value of air gap MMF $\mathcal{F}_{g(sat)}$ from the saturation curve (point 2 on the saturation curve). The location of the q -axis must now be determined. This step is usually accomplished by adding the voltage drop $jx_m I_s$ from the tip of the air gap voltage vector V_g . However the saturated value of $x_m I_s$ cannot be determined independently of the field MMF ($x_m I_{fr}$). Therefore, the location of the q -axis can not be found from saturated values. One can, however, locate the q -axis if one uses the corresponding unsaturated values. If the MMF acting in the gap $\mathcal{F}_{g(sat)}$ acted on unsaturated rather than saturated iron, the air gap voltage in the gap would take on the value $V_{g(unsat)}$ rather than $V_{g(sat)}$, as shown in Figure 4.22 (point #3).

Assuming linearity between excitation MMF and voltage drop, the unsaturated magnetizing reactance drop $jx_{m(unsat)} I_s$ (point 4) is now determined by measuring the proper distance along the air gap line. The appropriate value of $x_{m(unsat)}$ to use in this calculation must be determined from separate tests (to be discussed). This distance is then added to the tip of $V_{g(unsat)}$ in its correct phasor relationship. The unsaturated value of excitation voltage $E_{i(unsat)}$ as well as the location of the q -axis is thereby established. By projecting a line from the tip $V_{g(sat)}$ to the q -axis, the saturated values of $jI_s x_{m(sat)}$ and $E_{i(sat)}$ can now be determined. Note that the ratios $V_{g(unsat)}/V_{g(sat)}$, $E_{i(unsat)}/E_{i(sat)}$, and $x_{m(unsat)} I_s / (x_{m(sat)} I_s)$ are all equal. (It is an interesting trigonometric exercise to show this.)

For the purpose of obtaining a solution without resorting to the saturation curves, it is useful to define the saturation factor k_{sat} as

$$k_{sat} = \frac{V_{g(unsat)}}{V_{g(sat)}} \quad (4.163)$$

Then,

$$E_{i(sat)} = \frac{E_{i(unsat)}}{k_{sat}} \quad (4.164)$$

and

$$x_{m(sat)} = \frac{x_{m(unsat)}}{k_{sat}} \quad (4.165)$$

Figure 4.23 shows a typical plot of the saturation factor k_{sat} as a function of the excitation voltage for a fixed (rated) value of terminal voltage.

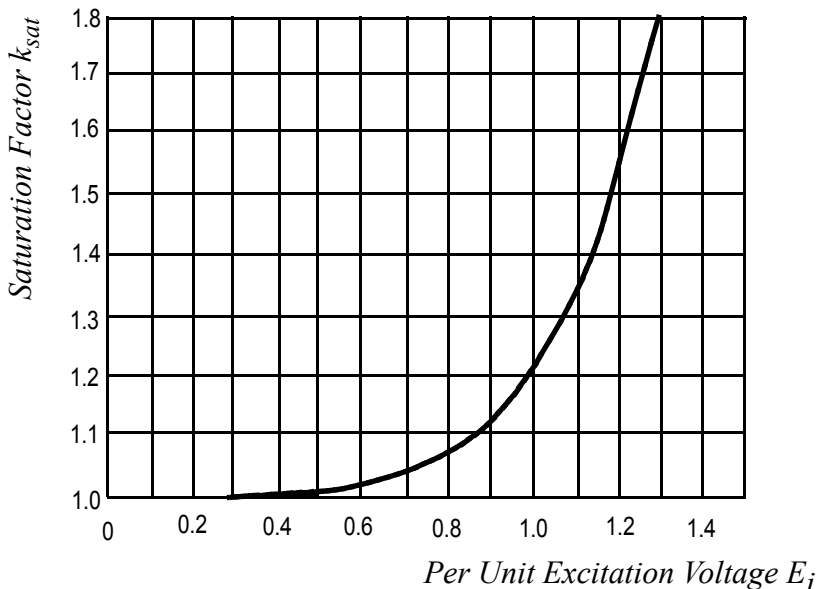


Figure 4.23 Saturation factor as a function of excitation voltage for rated terminal voltage for a typical round-rotor machine.

4.17 Calculation of the Phasor Diagram for a Saturated Salient-Pole Synchronous Machine

When the machine has a salient-pole construction, calculation of the vector diagram follows much the same procedure as for the round-rotor machine. If the terminal voltage and current are given, the air gap voltage $\tilde{V}_{g(sat)}$ can again be determined as shown in Figure 4.24 (point 1 on the saturation curve). In much the same manner as the previous round rotor case, it is now necessary to locate the q -axis so as to determine the reactance drop along the d - and q -axes. If saturation is assumed to occur only in the d -axis, the reactance drop $jx_{mq}\tilde{I}_s$ can again be used to locate the q -axis and the fictitious voltage \tilde{E}_q established in much the same manner as the unsaturated case. The projection $\tilde{V}_{gq(sat)}$ of \tilde{V}_g on the q -axis can then be determined. Reference to the corre-

sponding saturation curve now indicates the total d -axis MMF $\tilde{\mathcal{F}}_{gd}$ acting on the machine. Since the q -axis has now been located, the $d-q$ components of stator current can now be determined.

The next step is to determine the reactive drop $jx_{md}\tilde{I}_{ds}$ along the q -axis and thus establish \tilde{E}_i . However, in this case it is not possible to directly determine $jx_{md}\tilde{I}_{ds}$, since $x_{md(sat)}$ is not known. However, since the unsaturated value can be readily measured and the $d-q$ components of stator current are now known, the voltage $\tilde{V}_{gq(unsat)}$ can be found directly above $\tilde{V}_{gq(sat)}$ on the air gap line (point 2 on [Figure 4.24](#)). The reactance drop $x_{md(unsat)}\tilde{I}_{ds}$ can then be determined and the unsaturated value of the excitation voltage $E_{i(unsat)}$ can be identified on the air gap line. This point is marked as point 4. The saturated value of \tilde{E}_i lies directly below the unsaturated value on the saturation curve, point 5. Since distances along the q -axis in the phasor diagram and distances along the ordinate on the saturation curve are algebraic rather than vector quantities, the lengths corresponding to $x_{md(unsat)}\tilde{I}_{ds}$ and $x_{md(sat)}\tilde{I}_{ds}$ and the MMF needed to overcome this reactance drop can be established.

4.18 Zero Power Factor Characteristic and the Potier Triangle

An important step in the construction of the phasor diagrams for saturated machines is establishing the air gap voltage V_g by subtracting the leakage reactance drop (and resistance drop) from the terminal voltage. As yet, it has not been discussed how this leakage reactance can be determined. A case of special importance in this regard is that of a synchronous machine operating at zero power factor in a overexcited condition. Such a characteristic can be obtained by using a reactive load which can be adjusted to produce a constant (rated) terminal current when the excitation of the machine is varied over a wide range. Alternatively, the machine can be loaded with another synchronous machine of roughly equal size, as shown in [Figure 4.25\(a\)](#). By varying the two field currents, data can be obtained for a curve of terminal voltage as a function of generator field current when the armature current is constant at its rated full load value. This curve is known as the *zero power factor characteristic*.

From the phasor diagram of [Figure 4.25\(c\)](#), since the air gap emf voltage E_i and terminal voltage V_s during zero power factor operation are nearly in phase, the use of complex numbers can be dispensed with so that

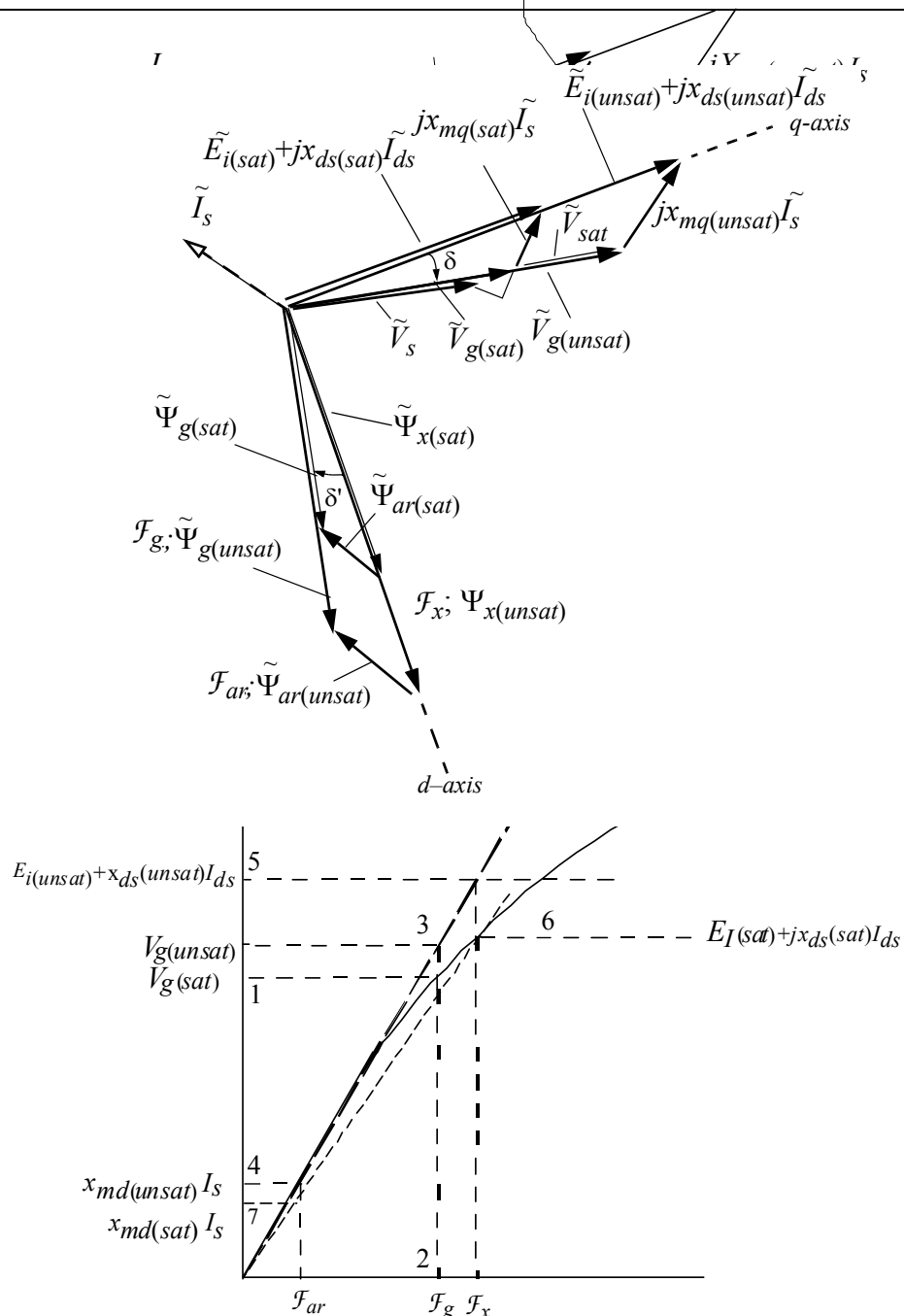


Figure 4.24 Construction diagram of saturated overexcited salient-pole synchronous generator.

$$V_s \cong E_{ig} - x_{dsg} I_s \quad (4.166)$$

or, alternatively in terms of the motor excitation voltage,

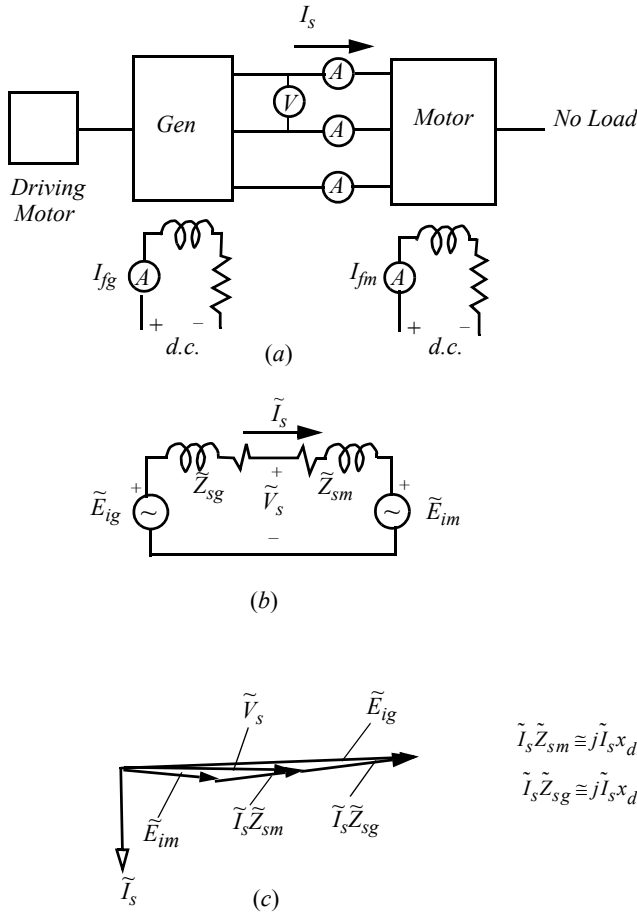


Figure 4.25 (a) Circuit connection for zero power factor test, (b) equivalent circuit and (c) resulting phasor diagram.

$$V_s \cong E_{im} + x_{dsm} I_s \quad (4.167)$$

The conditions of the circuit of Figure 4.25(b) for three values of \$V_s\$ are given in Figure 4.26. Assuming that it is the generator which is being tested, Eq. (4.167) can be written as

$$V_s = E_{ig} - x_{mdg} I_s - x_{lsg} I_s \quad (4.168)$$

$$= V_g - x_{lsg} I_s \quad (4.169)$$

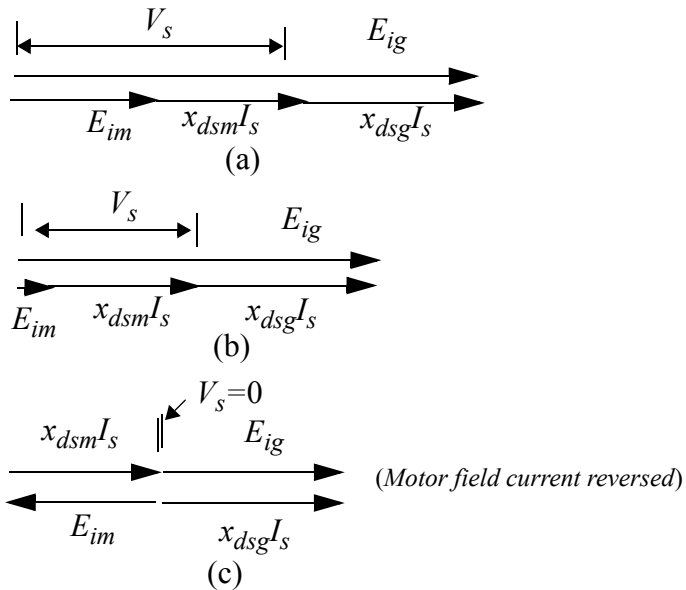


Figure 4.26 Conditions of the circuit of Figure 4.25(b) for three values of terminal voltage V_s . (a) large V_s , (b) medium V_s , (c) zero V_s .

where V_g is the generator air gap voltage under the zero power factor condition. The corresponding MMFs are now related by the simple algebraic equation

$$\mathcal{F}_{s(x)} = \mathcal{F}_s + \mathcal{F}_{s(ar)} \quad (4.170)$$

The armature reaction can be further broken down into two components, one which corresponds to the MMF, which corresponds to the flux through the main path of the d -axis and the second, which produces stator leakage flux,

$$\mathcal{F}_{s(ar)} = \mathcal{F}_{sm(ar)} + \mathcal{F}_{sl(ar)} \quad (4.171)$$

A typical curve is shown on Figure 4.27 together with its corresponding open-circuit characteristic. The equation describing the variation of open-circuit terminal voltage with excitation is simply

$$V_s = E_i \quad (4.172)$$

or, alternatively,

$$V_s = V_g \quad (4.173)$$

since, on open-circuit, V_g and E_i are identical. The resultant stator air gap MMF is clearly related to the excitation MMF simply by

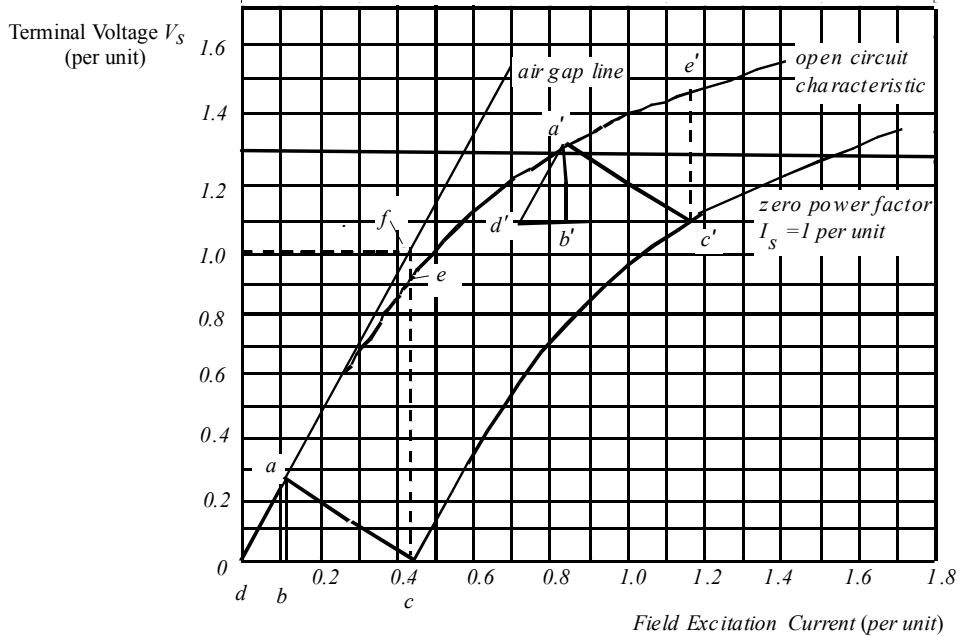


Figure 4.27 Open-circuit and zero power factor characteristics of a typical three-phase, wye connected, 100 KVA, 220 V, 60 Hz salient-pole synchronous machine.

$$\mathcal{F}_{s(x)} = \mathcal{F}_s \quad (4.174)$$

Comparison of Eq. (4.173) with (4.169) and Eq. (4.174) with (4.170) suggests that the excitation characteristic for zero power factor can be obtained by simply measuring the open-circuit characteristic and then moving this characteristic *down* by the generator leakage reactance $x_{lsg}I_s$ and *to the right* by the generator armature reaction MMF $\mathcal{F}_{s(ar)}$. If the motor rather than generator is the machine under test, the motion of the open-circuit curve down and to the right is the same even though the sign of the reactance drops, Eqs. (4.166) and (4.167), differ in sign from the generator. The effect is the same, since the polarity of the motor emf is reversed when $V_s = 0$ (see Figure 4.26). The motion of a given point in such a manner from the open-circuit curve to the zero power factor curves forms the triangles abc and $a'b'c'$ as shown on Figure 4.27.

The open-circuit and zero power factor curves can be used to determine many important parameters of the machine. For example, consider point c on

the zero power factor curve wherein the terminal voltage is equal to zero. From Eq. (4.166),

$$0 = E_i - I_s x_{ds} \quad (4.175)$$

Since the two terms must sum algebraically to zero, the distance from point c vertically to the open-circuit characteristic, point e , equals not only the value of E_i for this condition but also the value of $I_s x_{ds}$. If point f is located on the air gap line, then the unsaturated value of x_{ds} can be determined. That is,

$$x_{ds(unsat)} = \frac{V_{cf}}{I_{zpf}} \quad (4.176)$$

where I_{zpf} is the current selected for generating the zero power factor characteristic.

In a similar manner, consider point c' of the upper triangle. From Eq. (4.166) it is apparent that since point c' represents the terminal voltage V_s and point e corresponds to the internal voltage $E_{i(sat)}$, then the distance $c'-e'$ represents the voltage drop $I_s x_{ds(sat)}$. The saturated value of direct axis inductance is again found in the manner of Eq. (4.176).

The lower triangle located on the horizontal axis of Figure 4.27 has a special significance and forms what is called the *Potier triangle*. Although the field current is the implied variable, in general, the horizontal axis corresponds to the direct axis MMF. In fact, if one multiplies the field current by the effective number of field turns (the fundamental component of the winding function) this axis can be scaled in ampere turns (i.e., MMF) rather than amperes. Referring to Eq. (4.170), it is then apparent that the length cd is essentially proportional to the MMF $\mathcal{F}_{s(x)} = \mathcal{F}_{s(ar)} = \mathcal{F}_{sm(ar)} + \mathcal{F}_{sl(ar)}$, since the terminal voltage is zero for this case. While it is not possible at this point to separate $\mathcal{F}_{sm(ar)}$ and $\mathcal{F}_{sl(ar)}$, one can assume for the moment that this is possible and identify the additional point on the horizontal axis b . By the same reasoning process as used previously, it is possible to establish that the vertical distance $a-b$ then corresponds to the leakage reactance drop $I_s x_{ls}$. One can also realize that this is the case by comparing similar triangles dce and dba . In the case of dce , the horizontal side is proportional to the MMF to magnetize the leakage permeance plus that needed to magnetize the main direct axis air gap plus iron path. The vertical axis is the resulting voltage drops $I_s x_{ds} = I_s x_{ls} + I_s x_{md}$. In the case of the triangle dab , the horizontal axis is proportional to only the MMF needed to magnetize the leakage permeances. The triangles dab and dce are

similar triangles so that the vertical distance $a-b$ is clearly equal to the leakage reactance drop.

Since the point b is as yet unknown, the leakage reactance drop ab can not yet be determined. However, enough information is contained in its construction that a determination of the leakage reactance drop can be made. A geometrical construction for finding the triangle abc for any terminal voltage condition is as follows:

- 1) Select a point, say c' on the zero power factor characteristic at rated voltage (if this is the desired voltage operating point).
- 2) Draw the horizontal line $c'd'$ of equal length to the field excitation on short-circuit cd .
- 3) Through point d' draw the straight line $d'a'$ parallel to the air gap line, intersecting the open-circuit characteristic at a' .
- 4) Draw the vertical line $a'b'$. The Potier reactance x_p is then given by

$$x_p = \frac{\text{Voltage Drop } a'b'}{\text{Zero Power Factor Armature Current}} \quad (4.177)$$

The key to the Potier triangle is to note that the subtriangle dab must be equal to triangle $d'a'b$ whatever the operating point, presuming that the current remains constant and that the leakage inductance is essentially constant, independent of load. In practice, the size of the Potier triangle (specifically the length $a'b'$) varies slightly with excitation. This results from the fact that the stator leakage reactance and main flux component of the magnetizing inductance of the machine are not precisely constant but vary slightly as the iron saturates. While not precise, the value of x_p at rated voltage is usually taken as the (constant) value of leakage reactance for all operating conditions, provided that the air gap voltage does not become unusually large or small compared with the rated value.

4.19 Other Reactance Measurements

It is already apparent that the direct axis synchronous reactance can be obtained by a simple steady-state open-circuit and short-circuit test. Measurement of the quadrature axis synchronous reactance requires special techniques, however, to ensure that only the q -axis magnetic circuit is involved in the mea-

surement. One test, called the *slip test*, is accomplished by driving the machine mechanically at a speed slightly greater or less than synchronous speed. The field winding is open circuited, and balanced positive sequence voltages are applied to the stator windings. Under these conditions the armature *MMF* slowly moves past the field poles at what amounts to slip speed. Oscillograms are taken of the resulting armature current, together with the voltage applied to the stator and the voltage induced in the field winding.

Figure 4.28 shows the general shape of the oscillogram but, for simplicity, at a slip about five times larger than one recommended for this test. When the stator *MMF* wave is in line with the direct axis, the impedance of the machine equals x_{ds} . On the other hand, one quarter of a slip cycle later in time, the stator *MMF* is now in line with the q -axis and the impedance looking into the machine equals x_{qs} (in series, of course, with a stator *ir* drop). The instant when the stator *MMF* is lined up with the quadrature axis is generally taken to be the instant when the armature current reaches a maximum (this is not quite true when the stator resistive drop is significant). The quadrature reactance drop is then, approximately,

$$x_{qs} \approx \frac{V_{s(min)}}{I_{s(max)}} \quad (4.178)$$

The principal shortcoming of the slip test is that large errors may be produced by the effects of current induced in the rotor damper windings unless the slip is very small. This may be difficult to accomplish for all but very small machines because of the tendency of the machine to lock into synchronism as it nears synchronous speed. Better results are obtained at reduced values of armature voltage. However, in this case the effects of saturation on x_{qs} can not be determined.

Another test which can be used that avoids some of these difficulties is the loss of synchronism test. In this case the machine is run as an unloaded synchronous motor. Again balanced stator voltages are applied to the machine but in this case the field current is gradually reduced to zero. The machine then operates as a reluctance motor. The polarity of the field current is now reversed. The point at which zero torque is reached can be obtained by solving Eq. (4.51) when the left hand side has been set equal to zero, that is,

$$0 = \frac{3}{2} \left(\frac{P}{2\omega_b} \right) \left[\frac{V_s E_i}{x_{ds}} \sin \delta + V_s^2 \left(\frac{x_{ds} - x_{qs}}{2x_{ds}x_{qs}} \right) \sin(2\delta) \right] \quad (4.179)$$

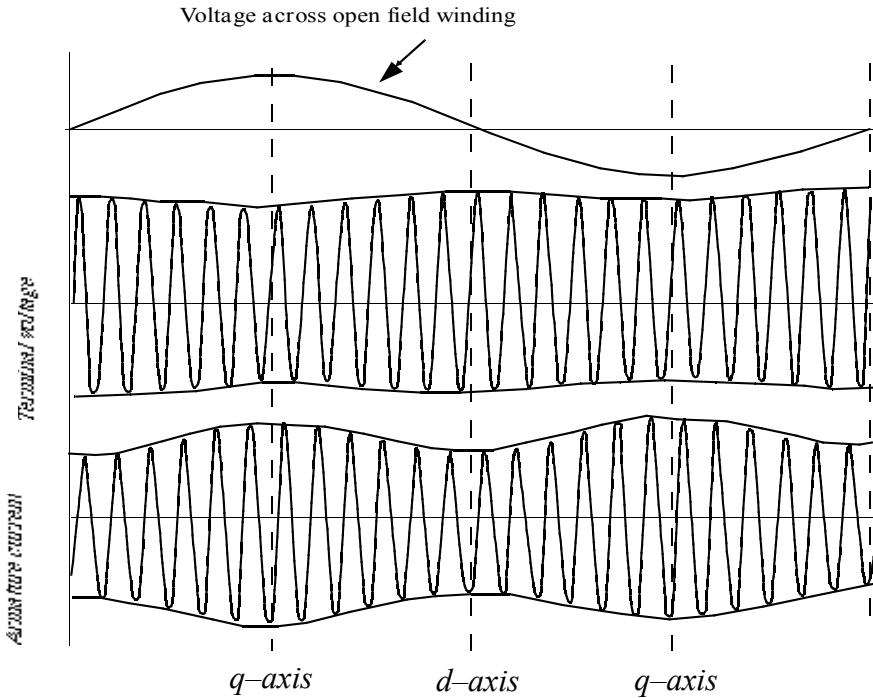


Figure 4.28 Terminal voltage and current of one phase during slip test.

Upon cancelling constants common to both terms and using the trig identity $\sin(2\delta) = 2\sin\delta\cos\delta$, one obtains

$$0 = \frac{E_i}{x_{ds}} + V_s \left(\frac{x_{ds} - x_{qs}}{2x_{ds}x_{qs}} \right) \cos\delta \quad (4.180)$$

The value of δ which corresponds to the point where this function reaches a maximum value of zero can be obtained by differentiating Eq. (4.60) with respect to δ , and setting the result equal to zero, so that

$$0 = V_s \left(\frac{x_{ds} - x_{qs}}{2x_{ds}x_{qs}} \right) \sin\delta \quad (4.181)$$

and the point at which the torque equals zero and is also the maximum value is when " $\delta = 0$ ". Setting $\delta = 0$ in Eq. (4.180) and solving for x_{qs} yields the final result,

$$x_{qs} = \frac{V_s}{V_s - E_i} x_{ds} \quad (4.182)$$

where E_i is a negative value. A plot of the torque vs. δ for progressively reducing values of E_i is plotted in Figure 4.29 which clearly indicates that the results obtained analytically are correct. An advantage of this test over the slip test is that the former can be carried out near rated voltage and therefore the variation of x_{qs} with saturation can be determined. A number of other methods exist and for these the reader is referred to the excellent treatment by Liwschitz-Garik and Whipple [2].

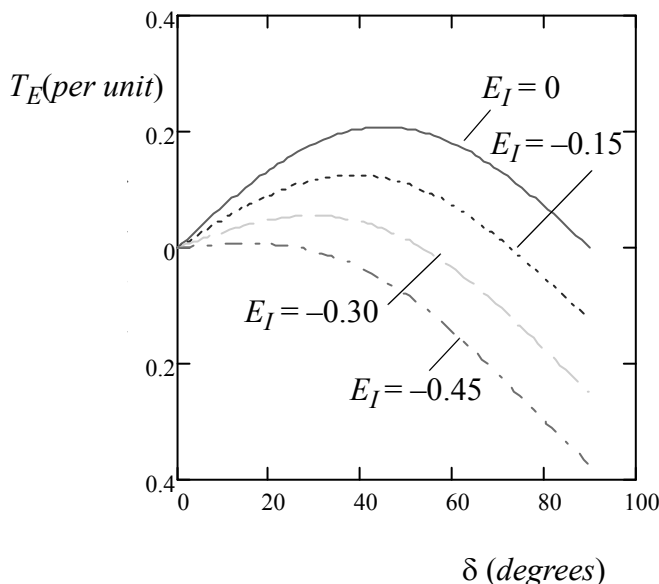


Figure 4.29 Torque vs. δ with negative values of excitation E_I for parameters $x_{DS} = 1.2$, $x_{QS} = 0.8$, and $V_S = 1.0$.

4.20 Steady-State Operating Characteristics

Numerous steady-state characteristics can be formed to aid in the application of synchronous machines. The computation of such characteristics is readily accomplished by repeated evaluation of the machine vector diagram presented in this chapter for the particular set of constraints of interest.

First of all, consider the case in which a synchronous generator delivers power at constant frequency to a constant power factor load. The curves showing the field current needed to maintain rated terminal voltage as the magnitude (but not phase) of the load is varied are called compounding curves. Three compounding curves are shown in Figure 4.30 for three power factors. When the load is leading the field current requirements can actually be reduced from the requirements at no load since the leading power factor reactive contributes reactive kVA to help magnetize the machine until the stator current roughly exceeds a value which depends on the load power factor.

Note that increasing excitation is required for lagging power factor loads to offset the need for reactive kVA to produce the desired flux in the machine as stator current increases. On the other hand, if the field current is held constant while the load varies, the terminal voltage will vary. Characteristic curves of terminal voltage as a function of armature current for fixed excitation are shown in Figure 4.31. In this case the field current used for the plots corre-

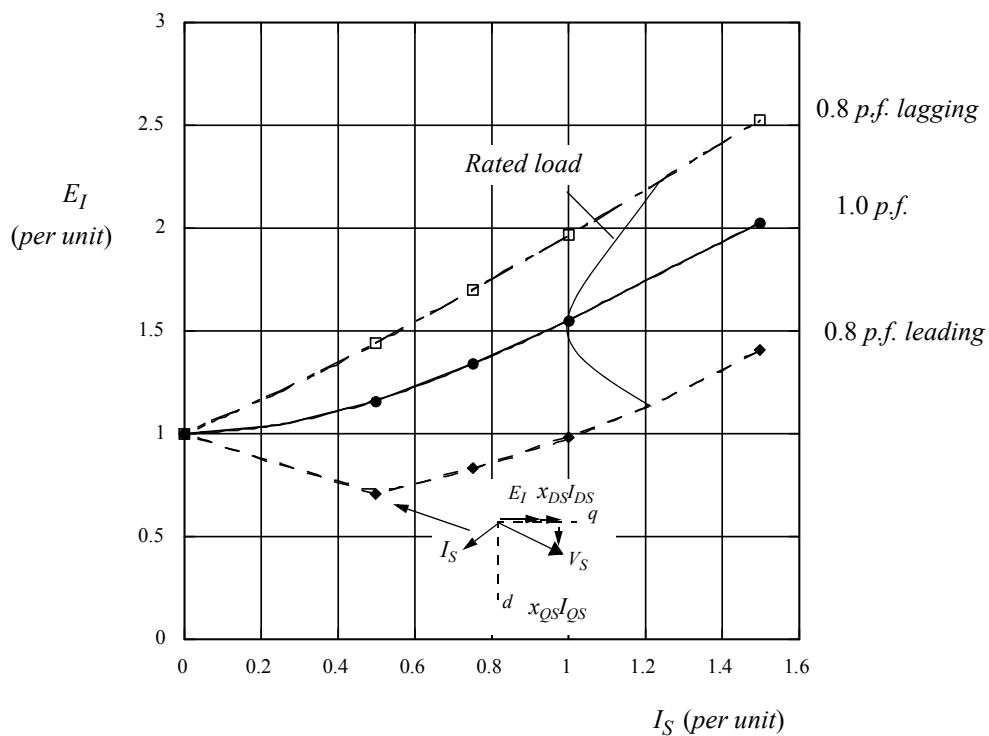


Figure 4.30 Generator compounding curves ($x_{DS} = 1.2$, $x_{QS} = 0.9$, $r_S = 0.01$ per unit).

sponds to that value required to produce rated voltage when rated current flows

at the power factor specified. The field current for the three curves is therefore not the same value.

Synchronous generators are usually rated in terms of a certain maximum MVA load at a specific voltage and power factor which they can supply without exceeding rated temperature. These power factors are typically 0.80, 0.85, or 0.90 lagging, meaning that the generator is typically called upon to supply reactive VA to the power system of prescribed amounts to magnetize magnetic components of the system such as transformers and induction motors. The active power output of a generator is typically limited to a value within (less than) its MVA rating. By virtue of the voltage regulating system, the machine normally operates at a constant voltage whose value is within $\pm 5\%$ of rated voltage. When active power loading and terminal voltage are fixed, the machine's reactive power loading is limited by armature and field heating. A typical set of reactive power capability curves for a large hydrogen cooled turbo generator is shown in [Figure 4.32](#). The curve gives the maximum reactive power loadings corresponding to various active power loadings with operation at rated voltage. Note that a higher value of reactive power can be supported with increased cooling (higher hydrogen pressure). Note the break in the continuous curve at the 85% power factor condition. For power factors lower than 0.85 the field heating of this machine is limiting, while at power factors greater than 0.85 the power output of the machine is limited by stator current.

The power factor of a synchronous motor can also be adjusted by changing its field excitation. A set of curves which shows the relation between armature current and field current at a constant terminal voltage for various loads is known as *V curves* because of their characteristic shape. A set of such curves is shown in [Figure 4.33](#). The dashed lines of Figure 4.33 are lines of constant power factor. It can be noted that for constant power output, the stator current reaches a minimum value at unity power factor and is larger for either leading or lagging power factor. Points to the right of the unit power factor curve correspond to overexcitation while points to the left produced underexcitation. Note that the synchronous motor compounding curves essentially the same as the generator compounding curves of Figure 4.32 except that the ordinate and abscissa are interchanged. Were it not for the small effects of armature resistance, the motor and generator compounding curves would clearly be identical except that the leading and lagging power factor curves would be reversed.

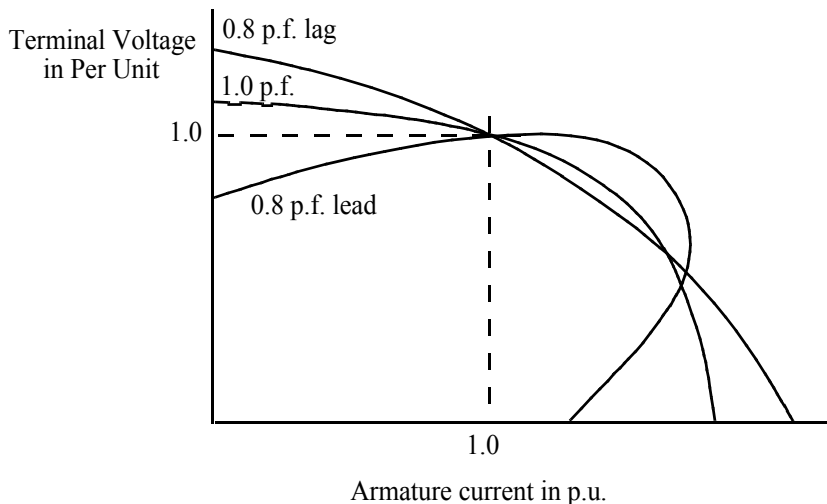


Figure 4.31 Generator volt-ampere characteristics for constant field current.

4.21 Calculation of Pulsating and Average Torque during Starting of Synchronous Motors

While operation at synchronous speed is, naturally, the condition of most interest, operation during asynchronous conditions provides valuable information concerning heating of the machine, torque pulsations, etc., which occur as the machine accelerates toward its rated speed. Strictly speaking, asynchronous operation should only be analyzed with the general form of Park's equations since the speed is rarely constant, making the equations non-linear. However, when the machine is large, the speed changes relatively slowly compared to the electrical time constants so that a "quasi-steady-state" operation can be assumed. That is, the machine variables can be determined from a series of steady-state solutions for speeds ranging from zero to synchronous speed [3].

The pertinent equations can be developed by again starting with Park's equations,

$$v_{ds} = \frac{p}{\omega_b} \psi_{ds} - \frac{\omega_r}{\omega_b} \psi_{qs} + r_s i_{ds} \quad (4.183)$$

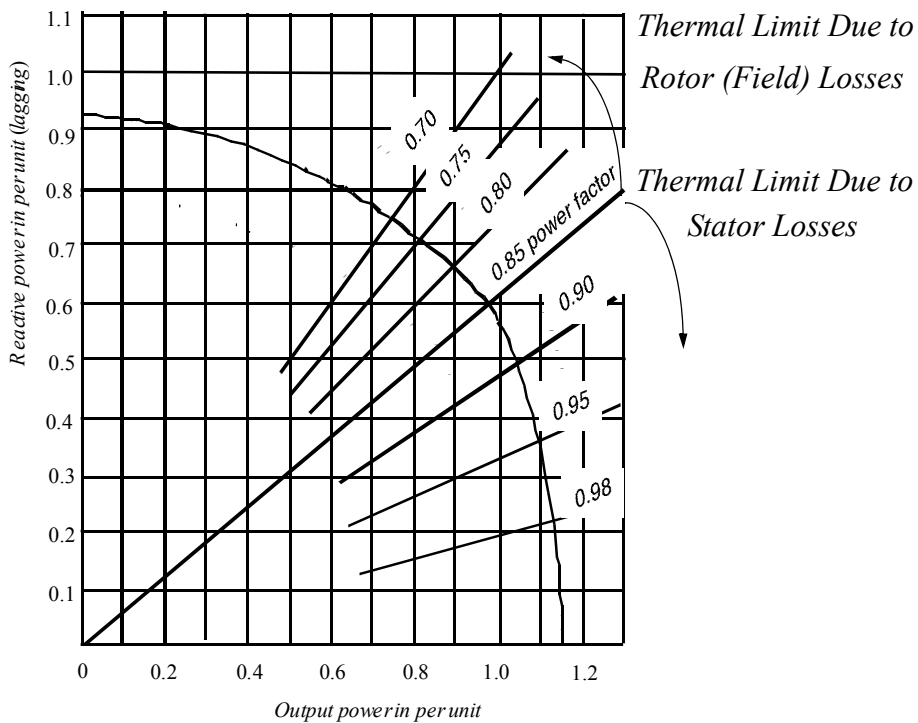


Figure 4.32 Reactive capability curves of a large turbo-generator, 0.85 power factor, 0.80 short-circuit ratio ($x_{DS} = 1.25$ p.u.).

$$\nu_{qs} = \frac{p}{\omega_b} \psi_{qs} + \frac{\omega_r}{\omega_b} \psi_{ds} + r_s i_{qs} \quad (4.184)$$

$$0 = \frac{p}{\omega_b} \psi_{dr} + r_{dr} i_{dr} \quad (4.185)$$

$$0 = \frac{p}{\omega_b} \psi_{qr} + r_{qr} i_{qr} \quad (4.186)$$

$$\nu_{fr} = \frac{p}{\omega_b} \psi_{fr} + r_{fr} i_{fr} \quad (4.187)$$

$$T_e = \frac{3}{2} \left(\frac{P}{2\omega_b} \right) [\psi_{ds} i_{qs} - \psi_{qs} i_{ds}] \quad (4.188)$$

where ω_r is the angular speed of the rotor, p is the time operator

$$p = \frac{d}{dt}$$

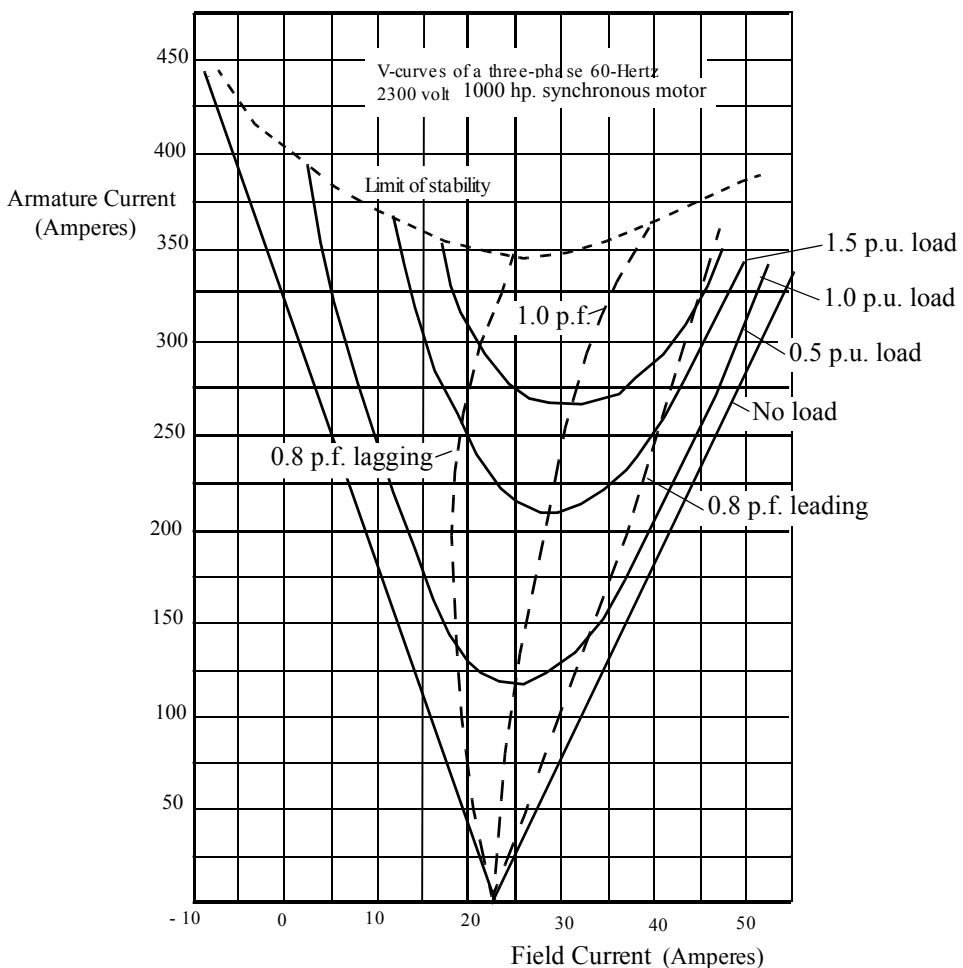


Figure 4.33 Synchronous motor V curves.

and ω_b is the angular frequency of the applied stator voltages. The flux linkages are defined by

$$\Psi_{ds} = x_{ls} i_{ds} + x_{md}(i_{ds} + i_{dr} + i_{fr}) \quad (4.189)$$

$$\Psi_{qs} = x_{ls} i_{qs} + x_{mq}(i_{qs} + i_{qr}) \quad (4.190)$$

$$\Psi_{dr} = x_{ldr} i_{dr} + x_{md}(i_{ds} + i_{dr} + i_{fr}) \quad (4.191)$$

$$\Psi_{qr} = x_{lqr} i_{qr} + x_{mq}(i_{qs} + i_{qr}) \quad (4.192)$$

$$\Psi_{fr} = x_{lfr} i_{fr} + x_{md}(i_{ds} + i_{dr} + i_{fr}) \quad (4.193)$$

During steady-state asynchronous operation at a slip S , the d - q axes quantities pulsate at slip frequency. Eqs. (4.183) to (4.187) may be written in phasor form

$$j\tilde{V}_s = jS\tilde{\psi}_{ds} - (1-S)\tilde{\psi}_{qs} + r_s\tilde{I}_{ds} \quad (4.194)$$

$$\tilde{V}_s = (1-S)\tilde{\psi}_{ds} + jS\tilde{\psi}_{qs} + r_s\tilde{I}_{qs} \quad (4.195)$$

$$0 = jS\tilde{\psi}_{dr} + r_{dr}\tilde{I}_{dr} \quad (4.196)$$

$$0 = jS\tilde{\psi}_{qr} + r_{qr}\tilde{I}_{qr} \quad (4.197)$$

$$0 = jS\tilde{\psi}_{fr} + r_{fr}\tilde{I}_{fr} \quad (4.198)$$

where

$$\nu_{fr} = 0$$

$$S = \frac{\omega_e - \omega_r}{\omega_e}$$

and $\omega_e = \omega_b$.

Assuming that the stator resistance r_s is sufficiently small, the ir drop can be neglected. If r_s is neglected in Eqs. (4.193) and (4.194), then Eq. (4.194) is multiplied by “ j ” and the right-hand sides of Eq. (4.193) are equated, one obtains

$$jS\psi_{ds} - (1-S)\psi_{qs} = j(1-S)\psi_{ds} - S\psi_{qs}$$

$$-j(1-2S)\psi_{ds} = (1-2S)\psi_{qs}$$

Hence

$$\tilde{\psi}_{qs} = -j\tilde{\psi}_{ds} \quad (4.199)$$

and

$$\psi_{ds} = j\psi_{qs} \quad (4.200)$$

Equations (4.194) and (4.195) therefore reduce to

$$j\tilde{V}_s = j\tilde{\psi}_{ds} \quad (4.201)$$

$$\tilde{V}_s = j\psi_{qs} \quad (4.202)$$

Note that Eqs. (4.196)–(4.198) contain inductive voltage drops proportional to slip S , whereas the simplified stator equations, Eqs. (4.201) and (4.202), have inductive voltage drops proportional to line frequency ω_e . This difficulty can be eliminated if Eqs. (4.196)–(4.198) are divided by slip S . Park's equations then reduce to the form

$$jV_s = jx_{ls}\tilde{I}_{ds} + jx_{md}(\tilde{I}_{ds} + \tilde{I}_{dr} + \tilde{I}_{fr}) \quad (4.203)$$

$$V_s = jx_{ls}\tilde{I}_{qs} + jx_{mq}(\tilde{I}_{qs} + \tilde{I}_{qr}) \quad (4.204)$$

$$0 = jx_{ldr}\tilde{I}_{dr} + jx_{md}(\tilde{I}_{ds} + \tilde{I}_{dr} + \tilde{I}_{fr}) + r_{dr}\tilde{I}_{dr}/S \quad (4.205)$$

$$0 = jx_{ldr}\tilde{I}_{dr} + jx_{md}(\tilde{I}_{qs} + \tilde{I}_{qr}) + r_{qr}\tilde{I}_{qr}/S \quad (4.206)$$

$$0 = jx_{lfr}\tilde{I}_{fr} + jx_{md}(\tilde{I}_{ds} + \tilde{I}_{dr} + \tilde{I}_{fr}) + r_{fr}\tilde{I}_{fr}/S \quad (4.207)$$

Equations (4.203)–(4.207) can be used to construct the equivalent circuit to the right of $A-A$ shown in Figure 4.34. The operational impedances seen looking into these two equivalent circuits are defined as $x_d(jS)$ and $x_q(jS)$, respectively. Although the stator resistance has been neglected in the development of this circuit, its effect can be approximated by simply reinserting this resistance in series with the impedances $x_d(jS)$ and $x_q(jS)$ as if they existed external to a machine having zero stator resistance. The terminal voltages V and jV now must appear at terminals $A'-A'$ rather than $A-A$. It should be noted that this manipulation is valid only if \tilde{I}_{ds} and \tilde{I}_{qs} as well as ψ_{ds} and ψ_{qs} are in time quadrature. It should be clear that this will be true only if the rotor is symmetrical. Although only approximately correct for salient-pole machines, the error is quite small and is considerably more accurate, particularly around half speed than if the stator resistance were neglected entirely.

Let the direct and quadrature axis currents be defined in complex notation as

$$\tilde{I}_{ds} = a + jb \quad (4.208)$$

$$\tilde{I}_{qs} = c + jd \quad (4.209)$$

Also let the operational impedances be denoted as the complex quantities

$$x_d(jS) = D_x - jD_r \quad (4.210)$$

$$x_q(jS) = Q_x - jQ_r \quad (4.211)$$

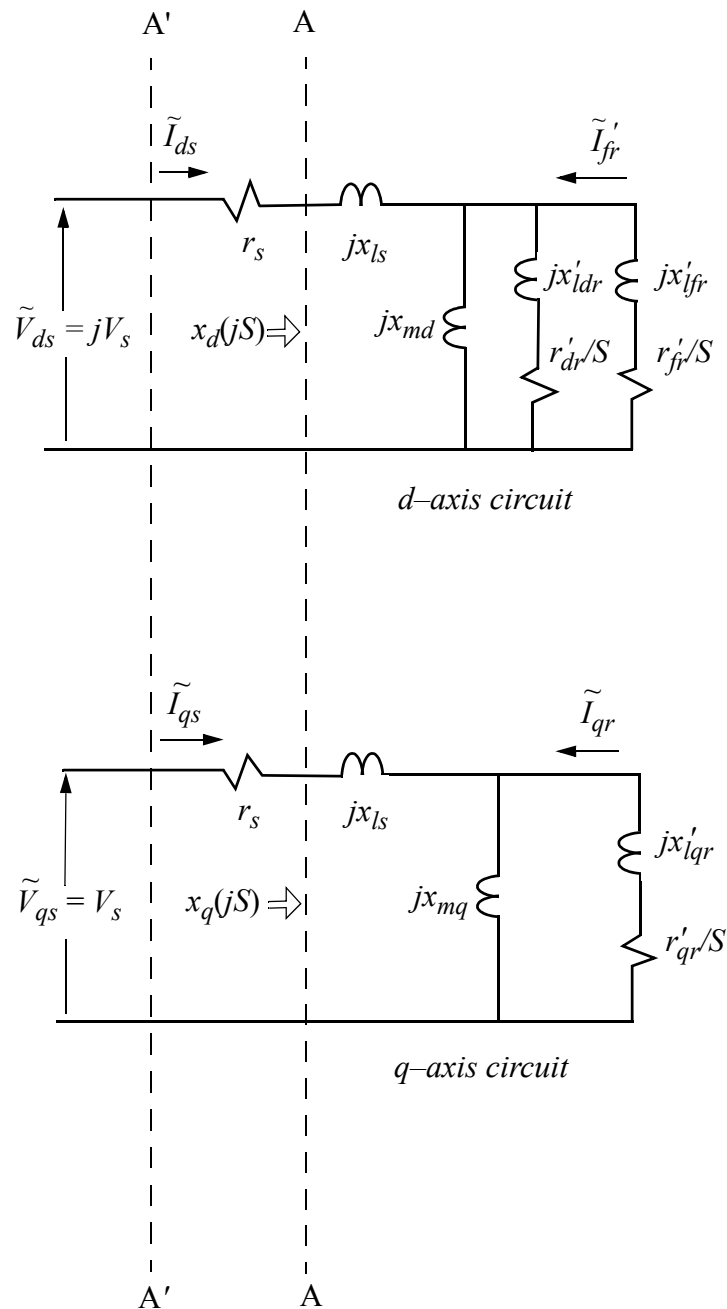


Figure 4.34 Equivalent circuit valid for steady-state asynchronous operation.

These impedances can be calculated from the usual direct and quadrature axis equivalent circuits. For example, $jx_d(jS)$ is the impedance calculated for slip s when looking into the direct axis circuit of Figure 4.34 at $A-A$.

In complex notation the flux linkages are found as

$$\tilde{\psi}_{ds} = (x_d jS) \tilde{I}_{ds} = aD_x + bD_r + j(bD_x - aD_r) \quad (4.212)$$

$$\tilde{\psi}_{qs} = x_q(jS) \tilde{I}_{qs} = cQ_x + dQ_r + j(dQ_x - cQ_r) \quad (4.213)$$

The real components (actual physical values) of current and flux can be calculated in the manner typified by

$$i_{ds} = \text{Real of } (\tilde{I}_{ds} e^{jS\omega_e t}) \quad (4.214)$$

where ω_e is the electrical angular line frequency and S is the per unit slip. The resulting real values are

$$i_{ds} = \cos S\omega_e t - b \sin S\omega_e t = |\tilde{I}_{ds}| \cos(S\omega_e t + \phi_d) \quad (4.215)$$

$$i_{qs} = c \cos S\omega_e t - d \sin S\omega_e t = |\tilde{I}_{qs}| \cos(S\omega_e t + \phi_q) \quad (4.216)$$

$$\begin{aligned} \psi_{ds} &= (aD_x + bD_r) \cos(S\omega_e t) + (aD_r - bD_x) \sin(S\omega_e t) \\ &\quad (4.217) \end{aligned}$$

$$\begin{aligned} \psi_{qs} &= (cQ_x + dQ_r) \cos(S\omega_e t) + (cQ_r - dQ_x) \sin(S\omega_e t) \\ &\quad (4.218) \end{aligned}$$

The instantaneous torque can now be computed from Eq. (4.188). The result is

$$\begin{aligned} T_e &= \left(\frac{3P}{4\omega_b} \right) \left(\frac{1}{2} \right) \{ [(ac + bd)(D_x - Q_x) + (bc - ad)(D_r + Q_r)] \\ &\quad + [(ac - bd)(D_x - Q_x) + (ad + bc)(D_r - Q_r)] \cos(2S\omega_e t) \\ &\quad + [(ac - bd)(D_r - Q_r) - (ad + bc)(D_x - Q_x)] \sin(2S\omega_e t) \} \end{aligned} \quad (4.219)$$

The first line of Eq. (4.219) is the average torque. The second and third lines together are the pulsating torque at twice slip frequency.

The amplitude of the pulsating torque T_{puls} is found by taking the square root of the sum of the squares of the amplitudes of the $\cos(2S\omega_e t)$ and $\sin(2S\omega_e t)$ terms. The similarity of terms permits one to write almost by inspection that

$$4T_{puls}^2 = K^2[(ac - bd)^2 + (ad + bc)^2][(D_x - Q_x)^2 + (D_r - Q_r)^2] \quad (4.220)$$

which is further reducible to

$$\begin{aligned} 4T_{puls}^2 &= K^2[(a^2 + b^2)(c^2 + d^2)][(D_x - Q_x)^2 + (D_r - Q_r)^2] \\ &\quad (4.221) \end{aligned}$$

By inspection of Eqs. (4.210), (4.211), and (4.215) it is seen that

$$a^2 + b^2 = |\tilde{I}_{ds}|^2 \quad (4.222)$$

$$c^2 + d^2 = |\tilde{I}_{qs}|^2 \quad (4.223)$$

$$(D_x - Q_x)^2 + (D_r - Q_r)^2 = |x_d(jS) - x_q(jS)|^2 \quad (4.224)$$

where $|...|$ means “absolute value of.” Thus the pulsating torque amplitude at any time is

$$T_{puls} = \left(\frac{3P}{4\omega_b}\right) \frac{1}{2} |\tilde{I}_{ds}| |\tilde{I}_{qs}| |x_d(jS) - x_q(jS)| \quad (4.225)$$

It is important to realize that the last member of the product is the absolute value of the difference between the complex impedances. It is not the difference between the absolute values of the impedances.

In a similar manner the average torque T_{ave} is

$$T_{ave} = \frac{1}{2} \left(\frac{3P}{4\omega_b}\right) [(ac + bd)(D_x - Q_x) + (bc - ad)(D_r + Q_r)] \quad (4.226)$$

Equation (4.226) can be reduced to the form

$$T_{ave} = \frac{1}{2} \left(\frac{3P}{4\omega_b}\right) Real[I_{ds}x_d(jS)I_{qs}^* - I_{qs}x_q(jS)I_{ds}^*] \quad (4.227)$$

where “*” means “conjugate of” and “Real” means the real part of the adjoining bracketed complex quantity.

Physical insight into the significance of Eq. (4.227) can be realized with the following approximation. From [Figure 4.34](#) it is apparent that if stator resistance is neglected, then approximately

$$\tilde{V}_{ds} = jx_d(jS)\tilde{I}_{ds} \quad (4.228)$$

$$\tilde{V}_{qs} = jx_q(jS)\tilde{I}_{qs} \quad (4.229)$$

Substituting into Eq. (4.227)

$$T_{ave} = \frac{1}{2} \left(\frac{3P}{4\omega_b} \right) \text{Im}[\tilde{V}_{qs}\tilde{I}_{ds}^* - \tilde{V}_{ds}\tilde{I}_{qs}^*] \quad (4.230)$$

which can be interpreted as the cross product between the axes stator voltages and currents. Equation (4.227) can be reduced still further if it is recalled that the $d-q$ axes stator voltages are in time quadrature. That is,

$$\tilde{V}_{ds} = jV_s = j\tilde{V}_{qs} \quad (4.231)$$

$$\tilde{V}_{qs} = V_s = -j\tilde{V}_{ds} \quad (4.232)$$

Substituting Eqs. (4.231) and (4.232) into Eq. (4.230), the average torque can be expressed approximately as

$$T_{ave} = \frac{1}{2} \left(\frac{3P}{4\omega_b} \right) \text{Real}[\tilde{V}_{ds}\tilde{I}_{ds}^* + \tilde{V}_{qs}\tilde{I}_{qs}^*] \quad (4.233)$$

which can be interpreted as the average value of the d - and q -axes air gap power.

In per unit the pulsating and average torque components are expressed as

$$T_{puls} = \frac{1}{2} |\tilde{I}_{DS}| |\tilde{I}_{QS}| |x_D(jS) - x_Q(jS)| \quad (4.234)$$

and

$$T_{AVE} = \frac{1}{2} \text{Re}[\tilde{V}_{DS}\tilde{I}_{DS}^* + \tilde{V}_{QS}\tilde{I}_{QS}^*] \quad (4.235)$$

It is important to remember that all phasor quantities are, in this text, always expressed in peak rather than *RMS* values. If phase quantities are used the “1/2” factor in these expressions is not necessary. A plot of the pulsating and average torque versus speed for the case of a small 60 Hz, 4 pole, 220 V., 10 kW machine where $x_{md} = 13.6$, $x_{mq} = 6.55$, $x_{ls} = 0.45$, $x_{ldr}' = 1.0$, $x_{lqr}' = 0.9$, $x_{lfr}' = 0.95$, $r_s = 0.31$, $r_{dr}' = 0.57$, $r_{qr}' = 0.08$, $r_{fr}' = 0.08$ is shown in [Figure 4.35](#).

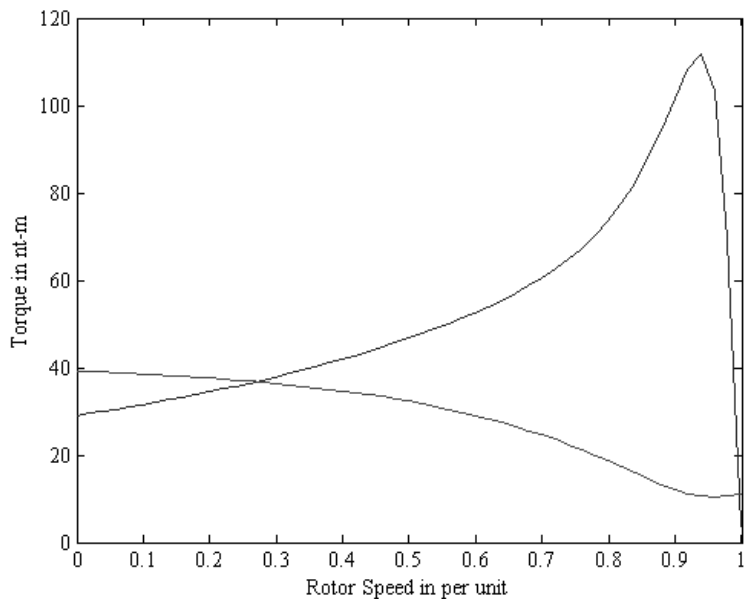


Figure 4.35 Average and pulsating components of torque as a function of speed for a small 10 kW salient-pole synchronous motor.

4.22 Conclusion

The study of the steady-state behavior of salient-pole and cylindrical rotor synchronous machines forms an essential body of knowledge for the power system analyst. Often, treatment of this subject is focused solely on a phasor representation. The approach taken in this chapter has attempted to emphasize rather the concept of a space vector interpretation which follows inherently from Park's equations. The phasor representation is introduced only as one of several tools for steady-state analysis. Rather than dwell on the phasor manipulations common for handling various steady-state special cases, the use of modern methods of solving non-linear equations such as using MathCAD has been emphasized. The steady-state representation has, finally, been extended to include the general case in which the rotor speed rotates asynchronously, allowing a means for readily calculating currents which flow during starting (*inrush currents*).

4.23 References

- [1] G.R. Slemmon and A. Straughen, "Electric Machines," Addison Wesley, Reading Mass, 1980.
- [2] M. Liwschitz-Garik and C.C. Whipple, "A-C Machines," 2nd Edition, D. Van Nostrand Co, Princeton, NJ, 1961.
- [3] E.L. Owen, H.D. Sniveley, and T.A. Lipo, "Torsional Coordination of High Speed Synchronous Motors-Part II," IEEE Trans. On Industry Applications, Vol. IA-17, Nov./Dec. 1981, pp. 572-580.

Chapter 5

Transient Analysis of Synchronous Machines

5.1 Introduction

Since the forces impressed on the windings of a synchronous machine due to excessive current are one of the limiting factors in its design, the study of synchronous machine faults is an essential topic in the study of synchronous machines. Analyses of this class of problems become intractable almost from the start unless certain assumptions are made. One of the most powerful techniques for the solution of such problems utilizes the *Theorem of Constant Flux Linkages*, sometimes referred to as *Doherty's Law* [1]. Robert E. Doherty was a renowned electrical engineer with the General Electric Company who wrote many classic papers on this topic during the 1920s.

5.2 Theorem of Constant Flux Linkages

In order to establish Doherty's Law, consider any group of coupled magnetic circuits. The voltage drop in any of the circuits consisting of a resistance, a self-inductance, and an arbitrary number of mutual inductances with adjacent stator and/or rotor coils may be written

$$e = ri + \frac{d\lambda}{dt} \quad (5.1)$$

where λ is the total flux linkages due to coupling with all the circuits in the system.

If this equation is solved for $d\lambda/dt$ and integrated from time t_1 to time t_2

$$\int_{t_1}^{t_2} \frac{d\lambda}{dt} dt = \lambda(t_2) - \lambda(t_1) = \int_{t_1}^{t_2} (e - ri) dt \quad (5.2)$$

If e , r , and i remain finite, it follows that the flux linkages can not change suddenly (i.e., have a discontinuity in the flux) but must change continuously since

the flux is the result of an integral. That is, a discontinuity is possible only in the time derivative of the flux.

If the circuit is suddenly short-circuited so that $e = 0$ and r is very small, the integral on the right hand side will always be small. Indeed, if at $t = t_1$ the voltage impression the circuit suddenly becomes zero and if $r = 0$, then

$$\lambda(t_2) = \lambda(t_1) \quad (5.3)$$

for any $t_2 > t_1$. Hence, the total flux linkages tend to remain constant if a circuit is short-circuited or if the voltage impressed on a closed circuit is zero both before and after a sudden voltage change in any other (coupled) circuit.

5.3 Behavior of Stator Flux Linkages on Short-Circuit

As a first approximation, the stator resistance will now be neglected. Let $\lambda_{as}(0)$, $\lambda_{bs}(0)$, and $\lambda_{cs}(0)$ be the flux linkages of the three stator phases as , bs , and cs at the moment the short-circuit occurs. From Doherty's Law, if e and r are both zero, then for any time thereafter,

$$\lambda_{as}(t) = \lambda_{as}(0) \quad (5.4)$$

$$\lambda_{bs}(t) = \lambda_{bs}(0) \quad (5.5)$$

$$\lambda_{cs}(t) = \lambda_{cs}(0) \quad (5.6)$$

Let $\theta_r = \omega_e t + \alpha$, which designates that the $d-q$ frame is rotating at synchronous speed with an arbitrary initial angle α at $t = 0$. The equations relating the as , bs , cs variables to the ds , qs variables in the rotor reference frame rotating at synchronous speed are then

$$\lambda_{qs} = \frac{2}{3} \left[\lambda_{as} \cos(\omega_e t + \alpha) + \lambda_{bs} \cos\left(\omega_e t + \alpha - \frac{2\pi}{3}\right) + \lambda_{cs} \cos\left(\omega_e t + \alpha + \frac{2\pi}{3}\right) \right] \quad (5.7)$$

$$\lambda_{ds} = \frac{2}{3} \left[\lambda_{as} \sin(\omega_e t + \alpha) + \lambda_{bs} \sin\left(\omega_e t + \alpha - \frac{2\pi}{3}\right) + \lambda_{cs} \sin\left(\omega_e t + \alpha + \frac{2\pi}{3}\right) \right] \quad (5.8)$$

Substituting for λ_{as} , λ_{bs} , and λ_{cs} in terms of the initial conditions $\lambda_{as}(0)$, $\lambda_{bs}(0)$, $\lambda_{cs}(0)$ and expanding, the following result is obtained:

$$\lambda_{qs} = \lambda_{qs}(0) \cos \omega_e t - \lambda_{ds}(0) \sin \omega_e t \quad (5.9)$$

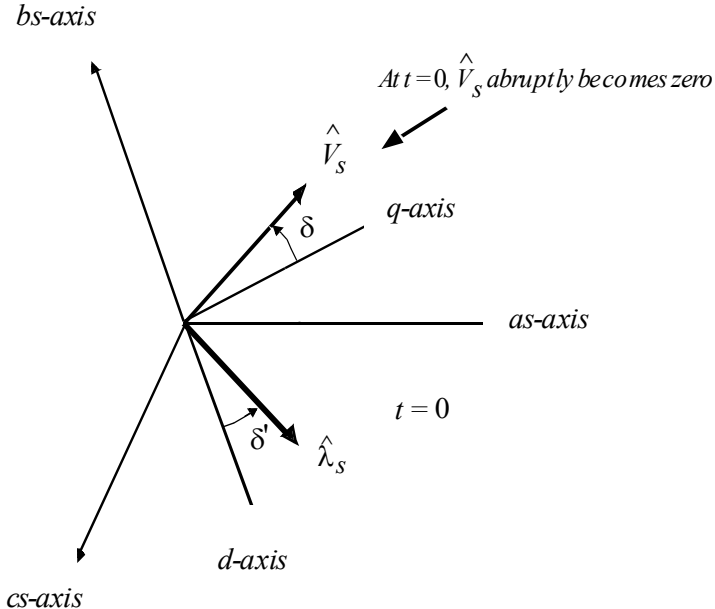


Figure 5.1 Voltage and flux linkage vector orientation at $t = 0$.

$$\lambda_{ds} = \lambda_{qs}(0) \sin \omega_e t + \lambda_{ds}(0) \cos \omega_e t \quad (5.10)$$

where

$$\lambda_{qs}(0) = \frac{2}{3} \left[\lambda_{as}(0) - \frac{1}{2} \lambda_{bs}(0) - \frac{1}{2} \lambda_{cs}(0) \right] \cos \alpha - \frac{1}{\sqrt{3}} [\lambda_{cs}(0) - \lambda_{bs}(0)] \sin \alpha \quad (5.11)$$

$$\lambda_{ds}(0) = \frac{2}{3} \left[\lambda_{as}(0) - \frac{1}{2} \lambda_{bs}(0) - \frac{1}{2} \lambda_{cs}(0) \right] \sin \alpha + \frac{1}{\sqrt{3}} [\lambda_{cs}(0) - \lambda_{bs}(0)] \cos \alpha \quad (5.12)$$

Note that whereas the flux linkages of the three stator phases remain constant during a short-circuit, the stator $d-q$ axis flux linkages in the rotor reference frame vary as sinusoidal functions of time. This is, in effect, accounted for by the speed voltage terms in Park's Equations.

5.4 Three-Phase Short-Circuit, No Damper Circuits, Resistances Neglected

It is now timely to proceed to find the solution for a practical short-circuit condition. Initially, the effects of the damper windings will be neglected (if they

exist) as well as assuming that the resistances of the machine are essentially zero. In this case the flux linkages are given for all time $t > 0$ as

$$\lambda_{qs} = \lambda_{qs}(0) \cos \omega_e t - \lambda_{ds}(0) \sin \omega_e t \quad (5.13)$$

$$\lambda_{ds} = \lambda_{qs}(0) \sin \omega_e t + \lambda_{ds}(0) \cos \omega_e t \quad (5.14)$$

$$\lambda_{fr} = \lambda_{fr}(0) \quad (5.15)$$

Note that the rotor flux linkage can also be considered as constant since the field voltage in the steady-state is dropped completely across the field resistance as illustrated in Figure 5.2. In addition, at this point, the use of the

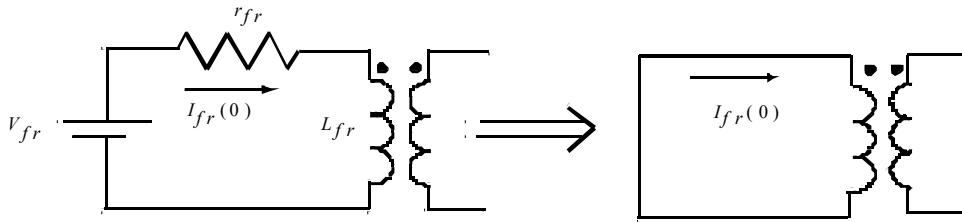


Figure 5.2 Equivalent field winding circuit after a disturbance.

upright prime ('') to denote the rotor/stator turns ratio transformation will be dropped (assumed) for the remainder of this text so as not to be confused with the use of the slanted prime ('') to be used for certain upcoming quantities in this chapter.

The flux linkages are related to the currents by

$$\lambda_{qs} = L_{qs} i_{qs} \quad (5.16)$$

$$\lambda_{ds} = L_{ds} i_{ds} + L_{md} i_{fr} \quad (5.17)$$

$$\lambda_{fr} = L_{fr} i_{fr} + L_{md} i_{ds} \quad (5.18)$$

Solving these equations for the three currents, one obtains

$$i_{ds} = \frac{-L_{md} \lambda_{fr}(0)}{L_{fr} \left[L_{ds} - \frac{L_{md}^2}{L_{fr}} \right]} + \frac{\left[\lambda_{ds}(0) \cos \omega_e t + \lambda_{qs}(0) \sin \omega_e t \right]}{\left[L_{ds} - \frac{L_{md}^2}{L_{fr}} \right]} \quad (5.19)$$

$$i_{qs} = \frac{\lambda_{qs}(0)\cos\omega_e t - \lambda_{ds}(0)\sin\omega_e t}{L_{qs}} \quad (5.20)$$

$$i_{fr} = \frac{L_{ds}\lambda_{fr}(0)}{L_{fr}\left[L_{ds} - \frac{L_{md}^2}{L_{fr}}\right]} - \frac{L_{md}[\lambda_{qs}(0)\sin\omega_e t + \lambda_{ds}(0)\cos\omega_e t]}{L_{fr}\left[L_{ds} - \frac{L_{md}^2}{L_{fr}}\right]} \quad (5.21)$$

Examining the form of Eqs. (5.19) and (5.21), it is useful to examine the term in the square brackets more carefully. Recall that the self inductance L_{ds} and L_{fr} can be expressed as the sum of a leakage plus a magnetizing inductance. Thus

$$L_{ds} - \frac{L_{md}^2}{L_{fr}} = L_{ls} + L_{md} - \frac{L_{md}^2}{L_{lfr} + L_{md}} \quad (5.22)$$

$$= \frac{L_{ls}L_{lfr} + L_{ls}L_{md} + L_{lfr}L_{md}}{L_{lfr} + L_{md}} \quad (5.23)$$

Rearranging,

$$L_{ds} - \frac{L_{md}^2}{L_{fr}} = \frac{L_{ls}(L_{lfr} + L_{md}) + L_{lfr}L_{md}}{L_{lfr} + L_{md}} \quad (5.24)$$

$$= L_{ls} + \frac{L_{lfr}L_{md}}{L_{lfr} + L_{md}} \quad (5.25)$$

$$= L_{ls} + \frac{1}{\frac{1}{L_{lfr}} + \frac{1}{L_{md}}} \quad (5.26)$$

Because this term often appears during the study of transient behavior, it is useful to define the *transient reactance* x_d'

$$x_d' \stackrel{\Delta}{=} \omega_e \left[L_{ds} - \frac{L_{md}^2}{L_{fr}} \right] = x_{ls} + \frac{1}{\frac{1}{x_{lfr}} + \frac{1}{x_{md}}} \quad (5.27)$$

as well as the *voltage behind transient reactance* E_q'

$$E_q' \stackrel{\Delta}{=} \frac{\omega_e L_{md}}{L_{fr}} \lambda_{fr}(0) = \frac{x_{md}}{x_{fr}} \psi_{fr}(0) \quad (5.28)$$

From the form of Eq. (5.27) it should be evident that the transient reactance is the Thevenin equivalent impedance viewed from the stator terminal obtained by short-circuiting the field winding and neglecting the stator and field resistances.

It is important to observe that E_q' is defined in terms of a flux linkage rather than in terms of current or another voltage. The voltage behind the transient reactance vector \hat{E}_q' is assumed to be oriented 90° CCW spatially with respect to ψ_{fr} in the same manner as the steady-state internal emf vector \hat{E}_i . Also note that at open circuit $\hat{E}_q = x_{md} \hat{I}_{fr}(0)$ which is, for the open circuit case only, the same amplitude and direction as the steady-state internal emf \hat{E}_i . In terms of these newly defined variables

$$i_{ds} = \frac{-E_q'}{x_d'} + \frac{\psi_{ds}(0) \cos \omega_e t + \psi_{qs}(0) \sin \omega_e t}{x_d'} \quad (5.29)$$

$$i_{qs} = \frac{\psi_{qs}(0) \cos \omega_e t - \psi_{ds}(0) \sin \omega_e t}{x_{qs}} \quad (5.30)$$

$$i_{fr} = \frac{x_{ds} E_q'}{x_d' x_{md}} - \frac{(x_{ds} - x_d') \psi_{ds}(0) \cos \omega_e t + \psi_{qs}(0) \sin \omega_e t}{x_{md}} \quad (5.31)$$

5.5 Three-Phase Short-Circuit with Resistances and Damper Windings Neglected

The simplest type of short-circuit occurs when the machine is open circuited before the fault. For no load to exist before the short-circuit, clearly $i_{ds} = i_{qs} = 0$. Hence

$$\psi_{qs}(0) = 0 \quad (5.32)$$

$$\psi_{ds}(0) = E_q' \quad (5.33)$$

$$\psi_{fr}(0) = \frac{x_{fr}}{x_{md}} E_q' \quad (5.34)$$

The solution, for the currents become

$$i_{ds} = \frac{-E'_q}{x'_d} (1 - \cos \omega_e t) \quad (5.35)$$

$$i_{qs} = \frac{-E'_q}{x'_{qs}} \sin \omega_e t \quad (5.36)$$

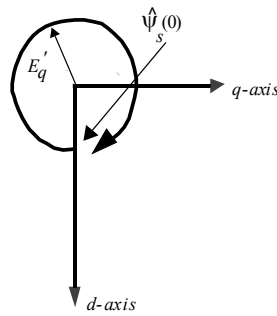
$$i_{fr} = \frac{E'_q}{x_{md}} \left[\frac{x_{ds}}{x'_d} - \frac{x_{ds} - x'_d}{x'_d} \cos \omega_e t \right] \quad (5.37)$$

The motion of the stator flux linkage and current vectors after the fault are illustrated by [Figure 5.3](#). It is interesting to observe that the d - q current trajectory rotates in the clockwise direction (opposite to the direction of rotation) so as to result in a stationary vector in the stator frame of reference.

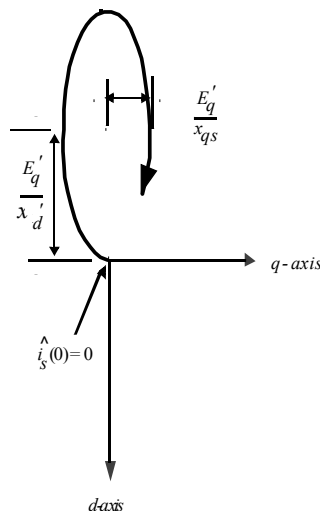
Upon utilizing the d - q transformation, the phase current i_{as} is

$$\begin{aligned} i_{as} &= i_{qs} \cos(\omega_e t + \alpha) + i_{ds} \sin(\omega_e t + \alpha) \\ &= \frac{E'_q}{2} \left(\frac{1}{x'_{qs}} + \frac{1}{x'_d} \right) \sin \alpha - \frac{E'_q}{x'_d} \sin(\omega_e t + \alpha) \\ &\quad + \frac{E'_q}{2} \left(\frac{1}{x'_d} - \frac{1}{x'_{qs}} \right) \sin(2\omega_e t + \alpha) \end{aligned} \quad (5.38)$$

where α is an arbitrary constant denoting, in this case, the angle that the q -axis makes with respect to the as -axis at $t = 0$. Similar equations apply for the currents in phases bs and cs . It is important to notice the appearance of a “double frequency” term in Eq. (5.38). This occurs, in effect, because the rotor is not symmetrical due to saliency and the presence of the field winding. In essence, the dc offset in currents in the stator produce an oscillating single-phase current in the rotor (i.e., in the field winding). This single-phase current can be broken up into positively and negatively rotating current vectors. The negatively rotating wave is stationary with respect to the stator and produces a flux component which is constant (i.e., no voltage is induced in the stator winding due to this component). The positively rotating wave rotates forward with respect to the rotor or at an angular velocity of twice synchronous speed with respect to the stator. This component results in a time rate of change of flux of twice synchronous speed, resulting in a current flow in the stator at an angular velocity of $2\omega_e$.



(a)



(b)

Figure 5.3 Motion of the (a) stator flux linkage Ψ_s and (b) current vector \hat{i}_s after a fault from an open circuit.

5.6 Short-Circuit from Loaded Condition, Stator Resistance and Dampers Neglected

Assume now that prior to the short-circuit, the machine has been carrying a set of balanced load currents. In this case initial conditions on i_{ds} and i_{qs} must be determined from a vector diagram such as the one shown in Figure 5.4. From this figure (as usual),

$$I_{ds}(0) = -I_s \sin(\delta + \phi) \quad (5.39)$$

$$I_{qs}(0) = I_s \cos(\delta + \phi) \quad (5.40)$$

where δ designates the torque angle existing at $t = 0$. From Figure 5.4, the flux linkages at $t = 0^-$ are then

$$\psi_{ds}(0) = \psi_s(0) \cos \delta = x_{ds} I_{ds}(0) + x_{md} I_{fr}(0) \quad (5.41)$$

$$\psi_{qs}(0) = -\psi_s(0) \sin \delta = x_{qs} I_{qs}(0) \quad (5.42)$$

$$\psi_{fr}(0) = x_{md} I_{ds}(0) + x_{fr} I_{fr}(0) \quad (5.43)$$

Note that in this case, in which $r_s = 0$, then $\delta' = \delta$. The field flux linkages can be written as

$$\frac{x_{md} \psi_{fr}(0)}{x_{fr}} = \frac{x_{md}^2}{x_{fr}} I_{ds}(0) + x_{md} I_{fr}(0) \quad (5.44)$$

or

$$E_q' = (x_{ds} - x_d') I_{ds}(0) + x_{md} I_{fr}(0) \quad (5.45)$$

Solving for $x_{md} I_{fr}(0)$, the stator flux linkages can then be written as

$$\psi_{ds}(0) = x_d' I_{ds}(0) + E_q' \quad (5.46)$$

$$\psi_{qs}(0) = x_{qs} I_{qs}(0) \quad (5.47)$$

Substituting Eqs. (5.46) and (5.47) into Eqs. (5.28) to (5.29) yields

$$i_{ds} = \frac{-E_q'}{x_d'} (1 - \cos \omega_e t) + I_{ds}(0) \cos \omega_e t + \frac{x_{qs}}{x_d'} I_{qs}(0) \sin \omega_e t \quad (5.48)$$

$$i_{qs} = -\frac{E_q'}{x_{qs}} \sin \omega_e t + I_{qs}(0) \cos \omega_e t - \frac{x_d'}{x_{qs}} I_{ds}(0) \sin \omega_e t \quad (5.49)$$

$$i_{fr} = \frac{E_q'}{x_{md}} \left[\frac{x_{ds}}{x_d'} - \frac{x_{ds} - x_d'}{x_d'} \cos \omega_e t \right] - \frac{(x_{ds} - x_d')}{x_{md}} I_{ds}(0) \cos \omega_e t$$

$$-\frac{x_q}{x_d'} \frac{(x_d - x_d')}{x_{md}} I_{qs}(0) \sin \omega_e t \quad (5.50)$$

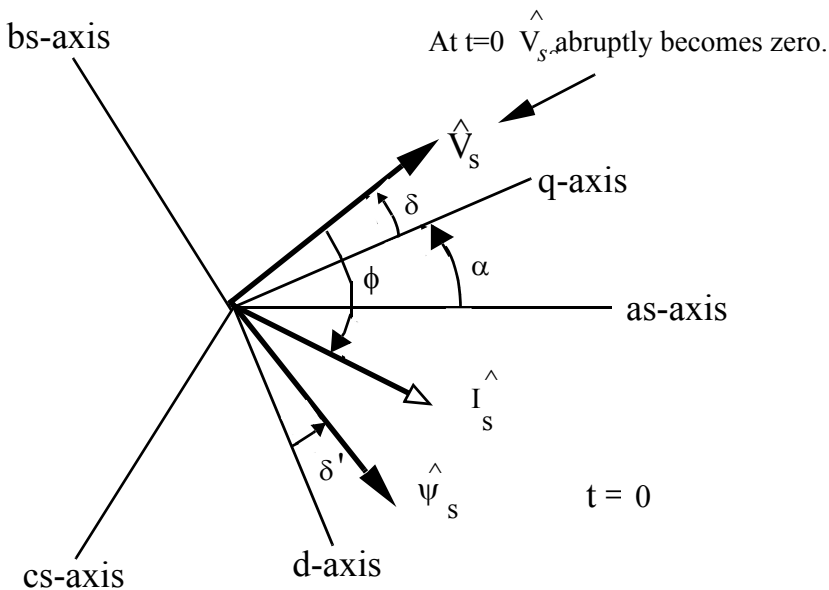


Figure 5.4 Voltage and flux linkage vector orientation at $t = 0$.

It is important to compare this result with that of Eqs. (5.34) to (5.36). A portion of the result is clearly the same as before with additional terms to account for the effect of loading.

The phase current i_{as} can be solved as (letting $\alpha = 0$ for simplicity)

$$\begin{aligned}
 i_{as} = & -\frac{E_q'}{x_d'} \sin \omega_e t + \frac{1}{2} \left(\frac{1}{x_q'} - \frac{1}{x_{qs}} \right) E_q' \sin 2\omega_e t + \frac{1}{2} I_{qs}(0)(1 + \cos 2\omega_e t) \\
 & - \frac{1}{2} \frac{x_d'}{x_{as}} I_{ds}(0) \sin 2\omega_e t + \frac{1}{2} \frac{x_{qs}}{x_d'} I_{qs}(0)(1 - \cos 2\omega_e t)
 \end{aligned} \tag{5.51}$$

or, alternatively,

$$\begin{aligned}
i_{as}(t) = & \frac{1}{2}x_{qs}I_{qs}(0)\left(\frac{1}{x_d'} + \frac{1}{x_{qs}}\right) - \frac{E_q'}{x_d'}\sin(\omega_e t) \\
& + \frac{1}{2}\left(\frac{1}{x_d'} - \frac{1}{x_{qs}}\right)[E_q' + x_d'I_{ds}(0)]\sin(2\omega_e t) \\
& + \frac{1}{2}\left(\frac{1}{x_d'} - \frac{1}{x_{qs}}\right)x_{qs}I_{qs}(0)\cos(2\omega_e t)
\end{aligned} \tag{5.52}$$

Again observe the presence of the constant, fundamental frequency, and double frequency terms. If $x_d' = x_{qs}$ (no transient saliency), the double frequency terms will drop out.

The electromagnetic torque can be obtained from Park's equations, derived in Chapter 3. Assuming that $\delta = 0$ (no-load) at the moment of the fault, the torque appearing after the short-circuit is

$$T_e = [E_q' + x_d'I_{ds}(0)]^2\left(\frac{1}{x_d'} + \frac{1}{X_{qs}}\right)\sin(2\omega_e t) + \frac{E_q'}{x_d'}[E_q' + x_d'I_{ds}(0)]\sin(\omega_e t) \tag{5.53}$$

Equation (5.53) shows that the torque for the first half cycle is positive, indicating a strong braking action occurs immediately after the fault. Should the machine have been generating just prior to the fault, the swing in the shaft torque from its normal negative value to the large positive value indicated by Eq. (5.53) clearly suggests that a very high stress occurs on the rotor shaft at the moment of the fault.

5.7 Three-Phase Short-Circuit, Effect of Resistances Included, No Dampers

Assume again that the machine without amortisseur windings is running at the no-load condition. The performance equations of the machine are ($\omega_r = \omega_e$)

$$v_{ds} = p\lambda_{ds} - \omega_e\lambda_{qs} + r_s i_{ds} \tag{5.54}$$

$$v_{qs} = p\lambda_{qs} + \omega_e\lambda_{ds} + r_s i_{qs} \tag{5.55}$$

$$v_{fr} = p\lambda_{fr} + r_{fr}i_{fr} \tag{5.56}$$

Transforming the three performance equations to Laplace variables results in

$$v_{ds}(s) = s\lambda_{ds}(s) - \lambda_{ds}(0) - \omega_e \lambda_{qs}(s) + r_s i_{ds}(s) \quad (5.57)$$

$$v_{qs}(s) = s\lambda_{qs}(s) - \lambda_{qs}(0) + \omega_e \lambda_{ds}(s) + r_s i_{qs}(s) \quad (5.58)$$

$$v_{fr}(s) = s\lambda_{fr}(s) - \lambda_{fr}(0) + r_{fr} i_{fr}(s) \quad (5.59)$$

wherein initial conditions exist

$$\lambda_{ds}(0) = L_{md} I_{fr}(0) \quad (5.60)$$

$$\lambda_{qs}(0) = 0 \quad (5.61)$$

$$\lambda_{fr}(0) = L_{fr} I_{fr}(0) \quad (5.62)$$

and, as applied voltages,

$$v_{ds}(s) = v_{qs}(s) = 0 \quad (5.63)$$

$$v_{fr}(s) = \frac{V_{fr}(0)}{s} = \frac{V_{fr}}{s} \quad (V_{fr} \text{ is constant}) \quad (5.64)$$

In terms of currents, Eqs. (5.57) to (5.59) can be written as

$$L_{md} I_{fr}(0) = (r_s + sL_{ds}) i_{ds}(s) + sL_{md} i_{fr}(s) - \omega_e L_{qs} i_{qs}(s) \quad (5.65)$$

$$0 = (r_s + sL_{qs}) i_{qs}(s) + \omega_e L_{ds} i_{ds}(s) + \omega_e L_{md} i_{fr}(s) \quad (5.66)$$

$$\frac{V_{fr}}{s} + L_{fr} I_{fr}(0) = (r_{fr} + sL_{fr}) i_{fr}(s) + sL_{md} i_{ds}(s) \quad (5.67)$$

where

$$I_{fr}(0) = \frac{V_{fr}}{r_{fr}} \quad (5.68)$$

Solving Eq. (5.67) for $i_{fr}(s)$,

$$i_{fr}(s) = \frac{\frac{V_{fr}}{s} + L_{fr} I_{fr}(0) - sL_{md} i_{ds}(s)}{sL_{fr} + r_{fr}} \quad (5.69)$$

Substituting this result into Eq. (5.65) yields

$$\begin{aligned}
L_{md}I_{fr}(0) &= \left[r_s + sL_{ds} - \frac{s^2 L_{md}^2}{sL_{fr} + r_{fr}} \right] i_{ds}(s) + \frac{L_{md}V_{fr} + sL_{fr}L_{md}}{sL_{fr} + r_{fr}} I_{fr}(0) \\
&\quad - \omega_e L_{qs} i_{qs}(s)
\end{aligned} \tag{5.70}$$

which can be written as

$$\frac{r_{fr}L_{md}I_{fr}(0) - L_{md}V_{fr}}{sL_{fr} + r_{fr}} = \left[r_s + s \left(L_{ds} - \frac{sL_{md}^2}{sL_{fr} + r_{fr}} \right) \right] i_{ds}(s) - \omega_e L_{qs} i_{qs}(s) \tag{5.71}$$

However, $r_{fr}I_{fr}(0) = V_{fr}$ so that the left hand side reduces to zero. The final form for the d -axis stator equation can now be written as

$$0 = [r_s + sL_d'(s)]i_{ds}(s) - \omega_e L_{qs} i_{qs}(s) \tag{5.72}$$

where $L_d'(s)$, the *transient operational inductance*, is defined as

$$L_d'(s) \stackrel{\Delta}{=} L_{ds} - \frac{sL_{md}^2}{sL_{fr} + r_{fr}} \tag{5.73}$$

Substituting the solution for $i_{fr}(s)$ into the q -axis equation,

$$\frac{-\omega_e L_{md} \left(\frac{V_{fr}}{s} + L_{fr}I_{fr}(0) \right)}{sL_{fr} + r_{fr}} = (r_s + sL_{qs})i_{qs}(s) + \omega_e L_d'(s)i_{ds}(s) \tag{5.74}$$

where $L_d'(s)$ is defined above. However, again, $I_{fr}(0) = V_{fr}/r_{fr}$ so that this equation reduces to

$$-\omega_e L_{md} \left(\frac{V_{fr}}{sr_{fr}} \right) \frac{sL_{fr} + r_{fr}}{sL_{fr} + r_{fr}} = (r_s + sL_{qs})i_{qs} + \omega_e L_d'(s)i_{ds} \tag{5.75}$$

or

$$-\frac{E_i}{s} = (r_s + sL_{qs})i_{qs} + \omega_e L_d'(s)i_{ds} \tag{5.76}$$

wherein $E_i = \omega_e L_{md} (V_{fr}/r_{fr})$. That is, the usual definition of E_i can be used. Alternatively, E_q' could be used since the two quantities are identical on short-circuits following an open circuit.

One can now proceed to solve for $i_{ds}(s)$ and $i_{qs}(s)$ from the two Laplace Eqs. (5.72) and (5.76). Thus,

$$i_{ds}(s) = \frac{-\omega_e L_{qs} \frac{E_i}{s}}{[s^2 + \omega_e^2]L_d'(s)L_{qs} + sr_s[L_d'(s) + L_{qs}] + r_s^2} \quad (5.77)$$

Neglecting the term r_s^2 ,

$$i_{ds}(s) = \frac{-\omega_e \frac{E_i}{s}}{L_d'(s)[s^2 + \omega_e^2 + sr_s\left(\frac{1}{L_{qs}} + \frac{1}{L_d'(s)}\right)]} \quad (5.78)$$

In addition, the following approximation in the coefficient of sr_s can be employed:

$$\begin{aligned} \frac{1}{L_{qs}} + \frac{1}{L_d'(s)} &= \frac{1}{L_{qs}} + \frac{1}{L_{ds} - \frac{sL_{md}^2}{sL_{fr} + r_{fr}}} \\ &\approx \frac{1}{L_{qs}} + \frac{1}{L_{ds} - \frac{L_{md}^2}{L_{fr}}} \\ &= \frac{1}{L_{qs}} + \frac{1}{L_d'} \end{aligned} \quad (5.79)$$

With this approximation one obtains

$$i_{ds}(s) = \frac{-\omega_e E_i}{sL_d'(s)(s^2 + 2as + \omega_e^2)} \quad (5.80)$$

where

$$2a = r_s \left(\frac{1}{L_{qs}} + \frac{1}{L_d'} \right) = \frac{2}{T_a} \quad (5.81)$$

so that an *armature transient time constant* T_a is defined as

$$T_a = \frac{2}{r_s \left(\frac{1}{L_{qs}} + \frac{1}{L_d'} \right)} \quad (5.82)$$

(5.83)

In terms of time constants, the quantity $L_d'(s)$ can be manipulated to form

$$L_d'(s) = L_{ds} - \frac{sL_{md}^2}{sL_{fr} + r_{fr}} \quad (5.84)$$

$$= \frac{L_{ds} \left[s \left(L_{fr} - \frac{L_{md}^2}{L_{ds}} \right) + r_{fr} \right]}{sL_{fr} + r_{fr}}$$

$$= \frac{L_{ds} \left(L_{fr} - \frac{L_{md}^2}{L_{ds}} \right)}{L_{fr}} \left[\frac{s + \frac{r_{fr}}{\left(L_{fr} - \frac{L_{md}^2}{L_{ds}} \right)}}{s + \frac{r_{fr}}{L_{fr}}} \right]$$

$$= \frac{\left[L_{ds} - \frac{L_{md}^2}{L_{fr}} \right] \left[s + \frac{r_{fr}}{\left(L_{fr} - \frac{L_{md}^2}{L_{ds}} \right)} \right]}{s + \frac{r_{fr}}{L_{fr}}}$$

$$= L_d' \left[\frac{s + \frac{1}{T_d'}}{s + \frac{1}{T_{do}'}} \right] \quad (5.85)$$

The quantity T_d' is defined as the field *d*-axis short-circuit transient time constant, whereas T_{do}' is defined to be the field *d*-axis open circuit transient time constant. The Laplace equation for i_{ds} can now be expressed

$$i_{ds}(s) = \frac{-\omega_e E_i}{L_d'} \left[\frac{s + \frac{1}{T_{do}'}}{s \left(s + \frac{1}{T_d'} \right) (s^2 + 2as + \omega_e^2)} \right] \quad (5.86)$$

Expanding by partial fractions,

$$i_{ds}(s) = -\frac{E_i}{\omega_e L_d'} \left[\frac{\frac{L_d'}{L_{ds}}}{s} + \frac{1 - \frac{L_d'}{L_{ds}}}{s + \frac{1}{T_d'}} + \frac{s + a}{s^2 + 2as + \omega_e^2} \right] \quad (5.87)$$

$$= -\frac{E_i}{\omega_e L_d'} \left[\frac{\frac{L_d'}{L_{ds}}}{s} + \frac{1 - \frac{L_d'}{L_{ds}}}{s + \frac{1}{T_d'}} + \frac{s + a}{(s + a)^2 + (\omega_e^2 - a^2)} \right] \quad (5.88)$$

Taking the inverse Laplace transform assuming $a^2 \gg \omega_e^2$, the time domain expression for $i_{ds}(t)$ is

$$i_{ds}(t) \cong -\frac{E_i}{x_{ds}} - E_i \left(\frac{1}{x_{d'}} - \frac{1}{x_{ds}} \right) e^{-\frac{t}{T_d'}} - \frac{E_i}{x_{d'}} e^{-\frac{t}{T_a}} \cos \omega_e t \quad (5.89)$$

Notice that at $t = 0$, $i_{ds}(t) = 0$ and that as $t \rightarrow \infty$, $i_{ds}(t) \rightarrow -E_i/x_{ds}$ as expected. It is useful to realize that this expression is approximate. In particular, the last term in Eq. (5.89) indicates that the sinusoidal component no longer rotates backward precisely synchronous with respect to rotor, but rather rotates forward with respect to the stator at the slip frequency so that

$$S_a = \frac{\omega_e - \sqrt{\omega_e^2 - a^2}}{\omega_e} \quad (5.90)$$

$$= 1 - \sqrt{1 - \left(\frac{a}{\omega_e}\right)^2} \quad (5.91)$$

$$\cong 1 - \left(1 - \frac{a}{\omega_e}\right) \quad (5.92)$$

$$= \frac{a}{\omega_e} \quad (5.93)$$

This result denotes the fact that the stator now acts as an equivalent “squirrel cage” to the negatively rotating wave and that braking in the form of induction motor torque is now created as well.

The solution for the q -axis armature current can be obtained by a similar procedure.

$$i_{qs}(s) = \frac{\frac{E_i}{s}[r_s + sL_d'(s)]}{[s^2 + \omega_e^2]L_d'(s)L_{qs} + sr_s[L_d'(s) + L_{qs}] + r_s^2} \quad (5.94)$$

Making the same approximations as before, i.e., $r_s^2 \approx 0$ and $L_d'(s) \approx L_d'$,

$$i_{qs}(s) \cong -\left(\frac{E_i}{L_{qs}}\right) \frac{1}{s^2 + 2as + \omega_e^2} \quad (5.95)$$

The above equation can be rewritten as

$$i_{qs}(s) \cong -\left(\frac{E_i}{L_{qs}}\right) \frac{1}{(s + a)^2 + (\omega_e^2 - a^2)} \quad (5.96)$$

Now, again assuming $\omega_e^2 - a^2 \cup \omega_e^2$, then the corresponding time domain expression is

$$i_{qs}(t) \cong -\frac{E_i}{x_{qs}} e^{-\frac{t}{T_a}} \sin \omega_e t \quad (5.97)$$

The armature current in phase as can be found from the inverse $d-q$ transformation wherein $\theta_r = \omega_e t + \alpha$.

$$\begin{aligned}
i_{as}(t) &= i_{qs} \cos(\omega_e t + \alpha) + i_{ds} \sin(\omega_e t + \alpha) \\
&= \frac{E_i}{2} \left(\frac{1}{x_{qs}} + \frac{1}{x_d'} \right) e^{-\frac{t}{T_d'}} \sin \alpha \\
&\quad - \left[\frac{E_i}{x_{ds}} + E_i \left(\frac{1}{x_d'} - \frac{1}{x_{ds}} \right) e^{-\frac{t}{T_d'}} \right] \sin(\omega_e t + \alpha) \\
&\quad - \frac{E_i}{2} \left(\frac{1}{x_{qs}} - \frac{1}{x_d'} \right) e^{-\frac{t}{T_a}} \sin(2\omega_e t + \alpha)
\end{aligned} \tag{5.98}$$

Using the same procedure, the field current can be solved as

$$i_{fr}(t) = E_i \left[\frac{1}{x_{md}} + \frac{x_{md}}{x_{fr} x_d'} e^{-\frac{t}{T_d'}} - \frac{x_{md}}{x_{fr} x_d'} e^{-\frac{t}{T_a}} \cos(\omega_e t) \right] \tag{5.99}$$

5.8 Extension of the Theory to Machines with Damper Windings

It is now possible to consider the total solution including the damper windings. The form of the equations for i_{ds} , i_{qs} , and i_{fr} remain the same as before. The complete solution, however, is quite tedious. When one additional rotor winding (damper or amortisseur winding) is added in each circuit, the results can be deduced by simple analogy to the previous solution without damper windings. The solutions are

$$\begin{aligned}
i_{ds}(t) &\equiv -\frac{E_i}{x_{ds}} - E_i \left(\frac{1}{x_d'} - \frac{1}{x_{ds}} \right) e^{-\frac{t}{T_d'}} \\
&\quad - E_i \left(\frac{1}{x_d''} - \frac{1}{x_d'} \right) e^{-\frac{t}{T_d''}} + \frac{E_i}{x_d''} e^{-\frac{t}{T_a}} \cos(\omega_e t)
\end{aligned} \tag{5.100}$$

$$i_{qs}(t) \equiv -\frac{E_i}{x_q''} e^{-\frac{t}{T_a}} \sin(\omega_e t) \quad (5.101)$$

$$i_{fr}(t) \equiv \frac{E_i}{x_{md}} + \frac{E_i}{x_{md}} \left(\frac{x_{ds} - x_d'}{x_d'} \right) \left[e^{-\frac{t}{T_d'}} - \left(1 - \frac{T_{ldr}}{T_d''} \right) e^{-\frac{t}{T_d''}} - \frac{T_{ldr}}{T_d''} e^{-\frac{t}{T_a}} \cos(\omega_e t) \right] \quad (5.102)$$

where

$$T_{ldr} = \frac{x_{ldr}}{\omega_e r_{dr}} \quad (5.103)$$

$$T_d'' = \frac{1}{\omega_e r_{dr}} \left(x_{ldr} + \frac{1}{\frac{1}{x_{lfr}} + \frac{1}{x_{ls}} + \frac{1}{x_{md}}} \right) \quad (5.104)$$

$$x_d'' = x_{ls} + \frac{1}{\frac{1}{x_{lfr}} + \frac{1}{x_{ldr}} + \frac{1}{x_{md}}} \quad (5.105)$$

$$x_q'' = x_{ls} + \frac{1}{\frac{1}{x_{lqr}} + \frac{1}{x_{mq}}} \quad (5.106)$$

The phase current and torque are

$$\begin{aligned} i_{as}(t) &\equiv -E_i \left[\frac{1}{x_{ds}} + \left(\frac{1}{x_d'} - \frac{1}{x_{ds}} \right) e^{-\frac{t}{T_d'}} + \left(\frac{1}{x_d''} - \frac{1}{x_d'} \right) e^{-\frac{t}{T_d''}} \right] \sin(\omega_e t + \alpha) \\ &+ \frac{E_i}{2} \left(\frac{1}{x_d''} + \frac{1}{x_q''} \right) e^{-\frac{t}{T_a}} \sin \alpha \\ &+ \frac{E_i}{2} \left(\frac{1}{x_d''} - \frac{1}{x_q''} \right) e^{-\frac{t}{T_a}} \sin(2\omega_e t + \alpha) \end{aligned} \quad (5.107)$$

$$T_e(t) \approx \frac{3P}{4\omega_b} \left\{ E_i^2 e^{-\frac{t}{T_a}} \left[\frac{1}{x_{ds}} + \left(\frac{1}{x_d'} - \frac{1}{x_{ds}} \right) e^{-\frac{t}{T_d'}} + \left(\frac{1}{x_d''} - \frac{1}{x_d'} \right) e^{-\frac{t}{T_d''}} \right] \sin \omega_e t \right. \\ \left. + \frac{E_i^2}{2} e^{-\frac{2t}{T_a}} \left(\frac{1}{x_q''} - \frac{1}{x_d''} \right) \sin 2\omega_e t \right\} \quad (5.108)$$

It is important to again mention here not to forget that these solutions are approximate and not exact. Note that the double frequency component of torque and armature current represented by the second term is small relative to the first term and decays more rapidly. The double frequency terms in the armature current and torque disappear if $x_d'' = x_q''$. [Table 5.1](#) illustrates the components of short-circuit current. Note also that if $\alpha = 0$, the q -axis is aligned with phase as at $t = 0$. In this case the short-circuit occurs when the voltage in phase as is a positive maximum (i.e., v_{as} is a cosine function). If the short-circuit occurs at this instant, the asymmetrical and second harmonic terms have a zero initial condition. Conversely, when $\alpha = \pm \pi/2$, the asymmetrical and second harmonics have a maximum influence on the solution.

A plot of the short-circuit armature and field currents of a typical 30 MVA generator is shown in [Figure 5.5](#). Also note that if phase as has a zero asymmetrical component $\alpha = 0$, then phases bs and cs have equal (and opposite) asymmetrical components. The second harmonic component in most machines is generally so small that it is barely detectable.

Because the rate at which the amplitude of the alternating component decreases is slow compared to one cycle, it is generally possible to plot the *RMS* value of the armature current vs. time. Alternatively, the positive peaks of the phase current can be connected as a smooth curve. When the asymmetrical component is extracted from the solution, a plot similar to curve *AB*, shown in [Figure 5.6](#), is produced.

The current amplitude given by curve *AB* can be divided into three parts. The steady-state short-circuit indicated by the dashed line *EF* is E_i/x_{ds} . The *transient component* shown by the dotted line *CD* has an initial value E_i/x_d' and decays with time constant T_d' . The *subtransient component* given by the difference between *AB* and *CD* has an initial value E_i/x_d'' and decays with

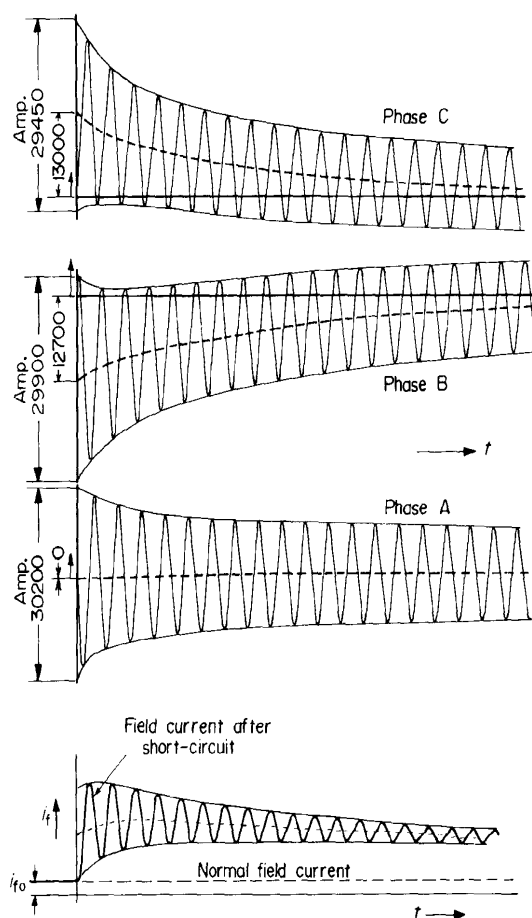


Figure 5.5 Armature currents and field current of 30 MVA synchronous machine after short-circuit.

the time constant T_d'' . It is apparent that the values of x_d'' , x_d' , x_{ds} , T_d'' , and T_d' can be deduced from the short-circuit characteristics of the machine.

Table 5.1 Components of the short-circuit current

Component	Initial Value	Frequency	Time Constant
Steady	$\frac{E_i}{x_{ds}}$	fundamental	∞
Transient	$E_i \left(\frac{1}{x_d'} - \frac{1}{x_{ds}} \right)$	fundamental	T_d'
Subtransient	$E_i \left(\frac{1}{x_d''} - \frac{1}{x_d'} \right)$	fundamental	T_d''
Asymmetrical	$\frac{-E_i}{2} \left(\frac{1}{x_d''} + \frac{1}{x_q''} \right) \sin \alpha$	fundamental	T_a
Second Harmonic	$\frac{-E_i}{2} \left(\frac{1}{x_d''} - \frac{1}{x_q''} \right)$	double fundamental	T_a

Figure 5.7 shows the transient components of the field current during the same short-circuit. Curve CB is obtained by joining the midpoints of the alternating components together and thus represents the behavior of the DC or asymmetrical components. From this figure and the solution that has been derived, it is possible to deduce that the symmetric component is composed of

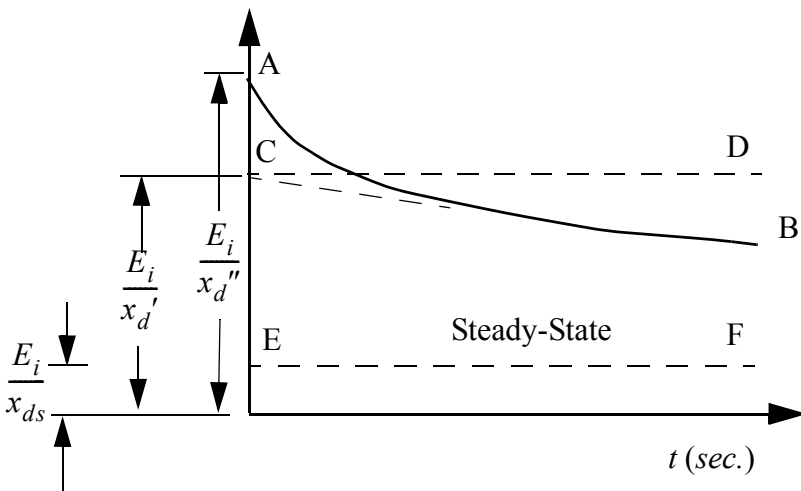


Figure 5.6 Alternating components of the short-circuit armature current.

three parts: (1) a steady-state value given by EF, (2) a transient component given as the difference between EF and CB, and (3) a subtransient component given by the difference between CB and AB.

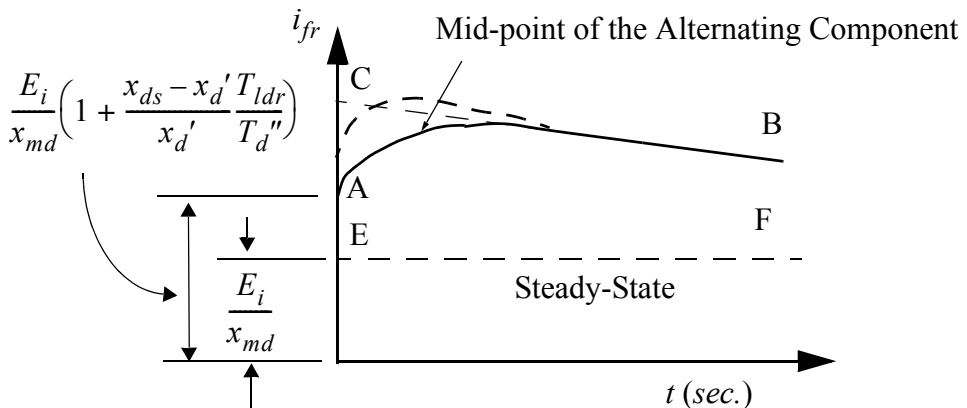


Figure 5.7 Unidirectional components of the field current.

In practice the dashed curve shown rather than the solid curve CB is obtained. In this case a more complicated analytical solution is indicated. This difference between theory and practice has been attributed to the fact that the

mutual inductance between field and damper is assumed equal to the mutual inductance between field and armature. In practice a mutual component of flux exists between field and damper which does not link the armature. A modified equivalent circuit can be derived which introduces such a term [3]. This equivalent circuit is shown in Figure 5.8. Precise knowledge of the field current transients is important in the selection of the discharge resistor used as part of the main field circuit breaker. To minimize damage to the machine in the event of an internal fault, a high ohmic resistance is desirable to hasten the flux decay after a trip-out. The value selected, however, is limited because of the hazard of excessive voltage imposed across the collector rings as the field breaker opens. Should the trip-out occur at the instant of a high transient field current peak, the IR drop across the discharge resistor becomes far more hazardous to the field winding insulation than under normal excitation.

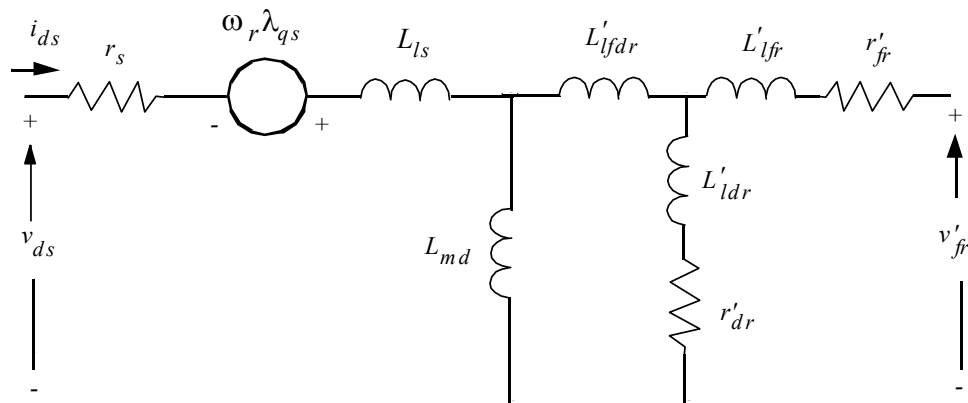


Figure 5.8 The d -axis equivalent circuit including damper-field coupling.

Reactances

Synchronous: d -axis

$$x_{ds} = x_{md} + x_{ls}$$

q -axis

$$x_{qs} = x_{mq} + x_{ls}$$

Transient: d' -axis

$$x_{d'} = \frac{x_{md}x_{lfr}}{x_{md} + x_{lfr}} + x_{ls}$$

Subtransient d -axis

$$x_d'' = \frac{x_{md}x_{lfr}x_{ldr}}{x_{md}x_{lfr} + x_{lfr}x_{ldr} + x_{ldr}x_{md}} + x_{ls}$$

Time constantsOpen-circuit transient: d -axis

$$T_{do'} = \frac{1}{\omega_b r_{fr}} [x_{md} + x_{lfr}]$$

Open-circuit subtransient: d -axis

$$T_{do}'' = \frac{1}{\omega_b r_{dr}} \left[\frac{x_{md}x_{lfr}}{x_{md} + x_{lfr}} + x_{ldr} \right]$$

 q -axis

$$T_{qo}'' = \frac{1}{\omega_b r_{qr}} [x_{mq} + x_{lqr}]$$

Short-circuit transient: d -axis

$$T_d' = \frac{1}{\omega_b r_{fr}} \left[\frac{x_{md}x_{ls}}{x_{md} + x_{ls}} + x_{lfr} \right] = (x_d' x_{ds}) T_{do}'$$

Short-circuit subtransient: d -axis

$$T_d'' = \frac{1}{\omega_b r_{dr}} \left[\frac{x_{md}x_{lfr}x_{ls}}{x_{md}x_{lfr} + x_{lfr}x_{ls} + x_{md}x_{ls}} + x_{ldr} \right] = \frac{x_d'' T_{do}' T_{do}''}{x_{ds} T_d'}$$

Short-circuit sub-transient: q -axis

$$T_q'' = \frac{1}{\omega_b r_{qr}} \left[\frac{x_{mq}x_{ls}}{x_{mq} + x_{ls}} + x_{lqr} \right] = \frac{x_q''}{x_{qs}} T_{qo}''$$

Short-circuited armature (DC):

$$T_a = \frac{1}{\omega_b r_s} \left[\frac{2x_d'' x_q''}{x_d'' + x_q''} \right]$$

Typical values of these quantities are summarized in [Table 5.2](#).

Table 5.2 Typical per unit values of synchronous machine constants

Parameter	Turbogenerator	Hydrogenerator	Synchronous Motor
x_{ds}	2.0	1.15	1.20
x_{qs}	2.0	0.75	0.90
x_{ls}	0.14	0.12	0.12
x_{lfr}	0.14	0.33	0.29
x_{ldr}	0.04	0.23	0.30
x_{lqr}	0.04	0.50	0.50
x_d'	0.27	0.37	0.35
x_d''	0.171	0.24	0.25
x_q''	0.179	0.25	0.28
x_{0s}	0.015	0.14	0.16
$r_{s(DC)}$	0.002	0.012	0.01
$r_{s(AC)}$	0.0033	0.02	0.016
r_{fr}	0.001	0.00058	0.00055
r_{dr}	0.003	0.02	0.025
r_{qr}	0.002	0.01	0.01
T_{do}'	6.37 s.	5.6 s.	6.0 s.
T_d'	0.86 s.	1.8 s.	1.4 s.
T_d''	0.114 s.	0.262 s.	0.255 s.
T_q''	0.181 s.	0.160 s.	0.160 s.
T_{ldr}	0.424 s.	0.030 s.	0.032 s.
T_a	0.278 s	0.062 s.	0.091 s.

5.9 Short-Circuit of a Loaded Generator, Dampers Included

When a synchronous machine is shorted from a loaded condition the same equations apply as for an unloaded machine. However, additional terms must be added to account for the new initial conditions. Let $v_{ds}(0)$ and $v_{qs}(0)$ be the voltages which prevailed at $t = 0$. The method of superposition can be used to determine the changes in current resulting from a sudden application of volt-

ages $-v_{ds}(0)$ and $-v_{qs}(0)$. The total solution then is obtained as the sum of (two) parts:

1. The original steady-state solution which prevailed before the fault.
2. The solution obtained by solving the machine equation with voltages $-v_{ds}(0)$ and $-v_{qs}(0)$ suddenly applied.

The total solution for the phase a s current is

$$i_{as} = i_{as1} + i_{as2} \quad (5.109)$$

where i_{as1} is the transient solution and i_{as2} is the steady-state solution. The solutions for i_{ds} , i_{qs} , i_{fr} and torque can be found in a similar manner.

5.10 Vector Diagrams for Sudden Voltage Changes

In power systems studies, the problem to be solved is often such that it is only necessary to determine the initial value of the alternating current after some disturbance (a symmetrical short-circuit being a typical disturbance). In such cases, vector or phasor diagrams can be constructed for this purpose. It is useful to return to the situation where dampers are neglected and resistances are set equal to zero. Also, neglect the stator $p\psi$ terms, which is equivalent to neglecting the asymmetrical component of stator currents. In this case, the equations reduce to

$$v_{ds} = -\omega_e \lambda_{qs} = -x_{qs} i_{qs} \quad (5.110)$$

$$v_{qs} = \omega_e \lambda_{ds} = x_{ds} i_{ds} + x_{md} i_{fr} \quad (5.111)$$

$$\lambda_{fr} = \lambda_{fr}(0) = L_{fr} i_{fr} + L_{md} i_{ds} \quad (5.112)$$

Solving the third equation for i_{fr} ,

$$i_{fr} = -\frac{L_{md}}{L_{fr}} i_{ds} + \frac{\lambda_{fr}(0)}{L_{fr}} \quad (5.113)$$

Substituting into the second equation,

$$v_{qs} = \left(x_{ds} - \frac{x_{md}^2}{x_{fr}} \right) i_{ds} + \frac{\omega_e x_{md}}{x_{fr}} \lambda_{fr}(0) \quad (5.114)$$

or simply

$$v_{qs} = x_d' i_{ds} + E_q' \quad (5.115)$$

where X_d' and E_d' have been defined previously. In addition, the d -axis stator equation is unchanged so that

$$v_{ds} = -x_{qs}i_{qs} \quad (5.116)$$

These two equations are valid for *arbitrary* changes in v_{qs} and v_{ds} (consistent with the stated assumptions). They approximately express the transient alternating component of i_{ds} and i_{qs} (coefficient of $e^{-t/T_d'}$) due to a sudden change in v_{qs} and v_{ds} . Assume, for example, that the machine is operating at steady-state and that the voltages v_{qs} and v_{ds} change suddenly to another (constant) value. The vector diagram which describes the transient behavior of the machine before and after the change is shown in [Figure 5.9](#) and [Figure 5.10](#). Generator action is assumed.

A similar result can be obtained if damper windings are included. In this case Park's equations are

$$v_{ds} = -\omega_e \lambda_{qs} \quad (5.117)$$

$$v_{qs} = \omega_e \lambda_{ds} \quad (5.118)$$

$$\lambda_{fr} = \lambda_{fr}(0) = L_{fr}i_{fr} + L_{md}(i_{ds} + i_{dr}) \quad (5.119)$$

$$\lambda_{dr} = \lambda_{dr}(0) = L_{dr}i_{dr} + L_{md}(i_{ds} + i_{fr}) \quad (5.120)$$

$$\lambda_{qr} = \lambda_{qr}(0) = L_{qr}i_{qr} + L_{mq}i_{qs} \quad (5.121)$$

Solving for the currents i_{fr} , i_{dr} , and i_{qr} in the last three equations and substituting the results in the two stator equations, one obtains

$$v_{qs} = x_d''i_{ds} + E_q'' \quad (5.122)$$

$$v_{ds} = -x_q''i_{qs} + E_d'' \quad (5.123)$$

where

$$x_d'' = x_{ls} + \frac{1}{\frac{1}{x_{lfr}} + \frac{1}{x_{ldr}} + \frac{1}{x_{md}}} \quad (5.124)$$

$$x_q'' = x_{ls} + \frac{1}{\frac{1}{x_{lqr}} + \frac{1}{x_{mq}}} \quad (5.125)$$

$$E_d'' = (x_d'' - x_{ls}) \left(\frac{\psi_{fr}(0)}{x_{lfr}} + \frac{\psi_{dr}(0)}{x_{ldr}} \right) \quad (5.126)$$

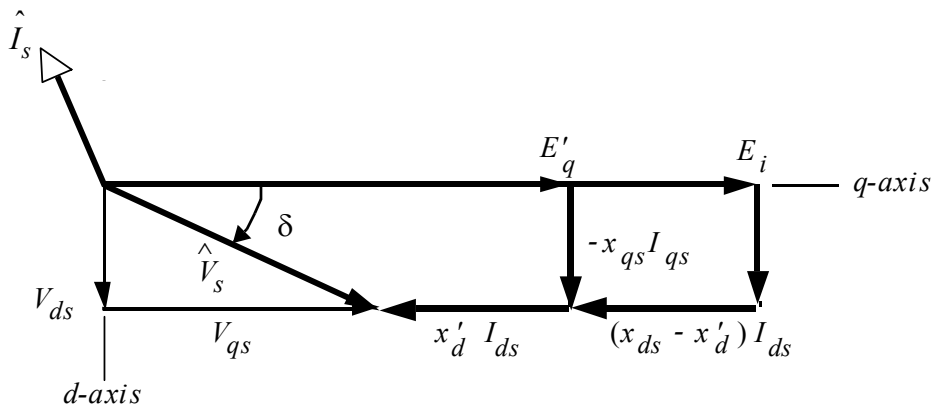
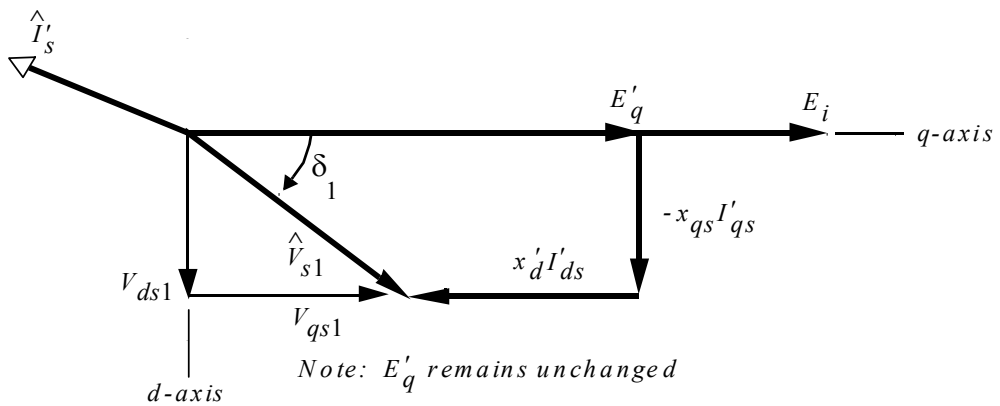


Figure 5.9 Vector diagram applicable before a sudden change.

Figure 5.10 Vector diagram applicable for calculating transient components after a change in voltage to \hat{V}_{s1} .

$$E_q'' = (x_q'' - x_{ls}) \left(\frac{\Psi_{qr}(0)}{x_{lqr}} \right) \quad (5.127)$$

The above equations can be used to find the subtransient components of currents both before and after a sudden change (coefficient of $e^{-t/T_d''}$). A typical case corresponding to the previous example is shown in Figure 5.11 and Figure 5.12. It is important to note that the approach includes, but is not limited to, a symmetrical short-circuit.

Having obtained the steady-state, transient, and subtransient components of stator current, the complete solution for an arbitrary voltage change can be

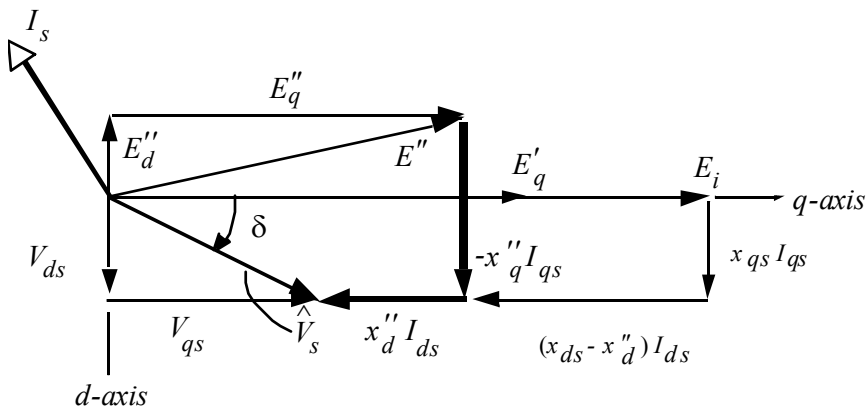


Figure 5.11 Vector diagram before the sudden change in voltage to \hat{V}_{s1} . The current voltage \hat{I}_s and \hat{V}_s are the same as Figure 5.9.

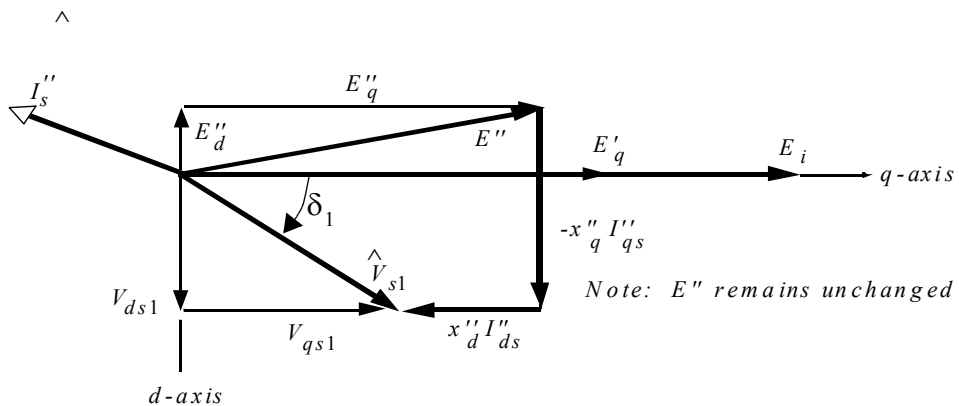


Figure 5.12 Vector diagram for calculating subtransient components after the change in voltage to \hat{V}_{s1} .

obtained if the armature, transient, and subtransient time constants are known. The solution is similar to Eqs (5.100) and (5.101). Assuming that the voltage changes from a nominal condition to an arbitrary but balanced voltage change,

$$i_{ds}(t) = \frac{V_{qs1} - E_i}{x_{ds}} + (V_{qs1} - E_i) \left(\frac{1}{x_{d'}'} - \frac{1}{x_{ds}} \right) e^{-\frac{t}{T_{d'}}}$$

$$+ (V_{qs1} - E_i) \left(\frac{1}{x_d''} - \frac{1}{x_d'} \right) e^{-\frac{t}{T_d''}} + \frac{E_i}{x_d''} e^{-\frac{t}{T_a}} \cos(\omega_e t) \quad (5.128)$$

$$i_{qs}(t) = \frac{V_{ds1}}{x_{qs}} - \left(\frac{V_{ds1} - E_i}{x_q''} \right) e^{-\frac{t}{T_q''}} \quad (5.129)$$

Alternatively, these two equations can be written as

$$i_{ds} = I_{ds1} + (I_{ds'} - I_{ds1}) e^{-\frac{t}{T_d'}} + (I_{ds''} - I_{ds'}) e^{-\frac{t}{T_d''}} + I_a e^{-\frac{t}{T_a}} \cos(\omega_e t) \quad (5.130)$$

$$i_{qs} = I_{qs1} + (I_{qs''} - I_{qs1}) e^{-\frac{t}{T_q''}} \quad (5.131)$$

where the primed and double primed quantities are obtained from [Figure 5.10](#) and [Figure 5.12](#), I_{ds1} and I_{qs1} are the steady-state currents after the change and $I_a = E_i/x_d''$ which corresponds to the DC decay of the asymmetrical component of current.

5.11 Effect of Exciter Response

Up to this point only cases in which the exciter field voltage V_{fr} (and consequently E_x) is constant have been examined. In most applications the exciter responds to any disturbance and attempts to maintain terminal voltage or some other terminal condition constant. In this case the field flux linkages no longer are considered constant. Considered here will only be the case where the damper windings can again be neglected. Also, it is again assumed that the asymmetrical component of stator current can be neglected so that the stator $p\Psi$ terms can be set equal to zero. Park's equations can then be written as

$$V_{qs} = r_s I_{qs} + x_{ds} I_{ds} + x_{md} I_{fr} \quad (5.132)$$

$$V_{ds} = r_s I_{ds} - x_{qs} I_{qs} \quad (5.133)$$

$$E_x = x_{md} I_{fr} + \frac{x_{md}}{\omega_b r_{fr}} \frac{d\Psi_{fr}}{dt} \quad (5.134)$$

Since the field flux linkage is no longer assumed constant, the $d\psi_{fr}/dt$ term in the field voltage equation must be retained. The field flux linkages are therefore

$$\psi_{fr} = x_{fr}I_{fr} + x_{md}I_{ds} \quad (5.135)$$

$$\frac{x_{md}}{x_{fr}}\psi_{fr} = x_{md}I_{fr} + \frac{x_{md}^2}{x_{fr}}I_{ds} \quad (5.136)$$

Recall from Eqs. 5.23 and 5.24, that by definition

$$x_{ds} - \frac{x_{md}^2}{x_{fr}} = x'_d \quad (5.137)$$

and

$$\frac{x_{md}}{x_{fr}}\psi_{fr} = E'_q \quad (5.138)$$

The field flux linkage equation can therefore be written in the form

$$E'_q = x_{md}I_{fr} + (x_{ds} - x'_d)I_{ds} \quad (5.139)$$

Solving this equation for $I_{fr}x_{md}$ and substituting into Eqs. (5.113) to (5.116), Park's equations, including the stator resistance drop, can be written

$$V_{qs} = r_s I_{qs} + x'_d I_{ds} + E'_q \quad (5.140)$$

$$V_{ds} = r_s I_{ds} - x_{qs} I_{qs} \quad (5.141)$$

$$E'_q = \frac{1}{T'_{do}} \int_0^t [E_x - E'_q + (x_d - x'_d)I_{ds}] dt \quad \left(T'_{do} = \frac{x_{fr}}{\omega_b r_{fr}} \right) \quad (5.142)$$

The voltage behind transient reactance E'_q must now be obtained as the solution to a first order differential equation. The input voltage E_x is now assumed to also be a variable, for example, in response to the error in a voltage regulator. The details of an excitation system which serves to regulate voltage will be discussed at a later time.

In general, a vector diagram with voltage regulator action can still be described. In this case the vector E'_q remains fixed immediately after the disturbance but then changes amplitude in response to the change in exciter voltage E_x , as shown in [Figure 5.13](#).

$$T_{d0}' \frac{dE'_g}{dt} = [E_x - E'_g + (x_d - x_d')I_{ds}] \quad (5.143)$$

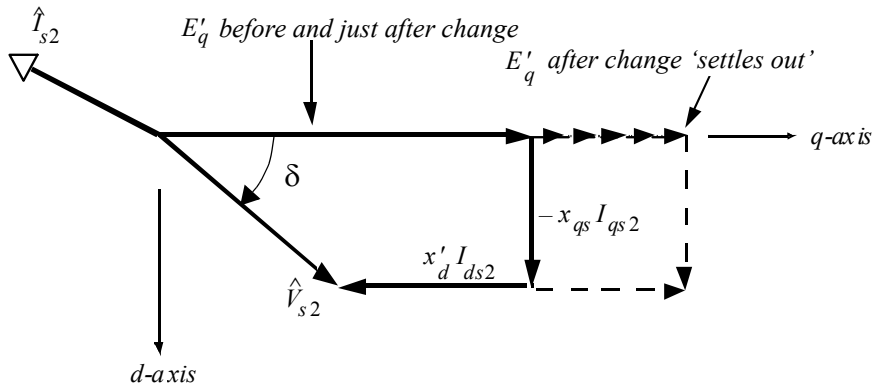


Figure 5.13 Showing the effect of exciter response on the short-circuit vector diagram.

5.12 Transient Solutions Utilizing Modal Analysis

It has been shown in this chapter that in order to carry out an explicit time domain solution to a synchronous machine transient, the circuit model must be simplified so that the algebra is kept within a manageable scale. For example, the square of stator resistance has been neglected in [Section 5.7](#) as well as the effect of field resistance in defining the transient reactance x_d' . These approximations are generally valid for large conventional machines equipped with definite amortisseur windings. However, some machines, for example, solid rotor turbo generators, necessitate more detailed rotor models having multiple rotor circuits [4]. The numerous time constants associated with each rotor circuit together with the extensive coupling among the circuits make the usual simplifying approximations difficult to justify. Also, smaller synchronous machines in the kilowatt range, even though constructed with definite amortisseur windings, typically have resistances which produce unsatisfactory answers for situations such as a three-phase short-circuit.

An alternative approach can be utilized which is based on modern eigenvalue-eigenvector techniques, often referred to as modal theory [5],[6]. This approach allows one to solve for the general case of a sudden change from a balanced, loaded, steady-state operating condition to an arbitrary unbalanced voltage condition. Hence, the correct result for most types of fault conditions can be obtained simply by specifying the proper winding voltages after the fault occurs. Moreover, solutions for other important transients can also be obtained without difficulty, including changes in load (assuming constant speed) or step changes in excitation which frequently result from sudden phase unbalances.

A simplified diagram of the system to be analyzed is given in Figure 5.14. In general, three sinusoidal voltages of arbitrary phase and amplitude are assumed connected to the terminals of a three-phase, four-wire salient-pole synchronous machine. The quantities r_g and x_g are the parameters of the neutral grounding reactor frequently connected between the machine neutral s and the ground point of the bus voltages g . For simplicity, no impedance is assumed external to the machine but, if desired, a balanced set of external impedances could easily be lumped with the stator resistance and leakage inductance of the machine. The case of unbalanced external impedances could be incorporated into the model with additional effort.

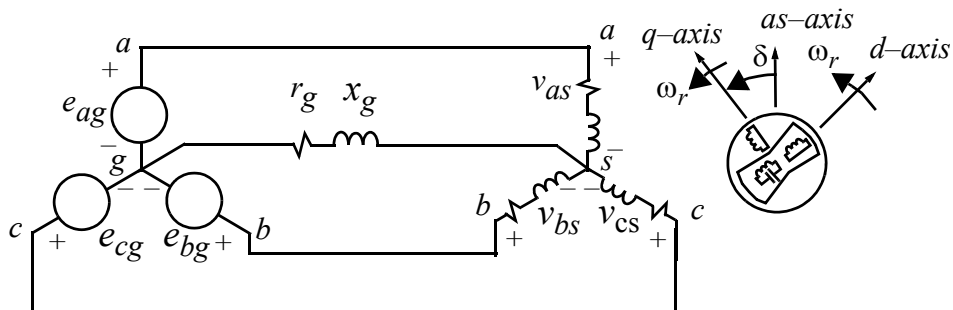


Figure 5.14 Synchronous machine with arbitrary set of sinusoidal applied voltages.

The three source voltages both before and after the transient are, in general, described by

$$e_{ag} = E_{a\alpha} \cos(\omega_e t) + E_{a\gamma} \sin(\omega_e t) \quad (5.144)$$

$$e_{bg} = E_{b\alpha} \cos(\omega_e t) + E_{b\gamma} \sin(\omega_e t) \quad (5.145)$$

$$e_{cg} = E_{c\alpha} \cos(\omega_e t) + E_{c\gamma} \sin(\omega_e t) \quad (5.146)$$

where the subscripts α and γ denote the cosine and sine terms of the source voltages, respectively. The three stator phase voltages are defined by

$$v_{as} = e_{ag} - v_{sg} \quad (5.147)$$

$$v_{bs} = e_{bg} - v_{sg} \quad (5.148)$$

$$v_{cs} = e_{cg} - v_{sg} \quad (5.149)$$

The equations relating the phase voltages to $d-q-n$ voltages expressed in a reference frame fixed on the stator can be found from Chapter 2 using Eq. (2.61), whereupon

$$\mathbf{v}_{dqns} = \mathbf{T}(0)\mathbf{v}_{abcs} \quad (5.150)$$

In scalar form

$$v_{ds}^s = \frac{1}{\sqrt{3}}(v_{cs} - v_{bs}) \quad (5.151)$$

$$v_{qs}^s = \frac{2}{3}v_{as} - \frac{1}{3}v_{bs} - \frac{1}{3}v_{cs} \quad (5.152)$$

$$v_{ns}^s = \frac{\sqrt{2}}{3}(v_{as} + v_{bs} + v_{cs}) \quad (5.153)$$

Substituting Eqs. (5.147) – (5.149) into these three equations yields

$$v_{ds}^s = \frac{1}{\sqrt{3}}(e_{cg} - e_{bg}) \quad (5.154)$$

$$v_{qs}^s = \frac{2}{3}e_{ag} - \frac{1}{3}e_{bg} - \frac{1}{3}e_{cg} \quad (5.155)$$

$$v_{ns}^s = \frac{\sqrt{2}}{3}(e_{ag} + e_{bg} + e_{cg} - 3v_{sg}) \quad (5.156)$$

Because the $d-q-n$ voltages in the stationary frame are linearly related to the actual supply voltages, they are of the same frequency as the source. Hence

$$v_{ds}^s = V_{d\alpha} \cos(\omega_e t) + V_{q\gamma} \sin(\omega_e t) \quad (5.157)$$

$$v_{qs}^s = V_{q\alpha} \cos(\omega_e t) + V_{q\gamma} \sin(\omega_e t) \quad (5.158)$$

$$v_{ns}^s = V_{n\alpha} \cos(\omega_e t) + V_{n\gamma} \sin(\omega_e t) \quad (5.159)$$

Also, the voltage between neutrals must be of the same frequency (neglecting effects of saturation) so that

$$v_{sg} = V_{sg\alpha} \cos(\omega_e t) + V_{sg\gamma} \sin(\omega_e t) \quad (5.160)$$

Equations (5.154) – (5.156) imply that

$$V_{d\alpha} = \frac{1}{\sqrt{3}}(E_{c\alpha} - E_{b\alpha}) \quad (5.161)$$

$$V_{d\gamma} = \frac{1}{\sqrt{3}}(E_{c\gamma} - E_{b\gamma}) \quad (5.162)$$

$$V_{q\alpha} = \frac{2}{3}E_{a\alpha} - \frac{1}{3}E_{b\alpha} - \frac{1}{3}E_{c\alpha} \quad (5.163)$$

$$V_{q\gamma} = \frac{2}{3}E_{a\gamma} - \frac{1}{3}E_{b\gamma} - \frac{1}{3}E_{c\gamma} \quad (5.164)$$

$$V_{n\alpha} = \frac{\sqrt{2}}{3}(E_{a\alpha} + E_{b\alpha} + E_{c\alpha} + 3V_{sg\alpha}) \quad (5.165)$$

$$V_{n\gamma} = \frac{\sqrt{2}}{3}(E_{a\gamma} + E_{b\gamma} + E_{c\gamma} + 3V_{sg\gamma}) \quad (5.166)$$

Since the inductances of the synchronous machine become time invariant only when expressed in the rotor reference frame, these stator voltages must be transformed to the rotor frame of reference. The necessary equations of transformation are illustrated by Figure 5.15 and expressed analytically as

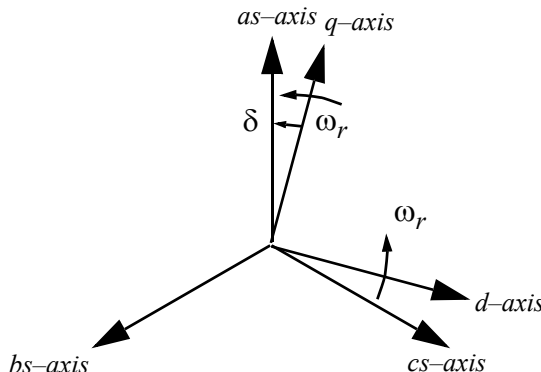


Figure 5.15 Reference frame orientation at $t = 0$.

$$v_{ds}^r = v_{qs}^s \sin(\omega_e t + \delta) + v_{ds}^s \cos(\omega_e t + \delta) \quad (5.167)$$

$$v_{qs}^r = v_{qs}^s \cos(\omega_e t + \delta) - v_{ds}^s \sin(\omega_e t + \delta) \quad (5.168)$$

$$v_{ns}^r = v_{ns}^s \quad (5.169)$$

In Eqs. (5.167) – (5.169) it has already been assumed that the rotor is synchronously rotating with the applied voltage vector ($\omega_r = \omega_e$). The quantity δ is the alignment of the rotating q -axis with respect to the stationary q -axis (as -axis) at $t = 0$. The superscript r denotes $d-q$ quantities in the rotor reference frame. When the stator phase voltages are a balanced sinusoidal set (i.e. $v_{as} = V_s \cos(\omega_e t)$, etc.) then the angle between the as - and q -axes corresponds to the conventional torque angle δ .

Upon performing the above indicated transformation of variables, the stator voltages can be expressed in the rotor reference frame as

$$\begin{aligned} v_{ds}^r &= \frac{1}{2}(V_{q\alpha} - V_{d\gamma}) \sin \delta + \frac{1}{2}(V_{q\gamma} + V_{d\alpha}) \cos \delta \\ &+ \frac{1}{2}(V_{q\alpha} + V_{d\gamma}) \sin(2\omega_e t + \delta) - \frac{1}{2}(V_{q\gamma} - V_{d\alpha}) \cos(2\omega_e t + \delta) \end{aligned} \quad (5.170)$$

$$\begin{aligned} v_{qs}^r &= \frac{1}{2}(V_{q\alpha} - V_{d\gamma}) \cos \delta - \frac{1}{2}(V_{q\gamma} + V_{d\alpha}) \sin \delta \\ &+ \frac{1}{2}(V_{q\alpha} + V_{d\gamma}) \cos(2\omega_e t + \delta) + \frac{1}{2}(V_{q\gamma} - V_{d\alpha}) \sin(2\omega_e t + \delta) \end{aligned} \quad (5.171)$$

$$v_{ns}^r = V_{n\alpha} \cos(\omega_e t) + V_{n\gamma} \sin(\omega_e t) \quad (5.172)$$

The stator voltages as defined by Eqs. (5.170)–(5.172) can now be “applied” to Park’s equations. By convention, the superscript r is generally omitted with writing Park’s equations since the rotor reference frame is implicit in their formulation. Using the motor conventions for stator currents, Park’s equations in matrix form can be written as

$$\begin{bmatrix} v_{ds} \\ v_{qs} \\ v_{ns} \\ e_x \\ 0 \\ 0 \end{bmatrix} = \begin{bmatrix} r_s & -\frac{\omega_e}{\omega_b} x_{qs} & 0 & 0 & 0 & -\frac{\omega_e}{\omega_b} x_{mq} \\ \frac{\omega_e}{\omega_b} x_{ds} & r_s & 0 & \frac{\omega_e}{\omega_b} x_{md} & \frac{\omega_e}{\omega_b} x_{md} & 0 \\ 0 & 0 & r_s + r_g & 0 & 0 & 0 \\ 0 & 0 & 0 & x_{md} & 0 & 0 \\ 0 & 0 & 0 & 0 & r_{dr} & 0 \\ 0 & 0 & 0 & 0 & 0 & r_{qr} \end{bmatrix} \times \begin{bmatrix} i_{ds} \\ i_{qs} \\ i_{ns} \\ i_{fr} \\ i_{dr} \\ i_{qr} \end{bmatrix}$$

$$+ \frac{p}{\omega_b} \begin{bmatrix} x_{ds} & 0 & 0 & x_{md} & x_{md} & 0 \\ 0 & x_{qs} & 0 & 0 & 0 & x_{mq} \\ 0 & 0 & x_{ls} + x_g & 0 & 0 & 0 \\ \frac{x_{md}^2}{r_{fr}} & 0 & 0 & \frac{x_{fr}x_{md}}{r_{fr}} & \frac{x_{md}^2}{r_{fr}} & 0 \\ x_{md} & 0 & 0 & x_{md} & x_{dr} & 0 \\ 0 & x_{mq} & 0 & 0 & 0 & x_{qr} \end{bmatrix} \times \begin{bmatrix} i_{ds} \\ i_{qs} \\ i_{ns} \\ i_{fr} \\ i_{dr} \\ i_{qr} \end{bmatrix} \quad (5.173)$$

where again, p denotes the operator d/dt and

$$e_x = \frac{v_{fr}}{r_{fr}} x_{md} \quad (5.174)$$

Equation (5.173) is equivalent to the matrix equation

$$\mathbf{v} = (\mathbf{R} + \mathbf{G})\mathbf{i} + \frac{p}{\omega_b} \mathbf{X}\mathbf{i} \quad (5.175)$$

where \mathbf{v} and \mathbf{i} are the 6×1 voltage and current vectors, \mathbf{R} and \mathbf{G} are 6×6 matrices corresponding respectively to the diagonal resistive elements and to the off-diagonal “speed voltage” terms of Eq. (5.173) and \mathbf{X} is the 6×6 reactance matrix given in Eq. (5.173).

It is assumed that before the transient occurs, only DC terms appear in the vector \mathbf{v} (balanced conditions so that the initial condition corresponding to Eq. (5.173) is found by setting $p\mathbf{i} = 0$, hence,

$$\mathbf{i}(0) = (\mathbf{R} + \mathbf{G})^{-1} \mathbf{v}(0) \quad (5.176)$$

After the disturbance occurs, the stator voltages v_{ds} , v_{qs} , and v_{ns} can contain components having zero frequency (DC), synchronous frequency (ω_e), and twice synchronous frequency ($2\omega_e$). In order to arrive at a compact solution, it is convenient to define auxiliary variables to express the sinusoidal part of the input voltages. If $x_{2\alpha}$ and $x_{2\gamma}$ are defined such that

$$x_{2\alpha} = \cos(2\omega_e t + \delta) \quad (5.177)$$

$$x_{2\gamma} = \sin(2\omega_e t + \delta) \quad (5.178)$$

then $x_{2\alpha}$ and $x_{2\gamma}$ can be obtained from the set of differential equations

$$\frac{p}{\omega_b} x_{2\alpha} = -2 \frac{\omega_e}{\omega_b} x_{2\gamma} \quad (5.179)$$

$$\frac{p}{\omega_b} x_{2\gamma} = 2 \frac{\omega_e}{\omega_b} x_{2\alpha} \quad (5.180)$$

where

$$x_{2\alpha}(0) = \cos \delta \quad (5.181)$$

$$x_{2\gamma}(0) = \sin \delta \quad (5.182)$$

In matrix form Eqs. (5.179) and (5.180) can be written

$$\frac{p}{\omega_b} \begin{bmatrix} x_{2\alpha} \\ x_{2\gamma} \end{bmatrix} = \begin{bmatrix} 0 & -2\omega_e/\omega_b \\ 2\omega_e/\omega_b & 0 \end{bmatrix} \times \begin{bmatrix} x_{2\alpha} \\ x_{2\gamma} \end{bmatrix} \quad (5.183)$$

or simply

$$\frac{p}{\omega_b} \mathbf{x}_2 = \mathbf{A}_2 \mathbf{x}_2 \quad (5.184)$$

where

$$\mathbf{x}(0) = [\cos \delta \ \sin \delta]^T \quad (5.185)$$

In a similar manner, if $x_{1\alpha} = \cos(\omega_e t)$ and $x_{2\gamma} = \sin(\omega_e t)$, then

$$\frac{p}{\omega_b} \mathbf{x}_1 = \mathbf{A}_1 \mathbf{x}_1 \quad (5.186)$$

where

$$\mathbf{x}_1(0) = [1 \ 0]^T \quad (5.187)$$

The quantities \mathbf{x}_1 and \mathbf{x}_2 are defined similar to \mathbf{x}_2 and \mathbf{x}_2 .

The voltage vector \mathbf{v} can now be written as the sum of three components corresponding to the DC, ω_e , and $2\omega_e$ components of the terminal voltage,

$$\mathbf{v} = \mathbf{v}_0 + \mathbf{v}_1 + \mathbf{v}_2 \quad (5.188)$$

The three voltage components are given by the vectors

$$\mathbf{v}_0 = \begin{bmatrix} \frac{1}{2}(V_{q\alpha} - V_{d\gamma})\sin\delta + \frac{1}{2}(V_{q\gamma} + V_{d\alpha})\cos\delta \\ \frac{1}{2}(V_{q\alpha} - V_{d\gamma})\cos\delta - \frac{1}{2}(V_{q\gamma} + V_{d\alpha})\sin\delta \\ 0 \\ 0 \\ 0 \\ E_x \end{bmatrix} \quad (5.189)$$

and

$$\mathbf{v}_1 = \mathbf{C}_1 \mathbf{x}_1 \quad (5.190)$$

where

$$\mathbf{C}_1 = \begin{bmatrix} 0 & 0 \\ 0 & 0 \\ V_{n\alpha} & V_{n\gamma} \\ 0 & 0 \\ 0 & 0 \\ 0 & 0 \end{bmatrix} \quad (5.191)$$

and

$$\mathbf{v}_2 = \mathbf{C}_2 \mathbf{x}_2 \quad (5.192)$$

where

$$\mathbf{C}_2 = \begin{bmatrix} \frac{1}{2}(V_{q\gamma} - V_{d\alpha}) & \frac{1}{2}(V_{q\alpha} + V_{d\gamma}) \\ \frac{1}{2}(V_{q\alpha} + V_{d\gamma}) & \frac{1}{2}(V_{q\gamma} - V_{d\alpha}) \\ 0 & 0 \\ 0 & 0 \\ 0 & 0 \\ 0 & 0 \end{bmatrix} \quad (5.193)$$

Substituting Eqs. (5.188) to (5.193) into Eq. (5.175) and rearranging into state variable form,

$$p\mathbf{i} = \omega_b X^{-1} [-(\mathbf{R} + \mathbf{G})\mathbf{i} + \mathbf{C}_2 \mathbf{x}_2 + \mathbf{C}_1 \mathbf{x}_1 + \mathbf{v}_0] \quad (5.194)$$

Combining Eqs. (5.184) and (5.186) with Eq. (5.194), the entire system can now be represented by the composite state variable matrix equation

$$p \begin{bmatrix} \mathbf{i} \\ \mathbf{x}_2 \\ \mathbf{x}_1 \end{bmatrix} = \omega_b \begin{bmatrix} -X^{-1}(\mathbf{R} + \mathbf{G}) & X^{-1}\mathbf{C}_2 & X^{-1}\mathbf{C}_1 \\ \mathbf{0}_{2 \times 6} & \mathbf{0}_{2 \times 2} & \mathbf{0}_{2 \times 2} \\ \mathbf{0}_{2 \times 6} & \mathbf{0}_{2 \times 2} & 1 \end{bmatrix} \times \begin{bmatrix} \mathbf{i} \\ \mathbf{x}_2 \\ \mathbf{x}_1 \end{bmatrix} + \begin{bmatrix} \omega_b X^{-1} \\ \mathbf{0}_{2 \times 6} \\ \mathbf{0}_{2 \times 6} \end{bmatrix} \mathbf{v}_0 \quad (5.195)$$

where $\mathbf{0}_{n \times m}$ is an $n \times m$ matrix of zeros.

Equation (5.195) is equivalent to the state variable matrix equation

$$p\mathbf{x} = \mathbf{A}\mathbf{x} + \mathbf{u} \quad (5.196)$$

where \mathbf{x} is the state vector given by

$$\mathbf{x} = \begin{bmatrix} \mathbf{i} \\ \mathbf{x}_2 \\ \mathbf{x}_1 \end{bmatrix} \quad (5.197)$$

The matrix \mathbf{A} is the 10×10 system matrix of Eq. (5.195) and \mathbf{u} is the 10×1 input vector of constant elements

$$\mathbf{u} = \begin{bmatrix} \omega_b X^{-1} \mathbf{v}_0 \\ \mathbf{0}_{4 \times 1} \end{bmatrix} \quad (5.198)$$

The system equations represented by Eq. (5.195) are now in a form amenable to a state variable solution. In particular, note that the input excitation vector \mathbf{u} is constant so that this equation may be integrated directly without difficulty. (Complications would have arisen if the two oscillators defining the auxiliary variables x_1 and x_2 had not been defined.) Using modal theory the complete solution can be expressed directly in terms of the eigenvalues and eigenvectors of the system. This solution is given in Appendix 2. It is further demonstrated in Appendix 2 how this result can be expanded such that the time domain expression for all state variables can be written simply as a weighted series of exponentials. The expansion method described in Appendix 2 is readily implemented with software such as MATLAB. Since the result is general, this formulation provides a convenient method for developing the solution to a wide variety of transient condition, including but not limited to the three-phase fault studied earlier in this chapter.

5.13 Comparison of Modal Analysis Solution with Conventional Methods

One of the most studied and best understood machine transients is the three-phase short-circuit previously considered using conventional techniques in [Section 5.7](#). The solution for a three-phase fault is readily obtained from the general solution by simply equating the source voltages e_{ag} , e_{bg} , and e_{cg} to zero. For simplicity the solution is normally given only for a short-circuit with the machine operating with an open circuit prior to the fault. The MATLAB printout for this condition is shown in [Figure 5.16](#). using the parameters of the 50 Hz 30 MW turbogenerator given in [Table 5.2](#). Here the solution has been presented so that it can be read directly in mathematical form without difficulty. Although only the $d-q$ currents are shown, solutions for the machine flux linkages can easily be obtained since they are merely algebraic combinations of the system state variables ($d-q$ currents). The time domain expression for per unit electromagnetic torque can also be calculated by means of Eq. (3.245). It should be mentioned that solutions for additional machine variables such as amortisseur winding currents, stator flux linkages, and the like are rarely given in the literature even for the simple case of a three-phase short-circuit.

The solution for I QS is:

$$\begin{aligned} & -0.4794E-3 \\ & + 0.5583E+01 * \text{EXP}(-0.3595E+01*T) * \text{SIN}(0.3141E+03*T - 0.1798E+03) \\ & - 0.4074E-01 * \text{EXP}(-0.9544E+01*T) \\ & + 0.5988E-01 * \text{EXP}(-0.5538E+01*T) \\ & + 0.5510E-02 * \text{EXP}(-0.1069E+01*T) \end{aligned}$$

The solution for I DS is:

$$\begin{aligned} & -0.5000E+00 \\ & + 0.5863E+01 * \text{EXP}(-0.3595E+01*T) * \text{SIN}(0.3141E+03*T + 0.8995E+02) \\ & - 0.1621E+01 * \text{EXP}(-0.9544E+01*T) \\ & - 0.33485E-03 * \text{EXP}(-0.5538E+01*T) \\ & - 0.3741E+01 * \text{EXP}(-0.1069E+01*T) \end{aligned}$$

The solution for I QR is:

$$\begin{aligned} & -0.2213E-04 \\ & + 0.5466E+01 * \text{EXP}(-0.3595E+01*T) * \text{SIN}(0.3141E+03*T + 0.3385E+00) \\ & + 0.4207E-01 * \text{EXP}(-0.9544E+01*T) \\ & - 0.6439E-01 * \text{EXP}(-0.5538E+01*T) \\ & - 0.9947E-02 * \text{EXP}(-0.1069E+01*T) \end{aligned}$$

The solution for I DR is:

$$\begin{aligned} & -0.5849E-06 \\ & + 0.4485E+01 * \text{EXP}(-0.3595E+01*T) * \text{SIN}(0.3141E+03*T - 0.8913E+02) \\ & + 0.3863E+01 * \text{EXP}(-0.9544E+01*T) \\ & - 0.5508E-03 * \text{EXP}(-0.5538E+01*T) \\ & + 0.6220E+00 * \text{EXP}(-0.1069E+01*T) \end{aligned}$$

The solution for I FR is:

$$\begin{aligned} & + 0.5376E+00 \\ & + 0.1284 * \text{EXP}(-0.3595E+01*T) * \text{SIN}(0.3141E+03*T - 0.9301E+02) \\ & - 0.2119 * \text{EXP}(-0.9544E+01*T) \\ & + 0.8611 * \text{EXP}(-0.5538E+01*T) \\ & + 0.3401 * \text{EXP}(-0.1069E+01*T) \end{aligned}$$

Figure 5.16 Computer printout for a three-phase fault from no load for a 50 Hz 30 MW Machine.

Table 5.3 Per unit parameters of a 30 MW, 11.86 kV, 50 Hz turbogenerator. The per unit parameters of this machine on a 37.5 MVA base are as follows

r_S	0.002	r_{FR}	0.001
x_{LS}	0.14	x_{FR}	2.0
$r_{DR} = r_{QR}$	0.003	x_{MQ}	1.86
$x_{QR} = x_{DR}$	1.9	x_{MD}	1.86
T_{d0}'	6.37 s.	T_d'	0.86 s.
T_d''	0.114 s.	T_q''	0.181 s.
H	2.65 s.		

The corresponding solutions for the direct and quadrature axis currents and the field winding are given by Eqs. (5.100) to (5.102). By comparing these solutions to the result shown in Figure 5.16 it is possible to identify x_{DS} , x_D' , x_D'' , x_Q'' and the time constants T_a , T_d' , T_d'' , and T_q'' . The parameters derived from the modal analysis are compared with the values in Table 5.2 as shown in Table 5.4.

Table 5.4 Comparison of transient parameters of a 50 Hz, 30 MW turbogenerator calculated by modal analysis compared with values derived from Eqs. (5.100) to (5.102).

Parameter	Conventional [2]	Modal Analysis	Parameter	Conventional [2]	Modal Analysis
x_{DS}	2.0	2.0	T_a	0.278	0.278
x_D'	0.27	0.236	T_d'	0.860	0.935
x_D''	0.171	0.171	T_d''	0.114	0.105
x_Q''	0.179	0.179	T_q''	0.181	0.181

For purposes of comparison the per unit machine current components in the time domain can be defined according to the equation

$$i_X = i_{XSS} + i_{XA} e^{-t/T_a} \sin(\omega_e t + \theta) + i_{XD'} e^{-t/T_d'} + i_{XD''} e^{-t/T_d''} + i_{XQ''} e^{-t/T_q''} \quad (5.199)$$

where X denotes D , Q or F . Table 5.5 shows a comparison of the various components of the $d-q$ stator currents computed by modal analysis and by Eqs. (5.100) to (5.102). Slight differences between the two sets of numbers are due to the approximations made in the conventional solution as a result of neglecting the circuit resistances when calculating the transient reactances from the complex operational impedances.

Table 5.5 Comparison of transient currents of a 50 Hz, 30 MW turbogenerator calculated with traditional method and with modal analysis (short-circuit from no load).

Current	Components	Conventional[2]	Modal Analysis
i_{DS}	i_{DSS}	-0.5	-0.5
	i_{DA}	5.85	5.86
	i_{DD}'	-3.20	-3.74
	i_{DD}''	-2.14	-1.62
	i_{DQ}''	0.0	0.0003
i_{FR}	i_{FSS}	0.54	0.54
	i_{FA}	1.17	1.28
	i_{FD}'	3.44	3.40
	i_{FD}''	-2.27	-2.12
	i_{FQ}''	0.0	0.0009
i_{QS}	i_{QSS}	0.0	0.0
	i_{QA}	5.58	5.58
	i_{QD}'	0.0	0.006
	i_{QD}''	0.0	-0.041
	i_{QQ}''	0.0	0.060

It has already been noted that since the modal solution has been formulated for an arbitrary sinusoidal voltage change, nearly any conventional type of transient associated with a one machine system can be solved by specifying the appropriate source voltages before and after the disturbance. As a typical example of the solution method, Figure 5.17 shows the result obtained for a line-to-ground fault wherein $e_{AG} = 0$. Again the 30 MW generator of Table 5.2 is assumed. However, in this case the machine is assumed to be loaded to

rated input power. The machine is operating with a 0.926 lagging power factor at the machine terminals at the instant of the fault. A three wire connection is assumed ($x_G = r_G = \infty$.) Neglecting the second order terms in the solution, the result obtained from the modal solution is

$$\begin{aligned} i_{QS} &= -0.277 + 1.86 \sin(2\omega_e t + 125^\circ) + 3.06 e^{-3.6t} \sin(\omega_e t - 89^\circ) \\ &\quad + 1.41 e^{-5.54t} - 0.007 e^{9.54t} \end{aligned} \quad (5.200)$$

$$\begin{aligned} i_{DS} &= -1.013 + 1.95 \sin(2\omega_e t + 35^\circ) - 3.21 e^{-3.6t} \sin(\omega_e t) \\ &\quad - 0.29 e^{-9.54t} + (-0.69) e^{-1.07t} \end{aligned} \quad (5.201)$$

$$\begin{aligned} i_{QR} &= 1.82 \sin(2\omega_e t - 54.8^\circ) + 3.0 e^{-3.6t} \sin(\omega_e t + 91^\circ) \\ &\quad - 1.51 e^{-5.54t} \end{aligned} \quad (5.202)$$

$$\begin{aligned} i_{DR} &= 1.49 \sin(2\omega_e t - 145^\circ) + 2.46 e^{3.6t} \sin(\omega_e t + 1.5^\circ) \\ &\quad + 0.70 e^{-9.54t} + 0.115 e^{1.07t} - 0.013 e^{5.54t} \end{aligned} \quad (5.203)$$

$$\begin{aligned} i_{FR} &= 1.29 + 0.43 \sin(2\omega_e t - 146.5^\circ) + 0.70 e^{-3.6t} \sin(\omega_e t - 2.4^\circ) \\ &\quad - 0.38 e^{9.54t} + 0.628 e^{-1.07t} + 0.02 e^{5.54t} \end{aligned} \quad (5.204)$$

In these equations $\omega_e = 2\pi(50)$. The functions are plotted in Figure 5.17 together with the instantaneous torque. The presence of the decaying 50 Hz transient and steady-state 100 Hz terms due to the phase unbalance are clearly evident. Comparison with an exact solution (to be discussed in detail in Chapter 11), assuming that the load angle δ can vary as a result of the fault, indicates that the solution is essentially the same as calculated by modal theory. The maximum deviation of any variable from the modal solution was 0.1 p.u. during the 0.12 second interval shown in Figure 5.17.

5.14 Unsymmetrical Short-Circuits

Thus far, only “symmetrical” short-circuits have been considered, in which case the impedances of the machine remain balanced so that a solution remains tractable. An unsymmetrical short-circuit occurs during a line to ground or double line to ground fault. When the non-grounded lines are open circuited, solution of these unsymmetrical faults is considerably more complicated than for a symmetrical fault. The solution must be obtained by introducing the

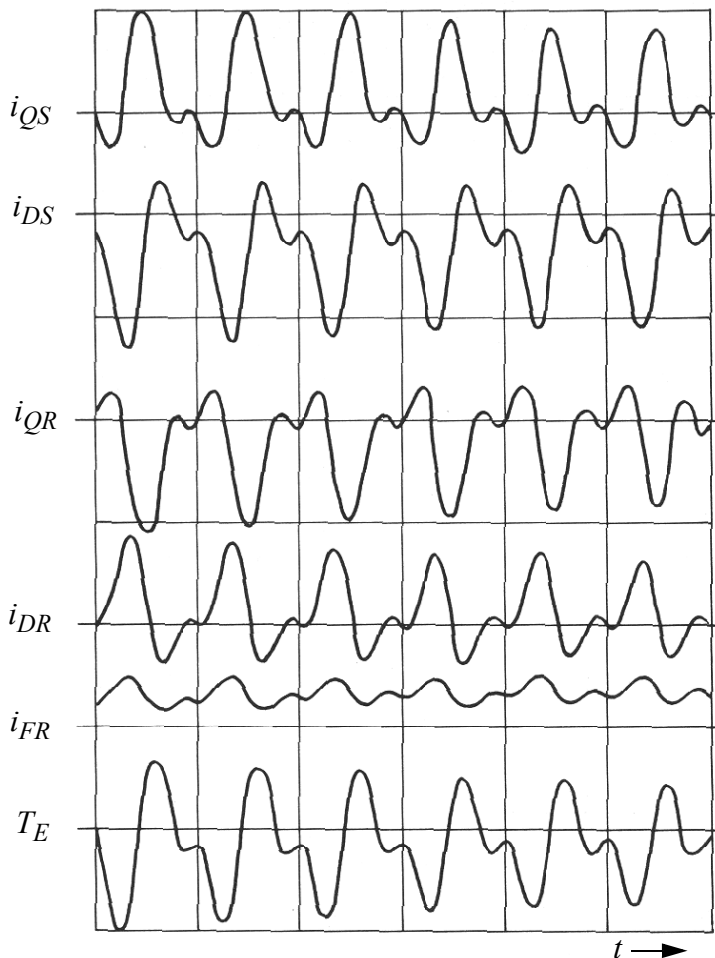


Figure 5.17 Machine currents and torque for a single-phase fault from rated load. Scale: vertical – 5.0 p.u. /div., horizontal – 0.02 sec/div.

applicable constraints into Park's equations. For example, if phases bs and cs are short-circuited when the generator is running on open circuit,

$$i_{as} = 0$$

and

$$i_{bs} = -i_{cs}$$

$$v_{bs} = -v_{cs}$$

In such cases the voltages and currents must be expressed as an infinite series of harmonics if resistances are included. A full theoretical treatment is

extremely difficult and numerous approximations must be made to arrive at a solution. The method of symmetrical components is generally used and employs the assumption that all harmonics can be neglected. A solution can be found in Ref. [9].

5.15 Conclusion

While synchronous machines normally operate in the steady-state, it is during the brief periods of time during which a transient occurs that the machine itself and its attendant parts such as circuit breakers, excitation systems, and the like reach their design limits. The traditional approach to analysis of this class of problems normally invokes the application of Doherty's Law, i.e., the Theorem of Constant Flux Linkages. This method has been covered in this chapter in some detail. However, more modern methods of analysis has, to a great extent, replaced this classical method. In particular, the use of eigenvector/eigenvalues has been introduced as a powerful means of computing constant speed transients, which eliminates the many assumptions invoked during the application of Doherty's Law.

5.16 References

- [1] C. Concordia, "Synchronous Machines," John Wiley, New York, 1951.
 - [2] B. Adkins and R.G. Harley, "The General Theory of Alternating Current Machines," Chapman and Hall, London, 1975.
 - [3] I.M. Canay, "Causes of Discrepancies on Calculation of Rotor Quantities and Exact Equivalent Diagrams of the Synchronous Machine," *IEEE Trans. on Power Apparatus and Systems*, vol. PAS-88, No. 7, July 1969, pp. 1114–1120.
 - [4] R.P. Schultz, W.D. Jones and D.W. Ewart, "Dynamic Models of Turbine Generators Derived from Solid Rotor Equivalent Circuits," *IEEE Trans. on Power Apparatus and Systems*, vol. PAS-92, May/June 1973, pp. 926–933.
 - [5] K. Ogata, "State Space Analysis of Control Systems," Prentice-Hall, Inc., Englewood Cliffs, NJ, 1967.
-

- [6] S.S. Kalsi and T.A. Lipo, "A Modal Approach to the Transient Analysis of Synchronous Machines," *Electric Machines and Electromechanics*, vol. 1, 1977, pp. 337–354.
- [7] G. Shackshaft, "General Purpose Turboalternator Model," *IEE Proceedings*, vol. 110, no. 4, April 1963, pp. 703–713.
- [8] M. Sarma, "Synchronous Machines," Gordon and Breach, New York, 1979.
- [9] R. Kerkman, P.C. Krause and T.A. Lipo, "Simulation of a Synchronous Machine with an Open Phase," *Electric Machines and Electromechanics*, vol. 1, no. 3, April–June 1977, pp. 245–254.

Chapter 6

Power System Transient Stability

6.1 Introduction

The transient state is defined as the operating state of a power system which is characterized by sudden changes in load or in the circuit conditions. The disturbances may include faults, switching events, as well as abrupt and significant changes in loading. Both the electrical system and the mechanical systems are in a transient state characterized by variations in electrical power, voltage, and so forth as well as variations in the rotor speed of the machine. The question to be answered by transient stability analysis is: “will any of the generators or groups of generators in an interconnected system lose synchronism as the result of a transient shock to the system?” This shock is most often assumed to be a fault which is cleared by removing the faulted equipment or circuits. The relay and circuit breaker characteristics dictate the duration of the fault as seen by the system and the breakers must open before a *critical clearing time* to remove the fault.

6.2 Assumptions

In general, the same assumptions are made for the analysis of transient stability as were made in the study of short-circuits.

(1) Only fundamental frequency currents and voltages will be considered. Hence, in the rotor frame of reference

$$p\Psi_{qs} = p\Psi_{ds} = 0 \quad (6.1)$$

(2) The effect of speed variations on the stator voltage will be neglected. This is accomplished by setting ω_r/ω_b equal to 1.0 in the two stator voltage equations. While the speed will still vary, since the torque angle δ must be permitted to vary, this variation is typically small over the period of time being analyzed. If this effect ever becomes large, synchronism has probably been lost anyway.

(3) The effect of the variation of speed on the electrical power will also be neglected. This is equivalent to assuming that in per unit

$$T_E = P_E + I_S^2 r_S \quad (6.2)$$

where:

T_E = per unit electrical torque,

P_E = per unit terminal electrical power,

r_S = per unit stator resistance

If the electrical power is measured behind the stator resistance, then it is equal to the air gap power P_E , which is therefore equal numerically to the electrical torque T_E , since speed variations are neglected.

(4) Saturation effects will be neglected initially. This allows one to still use the complex vector diagram as the basic tool for analysis.

(5) Amortisseur winding effects will be neglected. Although the amortisseur effects are significant in short-circuit current studies, the principal period of interest in transient stability analysis is after about three cycles and most often less than 60 cycles. Therefore, the amortisseur effects in the initial period after a disturbance are not of real significance. Should the machine begin to slip poles, currents will begin to be induced into the amortisseur windings which can not be neglected. This “induction motor” torque tends to help the machine regain or maintain synchronism by producing “damping torque” variations in rotor speed. This effect is almost always beneficial and neglecting its existence is considered as conservative.

(6) The mechanical torque input to the synchronous generator is assumed to be constant during the period being analyzed. This is equivalent to assuming that the time lags of the speed governor and the mechanical system are large enough so that the effects are not significant. Since any such effects should be beneficial to stability, this is again a conservative assumption. While it is possible to approximate these effects, the added complication and the increased time to make an analysis are great enough that it is very rarely attempted in hand calculations.

(7) Voltage regulator response is neglected (or idealized). Recall that the field voltage equation can be written as

$$e_x = x_{md} i_{fr} + \frac{x_{md}}{\omega_b r_{fr}} \left(\frac{d\psi_{fr}}{dt} \right), \quad (6.3)$$

As a result of any disturbance the field current will tend to be higher than its initial value. If e_x is constant, then $e_q' = (x_{md}/x_{fr})\psi_{fr}$ will clearly tend to decrease. However, this same current increase will tend to depress the terminal voltage. If an automatic voltage regulator is in service, the regulator will begin acting in order to increase e_x in order to raise the terminal voltage. The voltage regulator will act to restore or raise the value of e_q' . The net effect is that e_q' will tend to remain constant for a fairly long period of time. For major disturbances (such as a three-phase fault near the machine) which are cleared in about six cycles, the assumption is still reasonable. Less severe faults (unbalanced faults or remote faults) tend to make the assumption conservative.

In addition to these assumptions, transient saliency is often neglected. This assumption needs a little more elaboration. It has already been mentioned that the field flux linkages tend to remain constant during a transient disturbance and that the voltage regulator tends to maintain e_q' constant (and uniformly rotating). In many machines (particularly turbogenerators) the transient reactance x_d' is not sufficiently different from x_{qs} (or x_q') so that during the transient, the machine appears to be a round-rotor machine. In such cases it is useful to hold the voltage behind the reactance x_d' constant. In per unit the voltage E_S' is called the *per unit voltage behind transient reactance*. Note from the figure that E_S' is nearly the same amplitude as E_Q' , so that this assumption is often satisfactory, even when $x_D' \neq x_Q'$. It is typically a satisfactory assumption for overexcited operation but may lead to sizable differences at high power factor or underexcited operation, in which case the per unit value of E_Q' may be much smaller than E_S' . The use of the concept of constant voltage behind transient reactance permits the use of a simple round-rotor equivalent circuit, which is useful for purposes of illustration but may be used only with caution. The reader is referred to [Figure 6.1](#).

If E_S' is used to represent behavior of the rotor flux linkages rather than E_Q' then the machine representation is much simpler. In this case, assuming constant flux linkages, the machine is represented as shown. The magnitude of E_S' remains constant and equal to the magnitude $E_S'(0)$, the value at the instant of the fault, $t = 0$. The angle variation will be discussed in a succeeding section.

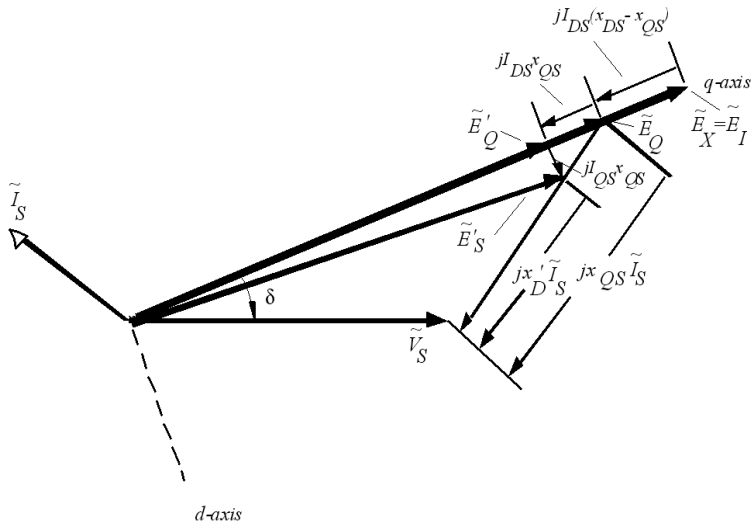


Figure 6.1 Phasor diagram showing the difference between E_Q' and E_S' (generator operation).

6.3 Torque Angle Curves

Neglecting resistance and variations in speed results in the electrical torque becoming numerically equal to the terminal power. In per unit, the electrical power is

$$P_E = v_{DS}i_{DS} + v_{QS}i_{QS} \quad (6.4)$$

where, from the phasor diagram, in steady-state

$$V_{DS} = V_S \sin \delta \quad (6.5)$$

$$V_{QS} = V_S \cos \delta \quad (6.6)$$

where δ is negative for generator operation.

Neglecting the stator resistance voltage drop $I_S r_S$, the amortisseur winding circuits, the voltages $p\psi_{QS}$, $p\psi_{DS}$, and assuming that $\omega_r / \omega_b = 1$, then Park's stator equations become simply

$$V_{DS} = -\psi_{QS} \quad (6.7)$$

$$V_{QS} = \psi_{DS} \quad (6.8)$$

where the stator fluxes are given by

$$\psi_{QS} = x_{QS} I_{QS} \quad (6.9)$$

$$\Psi_{DS} = x_{DS}I_{DS} + x_{MD}I_{FR} = x_{DS}I_{DS} + E_I \quad (6.10)$$

and, in addition,

$$\Psi_{FR} = x_{FR}I_{FR} + x_{MD}I_{DS} \quad (6.11)$$

Recall from Chapter 5 that if the field flux linkages are constant, one can write Eq. (6.11) as

$$E_Q' = E_I + (x_{DS} - x_{D'})I_{DS} \quad (6.12)$$

Substituting Eq. (6.12) into the expression for Ψ_{DS} , Eq.(6.10), then substituting this result into the equation for V_{QS} (Eq. (6.8)), and solving the two voltage equations for I_{QS} and I_{DS} , one obtains eventually

$$I_{DS} = \left(\frac{V_{QS} - E_Q'}{x_{D'}} \right) \quad (6.13)$$

$$I_{QS} = -\frac{V_{DS}}{x_{QS}} \quad (6.14)$$

Substituting these expressions for stator $d-q$ voltages and currents into the power equation and rearranging,

$$P_E = \frac{E_Q' V_S}{x_{D'}} \sin \delta + V_S^2 \frac{x_{D'}' - x_{QS}}{2x_{D'} x_{QS}} \sin 2\delta \quad (6.15)$$

Note that the power and torque are equal since it has been assumed that the per unit speed ω_r / ω_b is unity. If transient saliency is neglected (i.e., $x_{D'}' \equiv x_{QS}$) then this expression reduces to

$$T_E \equiv \frac{E_Q' V_S}{x_{D'}} \sin \delta \quad (6.16)$$

where δ is now the angle between E_Q' and V_S . Note the similarity between this equation and the expression for torque in the steady-state, (see Chapter 5). Note also that the angle δ is the same quantity as used for the steady-state phasor diagram since both E_Q and E_Q' lie on the q -axis.

Neglecting stator resistance, the per unit torque can also be calculated from

$$T_E = V_{DS}I_{DS} + V_{QS}I_{QS} \quad (6.17)$$

From Eqs. (6.13) and (6.14), another expression for per unit torque when the field flux linkages are constant is

$$T_E = [E_Q' + (x_D' - x_{QS})I_{DS}]I_{QS} \quad (6.18)$$

or simply

$$T_E = E_Q'I_{QS} \quad (6.19)$$

when there is no transient saliency.

6.4 Mechanical Acceleration Equation in Per Unit Form

It can be recalled from Chapter 4 that the equation which describes the electro-mechanical motion of the synchronous machine (neglecting damping) is given by

$$T_e + T_l = J \frac{d\omega_{rm}}{dt} \quad (6.20)$$

or, in terms of an equivalent electrical angular velocity,

$$T_e + T_l = \frac{2J}{P} \frac{d}{dt} \omega_r \quad (6.21)$$

If the angular speed is per unitized relative to base angular velocity, then

$$T_e + T_l = \frac{2J\omega_b}{P} \frac{d}{dt} (\omega_R) \quad (6.22)$$

where the per unit speed ω_R has been defined as

$$\omega_R = \frac{\omega_r}{\omega_b} \quad (6.23)$$

A corresponding expression in per unit is obtained by dividing this expression by base torque T_b where

$$T_b = \frac{VA_b}{\omega_{bm}} = \frac{(P)(VA_b)}{2\omega_b} \quad (6.24)$$

and VA_b denotes the power (or volt-ampere) base and $\omega_{bm} = (2/P)\omega_b$. Equation (6.22) can now be written in the form

$$\frac{T_e + T_l}{T_b} = \left(\frac{2}{P}\right)^2 \frac{J\omega_b^2}{VA_b} \frac{d\omega_R}{dt} \quad (6.25)$$

whereupon it is convenient to again define

$$H = \frac{\frac{1}{2}J\omega_{bm}^2}{VA_b} = \frac{\frac{1}{2}\left(\frac{2}{P}\right)^2 J\omega_b^2}{VA_b} \quad (6.26)$$

It is useful to realize that the quantity H is equal to the stored energy divided by the base time rate of change of energy and therefore has units of seconds (joules per watt).

In general, the torque angle δ is an equivalent electrical angle (as opposed to a physical mechanical angle) and is defined by

$$\delta = -\int \omega_r dt + \delta_o \quad (6.27)$$

Hence,

$$\frac{d\delta}{dt} = -\omega_r \quad (6.28)$$

and

$$\frac{d^2\delta}{dt^2} = -\frac{d\omega_r}{dt} \quad (6.29)$$

In terms of per unit angular speed,

$$\frac{d^2\delta}{dt^2} = -\omega_b \frac{d}{dt}(\omega_R) \quad (6.30)$$

As given, the torque angle δ is expressed in radians. It is often useful to express δ in electrical degrees. In this case, the second derivative of the torque angle is expressed in terms of the derivative of per unit speed as

$$\frac{d^2\delta}{dt^2} = -\left(\frac{180}{\pi}\right)(2\pi f_b) \frac{d}{dt}(\omega_R) \quad (6.31)$$

or, solving for $(d\omega_R)/(dt)$,

$$\frac{d\omega_R}{dt} = \left(-\frac{1}{360f_b}\right) \frac{d^2\delta}{dt^2} \quad (6.32)$$

Substituting this result into the per unit expression for the equation of motion, Eq. (6.25), results in

$$\frac{T_e}{T_b} + \frac{T_l}{T_b} = -\frac{2H}{360f_b} \frac{d^2\delta}{dt^2} = -\frac{H}{180f_b} \frac{d^2\delta}{dt^2} \quad (6.33)$$

or, alternatively,

$$\frac{t^2\delta}{dt^2} = -\frac{180f_b}{H}(T_E + T_L) \quad (6.34)$$

The quantity $T_E + T_L$ is called the accelerating torque and is formally defined as

$$T_A = T_E + T_L \quad (6.35)$$

Since δ is considered as negative for generator action, Eq. (6.16) verifies that T_E is negative for this case, so that T_L is positive. When T_E is balanced by an equal and oppositely impressed torque T_L , the accelerating torque T_A is zero. If the torque T_E suddenly drops as a result of a fault, the accelerating torque becomes positive, indicating a consequent positively increasing speed change and a negatively increasing value of δ . For the case of a generator Eq. (6.34) can also be written as

$$\frac{d^2\delta}{dt^2} = -\frac{180f_b}{H}(T_E + T_M) \quad (6.36)$$

where T_M represents the prime mover torque, which is again positive for generator action.

6.5 Equal Area Criterion for Transient Stability

Now let two machines be interconnected through an intertie. For each of the two interconnected machines, the acceleration equations may be written as

$$p^2\delta_1 = -\frac{180f_b}{H_1}T_{A1} \quad \text{for machine #1} \quad (6.37)$$

$$p^2\delta_2 = -\frac{180f_b}{H_2}T_{A2} \quad \text{for machine #2} \quad (6.38)$$

The angle between the quadrature axes of the two machines is

$$\delta_{12} = \delta_1 - \delta_2 \quad (6.39)$$

or

$$p^2\delta_{12} = p^2\delta_1 - p^2\delta_2 \quad (6.40)$$

$$= 180f_b\left(\frac{T_{A2}}{H_2} - \frac{T_{A1}}{H_1}\right) \quad (6.41)$$

Multiplying both sides by $2p\delta_{12}$, one has

$$(2p\delta_{12})p^2\delta_{12} = 2\frac{d\delta_{12}}{dt}\frac{d^2\delta_{12}}{dt^2} \quad (6.42)$$

which is equal to

$$= \frac{d}{dt}\left(\frac{d\delta_{12}}{dt}\right)^2 \quad (6.43)$$

Hence, the electromechanical equation can be written as

$$\frac{d}{dt}\left(\frac{d\delta_{12}}{dt}\right)^2 = 360f_b\left(\frac{T_{A2}}{H_2} - \frac{T_{A1}}{H_1}\right)\frac{d\delta_{12}}{dt} \quad (6.44)$$

Upon integrating both sides with respect to time,

$$\left(\frac{d\delta_{12}}{dt}\right)^2 = 360f_b\int\left(\frac{T_{A2}}{H_2} - \frac{T_{A1}}{H_1}\right)d\delta_{12} \quad (6.45)$$

In general, when a disturbance occurs, the angle δ_{12} becomes more negative and therefore $d\delta_{12}/dt$ is negative. Stability can only occur if the angle δ_{12} begins to get smaller (less negative). Otherwise the machine will begin to slip poles. When $d\delta_{12}/dt$ is equal to zero, the relative speed between the machines is equal to zero. The angle δ_{12} will subsequently start decreasing and stability (at least for the first swing) is preserved. On the other hand, if a condition whereby $d\delta_{12}/dt = 0$ can not be found for a given disturbance, then δ_{12} continues to increase and stability between the two machines is lost. Setting the right hand side of the above equation to zero forms an important condition called the *equal area criterion*.

$$0 = \int\left(\frac{T_{A2}}{H_2} - \frac{T_{A1}}{H_1}\right)d\delta_{12} \quad (6.46)$$

The need for the factor $360f_b$ has been dropped since the integral has been set equal to zero.

6.6 Transient Stability Analysis

It is instructive to consider first the system shown in [Figure 6.2](#), in which a generator is connected to a very large system compared to its own size. A constant voltage behind transient direct axis reactance model for the generator will be assumed as shown.

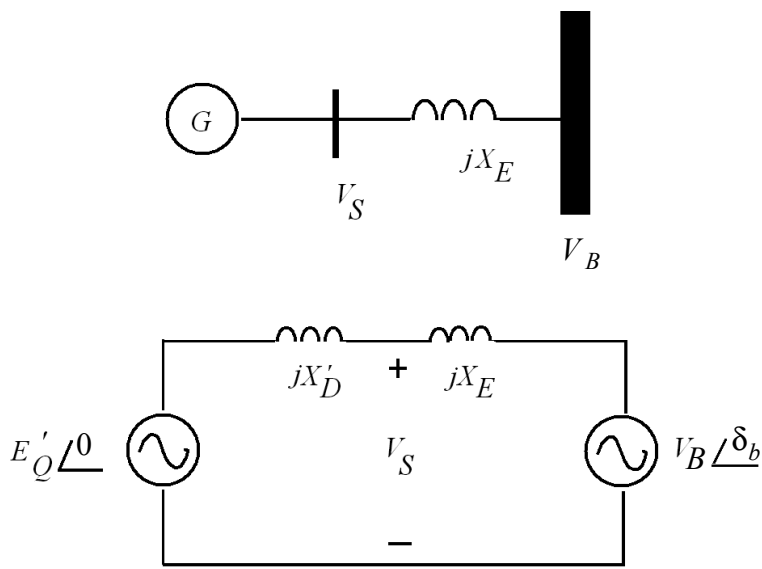


Figure 6.2 Simple single machine connected to an infinite bus via a transmission line represented by a lumped inductance and corresponding equivalent circuit.

The total angle between E_Q' located on the q -axis and the infinite bus voltage V_B is defined as δ_b , where the subscript b indicates that the torque angle is measured with respect to the infinite bus voltage rather than the terminal voltage of the machine. The torque-angle equation for this condition is equal to

$$T_E = \frac{E_Q' V_B}{x_{D'} + x_E} \sin \delta_b \quad (6.47)$$

The mechanical torque T_L is assumed to be constant and equal to the value of T_E at the instant prior to the disturbance, or

$$T_L = -T_E(0) \quad (6.48)$$

The equation that was derived in the previous section for stability is based on two interconnected machines but is also valid for one machine connected to an infinite bus. In this case the inertia of the second machine can be assumed to be infinite, in which case Eq. (6.46) becomes

$$0 = \int \frac{T_{A1}}{H_1} d\delta_{12} = \int \frac{T_{A1}}{H_1} d\delta_b \quad (6.49)$$

or, since H_1 is a simple constant,

$$0 = \int T_{A1} d\delta_b \quad (6.50)$$

The torque angle curve defined by the torque angle equation given above is shown below in Figure 6.3.

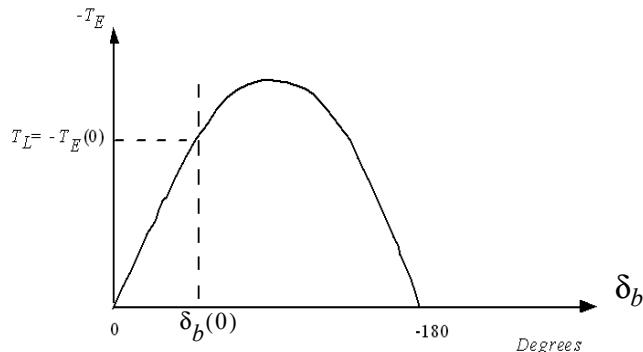


Figure 6.3 Torque–angle curve showing initial condition at instant of fault.

Assume now that a solid three-phase fault occurs at the generator terminals at $t = 0$ and is then removed at some later time $t = t_c$, without the value of X_E being affected. During the fault period, the short-circuit isolates the generator from the system. Neglecting resistance and any other generator losses, the electrical torque T_E during the fault is equal to zero, or

$$T_{A1} = T_L \quad (6.51)$$

The equal area criterion equation defines an area on the torque angle curve. For the period of the fault, this area is shown in Figure 6.4.

At the instant the fault is applied ($t = 0$) the electrical torque becomes zero and remains at zero until the fault is removed at a time corresponding to $\delta_{12}(t_c)$. During this period of time, the acceleration equation is

Per Unit Generating Torque

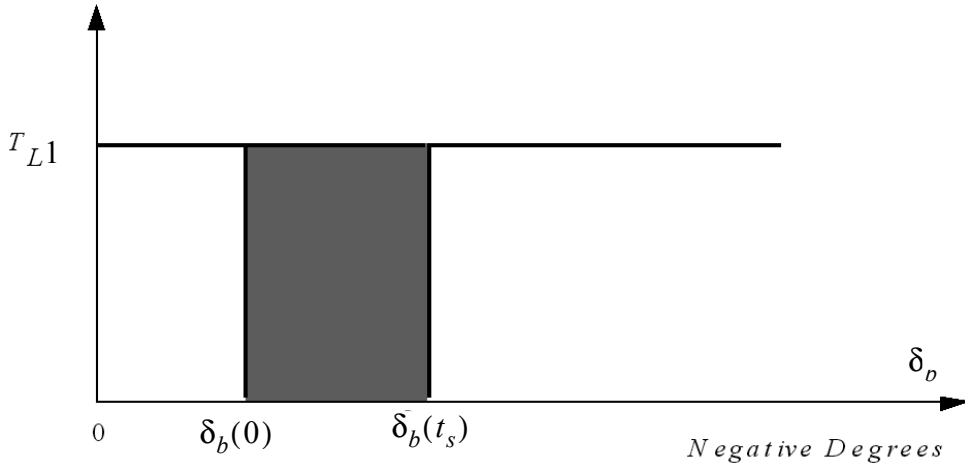


Figure 6.4 Area proportional to acceleration of a synchronous machine assuming a bolted three-phase fault and constant prime mover torque.

$$\frac{d^2\delta_b}{dt^2} = -\frac{180f_b}{H}T_{A1} \quad (6.52)$$

where T_{A1} is constant and equal to T_L . Upon integrating,

$$\frac{d\delta_b}{dt} = -\frac{180f_b}{H}T_L t + \frac{d\delta_b(0)}{dt} \quad (6.53)$$

where the last term represents an initial velocity of the torque angle.

Upon integrating a second time,

$$\dot{\delta}_b = -\frac{180f_bT_{A1}}{2H}t^2 + \frac{d\delta_b(0)}{dt}t + \delta_b(0) \quad (6.54)$$

If the fault is applied when the system is initially in the steady-state, then the term $d\delta_b(0)/dt$ is equal to zero. For this case, the above expression may be solved for the time t as

$$t = \sqrt{\frac{[\delta_b(0) - \delta_b]H}{90f_bT_{L1}}} \quad (6.55)$$

For a given switching time (time to interrupt the fault after the moment of the fault) the angle at the point of switching $\delta_b(t_s)$ can be calculated. In effect,

the shaded area in the previous figure represents energy which is converted from the prime mover to the inertia of the generating system. In this case, it is energy which is accelerating the rotor angle. That is, the rotor speed is increasing since the accelerating torque is positive. This area represents the energy which will tend to cause loss of synchronism between the generator and the system. The size of this area, then, is a measure of the severity of the fault as far as stability is concerned. A plot of the relative angle δ_b and the relative speed $d\delta_b/dt$ is shown in Figure 6.5 for the period during the fault.

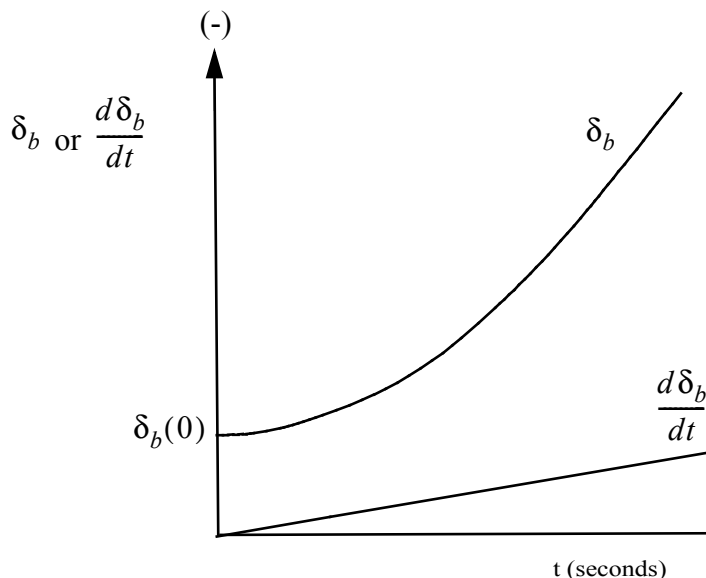


Figure 6.5 Generator torque angle and rate of change of torque angle for a bolted three-phase fault.

At the instant t_s the fault is removed and the machine again develops torque as defined by the voltage behind transient reactance. The torque available for braking the machine is shown below in Figure 6.6. Since the electrical torque is greater (numerically) than the mechanical torque, the accelerating torque is therefore negative and will attempt to decelerate or slow down the rotor speed as long as $-T_E$ is greater than T_L . The shaded area then, represents energy which tends to stabilize or synchronize the generator and system. The electrical torque during this period is often referred to as the *synchronizing torque*.

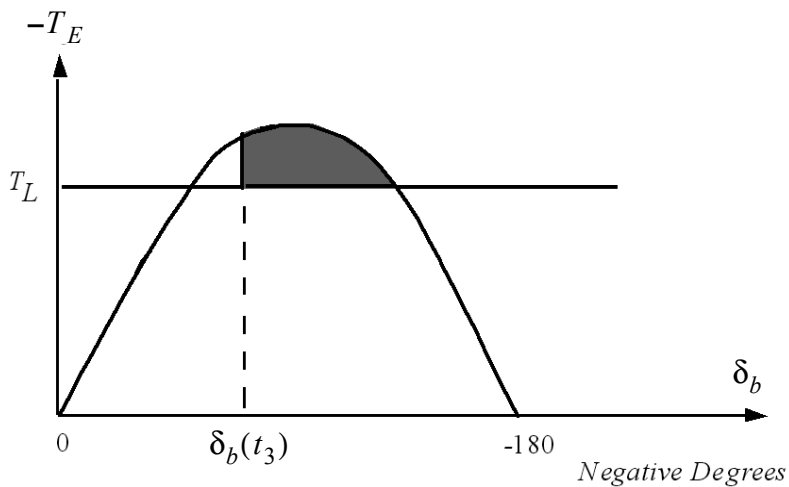


Figure 6.6 Portion of generator torque acting to brake the generator after a bolted three-phase fault.

If the areas of the two previous figures are drawn on the same diagram, the result is shown in Figure 6.7. The integral representing the area A_1 is positive

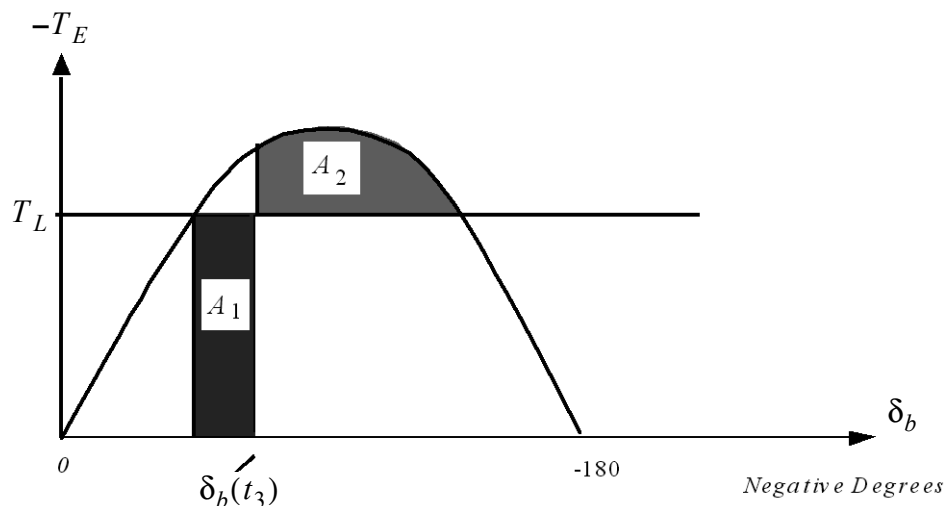


Figure 6.7 Torque versus angle curve showing equal accelerating component (A_1) and braking component (A_2) of torque.

and tends to produce instability and the integral represented by the area A_2 tends to produce stability. The sum of the two areas is the net solution to the integral,

$$A_1 + A_2 = \int T_A d\delta_b \quad (6.56)$$

When A_2 is greater than A_1 (and opposite in sign), the machine is transiently stable.

The condition shown in [Figure 6.7](#) for the case where the shaded areas above and below T_L are equal in magnitude. At the instant where these areas are equal, one obtains the solution to the equation

$$0 = \int T_A d\delta_b \quad (6.57)$$

and at this point the velocity $d\delta_b/dt$ between machines is zero. At the same time, the electrical torque is larger in magnitude than the mechanical torque, which results in a negative accelerating torque at this point. The angle δ_b will, therefore, begin to decrease. The behavior of the speed and angle for this condition is shown in [Figure 6.8](#).

When the area A_2 is less than A_1 in magnitude, the machine becomes transiently unstable as shown. When the angle $\delta_b(t_1)$ is reached, the machine still has a velocity greater than zero and the angle δ_{12} will continue to increase. Once past $\delta_{12}(t_1)$, the mechanical torque is again greater than the electrical torque and the machine will accelerate, increasing the velocity $d\delta_{12}/dt$ still further. The result is that the generator continuously has a velocity greater than the system and is therefore out of synchronism and unstable. Such characteristics are shown in [Figure 6.9](#).

The limiting case between being stable or unstable is a special case illustrated below. At this point, A_2 is just equal and opposite to A_1 . The theoretical performance of this system is shown in [Figure 6.10](#). For this limiting case, the angle $\delta_{12}(\text{max})$ is in the vicinity of 120 to 140 degrees. From this observation comes a rule of thumb: if the relative angle between two machines reaches a peak in the region of 120 electrical degrees, the system is near the transient stability limit.

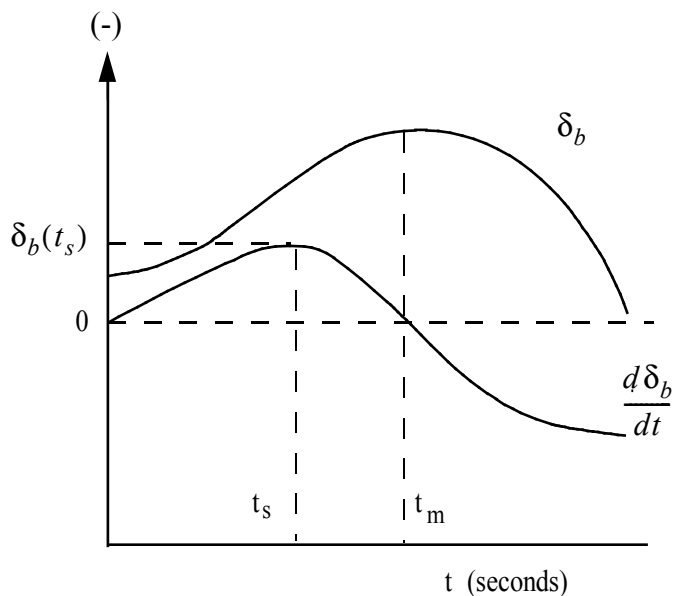


Figure 6.8 Progression of δ_{12} and $d\delta_{12}/dt$ for a stable three-phase fault condition.

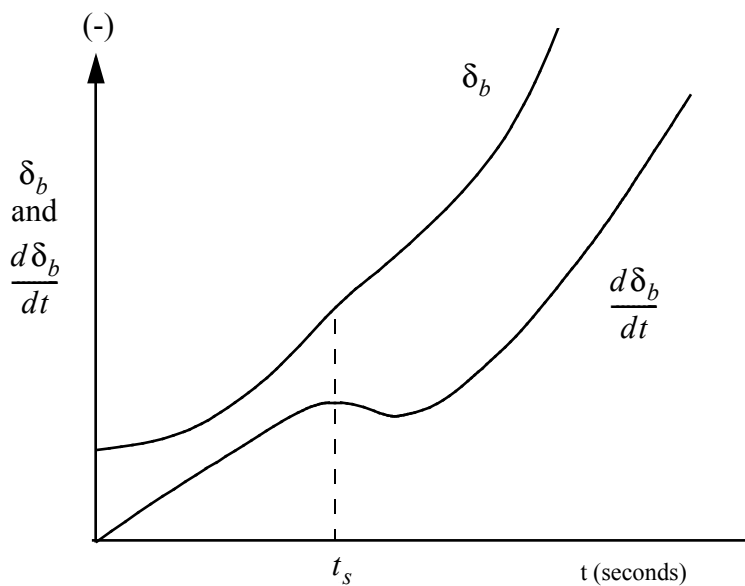


Figure 6.9 An unstable condition in which A_1 is greater than A_2 .

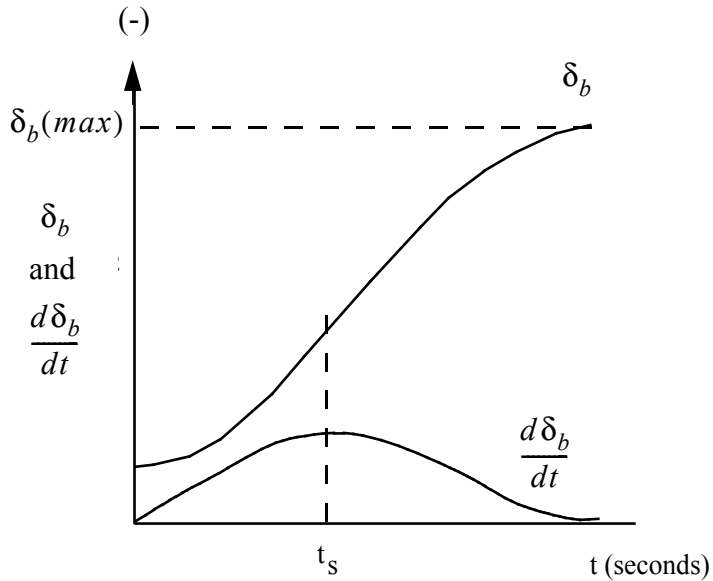


Figure 6.10 Limiting case in which A_2 is just equal to A_1 .

6.7 Transient Stability of a Two Machine System

For the more general case of a system having a finite inertia, the more general expression involving two inertias must be utilized, i.e.,

$$0 = \int \left(\frac{T_{A2}}{H_2} - \frac{T_{A1}}{H_1} \right) d\delta_{12}$$

For a given angle between machines $\delta_{12}(0)$, the accelerating torque for each machine is calculated as

$$T_{AG} = T_{LG} + T_{EG} \quad (6.58)$$

$$T_{AM} = T_{LM} + T_{EM} \quad (6.59)$$

The ratio between accelerating torque and the machine inertia is calculated for each machine. The resulting ratios are subtracted with the result plotted against the angle δ_{gs} , as shown in [Figure 6.11](#).

The areas A_1 and A_2 are again compared as was done previously in order to determine whether or not the system is transiently stable.

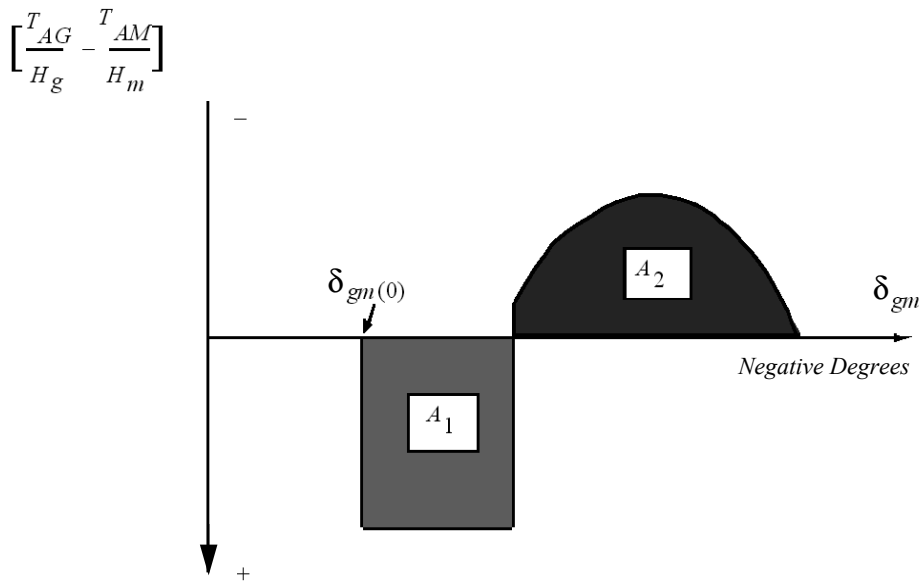


Figure 6.11 Integrand of the stability equation, Eq. (6.45) versus the torque angle δ_{gm} .

A special case for a two machine analysis arises where there is no system resistance of any kind. In this case, the electrical power (or torque) of the generator and the motor absorbing power are always equal and opposite in sign, or

$$T_{LM} = -T_{LG} \quad (6.60)$$

$$T_{EM} = -T_{EG} \quad (6.61)$$

Therefore, the stability equation becomes

$$\Im = \int \left(\frac{T_{AG}}{H_g} - \frac{T_{AM}}{H_m} \right) d\delta_{gm} \quad (6.62)$$

where

$$T_{AM} = -T_{AG} \quad (6.63)$$

in which case Eq. (6.62) becomes

$$\Im = \int T_{AG} \left(\frac{1}{H_g} + \frac{1}{H_m} \right) d\delta_{gm} \quad (6.64)$$

or simply

$$0 = \int T_{AG} d\delta_{gs} \quad (6.65)$$

This equation is the same as was used for a generator tied to an infinite bus. However, the apparent H of the equivalent generator is now

$$H_a = \frac{1}{\frac{1}{H_g} + \frac{1}{H_s}} = \frac{H_g H_s}{H_g + H_s} \quad (6.66)$$

The value of the two machine *Equal Area Criterion* for transient stability is in the ability to determine not only whether or not the machines are transiently stable, but also to determine stability limits for either power transfer or the time it takes to clear a fault. When a system is at the transient stability limit, the switching time t_s corresponding to the critical switching angle is called the *critical switching time* t_c . The angle $\delta(t_s)$ at which point the fault was removed is called the *critical switching (or clearing) angle* δ_c .

6.8 Multi-Machine Transient Stability Analysis

The equal area criterion can not be used directly in systems where three or more machines exist and the assumption of an “infinite” system is either completely wrong or where more accurate system representation is desired. However, the system behavior noted when analyzing two machines can be used to establish a criterion of stability of a system containing many machines.

The method of analysis most commonly used is as follows.

1. Represent the lines, transformers, etc., of the system in accordance with the conventional circuit analysis approaches.
2. Use circuit analysis (or a computer) to establish a complete steady-state operating condition for the system with all machine terminal conditions specified. This steady-state condition is to be tested for stability.
3. Represent each generator in the manner shown previously and determine E_q' for each machine.
4. Using step-by-step numerical methods, analyze the system for transient stability.

Previously, the assumption was inherently made that the angle of E_s' of each machine was equal to the angle between the quadrature axis of each

machine and a reference axis, typically the terminal voltage of the main generator of concern. When more than two machines are involved, this reference axis can be chosen more or less arbitrarily. Three generators are shown in Figure 6.12. Again the voltages \tilde{E}_{q1}' , \tilde{E}_{q2}' , and \tilde{E}_{q3}' are assumed proportional to

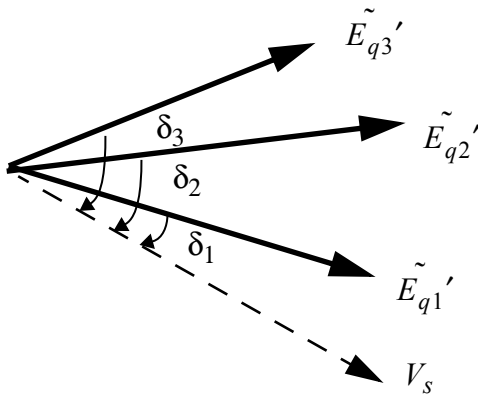


Figure 6.12 Phasor diagram for the internal voltages of three synchronous machines.

field flux linkages and transient saliency is neglected. The acceleration of any machine is expressed relative to a synchronously rotating reference axis. The acceleration equation is again, for any of the three machines,

$$\frac{d\omega_{rk}}{dt} = \frac{180f_b}{H_k} T_{Ak} \quad k = 1, 2, 3 \quad (6.67)$$

Using the definition of a derivative,

$$\frac{d\omega_{rk}}{dt} = \frac{\Delta\omega_{rk}}{\Delta t} \quad (6.68)$$

where $\Delta\omega_{rk}$ is a small change in ω_{rk} during the period Δt . By making Δt sufficiently small, the derivative is approximated by $\Delta\omega_{rk}/\Delta t$. Assuming specific values of time for the evaluation of this function, one may write

$$\Delta\omega_{rk}\Big|_{t_1 - \frac{\Delta t}{2}}^{t_1 + \frac{\Delta t}{2}} = \omega_{rk}\left(t_1 + \frac{\Delta t}{2}\right) - \omega_{rk}\left(t_1 - \frac{\Delta t}{2}\right) = \frac{180f_b\Delta t}{H_k} T_{Ak}(t_1) \quad (6.69)$$

where $T_{Ak}(t_1)$ is the per unit value of the accelerating torque of machine k at $t = t_1$. Therefore,

$$\delta_{rk}\left(t_1 + \frac{\Delta t}{2}\right) = \omega_{rk}\left(t_1 - \frac{\Delta t}{2}\right) + \frac{180f_b}{H_k} T_{Ak}(t_1)(\Delta t) \quad (6.70)$$

However,

$$\omega_{rk} = -\frac{\Delta\delta_k}{\Delta t} \quad (6.71)$$

and

$$\delta_k(t_1 + \Delta t) - \delta_k(t_1) = -\omega_{rk}\left(t_1 + \frac{\Delta t}{2}\right)\Delta t \quad (6.72)$$

Substituting for $\omega_{rk}(t_1 + \Delta t/2)$ from above,

$$\delta_k(t_1 + \Delta t) = \delta_k(t_1) - \frac{180f_b T_{Ak}(t_1)}{H_k} \cdot (\Delta t)^2 \quad (6.73)$$

At the very first interval ($t_1 = 0$) the equation for the speed change must be modified to include only one-half a time interval, so that

$$\Delta\omega_{rk}\Big|_{-\frac{\Delta t}{2}}^0 = 0 \quad (6.74)$$

$$\Delta\omega_{rk}\Big|_0^{\frac{\Delta t}{2}} = \frac{180f_b}{H_k} T_{Ak}\left(\frac{\Delta t}{4}\right) \frac{\Delta t}{2} \quad (6.75)$$

$$\delta_{rk}\left(\frac{\Delta t}{2}\right) = \frac{180f_b}{H_k} \cdot T_{Ak}\left(\frac{\Delta t}{4}\right) \frac{\Delta t}{2} + \omega_k(0) \quad (6.76)$$

$$\delta_k\left(\frac{\Delta t}{2}\right) = \delta_k(0) - \frac{180f_b}{H_k} \cdot T_{Ak}\left(\frac{\Delta t}{4}\right) \frac{\Delta t^2}{2} \quad (6.77)$$

The value of Δt should be chosen such that, for the sake of maintaining a reasonable degree of accuracy, the change in angular displacements between any two machines should not exceed approximately 5 degrees during a time interval.

The procedure for making this type of study is:

1. Hold e_Q' of each machine constant in magnitude ($e_Q' = E_Q$) and angle to the value which existed before the disturbance.

2. Calculate the new electrical torques for each machine.
3. Use the step-by-step equations, and determine the new angle δ for each machine.
4. Hold e_Q' constant in magnitude, and change its angle to the new value δ' .
5. Calculate the new electrical torques for each machine.

This procedure is repeated until a decision can be reached as to whether the system is transiently stable. This decision is usually based upon an examination of a plot of all the angles δ of the machines versus time (or the rotor slip $d\delta/dt$ versus time). In the discussion of the two machine problem solved by the equal area criterion, it was found that if the magnitude of the angle between machines decreased at some time after the disturbance, the system was considered transiently stable. If the angle magnitude continuously increased (and exceeded 180 degrees), the system was considered transiently unstable. If the angle began to increase at an angular difference between machines of 120 to 140 degrees, the system was shown to be near the stability limit. This knowledge can be applied directly to the analysis of the angle δ versus time plot. This curve is known as a *swing curve*.

As applied to systems containing several machines, the following criterion is used to determine transient stability: in order to be stable, the angular difference between all machines (including the machine with the slowest variations) must decrease after the final switching operation simulated. While the angle between the machine's rotor and a reference axis may be plotted, it is the relative angle between machines which is important. An example of a stable system and an unstable system is shown below in [Figure 6.13](#).

It should be emphasized that the criterion used in both the two machine analysis and the multi-machine system is based upon the examination of the *first swing* of the machine angles. In both cases, it is assumed that, if the machines satisfy the criterion on the first swing, then the system is transiently stable. The analysis, based upon this principle, is called *first swing transient stability analysis*. More rigorous and complete stability studies conducted upon computers indicate that the analysis of the first swing condition is sufficient except for a few cases. A swing curve for such a situation is shown in [Figure 6.14](#) and [Figure 6.15](#).

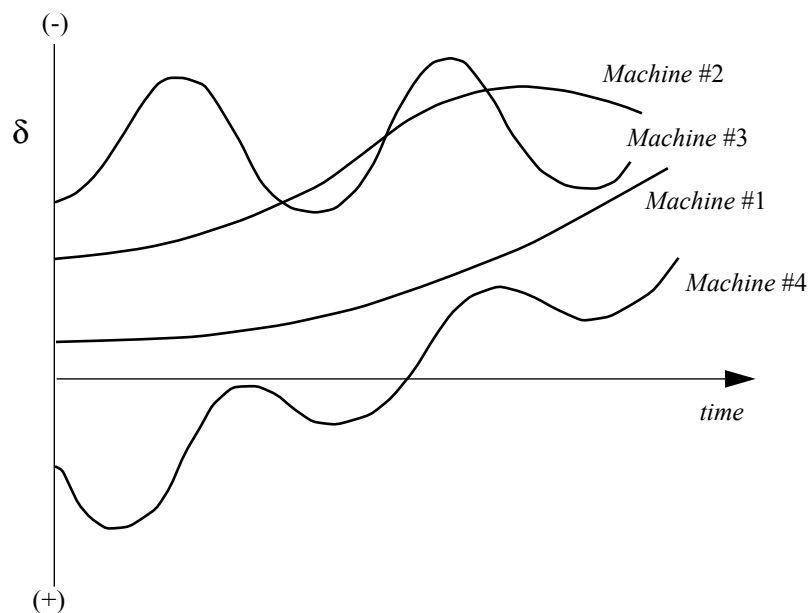


Figure 6.13 Torque angle versus time curves for a stable four machine system.

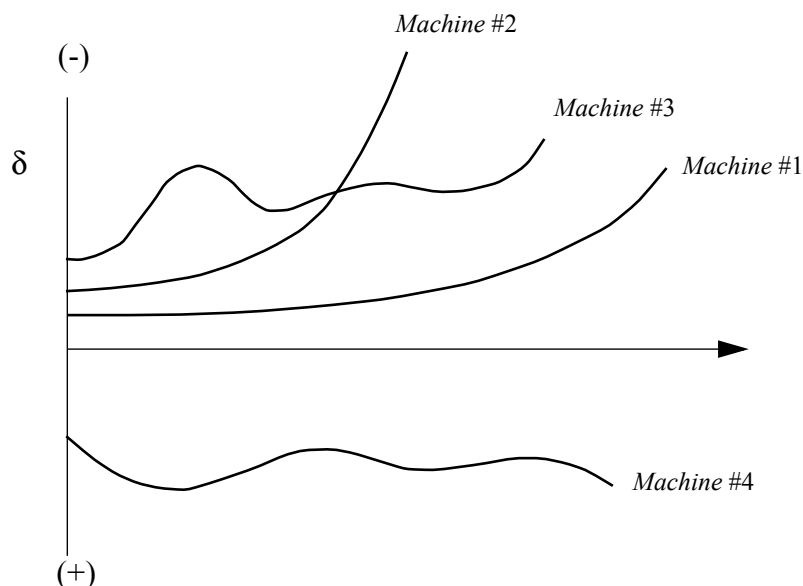


Figure 6.14 Torque angle versus time curves for an unstable four machine system.

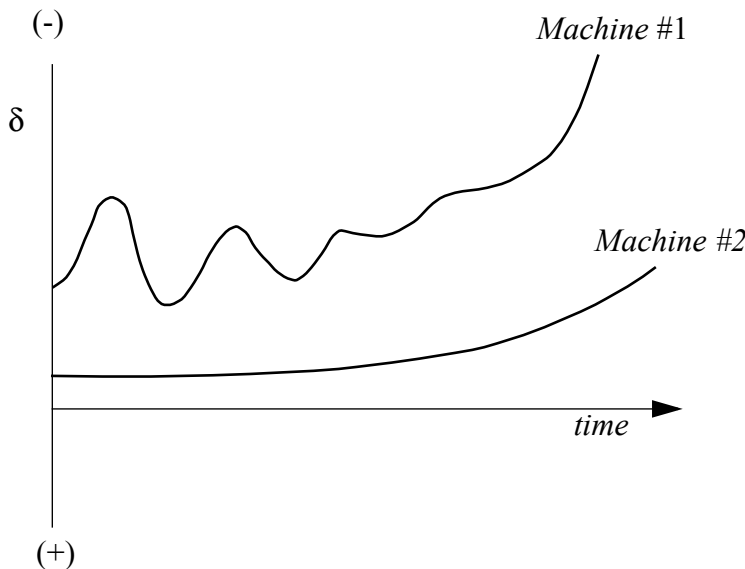


Figure 6.15 Swing curve of a generator which is initially stable but then ultimately becomes unstable after several swings.

6.9 Types of Faults and Effect on Stability

The most severe fault from the viewpoint of transient stability is a solid three-phase fault. This fault is the most severe since it reduces the voltage on all phases at the point of the fault to zero and eliminates any transfer of power past this point. In terms of decreasing severity on most power systems, are the following fault conditions.

1. Three-Phase Fault
2. Double-Line-to-Ground Fault (Machine Neutral Grounded)
3. Line-to-Line Fault
4. Line-to-Ground Fault (Machine Neutral Grounded).

A plot showing the critical clearing time for these four types of faults for a typical machine is shown in [Figure 6.16](#).

While the solid three-phase fault is the most severe, it is also the least likely to occur. Therefore, there is always the question of which fault to use to analyze transient stability. To partly help answer this question, the transient stabil-

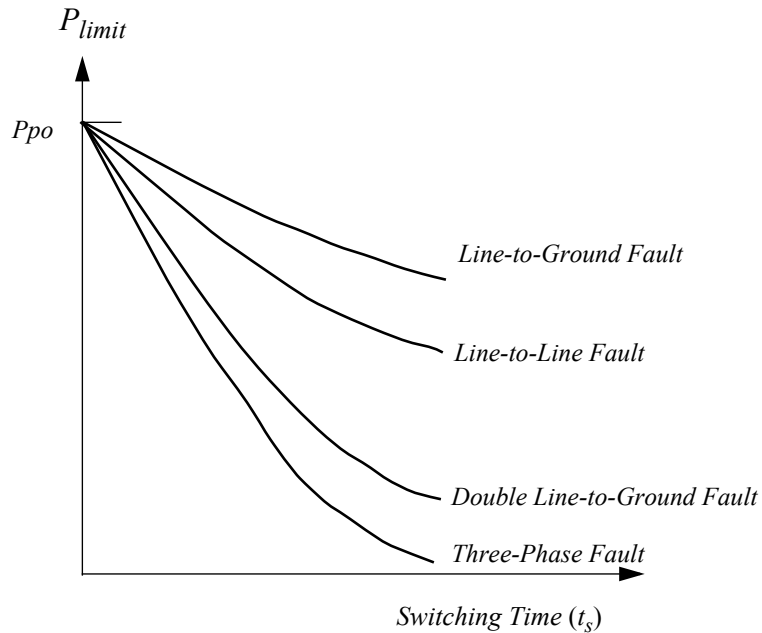


Figure 6.16 Comparison of the power limit for different types of faults as a function of the switching time t_s , P_{po} denotes the power at pull out.

ity power limits versus switching time for a two machine system is shown. As the switching time gets smaller, the difference between the severity of the faults also gets smaller and in the limit the condition that produces instability is the switching out of the line. Based on this reasoning, and also to protect the system against instability for *all* types of faults, most companies in the United States seem to use the three-phase fault for transient stability analysis. This is not true for all companies in the United States and is definitely not the case for Canada or Europe. The choice of the fault is principally a question of operating philosophy and is intimately associated with the economics of making additional expenditures for the purpose of making a system stable for a type of fault which occurs only rarely. Whatever the philosophy used, it is a question to be resolved by individual utilities.

6.10 Step-by-Step Solution Methods Including Saturation

Because of the complexity of the magnetic structure of a turbogenerator, the multiple circuits, and the varying degrees of saturation which may be encountered in different portions of the machine, the problem of accurately including the effects of saturation in machine analysis is a formidable one. Various methods of including the effects of saturation have been devised. Generally, each of these methods is intended for a specific type of problem. The methods which will be discussed here are fairly straightforward and can be readily used in conjunction with the “phasor” equations that have been developed.

Because transient stability deals with situations in which the machine is disturbed rather than at rest (i.e., in steady-state), the saturation of concern deals with the transient reactance and, to a lesser extent, the subtransient reactance rather than the steady-state synchronous reactances. However, reactances which limit short-circuit currents are definitely influenced by saturation as well. In fact, in tests taken to determine these reactances, saturation is an important variable. Because of the complex nature of the saturation effect, these reactances are usually calculated and then must be verified by tests. The correlation between calculation and test is often disturbingly poor.

The envelope of the fundamental frequency component of short-circuit current due to a three-phase fault applied at the terminals of an initially unloaded machine is shown in [Figure 6.17](#) and was described in Chapter 5.

As discussed in the previous section on faults, if the stator resistance is small, the subtransient value of current I_D'' is determined by the initial voltage and the subtransient reactance x_D'' . The transient current I_D' is determined by the initial voltage and by the transient reactance x_D' . If the initial voltage is changed to a new value, and the fault again applied, the apparent values of x_D' and x_D'' will change. If these reactances are plotted as a function of the transient current I_D' , a curve similar to that shown below will be determined ([Figure 6.18](#)).

It can be seen from this figure that the values of x_D' and x_D'' vary continuously with the values of the fault current. Therefore, the designation of “saturated” and “unsaturated” has no real meaning in terms of specifying the reactances. The degree of saturation must also be specified. Consequently, two specific values of reactance are commonly specified for industrial and utility

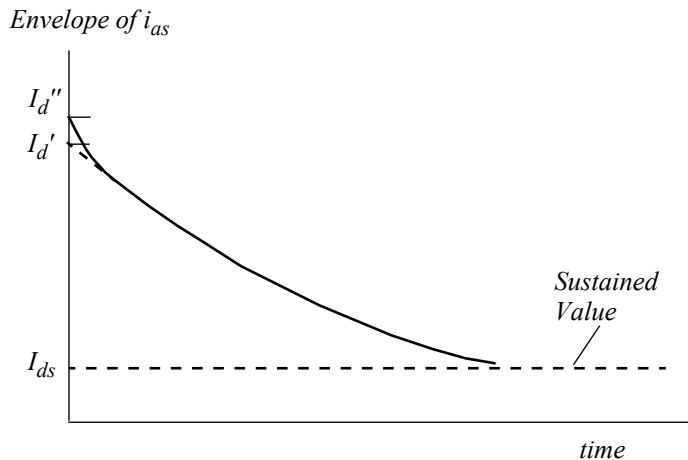


Figure 6.17 Envelope of fundamental component of short-circuit current resulting from a three-phase fault.

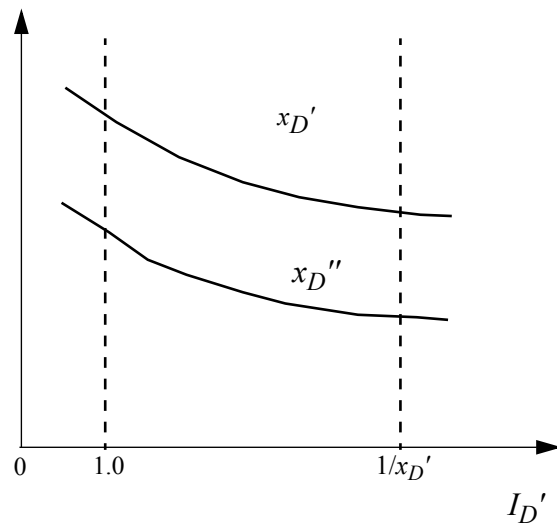


Figure 6.18 Variation of x_D' and x_D'' with the transient component of current I_D' .

machines: the rated current reactances x_{D_i}' , x_{D_i}'' , and the rated voltage reactances x_{D_v}' and x_{D_v}'' . When the initial terminal voltage of the machine is adjusted then the transient current I_D'' is equal to the rated current of the

machine upon application of the fault. The reactances so determined are designated the *rated current* values. When the initial terminal voltage is equal to the rated terminal voltage of the machine, the reactances determined are called the *rated voltage* values. In addition, the quadrature axis subtransient reactance x_Q'' is also defined with the same two degrees of saturation so that there is calculated a rated current value of quadrature axis reactance x_Q'' . If both rated current and rated voltage reactances are available, then for short-circuit studies, the most appropriate reactances would approach the “rated voltage” values. For voltage rise and voltage dip problems, the most appropriate reactances generally would be the rated current reactances.

The variation of these reactances from their “rated current” value to their “rated voltage” value is, in general, not very great for the salient-pole type of machine. Consequently, the inclusion of the effect of this type of saturation for salient-pole machines is of secondary importance. The purpose of pointing out the existence of these definitions of reactance is to emphasize that these quantities are, in fact, saturated reactances and the *usual assumption* is that the degree of saturation does not change during this initial period, that the variation of the degree of saturation in these reactances is of only secondary importance. These are not necessarily good assumptions.

6.11 Machine Model Including Saturation

In order to develop a technique for representing saturation, the first step is to obtain the Potier reactance x_P . Recall that the Potier reactance is essentially equal to the stator leakage reactance. Determination of the Potier reactance is obtained from short-circuit current conditions corresponding to an equivalent circuit, as shown in [Figure 6.19](#). The Potier voltage V_p is identified in this diagram. The per unit field excitation current E_I is equal to

$$\tilde{E}_I = \tilde{V}_S + jx_{DS}\tilde{I}_S \quad (6.78)$$

Since the vectors are co-linear, in terms of magnitudes

$$E_I = V_S + x_{DS}I_S \quad (6.79)$$

The terminal voltage in per unit is also equal to the per unit field current necessary to produce the same value of terminal voltage at no load measured on the air gap line. Or, in per unit from the open circuit saturation curve

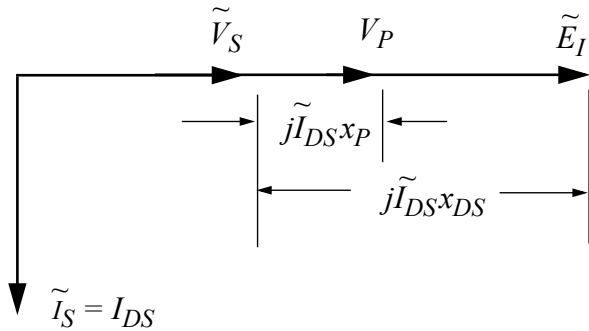


Figure 6.19 Phasor diagram showing terminal voltage, Potier voltage (air gap voltage), and excitation voltage for a short-circuit condition.

$$\tilde{V}_S = E_I \quad (6.80)$$

The per unit voltage drop $I_{DS}x_{DS}$ is equal to the per unit excitation required to overcome this voltage drop with zero terminal voltage, or

$$I_Ax_{DS} = E_{Iz} \quad (6.81)$$

The per unit field current can be written

$$E_I = E_{Iz} + E_{It} \quad (6.82)$$

Hence, the *actual* per unit excitation current E'_I necessary to produce E_A under this condition, *including saturation*, is equal to

$$E'_I = E_{Iz} + E_{It} + E_{Isat} \quad (6.83)$$

or, in terms of excitation current E_I ,

$$E'_I = E_I + E_{Isat} \quad (6.84)$$

The term E_{Isat} is the difference in field current due to the effect of saturation and is equal to the difference between the air gap line excitation and the actual no load excitation at a value of per unit terminal voltage equal in magnitude to the voltage behind Potier reactance V_P , which is equivalently the voltage at the air gap of the machine. The quantity E_{Isat} is identified in Figure 6.20. To extend this approach directly to power factors other than zero, it is necessary to assume that the MMF necessary to overcome saturation is proportional to E_P and that this MMF exists only in the direct axis. Test results indicate that

for the overexcited operating range of a synchronous machine this approach is entirely reasonable.

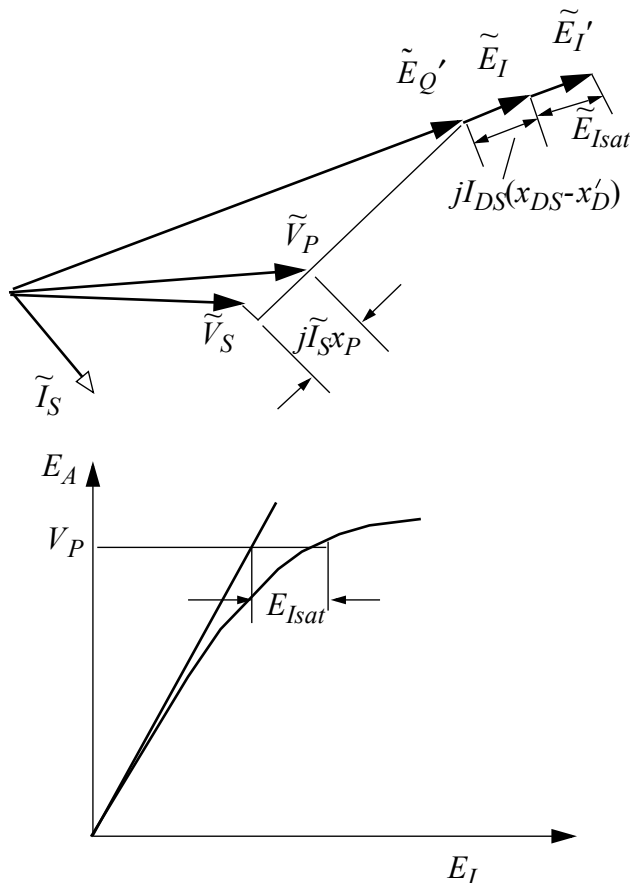


Figure 6.20 Phasor diagram and saturation curve identifying the voltage E_{Isat} .

In terms of the synchronous machine phasor diagram and the no load saturation curve, the procedure for construction is as follows:

1. The quantities in the phasor diagram are determined as discussed previously. The voltage V_P , which is the voltage behind Potier reactance x_P , is also determined.
2. From the no load saturation curve for a terminal voltage equal to V_P , the difference between the air gap excitation and the excitation including saturation effects is measured. This difference is equal to E_{Isat} .

3. The quantity E_{Isat} is added directly to E_I in order to determine the per unit field current including saturation effects E_I' .

Since both quadrature and direct axis quantities are used to calculate E_P , the existence of saturation in the quadrature axis, as well as in the direct axis, is recognized. The saturation principally associated with the quadrature axis arises from saturation of the stator core and teeth. The direct axis saturation is principally associated with the saturation of the stator core, stator teeth, and the rotor pole piece. The method discussed here basically assumes that the saturation characteristics in both axes are the same, with the correction for the effect of the saturation being applied in the direct axis.

There are more elaborate techniques for representing the effects of saturation. Most utilize load saturation curves in conjunction with calculations involving leakage reactance ($x_{LS} \approx x_P$). Even with these methods, if the no load saturation curve is used, the use of Potier reactance x_P is suggested. The use of Potier reactance, which is generally greater than the calculated leakage reactance, provides an empirical correction of the saturation MMF obtained from the open circuit saturation curve to allow for load saturation. Unfortunately, the test data necessary to calculate Potier reactance is not always available. In this situation, one approach would be to merely substitute x_D' for x_P in the method just discussed. The use of x_D' instead of x_{LS} (leakage reactance) is preferred when using the no load saturation curve. The approach appears to work well for turbine generators (solid pole round-rotor machines).

Another method for including saturation is very similar to the Potier reactance method, but does not require any “special” reactances other than the usual short-circuit reactances (x_D' specifically). The voltage proportional to the field flux linkages is E_Q' , since, by definition

$$E_Q' = \frac{x_{MD}}{x_{FR}} \Psi_{FR} \quad (6.85)$$

Since the field flux is typically much larger than the stator flux, it can also be used to determine the degree of saturation in the machine. If all of the saturation is assumed to take place in the path of the flux linking the field winding, then the degree of saturation is proportional to the magnitude of the flux. To state this differently, if the saturation effects are assumed to take place principally in the other paths taken by the flux linking the field circuit, then the

degree of saturation can be assumed to be proportional to the magnitude of the field flux linkages (proportional to E_Q').

The method used is as follows:

1. At any point in time, or under any steady-state condition of operation, calculate E_Q' .
2. Using the no load saturation curve as shown below, calculate the change in field current due to saturation E_{Isat} based upon the magnitude of E_Q' , as shown in Figure 6.21. The quantity E_{Isat} is added directly to E_I in order to determine the per unit field current including saturation effects, E_I' .

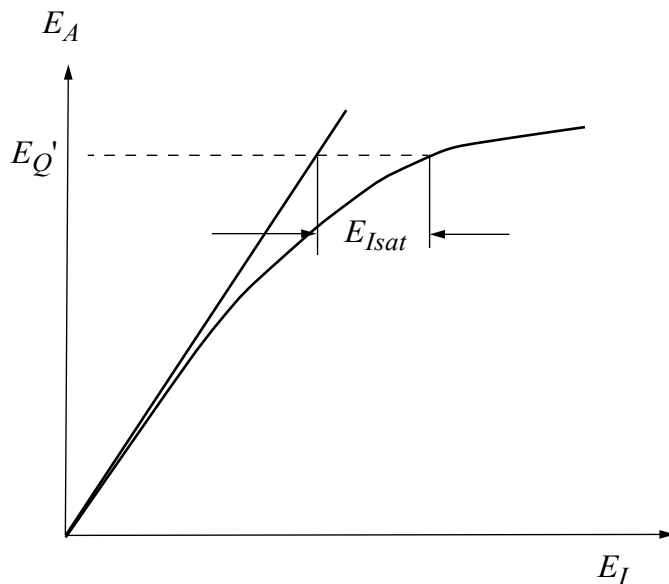


Figure 6.21 Saturation curve using E_Q' to find E_{Isat} .

The results of calculations using this method agree quite reasonably with test results for salient-pole generators. The choice of methods (Potier reactance or field flux linkages) is mostly a question of the type of machine and the data available.

In spite of the existence of the more elaborate techniques for representing the effects of saturation, in view of the problems associated with even specifying the no load saturating characteristics at high temperatures, the additional complexity introduced by more elaborate methods, and the type of saturation characteristics required for their use make their value questionable. Further-

more, as mentioned previously, the results obtained using the methods discussed here agree reasonably well with test results.

6.12 Summary Step-by-Step Method for Calculating Synchronous Machine Transients

Neglecting the effects of the damper windings and the DC offset in the stator currents, the equations to be solved are:

$$V_{DS} = -\Psi_{QS} + r_S I_{DS} \quad (6.86)$$

$$V_{QS} = \Psi_{DS} + r_S I_{QS} \quad (6.87)$$

$$pe_Q' = \frac{1}{T_{d0}}(E_X - E_I) \quad (6.88)$$

$$\Psi_{DS} = E_I + x_{DS} I_{DS} \quad (6.89)$$

$$\Psi_{QS} = x_{QS} I_{QS} \quad (6.90)$$

$$\varepsilon_Q' = E_I + (x_{DS} - x_D') I_{DS} \quad (6.91)$$

$$I_E = [E_Q' + (x_D' - x_{QS}) I_{DS}] I_{QS} \quad (6.92)$$

In situations where e_Q' is constant, the derivative pe_Q' can be set to zero and the equations solved simply as a set of algebraic equations. If the effect of the change in e_Q' is to be taken into account, one simply need integrate numerically the differential equation involving e_Q' .

A solution of a multi-machine problem with varying e_Q' would proceed as follows.

1. Using phasor equations (or phasor diagrams) determine the initial conditions of the system prior to the disturbance. The values of $e_Q'(0)$ are determined.
2. Applying the fault, maintaining $e_Q'(0)$ constant, use the phasor equations (or diagrams) to determine the initial value of the system and machine voltages and currents. These are the values at $t = 0^+$.

3. Evaluate $e_Q'(\Delta t)$ using $E_I(0)$ and $E_X(0)$ for each machine calculated in step (2). The value of E_X for any point in time would be based either upon an arbitrary curve of E_X versus time, or upon some function relating E_X to the terminal voltage. The value $E_I(t = 0)$ is calculated using the above set of equations.
4. Using the new values of e_Q' at $t = \Delta t$, evaluate the system and machine voltages and currents, including $E_I(\Delta t)$ for each machine.
5. Calculate $e_Q'(2\Delta t)$ for the pe_Q' differential equation, Eq. (6.84).

The entire process is then repeated, step-by-step until the solution has been carried out far enough in time.

In addition to solving for these “electrical” equations, the “mechanical” equations must also be solved, requiring integration of the differential equations

$$p\delta = -\omega_r \quad (6.93)$$

$$p\omega_r = \frac{180f_b\Delta t}{H}(T_E + T_M) \quad (6.94)$$

as described previously.

6.13 Conclusion

Transient stability involves those issues encountered by the slow speed transients produced by electromechanical motion as described by the swing equation. Because the torque produced by the machine varies sinusoidally with angular displacement, the describing differential equations remain non-linear even when the assumptions of constant flux linkages are invoked to help simplify the problem. Since the swing equation can be reduced to a second order differential equation, analysis of this class of problems is well suited to the graphical approach, as illustrated in this chapter.

6.14 References

- [1] E.W. Kimbark, “Power System Stability, vol. 1 Elements of Stability Calculations,” John Wiley & Sons, Inc., New York, 1948.
-

Chapter 7

Excitation Systems and Dynamic Stability

7.1 Introduction

In the previous chapter stability was investigated based on the concept of constant *voltage behind transient reactance* E_q' corresponding to an assumption of constant field flux linkages during the transient. Such machines are said to have a *non-continuously acting regulator* since the control of the field is then a manual procedure introduced by manual adjustment of a rheostat in the field circuit. In most cases in modern equipment, however, the machine is equipped with a terminal voltage regulator (in the case of a generator) or a power factor regulator (in the case of a motor). In effect, the voltage behind transient reactance is written as e_q' , which now varies in accordance with an error generated by sensing and feeding back either terminal voltage amplitude or phase angle. Such a machine is said to be equipped with a *continuously acting regulator*.

With the dominant use of continuously acting voltage regulators, the methods of analysis and concepts associated with transient stability no longer apply to modern power systems. Earlier excitation systems utilized rotating DC machines or so-called amplidyne (rotating DC amplifiers) to supply the field circuit. The time constant of these early regulators was sufficiently slow that the transient stability concept could be retained with relatively simple modifications. However, the introduction of modern solid-state rectifiers for control of field current has greatly increased the response of such regulating systems necessitating treating the system as a closed-loop control system. Because the effects of continuously acting voltage regulators are so significant on steady-state stability limits, because behavior of the system is so different, a new term was applied to this condition, namely, *dynamic stability*. Originally, dynamic stability was concerned only with the excitation system regulating loop when the power system was subjected to disturbances. However, the term has come to apply to any case where small signal analysis is applicable.

7.2 Generator Response to System Disturbances

In order to distinguish between the cases of continuously and non-continuously acting voltage regulators, it is useful to consider a typical case where a single large generator is connected by to large power system through a double circuit transmission line. If the system is sufficiently large, the problem can be reduced to a situation where the machine is connected to an infinite bus through a series reactance. If a severe disturbance occurs, a transient stability analysis is concerned with the first swing behavior. If the generator is stable on the first swing, then it is still necessary to determine the ultimate stability of the machine after numerous swings. When the machine is equipped with a non-continuously acting voltage regulator (manual control), it was found that the machine would typically lose synchronism on a subsequent swing only if the machine could not develop sufficient synchronizing power in the new steady-state operating condition. Typical responses of a stable and unstable machine during large swing transient stability are shown in Figure 7.1. Note that in both

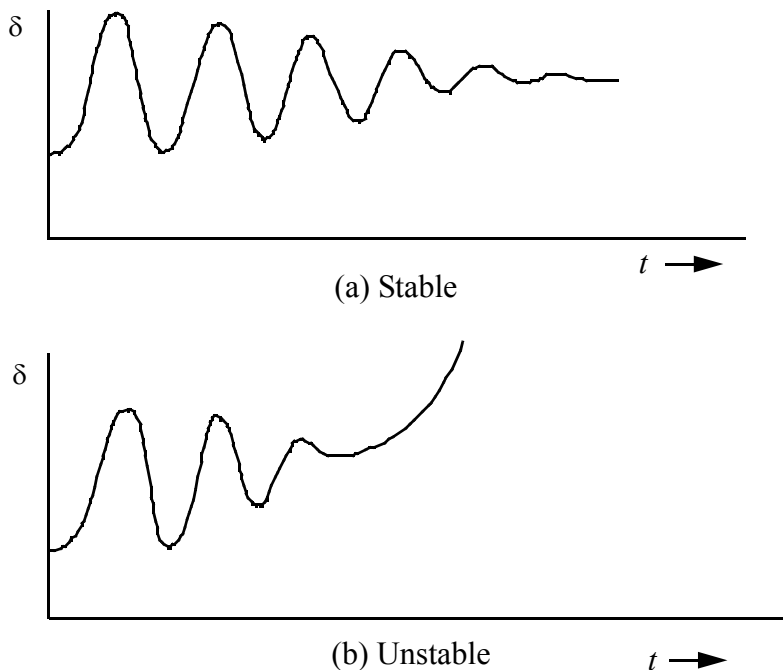


Figure 7.1 Illustration of (a) long term transient stability and (b) loss of stability after several swings due to loss of synchronizing torque.

cases the machine has decreasing oscillations (initially) but that the generator ultimately pulls out of step in the unstable case. In each case the machine possesses so-called *positive damping*, but this does not guarantee ultimate stability. The behavior of the machine over the long term falls under the domain of what is called *steady-state stability*.

Consider now the case shown in Figure 7.2 in which a very small disturbance is imposed on the machine. In the stable case the machine recovers from

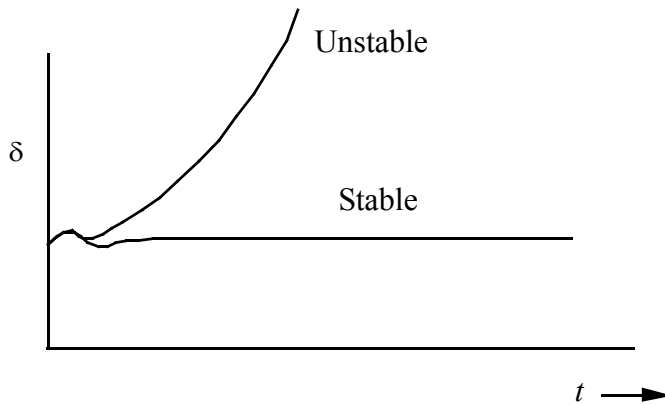


Figure 7.2 Monotonic loss of synchronism due to loss of synchronizing power.

the disturbance and returns to the steady-state condition existing before the disturbance, while for the unstable case the machine torque angle increases monotonically. Monotonic behavior during pull out is a symptom of not being able to develop sufficient positive synchronizing power in the steady-state.

If the generator has a continuously acting voltage regulator, the machine could possibly behave as shown in Figure 7.3. Note that the oscillations monotonically increase in this case until the machine *loses step*, i.e., pulls out of synchronism. The damping torque is now said to be *negative*. In some systems with weak interties, operating conditions sometimes arise where there is little net positive damping torque, which exists during a disturbance. In such cases, oscillations could persist over a long period of time. This problem is particularly important in remoter regions of the country such as in the mountain time zone (Idaho, Colorado, Montana, etc.). While such a system is not technically unstable it could well be just as intolerable. The amount of positive damping

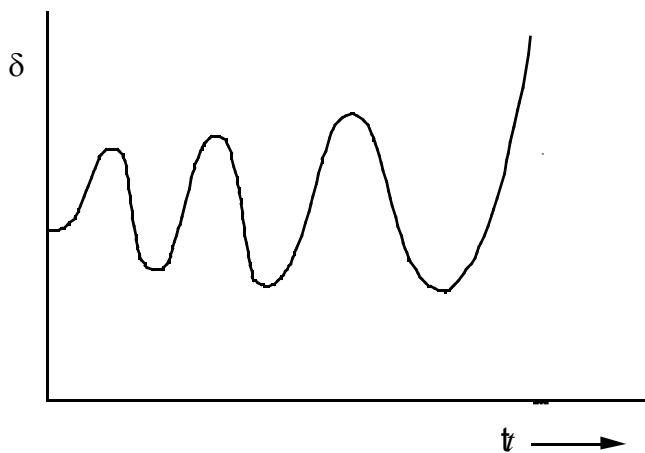


Figure 7.3 Unstable behavior with continuously acting voltage regulator.

therefore has an important influence on behavior of the system even if the overall system is not unstable.

7.3 Sources of System Damping

Because of the importance of system damping in dynamic stability, it is important to identify and account for significant sources of system damping. Some of the sources provide continuous damping, while some elements contribute either positive or negative damping depending upon the values of the parameters in the subsystem element. Generally, however, the important sources of damping a synchronous generator are

- 1) the synchronous machine itself,
- 2) the prime-mover, i.e., the steam or hydraulic turbine,
- 3) the excitation system of the machine,
- 4) the system load/frequency and load/voltage droop characteristics.

Damping occurs in the form of either mechanical torque (supplied by the prime mover) or electrical torque (supplied by the electrical components). Each of these sources of damping will now be discussed.

7.4 Excitation System Hardware Implementations

7.4.1 Basic Excitation System

In general, the three terminal voltages are transformed to signal level with a transformer and then rectified by means of a three-phase diode bridge as shown in Figure 7.4. The average value of the DC output voltage of the bridge is related to the input voltage by

$$\begin{aligned} V_{dc(ave)} &= \left(\frac{3}{\pi}\right) \int_{-\pi/6}^{\pi/6} \sqrt{3} \left(\frac{N_2}{N_1}\right) V_s \cos \theta d\theta \\ &= \frac{3\sqrt{3}N_2}{\pi N_1} V_s \end{aligned} \quad (7.1)$$

where N_2/N_1 is the turns ratio of the transformer. The quantities K_a and T_a are the regulator gain and time constant and K_g is the gain of the power amplifier. Recall that the output of the power amplifier V_{fr} without primes is the actual voltage applied to the physical field circuit.

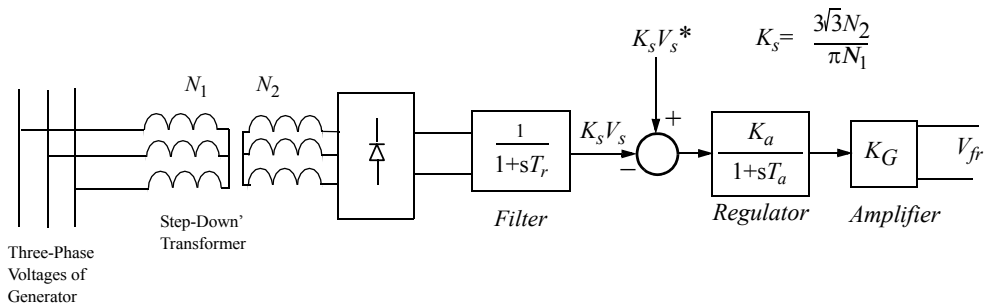


Figure 7.4 Basic synchronous machine excitation system.

7.4.2 Basic DC Exciter

Historically, synchronous machine excitation systems used a DC generator to power the field circuit and many of these systems are still in common use today. While somewhat out of date, the DC shunt field exciter forms the basis

for many of the models of excitation systems in common use today. IEEE has categorized modern excitation systems into four categories which are intended to cover most existing excitation systems. The first one describes the traditional DC machine used for the exciter. In order to understand the basic logic behind the block diagram of the so-called IEEE Type 1 Excitation System, consider first the equations defining the basic DC shunt field generator shown in Figure 7.5. The small machine traditionally used to produce the voltage v_{err} is the equivalent of a rotating amplifier and is called an *amplidyne*. A more modern approach would be to simply use a solid-state power amplifier, for example, a DC/DC converter.

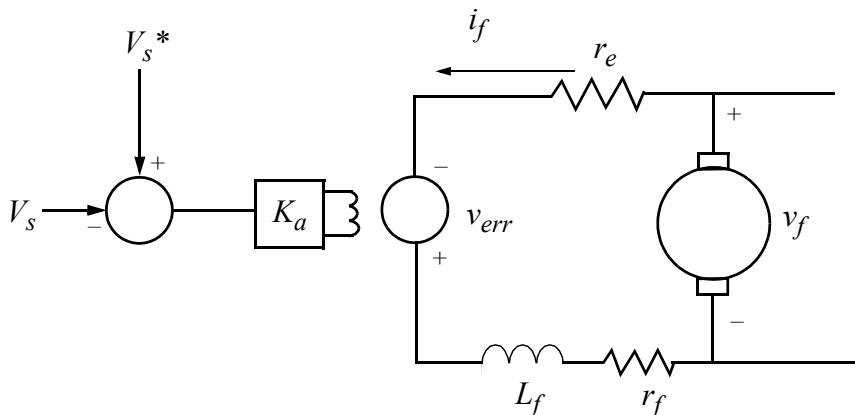


Figure 7.5 DC Shunt field exciter.

Neglecting saturation, the DC machine can be described by the equations

$$v_f + v_{err} = i_f(r_e + r_r) + L_f \frac{di_f}{dt} \quad (7.2)$$

and

$$v_f = \omega_{dcg} L_m i_f \quad (7.3)$$

These two equations suggest the block diagram shown in Figure 7.6. Note that both positive and negative feedback exists. If the field resistor r_e is adjusted such that

$$r_f + r_e = \omega_{dcg} L_m \quad (7.4)$$

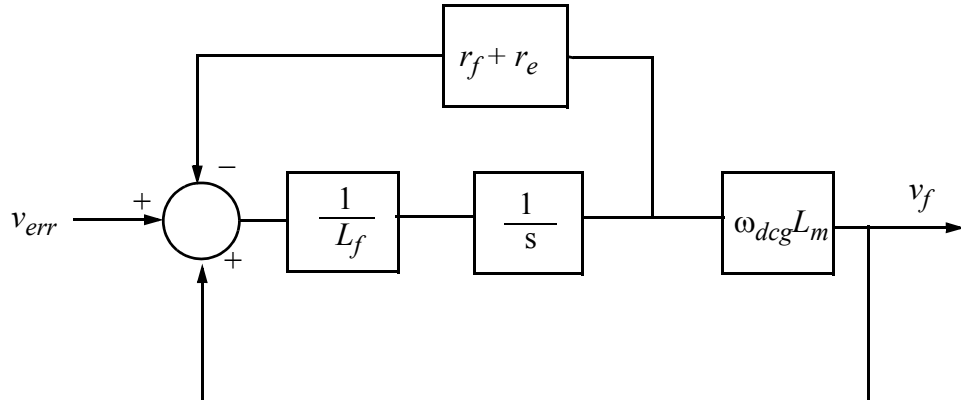
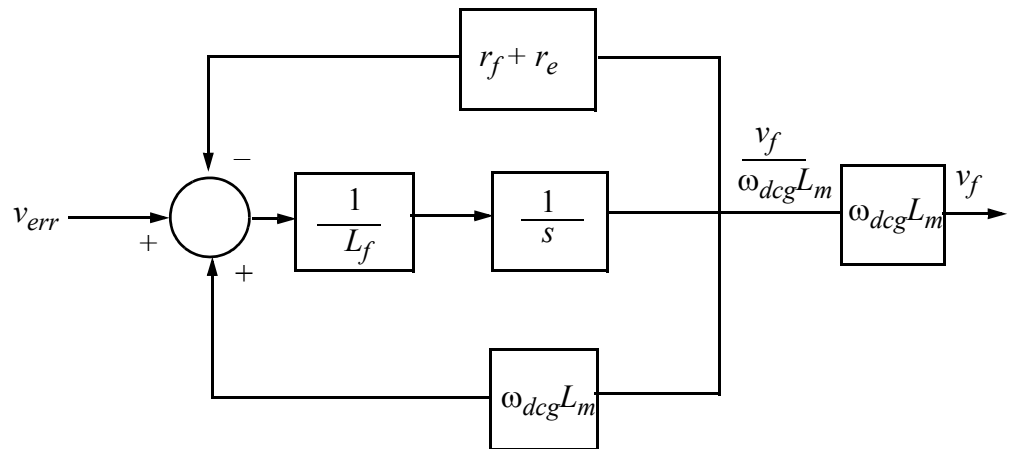
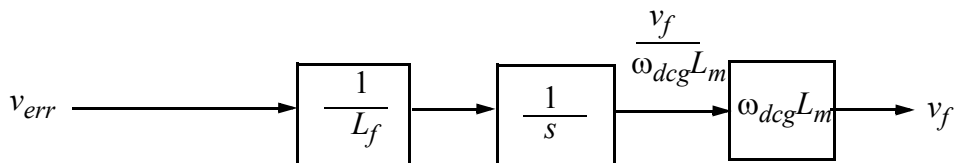


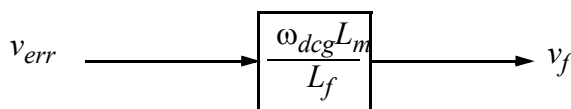
Figure 7.6 Block diagram of DC shunt field exciter.

then the block diagrams of Figure 7.7 are obtained. It can be seen that an electromechanical equivalent of an integrator has been formed. Hence, the output v_{fr} can exist even if there is no input (i.e., $v_{err} = 0$). Although an open-loop integrator can assume any output value, the DC shunt motor operating point is well defined due to the effects of saturation. More will be said concerning saturation later. If one combines this block with the excitation system of Figure 7.4 the closed-loop system of Figure 7.8 is obtained, wherein the effects of a change in torque angle $\Delta\delta$ have been neglected. The constants K_6 and K_7 in Figure 7.8 merely represent the scale factors needed to convert from actual units (as in Figure 7.6) to per unit (as in Figure 7.8). Note that if K_3 , representing the effect of the field resistance, were zero, the system would form an oscillator. That is, if the terminal voltage were suddenly commanded to change, the field circuit would oscillate forever. In practice, this does not happen of course, but the regulation is extremely poor and the system is unstable for nearly any gain K_A even with a relatively large field resistance. A sketch of the root locus of the system for changes in K_A is also shown in Figure 7.8.

This tendency to oscillate can be cured by introducing additional negative feedback into the regulating loop controlling the DC shunt motor. In Figure 7.9(a) additional negative feedback has been introduced via the block K_F . However, this leads to an inconsistency in the controller which is derived for small changes. In particular, assuming that the system is operating normally at the steady-state operating point, then $V_{err} = 0$. However, in the steady-state it must also be true that the sum of the inputs equal zero since the plant transfer

(a) Moving the Block $\omega_{dcg} L_m$ 

(b) After Cancelling Positive and Negative Feedback Terms



(c) Net Result

Figure 7.7 Cancellation of positive and negative feedback portions of DC shunt generator/amplidyne system.

function is a pure integrator. Hence, it becomes apparent that for steady-state to apply, $v_{err} + K_F v_f = 0$, which leads to the conclusion that $v_f = 0$, which is clearly impossible for any finite terminal voltage. Thus, it is necessary to make this feedback active only for *changes* in the field voltage. This is accomplished by introducing a differentiator in the block diagram, as in Figure 7.9(b).

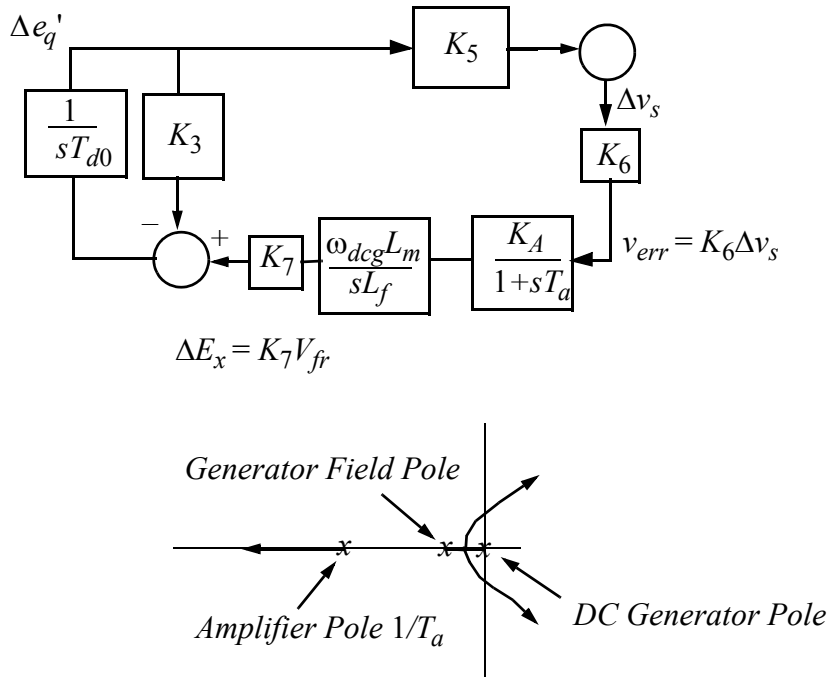


Figure 7.8 Closed-loop block diagram of excitation system and machine including the effects of a change in field flux linkage.

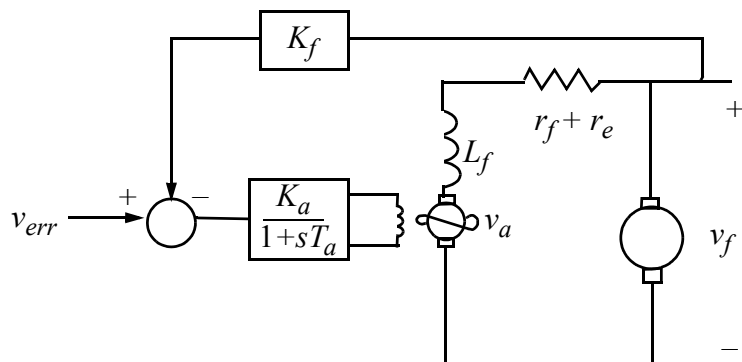
In general, the terms corresponding to negative (resistive) and positive (speed voltage) feedback in Figure 7.7 cannot entirely cancel or else net positive feedback is risked. The block diagram for the DC shunt motor can be reduced as shown in Figure 7.10.

7.4.3 Modeling of Saturation

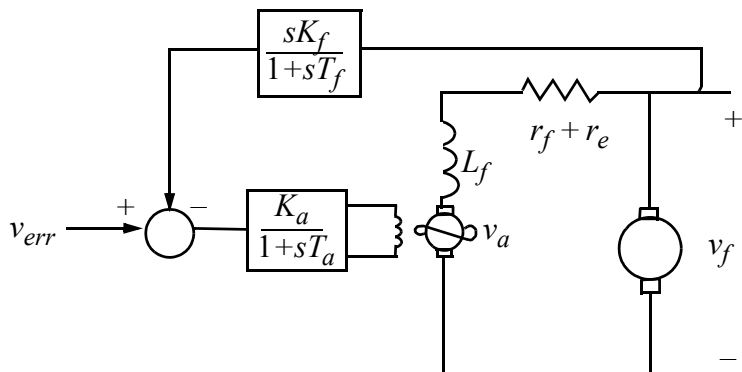
For large disturbances such as faults, the field voltage swings widely from its nominal value, and saturation of the shunt DC exciter can not be neglected. Figure 7.11(a) shows a typical saturation curve for the DC machine. In Figure 7.11(b) the abscissa of the curve has been multiplied such that the air gap line forms a 45° angle with respect to the abscissa. That is, when saturation is neglected,

$$v_f = \omega_{dcg} L_m i_{f(unsat)} \quad (7.5)$$

so that the abscissa and ordinate values are equal in Figure 7.11. The differential equation describing the shunt connection with the amplidyne is again



(a) Feedback Added to Exciter Loop



(b) Feedback Responding Only to the Change in Exciter Voltage

Figure 7.9 Stabilizing feedback strategies.

$$v_f + v_{err} = i_{f(sat)}(r_e + r_r) + L_f \frac{di_{f(sat)}}{dt} \quad (7.6)$$

In addition, because of saturation,

$$i_{f(sat)} = i_{f(unsat)} + \Delta i_f \quad (7.7)$$

where

$$i_{f(unsat)} = \frac{v_f}{\omega_{dcg} L_m} \quad (7.8)$$

Note also that if the air gap line forms a 45° angle, then

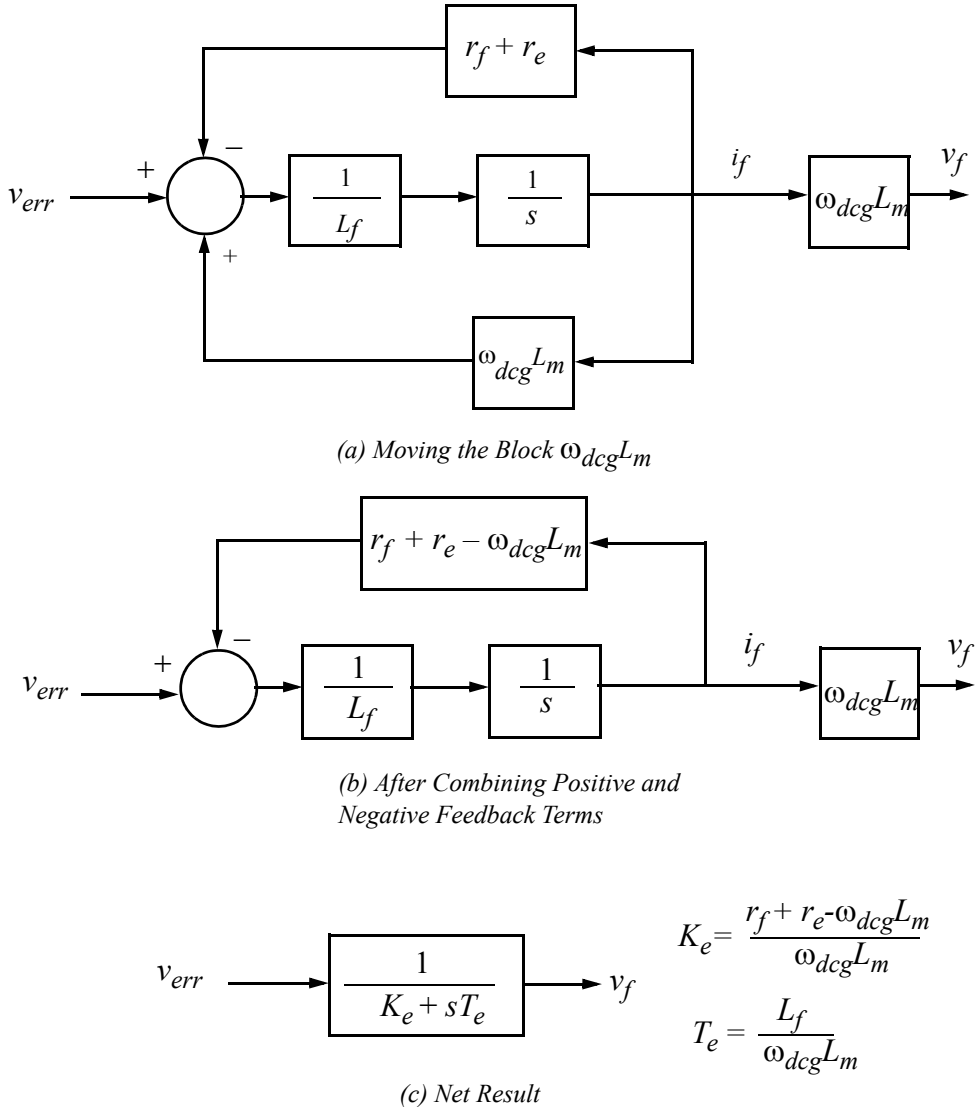


Figure 7.10 Manipulation of block diagram of shunt DC machine when positive and negative feedback terms do not cancel.

$$\Delta v_f = \omega_{dcg}L_m \Delta i_f \quad (7.9)$$

Finally, if the saturation effect of the field current is not changing rapidly (i.e., if deep saturation is avoided) then, approximately,

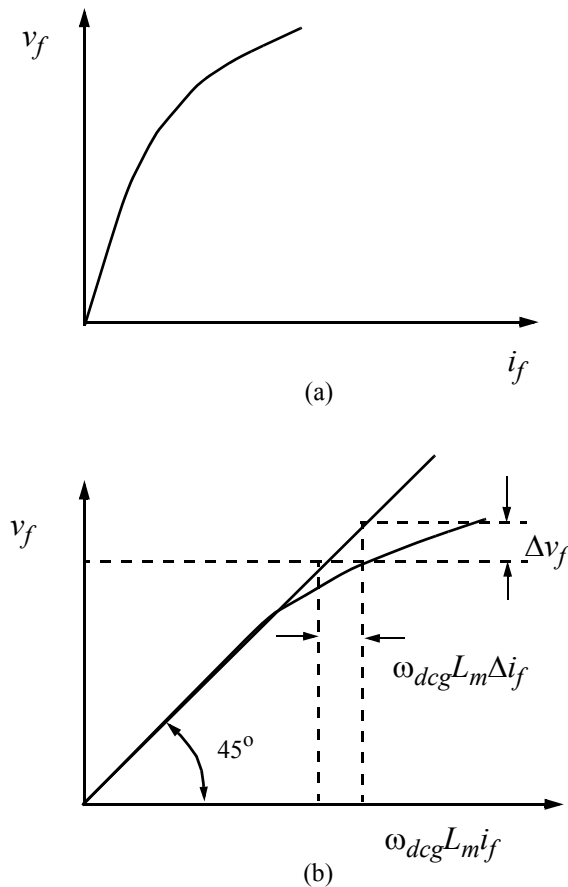


Figure 7.11 Normal and modified saturation curve of DC shunt connected machine.

$$\frac{di_{f(sat)}}{dt} \cong \frac{di_{f(unsat)}}{dt} \quad (7.10)$$

Substituting all of this into Eq. (7.6) it is possible to write

$$v_{err} + v_f = \frac{v_f}{\omega_{dcg} L_m} (r_f + r_e) + \Delta i_f (r_f + r_e) + \frac{L_f}{\omega_{dcg} L_m} \frac{dv_f}{dt} \quad (7.11)$$

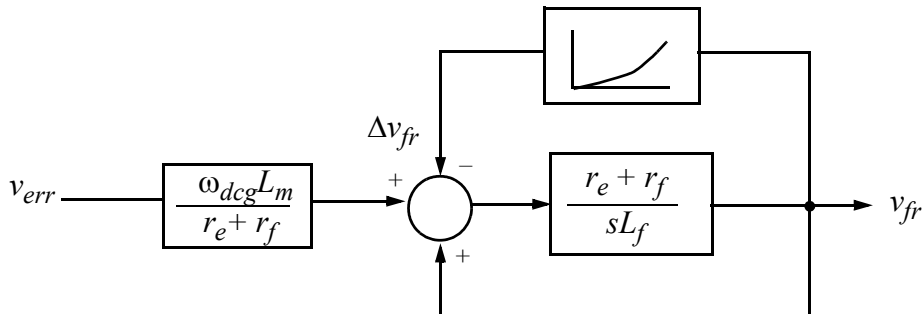
Solving for the derivative and integrating,

$$v_f = \frac{\omega_{dcg} L_m}{L_f} \int \left[v_{err} + v_f - \frac{r_f + r_e}{\omega_{dcg} L_m} v_f - \frac{(r_f + r_e)}{\omega_{dcg} L_m} \Delta v_f \right] dt \quad (7.12)$$

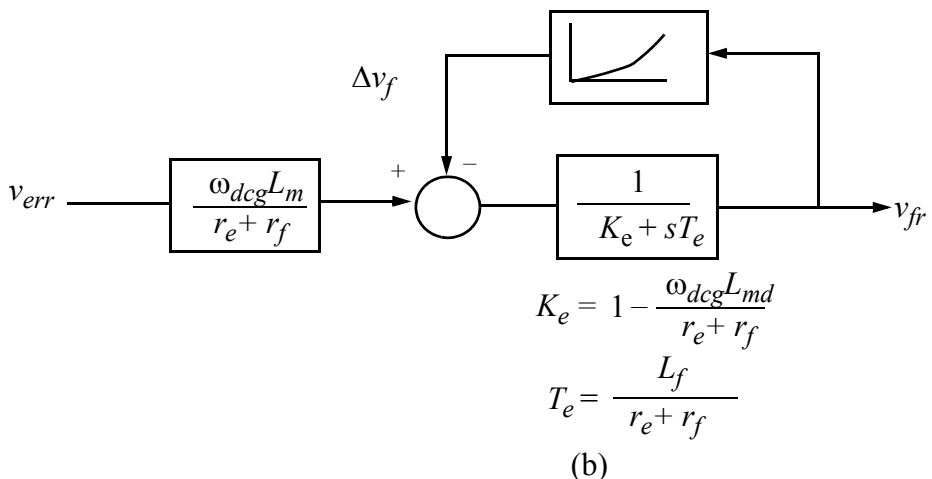
Combining terms and rearranging,

$$v_f = \frac{r_f + r_e}{L_f} \int \left[\frac{\omega_{dcg} L_m}{r_f + r_e} v_{err} - \frac{r_f + r_e - \omega_{dcg} L_m}{r_f + r_e} v_f - \Delta v_f \right] dt \quad (7.13)$$

Equation forms the block diagram shown in Figure 7.12(a). Upon combining blocks, the block diagram reduces to that shown in Figure 7.12(b). The functional relationship needed to form Δv_f is found by plotting the vertical distance



(a)



(b)

Figure 7.12 Block diagram of saturated shunt connected DC machine (a) in terms of parameters and (b) in reduced form.

from the voltage on the saturation curve to that on the air gap line as a function of the voltage on the saturation curve. See [Fig. 7.17](#).

7.4.4 AC Excitation Systems

AC excitation systems have basically replaced DC excitation systems in modern turbine generator installations. Systems of this type utilize AC machines as the main source of excitation power. Usually this machine is mounted on the same shaft as the turbine generator. The AC output is rectified to DC and then applied to the DC field winding via slip rings, as shown in Figure 7.13. The exciter is self excited with its own field power derived through a thyristor rectifier. As a variation, the diode bridge can also be mounted on the rotor and the AC power fed to the bridge via either slip rings or a rotating transformer. The configuration of Figure 7.13 is a somewhat simplified version of the General Electric ALTERREX excitation system [2].

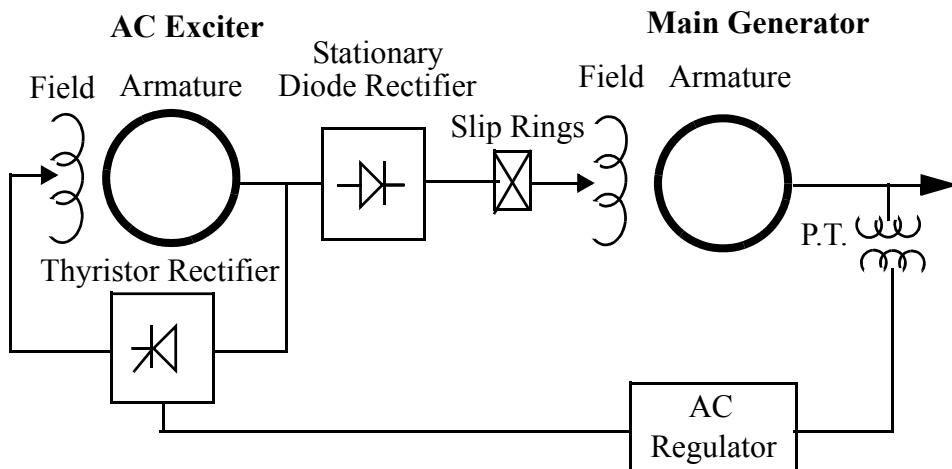


Figure 7.13 One line diagram of a field controlled alternator excitation system employing a diode bridge rectifier.

When controlled rectifiers (thyristors) are used in place of the diode bridge, the regulator directly controls the DC output voltage of the exciter as in [Figure 7.14](#). In this case the regulator directly controls the firing of the thyristors. The exciter alternator is again mounted on the main shaft and again uses a thyristor bridge to simply maintain rated AC voltage at its terminals. Since the thyristors directly control the exciter output, the arrangement is capable of a very fast response time. This diagram is representative of the General Electric ALTHY-REX excitation system [3]. Both types of system are commonly equipped with

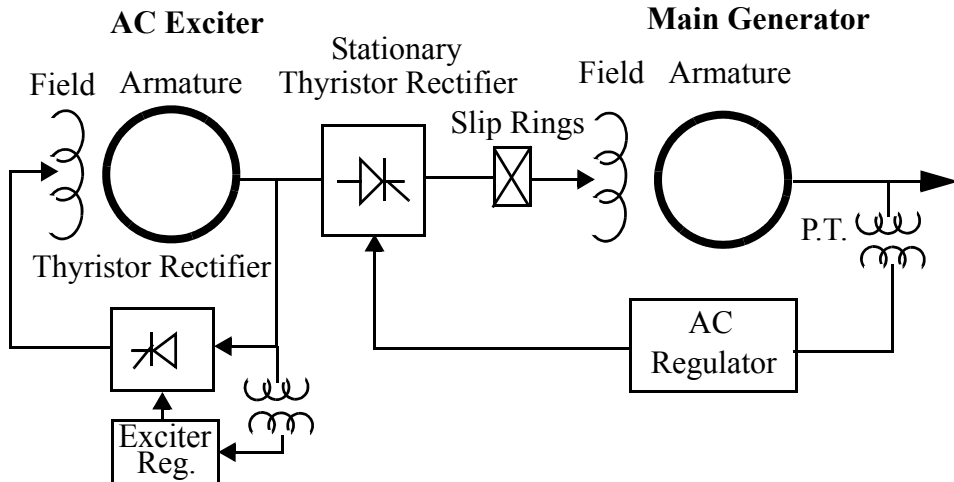


Figure 7.14 Controlled rectifier excitation system with alternator supply.

a manual override control system which functions when the AC regulator is faulty.

Another type of AC exciter is a rotating or “brushless” excitation system, as shown in [Figure 7.15](#). When the diode rectifiers are allowed to rotate the need for slip rings and brushes is eliminated. The armature of the AC exciter and the diode rectifier rotate with the main generator field winding. A small AC *pilot exciter* energizes the stationary field winding of the AC exciter. Fast response of such a system can be obtained since the stationary field winding of the exciter is controlled by a thyristor bridge. Manual control is again possible by an additional input to the regulator. One disadvantage of this approach is that direct measurement of the field voltage or field current is not allowed so that fast response can only be achieved by special design [4].

7.4.5 Static Excitation Systems

The term static excitation implies that all the active components of these systems are static or stationary. One such type of excitation system is commonly known as a transformer-fed static system and is shown in [Figure 7.16](#). In this system excitation power is supplied through a transformer either from the generator terminals or an auxiliary bus. Connection to an auxiliary bus which realizes its power from a source separate from the main bus ensures that the

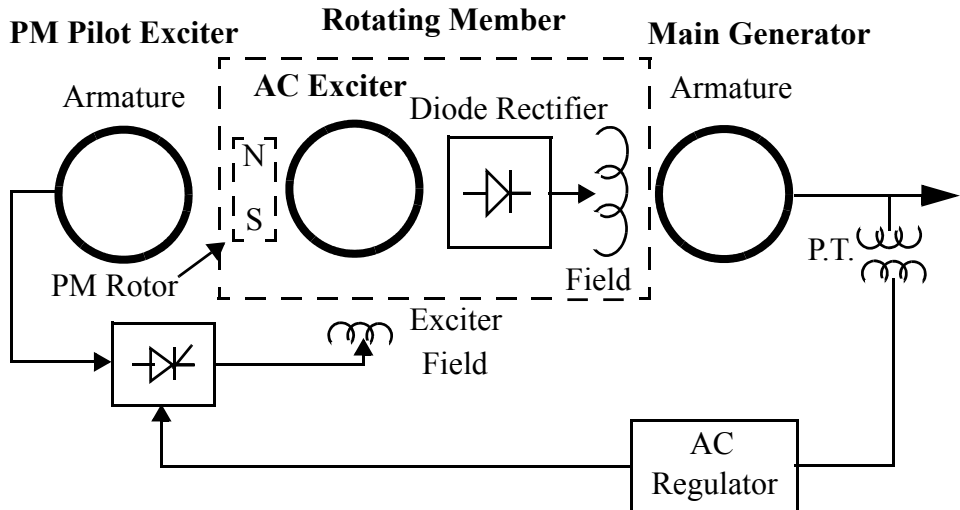


Figure 7.15 Brushless excitation system utilizing a pilot permanent magnet exciter.

machine can be energized in the event of a power failure. Since it is controlled by means of a thyristor bridge, this system again provides a very fast response. However, when the excitation power is obtained via the generator terminals, system fault conditions can cause depressed generator voltage and thus a reduction in the voltage fed to the excitation system. This type of excitation system is very popular in modern designs and is, in slight variations, produced by GE, ABB, Toshiba, and a number of other Japanese companies.

7.5 IEEE Type 1 Excitation System

In order to provide uniformity in modeling excitation systems, the IEEE defined four generic excitation systems termed Types 1,2 , 3, and 4 in 1967 and subsequent publications[5]–[8]. In general, the nomenclature of the IEEE Type 1 excitation system, shown in Figure 7.17 follows [5]. Over the years the Type 1 system has been extended to include most of the excitation systems presently produced. When applied to systems with a DC source, this type of system has recently been renamed IEEE Type DC1A [9]. The quantity V_{REF} is the input command. The voltage V_S (designated as V_T in [5]) is the generator terminal voltage amplitude fed back to the regulator input. The transfer function following V_S is a simple time constant T_R , which represents the regulator input filter-

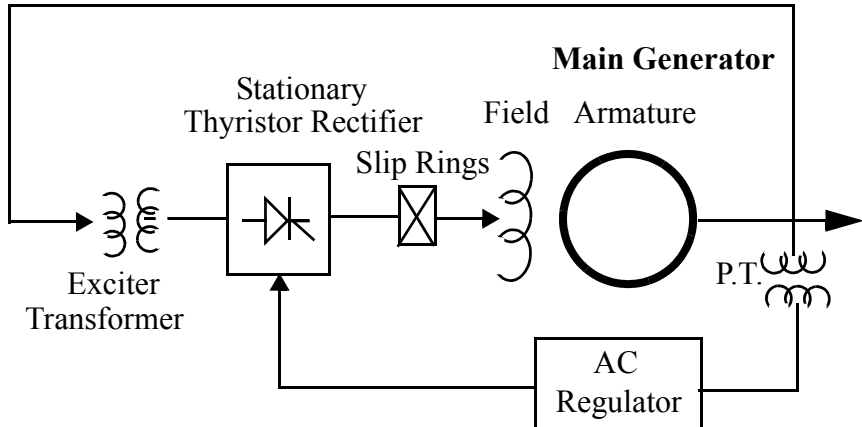


Figure 7.16 Controlled-rectifier excitation utilizing a transformer fed potential source.

ing of the 360 Hz ripple which occurs due to rectification of the feedback signal. For most systems T_R is very small and may be considered to be zero.

In each of the IEEE Type systems, a signal termed V_{PSS} is present. The generic term for such signals is “power system stabilizer.” These are auxiliary signals which are added to enhance the damping of the system to disturbances. Some of these signals are accelerating power, rotor speed, frequency, and rate of change of terminal voltage. Usually the stabilizing signal is inserted through a transfer function providing gain adjustment and a lead-lag compensation for phase shifting effects of the transducer.

The first summing point in the Type 1 system compares the regulator reference with the output of the terminal voltage filter to determine the voltage error input to the regulator amplifier. Most computer-based controllers do not require an input of V_{REF} but rather internally calculate the proper value of voltage. The second summing point combines voltage error input with the excitation major damping loop signal.

The main regulator transfer function is represented as a gain K_A and a time constant T_A , and in the basic controller of the previous section was the gain and time constant of an amplidyne. In more modern systems this block would correspond to the gain and time constant of a permanent magnet machine whose output is rectified by means of a thyristor bridge. This combination is today called a pilot exciter. Following this signal, the maximum and minimum limits of the regulator are imposed so that large input error signals cannot produce a

regulator output which exceeds practical limits and in modern system would represent the saturation of the rectifier (i.e., full rectification and full or partial inversion).

The next summing point subtracts a signal which represents the saturation function S_E of the exciter. The resultant is applied to the exciter transfer function. When a self excited shunt field is used, K_E represents the setting of the shunt field rheostat which provides a positive feedback of exciter output. To establish initial conditions, K_E is often chosen such that it is equal in magnitude to the saturation function at the initial value of E_X (E_{FD} in the original IEEE notation). For those systems with a separately excited exciter, regulator output is required to supply the exciter field and establish the initial value of E_X .

Major loop damping is provided by the feedback transfer function $sK_F/(1 + sT_F)$ from exciter output E_X to the first summing point. Note that in the steady-state (i.e., $s \rightarrow 0$)

$$\frac{1}{K_E}(V_S - S_E E_X) = E_X \quad (7.14)$$

or

$$V_S = (K_E + S_E)E_X \quad (7.15)$$

so that the proper steady-state excitation for a given terminal voltage can be determined. Depending upon the exact nature of the exciter, a second limiter bounding the excursion of the exciter, voltage E_X , may be used but is not shown in [Figure 7.17](#).

In addition to describing a traditional amplidyne/DC machine type excitation system, the Type 1 Excitation System is also representative of the majority of modern systems now in service and presently being supplied by manufacturers with relatively minor changes. The basic block diagram includes most continuously acting systems with rotating exciters such as

- General Electric Exciter with Amplidyne Regulator
- General Electric Alterrex Exciter
- General Electric Alterrex-Thyristor Exciter

In many cases the limits on E_X are given explicitly rather than the terminal voltage V_S and the corresponding limits on V_S must be inferred from the preceding steady-state relationship. The saturation function S_E is defined by the

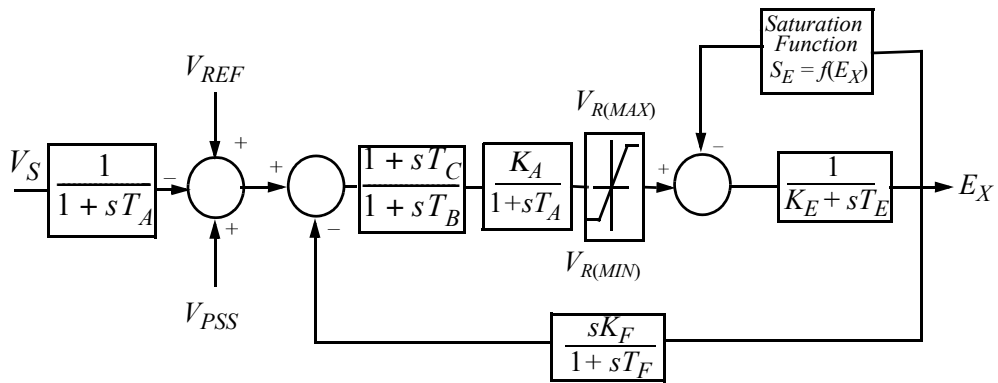


Figure 7.17 IEEE Type 1 (Type DC1A) excitation system.

IEEE Working Group as a multiplier of exciter output voltage E_X to represent the increase in exciter excitation requirements because of saturation. [Figure 7.18](#) illustrates the calculation of a particular value of S_E . The analysis procedure is much the same as in [Section 7.4.3](#). Note that the major difference is that the saturation curve used is under a loaded condition, i.e., with the main generator field excited so that the effects of the iR drop of the DC shunt generator can be incorporated.

At a given exciter output voltage, the quantities A and B are defined as the exciter excitation to produce the output voltage on the constant resistance load saturation curve and the air gap line, or

$$S_E = \frac{A - B}{B} = \frac{A}{B} - 1$$

In general, the saturation function is normally defined by two points. To be consistent, the points are chosen to be equal to maximum exciter voltage and 0.75 of maximum exciter voltage. The exact functional relationship is left up to the programmer, but whatever function is chosen, it is specified that it must pass through these two points.

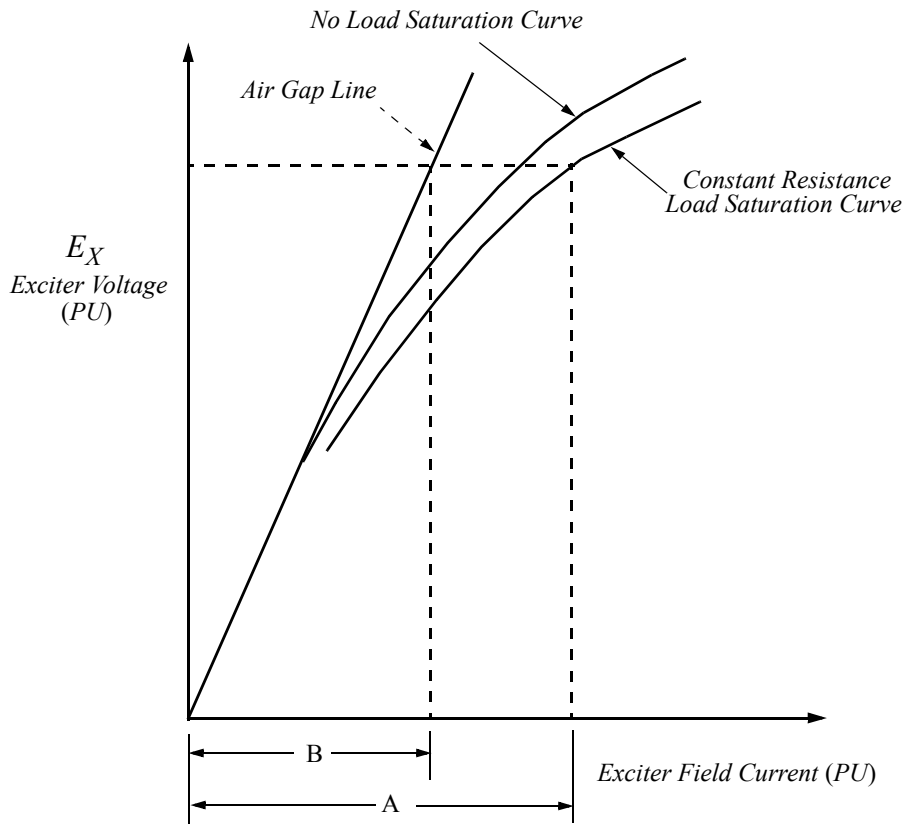


Figure 7.18 Exciter saturation curve.

The Type 1 system has been extended to include a limiter which comes into play only during extreme conditions [9] but is generally not needed for most studies. Typical data for this excitation system is shown in Table 7.1.

Table 7.1 Typical per unit data for an IEEE Type 1 DC exciter as shown in Figure 7.17.

$K_A = 187$	$T_A = 0.89$	$K_E = 1.0$	$T_E = 1.15$ s
$K_F = 0.058$	$T_F = 0.62$	$T_B = 0.06$	$T_C = 0.173$
$V_{R(MAX)} = 1.7$	$V_{R(MIN)} = -1.7$	$T_R = 0.015$	

Numerous other variations on the basic exciter model have been developed by IEEE Committees. A complete discussion of all of these variants is beyond the scope of this book and the reader is referred to [5]–[9].

7.6 Excitation Design Principles

The major elements of the large majority of excitation systems are shown in [Figure 7.19](#) and encompass

1. a voltage regulator to provide high gain at low frequency
2. a lead/lag (or lag/lead) circuit
3. an exciter which takes the voltage signal and converts the signal from a low to a high power signal
4. a feedback “washout” loop to reduce the tendency of E_X to help provide damping.

Other components such as the limiter shown in [Figure 7.17](#), are not key to selecting the gains of the basic controller and can be neglected here. Similarly, the input filter of the terminal voltage passes all important frequencies below the line frequency and can be neglected. Finally, the saturation feedback portion of the excitation model can usually be set aside until the basic gains of the controller have been established. It should be mentioned that numerous schemes have evolved to help compensate for the effects of load current, under and over current limitations of the exciter, and numerous other considerations which cannot be taken up here. Good references for these details are given in [10] and [11].

A basic exciter model incorporating the four items above is shown in [Figure 7.19](#). The basic control action is accomplished by means of the regulator which basically attempts to zero the voltage error combined with the exciter, which acts to boost the power level from a signal command to a voltage actually fed to the field circuit. The two additional components are often used to enhance the control action.

Consider first the operation of the components. The basic behavior of the controller can be examined by setting the constants $K_F = T_B = T_C = 0$. The gain K_A essentially determines the accuracy of the controller since in the steady-state the voltage error is the inverse of this gain. For purposes of an example, let $T_A = 0.04\text{ s}$ and choose $K_E = 1$ and $T_E = 1$. A root locus corresponding to these parameter values is shown in [Figure 7.20](#). A regulator gain of 200 is chosen as an example which would, in effect, result in a voltage error of 1/200 or 0.5%. [Figure 7.21](#) shows the corresponding Bode plot for this value of regulator gain, which indicates a phase margin of 20° . The phase margin is the value of phase which exists when the amplitude of the transfer function

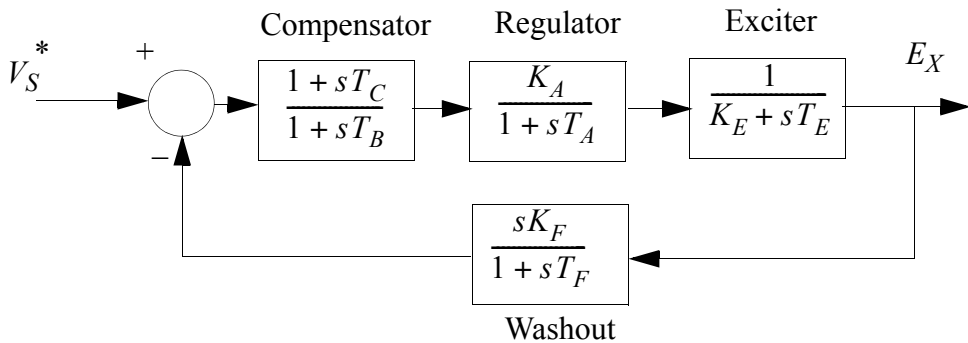


Figure 7.19 Basic excitation control system.

reaches unity. An acceptable value of phase margin is normally considered to be between 30° and 45° so that both the root locus and the Bode plot indicate a tendency for the output variable E_X to oscillate, a fact confirmed by Figure 7.22.

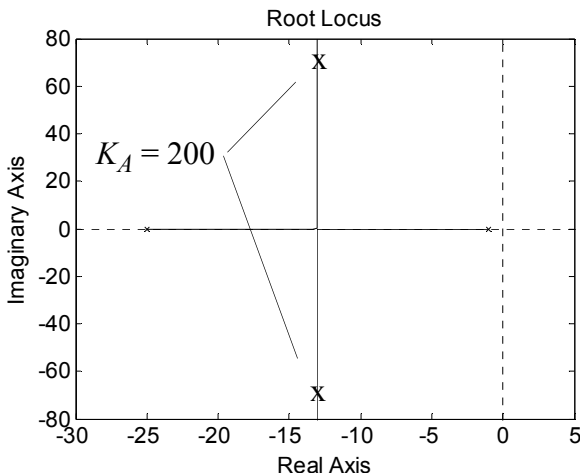


Figure 7.20 Root locus plot of basic regulator and exciter, $T_A = 0.04$ s., $K_E = 1.0$, $T_E = 1.0$ s., roots at point "x" denote a gain of $K_A = 200$.

The oscillatory response of most excitation systems has prompted the use of additional means to enhance their behavior. In Figure 7.23 the phase compensator shown in Figure 7.19 has been introduced to help increase the phase margin. This can be accomplished by choosing a lead lag circuit which provides a temporary phase lead in the frequency domain which the amplitude of

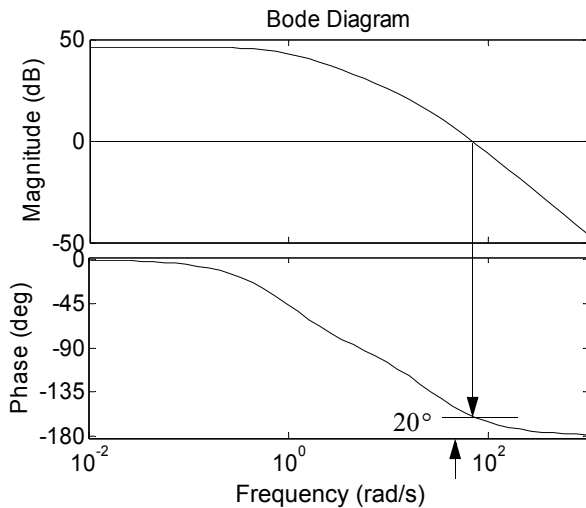


Figure 7.21 Bode plot corresponding to Figure 7.20 assuming a regulator gain of $K_A = 200$, phase margin = 20° .

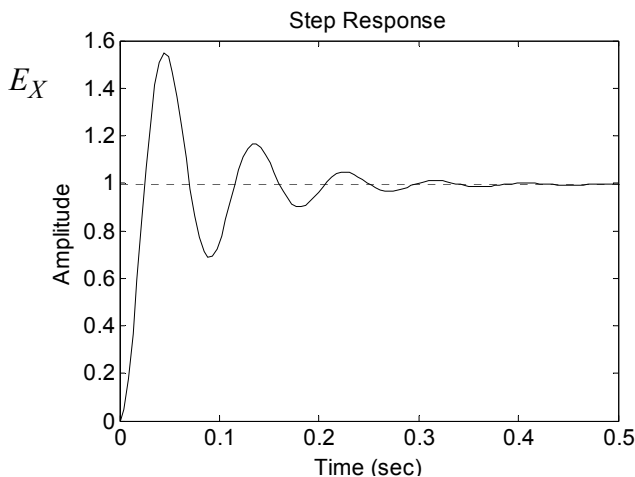


Figure 7.22 Step response of the exciter voltage E_X corresponding to Figure 7.20.

the overall transfer function passes through unity. The lead-lag circuit essentially adds an additional pole and zero to the overall open circuit transfer function. Since a phase lead is desired, the zero must be positioned to the right of the additional pole along the real axis. The positioning of the zero acts to “attract” the pole associated with the exciter and when the exciter pole is situated at the same point as the zero, the time response no longer has a significant time constant normally associated with an exciter (1.0 s. in this case). Much

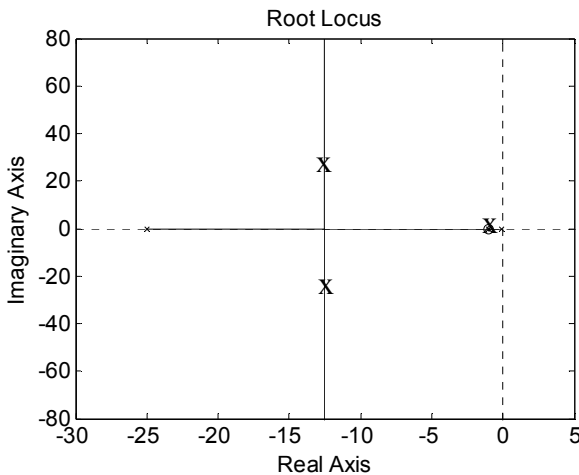


Figure 7.23 Root locus plot of regulator and exciter with phase compensation, $T_A = 0.04\text{ s.}$, $K_E = 1.0$, $T_E = 1.0\text{ s.}$, $T_B = 15\text{ s.}$, $T_C = 1.0\text{ s.}$, roots at point "x" denotes a gain of $K_A = 500$.

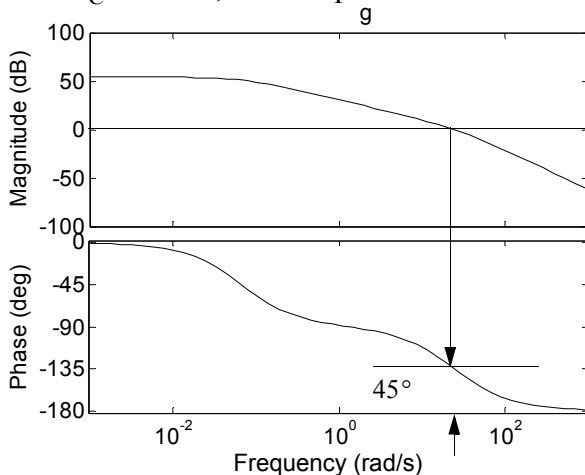


Figure 7.24 Bode plot corresponding to Figure 7.23 assuming a regulator gain of $K_A = 500$, phase margin = 45° .

higher gains can be achieved, as is evident from the root locus plot. The corresponding Bode plot is shown in Figure 7.24, which indicates a phase margin of 45° . The step response, shown in Figure 7.25, indicates a much improved transient response.

The term "washout" for the feedback compensator refers to the fact that only the change in the input is fed back and not its average value. In effect the

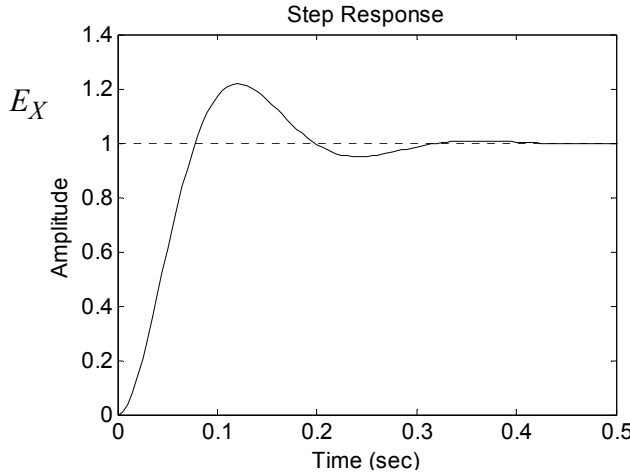


Figure 7.25 Step response of the exciter voltage E_X corresponding to Figure 7.23.

washout determines the time rate of change of E_X rather than its nominal value. The purpose of the washout feedback circuit can be illustrated by neglecting, for simplicity, the time constant associated with the regulator in addition to the phase compensator. The forward transfer function will then be

$$G = \frac{K_A}{1 + sT_E} \quad (7.16)$$

The feedback with washout is

$$H = \frac{sK_F}{1 + sT_F} \quad (7.17)$$

The closed-loop transfer function is clearly

$$\frac{G}{1 + GH} = \frac{\frac{K_A}{1 + sT_E}}{1 + \left(\frac{K_A}{1 + sT_E}\right)\left(\frac{sK_F}{1 + sT_F}\right)} \quad (7.18)$$

$$= \frac{K_A(1 + sT_F)}{1 + (T_E + T_F + K_A K_F)s + T_E T_F s^2} \quad (7.19)$$

Thus the overall effect is to place a zero at the location $-1/T_F$. The pole associated with the exciter has been replaced by two poles, one of which is shifted

to the left of $-1/T_E$ and one to the right of $1/T_E$. The overall effect is similar to the use of the phase compensator because of the presence of the zero.

7.7 Effect of the Excitation System on Dynamic Stability

When the use of digital computers became an important analysis tool in the 1950s, it was discovered that the response of the excitation system to large disturbances has an important effect upon the transient stability limits of a power system. It was learned that system conditions frequently exist where a very fast response excitation system is needed to guarantee the transient stability limits that would be predicted by assuming constant field flux linkages.

The effect of modern, fast response excitation systems on small signal dynamic stability has also been recognized. In most power systems this effect has typically been to allow for larger power limits than would be obtained with manual control. However, in certain rare cases, it has been found that an excitation system can actually be detrimental to system stability. Therefore, it is important to understand the contribution of the excitation system to both the synchronizing and damping torque components of a generator.

7.7.1 Generator Operating with Constant Field Flux Linkages

In order to develop the concepts associated with dynamic stability, it is convenient to return to the case of a single machine connected to an infinite bus through a reactance, [Figure 7.26](#). Initially, it will be assumed that the field flux linkages remain constant at a value determined by the operating condition of the machine before a disturbance occurs. From Chapter 6, Eq. (6.36), the expression for rotor acceleration is given by

$$\frac{\partial^2 \delta_b}{\partial t^2} = -\frac{180f_b}{H}(T_M + T_E) \quad (7.20)$$

where

H is the inertia constant of the generator, including the connected prime mover (($KW - SEC$)/(KVA))

δ_b is the angle between the generator quadrature axis and a reference axis defined by the voltage of the infinite bus (degrees)

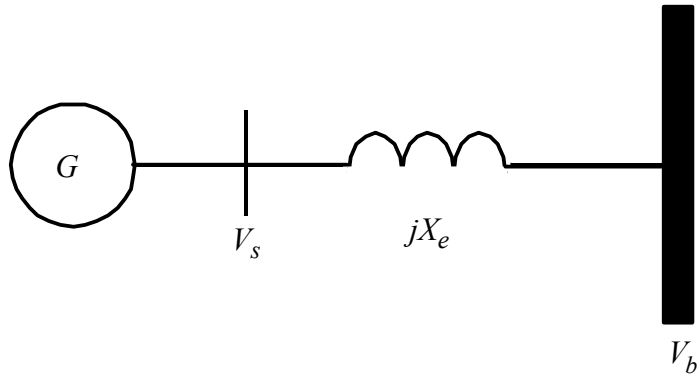


Figure 7.26 Single line diagram of a simple synchronous machine system connected to an infinite bus through a transmission line reactance.

f_b is the base frequency (hertz)

t is time (seconds)

T_M is the mechanical torque (per unit)

T_E is the electrical torque (per unit)

This equation may also be written in a different form where the angle is expressed in radians,

$$\frac{d^2\delta_b}{dt^2} = -\frac{\omega_b}{M}(T_M + T_E) \quad (7.21)$$

where

$$M = 2H$$

$$\omega_b = 2\pi f_b$$

Equation (7.21) omits the possibility of torque which may be proportional to the rate of change of the angle δ , i.e., slip frequency. This torque, which is a damping torque, is represented by a *damping coefficient* when the torque produced is linearly proportional to the slip frequency for the speed variations being considered. With this additional term, Eq. (7.21) becomes

$$\left(\frac{M}{\omega_b}\right)\frac{d^2\delta_b}{dt^2} + \left(\frac{D}{\omega_b}\right)\frac{d\delta_b}{dt} + T_E = -T_M \quad (7.22)$$

where D is the per unit *damping torque coefficient* (per unit torque per unit speed). Equation (7.22) is termed the *swing equation* of the synchronous machine.

In general, the electrical torque T_E also contains components of torque which are proportional to speed (damping torque). Consider first those damping torques which arise from the effect of the generator field and excitation system transients. All other damping torques are to be included in the coefficient D . These torques include the damping torque due to the prime mover and the damping torque due to the effect of the generator amortisseur windings.

If this analysis is restricted to small deviations away from an equilibrium condition, the variables in Eq. (7.22) can be segregated into two components:

$$\delta_b = \delta_{bo} + \Delta\delta_b$$

$$T_E = T_{Eo} + \Delta T_E$$

$$T_M = T_{Mo} + \Delta T_M$$

where the “ o ” subscript denotes the steady-state value which existed before the disturbance and “ Δ ” denotes the small change in the quantity. Since the time derivative of the steady-state portion of the torque angle δ_{bo} is zero, then $T_{Eo} = -T_{Mo}$. Eq. (7.22) becomes, for small changes,

$$\left(\frac{M}{\omega_b}\right) \frac{d^2(\Delta\delta_b)}{dt^2} + \frac{D}{\omega_b} \frac{d(\Delta\delta_b)}{dt} + \Delta T_E = -\Delta T_M \quad (7.23)$$

For the case where the field flux linkages of the machine are constant and the effect of damper windings is omitted, the electrical torque equation, obtained in Chapter 5, is, in per unit,

$$T_E = \frac{E_Q' V_S}{x_D'} \sin\delta + (V_S)^2 \frac{(x_D' - x_{QS})}{2x_D' x_{QS}} \sin 2\delta \quad (7.24)$$

When the machine is tied back to an infinite bus through a reactance, as in [Figure 7.26](#), then Eq. (7.24) may also be written as

$$T_E = \frac{E_Q' V_B}{x_D' + x_E} \sin\delta_b + V_B^2 \frac{(x_D' - x_{QS})}{2(x_D' + x_E)(x_{QS} + x_E)} \sin 2\delta_b \quad (7.25)$$

If the change in angle is sufficiently small, then

$$\sin \delta_b = \sin(\delta_{bo} + \Delta\delta_b) \approx \sin \delta_{bo} + \Delta\delta_b \cos \delta_{bo}$$

$$\sin 2\delta_b = \sin(2\delta_{bo} + 2\Delta\delta_b) \approx \sin 2\delta_{bo} + 2\Delta\delta_b \cos 2\delta_{bo}$$

so that Eq. (7.25) can be written as

$$\Delta T_E = \left(\frac{E_{Qo}' V_B}{x_D' + x_E} \cos \delta_{bo} + \frac{V_B^2 (x_D' - x_{QS})}{(x_D' + x_E)(x_{QS} + x_E)} \cos 2\delta_{bo} \right) \Delta\delta$$

(7.26)

or

$$\Delta T_E = K_1 \Delta\delta_b$$

(7.27)

where K_1 equals the term enclosed in the parentheses of Eq. (7.26). Note that this term is a function only of the initial condition, i.e., the conditions which prevailed before the disturbance.

Substituting Eq. (7.27) into Eq. (7.23) yields

$$\left(\frac{M}{\omega_b} \right) p^2 \Delta\delta_b + \left(\frac{D}{\omega_b} \right) p \Delta\delta_b + K_1 \Delta\delta_b = -\Delta T_M$$

(7.28)

The coefficient K_1 is usually called the per unit *synchronizing torque coefficient* and has the dimensions of per unit torque per radian of angular displacement. The constant K_1 is also the derivative of Eq. (7.25) with respect to delta. Equation (7.28) is frequently termed the *linearized form of the swing equation*.

To help visualize the significance of this equation, assume that variations in the mechanical torque are zero ($\Delta T_M = 0$) and that an initial displacement is introduced in $\Delta\delta_b$, i.e., $\Delta\delta_b(0)$. The resulting solution of the differential equation is

$$\Delta\delta_b = \Delta\delta_b(0) \left(e^{-\frac{Dt}{2M}} \right) \cos(\omega_n t - \beta)$$

(7.29)

where

$$\beta = \tan^{-1} \left(\frac{D}{2\omega_n M} \right)$$

(7.30)

$$\omega_n = \sqrt{\frac{K_1 \omega_b}{M} - \frac{D^2}{2M}}$$

(7.31)

The usual range of per unit damping torque coefficient D consists of very small values, so that

$$\omega_n \equiv \sqrt{\frac{K_1 \omega_b}{M}} \quad (7.32)$$

The quantity ω_n is called the *system natural frequency*, although its units in this equation remain radians per second.

Equation (7.29) indicates that the oscillation will eventually decay to zero if the damping torque coefficient D is positive. It is useful to note that the value of the machine inertia M also affects the rate of damping in much the same manner as an inductance in an $R-L$ circuit. The constant K_1 is called the *synchronizing torque coefficient* and, from Eq. (7.41), reaches zero when $\delta_b = 90^\circ$, as would be expected. The fact that K_1 varies with δ_b suggests the electrical equivalent of a spring with a variable spring constant. The higher the value of K_1 , that is, the higher the slope of the torque vs. angle curve, the higher the oscillation frequency. This fact is often used to gauge the degree of stability of a system when the oscillation frequencies are known but not the damping. In a power system, the frequency of oscillation is usually in the range of 0.5 to 2.0 hertz. It is important to remember, however, that if e_Q' changes, then Eq. (7.29) is not a valid solution of the differential equation, Eq. (7.28). However, the basic trends are still illustrative. Since the damping torque coefficient D is very small, the upper portion of the block diagram is essentially an oscillator with an angular frequency $\sqrt{\omega_b K_1 / M}$.

In the two machine example, only one natural frequency will exist. When a disturbance is introduced to a system of “ n ” synchronous machines, there will exist “ $n - 1$ ” natural frequencies. In block diagram form, Eq. (7.28) can be represented by [Figure 7.27](#). If all of the variables are assumed to be sinusoids at a frequency “ ω ” and if the p or (d/dt) operator in [Figure 7.26](#) is replaced by “ $j\omega$ ”, the variables can now be interpreted as being the complex number representation of a sinusoid, as shown in [Figure 7.28](#). Note that the electrical torque has been divided into two components, $\Delta\tilde{T}_{ES}$ and $\Delta\tilde{T}_{ED}$, called the *synchronizing torque* and *damping torque* respectively. If the damping torque coefficient D is zero, then this system will oscillate without any damping, and the only component of electrical torque will be the synchronizing torque $\Delta\tilde{T}_{ES}$, which is in phase with $\Delta\delta_b$. If positive damping exists, that is, if D is positive, then the damping torque component $\Delta\tilde{T}_{ED}$ will be in phase with the rotor slip fre-

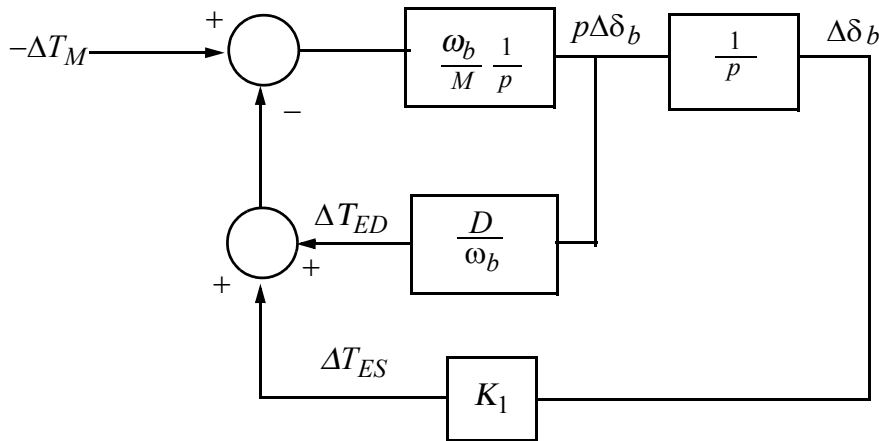


Figure 7.27 Block diagram of basic electromechanical system assuming constant field flux linkages.

quency $j\omega\Delta\delta_b$. Hence, the damping torque component leads the synchronizing torque by 90 electrical degrees. If it is desired to determine whether the damping component of electrical torque provides either positive or negative damping, it will be necessary to compare it to the phase of the frequency variation, and to determine either a positive or negative synchronizing component, it is necessary to compare its phase to the phase of the angular variation.

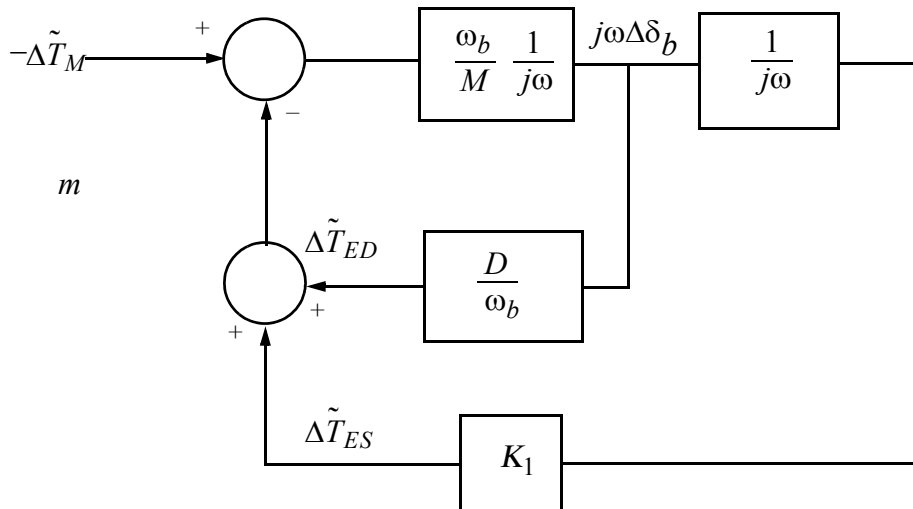


Figure 7.28 Block diagram in the frequency domain corresponding to Figure 7.27.

7.7.2 Generator with Variable Field Flux Linkages

During transient stability studies, the effect of a variation in the field flux linkages is found by solving the per unit equation,

$$v_{FR} = r_{FR}i_{FR} + \frac{d\lambda_{FR}}{dt} \quad (7.33)$$

which, after manipulation, becomes

$$e_X = e_I + T_{d0} \frac{de_Q'}{dt} \quad (7.34)$$

where

$$e_X = \frac{x_{MD}}{r_{FR}} v_{FR} \quad (7.35)$$

$$e_Q' = \frac{x_{MD}}{x_{FR}} \omega_b \lambda_{FR} \quad (7.36)$$

$$T_{d0} = \frac{x_{FR}}{\omega_b r_{FR}} \quad (7.37)$$

Since Eq. (7.34) is linear, it has the same form when written for small deviations around an operating point. In this case the small signal perturbation equation for the electromagnetic torque becomes

$$\begin{aligned} T_{Eo} + \Delta T_E &= \frac{(E_{Qo}' + \Delta e_Q')V_b}{x_D' + x_E} \sin(\delta_{bo} + \Delta\delta_b) \\ &+ \frac{V_B^2(x_D' - x_{QS})}{2(x_D' + x_E)(x_{QS} + x_E)} \sin 2(\delta_{bo} + \Delta\delta_b) \end{aligned} \quad (7.38)$$

Extracting the small change portion of the equation and discarding the average value of the expression results in

$$\begin{aligned} \Delta T_E &= \frac{V_B}{x_D' + x_E} \sin(\delta_{bo}) \Delta e_Q' + \left(\frac{E_{Qo}' V_B}{x_D' + x_E} \cos \delta_{bo} \Delta \delta_b \right) \\ &+ \frac{2 V_B^2 (x_D' - x_{QS})}{(x_D' + x_E)(x_{QS} + x_E)} \cos(2\delta_{bo}) \Delta \delta_b \end{aligned} \quad (7.39)$$

Inserting this result in Eq. (7.23) results in

$$\left(\frac{M}{\omega_b}\right) \frac{d^2(\Delta\delta_b)}{dt^2} + \frac{D}{\omega_b} \frac{d(\Delta\delta_b)}{dt} + \frac{V_B}{x_D' + x_E} \sin \delta_{bo} \Delta e_Q' + K_1 \Delta\delta_b = -\Delta T_M \quad (7.40)$$

where

$$K_1 = \left(\frac{E_{Qo}' V_B}{x_D' + x_E} \cos \delta_{bo} + \frac{2 V_B^2 (x_D' - x_{QS})}{(x_D' + x_E)(x_{QS} + x_E)} \cos(2\delta_{bo}) \right) \Delta\delta_b \quad (7.41)$$

Clearly, the term involving $\Delta e_Q'$ is the additional term resulting from a variation in field flux linkages. It is necessary to solve for $\Delta e_Q'$ in terms of the state variable $\Delta\delta_b$ and the input field voltage Δe_X .

In Chapter 6 it was shown that, neglecting resistance, the stator flux linkages can be written in either of two forms. That is, in linearized form

$$\Delta \psi_{DS} = \Delta v_{QS} = x_{DS} \Delta i_{DS} + \Delta e_I \quad (7.42)$$

or

$$= x_D' \Delta i_{DS} + \Delta e_Q' \quad (7.43)$$

The voltage v_{QS} is, in turn, related to the infinite bus voltage by

$$v_{QS} = V_B \cos \delta_{bo} - x_E i_{DS} \quad (7.44)$$

Upon linearizing this equation it can be determined that

$$\Delta v_{QS} = -V_B \sin \delta_{bo} \Delta\delta_b - x_E \Delta i_{DS} \quad (7.45)$$

so that one can now write that

$$-V_B \sin \delta_{bo} \Delta\delta_b = (x_{DS} + x_E) \Delta i_{DS} + \Delta e_I = (x_D' + x_E) \Delta i_{DS} + \Delta e_Q' \quad (7.46)$$

Solving for Δi_{DS} in terms of $\Delta e_Q'$ and $\Delta\delta_b$, it can be determined that

$$\Delta i_{DS} = -\frac{V_B \sin \delta_{bo}}{x_D' + x_E} \Delta\delta_b - \frac{1}{x_D' + x_E} \Delta e_Q' \quad (7.47)$$

However, from Eq. (7.46),

$$\Delta e_I = (x_D' - x_{DS}) \Delta i_{DS} + \Delta e_Q' \quad (7.48)$$

so that

$$\Delta e_I = \frac{(x_{DS} - x_D')}{x_D' + x_E} V_B \sin \delta_{bo} \Delta \delta_b + \frac{x_{DS} + x_E}{x_D' + x_E} \Delta e_Q' \quad (7.49)$$

Thus, finally, the small signal version of Eq. (7.34) can be written in the form

$$\Delta e_Q' = \frac{1}{pT_{d0}} (\Delta e_X - K_2 \Delta \delta_b - K_3 \Delta e_Q') \quad (7.50)$$

where $1/p$ denotes integration with respect to time and where

$$K_2 = \frac{x_{DS} - x_D'}{x_D' + x_E} V_B \sin \delta_{bo} \quad (7.51)$$

$$K_3 = \frac{x_{DS} + x_E}{x_D' + x_E} \quad (7.52)$$

Equations (7.49) and (7.50) suggest the block diagram representation of the synchronous machine, as shown in [Figure 7.29](#).

In most cases involving synchronous generators, the terminal voltage is the variable to be controlled by action of the field exciter. The terminal voltage amplitude in per unit is related to the d - and q -axis voltages by

$$v_S = \sqrt{v_{DS}^2 + v_{QS}^2} \quad (7.53)$$

Expanding about a steady-state equilibrium and discarding the “ $\Delta\Delta$ ” terms,

$$V_{So} + \Delta v_S = \sqrt{V_{DSo}^2 + V_{QSo}^2 + V_{DSo} \Delta v_{DS} + V_{QSo} \Delta v_{QS}} \quad (7.54)$$

Factoring out the steady-state terms from beneath the square root and making use of Eq. (7.53) results in

$$V_{So} + \Delta v_S = V_{So} \cdot \sqrt{1 + \frac{V_{DSo}}{V_{So}^2} \Delta v_{DS} + \frac{V_{QSo}}{V_{So}^2} \Delta v_{QS}} \quad (7.55)$$

However, from the power series expansion,

$$\sqrt{1 + X} = 1 + \frac{X}{2} - \frac{1 \cdot 1}{2 \cdot 4} X^2 + \frac{1 \cdot 1 \cdot 3}{2 \cdot 4 \cdot 6} X^3 - \frac{1 \cdot 1 \cdot 3 \cdot 5}{2 \cdot 4 \cdot 6 \cdot 8} X^4 + \dots$$

Eq. (7.55) becomes, approximately,

$$V_{So} + \Delta v_S = V_{So} + \frac{V_{DSo}}{2V_{So}} \Delta v_{DS} + \frac{V_{QSo}}{2V_{So}} \Delta v_{QS} \quad (7.56)$$

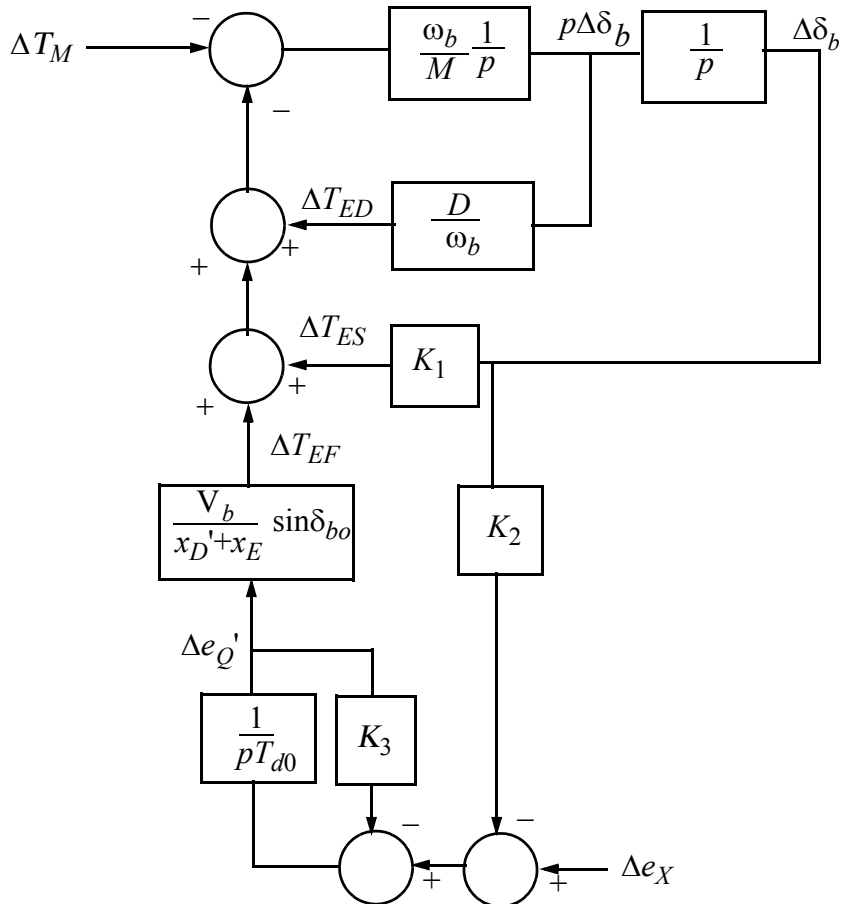


Figure 7.29 Block diagram of a synchronous machine with excitation control producing changes in field flux linkage.

Hence, for small changes,

$$\Delta v_S = \frac{V_{DSo}}{2V_{So}} \Delta v_{DS} + \frac{V_{QSo}}{2V_{So}} \Delta v_{QS} \quad (7.57)$$

From Eq. (7.45) it was shown that

$$\Delta v_{QS} = -V_B \sin\delta_{bo} \Delta\delta_b - x_E \Delta i_{DS} \quad (7.58)$$

where, from Eq. (7.47),

$$\Delta i_{DS} = -\frac{V_B \sin\delta_{bo}}{x_D' + x_E} \Delta\delta_b - \frac{1}{(x_D' + x_E)} \Delta e_Q' \quad (7.59)$$

In a similar manner it can be shown that

$$\Delta v_{DS} = -V_B \cos \delta_{bo} \Delta \delta_b - x_E \Delta i_{QS} \quad (7.60)$$

where

$$\Delta i_{QS} = -\frac{V_B \cos \delta_{bo}}{x_{QS} + x_E} \Delta \delta_b \quad (7.61)$$

Combining Eqs. (7.57), (7.45), (7.47), (7.60), and (7.61) one can express the change in terminal voltage as

$$\begin{aligned} \Delta v_S = & -\left[\frac{V_{QSo}}{2V_{So}} \left(\frac{x_D'}{x_D' + x_E} \right) V_B \sin \delta_{bo} + \frac{V_{DSo}}{2V_{So}} \left(\frac{x_{QS}}{x_{QS} + x_E} \right) V_B \cos \delta_{bo} \right] \Delta \delta_b \\ & + \frac{V_{QSo}}{2V_{So}} \left(\frac{x_E}{x_D' + x_E} \right) \Delta e_Q' \end{aligned} \quad (7.62)$$

or simply

$$\Delta v_S = -K_4 \Delta \delta_b + K_5 \Delta e_Q' \quad (7.63)$$

where the definitions of K_4 and K_5 are apparent. A complete system block diagram, including field regulation of the machine terminal voltage, is shown in [Figure 7.30](#). The “Excitation System” block refers to any of the many excitation system schemes, for example, [Figure 7.19](#).

The system equations may also be written in terms of complex variables if one sets $p = j\omega$. [Figure 7.31](#) then results. Note that the significant variable that has been introduced in this figure is the component ΔT_{EF} , arising from the variation in field flux linkage. As a complex number this torque is in phase with the variation of the field flux linkages $\Delta e_Q'$. If a component of this torque is in phase with the angular variation $\Delta \delta_b$, then this term will enhance the synchronizing torque component. If the other component (*out of phase* with $\Delta \delta_b$) is in phase with the speed variation $j\Delta \delta_b$, then the variation in field flux linkages will contribute *positive damping* to the system. On the other hand, if this component is in phase opposition to $j\Delta \delta_b$, then the system becomes less damped and ΔT_{EF} is said to contribute *negative damping*. In general, the phase of ΔT_{EF} with respect to $\Delta \delta_b$ lies in any of the four quadrants, depending upon the particular operating condition and the natural frequency of oscillation. In general, if negative damping occurs, the amplitude of ΔT_{EF} can never exceed ΔT_{ED} for any oscillation angular frequency ω or else instability will occur.

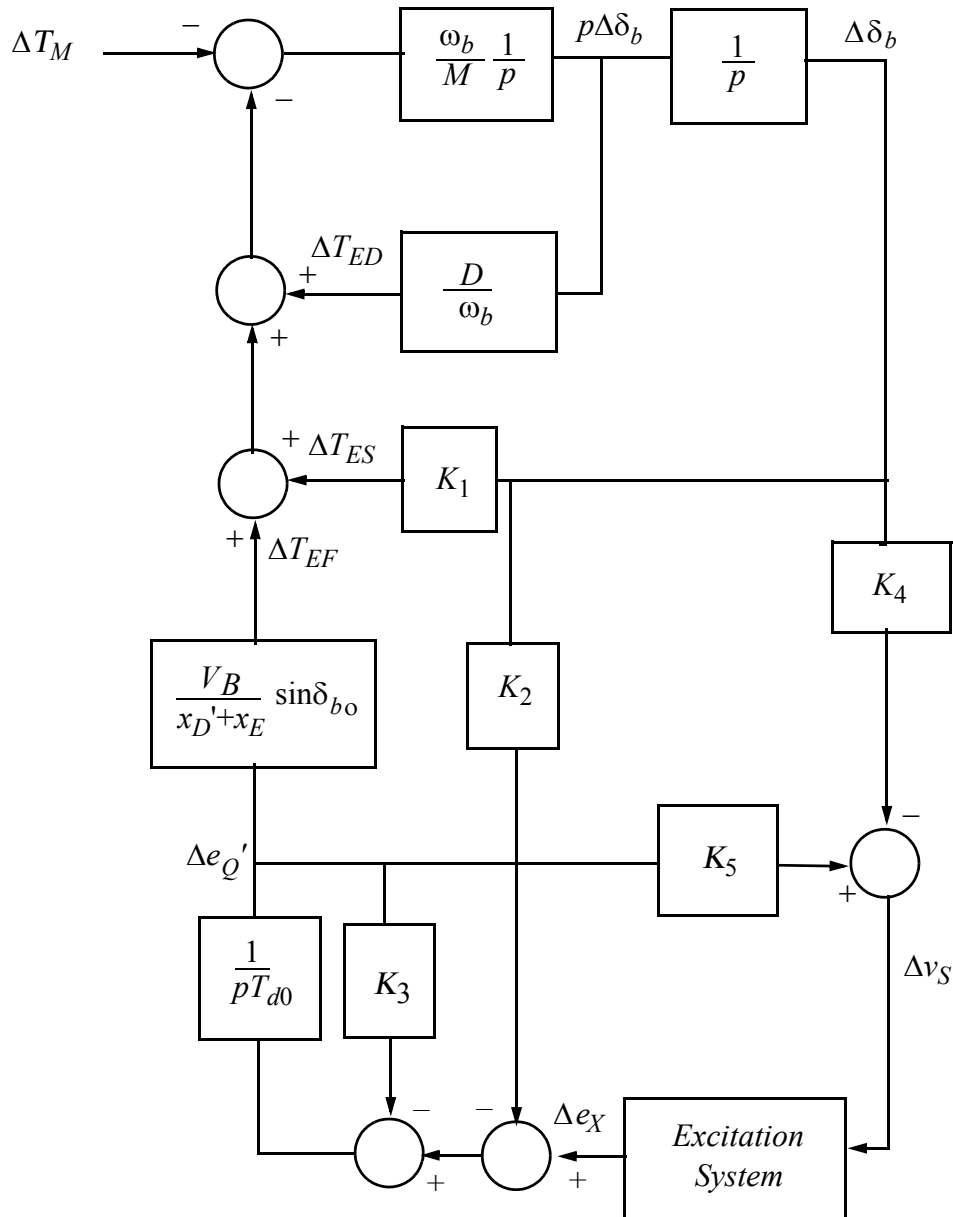


Figure 7.30 Overall block diagram showing regulation of stator terminal voltage amplitude.

Note that the coefficient K_4 can be either positive or negative, depending upon the load conditions and the size of the external reactance x_E . In general, K_4 is positive for light loadings (negative feedback) and small external reactances and is negative for heavy loadings and large external reactances (posi-

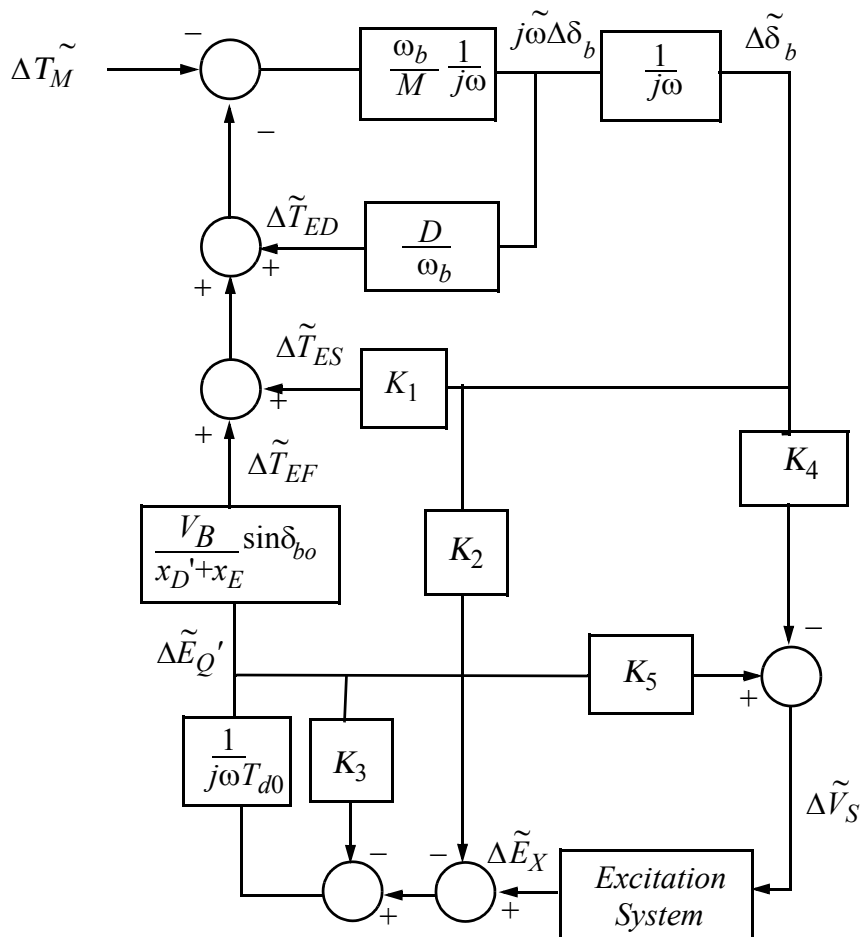


Figure 7.31 Frequency domain block diagram of closed-loop terminal voltage control system.

tive feedback). This latter case is therefore the area of concern for voltage regulated synchronous machines.

7.7.3 Closed-Loop Representation

While the block diagram of Figure 7.30 is useful from a conceptual point of view, it is not in one of the forms generally preferred by control designers. To be more useful, the equations expressing the block diagram of Figure 7.30 can then be accumulated into the state space matrix expression

$$P \begin{bmatrix} \Delta e_Q' \\ \Delta \delta \\ \frac{\Delta \omega_r}{\omega_b} \end{bmatrix} = \begin{bmatrix} -K_3 & -K_2 & 0 \\ \frac{-K_3}{T_{d0}} & \frac{-K_2}{T_{d0}} & 0 \\ 0 & 0 & 1 \\ -\frac{1}{M} \left(\frac{V_b \sin \delta_{bo}}{x_D' + x_E} \right) & -\frac{K_1}{M} & -\frac{D}{M} \end{bmatrix} \cdot \begin{bmatrix} \Delta e_Q' \\ \Delta \delta \\ \Delta \omega_r \end{bmatrix} + \begin{bmatrix} \frac{1}{T_{d0}} \\ 0 \\ 0 \end{bmatrix} \Delta e_X \quad (7.64)$$

together with the measurement equation

$$\Delta v_S = -K_4 \Delta \delta + K_5 \Delta e_Q' \quad (7.65)$$

This result can also be represented as a Laplace transfer function. If Eq. (7.64) is written in abbreviated form as

$$P \begin{bmatrix} \Delta e_Q' \\ \Delta \delta \\ \Delta \omega_r \end{bmatrix} = \begin{bmatrix} a_{11} & a_{12} & 0 \\ 0 & 0 & 1 \\ a_{31} & a_{32} & a_{33} \end{bmatrix} \cdot \begin{bmatrix} \Delta e_Q' \\ \Delta \delta \\ \Delta \omega_r \end{bmatrix} + \begin{bmatrix} \frac{1}{T_{d0}} \\ 0 \\ 0 \end{bmatrix} \Delta e_X \quad (7.66)$$

The transfer function representing the relationship between the excitation voltage and the terminal voltage can be expressed as

$$\frac{\Delta v_S}{\Delta e_X} = \frac{T_{d0}[a_{31}K_4 + (s^2 - a_{33}s - a_{32})K_5]}{s^3 - (a_{33} + a_{11})s^2 + (a_{11}a_{33} - a_{32})s + a_{11}a_{32} - a_{31}a_{12}} \quad (7.67)$$

In general it is easier to evaluate Eq. (7.66) numerically and then convert the numerical result to transfer function form.

[Figure 7.32](#) shows the root locus plot for a system in which the phase compensator, washout circuit, and exciter time constant have been neglected for simplicity. In practice such a regulator, without a delay for the exciter, is reasonably approximated by the modern static exciter shown in [Figure 7.16](#). The pole of the regulator was placed at $T_A = 0.05$ ms, resulting in a pole located at -20 sec^{-1} . Note that the poles associated with the electromechanical system are located very close to zeros of the transfer function, indicating that they have very little influence on the closed-loop behavior of the field circuit transfer function. However, it is interesting to notice that the effect of the closed-loop feedback terms K_2 and K_3 does somewhat affect the position of the open-loop pole located on the real axis near the origin. Without feedback of the

angle deviation in [Figure 7.30](#), this pole would be located at the value $1/T_{d0} = -0.157$ rather than at -0.6 . Probably more significant is the effect of loading on the DC (steady-state) gain. It sometimes supposed, for simplicity, that the transfer function of the generator is essentially defined by its open-circuit value [10]. That is, upon open-circuit, neglecting subtransient terms,

$$\frac{v_S}{e_X} \approx \frac{1}{1 + T_{d0}s} \quad (7.68)$$

The DC gain for a step function is obtain by supposing e_X to be a unit step function so that

$$e_X(s) = \frac{1}{s} \quad (7.69)$$

From the Final Value Theorem of Laplace Transforms

$$\lim_{t \rightarrow \infty} f(t) = \lim_{s \rightarrow 0} [sf(s)] \quad (7.70)$$

In this expression

$$f(s) \rightarrow \frac{e_X(s)}{1 + T_{d0}s} = \frac{1}{s(1 + T_{d0}s)} \quad (7.71)$$

in which case

$$\lim_{t \rightarrow \infty} v_s(t) = \lim_{s \rightarrow 0} \left(\frac{1}{1 + T_{d0}s} \right) = 1 \quad (7.72)$$

Upon applying the same principle to the example problem, the DC gain is, from Eq. (7.67),

$$\Delta v_S = \frac{T_{d0}[a_{31}K_4 - a_{32}K_5]}{a_{11}a_{32} - a_{31}a_{12}} = 0.664 \quad (7.73)$$

so that the simple model of Eq. (7.68) is considerably in error.

The system poles and zero for the case of zero closed-loop gain (open-loop) and for a closed-loop gain of 1000 are shown in [Table 7.2](#). The location of these roots on the root locus is shown in [Figure 7.32](#). The closed-loop gain of 1000 places the dominant poles very near to where the real and imaginary parts of the root are equal. This point is typically considered a near optimal case since it produces a damping ratio of 0.707 and a peak overshoot of 4.3%. The step response for unit step change in the voltage command v_S^* is shown in [Figure 7.33](#). It should be recognized here that the unit step change does nec-

essarily imply that a unit step change in voltage can, in fact, be accommodated in a practical sense. Almost certainly the machine will saturate since the nominal value of voltage was assumed to be one per unit and a second one per unit change command superimposed. The use of unit change is simply for purposes of convenience since the circuit is assumed to be linear and therefore the form of the response will be the same regardless of the amplitude of the command. The actual voltage command will, of course, be assumed to be sufficiently small that the assumptions made in linearizing Park's equations will remain valid.

Table 7.2 Location of open- and closed-loop poles and zeros corresponding to Figure 7.32.

Open-Loop	$K_A \rightarrow 0$
Poles	Zeros
-0.5996, -20.0	
$-0.1495 \pm j1.986$	$-0.00377 \pm j1.885$
Closed-Loop	$K_A = 1000$
-0.00935 ± 1.992	$-0.00377 \pm j1.885$
$-10.44 \pm j9.899$	

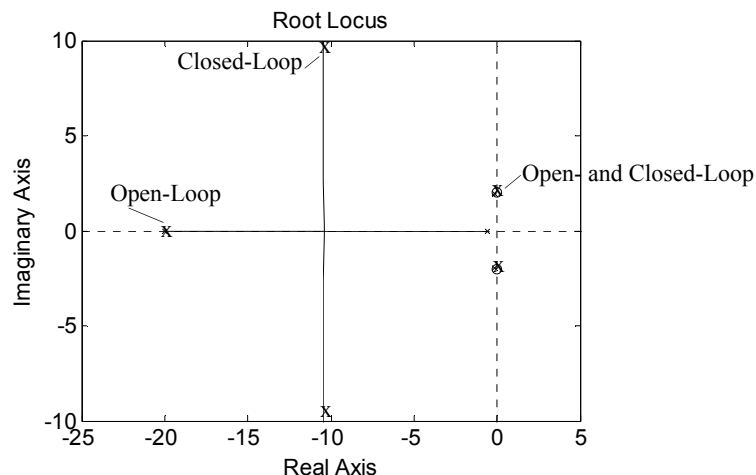


Figure 7.32 Root locus of 30 MW machine of Table 5.3 operating at unity power factor rated power and rated voltage. An external impedance of $x_E = 0.1$, $r_E = 0.01$ is assumed.

The simplified block diagrams developed in this section have been useful in visualizing the interaction between the key variables in the machine. In the past, such models have traditionally been used for the design of excitation con-

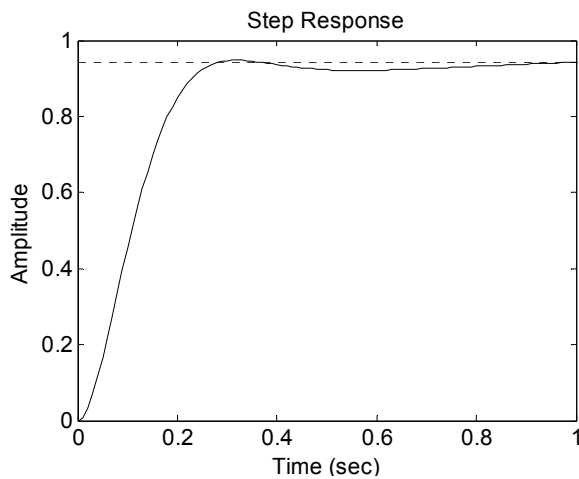


Figure 7.33 Step response of closed-loop exciter system with a regulator of the form $1000/(1 + 0.05s)$.

trollers [1]. However, the use of a simplified model inevitably produces simplified, i.e., inaccurate, results. A more detailed discussion of a design of a voltage controller will be deferred to Chapter 10, where a more suitable representation of the machine is developed and the power of modern computing tools can be brought to bear on the problem.

7.7.4 Excitation Control of Other Terminal Quantities

Control of terminal voltage is only one of many tasks that can be achieved by means of adjusting the excitation. Depending upon the application, it may be desirable to, instead, control the power factor, torque during motoring, reactive power, and numerous other quantities. As an example, consider the case where it is desired to control the phase angle of the current during motoring. In the synchronous reference frame, the phase angle ϕ can be expressed as the angular difference between the voltage vector and the current vector, both measured relative to the $d-q$ frame fixed to the rotor of the machine. The phase angle of the terminal voltage vector is

$$\delta = \arccos\left(\frac{v_{DS}}{\sqrt{v_{QS}^2 + v_{DS}^2}}\right) = \arccos\left(\frac{v_{QS}}{v_S}\right) \quad (7.74)$$

The phase angle of the current is

$$\gamma = \arccos\left(\frac{i_{QS}}{\sqrt{i_{QS}^2 + i_{DS}^2}}\right) = \arccos\left(\frac{i_{QS}}{i_S}\right) \quad (7.75)$$

The phase of the machine current with respect to the terminal voltage is

$$\phi = \delta - \gamma \quad (7.76)$$

For small changes about a steady-state condition

$$\Delta\gamma = \frac{\partial\gamma}{\partial i_{QS}}\Delta i_{QS} + \frac{\partial\gamma}{\partial i_{DS}}\Delta i_{DS} \quad (7.77)$$

$$= -\frac{I_{DS}}{I_S^2}\Delta i_{QS} + \frac{I_{QS}}{I_S^2}\Delta i_{DS} \quad (7.78)$$

However, from Eqs. (7.47) and (7.61),

$$\Delta i_{DS} = -\frac{V_B \sin \delta_{bo}}{x_{D'} + x_E} \Delta \delta_b - \frac{1}{x_{D'} + x_E} \Delta e_Q' \quad (7.79)$$

and

$$\Delta i_{QS} = -\frac{V_B \cos \delta_{bo}}{x_{QS} + x_E} \Delta \delta_b \quad (7.80)$$

whereupon

$$\Delta\gamma = \left(-\frac{I_{DS}}{I_S^2} - \frac{V_B \cos \delta_{bo}}{x_{QS} + x_E} + \frac{I_{QS}}{I_S^2} - \frac{V_B \sin \delta_{bo}}{x_{D'} + x_E} \right) \Delta \delta_b + \left(-\frac{I_{QS}}{I_S^2} \frac{1}{x_{D'} + x_E} \right) \Delta e_Q' \quad (7.81)$$

and

$$\Delta\phi = \left(-\frac{I_{DS}}{I_S^2} - \frac{V_B \cos \delta_{bo}}{x_{QS} + x_E} + \frac{I_{QS}}{I_S^2} - \frac{V_B \sin \delta_{bo}}{x_{D'} + x_E} - 1 \right) \Delta \delta_b + \left(-\frac{I_{QS}}{I_S^2} \frac{1}{x_{D'} + x_E} \right) \Delta e_Q' \quad (7.81)$$

Thus,

$$K_4 = -\frac{I_{DS}}{I_S^2} - \frac{V_B \cos \delta_{bo}}{x_{QS} + x_E} + \frac{I_{QS}}{I_S^2} - \frac{V_B \sin \delta_{bo}}{x_{D'} + x_E} - 1 \quad (7.82)$$

and

$$K_5 = -\left(\frac{I_{QS}}{I_S^2}\right) \frac{1}{x_{D'} + x_E} \quad (7.83)$$

The block diagram of Figure 7.30 clearly applies for a phase angle controller as well. Coefficients K_4 and K_5 can be derived for a wide variety of other control targets in a similar manner.

7.8 Conclusion

This chapter has introduced the concept of dynamic stability, the small signal performance of a synchronous machine about a steady-state operating point. The complexity of this situation has, traditionally, required the need to simplify the system by the classical assumption of constant (“trapped”) flux linkages in shorted windings. Second and third order models have resulted which are reasonably amenable to traditional analysis methods for the design of an excitation system. In general, such assumptions are no longer needed with modern computing tools, and a more general approach to small signal behavior will be considered in Chapter 10. The study of excitation systems also forms an important boundary between the study of electrical machines and issues dealing with power electronics as well as with control theory. This chapter has served only as a mere introduction to these important application considerations.

7.9 References

- [1] D.F.P. de Mello and C. Concordia, “Concepts of Synchronous Machine Stability as Affected by Excitation Control,” *IEEE Trans. on Power Apparatus and Systems*, Vol. 88, April 1969, pp. 316–329.
- [2] J.H. Bishop, D.H. Miller, and A.C. Shartrand, “Experience with ALTER-REX Excitation for Large Turbine-Generators,” *IEEE/ASME Power Conference*, Miami Beach, FL, Sept. 15–19, 1974.
- [3] P.H. Beagles, K. Carlsen, M.L. Crenshaw and M. Temoshok, “Generator and Power System Performance with GENERREX Excitation System,” *IEEE Trans. on Power Apparatus and Systems*, Vol. PAS-95, March/April 1976, pp. 489–493.
- [4] T.L. Dillman, J.W. Skoogland, F.W. Keay, W.H. Smith, and C. Raczkowski, “A High Initial Response Brushless Excitation System,” *IEEE Trans. on Power Apparatus and Systems*, Vol. PAS-90, Sept./Oct. 1971, pp. 2089–2094.

- [5] IEEE Working Group of Excitation Systems Subcommittee of the Power Generation Committee, "Computer Representation of Excitation Systems," *IEEE Trans. on Power Apparatus and Systems*, Vol. PAS-87, June 1968, pp. 1460–1464.
- [6] IEEE Working Group of Excitation Systems Subcommittee of the Power Generation Committee, "Proposed Excitation System Definitions for Synchronous Machines," *IEEE Trans. on Power Apparatus and Systems*, Vol. PAS-88, August 1969, pp. 1248–1258.
- [7] IEEE Working Group of Excitation Systems Subcommittee of the Power Generation Committee, "Excitation System Dynamic Characteristics," *IEEE Trans. on Power Apparatus and Systems*, Vol. PAS-92, Jan./Feb. 1973, pp. 64–75.
- [8] IEEE Working Group of Excitation Systems Subcommittee of the Power Generation Committee, "Excitation System Models for Power System Stability Studies," *IEEE Trans. on Power Apparatus and Systems*, Vol. PAS-100, February 1981, pp. 494–509.
- [9] IEEE Recommended Practice for Excitation System Models for Power System Stability Studies, IEEE Standard 421.5–1992.
- [10] P.M. Anderson and A.A. Fouad, "Power System Control and Stability," Second Edition, Wiley Interscience, New York, 2003.
- [11] P. Kundur, "Power System Stability and Control," McGraw Hill, Inc., New York, 1994.

Chapter 8

Naturally Commutated Synchronous Motor Drives

8.1 Introduction

In high horsepower applications, such as turbo-compressors, induced and forced draft fans and boiler feed pumps, very high mechanical efficiencies can be achieved through the use of adjustable speed motor drives, resulting in substantial energy savings. Such high horsepower applications are typically beyond the range of conventional DC motor drives as well as force-commutated induction motor drives. The *load commutated inverter* (LCI) fed synchronous motor drive has established itself as a leading choice for such applications, particularly for those with fan load type characteristics. Load commutation is made possible by the induced *emf* of the synchronous machine, which eliminates the need for the expensive forced commutation circuitry required in a conventional CSI drive. In addition, the synchronous motor is free from the high slip losses that are inherent in large induction motor drives.

8.2 Load Commutated Inverter (LCI) Synchronous Motor Drives

The basic LCI synchronous motor drive system is shown in [Figure 8.1](#). In this drive, two static converter bridges are connected on their DC side by means of a so-called DC current link having only a link inductor on the DC side. The line side converter ordinarily takes power from a constant frequency bus and produces a controlled DC voltage at its end of the DC link inductor. The DC link inductor effectively turns the line side converter into a current source as seen by the machine side converter. Current flow in the line side converter is controlled by adjusting the firing angle of the bridge and by natural commutation of the AC line.

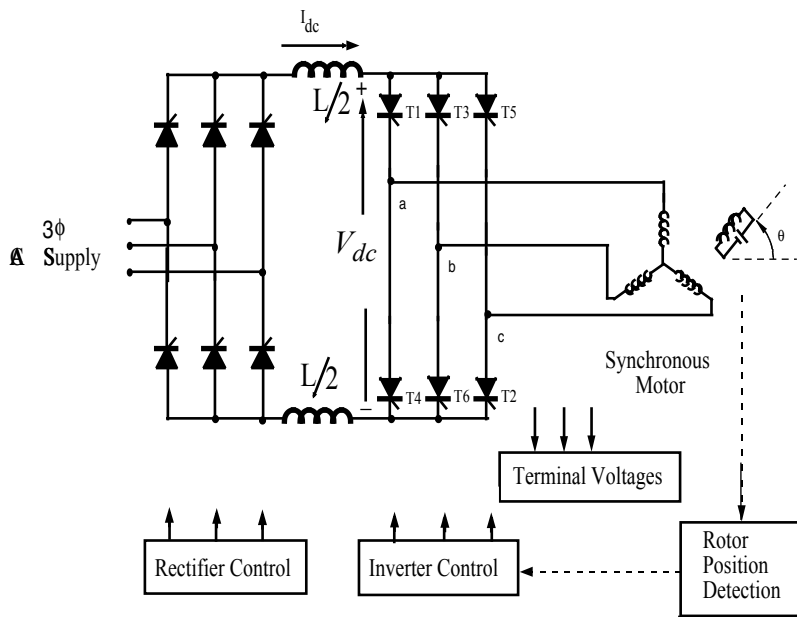


Figure 8.1 Basic load commutated inverter synchronous motor drive system.

The machine side converter normally operates in the inversion mode. Since the polarity of the machine voltage must be instantaneously positive as the current flows into the motor to commutate the bridge thyristors, the synchronous machine must operate at a sufficiently leading power factor to provide the volt-seconds necessary to overcome the internal reactance opposing the transfer of current from phase to phase (commutating reactance). Such load *emf* dependent commutation is called *load commutation*. As a result of the action of the link inductor, such an inverter is frequently termed a naturally commutated *current source inverter* (CSI).

Because the motor is separated from the AC supply by the DC link, it does not operate in a true synchronous mode where the mechanical speed is determined by the supply frequency. In the LCI drive, the inverter switching signals are derived from the rotor position [1] or from the stator terminal voltages [2] so that the inverter frequency is determined by the rotor speed, and the machine and inverter are always in synchronism. For this reason the LCI drive is sometimes called a *self-controlled synchronous machine*.

8.3 Principle of Inverter Operation

In order to rotate the stator magnetic field within the machine inverter, thyristors T1–T6 fire in sequence, one every 60 electrical degrees of operation. In this manner, the DC link current is distributed to the stator windings as balanced three-phase rectangular waves of current, illustrated in the idealized waveforms of Figure 8.2.

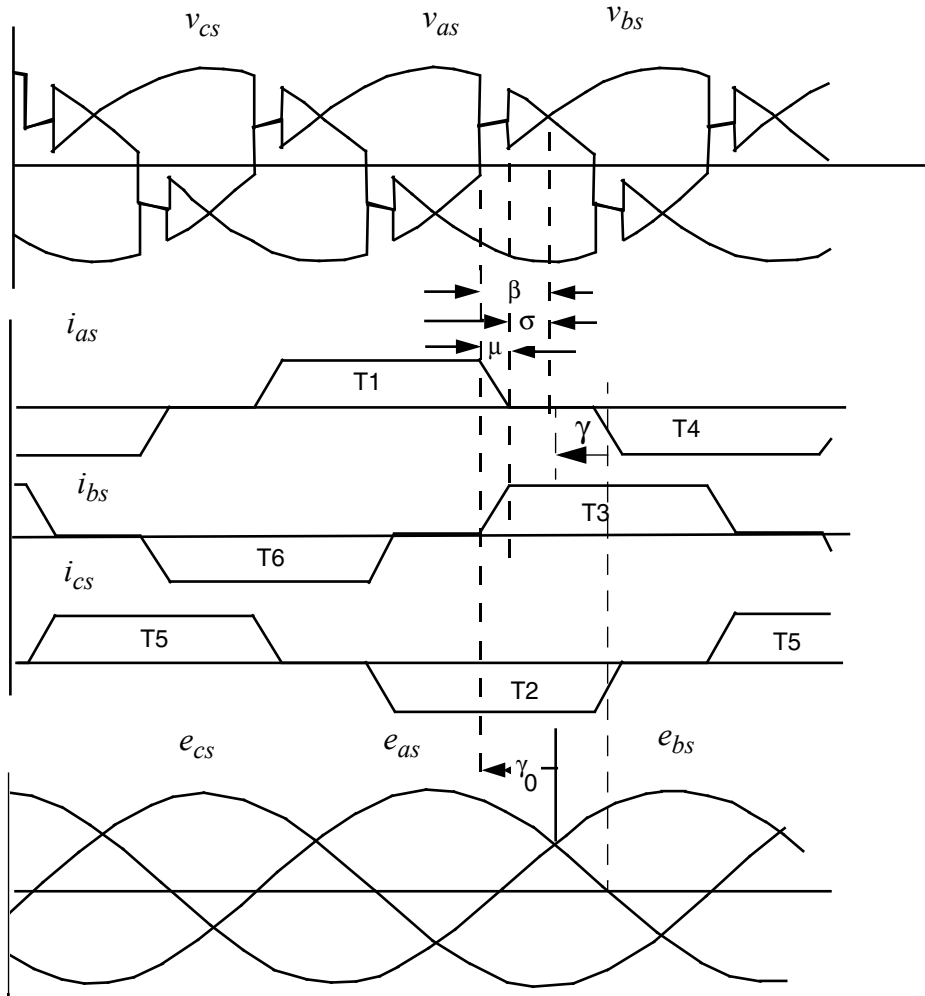


Figure 8.2 Idealized waveforms with synchronous motor operating with a load commutated inverter.

Operation of the inverter can best be illustrated by examining a single commutation event, say from thyristor T1 connected to phase *a* to T3 connected to phase *b*. The start of commutation is defined by the *commutation lead angle* β relative to the point at which machine terminal phase voltages v_{as} and v_{bs} become equal, as shown in [Figure 8.2](#). Once T3 is switched on, since v_{ab} is positive, the machine voltage v_{ab} forces current from phase *a* to phase *b*. The rate of rise of current in T3 is limited by the commutating reactance, which is approximately equal to the subtransient reactance of the machine.

During the interval defined by the *commutation overlap angle* μ , the current in T3 rises to a level of I_{dc} , while the current in T1 falls to zero. When the current in T1 goes to zero, v_{ab} appears as a reverse voltage across thyristor T1, for a period defined by the *commutation safety margin angle* σ . The commutation margin angle defines the time available to the thyristor to recover before it must again support forward voltage.

In practice, control of the inverter based on the lead angle β requires a signal proportional to the terminal voltage. Initiation of commutation can also be defined by the *mechanical firing angle*, γ_0 , relative to the internal voltage E_i . Since the internal voltage is induced by the rotation of the field flux, γ_0 is directly related to rotor position, and can be obtained from an appropriate rotor position transducer.

Successful commutation of the inverter requires first of all that the commutation process be completed within σ degrees of initiation. Otherwise the change in polarity of the machine voltage v_{ab} will drive the current in T1 positive again, resulting in a commutation failure. In addition, the time that the thyristor is reverse biased, defined by the safety margin angle σ , must be greater than the reverse recovery time of the solid state switching device (i.e., the thyristor). If the thyristor is forward biased before it has turned off completely, it will turn back on, again resulting in a commutation failure. In cases where the lead angle β is greater than 60 degrees, the overlap angle μ can not exceed 60 degrees. If it does, T4 will turn on before T1 turns off, resulting in a double overlap condition where the DC current is shunted past the machine and commutation failure ensues.

8.4 Fundamental Component Representation

In general, operation from a converter supply involves modes of operation in which the stator current is changing rapidly followed by intervals in which the current is essentially constant. A detailed solution of such a mode of operation will be attempted later in this chapter. If great accuracy is not required, the steady-state behavior of a synchronous machine can be described by the phasor diagram of its fundamental voltages and currents.

In the study of synchronous machines, it has been demonstrated that it is common to deal with brief transients by assuming that the flux linkages of the rotor circuits remain constant throughout the transient. This assumption is valid when the transient is short compared with the machine subtransient time constant and leads to a model of the machine as a constant voltage E'' behind subtransient reactance x'' . For most operating speeds of the LCI motor drive, the commutation transient is brief, in the sense that the subtransient time constant is of the order of a few cycles of rated frequency, while the commutation takes place in less than one sixth of a cycle.

In reference [3] it was assumed that the model of the machine as a voltage behind subtransient reactance is valid. This assumption reduces the problem of analyzing the machine/converter interaction to that of analyzing a current source inverter feeding into a voltage source of magnitude E'' with source reactance x'' . The pertinent results of reference [3] are summarized below, with suitable changes made for consistency in notation.

8.4.1 Phasor Diagram

A phasor diagram for an LCI synchronous machine, operating in the motoring mode at leading power factor, is shown in [Figure 8.3](#), where the resistive voltage drops have been neglected for simplicity. The internal voltage phasor E_i , which lies along the q -axis, is induced by the rotating field flux emanating from the rotor as a result of field current and is given by

$$E_i = x_{md} I_{fr} \quad (8.1)$$

Since leading power factor is needed to support commutation, the fundamental component of stator current is assumed to lead the internal voltage E_i by γ degrees. The angle γ is closely related to the firing angle γ_0 and is also

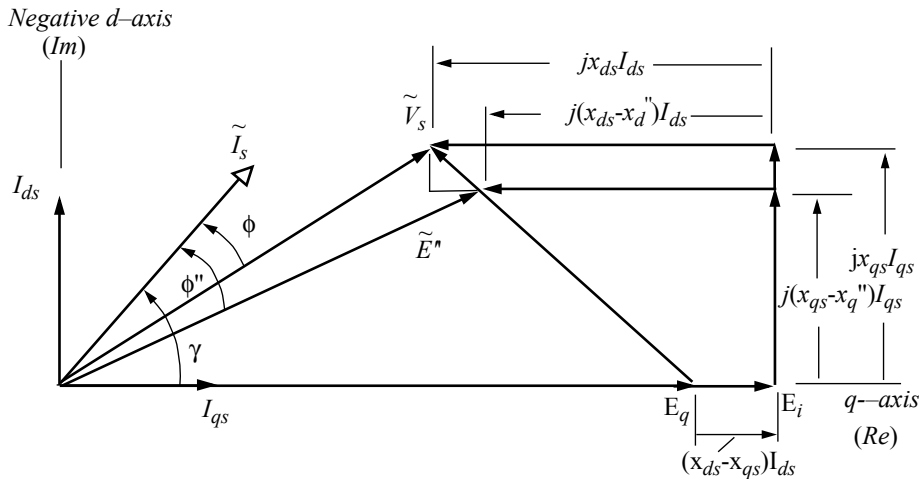


Figure 8.3 Fundamental component phasor diagram of synchronous motor operating from a load commutated inverter showing voltage behind sub-transient reactance E'' .

shown in [Figure 8.2](#). The components of current along the d - and q -axes are then

$$I_{qs} = I_s \cos \gamma \quad (8.2)$$

$$I_{ds} = -I_s \sin \gamma \quad (8.3)$$

It should be noted that, because the machine is overexcited, the d -axis component of current is negative, and hence tends to demagnetize the machine.

The fundamental component of terminal voltage V_s is expressed as

$$\tilde{V}_s = \tilde{E}_i + jI_{ds}x_{ds} + jI_{qs}x_{qs} \quad (8.4)$$

and, since \tilde{V}_s is also equal to

$$\tilde{V}_s = \tilde{E}'' + jI_{ds}x_d'' + jI_{qs}x_q'' \quad (8.5)$$

the voltage behind subtransient reactance may be expressed as

$$\tilde{E}'' = \tilde{E}_i + I_{ds}(x_{ds} - x_d'') + jI_{qs}(x_{qs} - x_q'') \quad (8.6)$$

It is often the case that the subtransient reactances are nearly equal on the two axes. If it is assumed that $x_d'' = x_q'' = x''$, then the voltage behind subtransient reactance may be simplified to

$$\tilde{E}'' = E_q + jI_s(x_{qs} - x'') \quad (8.7)$$

where E_q is a voltage phasor along the q -axis (real axis), defined as usual by

$$E_q = E_i + I_{ds}(x_{ds} - x_{qs}) \quad (8.8)$$

8.4.2 Inverter Operation

Commutation of a phase controlled converter delivering constant current to a voltage source of amplitude E'' can be analyzed by evaluating the volt-second integral necessary to commutate the current I_{dc} through the source reactance x'' [4]. Consider for example the commutation of current from the thyristor T1 to T3 as denoted in Figure 8.1 and illustrated in Figure 8.2. An equivalent circuit for this case is illustrated in Figure 8.4.

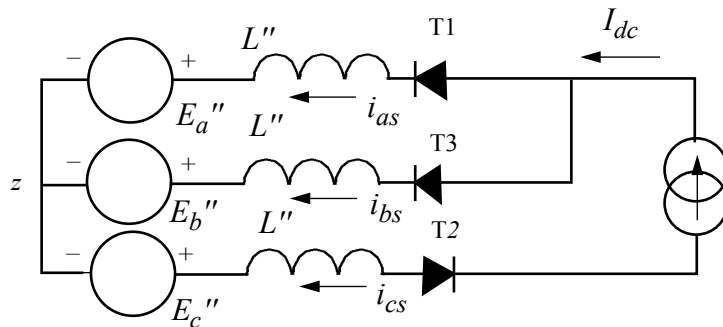


Figure 8.4 Equivalent circuit for commutation from phase a to phase b .

Immediately before the commutation event, T1 and T2 are assumed to be on. At time $t = 0$, thyristor T3 is fired. Since the internal voltage $E_a'' - E_b''$ is greater than zero at this instant, current will circulate such that i_{as} will tend to decrease and i_{bs} will tend to increase. The currents i_{as} and i_{bs} are described by

$$E_a'' - E_b'' = L'' \frac{di_{bs}}{dt} - L'' \frac{di_{as}}{dt} \quad (8.9)$$

where

$$i_{as} + i_{bs} = I_{dc} \quad (8.10)$$

where I_{dc} is assumed to be constant. By differentiating Eq. (8.10) with respect to time, it is evident that

$$\frac{di_{as}}{dt} + \frac{di_{bs}}{dt} = 0 \quad (8.11)$$

so that the $L''(di/dt)$ drop is shared equally between the two phases.

Eliminating i_{bs} from Eq. (8.10) using Eq. (8.11), the instantaneous voltage across the inductor of off-going phase a is therefore

$$\frac{E_b'' - E_a''}{2} = L'' \frac{di_{as}}{dt} \quad (8.12)$$

However,

$$E_b'' - E_a'' = \sqrt{3} E'' \sin(\omega_e t - \beta) \quad (8.13)$$

The current i_{as} is found by integrating Eq. (8.12), so that

$$i_{as} = \frac{\sqrt{3}}{2L''} \int_0^t E'' \sin(\omega_e t - \beta) dt + I_{dc} \quad (8.14)$$

Evaluation of this integral leads to the following

$$i_{as} = \frac{\sqrt{3} E''}{2\omega_e L''} [\cos \beta - \cos(\omega_e t - \beta)] + I_{dc} \quad (8.15)$$

and, from Eq. (8.10),

$$i_{bs} = \frac{\sqrt{3} E''}{2\omega_e L''} [\cos(\omega_e t - \beta) - \cos \beta] \quad (8.16)$$

The first portion of the angle β corresponds to the commutation overlap period. When $t = \mu/\omega_e$, the current has completely transferred from phase a to phase b , whereupon $i_{as} = 0$. Thus, from Eq. (8.15),

$$i_{as}(\mu/\omega_e) = 0 = \frac{\sqrt{3} E''}{2\omega_e L''} [\cos \beta - \cos(\mu - \beta)] + I_{dc} \quad (8.17)$$

and, since $\sigma = \beta - \mu$, finally,

$$\cos\sigma - \cos\beta = \frac{2\omega_e L''}{\sqrt{3}E''} I_{dc} \quad (8.18)$$

The angles β and σ are defined in [Figure 8.3](#).

Another relationship between β and σ can be obtained from power balance considerations. That is, if no power is consumed by the solid state power converter, then

$$V_{dc} I_{dc} = \frac{3}{2} E'' I_s \cos\phi'' \quad (8.19)$$

The terms on either side of Eq. (8.19) can be determined independently if one solves for the average voltage on the DC side in terms of the AC side voltage. If time $t = 0$ is taken to be the point where the phase a and c voltages intersect, then the average DC voltage is, on open circuit ($\mu = 0$),

$$\begin{aligned} V_{dc0} &= \frac{3}{\pi} \int_{-\beta}^{\frac{\pi}{3}-\beta} v_{ca} d\theta \\ &= \frac{3\sqrt{3}}{\pi} E'' \int_{\beta}^{\left(\frac{\pi}{3}-\beta\right)} \sin\left(\theta - \frac{2\pi}{3}\right) d\theta \\ &= \frac{3\sqrt{3}}{\pi} E'' \left[\cos\left(\beta + \frac{\pi}{3}\right) - \cos\left(\beta + \frac{2\pi}{3}\right) \right] \\ &= \frac{3\sqrt{3}}{\pi} E'' \cos\beta \end{aligned} \quad (8.21)$$

When current flows, a voltage drop occurs due to commutation. During the commutation interval, from Eq. (8.14),

$$\Delta V_{dc} = L'' \frac{di_{as}}{dt} \quad (8.22)$$

$$= \frac{\sqrt{3}E''}{2} \sin(\omega_e t - \beta) \quad (8.23)$$

The average value of ΔV_{dc} is

$$\hat{\Delta V_{dc}} = \left(\frac{3}{\pi}\right)\left(\frac{\sqrt{3}E''}{2}\right) \int_0^{(\beta - \sigma)} \sin(\omega_e t - \beta) d(\omega_e t) \quad (8.24)$$

$$= \left(\frac{3}{\pi}\right)\left(\frac{\sqrt{3}E''}{2}\right)(\cos\beta - \cos\sigma) \quad (8.25)$$

However, from Eq. (8.18),

$$\Delta V_{dc} = -\frac{3}{\pi}\omega_e L'' I_{dc} \quad (8.26)$$

The average DC voltage under load is

$$V_{dc} = V_{dc0} - \Delta V_{dc} \quad (8.27)$$

whereupon

$$V_{dc} = \frac{3}{\pi}(\sqrt{3}E'' \cos\beta + \omega_e L'' I_{dc}) \quad (8.28)$$

If it is assumed that the AC current remains quasi-rectangular 120 degree blocks of current, then the peak fundamental component of stator current is related to the DC current by

$$I_s = \frac{2}{\pi} \int_{-\frac{\pi}{3}}^{\frac{\pi}{3}} I_{dc} \cos\theta d\theta \quad (8.29)$$

$$I_s = \frac{2\sqrt{3}}{\pi} I_{dc} \quad (8.30)$$

Upon inserting Eqs. (8.28) and (8.30) into the expression for power balance,

$$V_{dc} I_{dc} = \frac{3}{\pi}(\sqrt{3}E'' \cos\beta + \omega_e L'' I_{dc}) I_{dc} \quad (8.31)$$

$$\frac{3}{2}E'' I_s \cos\phi'' = \frac{3}{2}E'' \left(\frac{2\sqrt{3}}{\pi} I_{dc}\right) \cos\phi'' \quad (8.32)$$

or

$$\sqrt{3}E'' \cos\beta + \omega_e L'' I_{dc} = E'' \sqrt{3} \cos\phi'' \quad (8.33)$$

so that

$$\cos \beta = \left(\frac{E'' \cos \phi'' - \frac{1}{\sqrt{3}} I_{dc} x''}{E''} \right) \quad (8.34)$$

where $x'' = \omega_e L''$. Thus, from Eq. (8.18),

$$\cos \sigma = \left(\frac{E'' \cos \phi'' + \frac{1}{\sqrt{3}} I_{dc} x''}{E''} \right) \quad (8.35)$$

If the internal state of the machine is known (i.e., E'', x'', ϕ'') the firing instant for each ongoing thyristor can be calculated from Eq. (8.34) together with a measurement of rotor position. It is important to note from Figure 8.3 that, since the stator resistances have been neglected, the entire phasor diagram grows or shrinks as speed (and hence frequency) increases or decreases. Therefore, the angles β and σ should remain constant. In practice, however, it is important to remember that these angles change drastically as frequency is reduced due to the stator resistive drop becoming a larger and larger portion of the voltage drop as frequency decreases.

8.4.3 Expression for Power and Torque

Definitions (8.7) and (8.8) lead to the following expressions for the power developed in the machine

$$P_e = \left(\frac{3}{2} \right) E'' I_s \cos \phi'' = \left(\frac{3}{2} \right) E_q I_s \cos \gamma \quad (8.36)$$

If the inverter losses and the machine resistances are neglected, the DC power will equal the input AC power, or

$$V_{dc} I_{dc} = \left(\frac{3}{2} \right) E'' I_s \cos \phi'' \quad (8.37)$$

From Eq. (8.30) it follows that the DC voltage is

$$V_{dc} = \frac{3\sqrt{3}}{\pi} E'' \cos \phi'' = \frac{3\sqrt{3}}{\pi} E_q \cos \gamma \quad (8.38)$$

The average torque developed by the machine is related to the power delivered to the internal *emf* E_q and, from Figure 8.3, can be written as

$$T_e = \left(\frac{3}{2}\right) \frac{E_q I_s \cos \gamma}{\omega_{rm}} \quad (8.39)$$

where ω_{rm} is the synchronous mechanical speed. Since E_q is speed dependent, the apparent speed dependence cancels. Thus, for a fixed value of the internal angle γ , the system behaves like a DC machine (as for field oriented drives) and direct steady-state torque control is possible by controlling $I_{qs} = I_s \cos \gamma$.

8.5 Control Considerations

Direct control of γ by use of a rotor position sensor has traditionally been applied in LCI drives but has largely been replaced by schemes using terminal voltage and current sensing to indirectly control γ . Direct control of the commutation margin angle σ (more correctly, the safety margin time σ / ω where ω is the motor angular frequency), illustrated in [Figure 8.2](#), has the advantage of causing operation at the highest possible power factor and hence gives the best utilization of the machine windings. The waveforms in Figure 8.2 also demonstrate that changes in the commutation overlap angle μ resulting from current or speed changes produce significant differences between the actual value of γ and the ideal value γ_0 . For this reason, compensators are required in direct γ controllers. This compensation is automatic in systems based on controlling the margin angle σ .

8.5.1 Firing Angle Controller

[Figure 8.5](#) shows a schematic diagram of a control circuit which can be used to determine the correct firing pulse instant. The principle of the controller is to compute the firing pulse instant so that the necessary volt-seconds are available to commutate the current between phases and also to ensure that sufficient time is available to allow recovery of the off-going thyristor. The computations of this figure can be explained by rearranging Eq. (8.18) as follows:

$$\frac{\sqrt{3} E''}{\omega_e} \cos \beta = \frac{\sqrt{3} E''}{\omega_e} \cos \sigma + 2 L'' I_{dc} \quad (8.40)$$

The left hand side of Eq. (8.40) represents the total volt-seconds available after triggering the on-going thyristor. This time is equal to the volt-seconds consumed by the commutation process (as illustrated by Eq. (8.26)) plus the volt-seconds available for thyristor recovery. The controller principle can be imple-

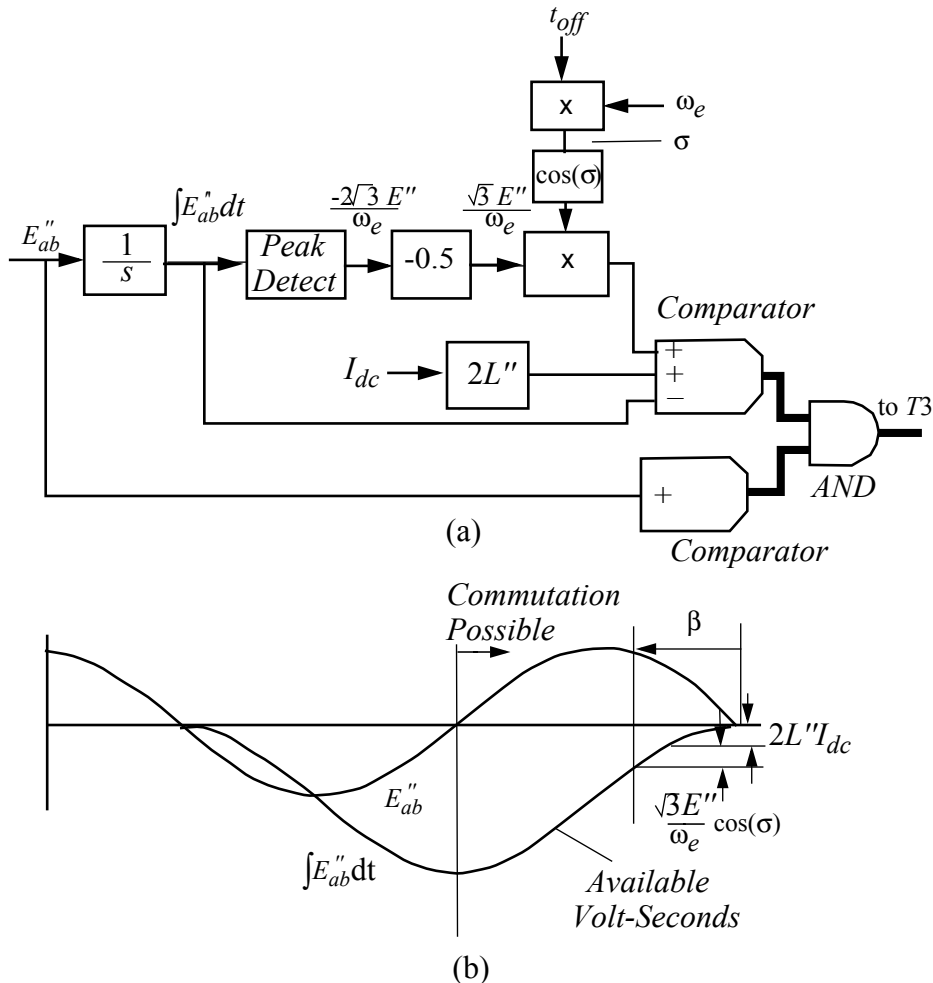


Figure 8.5 (a) Functional block diagram and (b) waveforms of firing pulse calculation.

mented by calculating the integral of the line-to-line voltage, which therefore corresponds to the voltseconds available for commutation. When the integral of this voltage becomes less than the recovery time volt–seconds plus the commutation time volt–seconds, then the thyristor is commanded to be fired. It should be noted that the computation of the integral uses “past history” information to predict the future. And sudden changes in speed, for example, could influence the accuracy of the prediction. Also, it is important to note that the stator iR drop is neglected in this computation, which may be valid for a large

machine but not for a smaller application. However, these problems are readily dealt with.

8.6 Starting Considerations

Load commutation of a synchronous machine is accomplished by adjusting the field current such that the *emf* is sufficiently large (and lagging the current) to ensure transfer of current from phase to phase. The *emf* is also proportional to rotor speed since this voltage is essentially due to “flux cutting action” of the rotor flux rotating past the stationary rotor conductors.

While load commutation is an effective and inexpensive method for commutating the machine side converter bridge, operation at or near zero speed is not possible since the *emf* approaches zero. Operation under these conditions is important since they occur during every start and stop of the machine. Commutation of the machine side bridge, however, can be maintained if the line side bridge, which always has sufficient commuting kVARs, is controlled to produce zero current intervals on the DC link, as shown in [Figure 8.6](#). Since the DC current becomes zero, the currents in all thyristors are also zero. The zero current intervals allow the previously conducting thyristors comprising the load side converter to recover their blocking ability. The bridge thyristors are sequentially fired in pairs to direct the current through the two appropriate phases and hence synchronize the stator MMF to the rotor as it begins to rotate. Since six commutations occur per cycle, the frequency of the DC link pulses must be six times the motor line frequency. Because of the inductance afforded by the DC link inductor, the pulsing procedure can only be continued to 2 or 3 Hz, at which time normal load commutation is initiated. In most cases rated motor torque can not be supported by artificial commutation even to 2–3 Hz. Fortunately, however, such drives find their greatest application in fan or pump type loads in which the torque requirements at low speed are relatively modest.

8.7 Detailed Steady-State Analysis

More detailed steady-state analyses of the LCI drive than presented thus far have been undertaken in the past. One approach is to assume a constant DC link current and to neglect the resistances in the machine [3],[4]. The methods of Ref. [3] have been found to yield accurate results in terms of the fundamen-

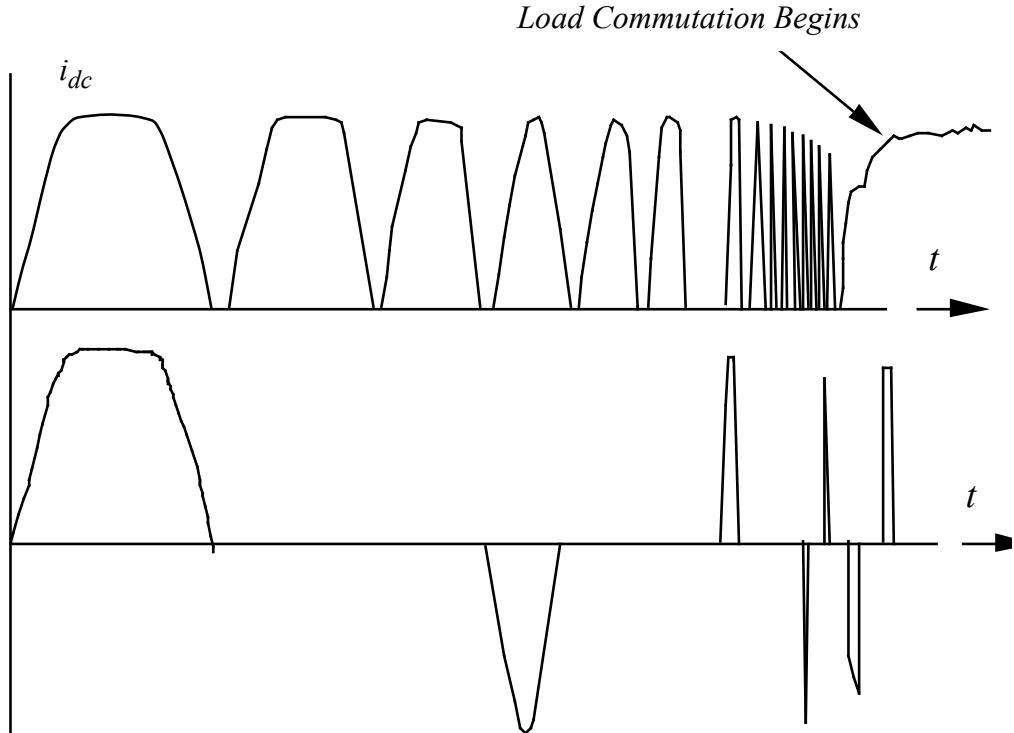


Figure 8.6 DC link current and motor phase current illustrating artificial commutation at low speed.

tal components of voltage and current, but do not provide detailed information on the waveforms. In addition, neglecting the resistances can make the results somewhat inaccurate at low operating frequencies, where the subtransient time constant is significant compared to the commutation time.

Analyses of the LCI drive that include machine resistances and finite DC link inductance are necessarily more involved than those employing simpler models. A state space formulation of the problem has been used in [5], but this method requires several iterations of the numerical integrations in order to find the boundary conditions. Reference [6] employs a Fourier series expansion of the voltage and current waveforms, and requires several terms in the series for accuracy, and several iterations of the solution to meet the boundary conditions. Computation times of the order of a few minutes are reported for this method.

The analysis developed here permits accurate calculation of voltage, current, and torque waveforms under the assumptions of constant shaft speed and constant DC link current. The problem is formulated in terms of the synchronous machine equations (Park's equations) making it relatively easy to investigate the influence of the machine parameters on the performance of the LCI drive.

Steady-state solutions are characterized by the firing angle γ_0 and the commutation overlap angle μ . The ratio of average field current to DC link current is calculated as one of the boundary conditions necessary to guarantee a solution at the specified values of γ_0 and μ . The symmetry of steady-state operation allows the proper boundary conditions to be found directly, without the need for iteration. This technique, which has been used previously in the study of induction motor drives [7],[8], is employed here to provide a substantial reduction in the computation time necessary to obtain a solution. The major portion of this development is taken from the M.S. thesis of R.S. Colby [9].

Although appearing to be extremely complex, because of the symmetry involved, the solution for steady-state operation can be found utilizing the state variable technique. In general, any time step solution that involves steady-state requires that the initial conditions be known. By employing the state transition matrix method and exploiting the inherent symmetry of the steady-state operation, the initial conditions can be found directly, without any iteration. After the initial conditions are found, the time step solution for the state variables becomes a straightforward matter.

The state variable solution presented here is carried out under two main assumptions. The first assumption is that the rotor speed is constant. This statement is equivalent to assuming that the mechanical load inertia is sufficiently large to prevent significant speed variations as a result of torque pulsations and is a reasonable approximation under most steady-state operating conditions.

The second assumption is that the DC link current is constant and is equivalent to assuming that the DC link inductance is large enough to prevent significant current ripple due to variations in the instantaneous voltages on the inverter and rectifier. The main advantage of this assumption is that it reduces the number of independent state variables, making the solution far easier than that for the case of a finite DC link inductor.

In addition to the above two assumptions, the usual assumptions concerning thyristors are made here. That is, device characteristics such as forward voltage drop and reverse recovery time are ignored, and the devices are treated as “ideal” thyristors which turn on when a gate signal is applied and turn off when the forward current goes to zero.

8.7.1 Modes of Converter Operation

When the LCI drive is operating in the steady-state, it can be recalled that inverter thyristors T1–T6 fire in sequence, one every 60 electrical degrees of operation, causing the stator *MMF* to advance 60° with each switching event. As a consequence, a complete steady-state solution can be obtained by analysis of any interval that is 60 electrical degrees in length.

The 60° interval chosen for this analysis begins when thyristor T5 turns off and ends when thyristor T6 turns off. This interval comprises two modes of operation, which will be denoted the *conduction* and *commutation* modes. During the conduction mode, thyristors T1 and T6 are on, and the DC link current flows from phase *a* to phase *b*, as seen in Figure 8.7. The commutation mode begins when thyristor T2 is gated on. A short-circuit is established between phases *b* and *c*, and a circulating current i_k flows from phase *c* to *b*, eventually turning off phase *b*, as shown in the right half of Figure 8.7. During this mode

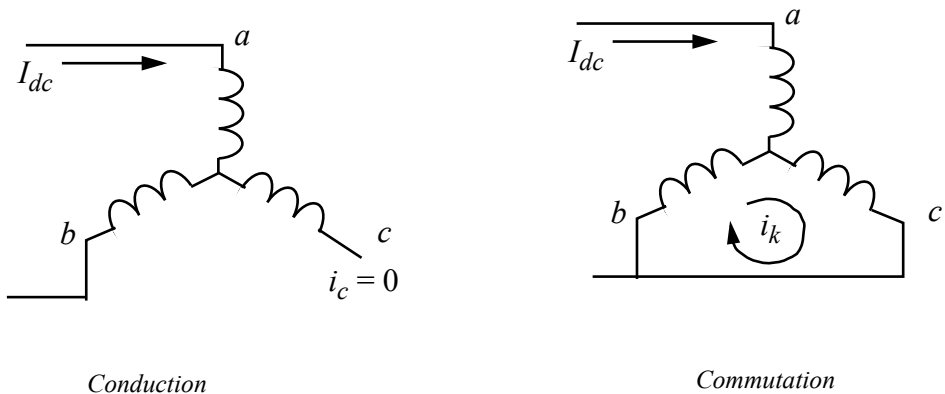


Figure 8.7 Conduction and commutation modes.

the DC link current is commuting from phase *b* to phase *c*. The commutation current is indicated by circulating current i_k , which starts at a value of zero and rises to a value of I_{dc} at the end of the commutation mode.

It is useful to define the two modes of operation in terms of the rotor position. At the transition from conduction to commutation mode, marked by the firing of thyristor T2, the rotor is at a negative angle

$$\theta = -\gamma_0$$

as indicated in Figure 8.8. This is equivalent to the definition of $-\gamma_0$, as indi-

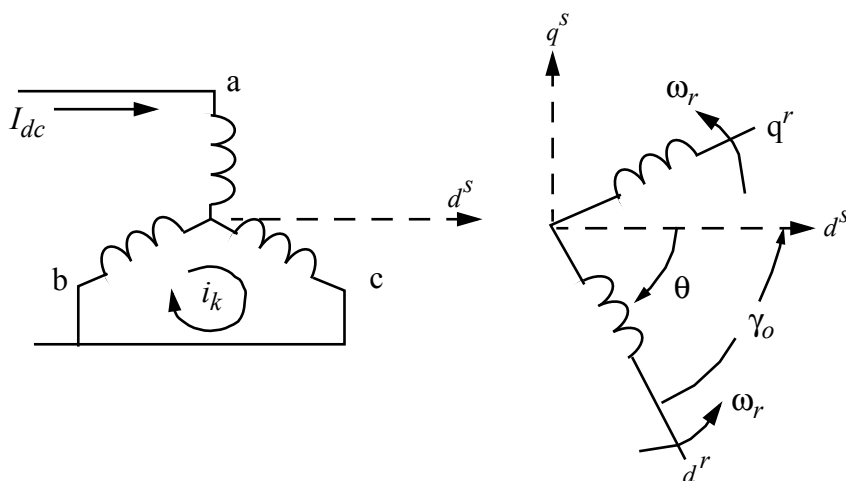


Figure 8.8 Rotor position at start of the commutation mode.

cated in Figure 8.3. During the commutation mode, the rotor advances through μ electrical degrees, where μ is the commutation overlap angle. Thus, at the end of the 60° interval, the rotor is at position

$$\theta = -\gamma_0 + \mu$$

and at the beginning of the interval it is at the position

$$\theta_0 = -\gamma_0 + \mu - \frac{\pi}{3}$$

The firing angle γ_0 is equivalent to the internal power factor angle neglecting overlap, i.e., it is the angle between the fundamental component of current, neglecting overlap, and the internal voltage of the synchronous machine.

8.7.2 State Equations

The synchronous machine used in this application is typically of salient-pole construction. Since damper windings have an important influence on the commutation time of the machine, such machines are usually equipped with a wound field together with one damper winding on each rotor axis. When the rotor rotates at synchronous speed, $\omega_r = \omega_e$. The circuit equations for this model are then expressed in the rotor reference frame as Eq. (8.41).

$$\begin{bmatrix} v_{qs} \\ v_{ds} \\ 0 \\ 0 \\ v_{fr} \end{bmatrix} = \begin{bmatrix} r_s + \frac{p}{\omega_b} x_{qs} & \frac{\omega_e}{\omega_b} x_{ds} & \frac{p}{\omega_b} x_{mq} & \frac{\omega_r}{\omega_b} x_{md} & \frac{\omega_r}{\omega_b} x_{md} \\ -\frac{\omega_r}{\omega_b} x_{qs} & r_s + \frac{p}{\omega_b} x_{ds} & -\frac{\omega_r}{\omega_b} x_{mq} & \frac{p}{\omega_b} x_{md} & \frac{p}{\omega_b} x_{md} \\ \frac{p}{\omega_b} x_{mq} & 0 & r_{qr} + \frac{p}{\omega_b} x_{qr} & 0 & 0 \\ 0 & \frac{p}{\omega_b} x_{md} & 0 & r_{dr} + \frac{p}{\omega_b} x_{dr} & \frac{p}{\omega_b} x_{md} \\ 0 & \frac{p}{\omega_b} x_{md} & 0 & \frac{p}{\omega_b} x_{md} & r_{fr} + \frac{p}{\omega_b} x_{fr} \end{bmatrix} \cdot \begin{bmatrix} i_{qs} \\ i_{ds} \\ i_{qr} \\ i_{dr} \\ i_{fr} \end{bmatrix} \quad (8.41)$$

The electromagnetic torque is written as

$$T_e = \frac{3P}{2} \frac{1}{2\omega_b} (\Psi_{ds} i_{qs} - \Psi_{qs} i_{ds}) \quad (8.42)$$

where Ψ_{ds} and Ψ_{qs} are the stator flux linkages,

$$\Psi_{ds} = x_{ds} i_{ds} + x_{md} (i_{dr} + i_{fr}) \quad (8.43)$$

$$\Psi_{qs} = x_{qs} i_{qs} + x_{mq} i_{qr} \quad (8.44)$$

At a constant rotor speed, the state of the machine is determined completely by the currents i_{qs} , i_{ds} , i_{qr} , i_{dr} , and i_{fr} . However, with a constant DC link current, the stator currents contain only one independent variable, the circulating current i_k , which is nonzero only during the commutation interval.

The stator currents, in the rotor reference frame, can be written in terms of the d -axis current in the stator frame by

$$\dot{i}_{ds}^s = \frac{1}{\sqrt{3}} (i_c - i_b) \quad (8.45)$$

$$= \frac{1}{\sqrt{3}}(-i_k - (i_k)) \quad (8.46)$$

$$= -\frac{2}{\sqrt{3}}i_k \quad (8.47)$$

while

$$i_{qs}^s = I_{dc} \quad (8.48)$$

The $d-q$ currents expressed in the rotor frame of reference are

$$i_{qs} = i_{qs}^s \cos \theta + i_{ds}^s \sin \theta \quad (8.49)$$

$$i_{ds} = i_{qs}^s \sin \theta - i_{ds}^s \cos \theta \quad (8.50)$$

or, since the commuting current lies along the negative stator frame d -axis,

$$i_{qs} = I_{dc} \cos \theta + \frac{2}{\sqrt{3}}i_k \sin \theta \quad (8.51)$$

$$i_{ds} = I_{dc} \sin \theta - \frac{2}{\sqrt{3}}i_k \cos \theta \quad (8.52)$$

Because the circulating current i_k is nonzero only during the commutation mode, the state equations must take on somewhat different forms during the two modes termed the conduction state and the commutation state.

8.7.3 Conduction Mode 1 State Equations

During the conduction mode the circulating current i_k is zero. This constraint is satisfied by defining a dummy state equation for this interval,

$$\left(1 + \frac{p}{\omega_b}\right)i_k = 0 \quad (8.53)$$

Clearly the solution of this equation is $i_k = 0$ provided that $i_k = 0$ at the beginning of the interval.

Setting $i_k = 0$ in Eq. (8.45) and (8.46) and substituting into the rotor circuit equations (the bottom three rows of (8.41)), yields terms proportional to $\cos \theta$ and $\sin \theta$, which are the result of the constant DC link current reflected to the moving rotor. Rather than have these terms appear as time varying inputs to the system, it is desirable to generate $\cos \theta$ and $\sin \theta$ as auxiliary state variables y_1

and y_2 . Since the rotor speed and initial position are known, this is easily accomplished by solving the auxiliary equations

$$\begin{bmatrix} p & \omega_e \\ \omega_b & \omega_b \\ -\omega_e & p \\ \omega_b & \omega_b \end{bmatrix} \cdot \begin{bmatrix} y_1 \\ y_2 \end{bmatrix} = \begin{bmatrix} 0 \\ 0 \end{bmatrix} \quad (8.54)$$

where $y_1(0) = 1$, $y_2(0) = 0$, making $y_1 = \cos[(\omega_e/\omega_b)\omega_b t] = \cos(\omega_e t)$, and $y_2 = \sin[(\omega_e/\omega_b)\omega_b t] = \sin(\omega_e t)$.

The functions y_1 and y_2 are combined with the currents to make up an augmented state vector,

$$x = [i_{qr} \ i_{dr} \ i_{fr} \ i_k \ y_1 \ y_2]^T \quad (8.55)$$

The three rotor circuit equations, the dummy state equation, Eqs. (8.53), and the auxiliary state equations (8.54) can now be cast in matrix form as Eq. (8.56).

$$\begin{bmatrix} r_{qr} + \frac{p}{\omega_b} x_{qr} & 0 & 0 & 0 & 0 & -\frac{\omega_e}{\omega_b} I_{dc} x_{mq} \\ 0 & r_{dr} + \frac{p}{\omega_b} x_{dr} & \frac{p}{\omega_b} x_{md} & 0 & \frac{\omega_e}{\omega_b} I_{dc} x_{md} & 0 \\ 0 & \frac{p}{\omega_b} x_{md} & r_{fr} + \frac{p}{\omega_b} x_{fr} & 0 & \frac{\omega_e}{\omega_b} I_{dc} x_{md} & 0 \\ 0 & 0 & 0 & 1 + \frac{p}{\omega_b} & 0 & 0 \\ 0 & 0 & 0 & 0 & \frac{p}{\omega_b} & \frac{\omega_e}{\omega_b} \\ 0 & 0 & 0 & 0 & -\frac{\omega_e}{\omega_b} & \frac{p}{\omega_b} \end{bmatrix} \times \begin{bmatrix} i_{qr} \\ i_{dr} \\ i_{fr} \\ i_k \\ y_1 \\ y_2 \end{bmatrix} = \begin{bmatrix} 0 \\ 0 \\ V_{fr} \\ 0 \\ 0 \\ 0 \end{bmatrix} \quad (8.56)$$

Since I_{dc} is as yet unknown, it must be moved to the right hand side of Eq. (8.56), resulting in the equivalent expression

$$\begin{bmatrix}
 r_{qr} + \frac{p}{\omega_b} x_{qr} & 0 & 0 & 0 & 0 & 0 \\
 0 & r_{dr} + \frac{p}{\omega_b} x_{dr} & \frac{p}{\omega_b} x_{md} & 0 & 0 & 0 \\
 0 & \frac{p}{\omega_b} x_{md} & r_{fr} + \frac{p}{\omega_b} x_{fr} & 0 & 0 & 0 \\
 0 & 0 & 0 & 1 + \frac{p}{\omega_b} & 0 & 0 \\
 0 & 0 & 0 & 0 & \frac{p}{\omega_b} & \frac{\omega_e}{\omega_b} \\
 0 & 0 & 0 & 0 & -\frac{\omega_e}{\omega_b} & \frac{p}{\omega_b}
 \end{bmatrix} \times \begin{bmatrix} i_{qr} \\ i_{dr} \\ i_{fr} \\ i_k \\ y_1 \\ y_2 \end{bmatrix} = \begin{bmatrix} \frac{\omega_e}{\omega_b} x_{mq} & 0 \\ -\frac{\omega_e}{\omega_b} x_{md} & 0 \\ -\frac{\omega_e}{\omega_b} x_{md} & 1 \\ 0 & 0 \\ 0 & 0 \\ 0 & 0 \end{bmatrix} \times \begin{bmatrix} I_{dc} \\ V_{fr} \end{bmatrix}$$

(8.57)

Letting

$$R_1 = \begin{bmatrix} r_{qr} & 0 & 0 & 0 & 0 & 0 \\ 0 & r_{dr} & 0 & 0 & 0 & 0 \\ 0 & 0 & r_{fr} & 0 & 0 & 0 \\ 0 & 0 & 0 & 1 & 0 & 0 \\ 0 & 0 & 0 & 0 & 0 & \frac{\omega_e}{\omega_b} \\ 0 & 0 & 0 & 0 & -\frac{\omega_e}{\omega_b} & 0 \end{bmatrix} \quad (8.58)$$

and

$$X_1 = \begin{bmatrix} x_{qr} & 0 & 0 & 0 & 0 & 0 \\ 0 & x_{dr} & x_{md} & 0 & 0 & 0 \\ 0 & x_{md} & x_{fr} & 0 & 0 & 0 \\ 0 & 0 & 0 & 1 & 0 & 0 \\ 0 & 0 & 0 & 0 & 1 & 0 \\ 0 & 0 & 0 & 0 & 0 & 1 \end{bmatrix} \quad (8.59)$$

and

$$B_1' = \begin{bmatrix} \frac{\omega_e}{\omega_b} x_{mq} & 0 \\ -\frac{\omega_e}{\omega_b} x_{md} & 0 \\ -\frac{\omega_e}{\omega_b} x_{md} & 1 \\ 0 & 0 \\ 0 & 0 \\ 0 & 0 \end{bmatrix} \quad (8.60)$$

During the conduction mode, mode 1, the state equations can be written

$$R_1 x + \frac{p}{\omega_b} X_1 x = B_1' u \quad (8.61)$$

where $u = [I_{dc} \ V_{fr}]^t$.

or, in the standard form,

$$\frac{p}{\omega_b} x = -X_1^{-1} R_1 x + X_1^{-1} B_1' u \quad (8.62)$$

or simply

$$px = A_1 x + B_1 u \quad (8.63)$$

where $A_1 = -\omega_b X_1^{-1} R_1$, and $B_1 = \omega_b X_1^{-1} B_1'$.

It should be noted that during the conduction mode, the system matrix A and the input coefficient matrix B are constants, i.e., the system is time-invariant.

8.7.4 Commutation Mode 2 State Equations

During the commutation interval, the circulating current i_k is no longer zero, so the full expressions for the stator currents Eqs. (8.45) and (8.46) must be used in the rotor circuit equations. In addition, the dummy state equation, (8.53), is no longer valid. The appropriate state equation for this mode is one that accounts for the short-circuit between phases b and c . Using Eq. (8.51), the differential equation corresponding to the third row of Eq. (8.41) becomes

$$0 = r_{qr}i_{qr} + \frac{p}{\omega_b}x_{qr}i_{qr} + \frac{p}{\omega_b}x_{mq}\left(I_{dc}\cos\theta + \frac{2}{\sqrt{3}}i_k\sin\theta\right) \quad (8.64)$$

Again terms appear containing sinusoidal quantities. The auxiliary matrix, Eq. (8.54), can again be constructed to generate these terms. The equations corresponding to the fourth and five rows of Eq. (8.41) can be obtained in a similar manner.

One additional equation must be generated to define the commutating current i_k . Transforming the stator voltage expressions to a stationary reference frame yields, for the d -axis voltage fixed in the stator,

$$v_{ds}^s = v_{ds}\cos\theta - v_{qs}\sin\theta \quad (8.65)$$

where v_{qs} and v_{ds} are given by the first and second rows of Eq. (8.41). After replacing the currents i_{qs} and i_{ds} in terms of their equivalents in the stationary frame using Eqs. (8.51) and (8.52) and, after a brief struggle, Eq. (8.65) becomes

$$\begin{aligned} v_{ds}^s &= \frac{1}{\sqrt{3}}(v_{cs} - v_{bs}) = 0 = -\frac{2}{\sqrt{3}}r_si_k - \frac{1}{\sqrt{3}}[x_{ds} + x_{qs} + (x_{ds} - x_{qs})\cos 2\theta]\frac{p}{\omega_b}i_k \\ &+ \frac{1}{\sqrt{3}}\frac{\omega_e}{\omega_b}(x_{ds} - x_{qs})i_k\sin 2\theta - x_{mq}\sin\theta\frac{p}{\omega_b}i_{qr} + x_{md}\cos\theta\frac{p}{\omega_b}(i_{dr} + i_{fr}) \\ &- \frac{\omega_e}{\omega_b}x_{mq}\cos\theta i_{qr} - \frac{\omega_e}{\omega_b}x_{md}\sin\theta(i_{dr} + i_{fr}) + \frac{\omega_e}{\omega_b}(x_{ds} - x_{qs})I_{dc}\cos 2\theta \end{aligned} \quad (8.66)$$

In this form double frequency terms also now appear explicitly as auxiliary state variables. The system equations valid during commutation can now be cast into matrix form, shown on the next page. Using trig identities, only one oscillator need again be used to generate the sinusoids of frequencies ω_r/ω_b and $2\omega_r/\omega_b$. The commutating mode state equations can be cast in matrix form as Eq. (8.67), on the next page, where the quantity a_{44} corresponds to

$$a_{44} = \frac{2}{\sqrt{3}}r_s - \frac{2}{\sqrt{3}}\frac{\omega_e}{\omega_b}(x_{ds} - x_{qs})y_1y_2 + \frac{2}{\sqrt{3}}[x_{ds}y_1^2 + x_{qs}y_2^2]\frac{p}{\omega_b} \quad (8.68)$$

By suitable matrix manipulation, these equations can also be put into standard form given by Eq. (8.63). The relevant R , X , and B' matrices are given by

$$\begin{bmatrix}
r qr + \frac{P}{\omega_b} x qr & 0 & 0 & -\frac{\omega_e}{\omega_b} I_{dc^x mq} \\
0 & r dr + \frac{P}{\omega_b} x dr & \frac{P}{\omega_b} x md & \frac{\omega_e}{\omega_b} I_{dc^x md} \\
0 & \frac{P}{\omega_b} x md & r fr + \frac{P}{\omega_b} x fr & \frac{\omega_e}{\omega_b} I_{dc^x md} \\
0 & x mq \left(\frac{\omega_e}{\omega_b} y_1 + y_2 \frac{P}{\omega_b} \right) & x md \left(\frac{\omega_e}{\omega_b} y_2 - y_1 \frac{P}{\omega_b} \right) & -\frac{\omega_e}{\omega_b} I_{dc^y 1} (x_{ds} - x_{qs}) \\
0 & 0 & 0 & \frac{\omega_e}{\omega_b} I_{dc^y 2} (x_{ds} - x_{qs}) \\
0 & 0 & 0 & \frac{\omega_e}{\omega_b} \\
0 & 0 & 0 & \frac{P}{\omega_b}
\end{bmatrix} = \begin{bmatrix}
0 \\
0 \\
0 \\
0 \\
0 \\
0
\end{bmatrix} \times \begin{bmatrix}
i qr \\
i dr \\
i fr \\
i k \\
y_1 \\
y_2
\end{bmatrix}$$

(8.67)

$$\mathbf{r}_2 = \begin{bmatrix} r_{qr} & 0 & 0 & \frac{2}{\sqrt{3}}x_{mq}\left(\frac{\omega_e}{\omega_b}y_1\right) & 0 & 0 \\ 0 & r_{dr} & 0 & \frac{2}{\sqrt{3}}x_{md}\left(\frac{\omega_e}{\omega_b}y_2\right) & 0 & 0 \\ 0 & 0 & r_{fr} & \frac{2}{\sqrt{3}}x_{md}\left(\frac{\omega_e}{\omega_b}y_2\right) & 0 & 0 \\ x_{mq}\left(\frac{\omega_e}{\omega_b}y_1\right)x_{md}\left(\frac{\omega_e}{\omega_b}y_2\right)x_{md}\left(\frac{\omega_e}{\omega_b}y_2\right)\frac{2}{\sqrt{3}}r_s - \frac{2}{\sqrt{3}}\frac{\omega_e}{\omega_b}(x_{ds} - x_{qs})y_1y_2 & 0 & 0 \\ 0 & 0 & 0 & 0 & 0 & \frac{\omega_e}{\omega_b} \\ 0 & 0 & 0 & 0 & -\frac{\omega_e}{\omega_b} & 0 \end{bmatrix} \quad (8.69)$$

$$\mathbf{Y}_2 = \begin{bmatrix} x_{qr} & 0 & 0 & \frac{2}{\sqrt{3}}x_{mq}y_2 & 0 & 0 \\ 0 & x_{dr} & x_{md} & -\frac{2}{\sqrt{3}}x_{md}y_1 & 0 & 0 \\ 0 & x_{md} & x_{fr} & -\frac{2}{\sqrt{3}}x_{md}y_1 & 0 & 0 \\ x_{mq}y_2 - x_{md}y_1 - x_{md}y_1 & \frac{2}{\sqrt{3}}[x_{ds}y_1^2 + x_{qs}y_2^2] & 0 & 0 & 1 & 0 \\ 0 & 0 & 0 & 0 & 0 & 0 \\ 0 & 0 & 0 & 0 & 0 & 1 \end{bmatrix} \quad (8.70)$$

and

$$B_2' = \begin{bmatrix} \frac{\omega_e}{\omega_b} x_{mq} & 0 \\ -\frac{\omega_e}{\omega_b} x_{md} & 0 \\ -\frac{\omega_e}{\omega_b} x_{md} & 1 \\ \frac{\omega_e}{\omega_b} (y_1^2 - y_2^2)(x_{ds} - x_{qs}) & 0 \\ 0 & 0 \\ 0 & 0 \end{bmatrix} \quad (8.71)$$

In this case the identity of the A and B matrices should now be clear from the context. During the commutation mode, the system matrix A and input coefficient matrix B are now time varying, being functions of the rotor angle θ . This is an inevitable consequence of having unbalanced components of stator current I_{dc} and i_k flowing in circuits that are in motion relative to an asymmetric rotor.

8.7.5 Calculation of Initial Conditions

The symmetry of steady-state operation provides a means to compute the boundary conditions for the steady-state operating point in closed form, without resorting to iterative calculations. This calculation requires that an expression be derived relating the initial values of the state variables to the final values, at the end of the 60° interval. The symmetry constraints are then applied to solve for the initial values of the rotor currents i_{qr} , i_{dr} , i_{fr} and for the field voltage v_{fr} .

For any linear, time invariant system with constant inputs, for example, the system described by Eq. (8.67), the state of the system at time t_1 is related to the initial state by [10]

$$x(t_1) = e^{At_1}x(0) + \lambda(t_1, 0)Bu \quad (8.72)$$

where e^{At} is the *state transition matrix*, and $\lambda(t_1, 0)$ is the integral,

$$\lambda(t_1, 0) = \int_0^{t_1} e^{At} dt \quad (8.73)$$

By formal integration, it can be shown that

$$\lambda(t_1, 0) = \int_0^{t_1} e^{At} dt = A^{-1}(e^{At_1} - I) \quad (8.74)$$

The validity of this expression is easily verified by taking the time derivative.

Let the entire solution interval now be divided as shown in Figure 8.9. If one denotes the initial state as x_0 , the state at the mode transition from conduction to commutation, where $t = T$, can be written as

$$x_1 = e^{A_1 T} x_0 + \lambda_1(T, 0) B_1 u \quad (8.75)$$

where

$$\lambda_1(T, 0) = A_1^{-1}(e^{A_1 T} - I)$$

The subscript 1 on the matrices indicates that they were evaluated for the conduction mode, (i.e., the increment T in Figure 8.9).

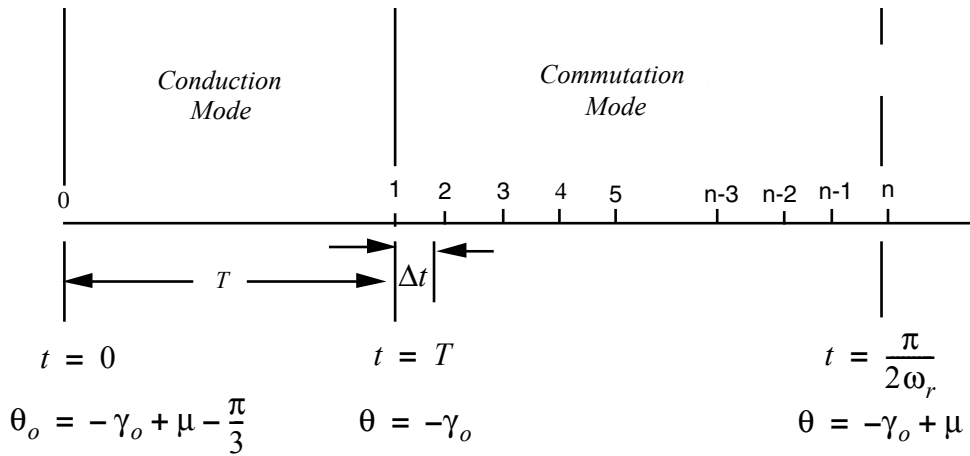


Figure 8.9 Discretization of commutation interval for initial condition calculation.

Since the system matrix A is time varying during the commutation mode, no simple calculation exists to find the final value of the state variables over this interval. Although it can be shown that a closed form solution exists for time variant systems [10], such solutions are generally impossible to find. However, reasonable accuracy can be obtained by dividing the commutation interval into small increments, say one degree, and treating the system as time

invariant over each increment. The value of the state vector at the end of any increment is related to the value at the end of the previous increment by

$$x_{2,n} = e^{A_{2,n-1}\Delta t}x_{2,n-1} + \lambda_{2,n-1}B_{2,n-1}u \quad (8.76)$$

where the state transition matrix and its integral are evaluated at the midpoint of each increment. Successive applications of Eq. (8.76) yield an expression for the final state, at the end of the 60° interval, in terms of its initial state,

$$x_2 = C_2x_1 + D_2u \quad (8.77)$$

where

$$C_2 = e^{A_{n-1}\Delta t}e^{A_{n-2}\Delta t}\dots e^{A_1\Delta t} \quad (8.78)$$

and $D_{2,n-1}$ is given recursively by

$$D_{2,n-1} = e^{A_{2,n-1}\Delta t}D_{2,n-2} + \lambda_{2,n-2}B_{2,n-2} \quad (8.79)$$

The overall solution is, over the entire 60° interval,

$$x_2 = C_2e^{A_1 T}x_0 + [C_2\lambda_1(T, 0)B_1 + D_2]u \quad (8.80)$$

or simply

$$x_2 = C_2C_1x_0 + [C_2D_1 + D_2]u \quad (8.81)$$

The top four rows of Eq. (8.80) are used to solve for the unknown currents and the field voltage. The symmetry obtained during steady-state operation requires that the rotor currents at the beginning and end of the 60 degree interval are related by

$$i_{qr_n} = i_{qr_0} \quad (8.82)$$

$$i_{dr_n} = i_{dr_0} \quad (8.83)$$

$$i_{fr_n} = i_{fr_0} \quad (8.84)$$

In addition, the commutation constraint requires

$$i_{k_0} = 0 \quad (8.85)$$

$$i_{k_n} = I_{dc} \text{ per unit} \quad (8.86)$$

These relations are substituted into the top four rows of Eq. (8.49) to obtain four equations in i_{QR} , i_{DR} , i_{FR} , and v_{FR} . From Eq. (8.82)–(8.86) one can write that

$$x_2 = \begin{bmatrix} 1 & 0 & 0 & 0 \\ 0 & 1 & 0 & 0 \\ 0 & 0 & 1 & 0 \\ 0 & 0 & 0 & 0 \end{bmatrix} x_0 + \begin{bmatrix} 0 & 0 \\ 0 & 0 \\ 0 & 0 \\ 1 & 0 \end{bmatrix} u \quad (8.87)$$

or, for simplicity,

$$x_2 = Sx_0 + Tu \quad (8.88)$$

Combining with Eq. (8.80),

$$\mathbf{0} = (C_2 C_1 - S)x_0 + [(C_2 D_1 + D_2) - T]u \quad (8.89)$$

This equation can now be used to solve for x_0 in terms of u as

$$x_0 = (S - C_2 C_1)^{-1} (C_2 D_1 + D_2 - T)u \quad (8.90)$$

Since $i_k(0) = x_0(4) = 0$, the fourth row of Eq. (8.90) can be written as

$$i_k(0) = x_0(4) = 0 = [a(4, 1), a(4, 2)] \times \begin{bmatrix} I_{dc} \\ v_{fr} \end{bmatrix} \quad (8.91)$$

where $a(4, 1)$ and $a(4, 2)$ are the elements in the first and second column of fourth row of the coefficient multiplying u in Eq. (8.91), so that

$$v_{fr}(0) = -\frac{a(4, 1)}{a(4, 2)} I_{dc} \quad (8.92)$$

Having solved for the field voltage in terms of the known input quantity I_{dc} , the remaining rows of Eq. (8.90) can now be solved. For example

$$i_{qr}(0) = x_0(1) = [a(1, 1), a(1, 2)] \times \begin{bmatrix} 1 \\ -\frac{a(4, 1)}{a(4, 2)} \end{bmatrix} I_{dc} \quad (8.93)$$

$$= \left(a(1, 1) - \frac{a(1, 2)a(4, 1)}{a(4, 2)} \right) I_{dc} \quad (8.94)$$

Similar expressions apply for the rotor currents $i_{dr}(0)$ and $i_{fr}(0)$.

8.8 Time Step Solution

Once the initial conditions have been found, it is a straightforward matter to integrate the state equations to find values for the state variables at convenient

time intervals. In particular, if the time interval is chosen to be the same as the increment for the initial condition calculation, the state transition matrices can be stored and used again, resulting in some saving of computation time.

Full-cycle 360° waveforms can easily be reconstructed from the waveforms calculated over 60°. Rotor quantities (currents and flux linkages) and electromagnetic torque simply repeat every 60°. Stator quantities (phase voltage, current, and flux linkages) exhibit half wave and three-phase symmetry, e.g.,

$$v_{as}(\theta + \pi) = -v_{as}(\theta) \quad (8.95)$$

and

$$v_{as}(\theta + \pi/3) = -v_{bs}(\theta) \quad (8.96)$$

$$v_{bs}(\theta + \pi/3) = -v_{cs}(\theta) \quad (8.97)$$

$$v_{cs}(\theta + \pi/3) = -v_{as}(\theta) \quad (8.98)$$

8.9 Sample Calculations

The steady-state performance of a 1000 hp LCI synchronous motor drive is calculated for an operating point characterized by $\gamma_0 = 55^\circ$, $\mu = 18^\circ$, and DC link current of 0.68 per unit. The parameters of the machine are given at the end of the chapter. All calculated quantities are given in per unit, with the machine rating as base power.

Rating: 1000 hp, 4 kV, 4 pole, 60 Hz.

Parameters:

$$x_{MD} = 1.28$$

$$x_{MQ} = 0.770$$

$$x_{LS} = 0.0932$$

$$x_{LDR} = 0.096$$

$$x_{LFR} = 0.1838$$

$$x_{LQR} = 0.115$$

$$r_S = 0.0051$$

$$I_{DR} = 0.085$$

$$I_{FR} = 0.001$$

$$I_{QR} = 0.032$$

Figure 8.10 shows voltage and current waveforms for one of the inverter thyristors. From this plot it is possible to deduce the thyristor voltage stress, the

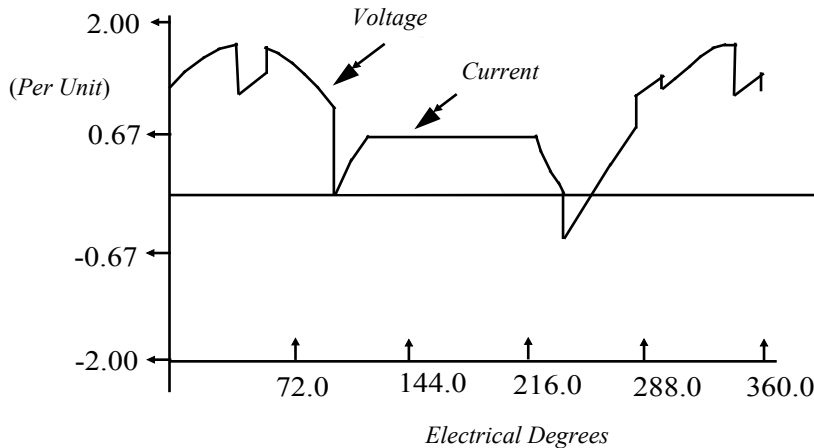


Figure 8.10 Thyristor voltage and current in per unit [11].

rate of forward current rise, and the commutation safety margin angle σ , which indicates how long the device is reverse biased before it must support forward voltage. [Figure 8.11](#) shows the solution for the stator voltages from line to neutral and from line to line.

Commutation notches in the inverter voltage are clearly visible in [Figure 8.12](#). The deviation of the inverter voltage from the average value can be used to estimate the current ripple that would occur with finite DC link inductance. The electromagnetic torque, [Figure 8.13](#), and field current, [Figure 8.14](#), both exhibit the sixth harmonic ripple components caused by inverter operation. These components are useful for identifying additional field heating caused by ripple current and provide a tool for evaluating the severity of torque oscillations imposed on the connected mechanical system.

Operation of the LCI drive at the minimum margin angle δ needed for safe commutation results in the highest power factor at the machine terminals and the best utilization of the machine windings [2]. Performance calculations for this type of operating scheme were carried out in [4]. For various values of fir-

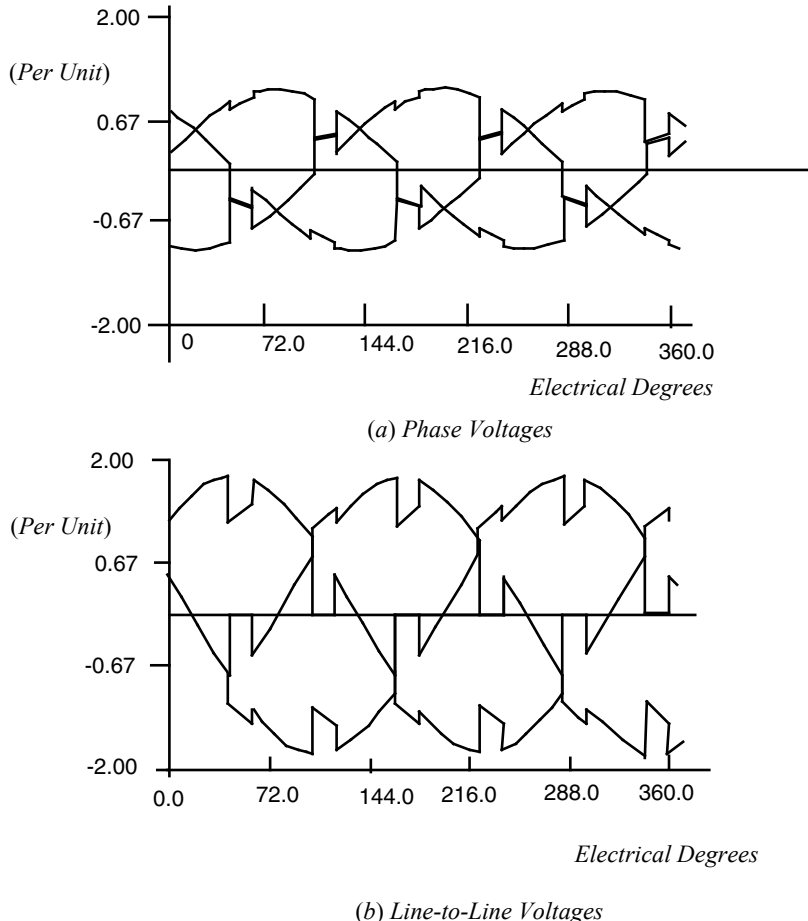


Figure 8.11 Phase voltages and line to line voltages [11].

ing angle γ_0 , an iterative technique was used to find the steady-state operating point (the value of μ) that yielded the desired value of commutation margin angle. Use of a binary search technique limited the number of iterations to a maximum of six for each operating point.

8.10 Torque Capability Curves

One useful measure of drive performance is a curve showing the maximum torque available over the entire speed range. A synchronous motor supplied from a variable voltage, variable frequency supply will exhibit a speed torque characteristic similar to that of a DC shunt motor, as shown in [Figure 8.15](#).

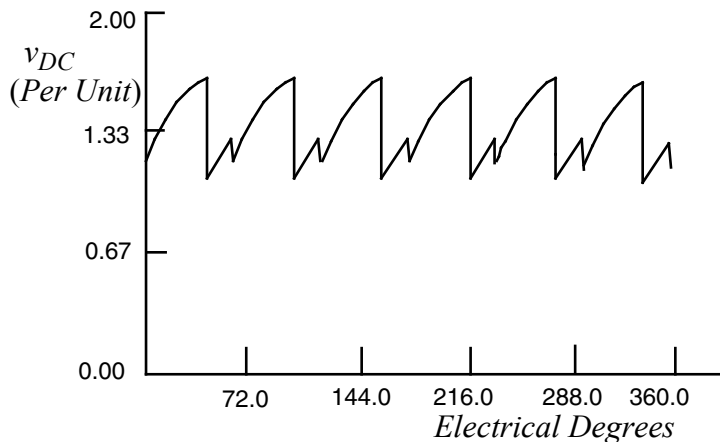


Figure 8.12 Inverter voltage[11].

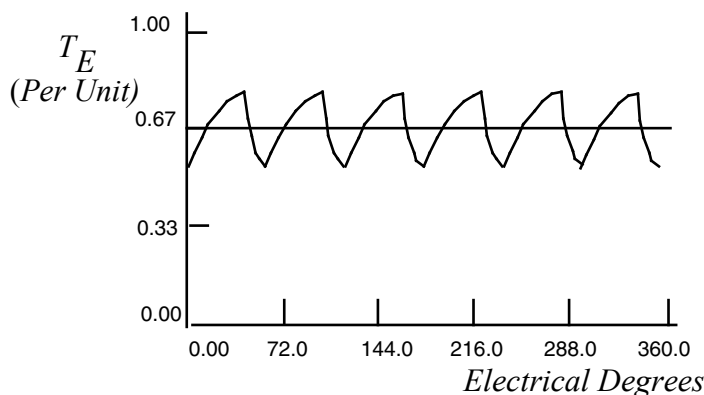


Figure 8.13 Electromagnetic torque [11].

Below rated speed, at constant armature current and field current, the machine voltage is proportional to speed and the motor operates in the *constant torque mode*. Above rated speed the field is weakened to maintain rated voltage and the drive operates in the *constant power mode*.

Torque in the LCI synchronous motor depends essentially on three factors: the armature current, the field current, and the internal power factor angle. If the internal power factor angle is held constant, it is possible to show that the speed torque characteristic will behave exactly as that of the DC motor [3]. However, operation at constant commutation margin time requires that the internal power factor angle change in order to maintain the minimum margin

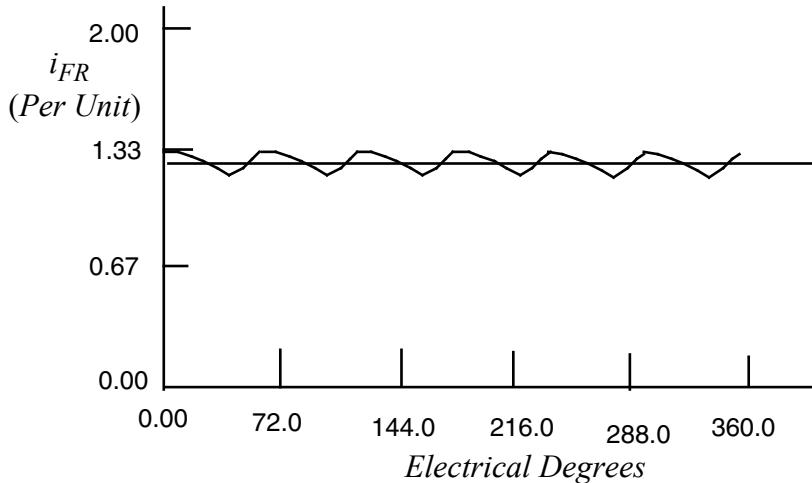


Figure 8.14 Field current [11].

angle. This will cause some deviation from the idealized torque capability curve of [Figure 8.15](#).

[Figure 8.16](#) shows a torque capability curve for the 1000 hp machine, operated at a constant commutation margin time corresponding to $\sigma = 10^\circ$ at rated speed. Calculations were made by the state variable method for a constant DC link current of 1.0 per unit on the machine base. Rated field current was set at the value that would achieve 1.0 per unit inverter voltage at rated speed, with a 10 degree margin angle.

For most of the region below rated speed, the developed torque exceeds its rated speed value. This is brought about by a slight increase in the internal power factor. Constant commutation margin time requires that the margin angle decreases as the speed is reduced. To achieve this, the firing angle γ_0 is reduced, giving a corresponding decrease in γ .

At very low speeds, where the commutation time is of the order of the sub-transient time constants, the machine resistances make up a significant part of the commutation impedance. The firing angle must now be increased to provide sufficient volt-seconds for commutation, and the resulting increase in the internal power factor angle reduces the torque capability. The behavior of the firing angle and internal power factor angle is shown in [Figure 8.17](#).

Above rated speed, the inverter voltage is maintained constant and the drive operates in a constant kVA mode. The DC voltage on the inverter is lim-

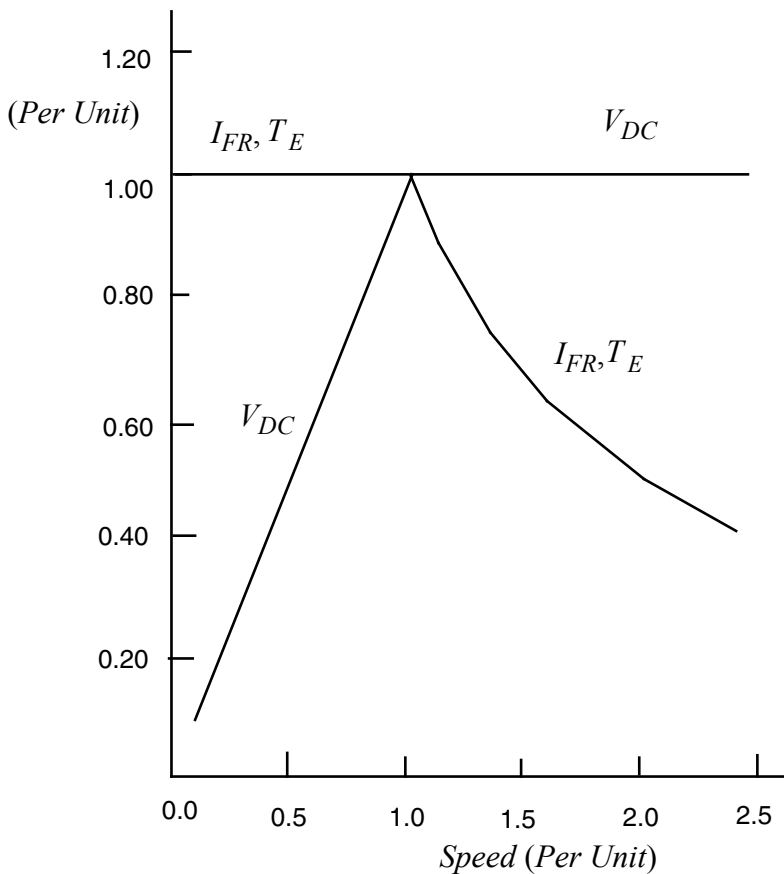


Figure 8.15 Ideal torque-speed curve corresponding to the speed-torque characteristic of a shunt wound DC motor [11].

ited by the device ratings and the maximum output of the input rectifier. Although Figure 8.16 shows a weakening of the field in the high speed region, the reduction in field current is not as great as the $1/N$ reduction indicated in Figure 8.14. This again is a consequence of the constant commutation margin time control. Since the margin angle increases with speed, the firing angle must also increase in order to achieve the higher margin angles. The corresponding increase in internal power factor angle results in a greater demagnetizing component of stator MMF. This partially offsets the need to weaken the field in the high speed region.

The high speed region of the capability curve terminates at 2.5 per unit speed. For the particular machine studied, this is the maximum speed at which

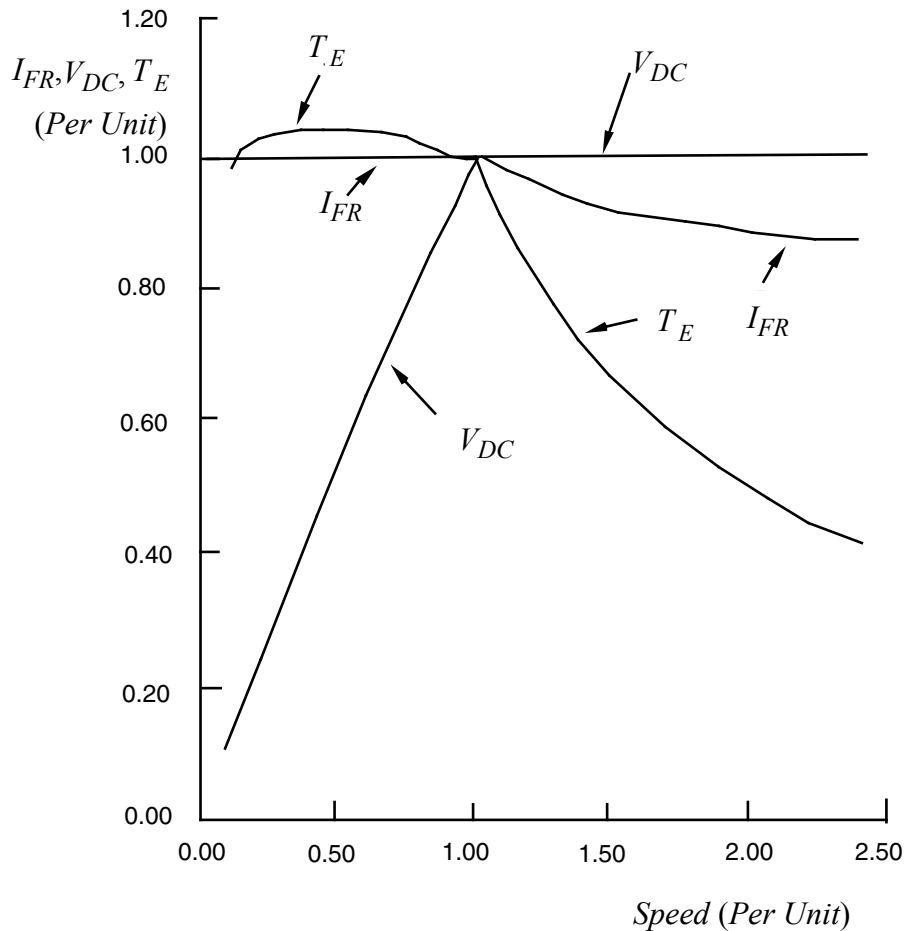


Figure 8.16 Speed-torque characteristic of an LCI synchronous motor drive with constant commutation safety margin time [11].

the rated kVA operation can be obtained while still maintaining the minimum commutation margin time. Operation at higher speeds would be possible only at lower DC link current or lower inverter voltage (corresponding to increased γ_0). The absolute maximum speed that could be obtained, assuming the same minimum margin time, is six times rated speed. In this limiting case, the margin angle takes up the entire 60 degrees between thyristor firings, leaving no time for commutation overlap.

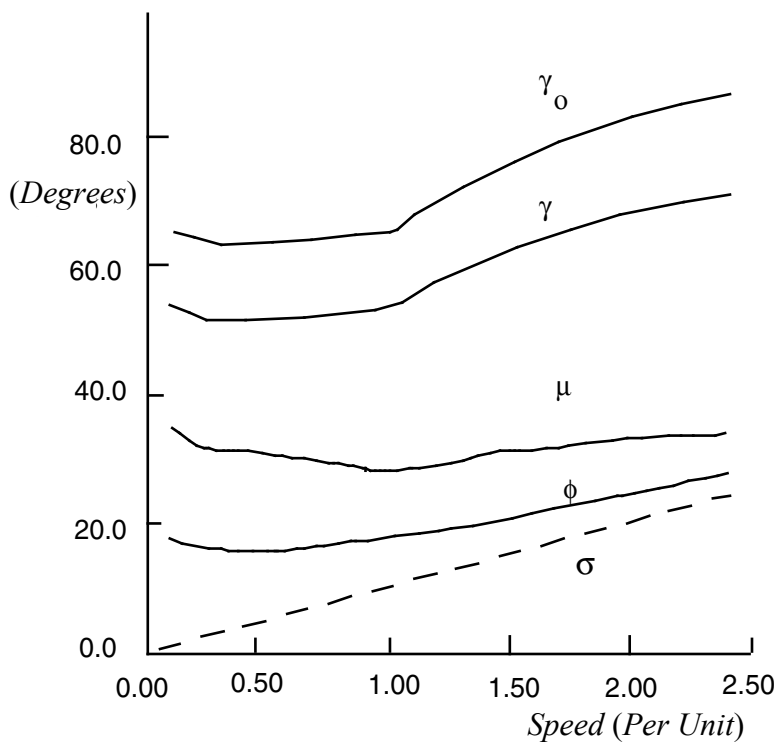


Figure 8.17 Characteristic electrical angles of an LCI synchronous motor drive with constant commutation margin time [11].

8.11 Constant Speed Performance

With DC current limited to the rated value, the maximum torque that can be obtained at a particular speed is indicated by the capability curve of [Figure 8.15](#). At any given speed, operation below maximum torque requires a reduction in the DC link current.

Steady-state performance curves for the LCI drive are shown in [Figure 8.18](#) and [Figure 8.19](#) for operation at rated speed and a margin angle of $\sigma = 10^\circ$. Figure 8.18 shows the average torque, fundamental AC voltage, and inverter voltage as a function of DC link current. Extreme overvoltage can be noted at low values of DC link current, indicating the need for some sort of field current control. The large voltages at low DC current arise from the reduction in the demagnetizing component of stator current. Not only is the

total stator current reduced, but the variation in the firing angle, necessary to maintain the minimum margin angle, reduces the proportion of stator *MMF* acting in the *d*-axis. The variation in firing angle and internal power factor angle is shown in Figure 8.19 as a function of the DC link current. Figure 8.19 shows a similar performance curve, with the field current adjusted to maintain the voltage at the rated value. The linearity of the solution made it possible to obtain the two plots from the same set of steady-state solutions simply by scaling the results to achieve either constant field current or constant voltage.

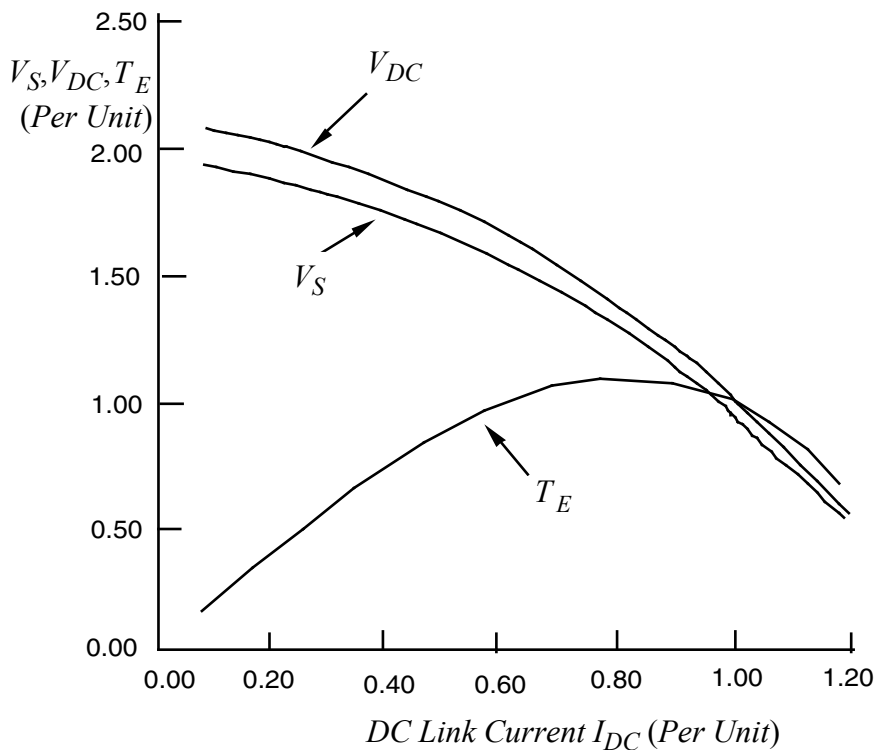


Figure 8.18 LCI synchronous motor drive torque, AC voltage, and DC voltage for operation at rated speed, rated field current, safety margin angle $\sigma = 10^\circ$ [11].

To operate the LCI synchronous motor drive at reduced torque without exceeding the inverter voltage ratings, it is necessary to control the field current and the DC link current simultaneously. Developed torque and field current are shown in Figure 8.20 for operation at rated DC voltage. The torque increases linearly with DC current, as would be expected, since at constant speed the torque is proportional to the power.

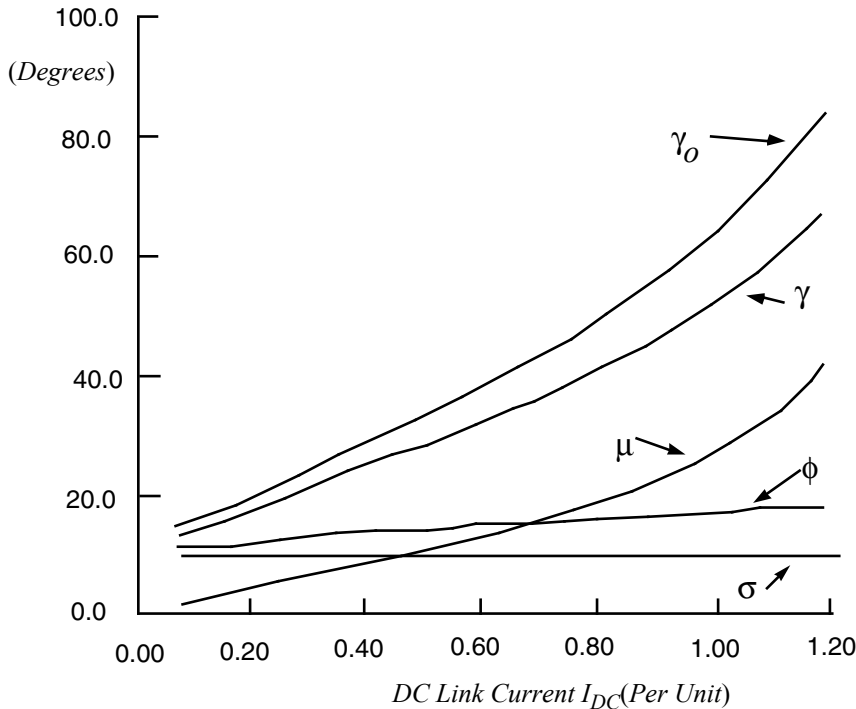


Figure 8.19 LCI synchronous motor drive electrical angles for operation at rated speed, rated field current. Margin angle $\sigma = 10^\circ$.

It can be seen that the variation in field current is nearly linear with DC current. This agrees with the results found in Ref [12], which discusses how the field current must be controlled to compensate for armature reaction as the load is varied. The slight nonlinearity in the field current can be explained by reference to the plot of γ in Figure 8.21. The need to maintain a constant margin angle requires that the firing angle, and consequently the internal power factor angle, increase along with the DC link current. The change in γ alters the proportion of demagnetizing stator current, hence the slight curvature in the field current plot.

8.12 Comparison of State Space and Phasor Diagram Solutions

Since the state space approach to determining the solution for the LCI synchronous motor drive generates an explicit time domain solution, many important

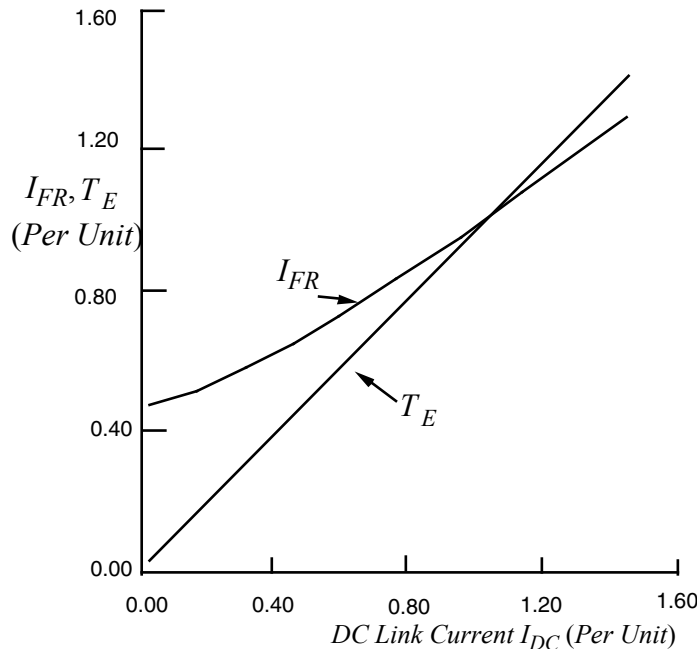


Figure 8.20 LCI synchronous motor drive torque and field current for operation at rated speed and rated inverter voltage. Safety margin angle $\sigma = 10^\circ$.

questions such as torque pulsations, amortisseur winding currents and associated losses, and voltage stresses on semiconductor switches, can best be obtained by these methods. Other characteristics such as overlap angle, margin angle, and power factor angle can be also obtained by using the phasor diagram approach developed in [Section 8.4](#). When precise values for these quantities are not required, the phasor approach offers an easy means to determine those quantities used in control, such as the firing angle γ_0 and the margin angle σ . [Figure 8.22](#) shows a comparison of the fundamental component approach of [Section 8.4](#) and the state variable approach. Recall that one of the key assumptions in the fundamental component approach is that $x_d'' \equiv x_q''$ as a worst case condition. Figure 8.22 assumes that the q -axis subtransient reactance is very large. It is evident that even with such an unreasonable assumption, the fundamental component is reasonably close to the state variable solution.

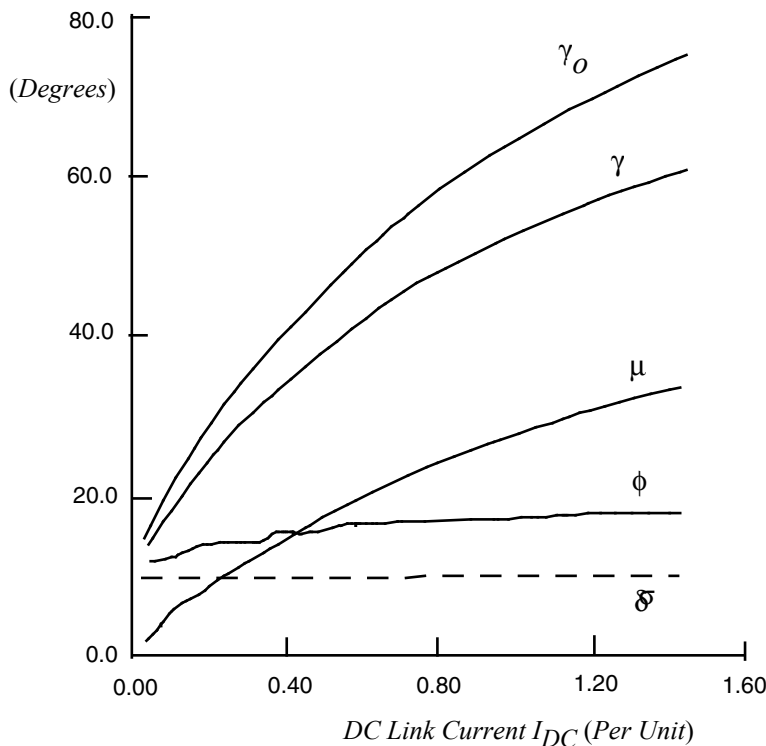


Figure 8.21 LCI synchronous motor drive electrical angles for operation at rated speed, rated field current, safety margin angle $\sigma = 10^\circ$.

8.13 Conclusion

Over the past several decades means for operation of electrical machines at variable speed, i.e., electrical drives, have made great strides. The cost associated with the manufacture of synchronous machines has meant that these machines, only become practical at very large ratings of 10 MW or more. At such power levels, the combination of low cost thyristor technology combined with the leading power factor capability of a synchronous machine becomes cost competitive to induction motor drives. This chapter has treated this important application of a synchronous machine in considerable depth to enable a deeper appreciation of the complexities involved. The chapter has also served as an introduction to the powerful state space approach for solving problems with complicated but periodic boundary conditions and it has been shown that

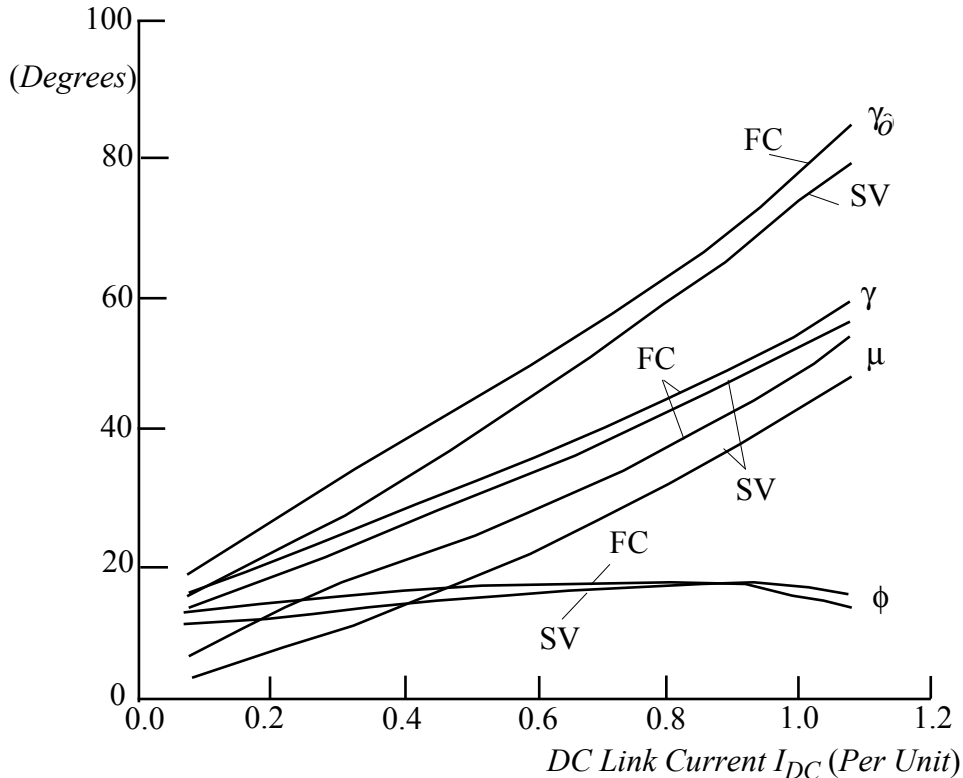


Figure 8.22 Electrical angles for LCI motor with $x_q'' \rightarrow \infty$. Comparison of fundamental component (FC) and state variable (SV) calculations for operation at rated speed and rated field current, margin angle $\sigma = 10$ degrees.

the method works quite well even when solving for non-linear systems with time varying coefficients. The approach obviates the need for invoking the numerous assumptions which are traditionally employed to make an analytical solution tractable.

8.14 References

- [1] N.A.H. Issa and A.C. Williamson, "Control of a Naturally Commutated Inverter-Fed Variable-Speed Synchronous Motor," *IEEE Proc. on Electric Power Applications*, Dec. 1979, vol. 2, No. 6.

- [2] H. Le-Huy, A. Jakubowicz, and R. Perret, "A Self-Controlled Synchronous Motor Drive Using Terminal Voltage Sensing," in *Conf. Record IEEE IAS Annual Meeting*, 1988, Part 2, pp. 562–569.
- [3] J. Rosa, "Utilization and Rating of Machine Commutated Inverter Fed Synchronous Motor Drives," *IEEE Trans. Ind. Appl.*, vol. IA-15, pp. 155–164, Mar./Apr. 1979.
- [4] F.C. Brockhurst, "Performance Equations for DC Commutatorless Motors Using Salient Pole Synchronous Type Machines," in *Conf. Rec. 1978 IEEE-IAS Annual Meeting*, pp. 861–868.
- [5] F. Harashima and T. Haneyoshi, "An Analysis of Commutatorless Motor with Salient Pole and DC Reactors of Finite Size," *Electrical Engineering in Japan*, vol. 97, No. 6, 1977, pp. 36–43.
- [6] S. Bolognani and G.B. Indri, "A Study of Converter-Fed Synchronous Machines by Means of Fourier Analysis," in *Conf. Rec. 1978 IEEE-IAS Annual Meeting*, pp. 869–875.
- [7] T.A. Lipo, "The Analysis of Induction Motors With Voltage Control by Symmetrically Triggered Thyristors," *IEEE Trans. Power Appl. and Syst.*, vol. PAS-90, pp.515–525, Mar./Apr. 1971.
- [8] T.A. Lipo and E.P. Cornell, "State-Variable Steady-State Analysis of a Controlled Current Induction Motor Drive," *IEEE Trans. Ind. Appl.*, vol. IA-11, pp.704–712, Nov./Dec. 1975.
- [9] R.S. Colby, "Steady-State Performance of Load Commutated Inverter Fed Synchronous Motor Drives," MSc Thesis, University of Wisconsin-Madison, August 1983.
- [10] G. Swisher, "Linear Systems Analysis," Champaign, Ill., Matrix Publishers, 1976.
- [11] R. S. Colby, T.A. Lipo, and D. W. Novotny, "A State-Space Analysis of LCI Fed Synchronous Motor Drives in the Steady-State," *IEEE Trans. on Industry Applications*, Vol. IA-21, No. 4, July/August 1985, pp. 1016–1022

Chapter 9

Extension of d - q Theory to Unbalanced Operation

9.1 Introduction

Balanced three-phase sinusoidal steady-state, studied in Chapter 4 is only an ideal, rarely achieved condition for either a motor or a generator. For example, in a power system, phase balance depends upon precise loading of distribution networks feeding various parts of a load network. The presence of non-linear loads such as rectifiers, computer power supplies, and the like also contribute harmonics which, while they may be filtered, continue to flow in small percentages in the phases of a large generator. Motors are generally tied to a distribution system which also has single phase loads, thereby producing unbalanced voltages across the lines of the motor. Harmonics produced by power electronic equipment in an industrial environment where such motors are located is a growing problem.

9.2 Source Voltage Formulation

It is useful to consider again the case of steady-state operation of a three-phase, three-wire synchronous machine this time for the general case wherein the three source voltages are arbitrary periodic functions. Although the solution method to be discussed is general, for simplicity, it is assumed that the three source voltages are periodic with the same fundamental frequency component. If this were not true, the solution for the currents could still be obtained by superposition by adding the solutions for each fundamental component.

Referring to [Figure 9.1](#), if periodic, the three source voltages can then be written in general as

$$e_{am} = \sum_{k=0}^{\infty} E_{ka\alpha} \cos k\omega_e t + \sum_{k=0}^{\infty} E_{ka\gamma} \sin k\omega_e t \quad (9.1)$$

$$e_{bm} = \sum_{k=0}^{\infty} E_{kb\alpha} \cos k\omega_e t + \sum_{k=0}^{\infty} E_{kb\gamma} \sin k\omega_e t \quad (9.2)$$

$$e_{cm} = \sum_{k=0}^{\infty} E_{kc\alpha} \cos k\omega_e t + \sum_{k=0}^{\infty} E_{kc\gamma} \sin k\omega_e t \quad (9.3)$$

where it is understood that $E_{0a\alpha}$, $E_{0b\alpha}$, and $E_{0c\alpha}$ are the DC components of the three source voltages and $E_{0a\gamma} = E_{0b\gamma} = E_{0c\gamma} = 0$.

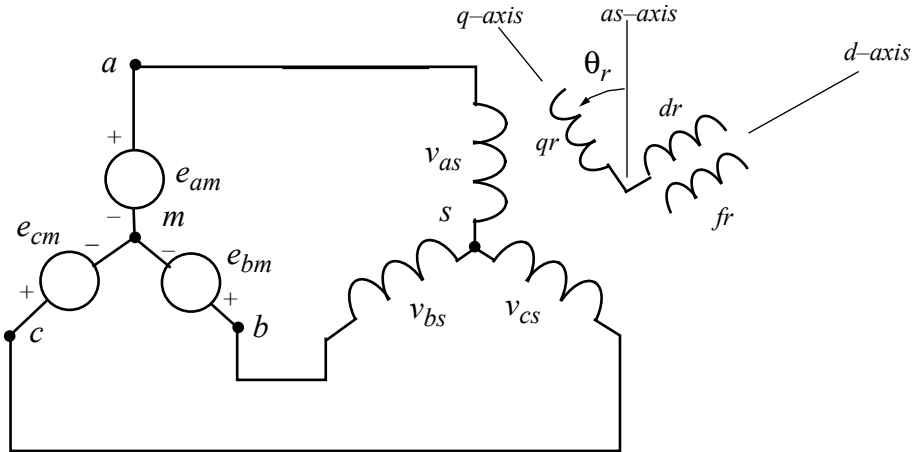


Figure 9.1 Synchronous machine with arbitrary periodic source voltages.

Following the same procedure as before, the $d-q$ voltages in the stationary reference frame are

$$v_{qs}^s = \sum_{k=0}^{\infty} V_{kq\alpha} \cos k\omega_e t + \sum_{k=0}^{\infty} V_{kq\gamma} \sin k\omega_e t \quad (9.4)$$

$$v_{ds}^s = \sum_{k=0}^{\infty} V_{kd\alpha} \cos k\omega_e t + \sum_{k=0}^{\infty} V_{kd\gamma} \sin k\omega_e t \quad (9.5)$$

wherein the harmonics of the v_{qs}^s , v_{ds}^s variables are related to the harmonics of the source voltages by

$$V_{kq\alpha} = \frac{2}{3}E_{ka\alpha} - \frac{1}{3}E_{kb\alpha} - \frac{1}{3}E_{kc\alpha} \quad (9.6)$$

$$V_{kq\gamma} = \frac{2}{3}E_{ka\gamma} - \frac{1}{3}E_{kb\gamma} - \frac{1}{3}E_{kc\gamma} \quad (9.7)$$

$$V_{kd\alpha} = \frac{1}{\sqrt{3}}(E_{kc\alpha} - E_{kb\alpha}) \quad (9.8)$$

$$V_{kd\gamma} = \frac{1}{\sqrt{3}}(E_{kc\gamma} - E_{kb\gamma}) \quad (9.9)$$

Since the inductances of a synchronous machine become time invariant only when expressed in the rotor reference frame, it is not practical to transform each of the stator voltages to synchronously rotating frames. Consider, however, the resulting set of equations which occur when the $d-q$ voltages are transformed to a reference frame rotating at rotor speed. The equations of transformation are

$$v_{qs}^r = v_{qs}^s \cos \omega_r t - v_{ds}^s \sin \omega_r t \quad (9.10)$$

$$v_{ds}^r = v_{qs}^s \sin \omega_r t + v_{ds}^s \cos \omega_r t \quad (9.11)$$

Substituting Eqs. (9.4) and (9.5) into Eqs. (9.10) and (9.11) one obtains

$$v_{qs}^r = \sum_{k=0}^{\infty} [V_{kq\alpha} \cos k\omega_e t \cos \omega_r t + V_{kq\gamma} \sin k\omega_e t \cos \omega_r t \quad (9.12)$$

$$- V_{kd\alpha} \cos k\omega_e t \sin \omega_r t - V_{kd\gamma} \sin k\omega_e t \sin \omega_r t]$$

$$\begin{aligned} v_{ds}^r = & \sum_{k=0}^{\infty} [V_{kq\alpha} \cos k\omega_e t \sin \omega_r t + V_{kq\gamma} \sin k\omega_e t \sin \omega_r t \quad (9.13) \\ & + V_{kd\alpha} \cos k\omega_e t \cos \omega_r t + V_{kd\gamma} \sin k\omega_e t \cos \omega_r t] \end{aligned}$$

Utilizing trigonometric identities #4, 5, and 6 of Appendix 1, Eqs. (9.12) and (9.13) can be expressed in the form

$$\begin{aligned} v_{qs}^r = & \sum_{k=0}^{\infty} \left[\frac{1}{2}(V_{kq\alpha} + V_{kd\gamma}) \cos(k\omega_e + \omega_r)t \right. \quad (9.14) \\ & + \frac{1}{2}(V_{kq\gamma} - V_{kd\alpha}) \sin(k\omega_e + \omega_r)t \\ & + \frac{1}{2}(V_{kq\alpha} - V_{kd\gamma}) \cos(k\omega_e - \omega_r)t \\ & \left. + \frac{1}{2}(V_{kq\gamma} + V_{kd\alpha}) \sin(k\omega_e - \omega_r)t \right] \end{aligned}$$

$$\begin{aligned} v_{ds}^r = & \sum_{k=0}^{\infty} \left[\frac{1}{2}(V_{kq\alpha} + V_{kd\gamma}) \sin(k\omega_e + \omega_r)t \right. \quad (9.15) \\ & - \frac{1}{2}(V_{kq\gamma} - V_{kd\alpha}) \cos(k\omega_e + \omega_r)t \\ & - \frac{1}{2}(V_{kq\alpha} - V_{kd\gamma}) \sin(k\omega_e - \omega_r)t \\ & \left. + \frac{1}{2}(V_{kq\gamma} + V_{kd\alpha}) \cos(k\omega_e - \omega_r)t \right] \end{aligned}$$

Note that for each value of k , the voltages have again been separated into four balanced sets. Two of the sets rotate relative to the rotor reference frame at an

angular velocity $k\omega_e + \omega_r$ (negative direction) and two of the sets rotate in the positive direction at the angular velocity $k\omega_e - \omega_r$.

9.3 System Equations to Be Solved

In general, regardless of the form of the source voltages, the synchronous machine equations, expressed in a reference frame rotating at any rotor speed are described by Park's equations. That is,

$$\nu_{qs} = r_s i_{qs} + \frac{p}{\omega_b} (x_{qs} i_{qs} + x_{mq} i_{qr}) + \frac{\omega_r}{\omega_b} (x_{ds} i_{ds} + x_{md} i_{dr} + x_{md} i_{fr}) \quad (9.16)$$

$$\nu_{ds} = r_s i_{ds} + \frac{p}{\omega_b} (x_{ds} i_{ds} + x_{md} i_{dr} + x_{md} i_{fr}) - \frac{\omega_r}{\omega_b} (x_{qs} i_{qs} + x_{mq} i_{qr}) \quad (9.17)$$

$$0 = r_{qr} i_{qr} + \frac{p}{\omega_b} (x_{qr} i_{qr} + x_{mq} i_{qs}) \quad (9.18)$$

$$0 = r_{dr} i_{dr} + \frac{p}{\omega_b} (x_{dr} i_{dr} + x_{md} i_{fr} + x_{md} i_{ds}) \quad (9.19)$$

$$\frac{r_{fr} E_x}{x_{md}} = r_{fr} i_{fr} + \frac{p}{\omega_b} (x_{fr} i_{fr} + x_{md} i_{dr} + x_{md} i_{ds}) \quad (9.20)$$

where

$$x_{ds} = x_{ls} + x_{md}$$

$$x_{qs} = x_{ls} + x_{mq}$$

$$x_{dr} = x_{ldr} + x_{md}$$

$$x_{qr} = x_{lqr} + x_{mq}$$

$$x_{fr} = x_{lfr} + x_{md}$$

In matrix form

$$\begin{bmatrix} v_{qs}^r \\ v_{ds}^r \\ 0 \\ 0 \\ \frac{r_{fr}E_x}{x_{md}} \end{bmatrix} = \begin{bmatrix} r_s & \frac{\omega_r}{\omega_b}x_{ds} & 0 & \frac{\omega_r}{\omega_b}x_{md} & \frac{\omega_r}{\omega_b}x_{md} \\ -\frac{\omega_r}{\omega_b}x_{qs} & r_s & -\frac{\omega_r}{\omega_b}x_{mq} & 0 & 0 \\ 0 & 0 & r_{qr} & 0 & 0 \\ 0 & 0 & 0 & r_{dr} & 0 \\ 0 & 0 & 0 & 0 & r_{fr} \end{bmatrix} \times \begin{bmatrix} i_{qs}^r \\ i_{ds}^r \\ i_{qr}^r \\ i_{dr}^r \\ i_{fr}^r \end{bmatrix}$$

$$+ \frac{p}{\omega_b} \begin{bmatrix} x_{qs} & 0 & x_{mq} & 0 & 0 \\ 0 & x_{ds} & 0 & x_{md} & x_{md} \\ x_{mq} & 0 & x_{qr} & 0 & 0 \\ 0 & x_{md} & 0 & x_{dr} & x_{md} \\ 0 & x_{md} & 0 & x_{md} & x_{fr} \end{bmatrix} \times \begin{bmatrix} i_{qs} \\ i_{ds} \\ i_{qr} \\ i_{dr} \\ i_{fr} \end{bmatrix} \quad (9.21)$$

Again the solution can be built up piecemeal using the principle of superposition. That contribution to the total solution resulting from field excitation can be found by setting v_{ds}^r and v_{qs}^r equal to zero in Equations (9.16)–(9.20). Assuming that the field voltage input E_i is a constant, the currents resulting from field excitation become constants in the steady-state and the solution is obtained from Equations (9.16)–(9.20) by setting all time derivatives equal to zero. The steady-state machine currents resulting from field excitation are then defined by the matrix

$$\begin{bmatrix} 0 \\ 0 \\ 0 \\ 0 \\ E_x \end{bmatrix} = \begin{bmatrix} r_s & \frac{\omega_r}{\omega_b} x_{ds} & 0 & \frac{\omega_r}{\omega_b} x_{md} & \frac{\omega_r}{\omega_b} x_{md} \\ -\frac{\omega_r}{\omega_b} x_{qs} & r_s & -\frac{\omega_r}{\omega_b} x_{mq} & 0 & 0 \\ 0 & 0 & r'_{qr} & 0 & 0 \\ 0 & 0 & 0 & r'_{dr} & 0 \\ 0 & 0 & 0 & 0 & x_{md} \end{bmatrix} \begin{bmatrix} I^r_{qs(x)} \\ I^r_{ds(x)} \\ I^r_{qr(x)} \\ I^r_{dr(x)} \\ I^r_{fr(x)} \end{bmatrix} \quad (9.22)$$

or, for simplicity,

$$V_{(x)} = Z_{(x)} I_{(x)} \quad (9.23)$$

where the subscript “*x*” has been appended to signify that this component of the solution arises from the “excitation.” In most practical cases involving asynchronous operation, the field voltage is set equal to zero so that Eq. (9.22) applies primarily for synchronous operation for which $\omega_r = \omega_e$. In general, however, it is clear that this component may exist for any rotor speed when $E_i \neq 0$.

The inversion of $Z_{(x)}$ is nearly trivial and it is possible to solve for $I_{(x)}$ simply by manual techniques. The result is

$$I^r_{fr(x)} = \frac{E_x}{x_{md}} \quad (9.24)$$

$$I^r_{dr(x)} = 0 \quad (9.25)$$

$$I^r_{qr(x)} = 0 \quad (9.26)$$

$$I^r_{ds(x)} = \frac{-\left(\frac{\omega_r}{\omega_b}\right)^2 x_{qs} E_x}{r_s^2 + \left(\frac{\omega_r}{\omega_b}\right)^2 x_{ds} x_{qs}} \quad (9.27)$$

$$I_{qs(x)}^r = \frac{-\frac{\omega_r}{\omega_b} r_s E_x}{r_s^2 + \left(\frac{\omega_r}{\omega_b}\right)^2 x_{ds} x_{qs}} \quad (9.28)$$

While not considered here, if E_x consists of harmonics as well as the DC value, the solution for the additional currents produced could be obtained by superimposing one harmonic frequency at a time on the system of equations defined by Eq. (9.21). The approach would follow the same form as will be taken up now for non-sinusoidal applied stator voltages.

9.4 System Formulation with Non-Sinusoidal Stator Voltages

Consider now only the currents which flow as a result of the stator excitation. Superposition will again be used and a particular k selected, say n , in the summation of Eqs. (9.14) and (9.15). In addition, consider initially only two balanced sets rotating in the positive direction. That is, first take into account vectors rotating at an angular velocity $n\omega_e - \omega_r$ relative to the rotor reference frame. These components will be denoted by $v_{qs(+n)}^r$ and $v_{ds(+n)}^r$. From Eqs. (9.14) and (9.15), selecting only those terms for which $k = n$ and are positively rotating

$$\begin{aligned} v_{qs(+n)}^r &= \frac{1}{2}(V_{nq\alpha} - V_{nd\gamma}) \cos(n\omega_e - \omega_r)t \\ &\quad + \frac{1}{2}(V_{nq\gamma} + V_{nda}) \sin(n\omega_e - \omega_r)t \end{aligned} \quad (9.29)$$

$$\begin{aligned} v_{ds(+n)}^r &= \frac{1}{2}(V_{nq\gamma} + V_{nda}) \cos(n\omega_e - \omega_r)t \\ &\quad - \frac{1}{2}(V_{nq\alpha} - V_{nd\gamma}) \sin(n\omega_e - \omega_r)t \end{aligned} \quad (9.30)$$

These voltages must be “applied” to Park’s equations. The equations to be solved are

$$\begin{aligned} v_{qs(+n)}^r &= r_s i_{qs(+n)}^r + \frac{p}{\omega_b} [x_{qs} i_{qs(+n)}^r + x_{mq} i_{qr(+n)}^r] \\ &\quad + \frac{\omega_r}{\omega_b} (x_{ds} i_{ds(+n)}^r + x_{md} i_{dr(+n)}^r + x_{md} i_{fr(+n)}^r) \end{aligned} \quad (9.31)$$

$$\begin{aligned} v_{ds(+n)}^r &= r_s i_{ds(+n)}^r + \frac{p}{\omega_b} [x_{ds} i_{ds(+n)}^r + x_{md} i_{dr(+n)}^r + x_{md} i_{fr(+n)}^r] \\ &\quad - \frac{\omega_r}{\omega_b} (x_{qs} i_{qs(+n)}^r + x_{mq} i_{qr(+n)}^r) \end{aligned} \quad (9.32)$$

$$0 = r'_{qr} i_{qr(+n)}^r + \frac{p}{\omega_b} (x'_{qr} i_{qr(+n)}^r + x_{mq} i_{qs(+n)}^r) \quad (9.33)$$

$$0 = r'_{dr} i_{dr(+n)}^r + \frac{p}{\omega_b} [x'_{dr} i_{dr(+n)}^r + x_{md} i_{ds(+n)}^r + x_{md} i_{fr(+n)}^r] \quad (9.34)$$

$$0 = r'_{fr} i_{fr(+n)}^r + \frac{p}{\omega_b} [x'_{fr} i_{fr(+n)}^r + x_{md} i_{ds(+n)}^r + x_{md} i_{dr(+n)}^r] \quad (9.35)$$

Observe that in this case the solution is not obtained by setting the $pi's = 0$, since the excitation is not "DC." However, the voltages which excite the system consist of a single frequency, namely, $n\omega_e - \omega_r$. Hence, in the steady-state all currents must be of this same frequency. Let

$$i_{qs(+n)}^r = I_{qs\alpha(+n)} \cos(n\omega_e - \omega_r)t + I_{qs\gamma(+n)} \sin(n\omega_e - \omega_r)t \quad (9.36)$$

with similar definitions for $i_{ds(+n)}^r$, $i_{dr(+n)}^r$, $i_{fr(+n)}^r$, $i_{qr(+n)}^r$. Substituting these equations together with Equations (9.29) and (9.30) into the system equations, Eqs. (9.31)–(9.35), one obtains, for the qs -circuit,

$$\begin{aligned}
& \frac{1}{2}(V_{nq\alpha} - V_{nd\gamma}) \cos(n\omega_e - \omega_r)t + \frac{1}{2}(V_{nq\gamma} + V_{nd\alpha}) \sin(n\omega_e - \omega_r)t \quad (9.37) \\
& = r_s I_{qs\alpha(+n)} \cos(n\omega_e - \omega_r)t + r_s I_{qs\gamma(+n)} \sin(n\omega_e - \omega_r)t \\
& + \frac{n\omega_e - \omega_r}{\omega_b} x_{qs} [-I_{qs\alpha(+n)} \sin(n\omega_e - \omega_r)t + I_{qs\gamma(+n)} \cos(n\omega_e - \omega_r)t] \\
& + \frac{n\omega_e - \omega_r}{\omega_b} x_{mq} [-I_{qr\alpha(+n)} \sin(n\omega_e - \omega_r)t + I_{qr\gamma(+n)} \cos(n\omega_e - \omega_r)t] \\
& + \frac{\omega_r}{\omega_b} x_{ds} [I_{ds\alpha(+n)} \cos(n\omega_e - \omega_r)t + I_{ds\gamma(+n)} \sin(n\omega_e - \omega_r)t] \\
& + \frac{\omega_r}{\omega_b} x_{md} [I_{dr\alpha(+n)} \cos(n\omega_e - \omega_r)t + I_{dr\gamma(+n)} \sin(n\omega_e - \omega_r)t] \\
& + \frac{\omega_r}{\omega_b} x_{md} [I_{fr\alpha(+n)} \cos(n\omega_e - \omega_r)t + I_{fr\gamma(+n)} \sin(n\omega_e - \omega_r)t]
\end{aligned}$$

In order for Equation (9.37) to be valid, the cosine component on the left hand side must equal the cosine component on the right hand side. The same reasoning applies for the sine component. Hence Eq. (9.37) implies that the following two equations must be valid.

$$\begin{aligned}
& \frac{1}{2}(V_{nq\alpha} - V_{nd\gamma}) = r_s I_{qs\alpha(+n)} + \frac{(n\omega_e - \omega_r)}{\omega_b} x_{qs} I_{qs\gamma(+n)} \quad (9.38) \\
& + \frac{(n\omega_e - \omega_r)}{\omega_b} x_{mq} I_{qr\gamma(+n)} mp + \frac{\omega_r}{\omega_b} x_{ds} I_{ds\alpha(+n)} \\
& + \frac{\omega_r}{\omega_b} x_{md} I_{dr\alpha(+n)} + \frac{\omega_r}{\omega_b} x_{md} I_{fr\alpha(+n)}
\end{aligned}$$

$$\begin{aligned}
& \frac{1}{2}(V_{nq\gamma} + V_{nd\alpha}) = r_s I_{qs\gamma(+n)} - \frac{(n\omega_e - \omega_r)}{\omega_b} x_{qs} I_{qs\alpha(+n)} \quad (9.39) \\
& - \frac{(n\omega_e - \omega_r)}{\omega_b} x_{mq} I_{qr\alpha(+n)} + \frac{\omega_r}{\omega_b} x_{ds} I_{ds\gamma(+n)} \\
& + \frac{\omega_r}{\omega_b} x_{md} I_{dr\gamma(+n)} + \frac{\omega_r}{\omega_b} x_{md} I_{fr\gamma(+n)}
\end{aligned}$$

The process of matching coefficients can be continued for the ds , dr , fr , qs , and qr circuits. This process will generate eight additional equations. All 10 equations are compactly described by the single matrix equation on the next page.

(9.40)

$$\begin{aligned}
& \left[\frac{\frac{1}{2}(V_{nq\alpha} - V_{nd\gamma})}{\omega_b x_{mq}} \right] = \\
& \left[\frac{\frac{1}{2}(V_{nq\gamma} + V_{nd\alpha})}{\omega_b x_{qs}} \right] + \left[\frac{\frac{1}{2}(V_{nq\gamma} + V_{nd\alpha})}{\omega_b x_{ds}} \right] + \left[\frac{\frac{1}{2}(V_{nq\alpha} - V_{nd\gamma})}{\omega_b x_{md}} \right] + \\
& \left[\frac{(n\omega_e - \omega_r)}{\omega_b x_{qs}} r_s \right] + \left[\frac{\frac{\omega_r x_{qs}}{\omega_b ds}}{\omega_b} \right] + \left[\frac{\frac{\omega_r x_{ds}}{\omega_b} r_s}{(n\omega_e - \omega_r)} \right] + \\
& \left[\frac{(n\omega_e - \omega_r)}{\omega_b x_{md}} \right] + \left[\frac{\frac{\omega_r x_{md}}{\omega_b} r_{qr}}{\omega_b} \right] + \left[\frac{\frac{\omega_r x_{md}}{\omega_b} (n\omega_e - \omega_r)}{(n\omega_e - \omega_r)} \right] + \\
& \left[\frac{(n\omega_e - \omega_r)}{\omega_b x_{fr}} \right] + \left[\frac{\frac{\omega_r x_{fr}}{\omega_b} r_{fr}}{\omega_b} \right] + \left[\frac{\frac{\omega_r x_{fr}}{\omega_b} (n\omega_e - \omega_r)}{(n\omega_e - \omega_r)} \right] + \\
& \left[\frac{\frac{1}{2}(V_{nq\alpha} - V_{nd\gamma})}{\omega_b x_{mq}} \right] = \\
& \left[\frac{\frac{1}{2}(V_{nq\alpha} - V_{nd\gamma})}{\omega_b x_{qs}} \right] + \left[\frac{\frac{1}{2}(V_{nq\alpha} - V_{nd\gamma})}{\omega_b x_{ds}} \right] + \left[\frac{\frac{1}{2}(V_{nq\alpha} - V_{nd\gamma})}{\omega_b x_{md}} \right] + \\
& \left[\frac{(n\omega_e - \omega_r)}{\omega_b x_{qs}} r_s \right] + \left[\frac{\frac{\omega_r x_{qs}}{\omega_b ds}}{\omega_b} \right] + \left[\frac{\frac{\omega_r x_{ds}}{\omega_b} r_s}{(n\omega_e - \omega_r)} \right] + \\
& \left[\frac{(n\omega_e - \omega_r)}{\omega_b x_{md}} \right] + \left[\frac{\frac{\omega_r x_{md}}{\omega_b} r_{qr}}{\omega_b} \right] + \left[\frac{\frac{\omega_r x_{md}}{\omega_b} (n\omega_e - \omega_r)}{(n\omega_e - \omega_r)} \right] + \\
& \left[\frac{(n\omega_e - \omega_r)}{\omega_b x_{fr}} \right] + \left[\frac{\frac{\omega_r x_{fr}}{\omega_b} r_{fr}}{\omega_b} \right] + \left[\frac{\frac{\omega_r x_{fr}}{\omega_b} (n\omega_e - \omega_r)}{(n\omega_e - \omega_r)} \right]
\end{aligned}$$

Equation (9.40) corresponds to a matrix of the following form,

$$V_{(+n)} = Z_{(+n)} I_{(+n)} \quad (9.41)$$

where $V_{(+n)}$, $I_{(+n)}$ are the 10 element vectors of voltages and currents of Equation (9.40). The current vector is readily found by inverting the $Z_{(+n)}$ matrix. That is,

$$I_{(+n)} = Z_{(+n)}^{-1} V_{(+n)} \quad (9.42)$$

In an entirely similar manner the solution for the negatively rotating set can be found corresponding to $k = n$. In essence, this simply involves replacing the quantity $n\omega_e - \omega_r$ in Equation (9.40) by $n\omega_e + \omega_r$ and defining the voltage vector for this case as

$$V_{(-n)} = \begin{bmatrix} \frac{1}{2}(V_{nq\alpha} + V_{nd\gamma}) \\ \frac{1}{2}(V_{nq\gamma} - V_{nd\alpha}) \\ -\frac{1}{2}(V_{nq\gamma} - V_{nd\alpha}) \\ -\frac{1}{2}(V_{nq\alpha} + V_{nd\gamma}) \\ 0 \\ 0 \\ 0 \\ 0 \\ 0 \\ 0 \end{bmatrix} \quad (9.43)$$

resulting in a matrix equation of the form

$$V_{(-n)} = Z_{(-n)} I_{(-n)} \quad (9.44)$$

Hence

$$I_{(-n)} = Z_{(-n)}^{-1} V_{(-n)} \quad (9.45)$$

9.5 Solution for Currents

The total solution is found by repeating the process for all $k = n, k = 0, 1, \dots, \infty$. In the rotor reference frame, the solution is therefore given by

$$i_{qs}^r = i_{qs(x)}^r + \sum_{k=0}^{\infty} [i_{qs(+k)}^r + i_{qs(-k)}^r] \quad (9.46)$$

$$i_{ds} = i_{ds(x)} + \sum_{k=0}^{\infty} [i_{ds(+k)} + i_{ds(-k)}] \quad (9.47)$$

$$i_{qr} = i_{qr(x)} + \sum_{k=0}^{\infty} [i_{qr(+k)} + i_{qr(-k)}] \quad (9.48)$$

$$i_{dr} = i_{dr(x)} + \sum_{k=0}^{\infty} [i_{dr(+k)} + i_{dr(-k)}] \quad (9.49)$$

$$i_{fr} = i_{fr(x)} + \sum_{k=0}^{\infty} [i_{fr(+k)} + i_{fr(-k)}] \quad (9.50)$$

where

$$i_{qs(+k)} = I_{qs\alpha(+k)} \cos(k\omega_e - \omega_r)t + I_{qs\gamma(+k)} \sin(k\omega_e - \omega_r)t \quad (9.51)$$

$$i_{qs(-k)} = I_{qs\alpha(-k)} \cos(k\omega_e + \omega_r)t + I_{qs\gamma(-k)} \sin(k\omega_e + \omega_r)t \quad (9.52)$$

and so forth. For $i_{ds(+k)}$, $i_{ds(-k)}$, $i_{fr(+k)}$, $i_{fr(-k)}$, $i_{dr(+k)}$, $i_{dr(-k)}$, $i_{qr(+k)}$, and $i_{qr(-k)}$.

Equations (9.48), (9.49), and (9.50) represent the total current flowing in the rotor circuits of the synchronous machine. Since these currents physically flow in the rotor, the solution for these currents is complete. However, since the stator currents actually flow in stationary circuits, the stator currents as defined by Equations (9.46) and (9.47) must be transformed to the stator.

Recall that the equations of transformation are

$$\dot{i}_{qs}^s = i_{qs} \cos \omega_r t + i_{ds} \sin \omega_r t \quad (9.53)$$

$$\dot{i}_{ds}^s = -i_{qs} \sin \omega_r t + i_{ds} \cos \omega_r t \quad (9.54)$$

Substituting Equations (9.46) and (9.47) into (9.53) and (9.54) results in the following equations for stator currents, after some simplification

$$\dot{i}_{qs}^s = I_{qs(x)} \cos \omega_r t + I_{ds(x)} \sin \omega_r t \quad (9.55)$$

$$\begin{aligned} &+ \sum_{k=0}^{\infty} \left\{ \frac{1}{2} [I_{qs\alpha(+k)} + I_{qs\alpha(-k)} - I_{ds\gamma(+k)} + I_{ds\gamma(-k)}] \cos k\omega_e t \right. \\ &+ \frac{1}{2} [I_{qs\gamma(+k)} + I_{qs\gamma(-k)} + I_{ds\alpha(+k)} - I_{ds\gamma(-k)}] \sin k\omega_e t \\ &+ \frac{1}{2} [I_{qs\alpha(+k)} + I_{ds\gamma(+k)}] \cos(k\omega_e - 2\omega_r)t \\ &+ \frac{1}{2} [I_{qs\gamma(+k)} - I_{ds\alpha(+k)}] \sin(k\omega_e - 2\omega_r)t \\ &\left. + \frac{1}{2} [I_{qs\alpha(-k)} - I_{ds\gamma(-k)}] \cos(k\omega_e + 2\omega_r)t \right\} \end{aligned}$$

$$\overset{s}{ds} = -I_{qs(x)} \sin \omega_r t + I_{ds(x)} \cos \omega_r t \quad (9.56)$$

$$\begin{aligned}
& + \sum_{k=0}^{\infty} \left\{ \frac{1}{2} [-I_{qs\alpha(+k)} + I_{qs\alpha(-k)} + I_{ds\gamma(+k)} + I_{ds\gamma(-k)}] \sin k\omega_e t \right. \\
& + \frac{1}{2} [I_{qs\gamma(+k)} - I_{qs\gamma(-k)} + I_{ds\alpha(+k)} + I_{ds\alpha(-k)}] \cos k\omega_e t \\
& + \frac{1}{2} [I_{qs\alpha(+k)} + I_{ds\gamma(+k)}] \sin(k\omega_e - 2\omega_r)t \\
& + \frac{1}{2} [-I_{qs\gamma(+k)} + I_{ds\alpha(+k)}] \cos(k\omega_e - 2\omega_r)t \\
& + \frac{1}{2} [-I_{qs\alpha(-k)} + I_{ds\gamma(-k)}] \sin(k\omega_e + 2\omega_r)t \\
& \left. + \frac{1}{2} [I_{qs\gamma(-k)} + I_{ds\alpha(-k)}] \cos(k\omega_e + 2\omega_r)t \right\}
\end{aligned}$$

It is important to realize that additional frequencies $k\omega_e - 2\omega_r$ and $k\omega_e + 2\omega_r$ appear in the expression for current which are not necessarily part of the source voltage spectrum. This feature distinguishes the analysis of synchronous machines from that of induction machines and makes the analysis of synchronous machines with load or source impedance unbalances very difficult.

9.6 Solution for Electromagnetic Torque

The final task remaining is to derive an analytical expression for electromagnetic torque. In general, the torque expression is (in physical SI units)

$$T_e = \frac{3P}{2} \frac{1}{2\omega_b} (\Psi_{ds} i_{qs} - \Psi_{qs} i_{ds}) \quad (9.57)$$

where

$$\Psi_{ds} = x_{ds} i_{ds} + x_{md} i_{dr} + x_{md} i_{fr}$$

$$\Psi_{qs} = x_{qs} i_{qs} + x_{mq} i_{qr}$$

and

$$x_{ds} = x_{ls} + x_{md}; \quad x_{qs} = x_{ls} + x_{mq}$$

Equation (9.57) can also be expressed in the form

$$T_e = \frac{3}{2} \frac{P}{2} \frac{1}{\omega_b} (\Psi_{md} i_{qs} - \Psi_{mq} i_{ds}) \quad (9.58)$$

where

$$\Psi_{md} = x_{md} (i_{ds} + i_{dr} + i_{fr}) \quad (9.59)$$

$$\Psi_{mq} = x_{mq} (i_{qs} + i_{qr}) \quad (9.60)$$

In the case where the current and fluxes are represented by an infinite series one has

$$T_e = \frac{3}{2} \frac{P}{2} \frac{1}{\omega_b} \sum_{k=0}^{\infty} \sum_{l=0}^{\infty} \{ [i_{qs(+k)} + i_{qs(-k)}] [\Psi_{md(+l)} + \Psi_{md(-l)}] \\ - [i_{ds(+k)} + i_{ds(-k)}] [\Psi_{mq(+l)} + \Psi_{mq(-l)}] \} \quad (9.61)$$

where

$$\Psi_{md(+l)} = x_{md} [i_{ds(+l)} + i_{dr(+l)} + i_{fr(+l)}]$$

$$\Psi_{md(-l)} = x_{md} [i_{ds(-l)} + i_{dr(-l)} + i_{fr(-l)}]$$

$$\Psi_{mq(+l)} = x_{mq} [i_{qs(+l)} + i_{qr(+l)}]$$

$$\Psi_{mq(-l)} = x_{mq} [i_{qs(-l)} + i_{qr(-l)}]$$

It is timely to now examine a particular harmonic:

$$T_{e(k, l)} = \frac{3}{2} \frac{P}{2} \frac{1}{\omega_b} \{ [i_{qs(+k)} + i_{qs(-k)}] [\Psi_{md(+l)} + \Psi_{md(-l)}] \\ - [i_{ds(+k)} + i_{ds(-k)}] [\Psi_{mq(+l)} + \Psi_{mq(-l)}] \}$$

(9.62)

In particular, consider the product of the first two bracketed terms. Due to symmetry, the product of the second pair of bracketed terms may then be obtained by inspection:

$$\begin{aligned}
 & [i_{qs(+k)} + i_{qs(-k)}] [\Psi_{md(+l)} + \Psi_{md(-l)}] \\
 &= [I_{qs\alpha(+k)} \cos(k\omega_e - \omega_r)t + I_{qs\gamma(+k)} \sin(k\omega_e - \omega_r)t \\
 &\quad + I_{qs\alpha(-k)} \cos(k\omega_e + \omega_r)t + I_{qs\gamma(-k)} \sin(k\omega_e + \omega_r)t] \\
 &\quad [\Psi_{md\alpha(+l)} \cos(l\omega_e - \omega_r)t + \Psi_{md\gamma(+l)} \sin(l\omega_e - \omega_r)t \\
 &\quad + \Psi_{md\alpha(-l)} \cos(l\omega_e + \omega_r)t + \Psi_{md\gamma(-l)} \sin(l\omega_e + \omega_r)t]
 \end{aligned} \tag{9.63}$$

Equation (9.63) can be written in the form shown on the next page.

$$\begin{aligned}
& [i_{qs(+k)} + i_{qs(-k)}][\Psi_{md(+l)} + \Psi_{md(-l)}] \\
&= I_{qs\alpha(+k)}\Psi_{md\alpha(+l)}\frac{1}{2}\{\cos(k-l)\omega_e t + \cos[(k+l)\omega_e - 2\omega_r]t\} \\
&+ I_{qs\gamma(+k)}\Psi_{md\alpha(+l)}\frac{1}{2}\{\sin(k-l)\omega_e t + \sin[(k+l)\omega_e - 2\omega_r]t\} \\
&+ I_{qs\alpha(-k)}\Psi_{md\alpha(+l)}\frac{1}{2}\{\cos(k+l)\omega_e t + \cos[(k-l)\omega_e + 2\omega_r]t\} \\
&+ I_{qs\gamma(-k)}\Psi_{md\alpha(+l)}\frac{1}{2}\{\sin(k+l)\omega_e t + \sin[(k-l)\omega_e + 2\omega_r]t\} \\
&+ I_{qs\alpha(+k)}\Psi_{md\gamma(+l)}\frac{1}{2}\{-\sin(k-l)\omega_e t + \sin[(k+l)\omega_e - 2\omega_r]t\} \\
&+ I_{qs\gamma(+k)}\Psi_{md\gamma(+l)}\frac{1}{2}\{\cos(k-l)\omega_e t - \cos[(k+l)\omega_e - 2\omega_r]t\} \\
&+ I_{qs\alpha(-k)}\Psi_{md\gamma(+l)}\frac{1}{2}\{\sin(k+l)\omega_e t - \sin[(k-l)\omega_e + 2\omega_r]t\} \\
&+ I_{qs\gamma(-k)}\Psi_{md\gamma(+l)}\frac{1}{2}\{-\cos(k+l)\omega_e t + \cos[(k-l)\omega_e + 2\omega_r]t\} \\
&+ I_{qs\alpha(+k)}\Psi_{md\alpha(-l)}\frac{1}{2}\{\cos(k+l)\omega_e t + \cos[(k-l)\omega_e - 2\omega_r]t\} \\
&+ I_{qs\gamma(+k)}\Psi_{md\alpha(-l)}\frac{1}{2}\{\sin(k+l)\omega_e t + \sin[(k-l)\omega_e - 2\omega_r]t\} \\
&+ I_{qs\alpha(-k)}\Psi_{md\alpha(-l)}\frac{1}{2}\{\cos(k-l)\omega_e t + \cos[(k+l)\omega_e + 2\omega_r]t\} \\
&+ I_{qs\gamma(-k)}\Psi_{md\alpha(-l)}\frac{1}{2}\{\sin(k-l)\omega_e t + \sin[(k+l)\omega_e + 2\omega_r]t\} \\
&+ I_{qs\alpha(+k)}\Psi_{md\gamma(-l)}\frac{1}{2}\{\sin(k+l)\omega_e t - \sin[(k-l)\omega_e - 2\omega_r]t\} \\
&+ I_{qs\gamma(+k)}\Psi_{md\gamma(-l)}\frac{1}{2}\{-\cos(k+l)\omega_e t + \cos[(k-l)\omega_e - 2\omega_r]t\} \\
&+ I_{qs\alpha(-k)}\Psi_{md\gamma(-l)}\frac{1}{2}\{-\sin(k-l)\omega_e t + \sin[(k+l)\omega_e + 2\omega_r]t\} \\
&+ I_{qs\gamma(-k)}\Psi_{md\gamma(-l)}\frac{1}{2}\{\cos(k-l)\omega_e t - \cos[(k+l)\omega_e + 2\omega_r]t\}
\end{aligned} \tag{9.64}$$

Note that terms occur having frequencies $(k \pm l)\omega_e \pm 2\omega_r$ and $(k \pm l)\omega_e$. Four of the terms are proportional to $\cos(k-l)\omega_e t$. Four additional terms arise from the second bracketed product of Eq. (9.62). These eight terms can be expressed in matrix form as

$$\Gamma_{e1c} = K_t \cos[(k - l)\omega_e t] \begin{bmatrix} I_{qs\alpha(+k)} \\ I_{qs\gamma(+k)} \\ I_{ds\alpha(+k)} \\ I_{ds\gamma(+k)} \\ I_{qs\alpha(-k)} \\ I_{qs\gamma(-k)} \\ I_{ds\alpha(-k)} \\ I_{ds\gamma(-k)} \end{bmatrix}^t \times \begin{bmatrix} 0 & 0 & 1 & 0 & 0 & 0 & 0 & 0 \\ 0 & 0 & 0 & 1 & 0 & 0 & 0 & 0 \\ -1 & 0 & 0 & 0 & 0 & 0 & 0 & 0 \\ 0 & -1 & 0 & 0 & 0 & 0 & 0 & 0 \\ 0 & 0 & 0 & 0 & 0 & 0 & 1 & 0 \\ 0 & 0 & 0 & 0 & 0 & 0 & 0 & 1 \\ 0 & 0 & 0 & 0 & 0 & -1 & 0 & 0 \\ 0 & 0 & 0 & 0 & 0 & 0 & -1 & 0 \end{bmatrix} \times \begin{bmatrix} \Psi_{mq\alpha(+l)} \\ \Psi_{mq\gamma(+l)} \\ \Psi_{md\alpha(+l)} \\ \Psi_{md\gamma(+l)} \\ \Psi_{mq\alpha(-l)} \\ \Psi_{mq\gamma(-l)} \\ \Psi_{md\alpha(-l)} \\ \Psi_{md\gamma(-l)} \end{bmatrix} \quad (9.65)$$

where

$$K_t = \frac{3P}{22} \frac{1}{\omega_b} \frac{1}{2} \quad (9.66)$$

or simply, in compressed form as

$$T_{e1c} = \frac{3P}{22} \frac{1}{\omega_b} \frac{1}{2} \cos[(k - l)\omega_e t] \quad I_k^t C_{1\alpha} \Psi_l \quad (9.67)$$

where

$$I_k = [I_{qs\alpha(+k)}, I_{qs\gamma(+k)}, \dots, I_{ds\gamma(-k)}]^t \quad (9.68)$$

$$\Psi_l = [\Psi_{mq\alpha(+k)}, \Psi_{mq\gamma(+k)}, \dots, \Psi_{md\gamma(-l)}]^t \quad (9.69)$$

and $C_{1\alpha}$ is the 8×8 matrix of Eq. (9.65).

In a similar fashion the remaining torque components can be expressed by the following matrix expressions:

$$T_{e1s} = \frac{3P}{22} \frac{1}{\omega_b} \frac{1}{2} \sin[(k - l)\omega_e t] \quad I_k^t C_{1\gamma} \Psi_l$$

where I_k and Ψ_l are defined by Eqs. (9.68) and (9.69) and

$$T_{e3c} = \frac{3P}{2} \frac{1}{2} \frac{1}{\omega_b^2} \cos\{(k+l)\omega_e - 2\omega_r]t\} I_k^t C_{3\alpha} \Psi_l \quad (9.75)$$

where

$$C_{3\alpha} = \begin{bmatrix} 0 & 0 & 1 & 0 & 0 & 0 & 0 & 0 \\ 0 & 0 & 0 & -1 & 0 & 0 & 0 & 0 \\ -1 & 0 & 0 & 0 & 0 & 0 & 0 & 0 \\ 0 & 1 & 0 & 0 & 0 & 0 & 0 & 0 \\ 0 & 0 & 0 & 0 & 0 & 0 & 0 & 0 \\ 0 & 0 & 0 & 0 & 0 & 0 & 0 & 0 \\ 0 & 0 & 0 & 0 & 0 & 0 & 0 & 0 \\ 0 & 0 & 0 & 0 & 0 & 0 & 0 & 0 \end{bmatrix} \quad (9.76)$$

$$T_{e3s} = \frac{3P}{2} \frac{1}{2} \frac{1}{\omega_b^2} \sin\{(k+l)\omega_e - 2\omega_r]t\} I_k^t C_{3\gamma} \Psi_l \quad (9.77)$$

where

$$C_{3\gamma} = \begin{bmatrix} 0 & 0 & 0 & 1 & 0 & 0 & 0 & 0 \\ 0 & 0 & 1 & 0 & 0 & 0 & 0 & 0 \\ 0 & -1 & 0 & 0 & 0 & 0 & 0 & 0 \\ -1 & 0 & 0 & 0 & 0 & 0 & 0 & 0 \\ 0 & 0 & 0 & 0 & 0 & 0 & 0 & 0 \\ 0 & 0 & 0 & 0 & 0 & 0 & 0 & 0 \\ 0 & 0 & 0 & 0 & 0 & 0 & 0 & 0 \\ 0 & 0 & 0 & 0 & 0 & 0 & 0 & 0 \end{bmatrix} \quad (9.78)$$

$$T_{e4c} = \frac{3P}{2} \frac{1}{2} \frac{1}{\omega_b^2} \cos\{(k+l)\omega_e + 2\omega_r]t\} I_k^t C_{4\alpha} \Psi_i \quad (9.79)$$

where

$$C_{4\alpha} = \begin{bmatrix} 0 & 0 & 0 & 0 & 0 & 0 & 0 & 0 \\ 0 & 0 & 0 & 0 & 0 & 0 & 0 & 0 \\ 0 & 0 & 0 & 0 & 0 & 0 & 0 & 0 \\ 0 & 0 & 0 & 0 & 0 & 0 & 0 & 0 \\ 0 & 0 & 0 & 0 & 0 & 0 & 1 & 0 \\ 0 & 0 & 0 & 0 & 0 & 0 & 0 & -1 \\ 0 & 0 & 0 & 0 & -1 & 0 & 0 & 0 \\ 0 & 0 & 0 & 0 & 0 & 1 & 0 & 0 \end{bmatrix} \quad (9.80)$$

$$T_{e4s} = \frac{3P}{2} \frac{1}{\omega_b} \frac{1}{2} \sin \{ [(k+l)\omega_e + 2\omega_r]t \} I_k^t C_{4\gamma} \Psi_l \quad (9.81)$$

where

$$C_{4\gamma} = \begin{bmatrix} 0 & 0 & 0 & 0 & 0 & 0 & 0 & 0 \\ 0 & 0 & 0 & 0 & 0 & 0 & 0 & 0 \\ 0 & 0 & 0 & 0 & 0 & 0 & 0 & 0 \\ 0 & 0 & 0 & 0 & 0 & 0 & 0 & 0 \\ 0 & 0 & 0 & 0 & 0 & 0 & 0 & 0 \\ 0 & 0 & 0 & 0 & 0 & 0 & 0 & 1 \\ 0 & 0 & 0 & 0 & 0 & 0 & 1 & 0 \\ 0 & 0 & 0 & 0 & 0 & -1 & 0 & 0 \\ 0 & 0 & 0 & 0 & -1 & 0 & 0 & 0 \end{bmatrix} \quad (9.82)$$

$$T_{e5c} = \frac{3P}{2} \frac{1}{\omega_b} \frac{1}{2} \cos \{ [(k-l)\omega_e - 2\omega_r]t \} I_k^t C_{5\alpha} \Psi_l \quad (9.83)$$

where

$$T_{e5s} = \frac{3P}{2} \frac{1}{2} \frac{1}{\omega_b^2} \sin \{[(k-l)\omega_e - 2\omega_r]t\} I_k^t C_{5\gamma} \Psi_l \quad (9.85)$$

where

$$C_{5\gamma} = \begin{bmatrix} 0 & 0 & 0 & 0 & 0 & 0 & 0 & -1 \\ 0 & 0 & 0 & 0 & 0 & 0 & 1 & 0 \\ 0 & 0 & 0 & 0 & 0 & 1 & 0 & 0 \\ 0 & 0 & 0 & 0 & -1 & 0 & 0 & 0 \\ 0 & 0 & 0 & 0 & 0 & 0 & 0 & 0 \\ 0 & 0 & 0 & 0 & 0 & 0 & 0 & 0 \\ 0 & 0 & 0 & 0 & 0 & 0 & 0 & 0 \\ 0 & 0 & 0 & 0 & 0 & 0 & 0 & 0 \end{bmatrix} \quad (9.86)$$

$$T_{e6c} = \frac{3P}{2} \frac{1}{2} \frac{1}{\omega_b^2} \cos \{[(k-l)\omega_e + 2\omega_r]t\} I_k^t C_{6\alpha} \Psi_l \quad (9.87)$$

where

$$C_{6\alpha} = \begin{bmatrix} 0 & 0 & 0 & 0 & 0 & 0 & 0 & 0 \\ 0 & 0 & 0 & 0 & 0 & 0 & 0 & 0 \\ 0 & 0 & 0 & 0 & 0 & 0 & 0 & 0 \\ 0 & 0 & 0 & 0 & 0 & 0 & 0 & 0 \\ 0 & 0 & 1 & 0 & 0 & 0 & 0 & 0 \\ 0 & 0 & 0 & 1 & 0 & 0 & 0 & 0 \\ -1 & 0 & 0 & 0 & 0 & 0 & 0 & 0 \\ 0 & -1 & 0 & 0 & 0 & 0 & 0 & 0 \end{bmatrix} \quad (9.88)$$

$$T_{e6s} = \frac{3P}{2} \frac{1}{2} \frac{1}{\omega_b^2} \sin \{[(k-l)\omega_e + 2\omega_r]t\} I_k^t C_{6\gamma} \Psi_l \quad (9.89)$$

where

$$C_{6\gamma} = \begin{bmatrix} 0 & 0 & 0 & 0 & 0 & 0 & 0 & 0 \\ 0 & 0 & 0 & 0 & 0 & 0 & 0 & 0 \\ 0 & 0 & 0 & 0 & 0 & 0 & 0 & 0 \\ 0 & 0 & 0 & 0 & 0 & 0 & 0 & 0 \\ 0 & 0 & 0 & -1 & 0 & 0 & 0 & 0 \\ 0 & 0 & 1 & 0 & 0 & 0 & 0 & 0 \\ 0 & 1 & 0 & 0 & 0 & 0 & 0 & 0 \\ -1 & 0 & 0 & 0 & 0 & 0 & 0 & 0 \end{bmatrix} \quad (9.90)$$

The total instantaneous torque is finally expressed as the sum of these terms, namely

$$\begin{aligned} T_e = \sum_{k=0}^{\infty} \sum_{l=0}^{\infty} [T_{e1c} + T_{e1s} + T_{e2c} + T_{e2s} + T_{e3c} + T_{e3s} & (9.91) \\ + T_{e4c} + T_{e4s} + T_{e5c} + T_{e5s} + T_{e6c} + T_{e6s}] \end{aligned}$$

9.7 Example Solutions

The above family of equations has been cast into a MATLAB program *smhb* (synchronous machine harmonic balance) which is included in this text as Appendix 5. It can again be assumed that the machine under study is the 30 MW, 50 Hz machine of Table 5.3. Also, it is supposed that the machine is located near an aluminum processing plant where a large number of AC/DC rectifiers are located. It has been determined that the harmonics produced by the aluminum plant are such that a fifth harmonic $V_5 = 1/5$, and a seventh harmonic, $V_7 = 1/7$ p.u., appears at the machine terminals. It is desired to determine the currents within the machine as well as the electromagnetic torque with the machine operating at unity power factor and rated load. A printout from *smhb* for this condition is shown in [Figure 9.2](#). It should be recalled that a three-phase balanced set of fifth harmonic voltages produces an *MMF* wave that travels in the negative direction (w.r.t. to rotor speed) rotating at $5\omega_e$ while the seventh produces a *MMF* that travels in the positive direction at $7\omega_e$. Thus the fifth and seventh harmonics both contribute to production of a sixth harmonic torque pulsation as well as sixth harmonic current flows in the rotor circuits. It is instructive to also observe that additional terms in the stator

current appear, the reason for which is not immediately apparent. These terms appear because the induced rotor emf is not symmetrical but produces both positive and negative rotating *MMF* components. For example, the fifth harmonic voltage applied to the stator produces a sixth harmonic *MMF* in the rotor which, in turn, results in *MMF* waves travelling forward and backward at six times the rotor speed. The negative rotating *MMF* induces currents in the stator at the fifth harmonic which corresponds to the fifth harmonic described in the previous paragraph. However, it also produces an positively rotating *MMF* which induces a seventh harmonic stator current. Similarly, the seventh harmonic voltage induces a sixth harmonic *MMF*, which also produces both fifth and seventh harmonic components of stator current.

Parameter Values in Per Unit

$$R_s = 0.002 \quad X_{ls} = 0.14$$

$$R_{dr} = 0.003 \quad X_{ldr} = 0.04$$

$$R_{fr} = 0.001 \quad X_{lfr} = 0.14$$

$$R_{qr} = 0.003 \quad X_{lqr} = 0.04$$

$$X_{md} = 1.86 \quad X_{mq} = 1.86$$

$$f_{\text{base}} = 50 \quad f_e = 50$$

$$E_x = 2.246 \quad \text{Delta} = -63.5 \text{ degrees}$$

Balanced Source Voltages Assumed? (Type yes or not)---yes

$$\begin{aligned} I_{as} &= & I_{bs} &= & I_{cs} &= \\ 1.00501 \cdot \cos(1we*t+116.496) & & 1.00501 \cdot \cos(1we*t+-3.50428) & & 1.00501 \cdot \cos(1we*t+-123.504) \\ + 0.228864 \cdot \cos(5we*t+-153.242) & & + 0.228864 \cdot \cos(5we*t+-33.2424) & & + 0.228864 \cdot \cos(5we*t+86.7576) \\ + 0.0056 \cdot \cos((5we+2wr)*t+25.7834) & & + 0.0056 \cdot \cos((5we+2wr)*t+-94.2166) & & + 0.0056 \cdot \cos((5we+2wr)*t+145.783) \\ + 0.116803 \cdot \cos(7we*t+-153.28) & & + 0.116803 \cdot \cos(7we*t+86.7202) & & + 0.116803 \cdot \cos(7we*t+-33.2798) \\ + 0.0028586 \cdot \cos((7we-2wr)*t+25.8) & & + 0.0028586 \cdot \cos((7we-2wr)*t+145.8) & & + 0.0028586 \cdot \cos((7we-2wr)*t+-94.2) \end{aligned}$$

$$\begin{aligned} I_{qr} &= & I_{dr} &= & I_{fr} &= \\ 6.06532e-016 \cdot \cos((0*we)*t+-178.845) & & 4.97711e-016 \cdot \cos((0*we)*t+91.4239) & & 1.2075 \cdot \cos((0*we)*t+6.7518e-015) \\ + 0.111546 \cdot \cos((6*we)*t+26.7588) & & + 0.091538 \cdot \cos((6*we)*t+116.851) & & + 0.026156 \cdot \cos((6*we)*t+116.203) \end{aligned}$$

Electromagnetic Torque

$$\begin{aligned} T_e &= -1.00716 \\ &+ 0.0457674 \cdot \cos((6*we)*t+-169.701) \\ &+ 0.000102338 \cdot \cos((12*we)*t+98.4863) \end{aligned}$$

Figure 9.2 Printout of solution of 30 MW synchronous generator when the rotor rotates at synchronous speed ($\omega_r = \omega_e$), unity power factor and rated load.

In Figure 9.3 this scenario is repeated at a speed of 0.4 p.u. The field is assumed to remain excited. In reality a turbo-generator would never be called upon to accelerate from rest, particularly when excitation is applied. This case is examined to simply illustrate the capability of this computational approach for solving a problem involving any combination of harmonics (balanced or unbalanced) and for any rotor speed. It is interesting to observe that the solution for the electromagnetic torque has become very complicated due to the fact that the speed is not synchronously rotating. Many small terms have not been printed. In this case, harmonic terms for the torque are produced of the form $(k \pm l) \pm 2(\omega_r/\omega_e)$, which do not neatly form integers when ω_r/ω_e is not itself an integer.

9.8 Conclusion

When a synchronous machine is subjected to an unbalanced supply, the resulting currents which flow can result in destructive heating within the machine. While such unbalances can be handled analytically with ease for an induction machine, the rotor of the synchronous machine does not present a balanced impedance to the stator of the machine, as does the induction machine. This results in a considerably more complicated solution. While the simple case of an unbalanced sinusoidal supply could be handled specifically, this chapter has presented a completely general approach to the analysis of such problems in which each of the phases of the machine is assumed to be composed of an arbitrary number of harmonics. The solution thus obtained can be used not only to investigate the effects of an unbalanced supply but also the effects of a supply with an arbitrary number of harmonics, either balanced or unbalanced. Again the treatment takes maximum advantage of modern computer techniques, which follows the theme of this text.

Parameter Values in Per Unit

 $R_s = 0.002 \quad X_{ls} = 0.14$ $R_{dr} = 0.003 \quad X_{ldr} = 0.04$ $R_{fr} = 0.001 \quad X_{lfr} = 0.14$ $R_{qr} = 0.003 \quad X_{lqr} = 0.04$ $X_{md} = 1.86 \quad X_{mq} = 1.86$ $f_{base} = 50 \quad f_e = 50$ $\Delta = -63.5 \text{ degrees} \quad E_x = 2.246$ Input the rotor speed in per unit (W_{rpu} .ne.1)---0.4

Balanced Source Voltages Assumed? (Type yes or not)--yes

$$\begin{aligned}
 I_{as} &= & I_{bs} &= & I_{cs} &= \\
 1.123 * \cos(0.4we*t + 90.1432) & & 1.123 * \cos(0.4we*t - 29.8568) & & 1.123 * \cos(0.4we*t - 149.857) \\
 5.71699 * \cos(1we*t - 151.58) & & 5.71699 * \cos(1we*t + 88.4205) & & 5.71699 * \cos(1we*t - 31.5795) \\
 +0.141498 * \cos((1we-2wr)*t + 21.0789) & & +0.141498 * \cos((1we-2wr)*t + 141.079) & & +0.141498 * \cos((1we-2wr)*t + 98.9211 \\
 0.228864 * \cos(5we*t - 153.228) & & 0.228864 * \cos(5we*t + -33.2283) & & 0.228864 * \cos(5we*t + 86.7717) \\
 +0.00560128 * \cos((5we+2wr)*t + 25.6981) & & +0.00560128 * \cos((5we+2wr)*t + -94.3019) & & +0.00560128 * \cos((5we+2wr)*t + 145.698 \\
 0.116803 * \cos(7we*t - 153.291) & & 0.116803 * \cos(7we*t + 86.7087) & & 0.116803 * \cos(7we*t + -33.2913) \\
 +0.00285851 * \cos((7we-2wr)*t + 25.8435) & & +0.00285851 * \cos((7we-2wr)*t + 145.844) & & +0.00285851 * \cos((7we-2wr)*t + -94.1565
 \end{aligned}$$

Stator Har. $I_{qr} =$ $I_{dr} =$ $I_{fr} =$

1.20753

$$\begin{aligned}
 5.45925 * \cos((1*we-W_{rpu}*we)*t - 28.75) & & 4.47785 * \cos((1*we-W_{rpu}*we)*t - 119.7) & & +1.28925 * \cos((1*we-W_{rpu}*we)*t - 113.3) \\
 0.218563 * \cos((5*we+W_{rpu}*we)*t + 116.8) & & 0.179359 * \cos((5*we+W_{rpu}*we)*t + 26.92) & & +0.0512505 * \cos((5*we+W_{rpu}*we)*t + 26.2 \\
 0.11155 * \cos((7*we-W_{rpu}*we)*t - 26.74) & & 0.091538 * \cos((7*we-W_{rpu}*we)*t - 116.82) & & +0.026155 * \cos((7*we-W_{rpu}*we)*t \\
 116.24)
 \end{aligned}$$

Electromagnetic Torque

$$\begin{aligned}
 T_e &= 0.100252 \\
 +0.161422 * \cos(2we-2wr)*t + 38.4475) & & \\
 +0.0265093 * \cos(6we)*t + 89.7275) & & \\
 +0.00560093 * \cos(-4we-2wr)*t + 88.7102) & & \\
 +0.023371 * \cos(-6we)*t + 84.4118) & & \\
 +0.0019618 * \cos(8we-2wr)*t + 61.9254) & & \\
 +0.0302478 * \cos(6we)*t - 91.5961) & & \\
 +0.00566189 * \cos(4we+2wr)*t - 98.5578) & & \\
 +0.000139099 * \cos(10we+2wr)*t - 99.2964) & & \\
 +0.000562132 * \cos(12we)*t - 90.1552) & & \\
 +0.000114335 * \cos(-2we-2wr)*t - 90.7632) & & \\
 +0.0234614 * \cos(6we)*t + 85.0418) & & \\
 +0.00279735 * \cos(8we-2wr)*t + 47.4446) & & \\
 +0.00056381 * \cos(12we)*t + 89.8219) & & \\
 +0.000114341 * \cos(2we-2wr)*t + 89.1216) & & \\
 +3.59801e-005 * \cos(14we-2wr)*t + 82.3507)
 \end{aligned}$$

Figure 9.3 Printout of solution when the rotor rotates as a sub-synchronous speed of 0.4 p.u.

Chapter 10

Linearization of the Synchronous Machine Equations

10.1 Introduction

Many problems exist in which the rotor speed can no longer be assumed as constant. The presence of the rotor speed dependant voltage term in Park's equations and the torque equations results in a non-linear set of differential equation to be solved. In many problems, however, the change in speed can be considered as sufficiently small that the equations can be shown to remain essentially linear. The resulting set of equations is generally termed the *small signal equations* and is particularly important for the design of controllers.

10.2 Park's Equations in Physical Units

Repeating here for convenience, Park's equations in physical units are,

$$v_{qs} = r_s i_{qs} + \frac{p}{\omega_b} \psi_{qs} + \frac{\omega_r}{\omega_b} \psi_{ds} \quad (10.1)$$

$$v_{ds} = r_s i_{ds} + \frac{p}{\omega_b} \psi_{ds} - \frac{\omega_r}{\omega_b} \psi_{qs} \quad (10.2)$$

$$v_{qr} = 0 = r_{qr} i_{qr} + \frac{p}{\omega_b} \psi_{qr} \quad (10.3)$$

$$v_{dr} = 0 = r_{dr} i_{dr} + \frac{p}{\omega_b} \psi_{dr} \quad (10.4)$$

$$e_x = x_{md} i_{fr} + \frac{x_{md}}{r_{fr}} \frac{p}{\omega_b} \psi_{fr} \quad (10.5)$$

$$T_e = \frac{3P}{22} \frac{1}{\omega_b} (\psi_{ds} i_{qs} - \psi_{qs} i_{ds}) \quad (10.6)$$

$$T_e - T_l = \frac{2J\omega_b}{P} \frac{d}{dt}(\omega_r/\omega_b) \quad (10.7)$$

where

$$\Psi_{qs} = x_{qs} i_{qs} + x_{mq} i_{qr} \quad (10.8)$$

$$\Psi_{ds} = x_{ds} i_{ds} + x_{md}(i_{dr} + i_{fr}) \quad (10.9)$$

$$\Psi_{qr} = x_{qr} i_{qr} + x_{mq} i_{qs} \quad (10.10)$$

$$\Psi_{dr} = x_{dr} i_{dr} + x_{md}(i_{ds} + i_{fr}) \quad (10.11)$$

$$\Psi_{fr} = x_{fr} i_{fr} + x_{md}(i_{ds} + i_{dr}) \quad (10.12)$$

and

$$e_x = \frac{x_{md} v_{fr}}{r_{fr}} \quad (10.13)$$

Assume that the machine is supplied from (or feeds) a balanced set of source voltages (i.e., from an infinite bus) through a lossy line reactance x_e . When the machine is synchronized (but not in the steady-state) it can be shown from the equations of transformation that

$$v_{qs} = v_b \cos \theta_b - \frac{p}{\omega_b} x_e i_{qs} - \frac{\omega_r}{\omega_b} x_e i_{ds} - r_e i_{qs} \quad (10.14)$$

$$v_{ds} = -v_b \sin \theta_b - \frac{p}{\omega_b} x_e i_{ds} + \frac{\omega_r}{\omega_b} x_e i_{qs} - r_e i_{ds} \quad (10.15)$$

where the infinite bus voltage amplitude and phase, v_b and θ_b , are possibly functions of time.

In the steady-state, v_b , θ_b , e_x , and T_l all become constants. Hence, i_{ds} , i_{qs} , i_{dr} , i_{qr} , i_{fr} , v_{ds} , v_{qs} and ω_r also become constants in the steady-state. In particular, i_{qr} and i_{dr} become zero since the forcing functions for these circuits (v_{qr} and v_{dr}) are zero. As in Chapter 7, a convention will be used here such that a subscript “o” denotes a variable in a steady-state operating condition.

In the steady-state, Park's equations reduce to

$$V_{qso} = r_s I_{qso} + \frac{\omega_{ro}}{\omega_b} \Psi_{dso} \quad (10.16)$$

$$V_{dso} = r_s i_{dso} - \frac{\omega_{ro}}{\omega_b} \Psi_{qso} \quad (10.17)$$

$$V_{qbo} = V_{bo} \cos \theta_{bo} = \frac{\omega_{ro}}{\omega_b} x_e I_{dso} + r_e I_{qso} + V_{qso} \quad (10.18)$$

$$V_{dbo} = -V_{bo} \sin \theta_{bo} = -\frac{\omega_{ro}}{\omega_b} x_e I_{qso} + r_e I_{dso} + V_{dso} \quad (10.19)$$

$$E_{io} = E_{xo} = x_{md} I_{fro} \quad (10.20)$$

$$T_{eo} = \frac{3}{2} \frac{P}{2} \frac{1}{\omega_b} (\Psi_{dso} I_{qso} - \Psi_{qso} I_{dso}) \quad (10.21)$$

$$T_{eo} = T_{lo} \quad (10.22)$$

where

$$\Psi_{qso} = x_{qs} I_{qso} \quad (10.23)$$

$$\Psi_{dso} = x_{ds} I_{dso} + x_{md} I_{fro} \quad (10.24)$$

$$\Psi_{qro} = x_{mq} I_{qso} \quad (10.25)$$

$$\Psi_{dro} = x_{md} (I_{dso} + I_{fro}) \quad (10.26)$$

$$E_{xo} = \frac{x_{md} V_{fro}}{r_{fr}} \quad (10.27)$$

In practical cases, the voltage at the terminals of the machine are specified so that V_{qso} and V_{dso} are assumed as known. Eqs. (10.16) and (10.17) are then used to solve for the stator currents and Eqs. (10.18) and (10.19) used to determine the voltage at the infinite bus.

10.3 Linearization Process

Consider again a small change from a balanced operating condition. In Eq. (10.14) let

$$\begin{aligned} V_{qso} + \Delta v_{qs} &= (V_{bo} + \Delta v_b) \cos(\theta_{bo} + \Delta \theta_b) - \frac{p}{\omega_b} x_e (I_{qso} + \Delta i_{qs}) \\ &\quad - \frac{(\omega_{ro} + \Delta \omega_r)}{\omega_b} x_e (I_{dso} + \Delta i_{ds}) - r_e (I_{qso} + \Delta i_{qs}) \end{aligned} \quad (10.28)$$

or, expanding the cosine function,

$$V_{qso} + \Delta v_{qs} = (V_{bo} + \Delta v_b)(\cos \theta_{bo} \cos \Delta \theta_b - \sin \theta_{bo} \sin \Delta \theta_b) \quad (10.29)$$

$$- \frac{p}{\omega_b} x_e (I_{qso} + \Delta i_{qs}) - \frac{(\omega_{ro} + \Delta \omega_r)}{\omega_b} x_e (I_{dso} + \Delta i_{ds}) - r_e (I_{qso} + \Delta i_{qs})$$

However, if the change of the angular displacement of the torque angle $\Delta \theta_{bo}$ is sufficiently small, then

$$\cos \Delta \theta_b \approx 1$$

$$\sin \Delta \theta_b \approx \Delta \theta_b$$

Upon substituting this result into Eq. (10.29) and eliminating the steady-state terms by virtue of Eq. (10.18),

$$\Delta v_{qs} \approx \Delta v_b \cos \theta_{bo} - V_{bo} \sin \theta_{bo} \Delta \theta_b - \frac{p}{\omega_b} x_e \Delta i_{qs}$$

$$- \frac{\Delta \omega_r}{\omega_b} x_e I_{dso} - \frac{\Delta \omega_r}{\omega_b} x_e \Delta i_{ds} - \frac{\omega_{ro}}{\omega_b} x_e \Delta i_{ds} + \frac{\Delta \omega_r}{\omega_b} x_e \Delta i_{ds} - r_e \Delta i_{qs} \quad (10.30)$$

If the change is sufficiently small, the product $\Delta \omega_r \Delta i_{ds}$ can be neglected in which case

$$\Delta v_{qs} \approx \Delta v_b \cos \theta_{bo} - V_{bo} \sin \theta_{bo} \Delta \theta_b - \frac{p}{\omega_b} x_e \Delta i_{qs} - x_e I_{dso} \frac{\Delta \omega_r}{\omega_b} - \frac{\omega_{ro}}{\omega_b} x_e \Delta i_{ds} - r_e \Delta i_{qs}$$

$$\quad (10.31)$$

In general, the angle θ_b is defined as

$$\theta_b = \int (\omega_e - \omega_r) dt \quad (10.32)$$

For a small change around a steady-state condition,

$$\Delta \theta_b = \int_{t_o}^{t_o + \Delta t} (\omega_{eo} + \Delta \omega_e - \omega_{ro} - \Delta \omega_r) dt \quad (10.33)$$

$$\quad (10.34)$$

So that, since $\omega_{eo} = \omega_{ro}$

$$\Delta \theta_b = \int \Delta \omega_e dt - \int \Delta \omega_r dt \quad (10.35)$$

$$= \Delta \delta_b - \Delta \theta_r \quad (10.36)$$

Therefore the deviation of the voltage vector can result from two sources, the first being the change in the angle of the source voltage itself, while the second is the change in angle due to the motion of the rotor.

Thus, finally,

$$\begin{aligned}\Delta v_{qs} \cong & \Delta v_b \cos \delta_{bo} - V_{bo} \sin \delta_{bo} \Delta \delta_b + V_{bo} \sin \delta_{bo} \Delta \theta_r - \frac{p}{\omega_b} x_e \Delta i_{qs} - x_e I_{dso} \frac{\Delta \omega_r}{\omega_b} \\ & - \frac{\omega_{ro}}{\omega_b} x_e \Delta i_{ds} - r_e \Delta i_{qs}\end{aligned}\quad (10.37)$$

Similarly, for the *d*-axis,

$$\begin{aligned}\Delta v_{ds} \cong & -\Delta v_b \sin \delta_{bo} - V_{bo} \cos \delta_{bo} \Delta \delta_b + V_{bo} \cos \delta_{bo} \Delta \theta_r - \frac{p}{\omega_b} x_e \Delta i_{ds} + x_e I_{qso} \frac{\Delta \omega_r}{\omega_b} \\ & + \frac{\omega_{ro}}{\omega_b} x_e \Delta i_{qs} - r_e \Delta i_{ds}\end{aligned}\quad (10.38)$$

where it has been noted that $\theta_{bo} = \delta_{bo}$ since the point of reference for the torque angle δ_b is the rotor *q*-axis.

Combining these results with linearized versions of Park's equations yields, finally

$$\begin{aligned}\Delta v_b \cos \delta_{bo} - V_{bo} \sin \delta_{bo} (\Delta \delta_b) = & -V_{bo} \sin \delta_{bo} \Delta \theta_r + (r_s + r_e) \Delta i_{qs} \\ & + \frac{p}{\omega_b} (\Delta \psi_{qs} + x_e \Delta i_{qs}) + \frac{\omega_{ro}}{\omega_b} (\Delta \psi_{ds} + x_e \Delta i_{ds}) + (\Psi_{dso} + x_e I_{dso}) \frac{\Delta \omega_r}{\omega_b}\end{aligned}\quad (10.39)$$

$$\begin{aligned}-\Delta v_b \sin \delta_{bo} - V_{bo} \cos \delta_{bo} (\Delta \delta_b) = & -V_{bo} \cos \delta_{bo} \Delta \theta_r + (r_s + r_e) \Delta i_{ds} \\ & + \frac{p}{\omega_b} (\Delta \psi_{qs} + x_e \Delta i_{qs}) - \frac{\omega_{ro}}{\omega_b} (\Delta \psi_{qs} + x_e \Delta i_{qs}) - (\Psi_{qso} + x_e I_{qso}) \frac{\Delta \omega_r}{\omega_b}\end{aligned}\quad (10.40)$$

$$0 = r_{qr} \Delta i_{qr} + \frac{p}{\omega_b} \Delta \psi_{qr}\quad (10.41)$$

$$0 = r_{dr} \Delta i_{dr} + \frac{p}{\omega_b} \Delta \psi_{dr}\quad (10.42)$$

$$\Delta e_x = x_{md} \Delta i_{fr} + \frac{x_{md}}{r_{fr}} \frac{p}{\omega_b} \Delta \psi_{fr}\quad (10.43)$$

$$\Delta T_e = \frac{3P}{2} \frac{1}{\omega_b} (\Psi_{dso} \Delta i_{qs} + \Delta \psi_{ds} i_{qso} - \Psi_{qso} \Delta i_{ds} - \Delta \psi_{qs} i_{dso}) \quad (10.44)$$

$$\Delta T_e - \Delta T_l = 2 \frac{J\omega_b}{P} p \left(\frac{\Delta \omega_r}{\omega_b} \right) \quad (10.45)$$

where

$$\Delta \psi_{qs} = x_{qs} \Delta i_{qs} + x_{mq} \Delta i_{qr} \quad (10.46)$$

$$\Delta \psi_{ds} = x_{ds} \Delta i_{ds} + x_{md} (\Delta i_{dr} + \Delta i_{fr}) \quad (10.47)$$

$$\Delta \psi_{qr} = x_{qr} \Delta i_{qr} + x_{mq} \Delta i_{qs} \quad (10.48)$$

$$\Delta \psi_{dr} = x_{dr} \Delta i_{dr} + x_{md} (\Delta i_{ds} + \Delta i_{fr}) \quad (10.49)$$

$$\Delta \psi_{fr} = x_{fr} \Delta i_{fr} + x_{md} (\Delta i_{ds} + \Delta i_{dr}) \quad (10.50)$$

$$\Delta e_x = \frac{x_{md} \Delta v_{fr}}{r_{fr}} \quad (10.51)$$

$$p = d/dt$$

Finally, an additional differential equation must be written to portray the angle produced by the change in speed as a state variable. Whereupon

$$p \theta_r = \omega_r \quad (10.52)$$

Equations (10.39)–(10.52) constitute seven differential and seven algebraic equations describing the behavior of a synchronous machine about a steady-state operating point. Substituting Eqs. (10.46)–(10.51) into Eqs. (10.39)–(10.45), one can eliminate the flux linkage variables from the differential equations. When flux linkages are eliminated, Eqs. (10.39)–(10.52) are equivalent to the matrix expression

$$\begin{bmatrix} \cos \delta_{bo} \\ -\sin \delta_{bo} \\ 0 \\ 0 \\ 0 \\ 0 \\ 0 \end{bmatrix} \Delta v_b + \begin{bmatrix} -V_{bo} \sin \delta_{bo} \\ -V_{bo} \cos \delta_{bo} \\ 0 \\ 0 \\ 0 \\ 0 \\ 0 \end{bmatrix} \Delta \delta_b + \begin{bmatrix} 0 \\ 0 \\ 0 \\ 1 \\ 0 \\ 0 \\ 0 \end{bmatrix} \Delta e_x + \begin{bmatrix} 0 \\ 0 \\ 0 \\ 0 \\ 0 \\ 1 \\ 0 \end{bmatrix} \Delta T_l =$$

$$\begin{bmatrix}
r_s + r_e & \frac{\omega_{ro}}{\omega_b}(x_{ds} + x_e) & 0 & \frac{\omega_{ro}}{\omega_b}x_{md} & \frac{\omega_{ro}}{\omega_b}x_{md} & \frac{\Psi_{dso} + x_e I_{dso}}{\omega_b} - V_{bo} \sin \delta_{bo} \\
-\frac{\omega_{ro}}{\omega_b}(x_{qs} + x_e) & r_s + r_e & -\frac{\omega_{ro}}{\omega_b}x_{mq} & 0 & 0 & -\frac{\Psi_{qso} + x_e I_{qso}}{\omega_b} - V_{bo} \cos \delta_{bo} \\
0 & 0 & r_{qr} & 0 & 0 & 0 \\
0 & 0 & 0 & r_{dr} & 0 & 0 \\
0 & 0 & 0 & 0 & x_{md} & 0 \\
C_t(\Psi_{dso} - x_{qs} I_{dso}) & -C_t(\Psi_{qso} - x_{ds} I_{qso}) & -C_t x_{mq} I_{dso} & C_t x_{md} I_{qso} & C_t x_{md} I_{qso} & 0 \\
0 & 0 & 0 & 0 & 0 & -1
\end{bmatrix} \times \begin{bmatrix} \Delta i_{qs} \\ \Delta i_{ds} \\ \Delta i_{qr} \\ \Delta i_{dr} \\ \Delta i_{fr} \\ \Delta \omega_r \\ \Delta \theta_r \end{bmatrix} \\
+ \frac{P}{\omega_b} \begin{bmatrix} x_{qs} + x_e & 0 & x_{mq} & 0 & 0 & 0 & 0 \\
0 & x_{ds} + x_e & 0 & x_{md} & x_{md} & 0 & 0 \\
x_{mq} & 0 & x_{qr} & 0 & 0 & 0 & 0 \\
0 & x_{md} & 0 & x_{dr} & x_{md} & 0 & 0 \\
0 & x_{md}^2/r_{fr} & 0 & x_{md}^2/r_{fr} & x_{fr} x_{md}^2/r_{fr} & 0 & 0 \\
0 & 0 & 0 & 0 & 0 & -\frac{2J\omega_b}{P} & 0 \\
0 & 0 & 0 & 0 & 0 & 0 & \omega_b
\end{bmatrix} \times \begin{bmatrix} \Delta i_{qs} \\ \Delta i_{ds} \\ \Delta i_{qr} \\ \Delta i_{dr} \\ \Delta i_{fr} \\ \Delta \omega_r \\ \Delta \theta_r \end{bmatrix} \quad (10.53)$$

where, for convenience, define

$$\Psi_{dso} = x_{ds} I_{dso} + x_{md} I_{fro} \quad (10.54)$$

$$= x_{ds} I_{dso} + E_{xo} \quad (10.55)$$

and

$$\Psi_{qso} = x_{qs} I_{qso} \quad (10.56)$$

and where the torque constant C_t has been defined as

$$C_t = \frac{3P}{22} \frac{1}{\omega_b}$$

The left-hand side of Eq. (10.53) can be written in the alternative form

$$\begin{bmatrix} \cos \delta_{bo} \\ -\sin \delta_{bo} \\ 0 \\ 0 \\ 0 \\ 0 \\ 0 \end{bmatrix} \Delta v_b + \begin{bmatrix} -V_{bo} \sin \delta_{bo} \\ -V_{bo} \cos \delta_{bo} \\ 0 \\ 0 \\ 0 \\ 0 \\ 0 \end{bmatrix} \Delta \delta_b + \begin{bmatrix} 0 \\ 0 \\ 0 \\ 0 \\ 1 \\ 0 \\ 0 \end{bmatrix} \Delta e_x + \begin{bmatrix} 0 \\ 0 \\ 0 \\ 0 \\ 0 \\ 1 \\ 0 \end{bmatrix} \Delta T_l = \begin{bmatrix} \cos \delta_{bo} & -V_{bo} \sin \delta_{bo} & 0 & 0 \\ -\sin \delta_{bo} & -V_{bo} \cos \delta_{bo} & 0 & 0 \\ 0 & 0 & 0 & 0 \\ 0 & 0 & 0 & 0 \\ 0 & 0 & 1 & 0 \\ 0 & 0 & 0 & 1 \\ 0 & 0 & 0 & 0 \end{bmatrix} \times \begin{bmatrix} \Delta v_b \\ \Delta \delta_b \\ \Delta e_x \\ \Delta T_l \end{bmatrix} \quad (10.57)$$

Eq. (10.53) can now be written in the form

$$\mathbf{A}_1 \Delta \mathbf{u} = \frac{p}{\omega_b} \mathbf{A}_2 \Delta \mathbf{x} + \mathbf{A}_3 \Delta \mathbf{x} \quad (10.58)$$

Hence

$$\frac{p}{\omega_b} \Delta \mathbf{x} = -\mathbf{A}_2^{-1} \mathbf{A}_3 \Delta \mathbf{x} + \mathbf{A}_2^{-1} \mathbf{A}_1 \Delta \mathbf{u} \quad (10.59)$$

Eq. (10.59) is of the form

$$\frac{p}{\omega_b} \Delta \mathbf{x} = \mathbf{A} \Delta \mathbf{x} + \mathbf{B} \Delta \mathbf{u} \quad (10.60)$$

where

$$\mathbf{A} = -\mathbf{A}_2^{-1} \mathbf{A}_3 \quad (10.61)$$

$$\mathbf{B} = \mathbf{A}_2^{-1} \mathbf{A}_1 \quad (10.62)$$

and

$$p = d/dt \quad (10.63)$$

10.4 Transfer Functions of a Synchronous Machine

With the use of MATLAB, transfer functions can be computed by first expressing the linearized synchronous machine equations in the state space form of Eq. (10.60). The vector $\mathbf{B}\Delta\mathbf{u} = \mathbf{b}\Delta u$ defines the input to the transfer function of interest. In addition, it is necessary to identify the desired output by forming the so-called measurement equation

$$y = \mathbf{c}^T \dot{\mathbf{x}} + d\mathbf{u} \quad (\text{measurement equation}) \quad (10.64)$$

where \mathbf{u} is the input of the desired transfer function and y is the output. The four possible inputs corresponding to the vector \mathbf{b} can be readily identified from Eq. (10.57).

10.4.1 Transfer Function Inputs

A desired transfer function input is defined by selecting the proper column of the matrix \mathbf{A} . For example, if Δv_b is selected as the input, then

$$\mathbf{b} = \begin{bmatrix} \cos\delta_{bo} \\ -\sin\delta_{bo} \\ 0 \\ 0 \\ 0 \\ 0 \end{bmatrix} \quad (10.65)$$

The \mathbf{b} vectors for the four most practical transfer function inputs are summarized in Table 10.1.

Table 10.1 Possible Synchronous Machine Transfer Function Inputs

Input	Vector \mathbf{b}
Change in Stator Bus Voltage Amplitude Δv_b	$\mathbf{b} = [\cos\delta_{bo}, -\sin\delta_{bo}, 0, 0, 0, 0]^t$
Change in Stator Bus Voltage Phase Angle (Torque Angle w.r.t. AC Bus Voltage) $\Delta\delta_b$	$\mathbf{b} = [-V_{bo}\sin\delta_{bo}, -V_{bo}\cos\delta_{bo}, 0, 0, 0, 0]^t$
Change in Field Voltage $\Delta e_x = (x_{md}/r_{fr})\Delta y_{fr}$ $= (x_{md}/r_{fr})(N_f/N_s)\Delta v_{fr}$	$\mathbf{b} = [0, 0, 0, 0, 1, 0]^t$
Change in Load Torque ΔT_l	$\mathbf{b} = [0, 0, 0, 0, 0, 1]^t$

10.4.2 Transfer Function Outputs

Transfer function outputs are defined by setting up the appropriate measurement equation. In the case of zero source impedance, the “ d ” portion of the measurement equation is zero, indicating that the output is not algebraically related to the input. Appropriate “ c ” vectors for a variety of outputs are summarized in Table 10.2. In practice the number of possible outputs is vast but is generally to those variables of interest in design of a feedback control loop. Many of the desired outputs, for example, the change in current amplitude, can be found by proper linearization. By definition

$$i_s = \sqrt{i_{ds}^2 + i_{qs}^2} \quad (10.66)$$

For small changes,

$$I_{so} + \Delta i_s = \sqrt{(I_{ds0} + \Delta i_{ds})^2 + (I_{qs0} + \Delta i_{qs})^2} \quad (10.67)$$

which can be written as

$$I_{so} + \Delta i_s \approx \sqrt{I_{so}^2 + 2I_{ds0}\Delta i_{ds} + 2I_{qs0}\Delta i_{qs}} \quad (10.68)$$

$$= I_{so} \sqrt{1 + 2\frac{I_{ds0}}{I_{so}^2}\Delta i_{ds} + 2\frac{I_{qs0}}{I_{so}^2}\Delta i_{qs}} \quad (10.69)$$

However, from the power series expansion

$$\sqrt{1+x} = 1 + \frac{x}{2!} + \frac{x^2}{4!} + \dots \quad (10.70)$$

and, neglecting the higher order terms, Eq/ (10.69) can be written

$$I_{so} + \Delta i_s \approx I_{so} + \frac{I_{ds0}}{I_{so}}\Delta i_{ds} + \frac{I_{qs0}}{I_{so}}\Delta i_{qs} \quad (10.71)$$

whereupon

$$\Delta i_s = \frac{I_{ds0}}{I_{so}}\Delta i_{ds} + \frac{I_{qs0}}{I_{so}}\Delta i_{qs} \quad (10.72)$$

The same procedure can clearly be used to determine flux linkage amplitudes $\Delta\psi_s$ and $\Delta\psi_m$ in terms of the state variables. However, the expression for the change in terminal voltage Δv_s requires more elaboration. Repeating Eqs. (10.31) and (10.38),

$$\begin{aligned} \Delta v_{qs} &= \cos\delta_{bo}\Delta v_b - V_{bo}\sin\delta_{bo}\Delta\delta_b + V_{bo}\sin\delta_{bo}\Delta\theta_r - \frac{p}{\omega_b}x_e\Delta i_{qs} - r_e\Delta i_{qs} \\ &\quad - \frac{\omega_{ro}}{\omega_b}x_e\Delta i_{ds} - x_e I_{ds0} \frac{\Delta\omega_r}{\omega_b} \end{aligned} \quad (10.73)$$

$$\begin{aligned} \Delta v_{ds} &\approx -\sin\delta_{bo}\Delta v_b - V_{bo}\cos\delta_{bo}\Delta\delta_b + V_{bo}\cos\delta_{bo}\Delta\theta_r - \frac{p}{\omega_b}x_e\Delta i_{ds} - r_e\Delta i_{ds} \\ &\quad + \frac{\omega_{ro}}{\omega_b}x_e\Delta i_{qs} + x_e I_{qs0} \frac{\Delta\omega_r}{\omega_b} \end{aligned} \quad (10.74)$$

The time derivatives in these expressions can now be found from the first and second row of the state equation, Eq. (10.60). In terms of the measurement equation

$$\Delta v_s = \left(\frac{V_{qso}}{V_{so}} c_{qs}^t + \frac{V_{dso}}{V_{so}} c_{ds}^t \right) \Delta x + \left(d - \frac{V_{qso}}{V_{so}} x_e b(1) - \frac{V_{dso}}{V_{so}} x_e b(2) \right) \Delta u \quad (10.75)$$

where

$$c_{qs} = \begin{bmatrix} -x_e A_{1,1} - r_e \\ -x_e A_{1,2} - (\omega_{ro}/\omega_b)x_e \\ -x_e A_{1,3} \\ -x_e A_{1,4} \\ -x_e A_{1,5} \\ -x_e (I_{dso} + A_{1,6}) \\ V_{bo} \sin \delta_{bo} - x_e A_{1,7} \end{bmatrix} \quad (10.76)$$

$$c_{ds} = \begin{bmatrix} -x_e A_{2,1} + (\omega_{ro}/\omega_b)x_e \\ -x_e A_{2,2} - r_e \\ -x_e A_{2,3} \\ -x_e A_{2,4} \\ -x_e A_{2,5} \\ x_e (I_{qso} - A_{2,6}) \\ V_{bo} \cos \delta_{bo} - x_e A_{2,7} \end{bmatrix} \quad (10.77)$$

$$d = \frac{V_{qso}}{V_{so}} \cos \delta_{bo} - \frac{V_{dso}}{V_{so}} \sin \delta_{bo} \quad \text{if } \Delta u = \Delta v_b \quad (10.78)$$

$$d = -\frac{V_{qso}}{V_{so}} V_{bo} \sin \delta_{bo} - \frac{V_{dso}}{V_{so}} V_{bo} \cos \delta_{bo} \quad \text{if } \Delta u = \Delta \delta_b \quad (10.79)$$

and the constants $A_{n,m}$ correspond to the n^{th} row and m^{th} column of the matrix \mathbf{A} defined by Eq. (10.61).

Table 10.2 Possible Synchronous Machine Transfer Function Outputs

Output	Vectors \mathbf{c}^t
Change in Stator Current Amplitude Δi_s	$\mathbf{c}^t = [I_{qso}/I_{so}, I_{dso}/I_{so}, 0, 0, 0, 0, 0]$ $I_{so} = \sqrt{I_{qso}^2 + I_{dso}^2}$
Change in Field Current Amplitude $\Delta i_{fr}' = (N_f/N_s)\Delta i_{fr}$	$\mathbf{c}^t = [0, 0, 0, 0, 1, 0, 0]$
Change in Air Gap Flux Amplitude $\Delta \Psi_m/\omega_b$	$\mathbf{c}^t = \left(\frac{1}{\omega_b \Psi_{mo}}\right) [\Psi_{mqo}, \Psi_{mdo}, \Psi_{mqo},$ $\Psi_{mdo}, \Psi_{mdo}, 0, 0]$ $\Psi_{mo} = \sqrt{\Psi_{mqo}^2 + \Psi_{mdo}^2}$
Change in Stator Flux Amplitude $(\Delta \Psi_s)/\omega_b$	$\mathbf{c}^t = \left(\frac{1}{\omega_b \Psi_{so}}\right) [\Psi_{qso}, \Psi_{dso}, \Psi_{qso},$ $\Psi_{dso}, \Psi_{dso}, 0, 0]$ $\Psi_{so} = \sqrt{\Psi_{qso}^2 + \Psi_{dso}^2}$
Change in Terminal Voltage Δv_s , ($r_e = x_e = 0$)	$\mathbf{c}^t = \frac{V_{qso}}{V_{so}} \mathbf{c}_{qs}^t + \frac{V_{dso}}{V_{so}} \mathbf{c}_{ds}^t$
Change in Electromagnetic Torque ΔT_e	$\mathbf{c}^t = C_t [(\Psi_{dso} - x_{qso} I_{dso}), (x_{ds} - x_{qs}) I_{qso},$ $-x_{mq} I_{dso}, x_{md} I_{qso}, x_{md} I_{qso}, 0, 0]$

Table 10.2 Possible Synchronous Machine Transfer Function Outputs

Output	Vectors c^t
Change in Mechanical Speed $\Delta\omega_{rm} = (2/P)\Delta\omega_r$	$c^t = [0, 0, 0, 0, 0, 2/P, 0]$
Change in Torque Angle $\Delta\delta$	$c^t = [0, 0, 0, 0, 0, 0, 1]$

10.5 Solution of the State Space and Measurement Equations

A listing of the MATLAB code, named TrafunSMPu, needed to compute the state space and measurement equations is given in Appendix 4. Once having computed these results, the poles and zeros of the transfer function can be computed in polynomial and in factored form by the functions “ss2tf” and “ss2zp”. The residues and poles of the transfer function can also be obtained by function “residue”. Finally the output time response for a step function input can be computed using the function “step.”

A typical printout of the computed results is shown in [Figure 10.1](#) for the case of a step decrease in the terminal voltage from rated voltage to zero. The per unit parameters of the 30 MVA machine of Table 5.3 have been used, the external impedance set to zero, and no load operation chosen, making the comparison of the results with Eq. (5.18) possible. The input chosen was the negative of the input voltage existing before the change, or $\Delta v_s = -V_{so}$, thereby resulting in a short-circuit at the terminals of the machine. The transfer function output was selected as Δi_{ds} . While the derivation of [Section 10.4](#) assumed conventional S.I. units, a per unit solution is easily obtained by setting the torque constant C_t equal to unity and the 6,6 element of the matrix A_2 , i.e., $-2J\omega_b/P$, replaced by $-2H$.

The time domain response can be determined by examining the poles and residues resulting from the partial fraction expansion of the transfer function. Seven poles are displayed plus a pole at the origin resulting from the Laplace transform of a unit step function. The residue and pole combine to form one of

the terms in the time domain response. For example, for the pole p_n and residue r_n of the n^{th} pole, the corresponding time response is $r_n e^{-p_n t}$.

It can be observed that residues of several of the poles are essentially zero so that these modes do not affect the time response and can be neglected. In particular, the third and fourth poles correspond to the state variables $\Delta\omega_r$ and $\Delta\theta_r$, have only a very small residue, indicating that these quantities have only a very marginal effect on the current response. Thus, the assumption of constant speed in the modal solution of Section 5.12 can be justified. The inverse transform of the remainder of the poles not containing complex parts should now be clear. The complex roots $3.6 \pm j314.1$ can be expanded in the manner described in Appendix 2 in which it is shown that

$$(a - jb)e^{(\sigma + j\omega)t} + (a + jb)e^{(\sigma - j\omega)t} = 2\sqrt{a^2 + b^2} \sin(\omega t + \phi)$$

where $\phi = \text{atan}(a/(-b))$. The complete solution is therefore

$$\Delta i_{ds} = -0.5 + 5.826e^{-3.6t} \sin(314.1t - 89.94) - 1.62e^{-9.54t} - 3.74e^{-1.07t}$$

which is the same as the result obtained in Figure 5.16. A computation of the current $\Delta i_{DS} = i_{DS}$ after the three-phase fault is shown in Figure 10.2.

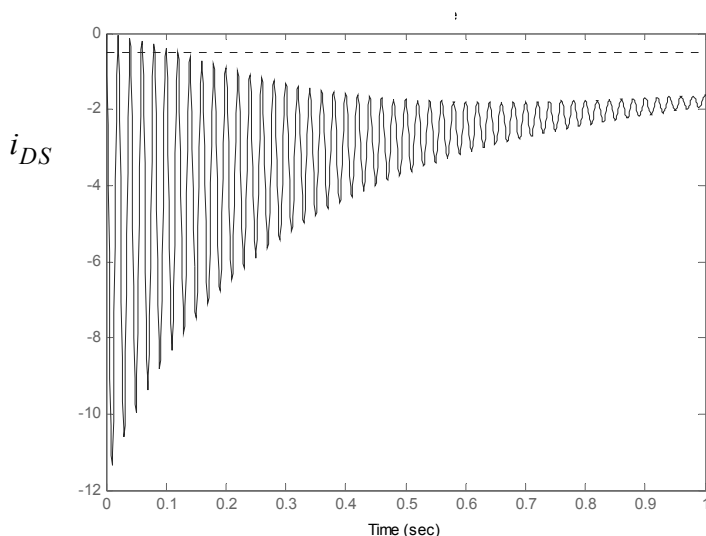


Figure 10.2 Per unit stator current i_{DS} after a three-phase fault computed using TrafunSMpu.

Parameter Values in Per Unit

$V_{l-l}(pu) = 1.2247$ V $F_{rated} = 50$ HZ Poles = 4
 $R_s = 0.002$ $R_{qr} = 0.003$ $R_{dr} = 0.003$ $R_{fr} = 0.001$
 $X_{ls} = 0.14$ $X_{mq} = 1.86$ $X_{md} = 1.86$
 $X_{lqr} = 0.04$ $X_{ldr} = 0.04$ $X_{lfr} = 0.14$ Inertia $H = 2.65$ s.

Steady-State Operating Point in Per Unit

Terminal Volts $V_{qs} = 1$ $V_{ds} = -0$ $V_s = 1$
 Inf. Bus Volts $V_{qb} = 1$ $V_{db} = 0$ $V_b = 1$
 $I_{qs} = 6.07153e-018$ $I_{ds} = 5.55112e-016$ $I_s = 5.55145e-016$
 $PSI_{qs} = 6.50521e-019$ $PSI_{ds} = 1$ $PSI_s = 1$
 $PSI_{Imq} = -4.11997e-018$ $PSI_{md} = 1$ $PSI_{fr} = 1.07527$
 $T_e = 6.07153e-018$
 Delta = 0 (deg) MMF Angle = -0.626648 (deg)
 Unsat. Field Amps I_{fr} (P.U.) = 0.537634 Unsat. Field Volts E_x (P.U.) = 1
 Power Factor = 0.0109368 (Leading) Power Factor Angle = 89.3734 (deg)

T.F. Input -- DELTA -V bus Units: P.U. Volts T.F. Output -- DELTA I_{ds} Units: P.U. Amperes
 Transfer Function (Polynomial Form):

$$-5.785e005 s^5 - 7.421e006 s^4 - 2.153e008 s^3 - 1.493e009 s^2 - 8.587e008 s - -8.258e007$$

$$s^7 + 23.34 s^6 + 9.919e004 s^5 + 1.599e006 s^4 + 3.947e007 s^3 + 3.683e008 s^2 + 5.049e008 s + 1.652e008$$

Factored Transfer Function:

$$-578490.9083 (s+7.17) (s+0.4998) (s+0.1213) (s^2 + 5.038s + 328.3)$$

$$(s+9.544) (s+1.069) (s+0.4998) (s^2 + 5.026s + 328.4) (s^2 + 7.201s + 9.868e004)$$

residues =

2.9311e+000 -2.7160e-003i	poles =
2.9311e+000 +2.7160e-003i	-3.6005e+000 +3.1411e+002i
-4.8420e-004 +1.8406e-003i	-3.6005e+000 -3.1411e+002i
-4.8420e-004 -1.8406e-003i	-2.5129e+000 +1.7946e+001i
-1.6206e+000	-2.5129e+000 -1.7946e+001i
-3.7407e+000	-9.5442e+000
1.3107e-009	-1.0685e+000
-4.9997e-001	-4.9985e-001

Figure 10.1 Output listing from TrafunSM corresponding to a short-circuit of the machine of Table 5.3.

Transfer functions for a wide variety of inputs and outputs can be obtained in a similar manner. For example, the response of the electromagnetic torque to a step increase in load torque can be computed by selecting ΔT_L as the input and ΔT_e as the output. The poles and residues corresponding to this transfer function are shown in Figure 10.3. The corresponding time response is shown in Figure 10.4. In this case the pair of complex poles which dominated the previous solution now have nearly zero residues, which indicates that their effect on the torque response is negligible, while the pair of complex poles corresponding to the deviation in speed and torque angle now dominate the solution. While the torque response suggests a slowly damped oscillation, it is important to keep in mind that the solution applies to relatively small deviations around an operating power, in this case no-load. In reality the differential equations are non-linear. In particular, the torque varies essentially sinusoidally with the torque angle δ . Excessively large step increases in load torque will lead to the machine pulling out of step (losing synchronism), as discussed in Chapter 6.

```

residues =
-0.0000 - 0.0000i
-0.0000 + 0.0000i
-0.5039 + 0.0708i
-0.5039 - 0.0708i
-0.0000
-0.0000
0.0077
1.0000

poles =
1.0e+002 *

-0.0360 + 3.1411i
-0.0360 - 3.1411i
-0.0251 + 0.1795i
-0.0251 - 0.1795i
-0.0954
-0.0107
-0.0050
0

```

Figure 10.3 Poles and residues corresponding to the response of the electromagnetic torque corresponding to a step load of one per unit.

Transfer functions are also an important tool for design of feedback control loops. For example, Chapter 7 dealt extensively with excitation control sys-

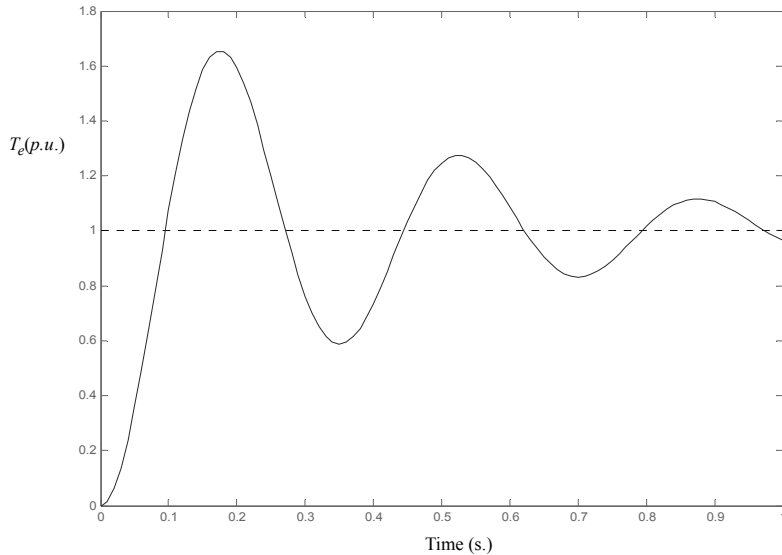


Figure 10.4 Time response of the electromagnetic torque to a step change in load.

tems for the purpose of regulating terminal voltage. The system of equations for the machine were considerably simplified to allow for a reasonably satisfactory solution. However, practical effects such as significant saliency, long amortisseur time constants, resistive line impedance, and so forth can make the simplified results deviate considerably from a proper regulator design. The full details of the relevant system transfer function for voltage control can be obtained by selecting Δe_X as the input to the program TrafunSMpu and Δv_S as the output. Values for an external line impedance $x_E = 0.1$ p.u. and $r_E = 0.01$ p.u. have been chosen. The generator is assumed to operate at rated load, rated terminal voltage, and unity power factor. A printout from the MATLAB program TrafunSM is presented in [Figure 10.5](#), which shows the transfer function in both polynomial and factored form as well as explicitly listing the poles and zeros.

It can be seen that the behavior of the complete transfer function is somewhat more complicated than that indicated by the simple block diagram of Figure 7.8. In particular, the presence of two zeroes in the right half plane indicates the possibility of a non-minimum phase solution. In such a case the step response of the output variable might begin with a negative value while ultimately ending up positively. The value of the change in terminal voltage at the instant of the step increase in field voltage can be found by examining the pole/

Steady-State Operating Point in Per Unit

Terminal Volts Vqs = 0.446198 Vds = 0.894934 Vs = 1
 Inf. Bus Volts Vqb = 0.351769 Vdb = 0.930776 Vb = 0.995031
 Iqs = -0.448367 Ids = -0.899453 Is = 1.00501
 PSIqs = -0.896733 PSIIds = 0.447095 PSIs = 1.00201
 PSImq = -0.833962 PSImd = 0.573018 PSIfr = 0.742072
 Te = -1.00703
 Delta = -63.5 (deg) MMF Angle = -26.4957 (deg)
 Unsat. Field Amps Ifr (P.U.) = 1.20753 Unsat. Field Volts Ex (P.U.) = 2.246
 Power Factor = 1 (Leading) Power Factor Angle = 0.00428332 (deg)
 T.F. Input -- DELTA Ex Units: P.U. Volts T.F. Output -- DELTA Vs Units: P.U. Volts

Transfer Function (Polynomial Form):

$$\begin{aligned}
 & 0.007308 s^6 + 0.3789 s^5 + 745 s^4 + 2.001e004 s^3 + 1.232e005 s^2 + 1.741e006 s \\
 & + 6.228e006
 \end{aligned}$$

$$\begin{aligned}
 & s^7 + 40.55 s^6 + 9.943e004 s^5 + 1.302e006 s^4 + 2.54e007 s^3 + 2.324e008 s^2 \\
 & + 5.439e008 s + 5.628e007
 \end{aligned}$$

Factored Transfer Function:

$$0.0073082 (s+23.56) (s+4.095) (s^2 - 0.6423s + 87.37) (s^2 + 24.84s + 1.011e005)$$

$$(s+7.633) (s+3.317) (s+0.1084) (s^2 + 2.02s + 207.5) (s^2 + 27.47s + 9.881e004)$$

poles =	zeros =
1.0e+002 *	1.0e+002 *
-0.1374 + 3.1404i	-0.1242 + 3.1772i
-0.1374 - 3.1404i	-0.1242 - 3.1772i
-0.0101 + 0.1437i	-0.2356
-0.0101 - 0.1437i	0.0032 + 0.0934i
-0.0763	0.0032 - 0.0934i
-0.0332	-0.0409
-0.0011	

Figure 10.5 Poles and zeros for the transfer function $\Delta v_S / \Delta e_X$.

zero/gain form of the transfer function of [Figure 10.5](#). Recall that the initial value theorem states that

$$\lim_{t \rightarrow 0} f(t) = \lim_{s \rightarrow \infty} s f(s) \quad (10.80)$$

If $f(s)$ corresponds to the transfer function corresponding to the step function response of the transfer function $\Delta v_S(s)/\Delta e_X(s) = G(s)$, then

$$\lim_{t \rightarrow 0} v_S(t) = \lim_{s \rightarrow \infty} s \frac{G(s)}{s} = \lim_{s \rightarrow \infty} G(s) \quad (10.81)$$

Letting s approach infinity in the factored form of the transfer function results in the initial condition being 0.0.

The final value of the terminal voltage after a unit step change is found in a similar manner. In this case the final value theorem can be used, i.e.

$$\lim_{t \rightarrow \infty} v_S(t) = \lim_{s \rightarrow 0} s \frac{G(s)}{s} = \lim_{s \rightarrow 0} G(s) \quad (10.82)$$

The final value of the terminal voltage after a step change can be easily found from the transfer function form of $\Delta v_S/\Delta e_X$. When s is set equal to zero in this expression, then

$$\lim_{t \rightarrow \infty} v_S(t) = \lim_{s \rightarrow 0} G(s) = \frac{6.228 \times 10^6}{5.628 \times 10^7} = 0.1107 \text{ p.u.} \quad (10.83)$$

[Figure 10.6](#) shows the response of the terminal voltage to a unit step change in field voltage as computed by its linearized transfer function. The very small negative initial value and trend to the positive final value can be verified from this result. The solution is almost entirely dominated by the field time constant $T_f = 1/0.11 = 9.03$ s. Note that the response initially moves in the negative direction before ultimately increasing in a positive direction. This type of behavior is characteristic of system which has open-loop zeros in the right half plane and their presence can be observed in [Figure 10.5](#).

10.6 Design of a Terminal Voltage Controller

It is useful to again consider the process of designing a voltage regulator, as introduced in Chapter 7, now that a more accurate representation of the transfer function has been determined. In the results to follow until the end of the chapter, the machine of Table 5.3 will again be used, with the machine operating at

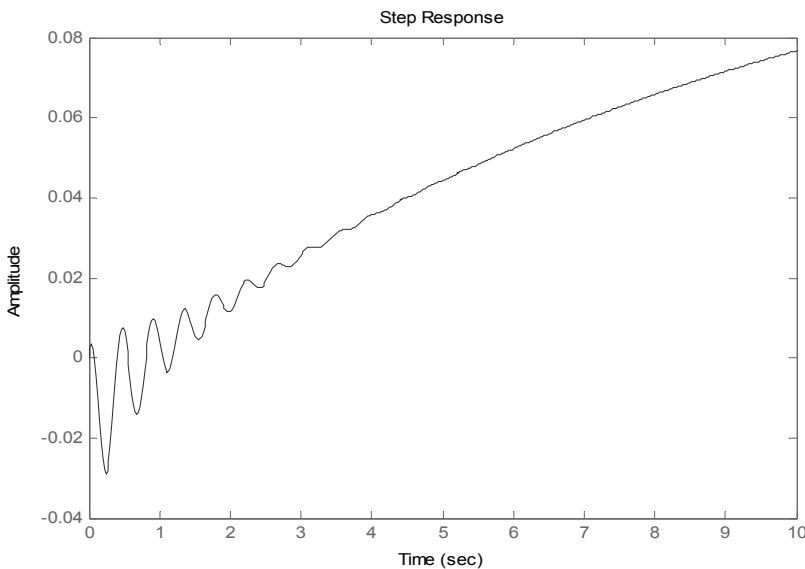
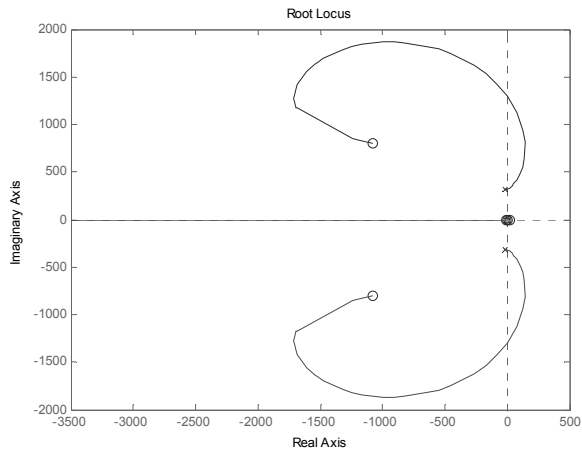


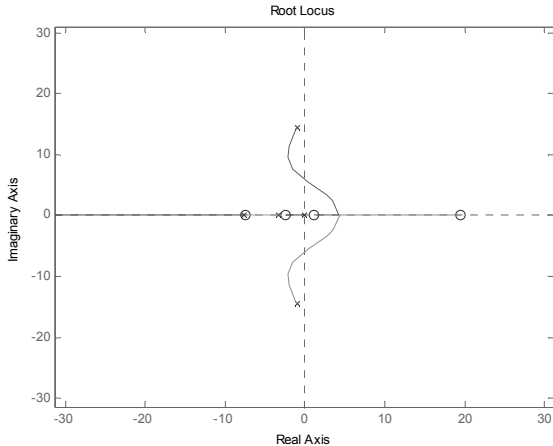
Figure 10.6 Change in stator terminal voltage to a unit step change in field voltage.

rated load with unity power factor. The system again is assumed to be connected to the infinite bus through an external impedance of $0.01 + j0.1$ ohms.

Figure 10.7 shows the root locus plot of the $G(s) = \Delta v_S / \Delta e_x$. The x 's and o 's show the open-loop location of the poles and zeros, respectively, and the loci show the paths of the poles toward the zeros as closed-loop gain is introduced. The pair of poles and zeros corresponding to the DC offset of the stator current in the stationary reference frame ($-13.7 \pm j314$, are in the right half plane until sufficient gain is introduced to move them toward their corresponding zeros. It is quite evident that with sufficient gain the poles associated with the electromechanical swing equation defined in Chapter 7 enter the right half plane. These poles are represented in this plot by their open-loop values $-1.01 \pm j14.37$. The critical DC gain in the overall transfer function that can be introduced before instability is reached is about 10. For reasonable transient response, the practical gain would be limited to about 2 to 3, indicating that the output v_S would follow the input e_X with a large steady-state error. This degree of tracking capability is generally considered as inadequate for most applications. It is clear that the complexity of the system transfer function limits the usefulness of the root locus technique when it comes to system design.



(a)



(b)

Figure 10.7 Root locus plots corresponding to the transfer function $(\Delta v_S)/(\Delta e_X)$ (a) showing all poles and zeros, (b) expanded version showing poles and zeros near the origin.

When the order of systems becomes more than three (seven in this case), the Bode frequency response method offers a preferred approach to closed-loop design. In this case the magnitude and phase of the transfer function is plotted in the frequency domain by replacing s with $j\omega$ in the open-loop transfer function. Figure 10.8 shows the Bode plot for the transfer function of the voltage ratio $G(j\omega) = \Delta v_S(j\omega)/\Delta e_X(j\omega)$ plotted in terms of its magnitude and phase.

The problem of insufficient DC gain for steady-state tracking can be overcome by introducing an integrator into the controller rather than a simple gain. In this case the output Δv_S will track the input command Δv_S^* with zero error since the integrator input (error) must be zero if the integrator output is expected to reach a constant steady-state value. However, the transfer function of the system has a pole very near the origin as a result of the time constant associated with the field circuit ($T_f = 1/0.108 = 9.26$ sec). It is interesting to note that this time constant is somewhat greater than the open circuit field time constant as a result of operating under a loaded condition rather than on open circuit as assumed in Chapter 7. As a result, the phase of the machine transfer function rapidly increases after the 0.108 rad/s break point produced by the field time constant. Since a simple integrator adds another 90 degree phase shift to the transfer function, very little margin is available to increase the system gain.

This problem can be somewhat overcome by more elaborate controllers. For example, a simple addition of a zero in addition to the integrator pole will reduce the effects of the -90 degree phase shift produced by the integrator and allows the DC gain to be increased. Such a controller is typically designated as a *proportional plus integrator control* (PI control). The gain that can ultimately be tolerated is limited by the resonance in the frequency plot caused by the location of the lightly damped poles produced by the electromechanical system equation (swing equation), the imaginary parts of which are located near ± 15 rad/s without feedback gain. The Bode plot of the transfer function $1.2*(1+j\omega)G(j\omega)/(j\omega)$ is also shown in [Figure 10.8](#), where $1/(j\omega)$ represents integration in the frequency domain and the constant 1.2 denotes the gain of the integrator. The function is also plotted in Figure 10.8. The unit step response for the control system containing an integrator pole as well as a zero with a gain of 1.2 is shown in [Figure 10.9](#).

The gain value of 1.2 has been chosen to produce a *phase margin* of 45 degrees. The phase margin is the difference between the 180 degrees and the phase angle of the transfer function when its magnitude reaches unity. When the phase margin is zero at the point where unit gain is reached, the system becomes unstable. This point is also termed the *crossover frequency*. A value of phase margin between 30 and 45 degrees is commonly considered as good design practice, in which case an integrator gain of 1.2 is roughly the most that can be tolerated for acceptable design. This value implies that the gain intro-

duced only amounts to 1.2 when the input frequency is 1 radian per second or 0.159 Hz so that the tracking of error even with a low frequency content will be poor.

The unit step response for the closed-loop system with a proportional plus integrator controller is shown in Figure 10.9. Whereas the terminal voltage reaches the desired value of one per unit, indicating tracking of the output with zero error in the steady-state, it is apparent that the response remains quite slow, reaching a value within 10% of its final value in about 40 sec.

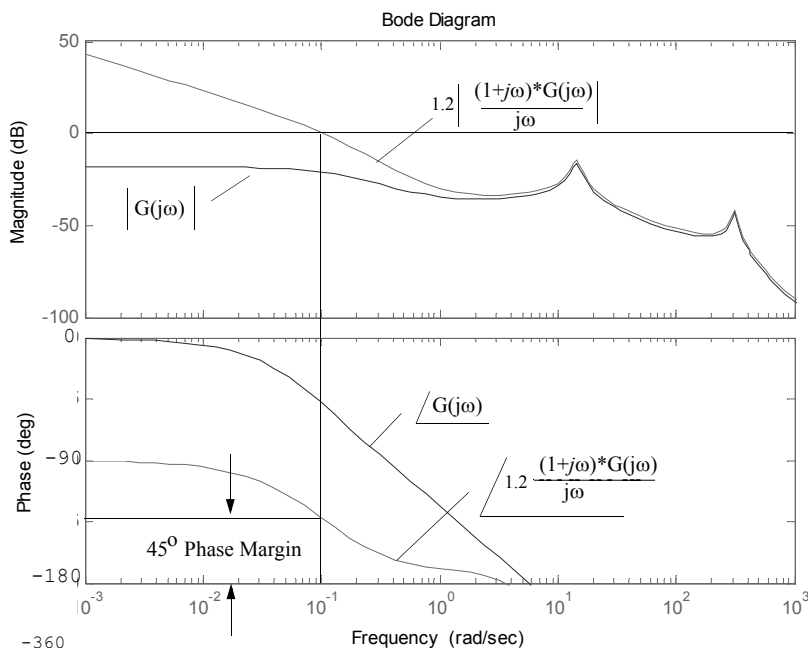


Figure 10.8 Bode plots of the voltage ratio transfer functions $G(j\omega) = \Delta v_S(j\omega)/\Delta e_X(j\omega)$ and $G(j\omega)$ plus PI regulator feedback terms.

It must be mentioned here that only the principles of voltage control have been covered in this section. A proper modeling of the problems would require that the excitation systems of Section 7.5 in Chapter 7 be modeled in complete detail. Nonetheless, the physical implementation of that section strives to accomplish in hardware the principles described here. Finally, it can be noted

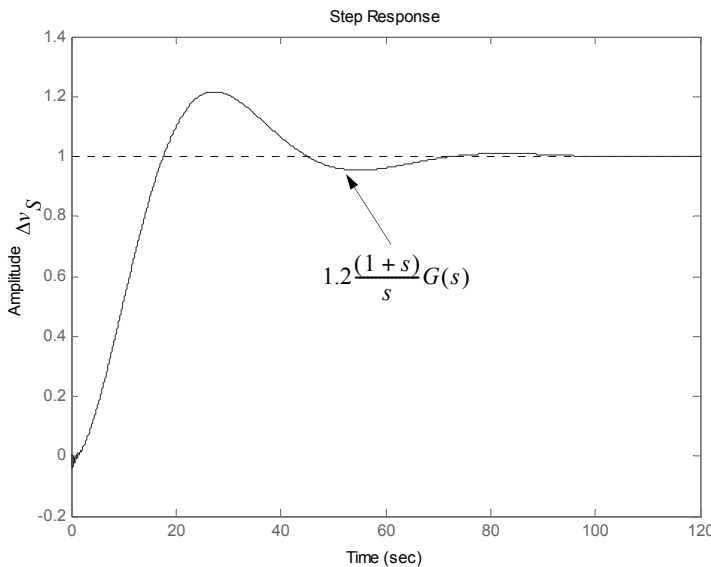


Figure 10.9 Time response of voltage controller as a result of a step command using proportional plus integral control.

that the exciter circuits described in Section 7.5 mention an additional input to the control system labeled V_{pss} . This additional signal is generically termed the power system stabilizer signal and is derived from such source as system frequency, accelerating power, and the like. These signals serve to enhance the damping of the system poles associated with the electromechanical swing equation. Clearly, the damping of these poles can be enhanced by feeding back the rotor speed, since the coefficient multiplying the speed appears as a damping term in the swing equation, Eq. (7.14).

An example of the use of speed feedback as a complement to the voltage regulator is shown in Figure 10.10 in which a small amount of speed feedback is provided. It is interesting to note that the zeros associated the electromechanical swing equation have now been moved to the left-hand plane. As a result, damping of the overall transfer function can be enhanced, as shown in Figure 10.11.

T.F. Input -- DELTA Ex+.5*DELTA wr Units: P.U.

T.F. Output -- DELTA Vs Units: P.U. Volts

Zero/pole/gain:

$$0.010306 (s+4.106) (s+0.2382) (s^2 + 5.248s + 384.9) (s^2 + 2499s + 1.766e006)$$

$$(s+7.633) (s+3.317) (s+0.1084) (s^2 + 2.02s + 207.5) (s^2 + 27.47s + 9.881e004)$$

poles =

$$\begin{aligned} -1.3737e+001 + 3.1404e+002i \\ -1.3737e+001 - 3.1404e+002i \\ -1.0102e+000 + 1.4369e+001i \\ -1.0102e+000 - 1.4369e+001i \\ -7.6326e+000 \\ -3.3166e+000 \\ -1.0844e-001 \end{aligned}$$

zeros =

$$\begin{aligned} -1.2495e+003 + 4.5196e+002i \\ -1.2495e+003 - 4.5196e+002i \\ -2.6242e+000 + 1.9443e+001i \\ -2.6242e+000 - 1.9443e+001i \\ -2.3815e-001 \\ -4.1057e+000 \end{aligned}$$

Figure 10.10 Poles and zeros of transfer function $\Delta v_S / (\Delta e_X + 0.5 * \Delta \omega_r)$.

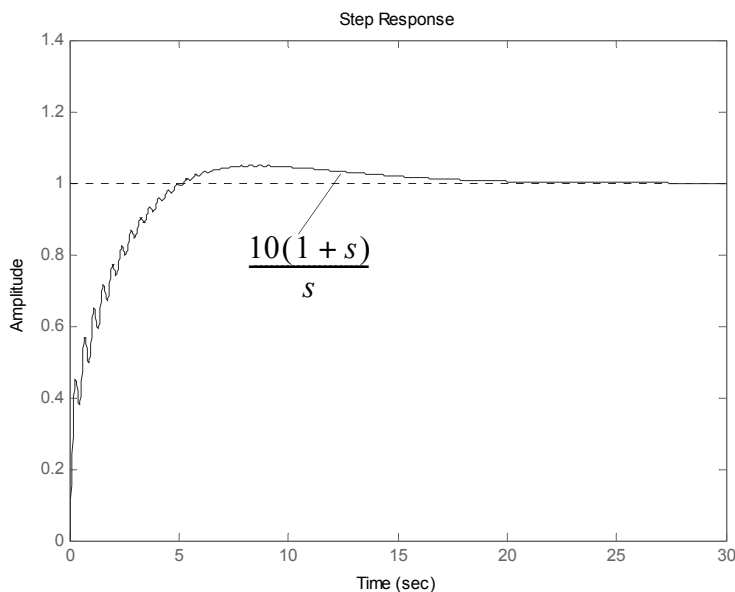


Figure 10.11 Step response of terminal voltage with input addition of speed feedback. System gain increased from 1.2 to 10 and with a unit step input command $\Delta e_X + 0.5 * \Delta \omega_r$

10.7 Design of a Classical Regulator

Having dealt with a PI regulator for control of terminal voltage, it is now useful to return to the theme of Chapter 7 and consider again the design of what can be considered as a classical regulator [1]. Figure 10.12(a) shows the block diagram of the relatively modern type of exciter which uses a thyristor bridge to form the regulator amplifier. Neglecting the peripheral components of the regulator such as limiters and the like, the equivalent circuit of Figure 10.12(b) is obtained.

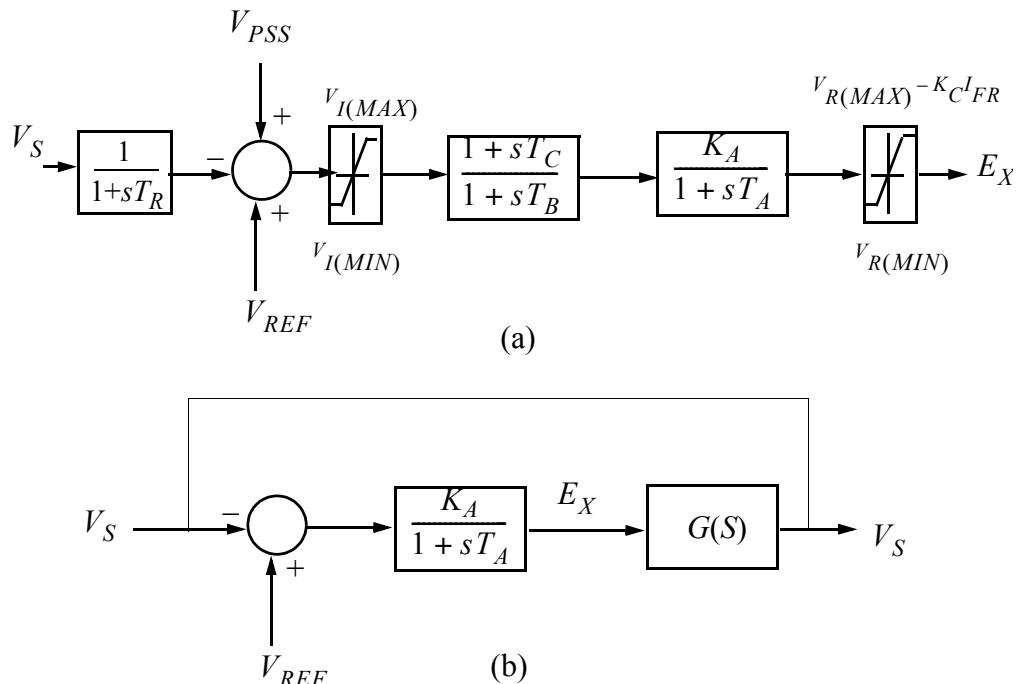


Figure 10.12 IEEE type AC4A excitation system model. (a) detailed model, (b) simplified model neglecting limiters, V_S input filter and lag/lead circuit and power system stabilizer signal.

[Figure 10.13](#) shows the Bode plots for two cases, one in which the machine itself is modeled and the second in which a simple regulator has been added. Again the machine of Table 5.3 operating a rated torque and unity power factor has been assumed. The gain and time constant of the regulator were selected to be $T_A = 0.05$ and $K_A = 30$. The phase margin of the system with the regulator was found to be 60 degrees, which indicates a slightly underdamped solution. The time domain solution for a step input is given is [Figure 10.14](#). The effects of right half plane zeros can again be noted.

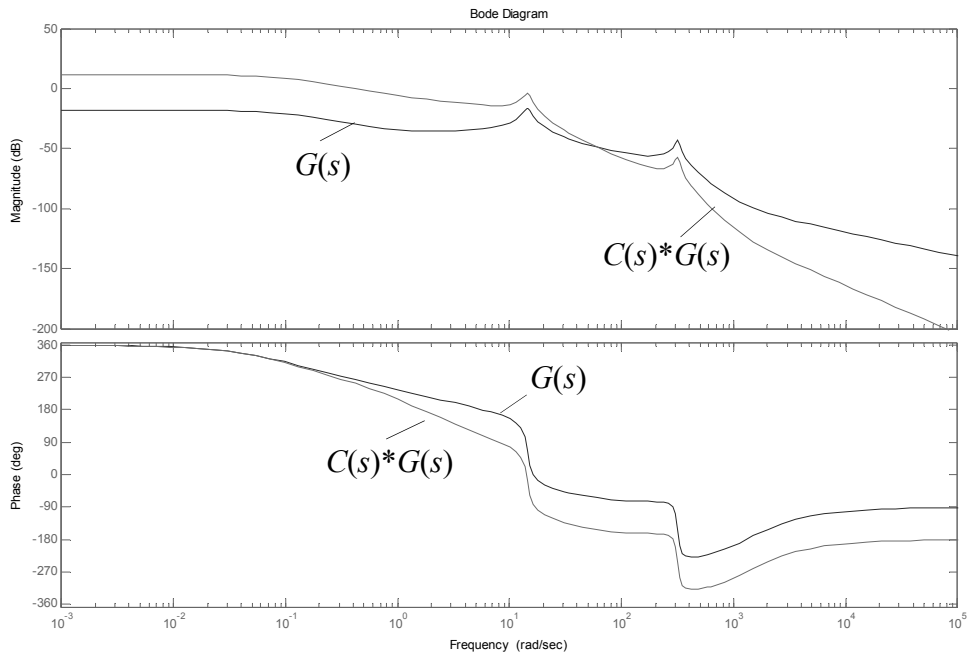


Figure 10.13 Bode plots of synchronous machine transfer function $G(s)$ and the synchronous machine plus regulator transfer function $C(s)*G(s)$, $C(s) = 30/(1+0.05s)$.

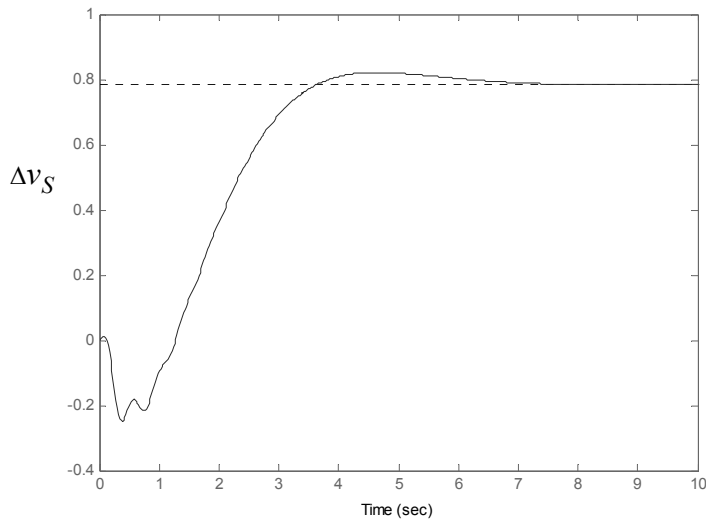


Figure 10.14 Response of terminal voltage to a unit step command for the system shown in Figure 10.12(b).

Increasing gain to values greater than 30 continues to improve the response but with a continuing decrease in damping. Addition of the lag/lead compensator of [Figure 10.12\(a\)](#) will act to improve the response by increasing the phase margin. Unfortunately, such increases in gain are not without their drawbacks. It can be readily shown that the transfer function describing the response of the excitation voltage Δe_X to the same step input in voltage command is given by

$$\frac{\Delta e_X(s)}{\Delta v_S^*(s)} = \frac{C(s)}{1 + G(s)C(s)} \quad (10.84)$$

where $C(s)$ corresponds to the transfer function of the regulator amplifier.

Plots of the step response of the excitation voltage to a unit step input voltage command are given in [Figure 10.15](#). When the gain of the PI controller is set to 30, the excitation voltage requirements reach roughly 30 per unit if saturation of the exciter is to be avoided! Clearly, a fast exciter response to a sudden voltage error comes at a quite a high price.

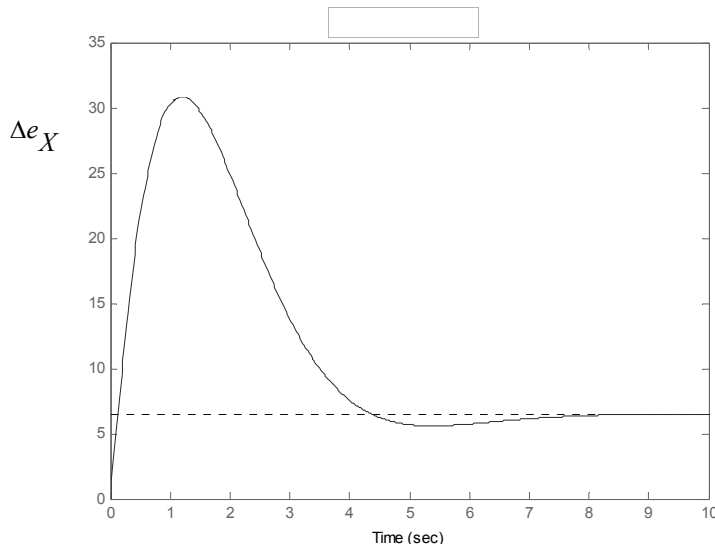


Figure 10.15 Time response of exciter voltage to a unit step command for the system shown in [Figure 10.12\(b\)](#).

The problem, in reality, is not quite as serious as suggested by [Figure 10.15](#). The unit step command assumed for [Figure 10.14](#) and [Figure 10.15](#) implies that a step command to rated voltage is required. This level of response is never required by a voltage controller, since the fluctuations in terminal volt-

age are typically only a few percent of rated voltage. If it is assumed that the maximum expected voltage change will be 10% of rated voltage, then, since the system differential equations are linear, the corresponding exciter voltage will be 3 per unit. [Figure 10.5](#) shows that the excitation voltage for rated, unity power factor operation is 2.25 per unit. Thus, in terms of the nominal excitation voltage for the rated condition, the total excitation voltage as a per unit of the nominal rated value is $3/2.25 + 1 = 2.33$. Hence, the price to pay for the headroom needed for the exciter to control variations in terminal voltage of $\pm 10\%$ is roughly to increase the voltage rating, and thus cost, of the exciter by about a factor of two (assuming that the current rating does not appreciably change). In reality, large increases in exciter voltage such as shown in [Figure 10.15](#) might not be allowed and explains the presence of the voltage limiters shown in [Figure 10.12](#).

Finally it should be observed that a noted difference is evident in the response of this controller compared to the PI controller of [Section 10.6](#). As shown by [Figure 10.9](#), the response of the PI controller is quite slow compared to the system with the simple regulator amplifier. However, while the terminal voltage reaches the commanded value in [Figure 10.9](#), the voltage of the simple regulator of [Figure 10.14](#) only reaches 0.8 of the desired voltage. Hence, because the DC gain is only 30, the regulator does a relatively poor job of regulating voltage. It might be questioned why such controls are in widespread use. First, with increased attention to phase margin, the gain of such regulators can be increased to higher values (100 or more) where the steady-state error is a few percent. Second, a certain amount steady-state voltage error amounts to a drop in the terminal volts vs. VAR characteristic, which is typically introduced into system control to enhance power system stability. Third, the steady-state error can be made vanishingly small if desired by simply slightly increasing the voltage command. This adjustment can be made on the basis of a slow update as part of the station operation.

It must be mentioned here that only the principles of voltage control have been covered in the last two sections. A proper modeling of the problems would require that the excitation systems in Chapter 7 be modeled in complete detail. Nonetheless, the physical implementations of that section strive to accomplish in hardware to follow the principles described here. A more detailed presentation of excitation control is beyond the scope of this book and the reader is referred to the (relatively) recent literature [2][3].

10.8 Conclusion

Transients constitute an key issue in the study of synchronous machines since it is during these relatively brief instants that catastrophic failures generally occur. In most cases, the inertia of the machine is sufficiently large that the speed of the machine can be considered as constant. In this case the approach of Chapter 5 can be profitably employed. In a substantial number of instances however, the disturbances are sufficiently large or the machine is sufficiently small that speed variations become important. This chapter serves to cover such cases in addition to those in which speed changes can be neglected. The use of these small signal equations has also been demonstrated to be useful in the design of a feedback control system, namely a stator terminal voltage regulator. The small signal equations, however, remain a linearized approximation of Park's Equations which are inherently non-linear. The last chapter will examine this class of problems.

10.9 References

- [1] F.P. de Mello and C. Concordia, "Concepts of Synchronous Machine Stability as Affected by Excitation Control," *IEEE Trans. on Power Apparatus and Systems*, Vol. 88, April 1969, pp. 316–329.
- [2] P.M. Anderson and A.A. Fouad, "Power System Control and Stability," First Edition 1977, Second Edition, John Wiley (IEEE Press), New York, 2003.
- [3] P. Kundur, "Power System Stability and Control," McGraw-Hill, Inc. New York, 1994.

Chapter 11

Computer Simulation of Synchronous Machines

11.1 Introduction

While a motor or generator runs at steady-state the vast majority of time, it is the brief instant where a transient occurs when most machines fail. There exist scenarios where the models leading up to this chapter fail to provide the needed accuracy, primarily because speed varies in such a manner that Park's equations remain non-linear. In this case a full simulation of the differential equations is required. The method by which one goes about solving these equations varies widely. This chapter will describe an approach based on using MATLAB. The solutions will be obtained using the hybrid flux linkage variable ψ introduced in Chapter 3. The hybrid flux linkage has units of flux linkages per second or volts but remains proportional to the proper flux linkage variable λ differing only by the constant ω_b .

11.2 Simulation Equations

Park's equations, derived in Chapter 3 and repeated in Chapter 10 as Eqs. (10.1)–(10.5) are a set of differential equations with mixed variables. That is, while the time derivatives in these equations are with respect to flux linkages, these equations also contain currents which are related to the flux linkages by auxiliary equations, Eqs. (10.8)–(10.12). Being expressed as time derivatives, flux linkages could be considered to be the natural set of state variables to be solved by time step integration. By virtue of these auxiliary equations, the flux linkages can be eliminated from Park's equations and replaced by currents as state variables. However, it has already been learned that flux linkages in a synchronous machine change slowly, limited by the open circuit time constants while currents change rapidly, limited by short-circuit time constants. Hence, Park's equations is most efficiently solved with flux linkages as the state variables in which case currents are best eliminated from these equations.

Solving the flux linkage equations, Eqs. (10.8)–(10.12), for currents yields

$$i_{ds} = \frac{\Psi_{ds} - \Psi_{md}}{x_{ls}} \quad (11.1)$$

$$i_{qs} = \frac{\Psi_{qs} - \Psi_{mq}}{x_{ls}} \quad (11.2)$$

$$i_{qr} = \frac{\Psi_{qr} - \Psi_{mq}}{x_{lqr}} \quad (11.3)$$

$$i_{dr} = \frac{\Psi_{dr} - \Psi_{md}}{x_{ldr}} \quad (11.4)$$

$$i_{fr} = \frac{\Psi_{fr} - \Psi_{md}}{x_{lfr}} \quad (11.5)$$

where

$$\Psi_{md} = x_{md}(i_{ds} + i_{dr} + i_{fr}) \quad (11.6)$$

and

$$\Psi_{mq} = x_{mq}(i_{qs} + i_{qr}) \quad (11.7)$$

Substituting Eqs. (11.1), (11.4), and (11.5) into Eq. (11.6) yields

$$\Psi_{md} = x_{md} \left(\frac{\Psi_{ds} - \Psi_{md}}{x_{ls}} + \frac{\Psi_{dr} - \Psi_{md}}{x_{ldr}} + \frac{\Psi_{fr} - \Psi_{md}}{x_{lfr}} \right) \quad (11.8)$$

or, rearranging,

$$\Psi_{md} \left(\frac{1}{x_{md}} + \frac{1}{x_{ls}} + \frac{1}{x_{ldr}} + \frac{1}{x_{lfr}} \right) = \frac{\Psi_{ds}}{x_{ls}} + \frac{\Psi_{dr}}{x_{ldr}} + \frac{\Psi_{fr}}{x_{lfr}} \quad (11.9)$$

It is useful to define

$$x_{md}^* = 1/(1/x_{md} + 1/x_{ls} + 1/x_{ldr} + 1/x_{lfr}) \quad (11.10)$$

in which case Eq. (11.9) can be written as

$$\Psi_{md} = \frac{x_{md}^*}{x_{ls}} \Psi_{ds} + \frac{x_{md}^*}{x_{ldr}} \Psi_{dr} + \frac{x_{md}^*}{x_{lfr}} \Psi_{fr} \quad (11.11)$$

In a very similar manner

$$\Psi_{mq} = \frac{x_{mq}^*}{x_{ls}} \Psi_{qs} + \frac{x_{mq}^*}{x'_{lqr}} \Psi_{qr} \quad (11.12)$$

It is now possible to proceed to eliminate currents as explicit variables from the machine voltage differential equations. The system equations prepared for computer solution (excluding the transformation equations) are

$$v_{qs} = \frac{r_s}{x_{ls}} (\Psi_{qs} - \Psi_{mq}) + \frac{p}{\omega_b} \Psi_{qs} + \frac{\omega_r}{\omega_b} \Psi_{ds} \quad (11.13)$$

$$v_{ds} = \frac{r_s}{x_{ls}} (\Psi_{ds} - \Psi_{md}) + \frac{p}{\omega_b} \Psi_{ds} - \frac{\omega_r}{\omega_b} \Psi_{qs} \quad (11.14)$$

$$v_{ns} = \frac{r_s}{x_{ls}} \Psi_{ns} + \frac{p}{\omega_b} \Psi_{ns} \quad (11.15)$$

$$v_{qr} (=0) = \frac{r_{qr}}{x'_{lqr}} (\Psi_{qr} - \Psi_{mq}) + \frac{p}{\omega_b} \Psi_{qr} \quad (11.16)$$

$$v_{dr} (=0) = \frac{r_{dr}}{x'_{ldr}} (\Psi_{dr} - \Psi_{md}) + \frac{p}{\omega_b} \Psi_{dr} \quad (11.17)$$

$$e_x = x_{md} \left(\frac{\Psi_{fr} - \Psi_{md}}{x'_{lfr}} \right) + \frac{x_{md}}{r'_{fr}} \frac{p}{\omega_b} \Psi_{fi} \quad (11.18)$$

together with the auxiliary air gap flux equations

$$\Psi_{md} = \frac{x_{md}^*}{x_{ls}} \Psi_{ds} + \frac{x_{md}^*}{x'_{ldr}} \Psi_{dr} + \frac{x_{md}^*}{x_{lfr}} \Psi_{fr} \quad (11.19)$$

$$\Psi_{mq} = \frac{x_{mq}^*}{x_{ls}} \Psi_{qs} + \frac{x_{mq}^*}{x'_{lqr}} \Psi_{qr} \quad (11.20)$$

where

$$x_{md}^* = 1/(1/x_{md} + 1/x_{ls} + 1/x_{ldr} + 1/x_{lfr}) \quad (11.21)$$

$$x_{mq}^* = 1/(1/x_{mq} + 1/x_{ls} + 1/x_{lqr}) \quad (11.22)$$

In addition, the speed is solved from Eq. (10.7),

$$T_e - T_l = \frac{2\omega_b J}{P} p(\omega_r/\omega_b) \quad (11.23)$$

where

$$T_e = \frac{3}{2} \frac{P}{2} \frac{1}{\omega_b} (\Psi_{ds} i_{qs} - \Psi_{qs} i_{ds}) \quad (11.24)$$

If desired, the electrical power input/output can be solved from

$$P_e = \frac{3}{2} (v_{qs} i_{qs} + v_{ds} i_{ds} + v_{ns} i_{ns} + v_{qr} i_{qr} + v_{dr} i_{dr} + v_{fr} i_{fr}) \quad (11.25)$$

where it should be recalled that the use of primes to denote the rotor/stator turns ratio transformation of Chapter 3 has been assumed in all subsequent chapters. In per unit these equations take the same form except that the coefficients in Eqs. (11.23)–(11.25) must be changed to the form

$$T_E - T_L = 2H_p(\omega_r/\omega_b) \quad (11.26)$$

where

$$T_E = (\Psi_{DS} i_{QS} - \Psi_{QS} i_{DS}) \quad (11.27)$$

and

$$P_E = (v_{QS} i_{QS} + v_{DS} i_{DS} + v_{NS} i_{NS} + v_{QR} i_{QR} + v_{DR} i_{DR} + v_{FR} i_{FR}) \quad (11.28)$$

11.3 MATLAB® Simulation of Park's Equations

Integrating Eqs. (10.1)–(10.5) results in the proper form for MATLAB/SIMULINK simulation:

$$\Psi_{qs} = \int \left[v_{qs} - \frac{\omega_r}{\omega_b} \Psi_{ds} + \frac{r_s}{x_{ls}} (\Psi_{mq} - \Psi_{qs}) \right] \omega_b dt \quad (11.29)$$

$$\Psi_{ds} = \int \left[v_{ds} + \frac{\omega_r}{\omega_b} \Psi_{ds} + \frac{r_s}{x_{ls}} (\Psi_{md} - \Psi_{ds}) \right] \omega_b dt \quad (11.30)$$

$$\Psi_{ns} = \int \left[v_{ns} - \frac{r_s}{x_{ls}} \Psi_{ns} \right] \omega_b dt \quad (11.31)$$

$$\Psi_{qr} = \int \left[\frac{r_{qr}}{x_{lqr}} (\Psi_{mq} - \Psi_{qr}) \right] \omega_b dt \quad (11.32)$$

$$\Psi_{dr} = \int \left[\frac{r_{dr}}{x_{ldr}} (\Psi_{md} - \Psi_{dr}) \right] \omega_b dt \quad (11.33)$$

$$\psi_{fr} = \int \left[\frac{r_{fr}}{x_{md}} e_x + \frac{r_{fr}}{x_{lfr}} (\psi_{md} - \psi_{fr}) \right] \omega_b dt \quad (11.34)$$

The SIMULINK simulation diagram can be assembled by implementing these equations one at a time. For example, the diagrams for calculating the d -axis flux linkages are shown in Figure 11.2. Solution of Eq. (11.29) requires three input quantities (“sources”), v_{qs} , $(\omega_r/\omega_b)\psi_{ds}$, and ψ_{mq} and produces one output quantity (“sink”), ψ_{qs} . Solution of Eq. (11.32) requires one input and produces one output. Figure 11.1 shows the implementation of the d -axis air gap flux. The coefficients of the equations are defined within the triangles but are repeated as a caption below each triangle for convenience. The numeric digits after these captions are an artifact of the SIMULINK program and can be ignored. The coefficients are expressed in their native form (i.e., as parameters such as rs/xls and not as a numerical values). It is generally more convenient to calculate the numerical value of each of the coefficients later by means of a MATLAB m-file. After constructing suitable simulation diagrams, they can be collapsed by selecting all elements and invoking the command Ctrl-G to realize the form shown on the right.

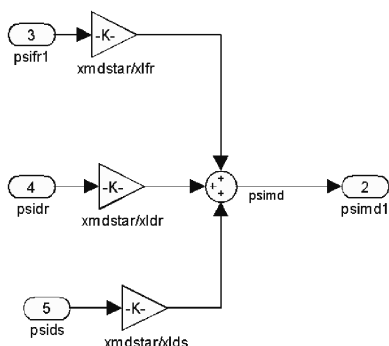
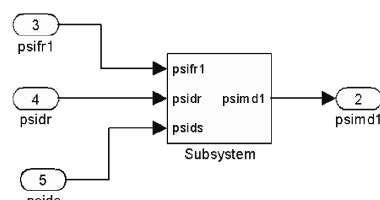
Solution for Ψ_{md} ExpandedSolution for Ψ_{md} Compressed

Figure 11.1 Simulation of direct axis air gap hybrid flux linkages.

The simulation of the q - and n -axis equations proceeds in the same manner. The next step is to interconnect the diagrams of the individual flux linkage equations so as to complete the modeling of the entire q -, d - and n -axis circuits. Figure 11.3 shows a diagram of the completed d -axis circuit. Three inputs to this circuit remain, one from the external voltage source, the second, the speed voltage from the d -axis circuit created from rotation, and the third from the field voltage supply.

If the n -axis circuit equations are neglected, since they are rarely required, the entire simulation of the synchronous machine can now be devised. The

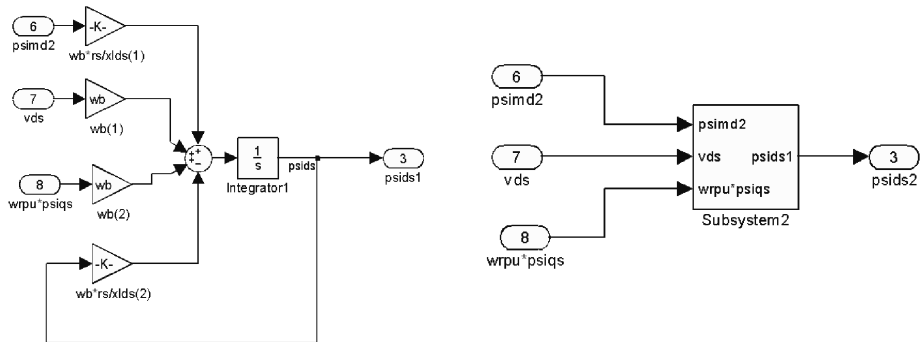
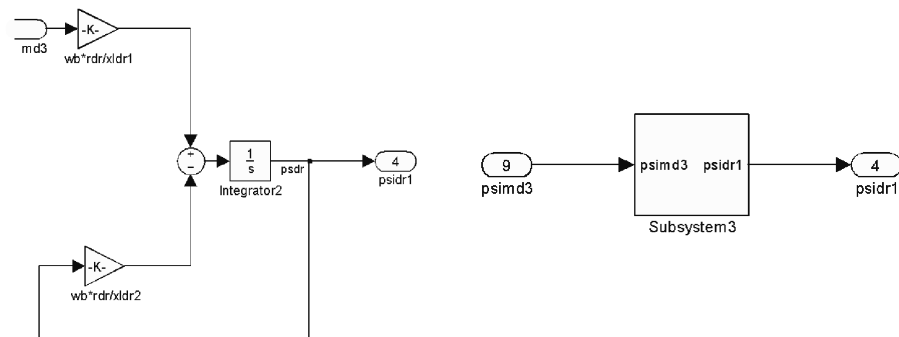
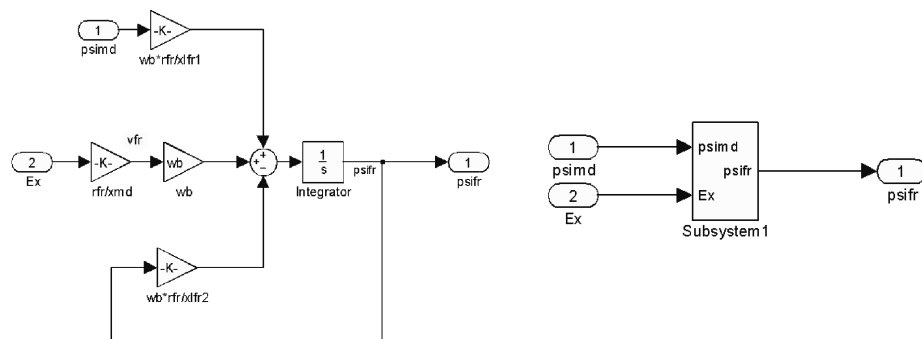
Solution for Ψ_{ds} ExpandedSolution for Ψ_{ds} CompressedSolution for Ψ_{dr} ExpandedSolution for Ψ_{dr} CompressedSolution for Ψ_{fr} ExpandedSolution for Ψ_{fr} Compressed

Figure 11.2 SIMULINK diagrams of Eqs. (11.29) and (11.32) showing expanded and compressed forms.

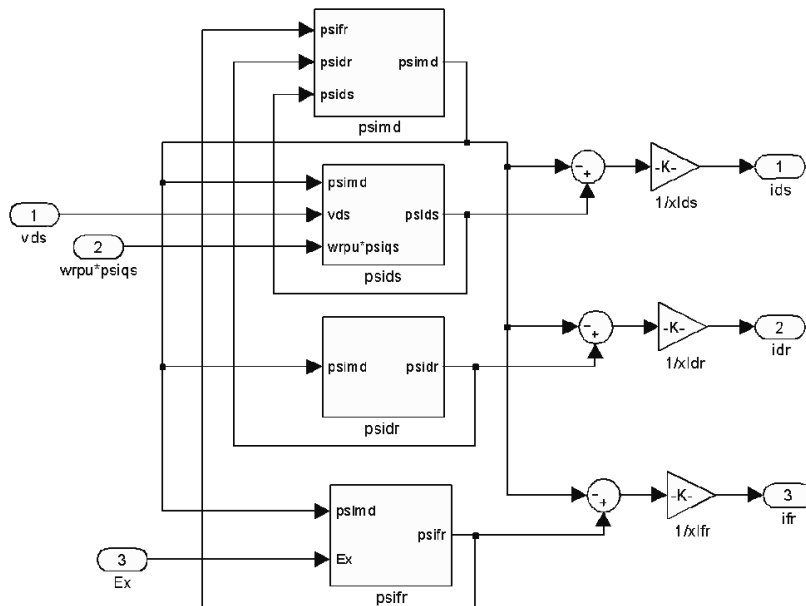


Figure 11.3 Completed simulation *d*-axis flux and current equations.

completed circuit, shown in [Figure 11.4](#), now includes simulation of the torque and speed by solving Eqs. (11.23) and (11.24). Once having obtained the speed, the non-linear product produced by the speed voltages can now be fed back to the *q*- and *d*- axis stator flux linkage equations. The four remaining inputs to the overall simulation are the *d*-*q* stator voltages, the field voltage (expressed in terms of e_x), and the load torque T_L . For generality, all of the five currents plus torque and speed have been identified as outputs. Scopes have been placed on a number of variables for ease in debugging. Also, data points associated with stator currents and voltages a well as torque and speed have been assigned to data files for later use with plotting using MATLAB.

The numerical values needed to be assigned to all of the coefficients of the differential and algebraic equations are best computed from a separate m-file. The script for this m-file for a 20 KW synchronous motor is shown in [Table 11.1](#).

11.4 Steady-State Check of Simulation

Confidence in computed simulation results can only be gained by exhaustive exercising of the algorithm under a multitude of conditions. While not a com-

Table 11.1 Matlab Data for Synchronous Motor Simulation

$rs = 0.1;$	$Llqr = Lqr - Lmq;$
$rqr = 0.2;$	$wb = 2*3.14159*60;$
$rdr = 0.10;$	$xlds = wb*Llds;$
$rfr = 0.016;$	$xlqs = wb*Llqs;$
$Lmd = 4.10e-3;$	$xmd = wb*Lmd;$
$Lds = 4.89e-3;$	$xmq = wb*Lmq;$
$Lqs = 2.39e-3;$	$xldr = wb*Lldr;$
$Lmq = 1.6e-3;$	$xlqr = wb*Llqr;$
$Lfr = 4.48e-3;$	$xlfr = wb*Llfr;$
$Lqr = 1.79e-3;$	$xmdstar = 1/(1/xlds + 1/xldr + 1/xlfr + 1/xmd);$
$Ldr = 4.39e-3;$	$xmqstar = 1/(1/xlqs + 1/xlqr + 1/xmq);$
$Llds = Lds - Lmd;$	$Vll = 240*sqrt(2);$
$Llqs = Lqs - Lmq;$	$Vln = Vll/sqrt(3);$
$Lldr = Ldr - Lmd;$	$J = 800/377;$
$Llfr = Lfr - Lmd;$	$P = 4;$
$Llqr = Lqr - Lmq;$	

pletely thorough test, confidence in the solution can be increased by a careful check of a steady-state condition, which can be determined by alternative means. The features of MATLAB allow a quick and easy way of assessing the machine variables at a steady-state condition. If it is assumed that the machine is in the steady-state under balanced conditions, then the time derivatives of all of the differentials are zero. Assuming operation at base speed, Equations (10.1)–(10.5) become

$$v_{qso} = r_s i_{qso} + \Psi_{dso} \quad (11.35)$$

$$v_{dso} = r_s i_{dso} - \Psi_{qso} \quad (11.36)$$

$$0 = r_{qr} i_{qro} \quad (11.37)$$

$$0 = r_{dr} i_{dro} \quad (11.38)$$

$$e_{xo} = x_{md} i_{fro} \quad (11.39)$$

where the subscript “o” is introduced to denote steady-state values.

Since the d - and q -axis damper winding currents are clearly zero, only the first, second, and third of these equations need be solved ((Eq. (11.39) of course being trivial). The other equations for the unknown currents are simply algebraic and can be again listed as

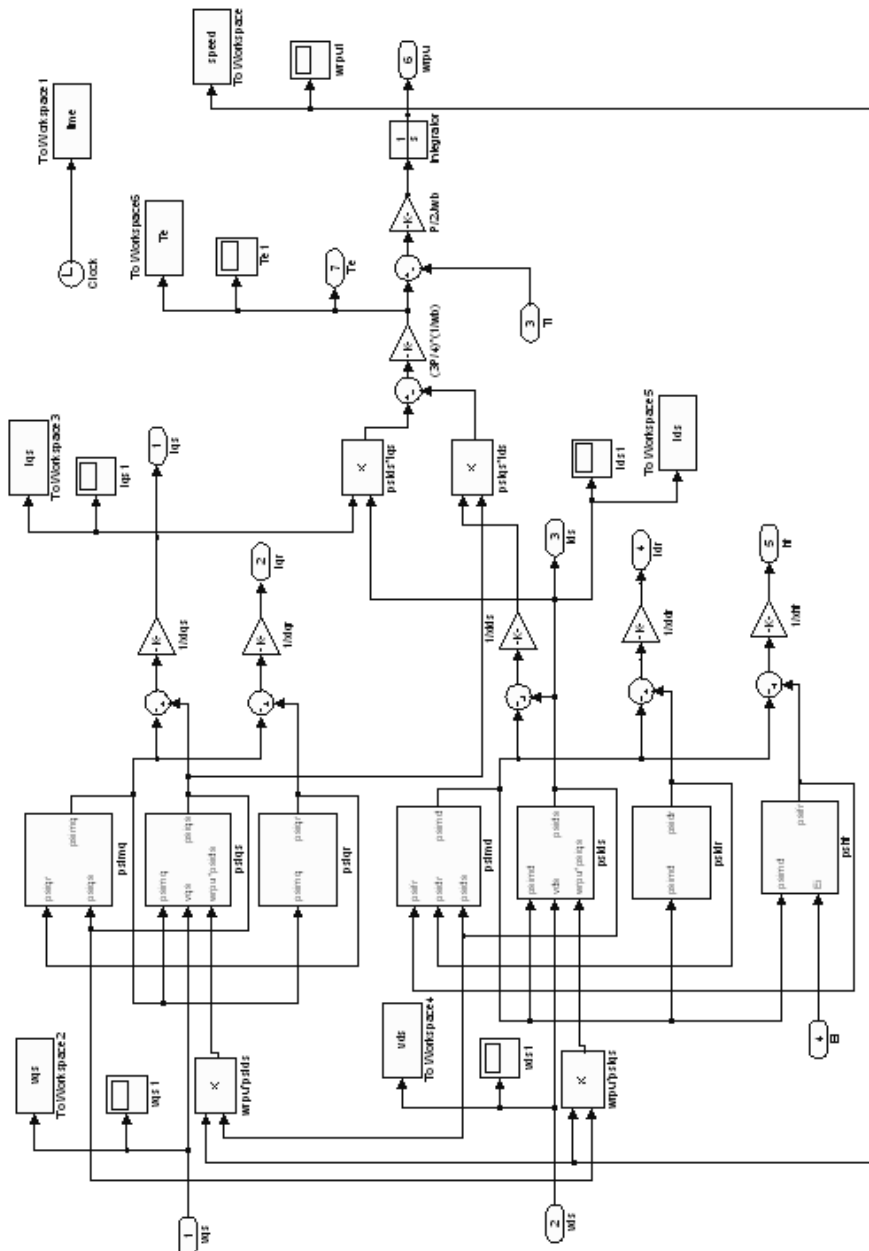


Figure 11.4 Completed simulation of a salient-pole synchronous machine.

$$i_{qso} = \frac{\Psi_{qso} - \Psi_{mqa}}{x_{ls}} \quad (11.40)$$

$$i_{dso} = \frac{\Psi_{dso} - \Psi_{mdo}}{x_{ls}} \quad (11.41)$$

$$i'_{fro} = \frac{\Psi'_{fro} - \Psi_{mdo}}{x'_{lfr}} \quad (11.42)$$

By virtue of the fact that i_{dro} and i_{gro} are zero, then $\Psi_{dro} = \Psi_{mdo}$ and $\Psi_{gro} = \Psi_{mqa}$. The equations relating the mutual flux linkages to the total flux linkages, Eqs. (11.19) and (11.20), become

$$0 = \frac{x^*_{md}}{x_{ls}} \Psi_{dso} + \left(\frac{x^*_{md}}{x'_{ldr}} - 1 \right) \Psi_{mdo} + \frac{x^*_{md}}{x'_{lfr}} \Psi_{fro} \quad (11.43)$$

$$0 = \frac{x^*_{mq}}{x_{ls}} \Psi_{qso} + \left(\frac{x^*_{mq}}{x'_{lqr}} - 1 \right) \Psi_{mqa} \quad (11.44)$$

These eight equations can be assembled in single matrix equation as

$$\begin{bmatrix} v_{qso} \\ v_{dso} \\ e_{xo} \\ 0 \\ 0 \\ 0 \\ 0 \\ 0 \end{bmatrix} = \begin{bmatrix} 0 & 1 & 0 & 0 & 0 & r_s & 0 & 0 \\ -1 & 0 & 0 & 0 & 0 & 0 & r_s & 0 \\ 0 & 0 & 0 & 0 & 0 & 0 & 0 & x_{md} \\ \frac{x^*_{mq}}{x_{ls}} & 0 & 0 & \frac{x^*_{mq}}{x'_{lqr}} - 1 & 0 & 0 & 0 & 0 \\ 0 & \frac{x^*_{md}}{x_{ls}} & \frac{x^*_{md}}{x'_{lfr}} & 0 & \frac{x^*_{md}}{x'_{ldr}} - 1 & 0 & 0 & 0 \\ 0 & \frac{1}{x_{ls}} & 0 & -\frac{1}{x_{ls}} & 0 & -1 & 0 & 0 \\ 0 & 0 & \frac{1}{x_{ls}} & 0 & -\frac{1}{x_{ls}} & 0 & -1 & 0 \\ 0 & 0 & \frac{1}{x_{lfr}} & 0 & -\frac{1}{x_{lfr}} & 0 & 0 & -1 \end{bmatrix} \times \begin{bmatrix} \Psi_{qso} \\ \Psi_{dso} \\ \Psi_{fro} \\ \Psi_{mqa} \\ \Psi_{mdo} \\ i_{qso} \\ i_{dso} \\ i_{fro} \end{bmatrix} \quad (11.45)$$

This equation is of the form

$$Y_o = Z_o X_o \quad (11.46)$$

where

$$X_o = [\Psi_{qso}, \Psi_{dso}, \Psi_{fro}, \Psi_{mbo}, \Psi_{mdo}, i_{qso}, i_{dso}, i_{fro}]^t \quad (11.47)$$

$$Y_o = [v_{qso}, v_{dso}, e_{xo}, 0, 0, 0, 0, 0]^t \quad (11.48)$$

and Z_o is the 7×7 impedance matrix,

The variables can be found by inverting Z_o , i.e.,

$$X_o = Z_o^{-1} Y_o \quad (11.49)$$

The inverted matrix generates all of the important steady-state quantities for comparison with the simulation except for the one non-linear equation, the electromagnetic torque. Having first solved Eq. (11.45), the torque is readily computed from Eq. (11.24). A short script, solving these equations, is given in [Figure 11.5](#), where it is assumed that $v_{qs} = 180$, $v_{ds} = 20$, and $e_x = 200$. Note that the first line of code runs the script defining the machine parameters. The computed result is also shown in [Figure 11.6](#).

[Figure 11.7](#) shows the transient which occurs when the same inputs are applied to the simulation, [Figure 11.4](#). Good correlation exists between the computed algebraic equations and simulated results. If desired, the simulated result can be examined more carefully using the Display device (a simulation equivalent of a digital voltmeter).

11.5 Simulation of the Equations of Transformation

The stator voltages in the $d-q$ rotor frame are only rarely known inputs. Generally, voltages expressed as physical (phase) variables in the stationary frame are defined either explicitly or implicitly as functions of stationary frame components. If the voltages are known explicitly, only a transformation from stationary to rotor frame is required. However, if these voltages vary with the machine currents, the voltage is known only implicitly, in which case the machine currents must be transformed back to the stationary frame in order to implement these implicit relationships. The equations relating the stationary and rotating frame variables is given by Eq. (2.145),

$$f_{dqns} = T(\theta) f_{abcs} \quad (11.50)$$

where

```

SynchronousMachineParameters
xds=wb*Lds;
xqs=wb*Lqs;
Matrix =[0 1 0 0 0 rs 0 0;
          -1 0 0 0 0 rs 0;
          0 0 0 0 0 0 0 xmd;
          xmqlstar/xlqs 0 0 xmqlstar/xlqr-1 0 0 0 0;
          0 xmdstar/xlds xmdstar/xlfr 0 xmdstar/xldr-1 0 0 0;
          1/xlqs 0 0 -1/xlqs 0 -1 0 0;
          0 1/xlds 0 0 -1/xlds 0 -1 0;
          0 0 1/xlfr 0 -1/xlfr 0 0 -1];
vqs = 180;
vds=20;
ex = 200;
Vector =[vqs; vds; ex; 0; 0; 0; 0; 0];
Matrixinv = inv(Matrix);
Answer = inv(Matrix)*Vector;
psiqs = Answer(1)
psids = Answer(2)
psifr = Answer(3)
psimq = Answer(4)
psiqr = psimq
psimd = Answer(5)
psidr = psimd
iqs = Answer(6)
ids = Answer(7)
ifr = Answer(8)
Te = (3/2)*(P/2)*(1/wb)*(psids*iqs - psiqs*ids)

```

Figure 11.5 MATLAB script *SteadyState* to calculate steady-state condition.

$$T(\theta) = \frac{2}{3} \begin{bmatrix} \sin\theta & \sin\left(\theta - \frac{2\pi}{3}\right) & \sin\left(\theta + \frac{2\pi}{3}\right) \\ \cos\theta & \cos\left(\theta - \frac{2\pi}{3}\right) & \cos\left(\theta + \frac{2\pi}{3}\right) \\ \frac{1}{\sqrt{2}} & \frac{1}{\sqrt{2}} & \frac{1}{\sqrt{2}} \end{bmatrix} \quad (11.51)$$

```
>> SteadyState
```

```
psiqs =
```

```
-20.9587
```

```
psids =
```

```
182.3261
```

```
psifr =
```

```
203.7180
```

```
psimq =
```

```
-14.0309
```

```
psiqr =
```

```
-14.0309
```

```
psimd =
```

```
185.1814
```

```
psidr =
```

```
185.1814
```

```
iqs =
```

```
-23.2614
```

```
ids =
```

```
-9.5872
```

```
ifr =
```

```
129.3944
```

```
Te =
```

```
-35.3491
```

Figure 11.6 Computer output after solution of script *SteadyState*.

and

$$f_{abcs} = \begin{bmatrix} f_{as} \\ f_{bs} \\ f_{cs} \end{bmatrix} \quad (11.52)$$

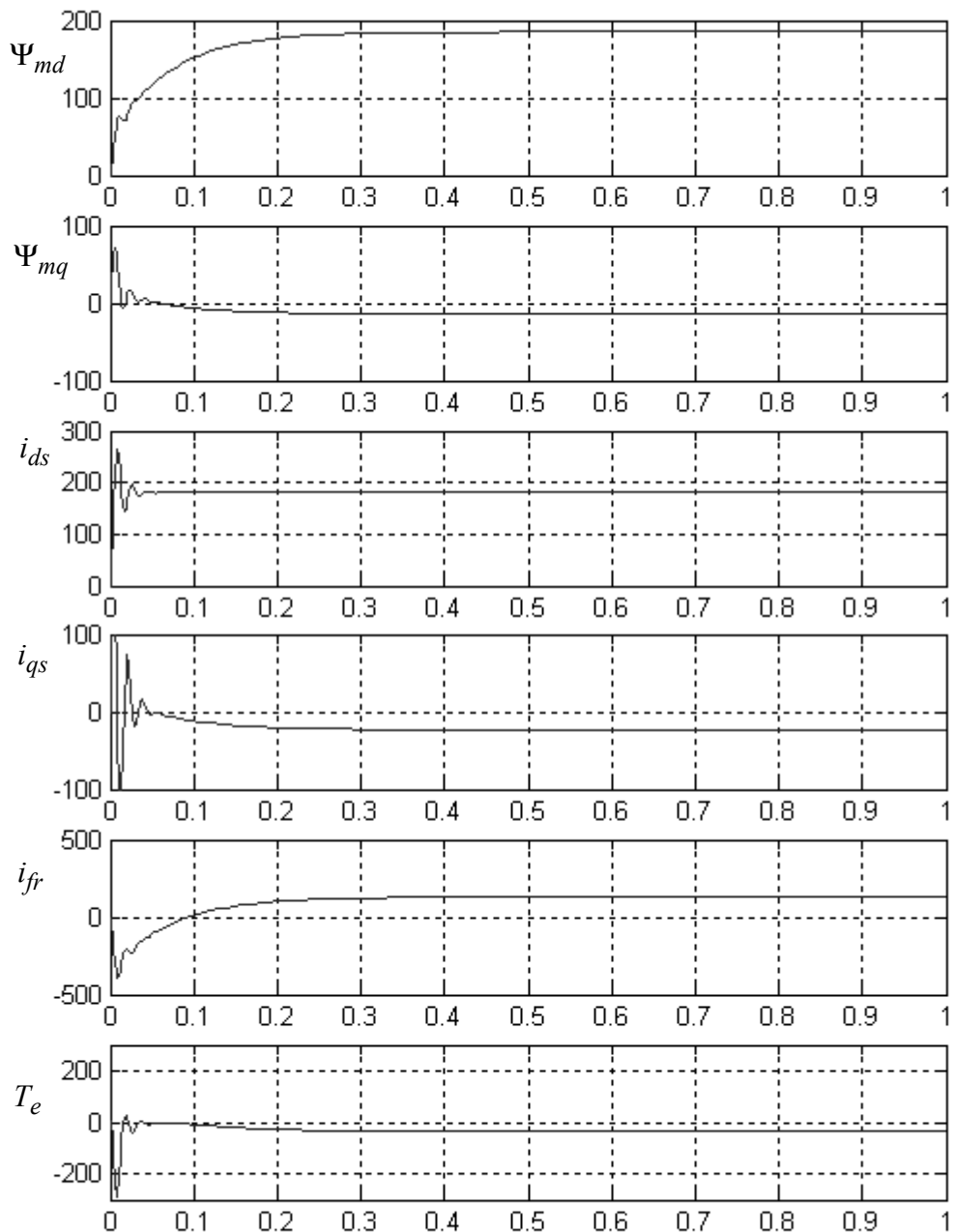


Figure 11.7 Simulation traces showing steady-state stabilization from zero flux initial conditions, $v_{qs} = 180$, $v_{ds} = 20$, $E_x = 200$, $\omega_r/\omega_b = 1.0$.

$$f_{dqns} = \begin{bmatrix} f_{ds} \\ f_{qs} \\ f_{ns} \end{bmatrix} \quad (11.53)$$

where “ f ” represents any three-phase variable such as voltage “ v ,” current “ i ,” flux linkage “ λ ,” or charge “ q .” From a computational point of view the transformation expressed by Eq. (11.50) is best accomplished in two steps. First a transformation is made from $a-b-c$ to $d-q-n$ variables expressed in the stator frame of reference. Second, a transformation is made from stationary frame $d-q-n$ to $d-q-n$ variables rotating with the rotor. The first transformation is made by simply setting $\theta = 0$ in Eq. (11.50).

$$f_{dqns}^s = T(0)f_{abcs} \quad (11.54)$$

from which it is readily determined that

$$T(0) = \frac{2}{3} \begin{bmatrix} 0 & -\frac{\sqrt{3}}{2} & \frac{\sqrt{3}}{2} \\ 1 & -\frac{1}{2} & -\frac{1}{2} \\ \frac{1}{\sqrt{2}} & \frac{1}{\sqrt{2}} & \frac{1}{\sqrt{2}} \end{bmatrix} \quad (11.55)$$

The second transformation is accomplished by a transformation of the form

$$f_{dqns}^r = R(\theta_r)f_{abcs}^s \quad (11.56)$$

It follows that

$$f_{dqns}^r = R(\theta_r)T(0)f_{abcs} \quad (11.57)$$

But from Eq. (11.50), setting $\theta = \theta_r$,

$$f_{dqns}^r = T(\theta_r)f_{abcs} \quad (11.58)$$

Clearly it must be true that

$$R(\theta_r)T(0) = T(\theta_r) \quad (11.59)$$

Solving for $R(\theta_r)$,

$$R(\theta_r) = T(\theta_r)T(0)^{-1} \quad (11.60)$$

From this point it is not difficult to show that

$$R(\theta_r) = \begin{bmatrix} \cos(\theta_r) & \sin(\theta_r) & 0 \\ -\sin(\theta_r) & \cos(\theta_r) & 0 \\ 0 & 0 & 1 \end{bmatrix} \quad (11.61)$$

This relationship can also be easily obtained by a simple sketch of the two sets of $d-q$ axes illustrating the trigonometric relationships, Figure 11.8. The imple-

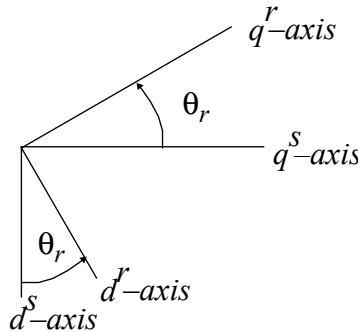


Figure 11.8 Stationary d^S-q^S and rotating d^R-q^R axes.

mentation of Eqs. (11.55) and (11.56) assuming $f \rightarrow v$ is shown in [Figure 11.9](#). In solving these equations it has been assumed that the zero sequence component is zero.

Inputs to Figure 11.9(a) assume that the three-phase voltages are known. However, since the neutral of the machine is floating with respect to the supply voltages, some difficulties still exist. The problem to be solved can be summarized by reference to [Figure 11.10](#). In this figure, e_{ag} , e_{bg} , and e_{cg} are known explicit functions of time, perhaps arising from outputs of another portion of the simulation, for example, an inverter simulation. In this case the neural “g” could, for example, represent the negative DC bus of the inverter. The three impedances $Z(p)$ represent any arbitrary network of inductances, capacitances and/or resistors. The important point to observe is that the three impedances are identical. In this case three loop equations can be written

$$e_{a'g} = Z(p)i_{as} + v_{as} + v_{sg} \quad (11.62)$$

$$e_{b'g} = Z(p)i_{bs} + v_{bs} + v_{sg} \quad (11.63)$$

$$e_{c'g} = Z(p)i_{cs} + v_{cs} + v_{sg} \quad (11.64)$$

Upon adding these three equations,

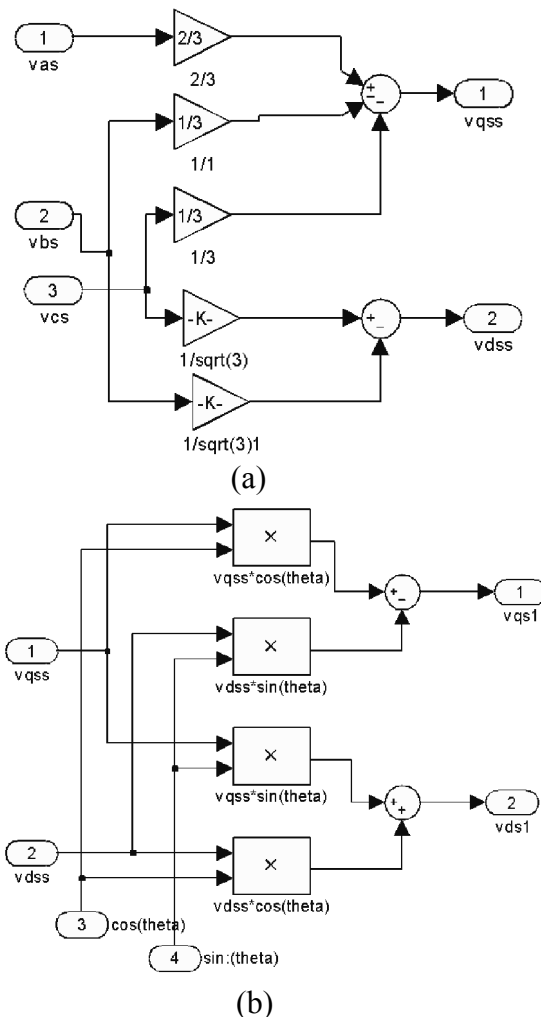


Figure 11.9 (a) Implementation of transformation from $a-b-c$ to $d-q$ reference frame, (b) transformation from $d-q$ stationary to $d-q$ rotating reference frame.

$$e_{ag} + e_{bg} + e_{cg} = Z(p)(i_{as} + i_{bs} + i_{cs}) + v_{as} + v_{bs} + v_{cs} + 3v_{sg} \quad (11.65)$$

Since the three-phase currents of a three wire system add to zero, the first term on the right hand side of Eq. (11.65) is clearly zero. It is more difficult to prove but still true that the sum of three machine phase voltages sum to zero even if the machine has saliency. Clearly it can easily be argued that the sum of the stator Ir drops and the sum of the stator leakage inductance drops are zero since the resistances and leakage inductance are identical in all three-phases. The fact the air gap voltages sum to zero is essentially a result of Gauss' Law,

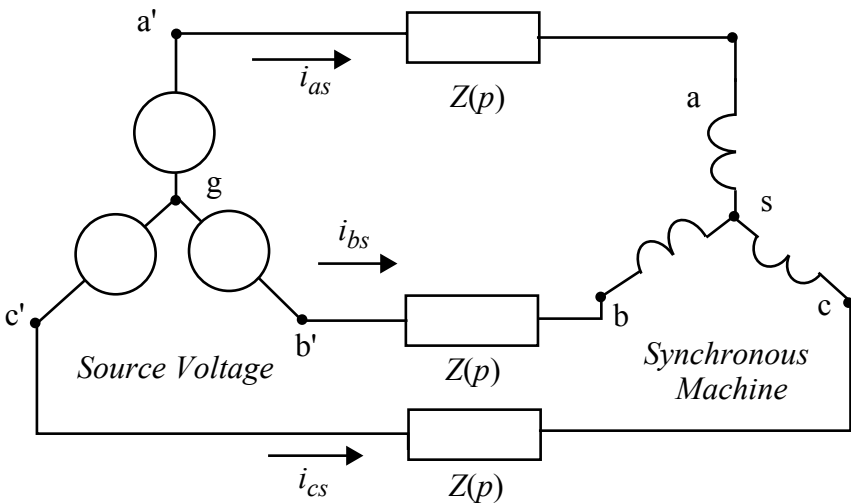


Figure 11.10 Typical simulation problem to be solved.

which in circuit form stipulates that the sum of the flux crossing a closed surface must be zero. The same is true for flux linkages since the turns are assumed the same for all phases. Thus the sum of the time derivatives of these flux linkages (i.e., the air gap voltage) must sum to zero. Equation (11.65) can therefore be written in the form,

$$v_{sg} = \frac{1}{3}(e_{a'g} + e_{b'g} + e_{c'g}) \quad (11.66)$$

Hence,

$$v_{as} = \frac{2}{3}e_{a'g} - \frac{1}{3}e_{b'g} - \frac{1}{3}e_{c'g} - Z(p)i_{as} \quad (11.67)$$

$$v_{bs} = \frac{2}{3}e_{b'g} - \frac{1}{3}e_{a'g} - \frac{1}{3}e_{c'g} - Z(p)i_{bs} \quad (11.68)$$

$$v_{cs} = \frac{2}{3}e_{c'g} - \frac{1}{3}e_{a'g} - \frac{1}{3}e_{b'g} - Z(p)i_{cs} \quad (11.69)$$

Solution of these equations depends, of course, upon the exact nature of the impedance $Z(p)$. In the frequently encountered case where the three source voltages sum to zero and there is no intermediate voltage drop to be solved, these equations simply reduce to $v_{as} = e_{ag}$, $v_{bs} = e_{bg}$, and $v_{cs} = e_{cg}$.

If $Z(p) = 0$, it is not necessary to transform the rotor frame $d-q$ currents back to the stationary frame. However, most problems concern the physical $a-$

b–c currents so that this conversion must take place. Solving Eq. (11.57) in the reverse sense,

$$f_{abcs} = [R(\theta_r)T(0)]^{-1} f_{dqns}^r \quad (11.70)$$

which can be written as

$$f_{abcs} = T(0)^{-1} R(\theta_r)^{-1} f_{dqns}^r \quad (11.71)$$

Also from Chapter 2

$$f_{abcs} = T(\theta)^{-1} f_{dqns}^r \quad (11.72)$$

so that

$$T(0)^{-1} R(\theta_r)^{-1} = T(\theta)^{-1} \quad (11.73)$$

or

$$R(\theta_r)^{-1} = T(0)T(\theta)^{-1} \quad (11.74)$$

From Eq. (2.147) $T(\theta)^{-1} = (3/2)T(\theta)^t$, from which

$$R(\theta_r)^{-1} = \frac{3}{2}T(0)T(\theta)^t \quad (11.75)$$

Or, finally in explicit form

$$R(\theta_r)^{-1} = \begin{bmatrix} \cos(\theta_r) & -\sin(\theta_r) & 0 \\ \sin(\theta_r) & \cos(\theta_r) & 0 \\ 0 & 0 & 1 \end{bmatrix} \quad (11.76)$$

This result is also readily surmised by investigation of Figure 11.8. Finally, the transformation needed in moving from the *d–q* stationary frame to *a–b–c* variables is obtained from $T(0)^{-1} = (3/2)T(0)^t$. Explicitly

$$T(0)^t = \begin{bmatrix} 0 & 1 & \frac{1}{\sqrt{2}} \\ -\frac{\sqrt{3}}{2} & -\frac{1}{2} & \frac{1}{\sqrt{2}} \\ \frac{\sqrt{3}}{2} & -\frac{1}{2} & \frac{1}{\sqrt{2}} \end{bmatrix} \quad (11.77)$$

For the sake of completeness, the implementation of these relationships, applied to current as a variable, is shown in Figure 11.11.

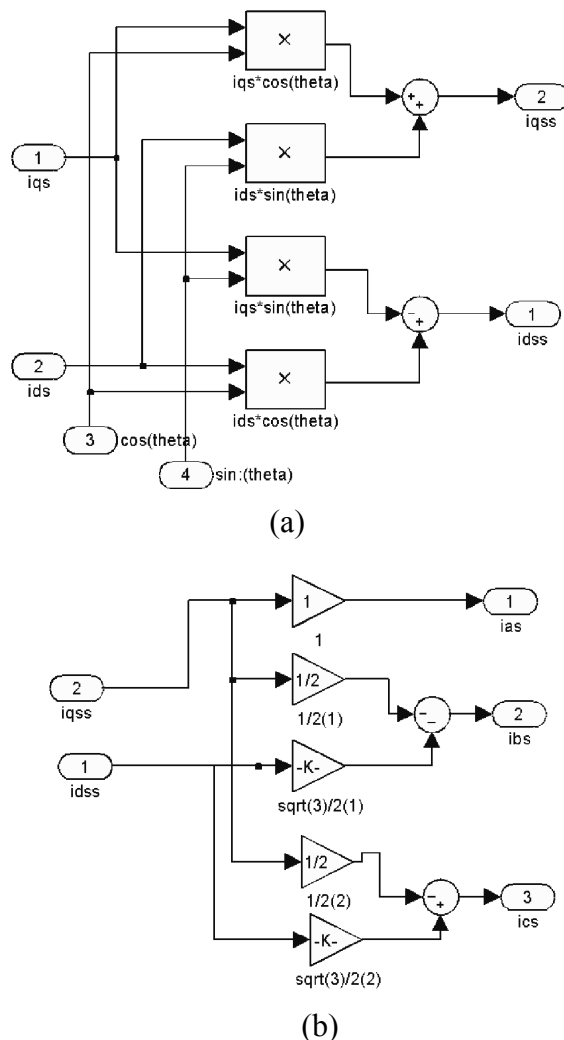


Figure 11.11 (a) Transformation of stator currents from $d-q$ rotor variables to $d-q$ stationary frame variables, (b) transformation for stationary $d-q$ currents to $a-b-c$ currents.

While the simulation process appears to be completed, one more item needs to be considered. It can be noted that input to the $R(\theta_r)$ and $R(\theta_r)^{-1}$ implementations required $\sin(\theta_r)$ and $\cos(\theta_r)$ as inputs. The per unit speed ω_r/ω_b is presumed known from the solution of Park's equations, so that this variable must be used for the simulation of these trigonometric functions. The

required equations are best uncovered by taking the time derivative of $\sin(\theta_r)$ and $\cos(\theta_r)$.

$$\frac{d}{dt}(\sin\theta_r) = \frac{d\theta_r}{dt}\cos\theta_r = \omega_b\left(\frac{\omega_r}{\omega_b}\right)\cos\theta_r \quad (11.78)$$

$$\frac{d}{dt}(\cos\theta_r) = -\frac{d\theta_r}{dt}\sin\theta_r = -\omega_b\left(\frac{\omega_r}{\omega_b}\right)\sin\theta_r \quad (11.79)$$

The integral equations to be solved are therefore,

$$\sin\theta_r = \int \omega_b\left(\frac{\omega_r}{\omega_b}\right)\cos\theta_r dt \quad (11.80)$$

$$\cos\theta_r = -\int \omega_b\left(\frac{\omega_r}{\omega_b}\right)\sin\theta_r dt \quad (11.81)$$

These equations can now be solved by use of the simulation diagram of Figure 11.12.

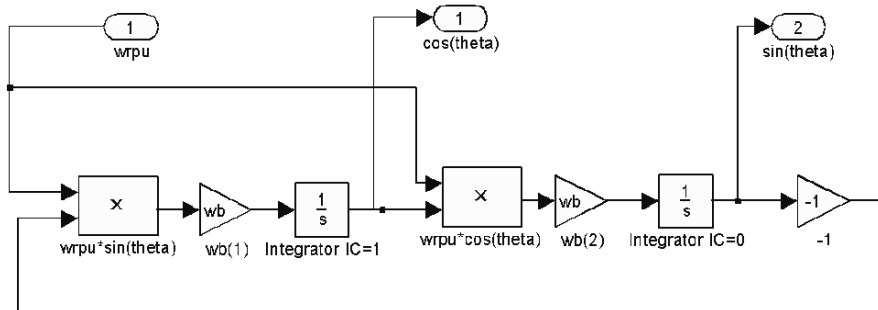


Figure 11.12 Variable frequency oscillator.

The overall computer simulation diagram is presented in [Figure 11.13](#). The identity of the various compressed blocks should be apparent from the context. The left most block represents the solution for the three machine phase voltages given the source voltages and details of the network incorporating Eqs. (11.67)–(11.69). Terminator “pins” are connected to variables not explicitly required to eliminate false error signals as the SIMULINK code solves the system of equations. Inputs to the problem to be defined are considered as the excitation e_x and load (or prime mover) torque T_l .

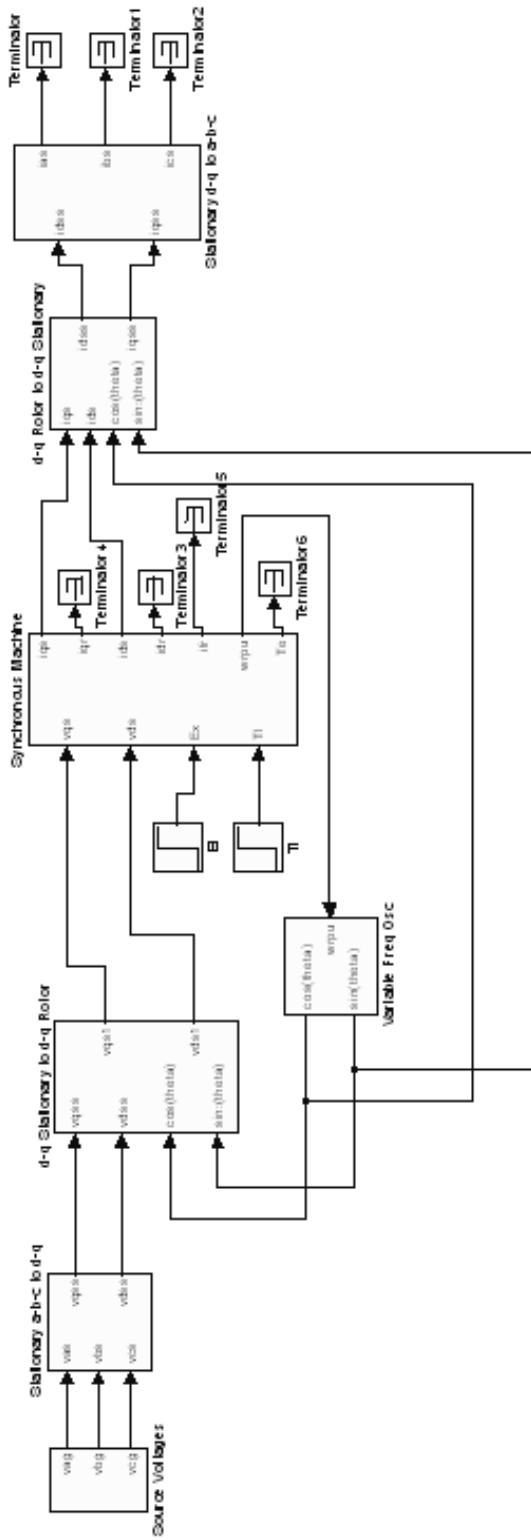


Figure 11.13 Overall simulation diagram for a salient-pole synchronous machine using SIMULINK.

11.6 Simulation Study

The same machine considered in [Section 11.4](#) is now assumed to be connected to a balanced three-phase supply through a zero impedance line. Rated voltage operation is assumed so that the amplitude of the supply voltage is $240\sqrt{2}/(\sqrt{3}) = 196$ V. Since balanced voltages are assumed, the source voltage block is greatly simplified. Details of the block used for this study are shown in Figure 11.14.

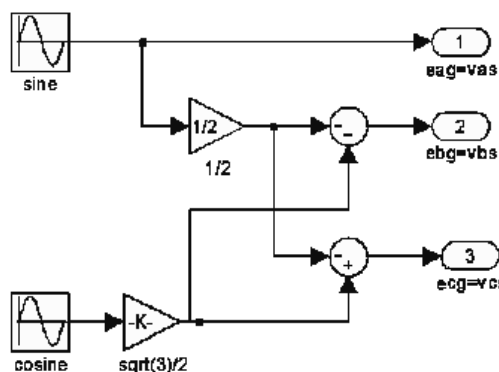


Figure 11.14 Source voltage block for developing balanced three-phase sinusoidal voltages.

In [Figure 11.15](#) the machine has been suddenly connected to the source voltages and allowed accelerate from rest without a torque load. At the same moment rated excitation (200 V.) is applied to the field winding. It is observed that the machine accelerates in about 4 seconds. A rather prolonged oscillation occurs as the machine pulls into synchronous speed.

In order to prevent this oscillatory effect, [Figure 11.16](#) shows the same case but with the field winding shorted. It can be noted that the machine now reaches synchronous speed in 3 seconds and the oscillations as the machine pulls into step, considerably reduced. Since the time to accelerate from rest has been reduced by 25%, losses incurred by inrush currents are also reduced by this factor, a considerable benefit which often translates to extended lifetime. However, it can be noted that the machine pulls into step with the q -axis voltage negative rather than positive. This result indicates that the negative q -axis is synchronized with the rotating stator voltage vector rather than the positive

q -axis. This results from the fact that the machine becomes synchronized solely by virtue of its reluctance torque. Thus either polarity can be obtained since the saliency is not polarity sensitive.

Figure 11.17 shows the transient that occurs when the excitation voltage is applied at the 8 second point after the machine reaches synchronous speed and begins to settle down. After a short delay during which time the positive reaction torque produced by the excitation must exceed the reluctance torque, the machine rapid swings to the “proper” polarity.

In Figure 11.18 the field voltage is applied at the instant that the machine reaches rated speed. In this case the machine synchronizes with the correct polarity, although the machine still exhibits oscillatory behavior as the synchronism is obtained.

11.7 Consideration of Saturation Effects

Due to the presence of the field winding, saturation effects in a synchronous machine are much more significant than for an induction machine. Because of the asymmetrical nature of the rotor, saturation is generally segregated into d -axis and q -axis saturation. Although fluxes in the two axes affect one another since there is one common path for both components in the stator (cross-magnetization), this effect is typically neglected. In general, q -axis saturation is less dominant than d -axis saturation due to the large effective q -axis air gap. The possibility of q -axis saturation will not be considered here but, if necessary, it is handled in the same manner as d -axis saturation.

Two methods exist for accommodating d -axis saturation. In general, saturation takes place over the entire rotor and stator path traversed by the d -axis mutual flux linkages. This case will be referred to as *air gap flux saturation*.

Another method of accounting for saturation looks at the problem in somewhat the reverse manner. It can be assumed that current flow in the machine depends only on the instantaneous net air gap flux linking the winding and not upon the individual contributions to the gap flux from the individual windings. If this is the case, then saturation can be accounted for by forcing extra field current to insure that the resultant gap flux is the same as when the machine is unsaturated. This saturation mechanism will be termed *field saturation*.

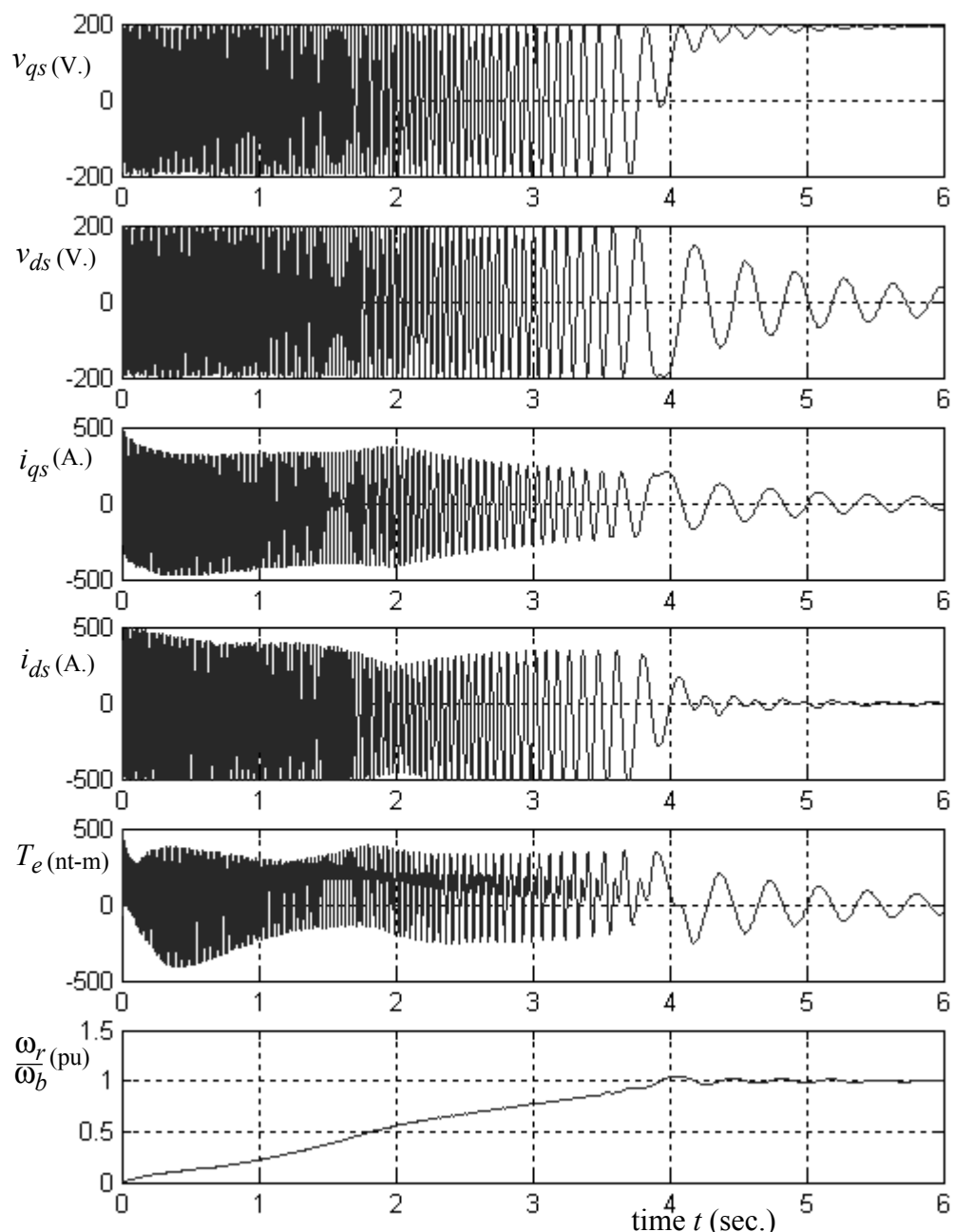


Figure 11.15 Acceleration of unloaded synchronous machine from rest with full excitation voltage applied.

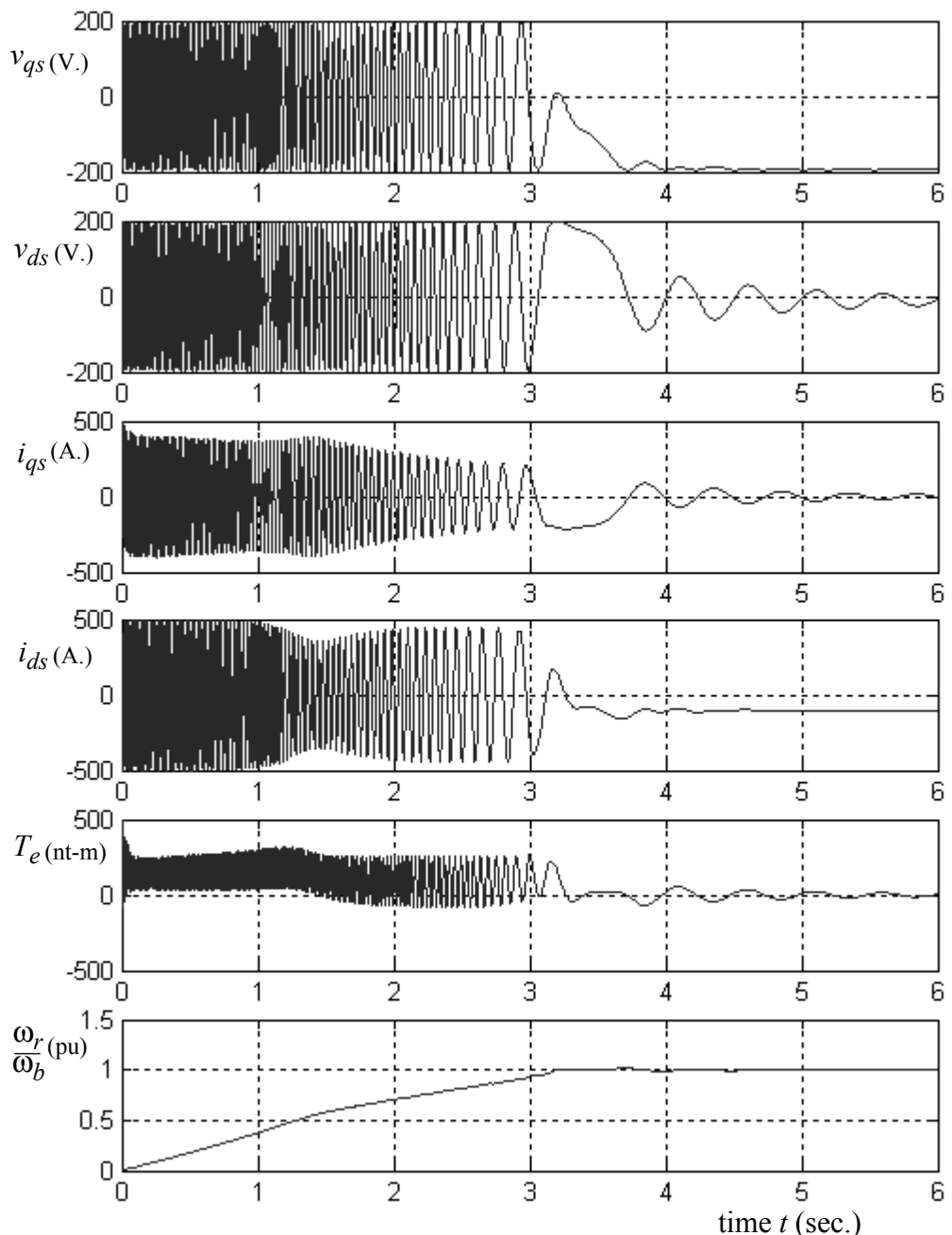


Figure 11.16 Acceleration of unloaded synchronous machine from rest with shorted field winding.

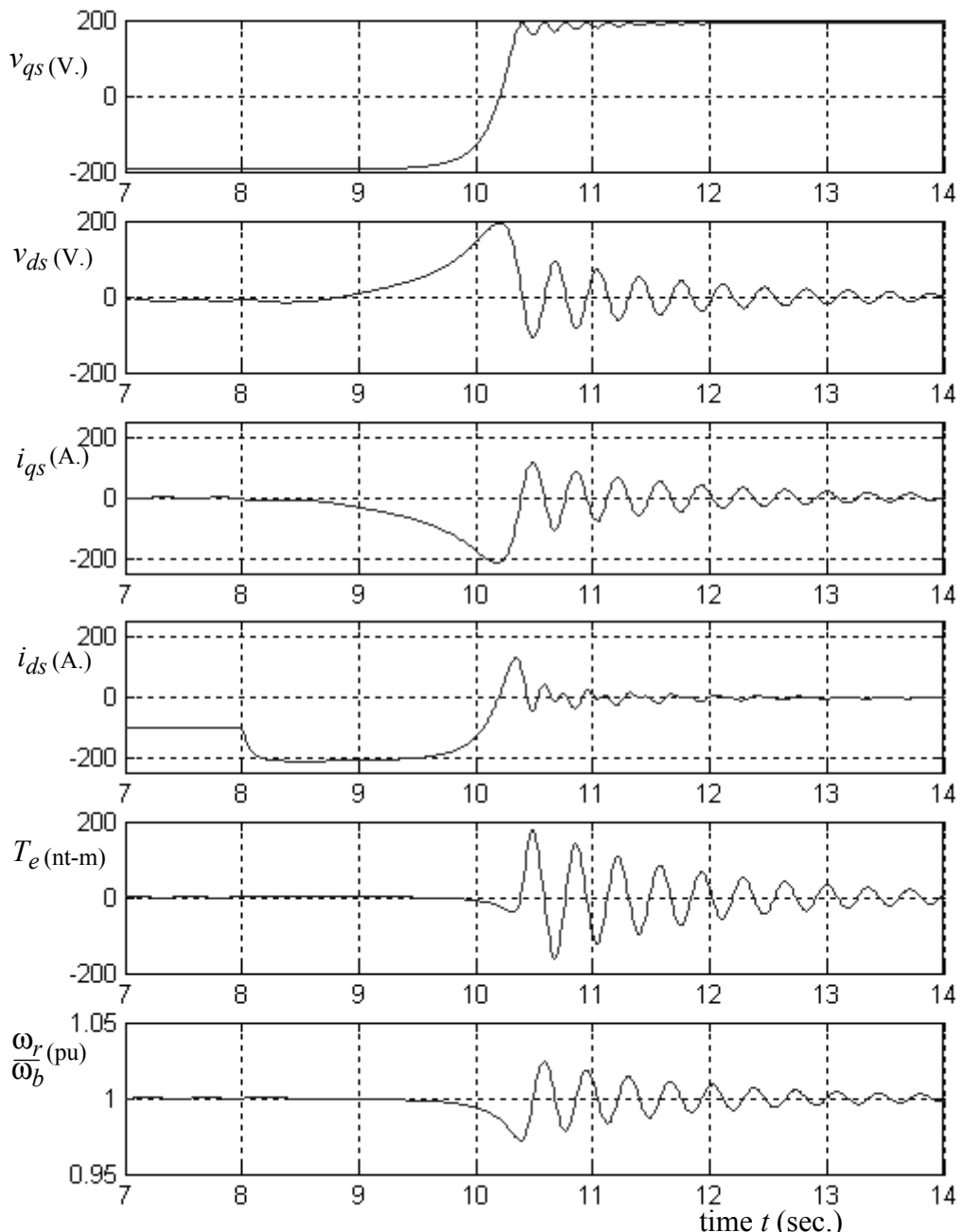


Figure 11.17 Sudden application of rated field voltage to machine of Figure 11.16 at the 8 second point.

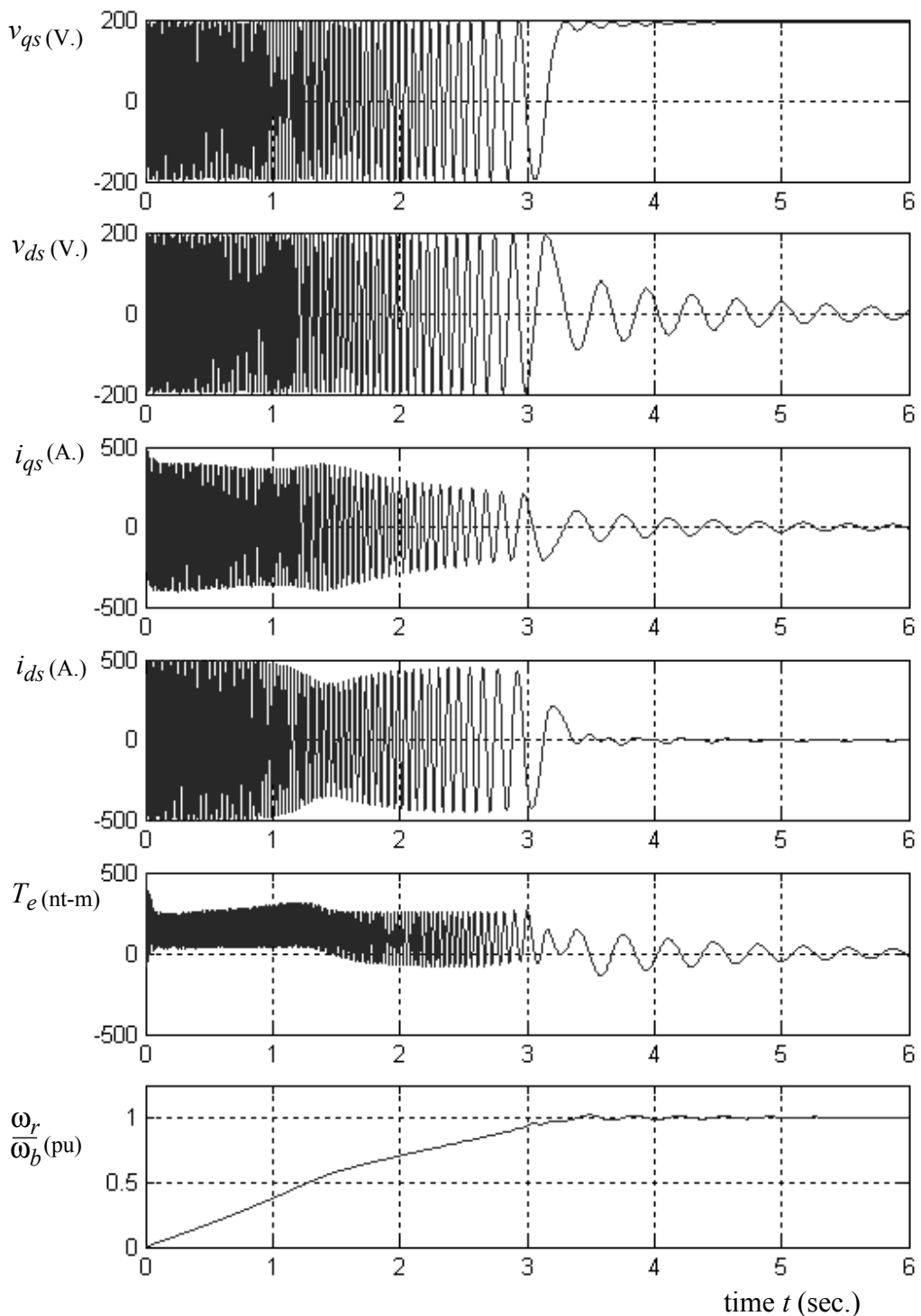


Figure 11.18 Acceleration from rest, field voltage applied as the machine reaches synchronous speed.

11.8 Air Gap Saturation

When air gap saturation occurs the d -axis mutual flux linkages are somewhat less than the value in the linear case. The relationship between the ideal (unsaturated) and actual (saturated) mutual flux linkages can be developed from the open circuit saturation curve of Figure 4.15 repeated here as [Figure 11.19](#). It can be recalled from the discussion of Potier Triangle, Chapter 4, Section 4.18, that with proper interpretation, the x -axis can be interpreted as the direct axis *MMF* while the y -axis is interpreted as the resulting flux linkage. This correspondence can be established by first multiplying the x -axis by the field turns N_f which converts the scale to an *MMF* quantity, and dividing the y -axis by the applied angular frequency, which produces a scale of flux linkage. Although the curve was measured with zero stator current, the curve can be extended to the general case with stator d -axis current by adding stator ampere turns $N_{s1}i_{ds}$ and d -axis amortisseur ampere turns $N_{dr1}i_{dr}$ to the x -axis. The argument is now made that multiplying these scale variables by constants does not change the essential meaning of the two axes variable, namely, *MMF*, for the x -axis and flux linkage for the y -axis. Remultiplying the y -axis by scaling factor ω_b converts the flux linkage to hybrid flux linkage, as utilized previously in this chapter, but does change the essential meaning of the variable. In a similar manner a multiplication of the *MMF* by the factor $\omega_b L_{md}/N_{s(1,p)}$ does not change the essential meaning but conveniently converts it to a quantity which again has voltage as the units. With the same manipulation carried out in Eq. (3.15), it can be shown that the x -axis quantity becomes $X_{md}(i_{ds} + i_{dr} + i_{fr})$. The revised plot is given in [Figure 11.20](#). It can be noted that since the unit of the two axes are the same the air gap line bisects the first quadrant.

From the saturation curve it is now possible to write

$$\Psi_{md(sat)} = \Psi_{md(unsat)} - \Delta\Psi_{md} \quad (11.82)$$

However, from previous work,

$$\Psi_{md(unsat)} = x_{md}(i_{ds} + i_{dr} + i_{fr}) \quad (11.83)$$

wherein

$$i_{ds} = [\Psi_{ds} - \Psi_{md(sat)}]/x_{ls} \quad (11.84)$$

$$i_{dr} = [\Psi_{dr} - \Psi_{md(sat)}]/x_{ldr} \quad (11.85)$$

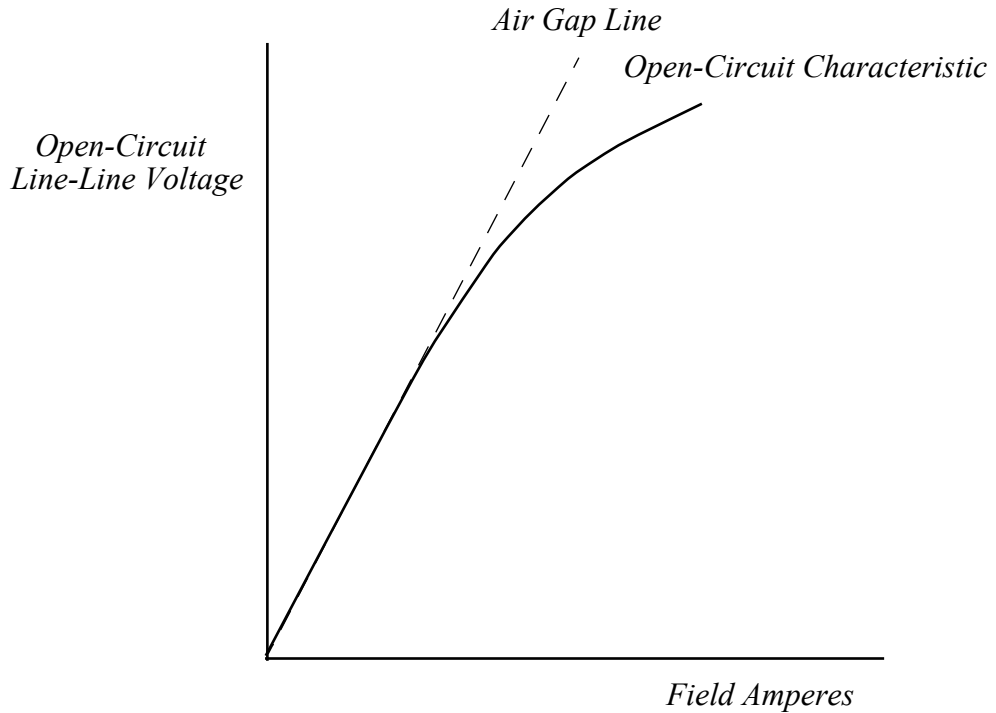


Figure 11.19 Open circuit saturation curve.

$$i_{fr} = [\Psi_{fr} - \Psi_{md(sat)}]/x_{lfr} \quad (11.86)$$

Substituting this into the equation for saturated field flux linkages, one has

$$\Psi_{md(sat)} = x_{md} \left(\frac{\Psi_{ds}}{x_{ls}} + \frac{\Psi_{dr}}{x'_{ldr}} + \frac{\Psi_{fr}}{x'_{lfr}} \right) - x_{md} \Psi_{md(sat)} \left(\frac{1}{x_{ls}} + \frac{1}{x_{ldr}} + \frac{1}{x_{lfr}} \right) - \Delta \Psi_{ma} \quad (11.87)$$

Dividing by x_{md} , and solving for $\Psi_{md(sat)}$,

$$\Psi_{md(sat)} \left(\frac{1}{x_{md}} + \frac{1}{x_{ls}} + \frac{1}{x'_{ldr}} + \frac{1}{x'_{lfr}} \right) = \frac{\Psi_{ds}}{x_{ls}} + \frac{\Psi_{dr}}{x_{ldr}} + \frac{\Psi_{fr}}{x_{lfr}} - \frac{\Delta \Psi_{ma}}{x_{md}} \quad (11.88)$$

where, by definition,

$$\frac{1}{x_{md}^*} = \frac{1}{x_{md}} + \frac{1}{x_{ls}} + \frac{1}{x_{ldr}} + \frac{1}{x_{lfr}} \quad (11.89)$$

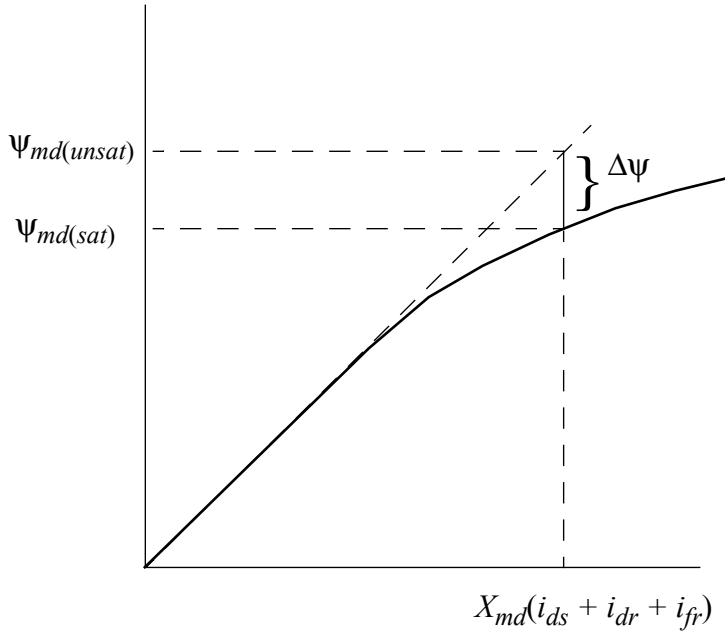


Figure 11.20 d -axis saturation curve with hybrid variables.

The equation for saturated flux linkages now assumes the form

$$\Psi_{md(sat)} = x_{md}^* \left(\frac{\Psi_{ds}}{x_{ls}} + \frac{\Psi_{dr}}{x'_{ldr}} + \frac{\Psi_{fr}}{x'_{lfr}} - \frac{\Delta\Psi_{md}}{x_{md}} \right) \quad (11.90)$$

The modification to the computer diagram implied by the above equation is given below in [Figure 11.21](#). The saturation function $\Delta\Psi_{md}$ vs. $\Psi_{md(unsat)}$ is obtained from the saturation curve of the machine.

One should note that if the ratio x_{md}^*/x_{md} is set equal to unity, then Eq. (11.90) becomes

$$\begin{aligned} \Psi_{md(sat)} &= x_{md} \left(\frac{\Psi_{ds}}{x_{ls}} + \frac{\Psi_{dr}}{x'_{ldr}} + \frac{\Psi_{fr}}{x'_{lfr}} \right) - \Delta\Psi_{md} \\ &= \Psi_{md(unsat)} - \Delta\Psi_{md} \end{aligned} \quad (11.91)$$

which now directly describes the curve of Figure 11.20. One might ask what happens if one simply models the saturation curve, Figure 11.20, described in equation form by Eq. (11.91), rather than by the use of Eq. (11.90). The simula-

tion of this representation of saturation is shown in Figure 11.22. However, the output is now only approximately $\psi_{md(sat)}$. Since the proper value for the ratio x_{md}^*/x_{md} is roughly 0.05, this simulation approach considerably overemphasizes the saturation effect.

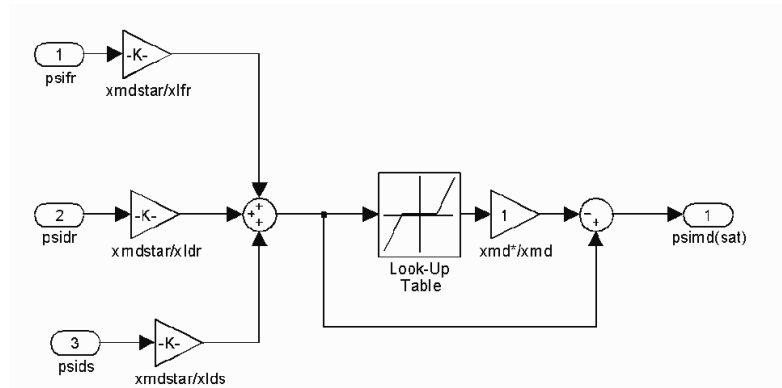


Figure 11.21 Simulation of d -axis air gap saturation using MATLAB/SIMULINK.

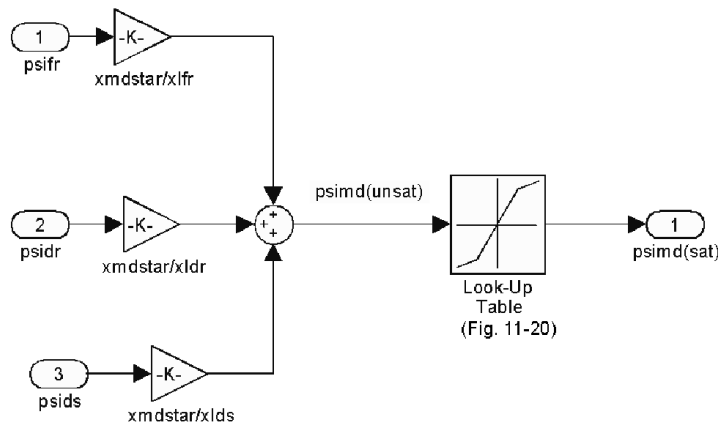


Figure 11.22 Approximate simulation of d -axis air gap saturation using MATLAB/SIMULINK assuming $x_{md}^* = x_{md}$.

11.9 Field Saturation

In the case of field saturation it is desired to replace the unsaturated value of $x_{md} i'_{fr}$ by a saturated value such that the instantaneous operating point is unchanged, but more field current is required to achieve the operating point. By definition, the field flux linkages are

$$\Psi_{fr} = (x_{lfr} + x_{md}) i_{fr} + x_{md} (i_{ds} + i_{dr})$$

Solving explicitly for $x_{md} i'_{fr}$,

$$(x_{md} i_{fr})_{unsat} = \frac{x_{md}}{x'_{lfr} + x_{md}} \Psi_{fr} - \frac{x_{md}^2}{x'_{lfr} + x_{md}} (i_{ds} + i_{dr}) \quad (11.92)$$

Recall that the first term above is defined in the literature as E'_q (voltage behind direct-axis transient reactance.)

$$E'_q = \frac{x_{md}}{x'_{lfr} + x_{md}} \Psi_{fr} \quad (11.93)$$

When the motor is saturated it is necessary add extra field current to achieve the same flux level

$$(x_{md} i_{fr})_{sat} = E'_q + \Delta E'_q - \frac{x_{md}^2}{x'_{lfr} + x_{md}} (i_{ds} + i_{dr}) \quad (11.94)$$

The voltage equation for the field winding is

$$\frac{r_{fr}}{x_{md}} e_x = \frac{p}{\omega_b} \Psi_{fr} + r_{fr} i_{fr(sat)} \quad (11.95)$$

Or, in terms of the variable $x_{md} i'_{fr}$

$$\frac{r_{fr} e_x}{x_{md}} = \frac{p}{\omega_b} \Psi_{fr} + \frac{r_{fr}}{x_{md}} (x_{md} i'_{fr})_{sat} \quad (11.96)$$

or

$$e_x = \frac{x_{md}}{r_{fr}} \frac{p}{\omega_b} \Psi'_{fr} + (x_{md} i'_{fr})_{sa} \quad (11.97)$$

These equations suggest the following modification to the basic computer simulation, the function $\Delta E'_q$ vs. E'_q is shown in [Figure 11.23](#). By definition,

$$E'_q = \frac{x_{md}}{x_{lfr} + x_{md}} \psi_{fr} \quad (11.98)$$

$$= \frac{x_{md}}{x_{lfr} + x_{md}} [(x'_{lfr} + x_{md}) i_{fr} + x_{md} (i_{ds} + i_{dr})] \quad (11.99)$$

When the machine is open circuited, then for steady-state $i_{ds} = i'_{dr} = 0$ and this expression reduces to

$$E'_q = x_{md} i'_{fr} \quad (11.100)$$

This result is nothing other than the amplitude of the open circuit voltage due to field excitation. Hence the function $\Delta E'_q$ vs. E'_q can also be found from the no-load excitation curve.

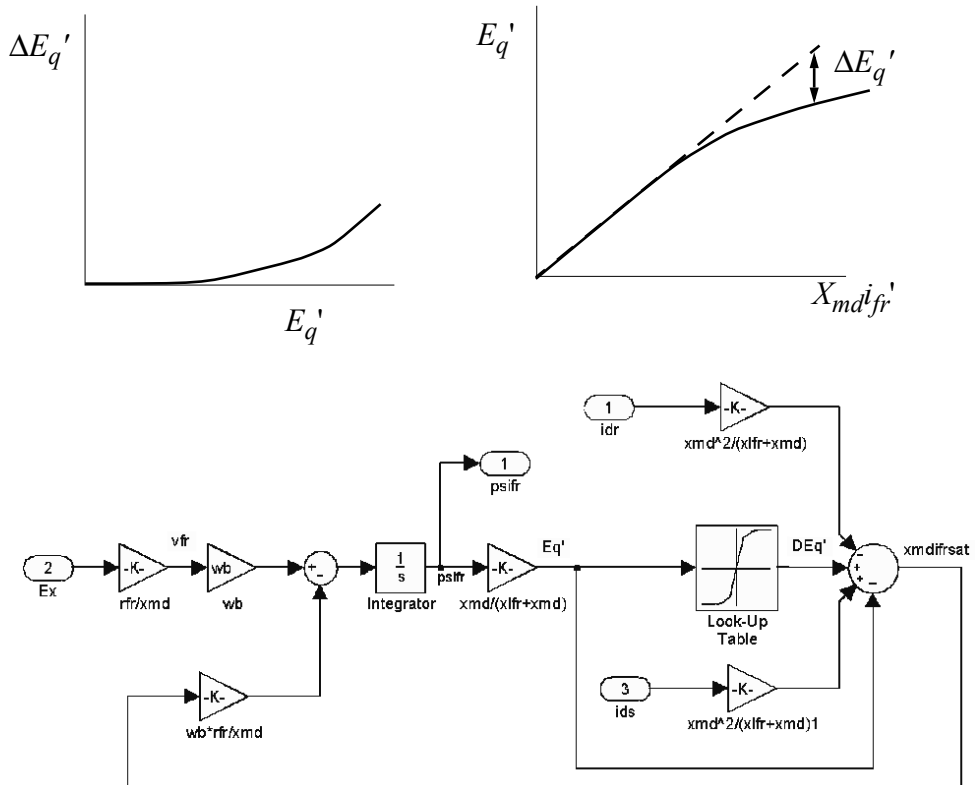


Figure 11.23 Modification to the basic simulation for field saturation.

It should be mentioned that generally a detailed representation of the saturation curve is not necessary. The simplest implementation follows that of Fred Rothe of the General Electric Company. Assume a no-load excitation curve as in [Figure 11.24](#). The field current (or $X_{md}i_{fr}$) is established for three points, 1) the value of field current at 1 per unit on the air gap line I_{fr0} , 2) the value of field current at 1 per unit on the saturation curve I_{fr1} , 3) the value of field current at 1.3 per unit voltage on the saturation curve I_{fr2} . Let V_b denote rated voltage. Utilizing the principle of least squares the function $\Delta E'_q$ can be approximated by the fourth order polynomial

$$\Delta E'_q = AV_b\left(\frac{E'_q}{V_b} - 0.7\right)^2 + BV_b\left(\frac{E'_q}{V_b} - 0.7\right)^4 \quad (11.101)$$

if $E'_q > V_b$ and

$$\Delta E'_q = 0$$

if $E'_q < V_b$ where

$$B = (2.7 + I_{fr2}/I_{fr0} - 4I_{fr1}/I_{fr0})/0.0975 \quad (11.102)$$

$$4 = (I_{fr2}/I_{fr0} - 1.3 - 0.1296B)/0.36 \quad (11.103)$$

Note that the saturation curve is assumed as linear until 0.7 p.u. volts. The saturation effect can be eliminated completely if one simply selects $I_{fr1} = I_{fr0}$ and $I_{fr2} = 1.3 I_{fr0}$. Care must be taken since the polynomial does not increase monotonically beyond a value of roughly 1.1 per unit.

11.10 Approximate Models of Synchronous Machines

In many applications a detailed solution of machine electrical transients is not required and only the electromechanical behavior of the machine is of concern. In other cases, the dimensionality of the interconnected system prohibits a detailed solution. In such cases it is possible to assume that the stator and/or rotor currents are in the “quasi-steady-state” throughout the transient solution.

It has already been learned from previous work that the steady-state is achieved from the $d-q$ equations by setting the rotor speed to synchronous speed ($\omega_r = \omega_e$) and setting the $d\lambda/dt$ terms equal to zero. In the synchronous reference frame, the machine stator $d-q$ equations are

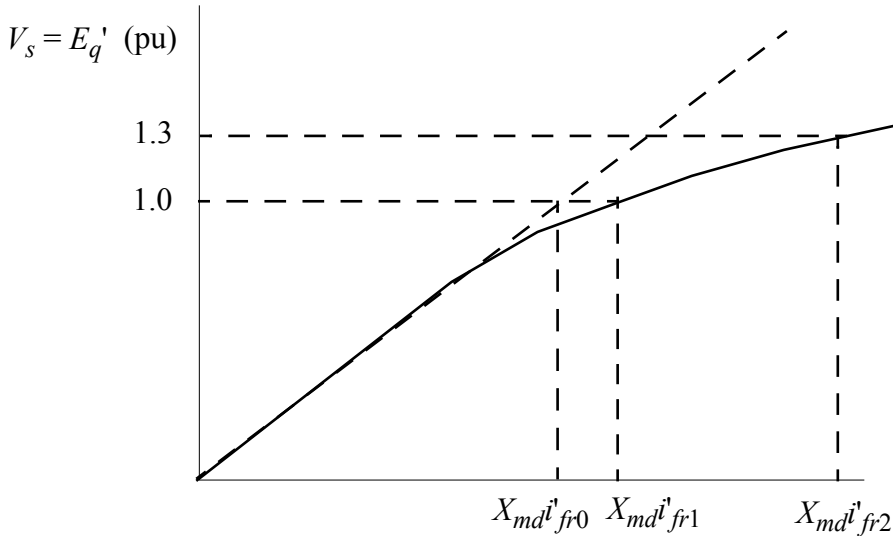


Figure 11.24 No load saturation curve illustrating points for least square approximation.

$$v_{qs}^e = r_s i_{qs}^e + \omega_e \lambda_{ds}^e + \frac{d\lambda_{qs}^e}{dt} \quad (11.104)$$

$$v_{ds}^e = r_s i_{ds}^e - \omega_e \lambda_{qs}^e + \frac{d\lambda_{ds}^e}{dt} \quad (11.105)$$

These equations remain valid, but difficult to solve, even if the rotor is not synchronously rotating. It is interesting to consider what happens if the derivative terms are set equal to zero, which forces the stator flux linkages to be in steady-state. While equations can be written for the stator flux linkage expressed in the synchronous frame, the voltage equations for the rotor circuits in this frame are not so simple, since the rotor is unsymmetrical. A simplified set of rotor voltage equations is obtained only if the d - q axis is fixed in the rotor. In order to get around this problem, it is necessary to determine how one can achieve the equivalent of setting $p\lambda_{ds}^e$ and $p\lambda_{qs}^e$ equal to zero in the rotor reference frame.

The equations relating the d - q stator flux linkages in the synchronous and arbitrary reference frames are

$$\lambda_{qs}^e = \lambda_{qs} \cos(\theta_e - \theta) - \lambda_{ds} \sin(\theta_e - \theta) \quad (11.106)$$

$$\lambda_{ds}^e = \lambda_{qs} \sin(\theta_e - \theta) + \lambda_{ds} \cos(\theta_e - \theta) \quad (11.107)$$

Hence

$$\begin{aligned} p\lambda_{qs}^e &= (p\lambda_{qs})\cos(\theta_e - \theta) - (p\lambda_{ds})\sin(\theta_e - \theta) \\ &\quad - (\omega_e - \omega)\lambda_{qs} \sin(\theta_e - \theta) - (\omega_e - \omega)\lambda_{ds} \cos(\theta_e - \theta) \end{aligned} \quad (11.108)$$

$$\begin{aligned} p\lambda_{ds}^e &= (p\lambda_{ds})\sin(\theta_e - \theta) + (p\lambda_{ds})\cos(\theta_e - \theta) \\ &\quad + (\omega_e - \omega)\lambda_{qs} \cos(\theta_e - \theta) - (\omega_e - \omega)\lambda_{ds} \sin(\theta_e - \theta) \end{aligned} \quad (11.109)$$

$$[p\lambda_{qs} - (\omega_e - \omega)\lambda_{ds}] \cos(\theta_e - \theta) = -[p\lambda_{ds} + (\omega_e - \omega)\lambda_{qs}] \sin(\theta_e) \quad (11.110)$$

$$[p\lambda_{qs} - (\omega_e - \omega)\lambda_{ds}] \sin(\theta_e - \theta) = [p\lambda_{ds} + (\omega_e - \omega)\lambda_{qs}] \cos(\theta_e) \quad (11.111)$$

Multiplying the first equation by $\cos(\theta_e - \theta)$ and the second by $\sin(\theta_e - \theta)$ and adding, one obtains

$$p\lambda_{qs} - (\omega_e - \omega)\lambda_{ds} = 0 \quad (11.112)$$

Multiplying the first equation by $-\sin(\theta_e - \theta)$ and the second by $\cos(\theta_e - \theta)$ and adding produces

$$p\lambda_{ds} + (\omega_e - \omega)\lambda_{qs} = 0 \quad (11.113)$$

Therefore, to neglect the stator transients the $p\lambda + (\omega_e - \omega)\lambda$ terms must be neglected (set equal to zero) in a non-synchronously rotating reference frame. The result reduces to the special case of $p\lambda = 0$ only in the case of the synchronous reference frame.

The $d-q$ equations of a synchronous machine in the rotor reference frame are (using the “ r ” superscript for clarity)

$$v_{qs}^r = r_s i_{qs}^r + \omega_r \lambda_{ds}^r + \frac{d\lambda_{qs}^r}{dt} \quad (11.114)$$

$$v_{ds}^r = r_s i_{ds}^r - \omega_r \lambda_{qs}^r + \frac{d\lambda_{ds}^r}{dt} \quad (11.115)$$

$$0 = r_{qr} i_{qr}^r + \frac{d\lambda_{qr}^r}{dt} \quad (11.116)$$

$$0 = r_{dr} i_{dr}^r + \frac{d\lambda_{dr}^r}{dt} \quad (11.117)$$

$$\varepsilon_x = x'_{md} i'_{fr}^r + \frac{x_{md}}{r_{fr}} \frac{d\lambda'_{fr}^r}{dt} \quad (11.118)$$

Substituting $\omega = \omega_r$ in the constraint equations that have been developed for neglecting stator transients, one obtains

$$p\lambda_{qs}^r = (\omega_e - \omega_r)\lambda_{ds}^r \quad (11.119)$$

$$p\lambda_{ds}^r = -(\omega_e - \omega_r)\lambda_{qs}^r \quad (11.120)$$

These two equations can be substituted into the two stator voltage equations. If the stator transients are neglected, the equations defining transient behavior of the machine are, in terms of hybrid flux linkages as state variables,

$$v_{qs}^r = r_s i_{qs}^r + \frac{\omega_e}{\omega_b} \psi_{ds}^r \quad (11.121)$$

$$v_{ds}^r = r_s i_{ds}^r - \frac{\omega_e}{\omega_b} \psi_{qs}^r \quad (11.122)$$

$$0 = r_{qr} i_{qr} + \frac{1}{\omega_b} \frac{d\psi_{qr}}{dt} \quad (11.123)$$

$$0 = r_{dr} i_{dr} + \frac{1}{\omega_b} \frac{d\psi_{dr}}{dt} \quad (11.124)$$

$$e_x = x_{md} i_{fr} + \frac{x_{md}}{\omega_b r'_{fr}} \frac{d\psi_{fr}}{dt} \quad (11.125)$$

In order to simulate these equations, the stator flux linkages must now be computed in terms of the remaining flux linkage state variables. From previous work, assuming the superscript “*r*” applies to all variables,

$$i_{qs} = \frac{\psi_{qs} - \psi_{mq}}{x_{ls}} \quad (11.126)$$

and

$$\psi_{mq} = x_{mq} * \left(\frac{\psi_{qs}}{x_{ls}} + \frac{\psi_{qr}}{x_{lqr}} \right) \quad (11.127)$$

These two equations can be substituted into Eq. (11.121) to form

$$v_{qs} + \frac{r_s}{x_{ls}} \left(\frac{x_{mq}^*}{x'_{lqr}} \right) \psi'_{qr} = \frac{r_s}{x_{ls}} \left(1 - \frac{x_{mq}^*}{x_{ls}} \right) \psi_{qs} + \frac{\omega_e}{\omega_b} \psi_{ds} \quad (11.128)$$

Similarly, one can find, from Eq. (11.122),

$$\psi'_{ds} + \frac{r_s}{x_{ls}} \left(\frac{x_{md}^*}{x'_{ldr}} \psi'_{dr} + \frac{x_{md}^*}{x'_{lfr}} \psi'_{fr} \right) = \frac{r_s}{x_{ls}} \left(1 - \frac{x_{md}^*}{x_{ls}} \right) \psi_{ds} - \frac{\omega_e}{\omega_b} \psi_{qs} \quad (11.129)$$

Upon solving these equations for stator flux linkages, in matrix form the solution is

$$\begin{bmatrix} \psi_{qs} \\ \psi_{ds} \end{bmatrix} = \frac{1}{\left(\frac{r_s}{x_{ls}} \right)^2 \left(1 - \frac{x_{mq}^*}{x_{ls}} \right) \left(1 - \frac{x_{md}^*}{x_{ls}} \right) + \left(\frac{\omega_e}{\omega_b} \right)^2} \times \begin{bmatrix} \frac{r_s}{x_{ls}} \left(1 - \frac{x_{md}^*}{x_{ls}} \right) & -\frac{\omega_e}{\omega_b} \\ \frac{\omega_e}{\omega_b} & \frac{r_s}{x_{ls}} \left(1 - \frac{x_{mq}^*}{x_{ls}} \right) \end{bmatrix}^{-1} \begin{bmatrix} v_{qs} + \frac{r_s}{x_{ls}} \left(\frac{x_{mq}^*}{x'_{lqr}} \right) \psi'_{qr} \\ v_{ds} + \frac{r_s}{x_{ls}} \left(\frac{x_{md}^*}{x'_{ldr}} \psi'_{dr} + \frac{x_{md}^*}{x'_{lfr}} \psi'_{fr} \right) \end{bmatrix} \quad (11.130)$$

or, in equivalent form,

$$\psi_{qs} = q_1 v_{qs} + q_2 \psi'_{qr} + q_3 v_{ds} + q_4 \psi'_{dr} + q_5 \psi'_{fr} \quad (11.131)$$

and

$$\psi_{ds} = d_1 v_{qs} + d_2 \psi'_{qr} + d_3 v_{ds} + d_4 \psi'_{dr} + d_5 \psi'_{fr} \quad (11.132)$$

where the definitions of the constants q_1, q_2, \dots, d_5 should be apparent from the context.

This expression is clearly complicated by the fact that the stator resistance is finite. In many cases the effect of the stator *ir* drop can be neglected, in which case Eq. (11.130) reduces to

$$\Psi_{qs} = -\frac{v_{ds}}{\left(\frac{\omega_e}{\omega_b}\right)} \quad (11.133)$$

$$\Psi_{ds} = \frac{v_{qs}}{\left(\frac{\omega_e}{\omega_b}\right)} \quad (11.134)$$

A simulation diagram implementing the exact form of these equations in MATLAB/SIMULINK is shown in [Figure 11.25](#). The constants are expressed by Eqs. (11.130)–(11.132) computed off-line. The following two computer traces repeat the case of [Figure 11.16](#) when stator transients are neglected. In the first trace, note the similarity of the results.

For the sake of completeness it should be noted that rotor transients can also be neglected in the synchronous machine equations. In this case $d\lambda_{qr}/dt = 0$ and $d\lambda_{dr}/dt = 0$ so that $i_{qr} = 0$ and $i_{dr} = 0$. Because of the long time constant, the field transient is nearly always retained. The equations to be solved when both stator and rotor transients are neglected are

$$v_{qs} = r_s i_{qs} + \frac{\omega_e}{\omega_b} \Psi_{ds} \quad (11.135)$$

$$v_{ds} = r_s i_{ds} - \frac{\omega_e}{\omega_b} \Psi_{qs} \quad (11.136)$$

$$e_x = x_{md} i'_{fr} + \frac{x_{md}}{\omega_b r_{fr}} \frac{d\Psi_{fr}}{dt} \quad (11.137)$$

Again

$$i_{qs} = \frac{\Psi_{qs} - \Psi_{mq}}{x_{ls}} \quad (11.138)$$

and

$$\Psi_{mq} = x_{mq} * \left(\frac{\Psi_{qs}}{x_{ls}} + \frac{\Psi_{qr}}{x_{lqr}} \right) \quad (11.139)$$

In this case, since $i_{qr} = i_{dr} = 0$,

$$\Psi_{qr} = \Psi_{mq} \quad (11.140)$$

in which case

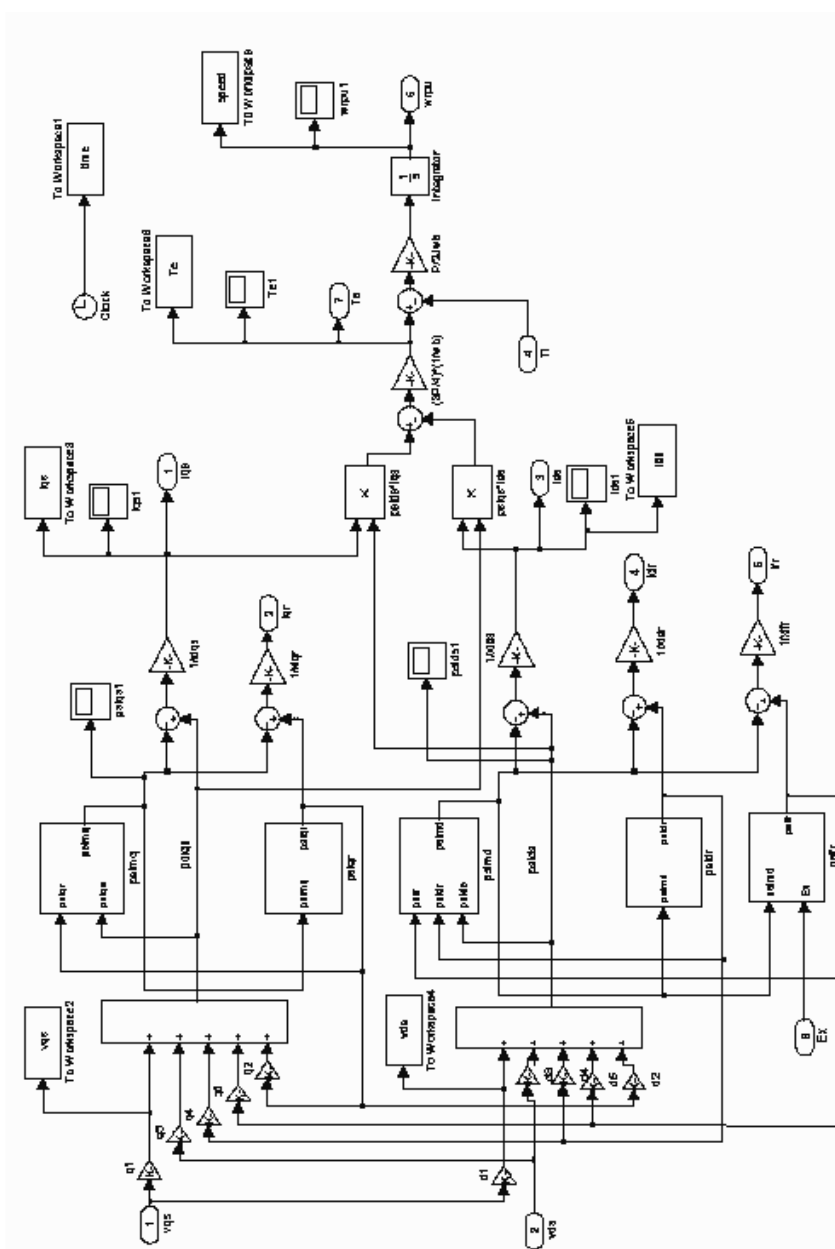


Figure 11.25 MATLAB/SIMULINK simulation of a synchronous machine neglecting stator transients.

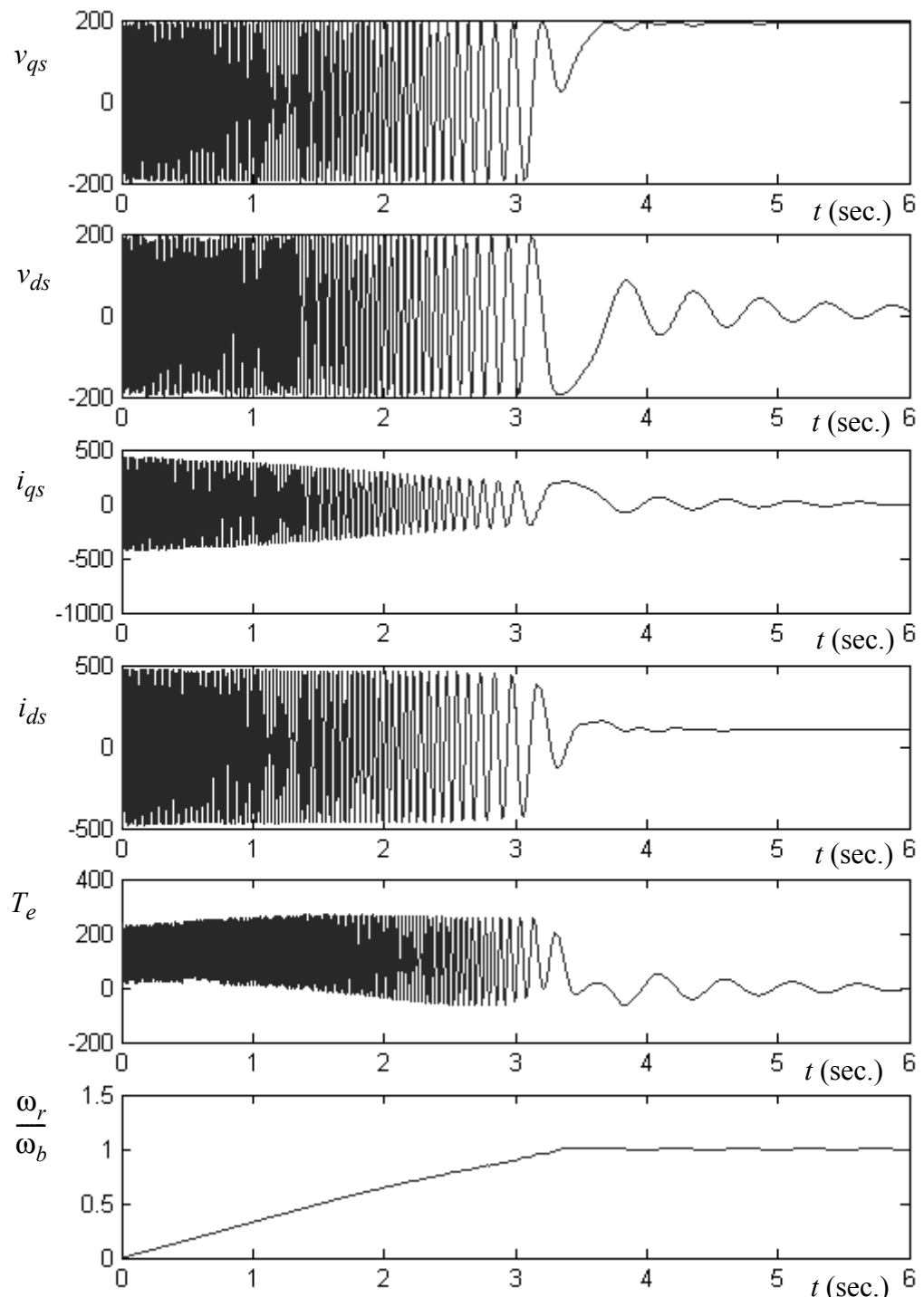


Figure 11.26 Acceleration from rest with shorted field winding neglecting stator $p\lambda$ terms (compare with Figure 11.16).

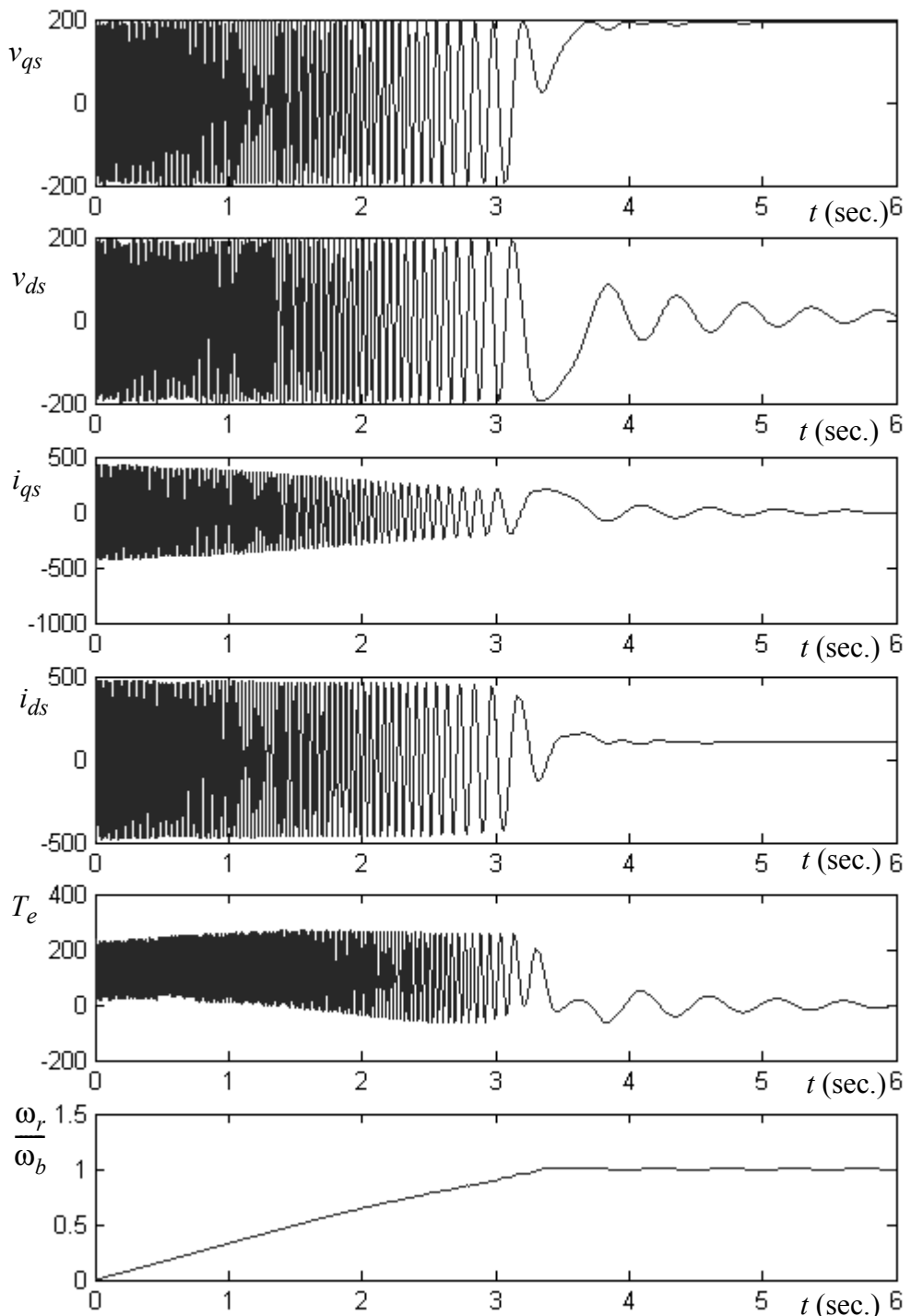


Figure 11.27 Acceleration from rest with shorted field winding neglecting stator $p\lambda$ terms and assuming $r_s = 0$ (compare with Figure 11.16).

$$\Psi_{mq} \left(1 - \frac{x_{mq}^*}{x_{lqr}} \right) = \frac{x_{mq}^*}{x_{ls}} \Psi_{qs} \quad (11.141)$$

Thus

$$i_{qs} = \frac{\Psi_{qs}}{x_{ls}} - \frac{x_{mq}^*}{x_{ls}} \frac{\Psi_{qs}}{\left(1 - \frac{x_{mq}^*}{x_{lqr}} \right)} \quad (11.142)$$

or

$$i_{qs} = \left[\frac{1 - x_{mq}^* \left(\frac{1}{x_{ls}} + \frac{1}{x_{lqr}} \right)}{1 - \frac{x_{mq}^*}{x_{lqr}}} \right] \frac{\Psi_{qs}}{x_{ls}} \quad (11.143)$$

so that

$$v_{qs} = \frac{r_s}{x_{ls}} \left[\frac{1 - x_{mq}^* \left(\frac{1}{x_{ls}} + \frac{1}{x_{lqr}} \right)}{1 - \frac{x_{mq}^*}{x_{lqr}}} \right] \Psi_{qs} + \frac{\omega_e}{\omega_b} \Psi_{ds} \quad (11.144)$$

Similarly

$$i_{ds} = \frac{\Psi_{ds} - \Psi_{md}}{x_{ls}} \quad (11.145)$$

and

$$\Psi_{md} = \frac{x_{md}^*}{x_{ls}} \Psi_{ds} + \frac{x_{md}^*}{x_{ldr}} \Psi_{dr} + \frac{x_{md}^*}{x_{lfr}} \Psi_{fr} \quad (11.146)$$

However,

$$\Psi'_{dr} = \Psi_{md} \quad (11.147)$$

so that

$$\Psi_{md} = \frac{1}{1 - \frac{x_{md}^*}{x_{ldr}}} \left(\frac{x_{md}^*}{x_{ls}} \Psi_{ds} + \frac{x_{md}^*}{x_{lfr}} \Psi_{fr} \right) \quad (11.148)$$

Eq. (11.145) becomes

$$i_{ds} = \frac{\Psi_{ds}}{x_{ls}} - \frac{1}{x_{ls} \left(1 - \frac{x_{md}^*}{x_{ldr}} \right)} \left(\frac{x_{md}^*}{x_{ls}} \Psi_{ds} + \frac{x_{md}^*}{x_{lfr}} \Psi_{fr} \right) \quad (11.149)$$

or

$$i_{ds} = \left(\frac{1 - \frac{x_{md}^*}{x_{ls}} - \frac{x_{md}^*}{x_{ldr}}}{1 - \frac{x_{md}^*}{x_{ldr}}} \right) \frac{\Psi_{ds}}{x_{ls}} - \frac{\frac{x_{md}^*}{x_{lfr}}}{\left(1 - \frac{x_{md}^*}{x_{ldr}} \right) x_{ls}} \Psi_{fr} \quad (11.150)$$

This result can be substituted into Eq. (11.135) to form

$$\dot{\psi}_{ds} + \frac{r_s}{x_{ls} \left(1 - \frac{x_{md}^*}{x_{ldr}} \right)} \frac{\frac{x_{md}^*}{x_{lfr}}}{x_{ls}} \Psi_{fr} = \frac{r_s}{x_{ls}} \left(\frac{1 - \frac{x_{md}^*}{x_{ls}} - \frac{x_{md}^*}{x_{ldr}}}{1 - \frac{x_{md}^*}{x_{ldr}}} \right) \Psi_{ds} - \frac{\omega_e}{\omega_b} \Psi_{qs} \quad (11.151)$$

Upon solving Eqs. (11.144) and (11.151) for stator flux linkages, the solution is, in matrix form,

$$\begin{bmatrix} \Psi_{qs} \\ \Psi_{ds} \end{bmatrix} = \frac{1}{\left(\frac{r_s}{x_{ls}} \right)^2 \left[1 - x_{mq}^* \left(\frac{1}{x_{ls}} + \frac{1}{x_{lqr}} \right) \right] \left[1 - x_{md}^* \left(\frac{1}{x_{ls}} + \frac{1}{x_{ldr}} \right) \right] + \left(\frac{\omega_e}{\omega_b} \right)^2} \times \begin{bmatrix} \frac{x_{md}^*}{x_{lfr}} \\ \frac{r_s}{x_{ls} \left(1 - \frac{x_{md}^*}{x_{ldr}} \right)} \end{bmatrix}$$

$$\begin{bmatrix}
 -\frac{r_s}{x_{ls}} \left[\frac{1 - x_{md}^* \left(\frac{1}{x_{ls}} + \frac{1}{x_{ldr}} \right)}{\left(1 - \frac{x_{md}^*}{x_{ldr}} \right)} \right] & \frac{\omega_e}{\omega_b} \\
 -\frac{\omega_e}{\omega_b} & \frac{r_s}{x_{ls}} \left[\frac{1 - x_{mq}^* \left(\frac{1}{x_{ls}} + \frac{1}{x_{lqr}} \right)}{\left(1 - \frac{x_{mq}^*}{x_{lqr}} \right)} \right]
 \end{bmatrix} \times \begin{bmatrix}
 v_{qs} \\
 \frac{x_{md}^*}{x_{lfr}} \Psi_{fr}
 \end{bmatrix} \\
 \begin{bmatrix}
 v_{ds} + \frac{r_s}{x_{ls}} \frac{x_{lfr}}{\left(1 - \frac{x_{md}^*}{x_{ldr}} \right)} \Psi_{fr}
 \end{bmatrix} \quad (11.152)$$

or, in equivalent form,

$$\Psi_{qs} = q_6 v_{qs} + q_7 v_{ds} + q_8 \Psi_{fr} \quad (11.153)$$

and

$$\Psi_{ds} = d_6 v_{qs} + d_7 v_{ds} + d_8 \Psi_{fr} \quad (11.154)$$

A simulation diagram neglecting both stator transients and fast rotor transients is shown in [Figure 11.28](#). In order to avoid algebraic loops, the air gap flux linkage calculation block must be modified to the form

$$\Psi_{mq} = \frac{1}{\left(1 - \frac{x_{mq}^*}{x_{lqr}} \right)} \frac{x_{mq}^*}{x_{ls}} \Psi_{qs} \quad (11.155)$$

and

$$\Psi_{md} = \frac{1}{\left(1 - \frac{x_{md}^*}{x_{ldr}} \right)} \left(\frac{x_{md}^*}{x_{ls}} \Psi_{ds} + \frac{x_{md}^*}{x_{lfr}} \Psi_{fr} \right) \quad (11.156)$$

A plot of an acceleration transient with the same parameters as [Figure 11.16](#) is given in [Figure 11.29](#). Clearly this model is not a good approximation to predict starting currents, since it is the current flow in the amortisseur windings that produces the major portion of the starting torque.

The model neglecting rotor $p\lambda$ terms is better suited to problems in which the rotor is swinging slowly such that the induced rotor currents are relatively small. In effect, the model of Figure 11.28 neglects the sub-transient components of torque.

11.11 Conclusion

This text is an attempt to provide a sound introduction to the fascinating subject of synchronous machines. The understanding of the intricacies of synchronous machines will surely be of importance as long as electrical power is derived from a mechanical source. It is hoped that a few photons of light have been shed on this subject.

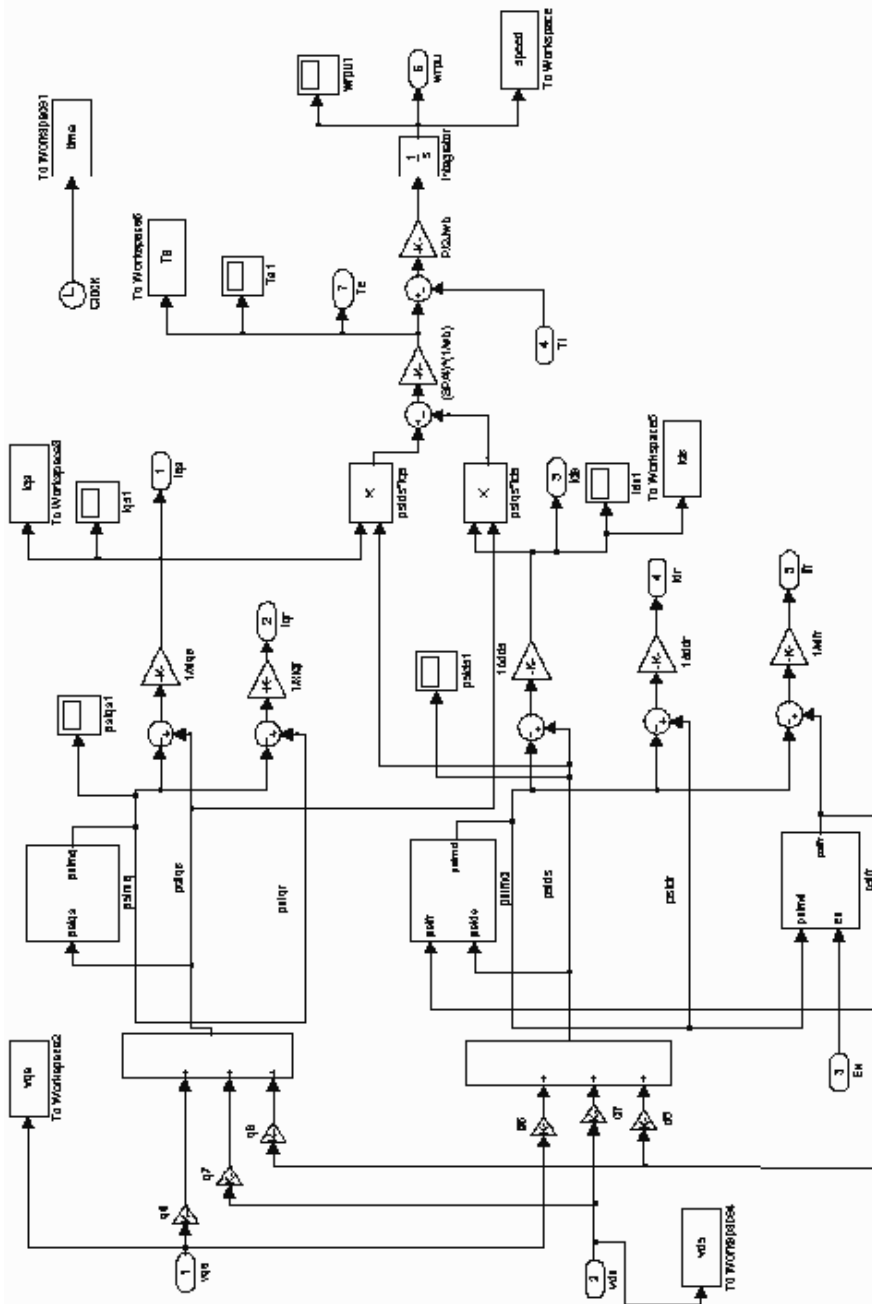


Figure 11.28 MATLAB/SIMULINK simulation of a synchronous machine neglecting both stator transients and fast rotor transients.

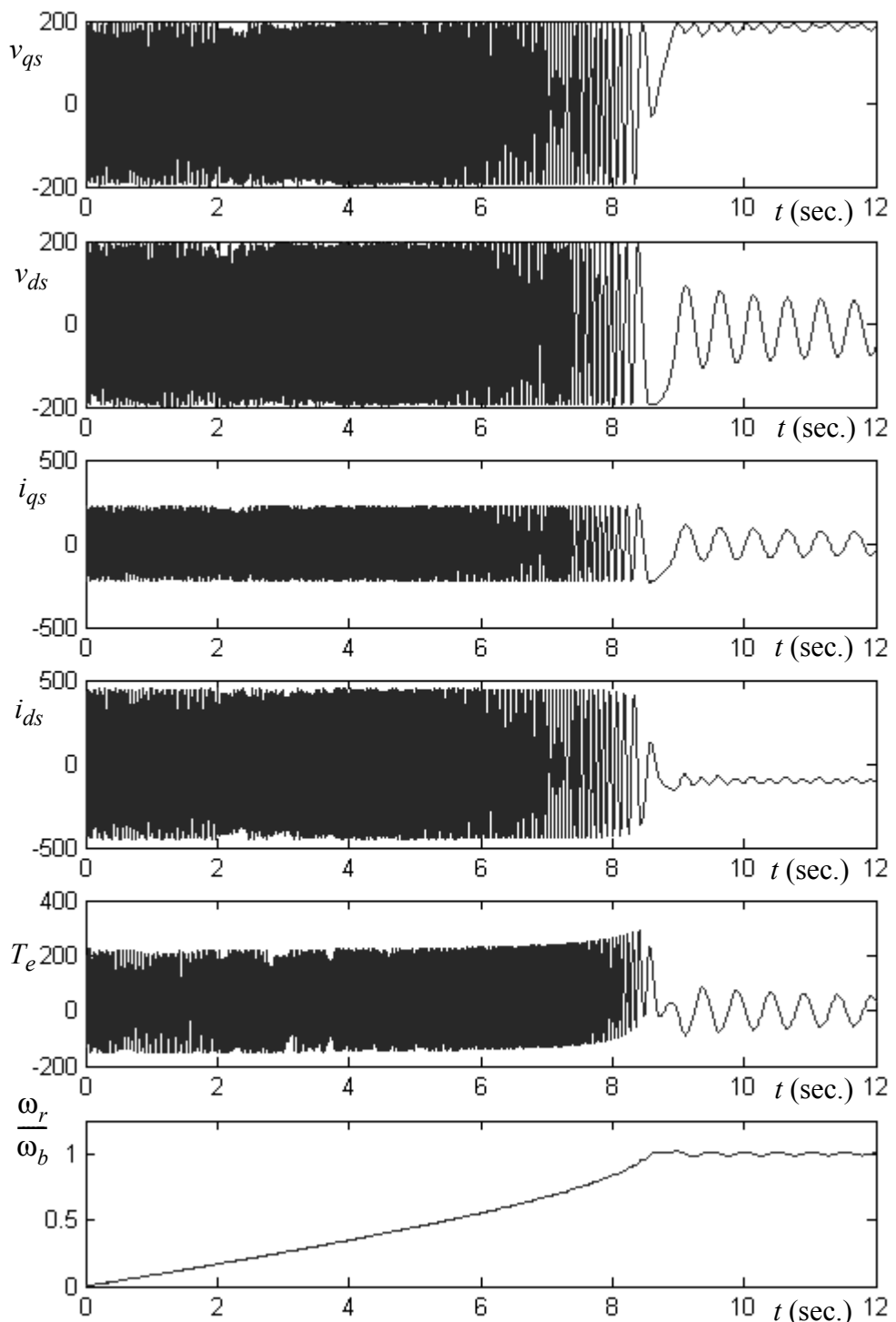


Figure 11.29 Acceleration from rest with shorted field winding neglecting stator and rotor amortisseur $p\lambda$ terms (compare with Figure 11.16).

Appendix 1

Identities Useful in AC Machine Analysis

1. $\sin^2 A + \cos^2 A = 1$
2. $\sin(A \pm B) = \sin A \cos B \pm \cos A \sin B$
3. $\cos(A \pm B) = \cos A \cos(B) \mp \sin A \sin B$
4. $\sin A \cos B = \frac{1}{2}[\sin(A + B) + \sin(A - B)]$
5. $\cos A \cos B = \frac{1}{2}[\cos(A + B) + \cos(A - B)]$
6. $\sin A \sin B = \frac{1}{2}[\cos(A - B) - \cos(A + B)]$
7. $\cos A + \cos\left(A - \frac{2\pi}{3}\right) + \cos\left(A + \frac{2\pi}{3}\right) = 0$
8. $\sin A + \sin\left(A - \frac{2\pi}{3}\right) + \sin\left(A + \frac{2\pi}{3}\right) = 0$
9. $\cos^2 A + \cos^2\left(A - \frac{2\pi}{3}\right) + \cos^2\left(A + \frac{2\pi}{3}\right) = \frac{3}{2}$
10. $\sin^2 A + \sin^2\left(A - \frac{2\pi}{3}\right) + \sin^2\left(A + \frac{2\pi}{3}\right) = \frac{3}{2}$
11. $\sin A \sin\left(A - \frac{2\pi}{3}\right) + \sin\left(A - \frac{2\pi}{3}\right)\sin\left(A + \frac{2\pi}{3}\right) + \sin\left(A + \frac{2\pi}{3}\right)\sin A = -\frac{3}{4}$
12. $\cos A \cos\left(A - \frac{2\pi}{3}\right) + \cos\left(A - \frac{2\pi}{3}\right)\cos\left(A + \frac{2\pi}{3}\right) + \cos\left(A + \frac{2\pi}{3}\right)\cos A = -\frac{3}{4}$
13. $\sin A \cos A + \sin\left(A - \frac{2\pi}{3}\right)\cos\left(A - \frac{2\pi}{3}\right) + \sin\left(A + \frac{2\pi}{3}\right)\cos\left(A + \frac{2\pi}{3}\right) = 0$
14. $\sin A \cos\left(A + \frac{2\pi}{3}\right) + \sin\left(A - \frac{2\pi}{3}\right)\cos A + \sin\left(A + \frac{2\pi}{3}\right)\cos\left(A - \frac{2\pi}{3}\right) = -\frac{3\sqrt{3}}{4}$
15. $\sin A \cos\left(A - \frac{2\pi}{3}\right) + \sin\left(A - \frac{2\pi}{3}\right)\cos\left(A + \frac{2\pi}{3}\right) + \sin\left(A + \frac{2\pi}{3}\right)\cos A = \frac{3\sqrt{3}}{4}$

$$16. \cos A \cos B + \cos\left(A - \frac{2\pi}{3}\right)\cos\left(B - \frac{2\pi}{3}\right) + \cos\left(A + \frac{2\pi}{3}\right)\cos\left(B + \frac{2\pi}{3}\right) = \frac{3}{2}\cos(A - B)$$

$$17. \sin A \sin B + \sin\left(A - \frac{2\pi}{3}\right)\sin\left(B - \frac{2\pi}{3}\right) + \sin\left(A + \frac{2\pi}{3}\right)\sin\left(B + \frac{2\pi}{3}\right) = \frac{3}{2}\cos(A - B)$$

$$18. \sin A \cos B + \sin\left(A - \frac{2\pi}{3}\right)\cos\left(B - \frac{2\pi}{3}\right) + \sin\left(A + \frac{2\pi}{3}\right)\cos\left(B + \frac{2\pi}{3}\right) = \frac{3}{2}\sin(A - B)$$

Appendix 2

Time Domain Solution of the State Equation

A2.1 Reduction to Explicit Form

It has been shown in Chapter 5 that a synchronous machine can be expressed in the form

$$px = Ax + u \quad (\text{A2.1})$$

where p is time derivative operator d/dt and x is the state vector given by

$$x = \begin{bmatrix} i \\ x_2 \\ x_1 \end{bmatrix} \quad (\text{A2.2})$$

The matrix A is the 10×10 system matrix of Eq. (5.184) and u is the 10×1 input vector of constant elements

$$u = \begin{bmatrix} \omega_b X^{-1} v_0 \\ \mathbf{0}_{4 \times 1} \end{bmatrix} \quad (\text{A2.3})$$

The vector i denotes the element vector of machine current, x_2 , and x_1 represent oscillators which oscillate at two times the source frequency and at the source frequency, respectively. The vector v_0 represents the voltages applied to the six machine terminals corresponding to the elements of i .

Since the forcing function of Eq. (A2.1) is a vector of constants, the solution can be found by direct integration. It is well known that the solution to Eq. (A2.1) is [1]

$$x(t) = PQ(t)Rx(0) + \Lambda^{-1}P[Q(t) - I]Ru \quad (\text{A2.4})$$

where

$$P = [p_1, p_2, p_3, \dots, p_m] \quad (\text{A2.5})$$

$$R = P^{-1} \quad (\text{A2.6})$$

$$\Lambda = \begin{bmatrix} \lambda_1 & 0 & 0 & \cdots & 0 \\ 0 & \lambda_2 & 0 & \cdots & 0 \\ 0 & 0 & \lambda_3 & \cdots & \cdot \\ \cdot & \cdot & \cdot & \cdots & \cdot \\ \cdot & \cdot & \cdot & \cdots & 0 \\ \cdot & \cdot & \cdot & \cdots & \lambda_m \end{bmatrix} \quad (\text{A2.7})$$

$$Q(t) = \begin{bmatrix} e^{\lambda_1 t} & 0 & 0 & \cdots & 0 \\ 0 & e^{\lambda_2 t} & 0 & \cdots & 0 \\ 0 & 0 & e^{-\lambda_3 t} & \cdots & 0 \\ \cdot & \cdot & \cdot & \cdots & \cdot \\ \cdot & \cdot & \cdot & \cdots & 0 \\ \cdot & \cdot & \cdot & \cdots & 0 & e^{-\lambda_m t} \end{bmatrix} \quad (\text{A2.8})$$

The quantity P is the matrix of eigenvectors p_1, p_2, \dots, p_m corresponding to the eigenvalues $\lambda_1, \lambda_2, \dots, \lambda_m$ contained in the eigenvalue matrix Λ . The integer m is the order of the system (rank of A). In this case $m = 10$. The matrix $Q(t)$ is the response matrix of the uncoupled system. It will be assumed that no repeated eigenvalues occur so that both Λ and $Q(t)$ are diagonal. The quantity I is the identity matrix.

The first term of Eq. (A2.4) can be recognized as the homogeneous part of the solution resulting from the initial conditions at $t = 0$. The second part of Eq. (A2.4) corresponds to the complementary solution resulting from the excitation u .

The first term of Eq. (A2.4) can be written as

$$PQ(t)Rx(0) = RQ(t) \begin{bmatrix} r_1 \cdot x(0) \\ r_2 \cdot x(0) \\ \vdots \\ r_m \cdot x(0) \end{bmatrix} \quad (\text{A2.9})$$

where, for example, $r_1 \cdot x(0)$ denotes the dot (inner) product of r_1 and $x(0)$ and r_1, r_2, \dots, r_m are the rows of the matrix R .

Multiplying the response matrix $Q(t)$ by $Rx(0)$, the first term in Eq. (A2.4) can be expressed as

$$PQ(t)Rx(0) = [p_1, p_2, \dots, p_m] \begin{bmatrix} e^{\lambda_1 t} r_1 \cdot x(0) \\ e^{\lambda_2 t} r_2 \cdot x(0) \\ \vdots \\ e^{\lambda_m t} r_m \cdot x(0) \end{bmatrix} \quad (\text{A2.10})$$

Equation (A2.10) can be written in the alternative form

$$PQ(t)Rx(0) = \{[r_1 \cdot x(0)]p_1, [r_2 \cdot x(0)]p_2, \dots, [r_m \cdot x(0)]p_m\} \begin{bmatrix} e^{\lambda_1 t} r_1 \cdot x(0) \\ e^{\lambda_2 t} r_2 \cdot x(0) \\ \vdots \\ e^{\lambda_m t} r_m \cdot x(0) \end{bmatrix} \quad (\text{A2.11})$$

Equation (A2.11) is of the form

$$PQ(t)Rx(0) = Sq \quad (\text{A2.12})$$

where

$$q = [e^{\lambda_1 t}, e^{\lambda_2 t}, \dots, e^{\lambda_m t}]^t \quad (\text{A2.13})$$

Using the same manipulation technique, it can be shown that the second term of Eq. (A2.4) can be reduced to

$$\Lambda^{-1} P[Q(t) - I] R u = - \begin{bmatrix} p_{11}(r_1 \cdot u)/\lambda_1 & p_{12}(r_2 \cdot u)/\lambda_1 & \cdots & p_{1m}(r_m \cdot u)/\lambda_1 \\ p_{12}(r_1 \cdot u)/\lambda_2 & p_{22}(r_2 \cdot u)/\lambda_2 & \cdots & p_{2m}(r_m \cdot u)/\lambda_1 \\ \vdots & \vdots & \ddots & \vdots \\ p_{m1}(r_1 \cdot u)/\lambda_m & p_{m2}(r_2 \cdot u)/\lambda_m & \cdots & p_{mm}(r_m \cdot u)/\lambda_1 \end{bmatrix} \quad (\text{A2.14})$$

Equation (A2.14) can be expressed as

$$\Lambda^{-1} P[Q(t) - I] R u = T[\mathbf{1} - q(t)] \quad (\text{A2.15})$$

where

$$\mathbf{1} = [1, 1, 1, \dots, 1]^t \quad (m \times 1 \text{ vector of ones}) \quad (\text{A2.16})$$

Hence the solution for $x(t)$ given by Eq. (A2.4) can be written in the alternative form

$$x(t) = (S - T)q(t) + T\mathbf{1} \quad (\text{A2.17})$$

It should be clear that when $t = 0$ then $x(0) = S\mathbf{1}$. If the eigenvalues of A have negative real parts, then when $t \rightarrow \infty$, $x(\infty) \rightarrow T\mathbf{1}$.

A2.2 Complex Eigenvalues

When the eigenvalues $\lambda_1, \lambda_2, \dots, \lambda_m$ are not all real, complex terms appear in the S and T matrices and it is useful to rewrite these terms in a different form. Consider first the homogeneous part of the solution. Because the roots are complex conjugates, two terms in the solution will appear typically as

$$x_h = (a + jb)e^{(\sigma + j\omega)t} + (a - jb)e^{(\sigma - j\omega)t} \quad (\text{A2.18})$$

This equation can be written in the form

$$x_h = 2ae^{\sigma t} \left(\frac{e^{j\omega t} + e^{-j\omega t}}{2} \right) - 2be^{\sigma t} \left(\frac{e^{j\omega t} - e^{-j\omega t}}{2j} \right), \quad (\text{A2.19})$$

Equation (A2.19) is equivalent to

$$x_h = e^{\sigma t} [2 \cos(\omega t) - 2b \sin(\omega t)] \quad (\text{A2.20})$$

or, alternatively,

$$x_h = ce^{\sigma t} \sin(\omega t + \phi) \quad (\text{A2.21})$$

where

$$c = \sqrt{a^2 + b^2} \quad (\text{A2.22})$$

and

$$\phi = \arctan\left(\frac{a}{-b}\right) \quad (\text{A2.23})$$

In a similar manner, it can be shown that the two complex conjugate terms in the complementary part of the solution reduce to

$$x_c = 2a - ce^{\sigma t} \sin(\omega t + \phi) \quad (\text{A2.24})$$

where c and ϕ are the same as defined above.

A2.3 References

- [1] K. Ogata, "State Space Analysis of Control Systems," Prentice-Hall, Inc., Englewood Cliffs, N.J., 1967.

Appendix 3

Three-Phase Fault

```
%%%%%%%%%%%%%%  
% T.A. Lipo  
% Three-phase synchronous machine fault equations  
% My thanks to Ricky White for his generous help  
%%%%%%%%%%%%%
```



```
%%%%%%%%%%%%%%  
%Things that you must input!  
%%%%%%%%%%%%%  
%stator, Xls, rqr, rdr, rfr, Xqr, Xdr, Xfr, Xmq, Xmd, Xg, rg  
Param=[0.002 0.14 0.003 0.001 1.9 1.9 2 1.86 0 0];
```



```
Vph =1; %Phase source voltage pre-transient (pu)  
we = 2*pi*50; %Angular frequency (rad/s), assumed equal to wb  
pf= 1; %Power Factor pre-transient;  
LagorLead = 1; %LagorLead equals 1 for lagging power factor  
 %and LagorLead equals -1 for leading power factor  
 %prior to transient  
MotororGen = -1; %MotororGen equals 1 for motor and -1 for generator  
I=0.0; %Phase current amplitude pre-transient (pu)
```



```
%Source voltages during transient transient (complex notation)  
Eag=0; %1 ;  
Ebg=0; %-0.5 - i*(sqrt(3)/2);  
Ecg=0; %-0.5 + i*(sqrt(3)/2);  
ex2=1;
```



```
%%%%%%%%%%%%%%  
%Phasor current pre-transient  
%%%%%%%%%%%%%  
phi=acos(pf)*-(LagorLead); %Angle between voltage and current  
Iph=I*exp(i*phi);
```



```
%%%%%%%%%%%%%%  
%Input values from data file  
%%%%%%%%%%%%%  
%MWbase=Base(1);  
%Vbase=Base(2);
```

```
%fbase=Base(3 );
rs=Param(1);
Xls=Param(2);
rqr=Param(3);
rdr=Param(4);
rfr=Param(5);
Xlqr=Param(6);
Xldr=Param(7);
Xfr=Param(8);
Xmq=Param(9);
Xmd=Param(10);
Xg=Param(11);
rg=Param(12);

%%%%%%%%%%%%%
%Begin calculations
%%%%%%%%%%%%%
%Calculated constants %
%%%%%%%%%%%%%
Xq=Xls+Xmq;
Xd=Xls+Xmd;
wb=we;

%%%%%%%%%%%%%
%Calculate steady-state just before the transient.
%In this exercise, it is always assumed that the
%steady-state is initially balanced
%%%%%%%%%%%%%

%Source phase voltage phasors before transient
Va=Vph; %Phase A voltage phasor
Vb=Vph*(-0.5-i*(sqrt(3)/2)); %Phase B voltage phasor
Vc=Vph*(-0.5+i*(sqrt(3)/2)); %Phase C voltage phasor

%Source phasor currents before transient
Ia=Iph*MotororGen; %Phase A current
Ib=Iph*(-0.5 - i*(sqrt(3)/2))*MotororGen; %Phase B current
Ic=Iph*(-0.5 + i*(sqrt(3)/2))*MotororGen; %Phase C current

%Torque angle before transient
Eq = Va-Ia*(rs+i*Xq)
```

```
delta = -angle(Eq);

% D-Q currents
iqs=real(Ia*exp(i*delta));
ids=imag(Ia*exp(i*delta));
ios=(Ia+Ib+Ic)/3;
ikq=0;
ikd=0;

% Excitation before transient (assumed the same after transient)
Ex=Va+Ia*rs+i*Ia*Xls+i*ids*i*Xmd+i*iqs*Xmq;
ifr=abs(Ex)/Xmd;

%%%%%%%%%%%%%
% Calculations of voltages defining the transient.
%%%%%%%%%%%%%

Eaalpha=real(Eag);
Ebalpha=real(Ebg);
Ecalpha=real(Ecg);

Eabeta=-imag(Eag);
Ebbeta=-imag(Ebg);
Ecbeta=-imag(Ecg);

Vdalpa=(1/sqrt(3))*(Ecalpha-Ebalpha);
Vdbeta=(1/sqrt(3))*(Ecbeta-Ebbeta);

Vqalpha=(2/3)*Eaalpha-(1/3)*Ebalpha-(1/3)*Ecalpha;
Vqbeta=(2/3)*Eabeta-(1/3)*Ebbeta-(1/3)*Ecbeta;

Voalpha=(1/3)*(Eaalpha+Ebalpha+Ecalpha);
Vobeta=(1/3)*(Eabeta+Ebbeta+Ecbeta);

Vqr=0.5*(Vqalpha-Vdbeta)*cos(delta)-0.5*(Vqbeta+Vdapha)*sin(delta)...
+0.5*(Vqalpha+Vdbeta)*cos(2*we*t+delta)+0.5*(Vqbeta-Vdapha)*sin(2*we*t+delta);

Vdr=0.5*(Vqalpha-Vdbeta)*sin(delta)+0.5*(Vqbeta+Vdapha)*cos(delta)...
+0.5*(Vqalpha+Vdbeta)*sin(2*we*t+delta)-0.5*(Vqbeta-Vdalpa)*cos(2*we*t+delta);

Vog=Voalpha*cos(we*t)+Vobeta*sin(we*t)
```

%Xbar from the Paper...

```
Xbar=[Xq 0 0 Xmq 0 0
      0Xd 0 0 Xmd Xmd
      0 0 Xls+Xg 0 0 0
      Xmq 0 0 Xlqr 0 0
      0 Xmd 0 0 Xldr Xmd
      0 (Xmd*Xmd)/rfr 0 0 (Xmd*Xmd)/rfr (Xfr*Xmd)/rfr];
```

```
InvXbar=inv(Xbar);
```

% Rbar plus Gbar

```
RbarplusGbar=[rs Xd 0 0 Xmd Xmd
-Xq rs 0 -Xmq 0 0
0 0 rs+rg 0 0 0
0 0 0 rqr 0 0
0 0 0 0 rdr 0
0 0 0 0 Xmd];
```

%The 0megas...

```
Omega1=[0 -1
1 0];
```

```
Omega2=[0 -2
2 0];
```

%and the C matrices...

```
C1=[0 0
0 0
Voalpha Vobeta
0 0
0 0
0 0];
```

```
C2=[(Vqalpha+Vdbeta)/2 (Vqbeta-Vdalpah)/2
(Vqbeta-Vdalpah)/2 (Vqalpha+Vdbeta)/2
0 0
0 0
0 0
0 0];
```

% State space matrices

```
A=wb*-inv(Xbar)*RbarplusGbar;
```

```
Aprim=wb*[-inv(Xbar)*RbarplusGbar inv(Xbar)*C2 inv(Xbar)*C1  
zeros(2,6) Omega2 zeros(2,2)  
zeros(2,6) zeros(2,2) Omega1];
```

```
B=wb*InvXbar;
```

```
Bprim=[B  
zeros(4,6)];
```

```
%%%%%%  
%Eigenvectors and Eigenvalues  
%%%%%%  
%%%%%%  
%%%%%S
```

```
[Eigvec,Eigval]=eig(Aprim);
```

```
%%%%%%  
%Vectors  
%%%%%%  
%%%%%
```

```
%State variable initial conditions
```

```
Ixoprim=[iqs  
ids  
ios  
ikq  
ikd  
ifr];
```

```
x1=[1  
0];
```

```
x2=[cos(delta)  
sin(delta)];
```

```
vo=[0.5*(Vqalpha-Vdbeta)*cos(delta)-0.5*(Vqbeta+Vdalpa)*sin(delta)  
0.5*(Vqalpha-Vdbeta)*sin(delta)+0.5*(Vqbeta+Vdalpa)*cos(delta)  
0  
0  
0  
Ex];
```

```

v = vo + C1*x1 + C2*x2;

%%%%%%%%%%%%%
%The big ones for the solution
%%%%%%%%%%%%%

Pbar=Eigvec;
Rbar=inv(Pbar);
u=[(wb*InvXbar)*v
    zeros(4,1)];
xo=[Ixoprim
    x1
    x2];

%S matrix calculation
for ii=1:length(Aprim(1,:))
% S(:,ii)=(Rbar(ii,:)*xo)*Pbar(:,ii);
S(:,ii)=Pbar(:,ii)*(Rbar(ii,:)*xo);
end

%T matrix calculation
for jj=1:length(Aprim(1,:))
tempT(jj,jj)=Rbar(jj,:)*u;
end
T=-Pbar.*((ones(10,10)*inv(Eigval)).*(ones(10,10)*tempT));

%%%%%%%%%%%%%
%Output matrices (The dreaded S and T matrices)
%%%%%%%%%%%%%

SminusT=S-T;
TbyOne=T*ones(10,1);
TbyOnemat=TbyOne([1 2 3 4 5 6]);
%%%%%%%%%%%%%
%Calculate currents
%%%%%%%%%%%%%
iii=1;
for time=0:0.001:2
q=exp((Eigval*ones(10,1))*time);
Output(:,iii)=[TbyOne+SminusT*q

```

```
time];
```

```
iii=iii+ 1;  
end
```

```
%%%%%%%%%%%%%%%%%%%%%%%%%%%%%%%%%%%%%%
```

```
% Calculate Torque
```

```
%%%%%%%%%%%%%%%%%%%%%%%%%%%%%%%%%%%%%%
```

```
PhiD=Xd*Output(2,:)+Xmd*(Output(5,:)+Output(6,:));% D-Axis Flux Voltage
```

```
PhiQ=Xq*Output(1,:)+Xmq*Output(5,:);% Q-Axis Flux Voltage
```

```
torque=PhiD.*Output(1,:)-PhiQ.*Output(2,:);
```

```
%%%%%%%%%%%%%%%%%%%%%%%%%%%%%%%%%%%%%%
```

```
%Screen Stuff
```

```
%%%%%%%%%%%%%%%%%%%%%%%%%%%%%%%%%%%%%%
```

```
%Compute Analytical Exponential Coefficients and Phase Angles (in Degrees)
```

```
for nn=1: 10
```

```
for kk=1: 10
```

```
    a(nn,kk)=real(SminusT(nn,kk));
```

```
    b(nn,kk)=imag(SminusT(nn,kk));
```

```
    c(nn,kk)=2*sqrt(a(nn,kk)^2+b(nn,kk)^2);
```

```
if ~ (b(nn,kk)==0)
```

```
    theta(nn,kk)=180*atan2(a(nn,kk),-b(nn,kk))/pi;
```

```
else
```

```
    theta(nn,kk)=0;
```

```
end
```

```
sig(nn,kk)=real(Eigval(kk,kk));
```

```
end
```

```
end
```

```
SolutionText=['The Solution for Iqs is:\n',...
```

```
'The Solution for Ids is:\n',...
```

```
'The Solution for Igs is:\n',...
```

```
'The Solution for Iqr is:\n',...
```

```
'The Solution for Idr is:\n',...
```

```
'The Solution for Ifr is:\n'];
```

```
no=0;
for nn= 1:6
fprintf(SolutionText((1+no):(24+no)))
no=no+26;
fprintf(1,' \n\n%0.3E\n',real(TbyOnemat(nn)))
for kk=1:5
if~(imag(Eigval(kk,kk))==0)
if imag(Eigval(kk,kk))<0
fprintf(
%0.4E*exp(%0.4g*t)*sin(%0.4g*t+%0.4g)\n',c(nn,kk),sig(nn,kk),imag(Eigval(kk,kk)),theta(nn))
%else
%fprintf(
%0.4E*exp(%0.4g*t)*sin(%0.4g*t+%0.4g)\n',c(nn,kk),sig(nn,kk),imag(Eigval(kk,kk)),theta(nn))
end
else
fprintf(' %0.4E*exp(%0.4g*t))\n',SminusT(nn,kk),sig(nn,kk))
end
fprintf('\n')
end
end

%%%%%%%%%%%%%%%
%Pretty pictures
%%%%%%%%%%%%%%%
figure
plot(Output(11,:),real(Output([6],:)))
legend('ifr')

figure
plot(Output(11,:),real(Output([4 5],:)))
legend('iqr','idr')

figure
plot(Output(11,:),real(Output([1 2],:)))
legend('iqs','ids')

figure
plot(Output(11,:),real(torque))
legend('torque')
```

Appendix 4

TrafunSM

```
%*****  
%*      TRANSFER FUNCTIONS OF A SYNCHRONOUS MACHINE      *  
%*      ALL VARIABLES AND PARAMETERS ARE IN PER UNIT      *  
%*      My thanks to Mr. Yang Wang for his help          *  
%*****  
  
clear  
  
A = zeros(7,7); AINV = zeros(7,7); YSS = zeros(7,1); XSS = zeros(7,1);  
A1 = zeros(7,4); A2 = zeros(7,7); A2inv = zeros(7,7); A3 = zeros(7,7);  
B = zeros(7,4);  
X = zeros(7,1); BB = zeros(7,1); C = zeros(7,1); cds = zeros(7,1); ...  
cqs = zeros(7,1);cwr = zeros(7,1);  
  
% READ MOTOR PARAMETERS FROM FILE INPUT  
file_input = fopen('input.txt','r');  
data_buf = fscanf(file_input, '%g', [1,22]);  
data_buf = data_buf';  
fprintf('Parameter Values in Per Unit\r\n')  
fprintf('V_l-1(pu) = %g V      F_rated = %g HZ      Poles = %g...  
\r\n',data_buf(1:3));  
fprintf('Rs = %g      Rqr = %g      Rdr = %g    Rfr = %g...  
\r\n',data_buf(4:7));  
fprintf('Xls = %g      Xmq = %g      Xmd = %g \r\n',data_buf(8:10));  
fprintf('Xlqr = %g      Xldr = %g      Xlfr = %g \r\n',data_buf(11:13));  
fprintf('Xe = %g      Re = %g \r\n',data_buf(14:15));  
fprintf('Inertia H = %g s.\r\n', data_buf(16));  
Vll = data_buf(1);Fb = data_buf(2);Poles = data_buf(3);  
Rs = data_buf(4);Rqr = data_buf(5);Rdr = data_buf(6);Rfr =...  
    data_buf(7);  
Xls = data_buf(8);Xmq = data_buf(9);Xmd = data_buf(10);  
Xlqr = data_buf(11);Xldr = data_buf(12);Xlfr = data_buf(13);  
Xe = data_buf(14);Re = data_buf(15);  
H = data_buf(16);  
  
% CONVERT Vll TO PEAK PHASE VOLTAGE  
Vb = Vll*sqrt(2/3);  
% DEFINE REMAINING PARAMETERS  
Wb = 2*pi*Fb;  
  
Xds = Xls+Xmd;
```

```

Xqs = Xls+Xmq;
Xdr = Xldr+Xmd;
Xqr = Xlqr+Xmd;
Xfr = Xlfr+Xmd;
Xqstar = 1.0/(1.0/Xmq+1.0/Xls+1.0/Xlqr);
Xdstar = 1.0/(1.0/Xmd+1.0/Xls+1.0/Xlfr+1.0/Xldr);

% PREPARE MATRICES
A(5,1)=-1;
A(6,2)=-1;
A(1,3)=-Rs/Xls;
A(2,4)=A(1,3);
A(1,5)=-A(1,3);
A(2,6)=A(1,5);
A(3,3)=-Xqstar/Xls;
A(3,5)=1-Xqstar/Xlqr;
A(4,4)=-Xdstar/Xls;
A(4,6)=1-Xdstar/Xldr;
A(4,7)=-Xdstar/Xlfr;
A(5,3)=1/Xls;
A(6,4)=A(5,3);
A(5,5)=-A(5,3);
A(6,6)=A(5,5);
A(7,6)=-Xmd/Xlfr;
A(7,7)=-A(7,6);

% READ THE MOTOR STATE
% Vs Inputted in p.u., Deltad in degrees, Fe in Hertz, Ex in Pu
Vso = data_buf(17); Deltad = data_buf(18); Fe = data_buf(19); Ex =...
data_buf(20);
Deltar = Deltad*pi/180;
Wr = 2*pi*Fe;
A(1,4) = -Wr/Wb;
A(2,3) = Wr/Wb;
Vqso = Vso*cos(Deltar);
Vdso = -Vso*sin(Deltar);
YSS(1) = -Vqso;
YSS(2) = -Vdso;
YSS(7) = Ex;

% PROCESS MATRICES
AINV = inv(A);
XSS = XSS+AINV*YSS;
% XSS(1)=Iqso, XSS(2)=Idso, XSS(3)=PSIqso, XSS(4)=PSIdso,
% XSS(5)=PSIqro, XSS(6)=PSIdro, XSS(7)=PSIfro

Iso = sqrt(XSS(1)^2+XSS(2)^2);
Vqbo = Wr/Wb*Xe*XSS(2) + Re*XSS(1) + Vqso;
Vdbo = -Wr/Wb*Xe*XSS(1) + Re*XSS(2) + Vdso;

```

```

Vbo = sqrt(Vqbo^2+Vdbo^2);
Vso = sqrt(Vqso^2+Vdso^2);
Deltabo = atan(-Vdbo/Vqbo);
TORQ = XSS(1)*XSS(4)-XSS(2)*XSS(3);
PSIso = sqrt(XSS(3)^2+XSS(4)^2);
MMFANG = 180/pi*atan(-XSS(1)/XSS(2));
PF = sin(MMFANG*pi/180+Deltar);

fprintf('\r\nSteady-State Operating Point in Per Unit \r\n')
Ifr = (XSS(7)-XSS(6))/Xlfr;
fprintf('Terminal Volts Vqs = %g           Vds = %g           Vs = %g...
\r\n', Vqso, Vdso, Vso);
fprintf('Inf. Bus Volts Vqb = %g           Vdb = %g           Vb = %g...
\r\n', Vqbo, Vdbo, Vbo);
fprintf('Iqs = %g     Ids = %g     Is = %g \r\n', XSS(1), XSS(2), Iso);
fprintf('PSIqs = %g     PSIIds = %g     PSIs = %g \r\n', XSS(3), ...
XSS(4), PSIso);
fprintf('PSImq = %g     PSImd = %g     PSIfr = %g \r\n', XSS(5), ...
XSS(6), XSS(7));
fprintf('Te = %g \r\n', TORQ);
fprintf('Delta = %g (deg)   MMF Angle = %g (deg) \r\n', Deltad,MMFANG);
fprintf('Unsat. Field Amps Ifr (P.U.) = %g   Unsat. Field Volts...
Ex (P.U.) = %g \r\n', Ifr, Ex);
PF = abs(PF);
fprintf('Power Factor = %g ', PF);
if MMFANG-Deltad > 90
    fprintf('(Lagging) ');
end
if MMFANG-Deltad < 90
    fprintf('(Leading) ');
end
Phid = MMFANG+Deltad + 90;
fprintf('Power Factor Angle = %g (deg) \r\n', Phid);
% SET UP A1 MATRIX
A1(1,1)=cos(Deltabo);
A1(1,2)=-Vbo*sin(Deltabo);
A1(2,1)=-sin(Deltabo);
A1(2,2)=-Vbo*cos(Deltabo);
A1(5,3)=1;
A1(6,4)=-1;

% SET UP A2 MATRIX
A2(1,1)=Xqs + Xe;
A2(1,3)=Xmq;
A2(2,2)=Xds + Xe;
A2(2,4)=Xmd;
A2(2,5)=Xmd;
A2(3,1)=Xmq;
A2(3,3)=Xqr;

```

```

A2(4,2)=Xmd;
A2(4,4)=Xdr;
A2(4,5)=Xmd;
A2(5,2)=Xmd^2/Rfr;
A2(5,4)=Xmd^2/Rfr;
A2(5,5)=Xmd*Xfr/Rfr;
A2(6,6)=-2*H;
A2(7,7)=Wr;

% SET UP A3 MATRIX
A3(1,1)= Rs + Re;
A3(1,2)= Wr/Wb*(Xds+Xe);
A3(1,4)= Wr/Wb*Xmd;
A3(1,5)= Wr/Wb*Xmd;
A3(1,6)= (XSS(4)+Xe*XSS(2))/Wb;
A3(1,7)= -Vbo*sin(Deltabo);
A3(2,1)=-Wr/Wb*(Xqs+Xe);
A3(2,2)= Rs + Re;
A3(2,3)=-Wr/Wb*Xmq;
A3(2,6)=- (XSS(3)+Xe*XSS(1))/Wb;
A3(2,7)= -Vbo*cos(Deltabo);
A3(3,3)= Rqr;
A3(4,4)= Rdr;
A3(5,5)= Xmd;
Ct = 1;
A3(6,1)=Ct*(XSS(4)-Xqs*XSS(2));
A3(6,2)=-Ct*(XSS(3)-Xds*XSS(1));
A3(6,3)=-Ct*Xmq*XSS(2);
A3(6,4)=Ct*Xmd*XSS(1);
A3(6,5)=Ct*Xmd*XSS(1);
A3(7,6)=-1;

% SOLVE FOR THE A MATRIX
A2INV = inv(A2);
A = zeros(7,7);
for ii=1:7
    for jj=1:7
        for kk=1:7
            A(ii,jj) = A(ii,jj)-Wb*A2INV(ii,kk)*A3(kk,jj);
        end
    end
end

% SOLVE FOR THE B MATRIX
for ii=1:7
    for jj=1:4
        for kk=1:7
            B(ii,jj) = B(ii,jj)+Wb*A2INV(ii,kk)*A1(kk,jj);
        end
    end
end

```

```
    end
end

%Read from file INPUT to determine input and output desired
IB =data_buf(21); ICD=data_buf(22);
fclose(file_input);
% DEFINE 'B' VECTOR
if IB==1
    fprintf('T.F. Input -- DELTA V bus      Units: P.U. Volts')
end
if IB==2
    fprintf('T.F. Input -- DELTA Delta bus     Units: Degrees')
end
if IB==3
    fprintf('T.F. Input -- DELTA Ex      Units: P.U. Volts')
end
if IB==4
    fprintf('T.F. Input -- DELTA Tload     Units: P.U. Torque')
end
if IB<1 || IB>4
    err=1;
    return
end
for ii=1:7
    BB(ii)=B(ii,IB);
    if IB==2
        BB(ii)=180*BB(ii)/pi;
    end
end

% SET UP THE 'C' VECTOR and 'D' SCALAR
D = 0;
if ICD<1 || ICD>8
    err=1;
    return
end
if ICD==1
    fprintf('    T.F. Output -- DELTA Is      Units: P.U. Amperes\r\n')
    C(1)=XSS(1)/Iso;
    C(2)=XSS(2)/Iso;
end
if ICD==2
    fprintf('    T.F. Output -- DELTA Ifr     Units: P.U. Amperes\r\n')
    C(5)=1;
end
if ICD==3
    fprintf('    T.F. Output -- DELTA Air Gap Flux     Units: P.U. ...
Flux Linkage\r\n')
    PSIm=sqrt(XSS(5)^2+XSS(6)^2);
```

```

C(1)=XSS(5)/(PSIm);
C(2)=XSS(6)/(PSIm);
C(3)=XSS(5)/(PSIm);
C(4)=XSS(6)/(PSIm);
C(5)=XSS(6)/(PSIm);

end
if ICD==4
    fprintf('      T.F. Output -- DELTA Te      Units: P.U. Torque\r\n')
    C(1)=A3(6,1);
    C(2)=A3(6,2);
    C(3)=A3(6,3);
    C(4)=A3(6,4);
    C(5)=A3(6,5);
end
if ICD==5
    fprintf('      T.F. Output -- DELTA Wrm      Units: Mechanical ...
Rad/s\r\n')
    C(6)=1/(Poles/2);
end
if ICD==6
    fprintf('      T.F. Output -- DELTA Delta      Units: ...
Degrees\r\n')
    C(7)=180/pi;
end
if ICD==7
    fprintf('      T.F. Output -- DELTA Ids      Units: P.U. ...
Amperes\r\n')
    C(2)=1;
end
if ICD==8
    fprintf('      T.F. Output -- DELTA Vs      Units: P.U. ...
Volts\r\n')
    for ij=1:7
        cqs(ij)=-Xe*A(1,ij)/Wb;
    end
    cqs(1) = cqs(1) - Re;
    cqs(2) = cqs(2) - Wr/Wb*Xe;
    cqs(6) = cqs(6) - Xe*XSS(2);
    cqs(7) = cqs(7) + Vbo*sin(Deltabo);
    for ij = 1:7
        cds(1) = -Xe*A(2,ij)/Wb;
    end
    cds(1) = cds(1) + Wr/Wb*Xe;
    cds(2) = cds(2) - Re;
    cds(6) = cds(6) + Xe*XSS(1);
    cds(7) = cds(7) + Vbo*cos(Deltabo);
    %cwr(6) = 0.01;%Setting cwr(6)=1 introduces speed feedback
    C = Vqso/Vso*cqs + Vdso/Vso*cds - cwr;
    if IB>2

```

```
D = 0;
end
if IB==1
    D = Vqso/Vso*cos(Deltabo)-Vdso/Vso*sin(Deltabo)...
-Vqs/Vso*Xe*BB(1)-Vdso/Vso*Xe*BB(2);
end
if IB==2
    D = -Vqso/Vso*Vbo*sin(Deltabo)-Vdso/Vso*Vbo*cos(Deltabo)...
-Vqso/Vso*Xe*BB(1)-Vdso/Vso*Xe*BB(2);
end
end
[b,a] = ss2tf(A,BB,C',D,1);
SYS = tf(b,a)
figure(1)
bode(SYS)
figure(2)
rlocus(SYS)
figure(3)
T = feedback(SYS,1)
step(T,50)
figure(4)
T = feedback(1,SYS)
step(T,50)
[z,p,k] = ss2zp(A,BB,C',D,1);
SYS2 = zpk(z,p,k)
[residues,poles,kk] = residue(b,a);
residues
poles
z
```


Appendix 5

SMHB—Synchronous Machine Harmonic Balance

% CALCULATION OF SYNCHRONOUS MACHINE QUASI-STEADY-STATE BEHAVIOR

% DURING ASYNCHRONOUS OPERATION.

% ALL PARAMETERS ARE IN PER UNIT. THE FIELD IS ASSUMED TO BE SHORTED.

% T.A.L.

% SOURCE VOLTAGES ARE ENTERED AS HARMONIC COMPONENTS.

% ONLY HARMONICS THAT ARE OF INTEREST NEED BE ENTERED.

% THE HIGHEST HARMONIC THAT CAN BE CALCULATED IS THE 50TH.

% THE ANGLE DELTA IS THE ROTOR Q-AXIS POSITION W.R.T. PHASE A AT T=0.

% IF THE VOLTAGES ARE BALANCED AND COSINUSOIDAL, THEN DELTA IS THE TORQUE ANGLE.

% DELTA .LT. 0 IMPLIES MOTOR OPERATION.

% IMIN AND TMIN ARE TOLERANCES FOR PRINTING THE STATOR CURRENT AND TORQUE.

% COMPONENTS OF CURRENT AND TORQUE .LT. IMIN AND TMIN WILL NOT BE PRINTED.

% IF SOURCE VOLTAGES CONTAIN HARMONICS BUT ARE BALANCED

% ONLY COMPONENTS OF PHASE A NEED BE ENTERED.

% A TYPICAL DATA FILE WHICH MUST BE NAMED smhb_input.txt IS:

% 0.0542 0.07832 0.0993 0.1706	Rs, Xls, Rdr, Xldr
% 0.014 0.163 0.0904 0.1611	Rfr, Xlfr, Rqr, Xlqr
% 2.364 1.383	Xmd, Xmq
% 60. 60.	f base, f fund.
% 2.0 -30	Ex, Delta (+motor, -gen)
% 0.0001 .00001	Imin, Tmin
% 2	Total Number of Harmonics
% 1	Harmonic number
% 1. 0.	Ea mag, Ea phase (Ephase set to zero zero by convention - Delta inputed above)
%	Harmonic number
% 5	Ea mag, Ea phase
% 0.2 -20.	-1 to stop read

% IF SOURCE VOLTAGES ARE UNBALANCED

% A TYPICAL DATA FILE IS:

```
% 0.0542 0.078329 0.0993 0.1706
% 0.014 0.163 0.0904 0.1611
% 2.364 1.383
% 60. 60.
% 2.0 0.0          Delta undefined, input phase angles
%                   separately below
% 0.0001 .00001
% 2                  Total Number of Harmonics
% 1                  Harmonic number
% 0.5 0. 1. -120. 1. 120.    Ea mag, Ea phase, Eb mag, Eb phase, Ec mag, Ec phase
% 7                  Harmonic number
% 0.1 0 0.2 -150 0.0 0.0    Ea mag, Ea phase, Eb mag, Eb phase, Ec mag, Ec phase
% -1                 -1 to stop read
```

clear

```
Vpos = zeros(10,1); Ipos = zeros(10,1); Vneg = zeros(10,1); Ineg = zeros(10,1);
Zpos = zeros(10,10); Zneg = zeros(10,10); klist = zeros(50);
Ivec = zeros(8,50); Psivec = zeros(8,50); Irotor = zeros(12,50);
data_buf = zeros(1000);
```

%Read Motor Parameters

```
file_input = fopen('smhb_input2.txt','r');
data_buf = fscanf(file_input, "%g", [1,1000]);
data_buf = data_buf';
fprintf('Parameter Values in Per Unit\r\n')
fprintf('Rs = %g   Xls = %g \r\n',data_buf(1:2));
fprintf('Rdr = %g   Xldr = %g \r\n',data_buf(3:4));
fprintf('Rfr = %g   Xlfr = %g \r\n',data_buf(5:6));
fprintf('Rqr = %g   Xlqr = %g \r\n',data_buf(7:8));
fprintf('Xmd = %g   Xmq = %g \r\n',data_buf(9:10));
fprintf('f_base = %g   f_e = %g \r\n',data_buf(11:12));
fprintf('Delta = %g degrees  Ex = %g\r\n',data_buf(14),data_buf(13));
Rs = data_buf(1); Xls = data_buf(2); Rdr = data_buf(3); Xldr = data_buf(4);
Rfr = data_buf(5); Xlfr = data_buf(6); Rqr = data_buf(7); Xlqr = data_buf(8);
Xmd = data_buf(9); Xmq = data_buf(10);
Fb = data_buf(11); Fe = data_buf(12);
Ex = data_buf(13); Delta = data_buf(14);
Imin = data_buf(15); Tmin = data_buf(16);
```

% DEFINE REMAINING PARAMETERS

```
Deltar = Delta*180/pi;
Wb = 2*pi*Fb;
We = 2*pi*Fe;
Wr = We;
```

```

Wrpu = Wr/We; %Operation with rotor at synchronous speed of fund. assumed
Xds = Xls+Xmd;
Xqs = Xls+Xmq;
Xdr = Xldr+Xmd;
Xqr = Xlqr+Xmd;
Xfr = Xlfr+Xmd;
sqrt3 = sqrt(3.);
pi = 4.*atan(1.);
ans = input('Balanced Source Voltages Assumed? (Type yes or not)---','s');
if ans=='yes'
    ioption = 1;
end
if ans=='not'
    ioption = 0;
end
ktotal = data_buf(17);
for main = 1:ktotal
    k = data_buf(17+3*main-2);
    klist(k) = 1;
    if main == ktotal
        kmax = k;
    end
% Read in Source Voltage Components for Harmonic k
if ioption==1 %Balanced Voltages
    k = data_buf(17+3*main-2);
    Eamag = data_buf(17+3*main-1); Thetaa = data_buf(17+3*main)+Deltar;
    Ebmag = Eamag;
    Ecmag = Eamag;
    Thetab = Thetaa - k*120;
    Thetac = Thetaa + k*120;
end
if ioption~=1 %Unbalanced Voltages
    k = data_buf(17+7*main-6);
    Eamag = data_buf(17+7*main-5); Thetaa = data_buf(17+7*main-4);
    Ebmag = data_buf(17+7*main-3); Thetab = data_buf(17+7*main-2);
    Ecmag = data_buf(17+7*main-1); Thetac = data_buf(17+7*main);
end
Eaalpha = Eamag*cos(Thetaa*pi/180);
Eagamma = -Eamag*sin(Thetaa*pi/180);
Ebalpha = Ebmag*cos(Thetab*pi/180);
Ebgamma = -Ebmag*sin(Thetab*pi/180);
Ecalpha = Ecmag*cos(Thetac*pi/180);
Ecgamma = -Ecma
%Solve for Vq and Vd Components
Vqalpha = 2/3*Eaalpha-1/3*Ebalpha-1/3*Ecalpha;

```

```
Vqgamma = 2/3*Eagamma-1/3*Ebgamma-1/3*Ecgamma;
Vdalpa = 1/sqrt3*(Ecalpha - Ebalpha);
Vdgamma = 1/sqrt3*(Ecgamma - Ebgamma);
```

```
%Define Vpos and Vneg Voltage Vectors;
```

```
Vpos = zeros(10,1);
```

```
Vneg = zeros(10,1);
```

```
Vpos(1) = 0.5*(Vqalpha-Vdgamma);
```

```
Vpos(2) = 0.5*(Vqgamma+Vdalpa);
```

```
Vpos(3) = 0.5*(Vqgamma+Vdalpa);
```

```
Vpos(4) = -0.5*(Vqalpha-Vdgamma);
```

```
if k==1
```

```
    Vpos(9) = Rfr*Ex/Xmd;
```

```
end
```

```
Vneg(1) = 0.5*(Vqalpha+Vdgamma);
```

```
Vneg(2) = 0.5*(Vqgamma-Vdalpa);
```

```
Vneg(3) = -0.5*(Vqgamma-Vdalpa);
```

```
Vneg(4) = 0.5*(Vqalpha+Vdgamma);
```

```
%Set Up Zpos and Zneg Matrices
```

```
%First Pass Sets Up Zneg; Second Pass Sets Up Zpos
```

```
for loop = 1:2
```

```
    if loop==1
```

```
        seq = -1;
```

```
    end
```

```
    if loop==2
```

```
        seq = 1;
```

```
    end
```

```
Zpos(1,1) = Rs;
```

```
Zpos(1,2) = (k*We-seq*Wr)/Wb*Xqs;
```

```
Zpos(1,3) = Wr/Wb*Xds;
```

```
Zpos(1,6) = (k*We-seq*Wr)/Wb*Xmq;
```

```
Zpos(1,7) = Wr/Wb*Xmd;
```

```
Zpos(1,9) = Wr/Wb*Xmd;
```

```
Zpos(2,1) = -(k*We-seq*Wr)/Wb*Xqs;
```

```
Zpos(2,2) = Rs;
```

```
Zpos(2,4) = Wr/Wb*Xds;
```

```
Zpos(2,5) = -(k*We-seq*Wr)/Wb*Xmq;
```

```
Zpos(2,8) = Wr/Wb*Xmd;
```

```
Zpos(2,10) = Wr/Wb*Xmd;
```

```
Zpos(3,1) = -Wr/Wb*Xqs;
```

```
Zpos(3,3) = Rs;
```

```
Zpos(3,4) = (k*We-seq*Wr)/Wb*Xds;
```

```
Zpos(3,5) = - Wr/Wb*Xmq;
```

```
Zpos(3,8) = (k*We-seq*Wr)/Wb*Xmd;
```

```

Zpos(3,10) = (k*We-seq*Wr)/Wb*Xmd;
Zpos(4,2) = -Wr/Wb*Xqs;
Zpos(4,3) = -(k*We-seq*Wr)/Wb*Xds;
Zpos(4,4) = Rs;
Zpos(4,6) = -Wr/Wb*Xmq;
Zpos(4,7) = -(k*We-seq*Wr)/Wb*Xmd;
Zpos(4,9) = -(k*We-seq*Wr)/Wb*Xmd;
Zpos(5,2) = (k*We-seq*Wr)/Wb*Xmq;
Zpos(5,5) = Rqr;
Zpos(5,6) = (k*We-seq*Wr)/Wb*Xqr;
Zpos(6,1) = -(k*We-seq*Wr)/Wb*Xmq;
Zpos(6,5) = -(k*We-seq*Wr)/Wb*Xqr;
Zpos(6,6) = Rqr;
Zpos(7,4) = (k*We-seq*Wr)/Wb*Xmd;
Zpos(7,7) = Rdr;
Zpos(7,8) = (k*We-seq*Wr)/Wb*Xdr;
Zpos(7,10) = (k*We-seq*Wr)/Wb*Xmd;
Zpos(8,3) = -(k*We-seq*Wr)/Wb*Xmd;
Zpos(8,7) = -(k*We-seq*Wr)/Wb*Xdr;
Zpos(8,8) = Rdr;
Zpos(8,9) = -(k*We-seq*Wr)/Wb*Xmd;
Zpos(9,4) = (k*We-seq*Wr)/Wb*Xmd;
Zpos(9,9) = Rfr;
Zpos(9,8) = (k*We-seq*Wr)/Wb*Xmd;
Zpos(9,10) = (k*We-seq*Wr)/Wb*Xfr;
Zpos(10,3) = -(k*We-seq*Wr)/Wb*Xmd;
Zpos(10,7) = -(k*We-seq*Wr)/Wb*Xmd;
Zpos(10,9) = -(k*We-seq*Wr)/Wb*Xfr;
Zpos(10,10) = Rfr;
if loop==1
    Zneg = Zpos;
end
end
%Solve for Ipos and Ineg Vectors
%if k==1
%Vpos = [Vqalpha 0 Vdalpha 0 0 0 0 Ex 0]';
%end
Ipos = inv(Zpos)*Vpos;
Ineg = inv(Zneg)*Vneg;

% Calculate D-Q Stator Currents in the Stationary Frame
if k==1
    Iqalpha1 = Ipos(1) + Ineg(1) + Ineg(4);
    Iqgamma1 = Ipos(3) + Ineg(2) - Ineg(3);
    Idalpha1 = Ipos(3) - Ineg(2) + Ineg(3);
    Idgamma1 = -Ipos(1) + Ineg(1) + Ineg(4);

```

```

Iqalpha2 = 0;
Iqgamma2 = 0;
Idalpha2 = 0;
Idgamma2 = 0;
else
Iqalpha1 = 0.5*(Ipos(1)+Ineg(1)-Ipos(4)+Ineg(4));
Iqgamma1 = 0.5*(Ipos(2)+Ineg(2)+Ipos(3)-Ineg(3));
Idalpha1 = 0.5*(Ipos(2)-Ineg(2)+Ipos(3)+Ineg(3));
Idgamma1 = 0.5*(-Ipos(1)+Ineg(1)+Ipos(4)+Ineg(4));
Iqalpha2 = 0.5*(Ipos(1)+Ipos(4));
Iqgamma2 = 0.5*(Ipos(2)-Ipos(3));
Idalpha2 = 0.5*(-Ipos(2)+Ipos(3));
Idgamma2 = 0.5*(Ipos(1)+Ipos(4));
end
Iqalpha3 = 0.5*(Ineg(1)-Ineg(4));
Iqgamma3 = 0.5*(Ineg(2)+Ineg(3));
Idalpha3 = 0.5*(Ineg(2)+Ineg(3));
Idgamma3 = 0.5*(-Ineg(1)+Ineg(4));

```

% Calculate the A-B-C Currents in the Stationary Frame

```

Iaalpha1 = Iqalpha1;
Ibalpha1 = -0.5*Iqalpha1-sqrt3/2*Idalpha1;
Icalpha1 = -0.5*Iqalpha1+sqrt3/2*Idalpha1;
Iagamma1 = Iqgamma1;
Ibgamma1 = -0.5*Iqgamma1-sqrt3/2*Idgamma1;
Icgamma1 = -0.5*Iqgamma1+sqrt3/2*Idgamma1;
Iaalpha2 = Iqalpha2;
Ibalpha2 = -0.5*Iqalpha2-sqrt3/2*Idalpha2;
Icalpha2 = -0.5*Iqalpha2+sqrt3/2*Idalpha2;
Iagamma2 = Iqgamma2;
Ibgamma2 = -0.5*Iqgamma2-sqrt3/2*Idgamma2;
Icgamma2 = -0.5*Iqgamma2+sqrt3/2*Idgamma2;
Iaalpha3 = Iqalpha3;
Ibalpha3 = -0.5*Iqalpha3-sqrt3/2*Idalpha3;
Icalpha3 = -0.5*Iqalpha3+sqrt3/2*Idalpha3;
Iagamma3 = Iqgamma3;
Ibgamma3 = -0.5*Iqgamma3-sqrt3/2*Idgamma3;
Icgamma3 = -0.5*Iqgamma3+sqrt3/2*Idgamma3;

```

% Calculate the Amplitudes of Stator Currents

```

Iamax1 = sqrt(Iaalpha1^2+Iagamma1^2);
Ibmax1 = sqrt(Ibalpha1^2+Ibgamma1^2);
Icmax1 = sqrt(Icalpha1^2+Icgamma1^2);
Iamax2 = sqrt(Iaalpha2^2+Iagamma2^2);
Ibmax2 = sqrt(Ibalpha2^2+Ibgamma2^2);
Icmax2 = sqrt(Icalpha2^2+Icgamma2^2);

```

```

Iamax3 = sqrt(Ialpha3^2+Igamma3^2);
Ibmax3 = sqrt(Ialpha3^2+Ibeta3^2);
Icmax3 = sqrt(Ialpha3^2+Igamma3^2);
Iphase1 = 180.*atan2(-Igamma1,Ialpha1)/pi;
Ibphase1 = 180.*atan2(-Ibeta1,Ialpha1)/pi;
Icphase1 = 180.*atan2(-Igamma1,Ialpha1)/pi;
Iphase2 = 180.*atan2(-Igamma2,Ialpha2)/pi;
Ibphase2 = 180.*atan2(-Ibeta2,Ialpha2)/pi;
Icphase2 = 180.*atan2(-Igamma2,Ialpha2)/pi;
Iphase3 = 180.*atan2(-Igamma3,Ialpha3)/pi;
Ibphase3 = 180.*atan2(-Ibeta3,Ialpha3)/pi;
Icphase3 = 180.*atan2(-Igamma3,Ialpha3)/pi;

if k==1
fprintf(' Ias = %g Ibs = %g Ics = %g\r\n')
end

if Iamax1>Imin|Ibmax1>Imin|Icmax1>Imin
    fprintf('%g*cos(%g*w*t+%g) %g*cos(%g*w*t+%g)
%g*cos(%g*w*t+%g) \r\n', Iamax1,k,Iphase1,Ibmax1,k,Ibphase1,Icmax1,k,Icphase1);
end

if Iamax2>Imin|Ibmax2>Imin|Icmax2>Imin
    fprintf('+%g*cos(%g*(w-2wr)*t+%g) +%g*cos(%g*(w-2wr)*t+%g) +%g*cos(%g*(w-
2wr)*t+%g) \r\n', Iamax2,k,Iphase2,Ibmax2,k,Ibphase2,Icmax2,k,Icphase2);
end

if Iamax3>Imin|Ibmax3>Imin|Icmax3>Imin
    fprintf('+%g*cos(%g*(w+2wr)*t+%g) +%g*cos(%g*(w+2wr)*t+%g)
+%g*cos(%g*(w+2wr)*t+%g) \r\n', Iamax3,k,Iphase3,Ibmax3,k,Ibphase3,Icmax3,k,Icphase3);
end

% Store Stator Currents and Fluxes for Torque Calculation
for i=1:4
    Ivec(i,k) = Ipos(i);
    Ivec(i+4,k) = Ineg(i);
end

for i = 1:2
    Psivec(i,k) = Xmq*(Ipos(i)+Ipos(i+4));
    Psivec(i+2,k) = Xmd*(Ipos(i+2)+Ipos(i+6)+Ipos(i+8));
    Psivec(i+4,k) = Xmq*(Ineg(i)+Ineg(i+4));
    Psivec(i+6,k) = Xmd*(Ineg(i+2)+Ineg(i+6)+Ineg(i+8));
end

% Store Rotor Current for Later Printout
for i=1:6
    Irotor(i,k) = Ipos(i+4);
    Irotor(i+6,k) = Ineg(i+4);

```

```

end
end %main loop
fprintf(' \r\n')
ans = input('Print Out Rotor Currents? (Type yes or not)---''s');
if ans=='yes'
    ioption1 = 1;
end
if ans~='yes'
    ioption1 = 0;
end
if ioption1==1
fprintf('Stator Har. Iqr =           Idr =           Ifr =   \r\n')
for ii=1:kmax
    if ii==1|ii==4|ii==7|ii==10|ii==13|ii==16|ii==19|ii==22|ii==25
        kr = ii-1;
    end
    if ii==2|ii==5|ii==8|ii==11|ii==14|ii==17|ii==20|ii==23|ii==26
        kr = ii+1;
    end
    if ii==3|ii==6|ii==9|ii==12|ii==15|ii==18|ii==21|ii==24|ii==27
        kr = ii;
    end
    Iqrmax = sqrt((Irotor(1,ii)+Irotor(7,ii))^2+(Irotor(2,ii)+Irotor(8,ii))^2);
    Idrmax = sqrt((Irotor(3,ii)+Irotor(9,ii))^2+(Irotor(4,ii)+Irotor(10,ii))^2);
    Ifrmax = sqrt((Irotor(5,ii)+Irotor(11,ii))^2+(Irotor(6,ii)+Irotor(12,ii))^2);
    Iqrphase = 180.*atan2(-(Irotor(2,ii)+Irotor(8,ii)),(Irotor(1,ii)+Irotor(7,ii)))/pi;
    Idrphase = 180.*atan2(-(Irotor(4,ii)+Irotor(10,ii)),(Irotor(3,ii)+Irotor(9,ii)))/pi;
    Ifrphase = 180.*atan2(-(Irotor(6,ii)+Irotor(12,ii)),(Irotor(5,ii)+Irotor(11,ii)))/pi;
    if Iqrmax>Imin|Idrmax>Imin|Ifrmax>Imin
        fprintf(' %g ',ii)
        fprintf(' %g*cos((%g*we)*t+%g)   %g*cos((%g*we)*t+%g)   %g*cos((%g*we)*t+%g)\r\n',...
        Iqrmax,kr,Iqrphase,Idrmax,kr,Idrphase,Ifrmax,kr,Ifrphase);
    end
end
fprintf(' \r\n');
fprintf('Instantaneous Torque \r\n');
fprintf(' \r\n');
Teave = 0;
Istop = 0;
for k=1:kmax
    for l = 1:kmax
% Set Up C Matrix for Torque Prop. to cos((k-l)we*t)
        C = zeros(8,8);
        C(1,3) = 1.;
        C(2,4) = 1.;


```

```
C(5,7) = 1.;  
C(6,8) = 1.;  
C = asym(C);  
Te1cos = Tcalc(C,Ivec,Psivec,k,l);  
if k-l==0  
    Teave = Teave + Te1cos;  
end  
% Set Up C Matrix for Torque Prop. to sin((k-l)we*t)  
C = zeros(8,8);  
C(1,4) = -1;  
C(2,3) = 1.;  
C(3,2) = 1.;  
C(4,1) = -1;  
C(5,8) = -1;  
C(6,7) = 1;  
C(7,6) = 1.;  
C(8,5) = -1;  
Te1sin = Tcalc(C,Ivec,Psivec,k,l);  
% Set Up C Matrix for Torque Prop. to cos((k+l)we*t)  
C = zeros(8,8);  
C(1,7) = 1.;  
C(2,8) = -1;  
C(3,5) = -1;  
C(4,6) = 1.;  
C = asym(C);  
Te2cos = Tcalc(C,Ivec,Psivec,k,l);  
if k+l==0  
    Teave = Teave + Te2cos;  
end  
% Set Up C Matrix for Torque Prop. to sin((k+l)we*t)  
C = zeros(8,8);  
C(1,8) = 1;  
C(2,7) = 1.;  
C(3,6) = -1;  
C(4,5) = -1;  
C = asym(C);  
Te2sin = Tcalc(C,Ivec,Psivec,k,l);  
% Set Up C Matrix for Torque Prop. to cos(((k+l)We-2wr)*t)  
C = zeros(8,8);  
C(1,3) = 1.;  
C(2,4) = -1.;  
C = asym(C);  
Te3cos = Tcalc(C,Ivec,Psivec,k,l);  
if k+l-2*Wrpu==0  
    Teave = Teave + Te3cos;  
end
```

```

% Set Up C Matrix for Torque Prop. to sin(((k+l)we-2wr)*t)
C = zeros(8,8);
C(1,4) = 1.;
C(2,3) = 1.;
C = asym(C);
Te3sin = Tcalc(C,Ivec,Psivec,k,l);

% Set Up C Matrix for Torque Prop. to cos(((k+l)we+2wr)*t)
C = zeros(8,8);
C(5,7) = 1;
C(6,8) = -1;
C = asym(C);
Te4cos = Tcalc(C,Ivec,Psivec,k,l);
if k+l+2*Wrpu==0
    Teave = Teave + Te4cos;
end

% Set Up C Matrix for Torque Prop. to sin(((k+l)we+2wr)*t)
C = zeros(8,8);
C(5,8) = 1.;
C(6,7) = 1.;
C = asym(C);
Te4sin = Tcalc(C,Ivec,Psivec,k,l);

% Set Up C Matrix for Torque Prop. to cos(((k-l)we-2wr)*t)
C = zeros(8,8);
C(1,7) = 1.;
C(2,8) = 1.;
C(3,5) = -1.;
C(4,6) = -1.;
Te5cos = Tcalc(C,Ivec,Psivec,k,l);
if k-l-2*Wrpu==0
    Teave = Teave + Te5cos;
end

% Set Up C Matrix for Torque Prop. to sin(((k-l)we-2wr)*t)
C = zeros(8,8);
C(1,8) = -1;
C(2,7) = 1.;
C(3,6) = 1.;
C(4,5) = -1.;
Te5sin = Tcalc(C,Ivec,Psivec,k,l);

% Set Up C Matrix for Torque Prop. to cos(((k-l)we+2wr)*t)
C = zeros(8,8);
C(5,3) = 1.;
C(6,4) = 1.;
C(7,1) = -1;
C(8,2) = -1;
Te6cos = Tcalc(C,Ivec,Psivec,k,l);
if k-l+2*Wrpu==0

```

```

Teave = Teave + Te6cos;
end
% Set Up C Matrix for Torque Prop. to sin(((k-l)we+2wr)*t)
C = zeros(8,8);
C(5,4) = -1;
C(6,3) = 1.;
C(7,2) = 1.;
C(8,1) = -1;
Te6sin = Tcalc(C,Ivec,Psivec,k,l);
Te1 = sqrt(Te1sin^2+Te1cos^2);
Te2 = sqrt(Te2sin^2+Te2cos^2);
Te3 = sqrt(Te3sin^2+Te3cos^2);
Te4 = sqrt(Te4sin^2+Te4cos^2);
Te5 = sqrt(Te5sin^2+Te5cos^2);
Te6 = sqrt(Te6sin^2+Te6cos^2);
if abs(Teave)>Tmin&Istop==0
    fprintf('Te = %g\n',Teave);
    Istop = 1;
end
if Te1>Tmin&k-l~=0
    fprintf('+ %g*cos((%gwe)*t) + %g*sin((%gwe)*t)\n',Te1cos,k-l,Te1sin,k-l);
end
if Te2>Tmin&k+l~=0
    fprintf('+ %g*cos((%gwe)*t) + %g*sin((%gwe)*t)\n',Te2cos,k+l,Te2sin,k+l);
end
if Te3>Tmin&k+l-2*Wrpu~=0
    fprintf('+ %g*cos((%gwe-2wr)*t) + %g*sin((%gwe-2wr)*t)\n',Te3cos,k+l,Te3sin,k+l);
end
if Te4>Tmin&k+l+2*Wrpu~=0
    fprintf('+ %g*cos((%gwe+2wr)*t) + %g*sin((%gwe+2wr)*t)\n',Te4cos,k+l,Te4sin,k+l);
end
if Te5>Tmin&k-l-2*Wrpu~=0
    fprintf('+ %g*cos((%gwe-2wr)*t) + %g*sin((%gwe-2wr)*t)\n',Te5cos,k-l,Te5sin,k-l);
end
if Te6>Tmin&k-l+2*Wrpu~=0
    fprintf('+ %g*cos((%gwe+2wr)*t) + %g*sin((%gwe+2wr)*t)\n',Te6cos,k-l,Te6sin,k-l);
end
end
end
end

```


A

- AC machine equations, 78
Accelerating torque, 327, 331
Air gap flux saturation, 520, 525–527
Air gap line, 227
Air gaps, 5, 25, 64, 229, 244, 358, 501
Ampere's Law, 3, 66
Amplidynes, 349, 357, 366
Arbitrary reference frame, 88, 107
Armature flux, 228
Armature reaction flux, 233, 244
Armature resistance, 229
Armature terminals, 228
Armature windings, 137

B

- Base quantities, 182
Belt harmonics, 145
Belt leakage, 67
Bode plots, 488

C

- C circuits
general case of windings, 49–53
sinusoidal winding distribution, 50
- Capability curves, 252
- Classical regulator, 490, 492, 494–495
- Commutation lead angle beta, 396
- Commutation overlap angle mu, 396
- Commutation safety margin angle, 396
- Compounding curves, 248
- Computer simulation of synchronous machines. See Simulation of synchronous machines
- Concentrated windings, 10
cosine components, 20
full pitch, 15
harmonic components of, 13, 14, 20
mutual inductances of, 29
- Consequent pole winding, 72

- Continuously acting regulators, 349
Crossover frequency, 488
Current source inverter, 396

D

- D axis amortisseur winding function, 148–154
- D axis synchronous reactance, 229
- D-q axis orientation, 194–196, 200
- D-q-n reference frame
cylindrical three-phase inductor, in, 131–134
matrix approach to, 112, 114–117, 118–121
power flow in, 95–96, 111
rotating, 161
simple three-phase cylindrical inductor, applied to, 121–125
stationary three-phase r-L circuits in, 96–104
stator magnetizing inductances in, 160–164
system equations in, 92–95
winding functions in, 125–131, 146–148
- D-q-n stator windings, 165
- Damper windings, 267–268, 269–270, 270, 282–284, 286–288
- Damping torque, 378
- Damping torque coefficient, 376, 378
- DC excitor, 353–357
- Demagnetizing armature reaction, 210
- Differential leakage, 67, 139
- Direct axis, 164, 308
- Doherty's Law, 266, 312. See also Flux linkages
- Doherty, Robert E., 265
- Double-layer windings, 71, 73–74
- Doubly cylindrical machine, 2
air gap of, 25
flux linking coils of, 26, 27, 28

- inductances, 25–29
winding of, 25
- Dynamic stability, 349
excitation systems; see Excitation systems
system damping, importance of, 352
- E**
- Effective gap, 5
- Eigen-value-eigenvector techniques, 298
- Electromagnetic torque, 185–186, 275, 380, 426, 453–455, 456–462
- End-winding leakage, 64–65
- Equal area criterion, 322–323
- Equivalent circuits, 217–221
- Excitation systems
AC systems, 362–363
basic, 353
closed-loop representation, 386–390
DC excitor, basic, 353–357
design principles, 369–374
dynamic stability, effect on, 374–379, 380–386
IEEE type 1 systems, 364–368
static systems, 363–364
- Excitor field voltage, 295–296
- F**
- Field circuit winding functions, 159–160
- Field flux, 228, 374, 380, 384
- Field saturation, 520, 529–531
- Field winding circuits, 159
- Field windings, 137
- Flux linkages, 497–498
constant, theorem of, 265–266
equations, 123, 124, 125, 142, 172–177, 184–185, 255
rotor, 268
short-circuit from loaded condition, stator resistance and dampers neglected, 272–275
- short-circuit of a loaded generator, dampers included, 290–291
short-circuit, behavior on, 266–267
three-phase short-circuit with no damper circuits, on, 267–268
three-phase short-circuit with resistances and damper windings neglected, 269–270
three-phase short-circuit, effect of resistances included, no dampers, 275–282
- Flux linking coils, 26, 27, 28
- Flux plot, 57, 58
- Flux tube, 57
- Fortescue's zero sequence, 91, 92
- Fractional pitch windings. See Short pitch windings
- Fractional slotting, 73, 74
- Full pitch windings, 8–10, 15
- G**
- Gap leakage, 64, 65–66
- Gap, air. See Air gaps
- Gauss' Law, 55
- General Electric ALTERREX excitation system, 362, 366
- General Electric ALTHY-REX excitation system, 362
- Generator leakage reactance, 245
- Generator response to system disturbance, 350–352
- H**
- Harmonic elimination, 14, 15
- Harmonic leakage, 67
- Harmonic voltages, 462
- Harmonic winding factor, 20
- Hybrid flux linkages, 180–181
- I**
- Inductance matrix, 129, 130

Inductances, machine, 8. See also Winding inductances

Internal torque angle, 210

Inverse gap function, 63, 161, 164

Inverter current source, 394

Inverter operation, 397–398

L

Laplace variables, 276

Laplace's equation, 1

LCI. See Load commutated inverter (LCI)
synchronous motor drives

Leakage inductances

belt leakage, 67

d-q-n reference frames, in, 126

differential leakage, 67, 68–69

end-winding leakage, 64–65

gap leakage, 64

harmonic leakage, 67

slot leakage, 69

synchronous machine stators, in, 64–69

tooth-top leakage, 69

zig-zag leakage, 67, 69

Leakage reactance, 247

Linearization of synchronous machine

equations

measurement equations, 479–480, 482–483, 485

overview, 467

process of, 469–474

state space equations, 479–480, 482–483, 485

transfer functions of synchronous machines; see Transfer functions of synchronous machines

Load commutated inverter (LCI)

synchronous motor drives

basic system, 395–396

commutation mode 1 state equation, 414–417

commutation mode 2 state equation, 417–421

constant power mode, 426

constant torque mode, 426

converter operations, 411–412

firing angle controller, 406–408

initial conditions, calculation of, 421–424

inverter operation, 397–398, 401–405

phasor diagram of, 399–401, 434–435

power expressions, 405–406

speed performance, 430

starting considerations, 408

state equations, general, 413–414

state space approach to, 434–435

steady-state analysis of, 408–411

steady-state performance curves, 432–434

time step solution, 424–425

torque expressions, 405–406

Load commutation, 396, 408

M

Magnetic axis, 8

Magnetizing armature reaction, 210

Magnetizing inductance, 131–132

MathCAD, 223

MATLAB, 223, 479, 483, 497, 500–501, 503, 536. See also Simulation of synchronous machines

Mechanical acceleration, per unit, 320–322

Modal analysis

conventional methods, versus, 306, 308–310

description, 297

overview, 297–298

stator voltages, of, 301–302

transient solutions utilizing, 298–306

unbalanced external impedances, of, 298–299

Motional equations, 186–187

Motor excitation voltage, 242–243

N

Neutral axis, 8, 92

Non-continuously acting regulators, 349

Non-sinusoidal stator voltages, 446–448, 449, 450

O

Open-circuit characteristics, 226–228, 229, 244, 245

Open-circuit subtransient, 289

Open-circuit test, 247

Open-circuit transient, 289

Open-circuit voltage, 227

Oscillogram, 248

Overexcited condition, 204

Overexcited generator, 206

Overexcited motor, 205

P

Park's equations, 77, 171–172, 188, 194, 267, 275. See also specific equations

excitor field voltages, 295

MATLAB simulation equations, 500–501, 503

physical units, in, 467–469

reference frame rotating, for, 443–445

simulation equations, 497–500

stator voltages, 301–302

steady-state form of, 196–200, 216–217

vector descriptions of, 211–212

Peak reluctance torque, 220

Phasor equations, 220–223

Poisson's equation, 1

Positive damping, 351

Potier reactance, 343

Potier triangles, 241–247

Power equations, 178–179, 187

steady-state, 202–203

vector interpretation of, 210–214

Power factor curves, 252

Power input to machines, 168–169

Proportional plus integrator control, 488

Q

Q axis amortisseur circuit winding function, 155–157, 159, 166

Quadrature axis, 92, 257, 308, 374

form factors, 164

magnetizing inductance, 160–164, 176, 237

R

r-L circuits, vector approach to, 81–84

Reaction torque, 201

Reactive power, steady-state. See Steady-state reactive power

Reference frame theory

arbitrary reference frame, 88, 107

d-q-n reference frame; see D-q-n reference frame

freely floating reference frame, 88

overview, 77, 78

r-L circuits, vector approach to, 81–84

rotating reference frames, 78–81, 89, 143–144, 442, 443–445

speed of reference frames, 111

stationary reference frames, 109, 111

transformation equations; see

transformation equations

unbalanced voltages, in, 104, 106–111

Reluctance torque, 201

Rotating stator flux, 193

Rotor flux linkage, d-q transformation of, 167–168

Rotor reference frame, 163

Rotor-stator mutual inductance. See Stator-rotor mutual inductance

Round-rotor machines, 69

phasor diagram for a saturated machine,

237, 239–240

S

- Saliency torque, 199, 201–202
Salient-pole machines, 202, 413
 interpole leakage, 69–70
 leakage components, 69
 saturated, phasor diagrams for, 240–241
 slot leakage, 69
 stator windings in, 138
 symmetric winding distribution, 54, 56
 tooth-top leakage, 69
 winding function modifications for, 53–64
 zig-zag leakage, 69
Saturation effects, 520
Saturation modeling
 DC excitor, 357–362
 synchronous machines under load, 233–237
Self-controlled synchronous machines, 396
Short-circuits, unsymmetrical. See
 Unsymmetrical short-circuits
Short pitch windings, 12, 16–17
Short-circuit armature, 289
Short-circuit characteristics, 226, 228–229, 230–231
Short-circuit load loss, 232
Short-circuit ratio, 230–231
Short-circuit subtransient, 289
Short-circuit test, 247
Short-circuit transient, 289
Shorted coil, 46–49
Simulation of synchronous machines. See
 also MATLAB
 air gap saturation, 525–527
 approximate models of, 531–536, 540–543
 equations of transformation, 507–509, 511–517
 field saturation, 529–531
 MATLAB SIMULINK, 500–501, 503, 517, 536
 overview, 497
 Park's equations, 497–500
 saturation effects, 520
 simulation case study, 519–520
 steady-state check of simulation, 503–504, 506–507
 SIMULINK, 109, 501, 517, 536
Single-layer windings, 71, 75
Sinusoidal voltage, 30
Slip frequency, 256, 378–379
Slip test, 248
Slot leakage, 69
Small signal equations, 467. See also
 linearization of synchronous machine
 equations
Source voltage formulation, 439–443
Spatial field distribution, 7
Spatial harmonics, 145
State transition matrix, 421–422
Static networks, 98–99
Stationary reference frame, 87, 109, 111
Stator flux linkages, 144–146, 318–319
Stator magnetizing inductances, 160–164
Stator phase voltages, 301–302
Stator resistance, 220, 256, 257, 318, 340
Stator voltages, 255
Stator-rotor mutual inductance, 164–167, 169
Steady-state equations
 equivalent circuit, 215
 graphical interpretations of, 204–207
 MATHCAD, solutions using, 223–225
 Park's equations; see Park's equations
 phasor form of, 216–217, 318
 power equations, 200, 202–203
 torque, 200–202
 vector diagrams, 207–210
Steady-state operating characteristics, 250–252
Steady-state reactive power, 204

- Steady-state stability, 351
 Steady-state synchronous operations, 256
 Subtransient component, 284, 286, 289
 Swing curve, 336
 Swing equation, 376
 Synchronism test, 248
 Synchronizing torque, 327, 378
 Synchronous generators, 250–252
 Synchronous machines
 base quantities for equations, 182–183
 computer simulation of; see Simulation of synchronous machines
 defining, 137
 electrical equivalent circuit for, 189
 flux linkage equations; see Flux linkages
 inductance calculations, 138–139
 leakage inductances in stator, 64–69
 overview, 137–138
 pulsating and average torque during startup of motors, 253–257, 259–261
 rotor configurations, 137–138, 139, 140
 saturation modeling of, 233–237
 self-controlled; see Self-controlled synchronous machines
 transfer function inputs; see Transfer functions of synchronous machines
 voltage equations; see Voltage equations
 Synchronous reactance, 218
 Synchronous speed, 194
 Synchronous torque, 201
 System damping, 352. See also Dynamic stability
 System disturbances, generator response to, 350–352
- T**
- Tapered gap, 164
 Terminal voltage, 245, 390–392
 Terminal voltage controller, 485–490
 Theorem of Constant Flux Linkages. See under Flux linkages
- Thyristors, 362, 401, 406, 426
 Tooth-top leakage, 69
 Torque
 accelerating, 327, 331
 angle curve, 316
 capability curves, 427–431
 damping; see Damping torque
 electromagnetic, 185–186, 222, 275, 380, 426, 453–455, 456–462
 equations, 169–171, 177
 instantaneous, 259
 pulsating, 259
 pulsating amplitude, 260
 steady-state, 200–202
 synchronizing torque; see Synchronizing torque
 vector interpretation of, 210–214
- Torque angle curves, 318–320
 TranfunSMPu, 479
 Transfer functions of synchronous machines
 inputs, 474–475
 outputs, 475–477
 overview, 474
- Transformation equations. See also reference frame theory
 excitation vectors, 89
 Fortescue's zero sequence, 91, 92
 plane of rotation, 88
 power flow in the d-q-n equivalent circuits, 95–96
 system equations in the d-q-n coordinate system, 92–95
 unit vectors, 85, 86, 87–88
- Transient component, 284, 286, 288
 Transient reactance, 269
 Transient resistance, 327
 Transient stability
 analysis of, 323–329, 333–336, 338
 assumptions regarding, 315, 316–317

- double line to ground fault, impact of, 338
 equal area criterion, 322–323
 line to ground fault, impact of, 338
 line to line fault, impact of, 338
 machine modeling, including saturation, 342–347
 mechanical acceleration, per unit, 320–322
 multi-machines, of, 333–336, 338
 overview, 315
 saturation issues, 340–342
 synchronous machine transients, step-by-step method for calculating, 347–348
 three-phase fault, impact of, 338, 339
 two-machine system, of, 331–333
- Turns function, 3
 doubly cylindrical machines, in, 27
 multiple circuit configurations, 39
 multipole configurations, 22–23
 salient-pole machines, 59
- Two-pole stator-rotor, 53
- U**
- Uniform air gap, 53
 Unit matrix, 119
 Unsymmetrical short-circuits, 310–312
- V**
- V curves, 250
 Vector amplitude, 90
 Vector diagrams
 field voltages, 295
 overexcited generator, 206
 overexcited motor, 196, 205
 steady-state, 207–210
 transients, for, 289
 voltage changes, sudden, 291–295
- Voltage behind quadrature axis resistance, 222
 Voltage behind synchronous reactance, 218
 Voltage behind transient reactance, 269, 323–324, 349
 Voltage equations, 140–141, 176–177, 184
 transformation of stator voltage equations to rotating reference frame, 143–144
 Voltage vector differential equation, 123
- W**
- Wave windings, 73
 Winding functions
 amortisseur winding functions, 282
 d axis amortisseur winding function, 148–154
 d-q-n reference frame, in; see under D-q-n reference frame
 field circuit, 159–160
 q axis amortisseur circuit winding function, 155–157, 159, 166
- Winding inductances
 calculating, 29–32
 mutual, between two circuits, 42, 44, 45, 48
 mutual, between two windings, 45, 121, 123, 130
 mutual, in concentrated windings, 29, 32–38
 rotor-associated, 33
 self-inductance, 30, 41, 44, 47, 50
 stator-associated, 33
- Winding magnetic axis, 8
 Winding series, 11, 31, 37
- Windings
 armature; see Armature windings
 arrangement of, 1
 concentrated; see Concentrated windings
 consequent pole winding, 72
 damper, 267–268, 269–270, 270, 282–284, 286–288
 derivations of function, 7
 design basics, 70, 71–75

distributed, 29
distribution of, 2
double-layer, 71, 73–74
doubly cylindrical machine, of, 25–26, 28,
29
field; see Field windings
fractional pitch; see Short pitch windings
full pitch; see Full pitch windings
function of, 2–8
generator amortisseur, 376
inductances; see Winding inductances
multiple circuit configurations, 39–45
multipole configurations, 22–23, 25
non-sinusoidally distributed, 52
series; see Winding series
short pitch; see Short pitch windings
single-layer, 71, 75
sinusoidally distributed, 19, 30–31, 52
turns, number of, 8
two-pole, 12, 21, 29
uniformly distributed, 15, 16, 18
wave; see Wave windings
wye windings; see Wye windings
Wye windings, 137

Z

Zero power characteristics, 226, 241–247,
245
Zero sequence, Fortescue's, 91, 92
Zero terminal voltage, 243
Zig-zag leakage, 67, 69

Second Edition

Analysis of Synchronous Machines

Analysis of Synchronous Machines, Second Edition is a thoroughly modern treatment of an old subject. Courses generally teach about synchronous machines by introducing the steady-state per-phase equivalent circuit without a clear, thorough presentation of the source of this circuit representation, which is a crucial aspect. Taking a different approach, this book provides a deeper understanding of complex electromechanical drives.

Focusing on the terminal rather than on the internal characteristics of machines, the book begins with the general concept of winding functions, describing the placement of any practical winding in the slots of the machine. This representation enables readers to clearly understand the calculation of all relevant self- and mutual inductances of the machine. It also helps them to more easily conceptualize the machine in a rotating system of coordinates, at which point they can clearly understand the origin of this important representation of the machine.

- Provides numerical examples
- Addresses Park's equations starting from winding functions
- Describes operation of a synchronous machine as an LCI motor drive
- Presents synchronous machine transient simulation, as well as voltage regulation

Applying his experience from more than 30 years of teaching the subject at the University of Wisconsin, author T.A. Lipo presents the solution of the circuit both in classical form using phasor representation and also by introducing an approach that applies MathCAD®, which greatly simplifies and expands the average student's problem-solving capability. The remainder of the text describes how to deal with various types of transients—such as constant speed transients—as well as unbalanced operation and faults and small signal modeling for transient stability and dynamic stability. Finally, the author addresses large signal modeling using MATLAB®/Simulink®, for complete solution of the non-linear equations of the salient pole synchronous machine. A valuable tool for learning, this updated edition offers thoroughly revised content, adding new detail and better-quality figures.

K13792

ISBN: 978-1-4398-8067-8

90000



9 781439 880678



CRC Press
Taylor & Francis Group
an Informa business
WWW.CRCPRESS.COM

6000 Broken Sound Parkway, NW
Suite 300, Boca Raton, FL 33487
711 Third Avenue
New York, NY 10017
2 Park Square, Milton Park
Abingdon, Oxon OX14 4RN, UK

WWW.CRCPRESS.COM